Structure and function of the external ciliation of larval bivalves with different life history strategies

Samuel Andrew Stanton

The thesis is submitted in partial fulfilment of the requirements for the award of the degree of Doctor of Philosophy of the University of Portsmouth

March, 2012

Abstract

Cilia are of particular importance to the planktonic veliger larva, fulfilling feeding, locomotory and sensory roles. This study concentrates on the ciliation of the larval mantle and velum. The mantle is an important adult organ yet one scarcely studied in the larval form. The larval velum is the characteristic swimming and feeding organ of the veliger larval form. Knowledge of the ciliary arrangement of larval bivalves, especially in relation to different life history strategies, provides important information for arguments over the phylogeny of such characteristics within the Mollusca. Anatomical work explored the possibility of ciliary sense organs being found on the mantle and further elucidates the pattern of distribution of cilia on the velum. Larval ciliary swimming in varying water temperatures has been investigated via the development of a filming methodology, revealing the thermal tolerance of swimming using velar ciliation and the ability of the larva to detect and respond to temperature stimuli.

Cilia were investigated throughout larval development from veliger stage to metamorphosis in two bivalve families, the Ostreidae (*Crassostrea gigas* and *Ostrea edulis*) and the Teredinidae (*Lyrodus pedicellatus*). The three larvae represented three developmental modes with *C. gigas* planktonic, *O. edulis* partly brooded and *L. pedicellatus* long-term brooded. Scanning electron microscopy (SEM) and light microscopy was used for anatomical investigations. Confocal laser scanning microscopy was used to locate catecholamines and serotonin in *C. gigas* larvae, with reference to the cilia locations identified by SEM. Swimming larvae were filmed in fixed and changing temperatures to identify behavioural or physiological reactions.

The mantle of the ostreid larvae had 13 different cilia groups which have been identified and photographed in *C. gigas* and *O. edulis*. Two of these groups appear to be sensory. One group is associated with the developing gill bud, and the other is located directly under the posterodorsal shell notch. The location of this group under the shell notch also was the location for several cells containing catecholamines. The ventral inner mantle rim of ostreid larvae has large tracts of cilia, probably primitive larval versions of adult rejection tracts. There were several flask-shaped cells with catecholamines and two long serotonin containing fibres in the mantle

where these tracts were found. The mantle of *L. pedicellatus* had 2 distinct groups of cilia. One of these groups formed discrete clumps on the inner mantle fold and featured sensory structures. The velar ciliation of both the ostreid species larvae was almost identical, and both revealed a previously unreported band of cilia. This band may increase the efficiency of the opposed band particle capture system. The velum of *L. pedicellatus* was different from the ostreid larvae; its velar ciliature was similar to other long-term brooded larvae recorded in the literature with a large adoral tract and the loss of the post-oral band.

Larval swimming velocity increased with increasing water temperature. Acclimated larvae were able to swim in water temperatures where larval activity stopped during sudden temperature changes. Changes in larval swimming during sudden temperature changes are probably due to an interaction of three factors: water viscosity changes affecting cilia efficiency, the physiological effect of temperature and behavioural responses.

The additional ciliary band on the ostreid velum probably increases particle capture efficiency, and further investigations are needed to determine if this is a characteristic unique to the ostreids. The velar ciliation of the brooded *L. pedicellatus* is, by the pediveliger stage, similarly modified to the velum of other brooded larvae from widely separated taxonomic groups. Mantle ciliation is more extensive in ostreids than in teredinids, but both have sensory stereocilia on the mantle. The presence of catecholamines and serotonin suggests that the larva has a measure of control both of mantle and velar ciliary beat, seen in the variation in swimming patterns and particle rejection.

The filming and analytical techniques developed offer an accessible method for gathering laboratory data on larval behaviours. Analysis of swimming suggested larvae can sense changes in temperature and effect a behavioural response to it. Such responses may enable larvae to control their vertical position in the water column when encountering environmental discontinuities or heterogeneities such as thermoclines. Variation in larval swimming velocity between larval batches suggests this method could also be used as a quick assay to determine the fitness of different larval batches within a hatchery.

Contents

Declaration

Whilst registered as a candidate for the above degree, I have not been registered for any other research award. The results and conclusions embodied in this thesis are the work of the named candidate and have not been submitted for any other academic award.

Samuel Stanton

List of tables

List of figures

Abbreviations

Table 0.1 - Key to mantle cilia abbreviations

Mantle Cilia				
Feature	Description	Location	Species	Stage
C1	Tract of cilia clumps, arranged as a single row	Inner mantle fold rim, posterodorsal region	*Crassostrea gigas* & *Ostrea edulis*	Veliger, pediveliger and early spat
C2	Short lines of approximately 6 cilia.	Gill bud/mantle junction on inner mantle fold rim	*Crassostrea gigas*	Veliger & pediveliger
C3	Large, round group of cilia, occasionally stiff in appearance, featuring C9 cilia	On mantle below gill bud	*Crassostrea gigas* & *Ostrea edulis*	Veliger & pediveliger
C4	Loosely organised clump of cilia	On mantle below the gill bud, next to C3	*Crassostrea gigas* & *Ostrea edulis*	Veliger & pediveliger
C5	Clusters of cilia aligned to form 2 rows on the inner mantle rim	Inner mantle fold rim from gill bud to antero-ventral	*Crassostrea gigas* & *Ostrea edulis*	Veliger, pediveliger and early spat
C5a	Lines of cilia not organised as C5, but still in two rows forming a transition between C5 and C6 or C10	Inner mantle fold rim - ventral region and antero-ventral	*Crassostrea gigas* & *Ostrea edulis*	Early veliger through to late pediveliger
C6	Scattered individual cilia loosely forming a single tract	Inner mantle fold rim - ventral region	*Crassostrea gigas*	Early veliger
C7	Short individual cilia	Anywhere on the inner mantle fold rim	*Crassostrea gigas* & *Ostrea edulis*	All stages, limited numbers
C8	Single tract of cilia	On the mantle below the C5 cilia	*Crassostrea gigas*	Late pediveliger and early spat
C9	Cilium bearing a ring of microvilli at the base	On the mantle directly below the posterodorsal shell notch and dorsal of the anal tuft.	*Crassostrea gigas* & *Ostrea edulis*	Veliger & pediveliger
C10	Single tract of cilia	Anterior and antero-dorsal inner mantle fold rim after the C5/C5a ciliation	*Crassostrea gigas* & *Ostrea edulis*	Veliger, pediveliger and early spat
C11	Cilia tract	Within the periostracal groove	*Crassostrea gigas* & *Ostrea edulis*	Pediveliger
C12	Long cilia, singly or in groups of 2-4	Anywhere on outer mantle fold rim, arising from within the periostracal groove	*Crassostrea gigas* & *Ostrea edulis*	Veliger & pediveliger
C13	Short, discrete lines of approx 15-30 cilia	Ventral to anterior region of the mantle, between C5 and C8	*Crassostrea gigas* & *Ostrea edulis*	Pediveliger and early spat
L1	Round group of cilia, often with associated stereocilia	On the inner mantle fold rim, from the hinge to the ventral region	*Lyrodus pedicellatus*	Pediveliger
L2	Line of cilia	On the mantle below the inner mantle fold rim	*Lyrodus pedicellatus*	Pediveliger

Table 0.2 - Key to mantle abbreviations

Mantle Features				
Feature	Description	Location	Species	Stage
At	Anal tuft/Post-anal tuft	Tuft of cilia located at the anus, and a second just after anus	All ostreid	Early veliger to metamorphosis
M	Mantle	Envelope of tissue enclosing the body cavity	All	D-larva to metamorphosis
iF	Inner mantle fold	Inner fold of the mantle rim	All	D-larva to metamorphosis
oF	Outer mantle fold	Outer fold of the mantle rim	All	D-larva to metamorphosis
T	Tract between the C5 type cilia rows	Un-ciliated tract between cilia rows	All	Any

Table 0.3 - Key to velum abbreviations

Velar Features				
Feature	Description	Location	Species	Stage
IPO	Inner pre-oral compound cilia	Top surface of velum, around the outer margin	All	Early veliger to metamorphosis
PO	Pre-oral compound cilia	Top ciliary band of the velar edge	All	Early veliger to metamorphosis
mPO	Minor pre-oral band	Below the pre-oral band and above the adoral band on the velar edge	*Crassostrea gigas* & *Ostrea edulis*	Early veliger to metamorphosis
AD	Adoral band	Central ciliary band running around velar edge	All	Early veliger to metamorphosis
PsO	Post-oral band	Lowest ciliary band of the velar edge	*Crassostrea gigas* & *Ostrea edulis*	Early veliger to metamorphosis
AT	Apical tuft	Located centrally on the top of the velum	All	Early veliger to metamorphosis
Mo	Mouth	At anterior edge of the velum	All	Early veliger to metamorphosis
V	Velum	Exits the shell valves opposite the hinge	All	Early veliger to metamorphosis

Table 0.4 - Key to additional abbreviations for relevant larval anatomy

Additional larval anatomy				
Feature	Description	Location	Species	Stage
Foot				
Bg	Byssal groove	From tip of foot to heel	All	Pediveliger
F	Foot	n/a	All	Pediveliger
hF	Heal of the foot	n/a	All	Pediveliger
Musculature				
aAD	Anterior adductor muscle	Anterior of shell valve	All	Early veliger to metamorphosis
pAD	Posterior adductor muscle	Posterior of shell valve	All	Early veliger to metamorphosis
MM	Mantle musculature	Behind outer fold of mantle, attaching to shell	All	Early veliger to metamorphosis
Shell features				
P1	Prodissoconch 1	n/a	All	Very early veliger
P2	Prodissoconch 2	n/a	All	Veliger to metamorphosis where the shell becomes the adult dissoconch
Pn	Posterodorsal shell notch	Posterodorsal region of shell valve, on the shell edge above the hinge	*Crassostrea gigas* & *Ostrea edulis*	From prodissoconch 1/2 boundary to metamorphosis
H	Hinge	Dorsal region of shell	All	From D-larva
Additional features				
G	Gill bud/Gill	Posterodorsal region	All	Veliger to metamorphosis
Gb	Gill bridge between mantle of each shell valve	Posterior region	All	Veliger to metamorphosis
Mu	Mucus	Velum/occasional around any ciliation	All	All
M1	Microvilli	Surface of velum and mantle	All	Veliger to metamorphosis
M2	Longer microvilli	Between the IPO and PO on the top surface of the velar edge	All	Veliger to metamorphosis
P	Periostracum	Emerges from within periostracal groove, over the outer mantle fold and over the shell	All	Veliger to metamorphosis
Pg	Periostracal groove	Between inner and outer fold of the mantle	All	Veliger to metamorphosis

Acknowledgements

Throughout my PhD I have tried to juggle the responsibilities of work at Emu Ltd with the labours of my thesis. This would not be possible without the unwavering support of my friends, family and colleagues.

Malacological Society of London supported my work through the award of the Centenary Research Grant, 2003. This grant enabled me to purchase the stains for the confocal work and various consumables for the electron microscopy work.

Firstly I would like to thank my supervisor, Dr Simon Cragg, whose enthusiasm for the topic and wonderful breadth of knowledge has generated a wealth of ideas throughout the course of my project. I have genuinely enjoyed our discussions and hope they continue in the future as we look to publish together.

I would also like to thank my second supervisor, Dr Gordon Watson, whose advice was always freely given and gratefully received. Gordon's support and belief that I would finish my thesis has always been resolute, I would like to take this opportunity to say thank you.

The shellfish hatchery, SeaSalter Shellfish at Reculver in Kent deserves a special mention. John Bayes, Antoine Pennec and Darryl Arnold allowed me to use their facilities to film their larvae with a refreshing mixture of enthusiasm and mild amusement! I was always comfortable working there and I am indebted to them for the interest they had in my work and the laboratory space they allowed me to use.

I would like to sincerely thank Richard Greenwood, who has been fantastically generous with his time in helping me with my statistics.

I would also like to thank Alex Ball at the Natural History Museum for allowing me to use the FEG SEM to view some of my samples.

My friends at the University and at Emu have been both a sounding board for ideas and a collection of friendly ears to listen when experiments have proven frustrating! While I cannot list everyone here I would particularly like to thank a few. Matt Harris was invaluable in the conducting of my filming work, being both a source of ideas and a fantastically willing pair of hands! Thank you to Gervis Sawyer who built my filming chamber and offered many useful insights into the design of my filming experiments. Thanks to Adam Bonner for his help maintaining my adult oysters. Ryan Coombes, Jo Murray, Graham Malyon, Peter Coxhead, Lucy Crooks and Neil Crooks have all been fantastic, thank you. A special mention must go to Martin Schaefer, always willing to listen to me, "thanks mate".

I would also like to thank my parents, Jo and Roy, and my brother Matthew who, while always nervous when asking "how's it going?" always cared enough to ask and listen to troubles. They have been unflinching in their support of my pursuit of a PhD, and have always believed I would succeed. All I can do is say thank you.

Finally I must thank my wife, Alison Stanton, who has put up with the weekends at work, the swings of mood whilst writing, and a myriad of other unpredictable ups and downs. In 8 years you have never once complained, never been anything but positive, and endlessly supplied me with tea and biscuits!

Quite simply I could not have finished this thesis without your love and support, thank you Ali.

Chapter 1 - General Introduction

The bivalve veliger larva is a superbly adapted marine invertebrate larva, subtly hiding its anatomical complexity under its shell and given further human interest due to the importance of many bivalve species in aquaculture and ecotoxicology. Investigations of bivalve larvae often are concentrated on survivability studies for the hatchery production of larvae as seed stock, with such studies focusing on the effects of temperate and salinity on larval development (Dove & O'Connor, 2007, Drent, 2002, His et al., 1989, Robert et al., 1988), or the effects of diet and starvation (His & Seaman, 1992, Rico-Villa et al., 2009). As a result of this focus on larval rearing there still are gaps in the anatomical and behavioural knowledge of larval stages, where comparative and functional understanding lags behind that of the adult forms. The structure and function of the external ciliation of larval bivalves, especially the ciliation of the mantle and velum, are important aspects of larval biology and phylogeny that still require further study.

1.1 A brief overview of life histories

This study focuses on the larvae of three marine bivalve species - *Crassostrea gigas, Ostrea edulis* and *Lyrodus pedicellatus*. These three species are of both economic and ecosystem importance, and provide examples of the variation in marine bivalve reproductive strategy. Consequently the demands placed on the remarkably similar larval stages of these species are quite different, with variation in development site, length of the planktonic phase and differing larval nutrition.

1.1.1 *Crassostrea gigas* (Thunberg, 1793)

Adult *Crassostrea gigas*, the Pacific Oyster, attach to hard surfaces, principally in the intertidal region where it filter feeds. While the adults have a wide tolerance range of both salinity (10-42psu) and temperature (4-35^{o}C) they require an optimal temperature of 20-23^{o}C for reproduction (Quayle, 1988), although spawning has been observed in 15^{o}C water in British Columbia (Quayle, 1988), and 18^{o}C in UK waters (Spencer et al., 1994). Adult *C. gigas*, like many ostreids, are protandric hermaphrodites, initially spawning as males, before spawning as females

when older (Galtsoff, 1964, Helm & Bourne, 2004). *C. gigas* reaches sexual maturity approximately one year after settlement, with spawning in UK waters in the summer months, usually July-August (Spencer et al., 1994). *C. gigas* broadcast spawn, releasing eggs and sperm into the water column, with fertilisation thus occurring externally. Females release 50-100 million eggs in several spawning bursts, and fertilisation must occur ~15 hours after spawning for eggs to remain viable (Mackie, 1984). All subsequent development occurs in the plankton via a feeding larval stage (planktotrophic nutrition), prior to settlement of the final larval stage onto a suitable substrata (usually a hard surface, for example *C. gigas* can be locally abundant on intertidal coastal defence structures) and metamorphosis into the adult form (Young, 2002).

1.1.2 *Ostrea edulis* (Linnaeus, 1758)

Ostrea edulis, the European Flat Oyster, is also a protandric hermaphrodite, beginning as males and at the onset of sexual maturity alternating between male and female states for the remainder of their life cycle (Laing et al., 2006). Spawning occurs in water temperatures of ≥14^{o}C (usually May-August in UK waters), males releasing sperm into the water column and females filtering sperm from the phytoplankton (Helm & Bourne, 2004). Fertilisation occurs in the mantle cavity of the adult female, and the first 7-10 days of larval development occurs within the adult, utilising nutrition from the egg (lecithotrophic nutrition). Subsequently *O. edulis* larvae are brooded for their early development (Foighil & Taylor, 2000), in contrast to the purely planktonic larval development of *C. gigas,* before having a short planktonic larval stage with planktotrophic nutrition (Young, 2002). As with *C. gigas*, final larval development and dispersal occurs within the plankton prior to benthic settlement and metamorphosis into the adult form.

1.1.3 *Lyrodus pedicellatus* (Quatrefages, 1849)

Lyrodus pedicellatus, the Siamese Shipworm, is an intertidal and shallow subtidal wood boring bivalve mollusc (Turner & Boyle, 1974). *L. pedicellatus* fertilisation occurs as for *O. edulis*, within the female mantle cavity after filtering sperm from the phytoplankton. Larvae then brooded within the mantle cavity in specialised brood pouches around the adult gill (Turner & Boyle, 1974, Turner & Johnson, 1971, Young, 2002). Larvae are presumed to utilise lecithotrophic

nutrition, using reserves from the egg (Turner & Johnson, 1971). Upon release the larvae of *L. pedicellatus* do not feed in the plankton (they have no planktotrophic phase), with this planktonic phase varying in length according to the presence/absence of suitable wood for settlement (Pechenik et al., 1979).

1.2The marine invertebrate larva

The marine environment is a buoyant and non-desiccating environment in which diverse behaviours and development modes have evolved (Young, 2002). The larval form serves as a dispersal stage for the adult (Strathmann, 1980), with this role being especially important in groups such as the Bivalvia that have largely immobile adult forms. The life histories of the study organisms described above represent some examples of differing larval strategies, and their utilisation within the Bivalvia, probably for dispersal (Strathmann, 1980). For successful dispersal the larva needs to be able to survive, function, and grow within the planktonic environment by utilising a suite of locomotory, sensory and behavioural abilities often independent of those found in the adult form. There is evidence for these pelagic larval stages being positively linked to passive dispersal, both in distance and scale (Levin, 2006, Scheltema, 1995). However, dispersal may alternatively be regarded as a consequence of having a larval form within the marine environment that is, an unavoidable a consequence of being pelagic (Todd et al., 1998).

The established view that a larval phase is advantageous for dispersal is being increasingly challenged (Levin, 2006). For example there is significant retention of larvae within natal populations (Levin, 2006, Todd et al., 1998). Furthermore, long planktonic phases suffer significant disadvantages, such as high mortality rates, and force trade-offs in the larval form (for example restricting cilia length to fulfil both swimming and particle capture functions, Chia et al., 1984) involved in utilising this strategy (Levin, 2006, Strathmann & Grunbaum, 2006). Understanding larval dispersal has become increasingly important, especially in the management of commercially important bivalves such as oysters (or those of ecological and economic importance such as the wood-boring Teredinids). Knowledge of populations that may act as sources, sinks, or those connected by larval exchange is important in fisheries management, in the

design of Marine Protected Areas (Levin, 2006), or for predicting the spread of non-native species such as *Crassostrea gigas* in UK waters (Child et al., 1995, Spencer et al., 1994). Furthermore, recent models of larval dispersal have become increasingly complex through the inclusion of larval swimming behaviours as mathematical factors influencing the prediction outcomes (Stobutzki, 2001).

The subject of whether dispersal is the main function of a pelagic larva is still subject to considerable debate, one that is too large to be fully considered in the scope of this introduction. Within the context of this work it is important to consider that dispersal is unavoidable when marine life histories include a pelagic larval phase. The marine invertebrate larval form must therefore be one suitable to survive the rigours of the planktonic phase regardless of the length of this phase. Investigations into that larval form and its behaviour, especially in relation to the use of cilia, contribute to the understanding of larval competence whilst within the plankton. This is especially relevant in the case of the species focused on in this study where there is little information available concerning larval anatomy or behaviours.

1.2.2 An overview of marine invertebrate larval forms

Many invertebrate phyla feature trochal larvae: those larvae that have cilia organised into discrete bands (Young, 2002). Broadly, these ciliated larvae may be divided into two larval forms – those having protostomian or deuterostomian development (Young, 2002). Protostomian development generally features a trochophore stage with a characteristic top-shaped body form, complete gut, a pair of protonephridia, ventral anus and the presence of an apical organ, typically in the form of a dorsal tuft of cilia (Fioroni, 1982). The trochophore plan has two opposed bands of cilia running around the equator of the larva – the prototroch and the metatroch - functioning as a downstream particle collection system (Nielsen & Nielsen, 1995). The multiciliated cells forming bands of different types of cilia are characteristic of protostomian development. The Mollusca, and therefore the Bivalvia species featured in this study, feature protostome development (Morse & Zardus, 1997).

Deuterostomian development is characteristic of the echinoderms and hemichordate phyla and has a dipleurula larval plan. The dipleurula has a single band of cilia, the neotroch, which functions as an up-stream particle capture system (Nielsen & Nielsen, 1995). Larvae following deuterostome development have a single flagellum arising from a single cell, forming undifferentiated ciliation. Some deuterostome, such as the urochordates and chordates, do not have ciliated larvae.

It should be noted here that this description is in no way sufficient to cover all the larval forms of the marine invertebrates, which exhibit great variety, but does encompass the major forms of invertebrate larvae that rely on cilia.

1.2.3 Classification of marine invertebrate larval development

There is some variation in the classification schemes used by different authors to examine marine invertebrate larval development. These schemes have variations of nomenclature or broad nomenclature that other authors have expanded into separate categories. For example, the broader classifications use three categories: direct development, lecithotrophic development (larval development utilising energy from yolk) and planktonic development (a feeding larval stage, although lecithotrophic larvae can still feature a planktonic phase), all of which occur in the Mollusca (Fioroni, 1982). However, this nomenclature fails to convey the true variety and complexity of marine invertebrate development. Levin and Bridges (1995) offer a more comprehensive classification scheme based on the following four categories.

1 – Larval nutrition

2 – Site of development

3 – Dispersal potential

4 – Morphogenesis

The system of Levin and Bridges (1995) will be used as framework for this brief overview of larval development as the classification system fits well with the larval development strategies used by the bivalve species examined within this study.

Larval nutrition

Larval nutrition, combined with the length of the planktonic phase, was an early classification criterion of larval development (Thorson, 1950). Primarily this was through the distinction of planktotrophy (oviparous species - the release of eggs not larvae or juveniles) and lecithotrophy.

Planktotrophic larvae develop entirely in the plankton, feeding and swimming within the planktonic environment. Lecithotrophic larvae derive at least some (usually most) nutrition from yolk, show variation in the length of the planktonic phase, can be brooded or not and can be encapsulated or not (Strathmann, 1985).

The species focused on in this study - *Crassostrea gigas, Ostrea edulis* and *Lyrodus pedicellatus* - feature a planktonic larval phase, of varying length, although the larvae of *Lyrodus pedicellatus* do not feed in the plankton (Pechenik et al., 1979). *Crassostrea gigas* is an oviparous species whose larvae develop solely in the plankton. *Ostrea edulis* larvae have lecithotrophic nutrition followed by planktotrophic nutrition (Gabbot, 1973, Waller, 1981), with larvae taking nutrition from egg yolk and then later from planktonic feeding when the larvae are released after a period of brooding. *Lyrodus pedicellatus* larvae have lecithotrophic nutrition (Isham & Tierney, 1953), with no larval feeding having been documented (Pechenik et al., 1979). However, the large prodissoconch II of the *Lyrodus pedicellatus* shell (Young, 2002) does suggest considerable growth after yolk reserves have been used, as the presence of a large prodissoconch II is typically associated with planktotrophic rather than lecithotrophic nutrition.

The classification structure of Levin and Bridges (1995) allows for the full complexity of larval nutrition to be considered, utilising all the factors discussed here and extending beyond the traditional split between planktotrophy and lecithotrophy. For example, direct uptake of dissolved organic matter (DOM) is a factor not taken into account by the more basic classifications of marine invertebrate larval development, but available to be considered within the system of Levin & Bridges (1995). Both non-feeding and feeding larvae can increase in biomass in the absence of particulate food, through the absorption of DOM (Manahan, 1990). In the case of the

bivalve larva, DOM take-up starts from fertilised embryo and continues throughout development (Manahan, 1983). The primary site of amino acid absorption and transport for the bivalve larva is through the larval swimming and feeding structure, the velum (Manahan, 1983), before the gills take over this role at metamorphosis (Manahan & Crisp, 1983). Molluscan larva can obtain 55% of their metabolic requirement from uptake of amino acids (Jaeckle & Manahan, 1989). This is not the case for all invertebrate larvae – crustacean larvae do not have the necessary transport systems in their integument to utilise DOM (Manahan, 1990). Interestingly both planktotrophic and lecithotrophic larvae will use DOM during their development, with even strongly lecithotrophic (relying entirely on yolk), encapsulated larvae such as those of the gastropod *Chorus giganteus* showing significant ability to utilise DOM (Martinez et al., 2008), and some non-feeding larvae supply up to 30% of their nutrient requirement from DOM (Jaeckle & Manahan, 1989). DOM uptake is a factor in nutritional systems, not a separate classification in itself.

Finally some invertebrate larvae utilise autotrophy – the ability to synthesise food, commonly through the utilisation of symbiotic bacteria. This is found in other invertebrate groups such as the cnidarians, but not in molluscan larvae (Young, 2002).

Development site

It is important to consider the site of larval development when considering the adaptations of the larva to its role and its environment. Development may occur in the planktonic environment or the benthic environment.

Planktonic larvae, such as those of *Crassostrea gigas*, develop entirely in the water column. Many lecithotrophic larvae, whilst generally encapsulated or brooded within the adult, will also have planktonic development, either after a brooded stage or when egg yolk has been used up, complicating the definition of development site. This issue of development site is one that is particularly relevant within the Bivalvia, with both planktonic and benthic types being found.

Benthic development can be broadly divided into 2 modes – parental and aparental (Levin & Bridges, 1995). Both *Ostrea edulis* and *Lyrodus pedicellatus* have at least some benthic development through the presence of brooding.

Aparental development shows development distinct from the parent, either from larvae attaching to the benthos, or more commonly through the use of encapsulated larvae. The gastropod and cephalopod molluscs show well-developed use of encapsulated development. Encapsulated benthic development generally shows lower mortality rates than planktonic development, however the energetic cost to the adult is significantly higher (Strathmann, 1985).

Parental development indicates that larvae are brooded by the adult. This can be either internal or external. Both *Ostrea edulis* and *Lyrodus pedicellatus* brood their larvae. *Ostrea edulis* broods until the veliger stage and release early prodissoconch II veliger stage larvae (Acarli & Lok, 2009, Waller, 1981). *Lyrodus pedicellatus* development can be considered to be almost entirely benthic with larvae being brooded for a longer period (Turner & Johnson, 1971) before being released as non-feeding pediveliger larvae ready for settlement (Pechenik et al., 1979). Brooding is an important trait within the Mollusca, and the bivalves particularly where early larvae are held (either free-swimming or in brood pouches) within the mantle cavity, usually in the region of the adult gill. This will be discussed further in **1.2**.

Dispersal potential

This classification term clarifies any confusion caused by using the terms planktotrophy or lecithotrophy to encompass the length of the planktonic phase. These terms on their own do not allow for definition between strategies such as the strategy of lecithotrophic larvae with brooding and pelagic phases of varying length, against strategies where full development occurs in the water column.

Thus larval dispersal potential is classified using the terms (Levin & Bridges, 1995):

Teleplanic – planktonic phase (arbitrarily) 2 months to over a year.

Actaeplanic – planktonic phase 1 week to less than 2 months – covers 70% of sublittoral species, including those used in this study, with typical development times of 4 to 6 weeks. All of the species focused on in this study have actaeplanic dispersal potential, with *Crassostrea gigas* having the longest planktonic stage and *Lyrodus pedicellatus* having the shortest.

Anchiplanic – short larval phase of few hours to a few days. *Lyrodus pedicellatus* can also be assigned to this category as the presence of wood will reduce the length of the planktonic phase to just days or even hours (Gallager, 1993, Pechenik et al., 1979).

Aplanic – non-planktonic larvae.

Morphogenesis

This classification of morphogenesis type provides a mechanism for including those species which undergo direct as opposed to indirect development. Indirect development sees the use of a larval stage which undergoes metamorphosis into the adult form - all of the species used in this study are examples of indirect development. Direct development rarely features a larval stage: embryonic stages are followed directly by morphogenesis into juveniles, or via highly modified larval forms, such as in the clam *Lasaea adansonii* (Altnoder & Haszprunar, 2008).

1.3 Bivalve spawning strategy

The adults of the Bivalvia often have limited mobility making spawning strategy highly important for dispersal of populations. Broadly two strategies predominate - those with entirely planktonic development and those that show a higher parental investment with lecithotrophic larval nutrition and larval brooding. The species focused on in this study are examples of variations of spawning strategy within the Bivalvia. Bivalves such as *Crassostrea gigas* and *Pecten maximus* show an entirely planktotrophic strategy with fertilisation and larval development all occurring in the planktonic environment (oviparous reproduction, as illustrated in *Pecten maximus* in Figure 1.1) with small, <50µm eggs released in large numbers (Helm & Bourne, 2004, Le Pennec et al., 2003, Mackie, 1984). Other bivalves such as *Ostrea edulis* and *Lyrodus pedicellatus* have larger eggs of approximately 150µm diameter; these eggs contain more yolk

and are produced in smaller numbers (Culliney, 1975, Waller, 1981). Larvae are then brooded free within the adult mantle cavity, prior to release of larvae for dispersal and settlement site searching.

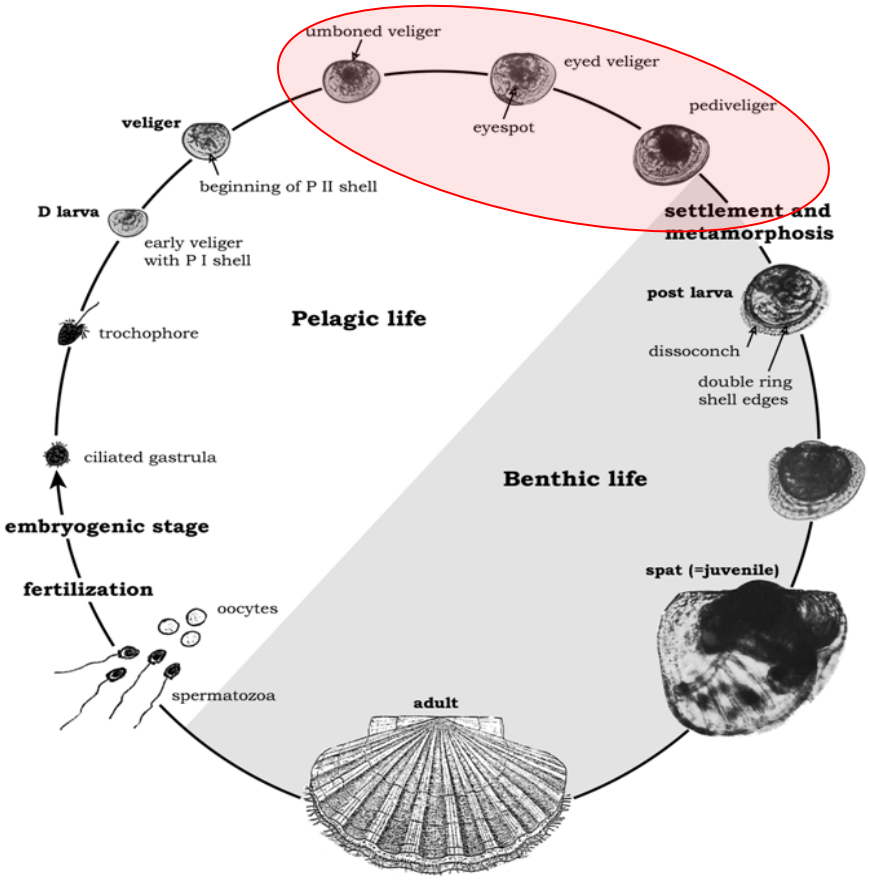

Figure 1.1 - *Pecten maximus* life cycle (Le Pennec et al., 2003).

Pecten maximus (as with *Crassostrea gigas*) is a broadcast spawner. All larval development occurs in the plankton during the pelagic stages of the life cycle prior to settlement and metamorphosis into the post larval spat. The ringed area above illustrates the larval stages investigated during this study.

Planktotrophy generally is considered an ancestral trait within the Bivalvia, with brooding and/or lecithotrophy representing a newer evolutionary strategy (Foighil & Taylor, 2000, Strathmann, 1985). However it has been proposed that within the Mollusca lecithotrophic larvae using energy from egg yolk may be the plesiomorphic condition, and that planktotrophy is the product of parallel evolution in the gastropods and the bivalves (Haszprunar et al., 1995). The author suggests that the shared ciliary arrangement in planktotrophic larvae may have arisen from an adult feeding system, and that this is probably not the plesiomorphic condition, with lecithotrophic nutrition being a plausible alternative. However, both arguments are hindered by

gaps in anatomical details concerning the ciliary bands of invertebrate larvae. Any new or expanded description of invertebrate larvae ciliary arrangements will add evidence to these discussions.

Brooding is a trait that does not appear positively linked with either lecithotrophic or planktotrophic development, and thus should be considered separately to the arguments surrounding the ancestral nature of either. Some non-lecithotrophic brooders such as *Ostrea chilensis* or *Ostrea circumpicta* have feeding planktotrophic larvae held within the mantle cavity but activity is confined to swimming and feeding around the adult gill, either by collecting particles or possibly exploiting mucal strings from the adult (Chaparro et al., 1993, Kang et al., 2004). Other brooding species, such as *Lyrodus pedicellatus* (personal observations) and *Teredo* sp. (Morse & Zardus, 1997), retain larvae in brood pouches in the adult gill. Brooding species, such as the teredinid *Teredo navalis* or the ostreid *Ostrea edulis*, produce larger, more yolky eggs than their planktotrophic relatives (for example the sizes given for *Ostrea* and *Crassostrea* eggs earlier). These eggs are fewer in number, and represent the higher energetic cost to parent typical of lecithotrophy (Pechenik, 1999), and still are followed by a period of planktotrophic larval nutrition. However, variation in egg hydration makes egg size a less consistent definition of nutrition in marine invertebrates generally. Echinoderm eggs particularly show comparable energy concentrations between planktotrophic and lecithotrophic species (McEdward & Chia, 1991).

Despite the general similarity in planktotrophic larval form, there is significant variation in brooding time, brooding style (free swimming larvae or pouches) and the capabilities of the larvae when released - for example the larvae of *Lyrodus pedicellatus* will not feed once released (Pechenik et al., 1979), whereas the larvae of *O. edulis* have to feed within the plankton (Waller, 1981). Those adults showing longer brooding time tend to have larvae with a shorter planktonic phase. In addition some brooded larvae show significant differences in appearance throughout the early or brooded stages of development with some larvae having altered larval morphology during the late trochophore and early veliger stages of development. For example larvae of some

Teredo sp, have a modified velum for absorbing nutrition from the adults whilst being brooded (Turner & Boyle, 1974). Brooding versus non-brooding also represents a difference in the site of fertilisation. In brooding adults, fertilisation tends to take place in the mantle cavity as is the case for *Lyrodus pedicellatus* (Nair, 1971) and *Ostrea edulis* (Waller, 1981) and subsequently some or all of the larval development occurs within the adult. Non-brooding adults tend to be broadcast spawners, for example *Crassostrea gigas,* (Helm & Millican, 1977) and *Pecten maximus* (Le Pennec et al., 2003), which release eggs and sperm into the plankton and rely on external fertilisation (Figure 1.1).

Brooding represents a significant parental investment; it is a strategy suffering from a higher energetic demand with lower larval dispersal potential, but resulting in better larval recruitment (Strathmann, 1980, Strathmann, 1985). The genera *Ostrea* and *Crassostrea* provide a good example of quite closely related species with different larval strategies showing the effect of these strategies in the adult form - in this case the increased parental investment in brooding leads to smaller adult size in *Ostrea* against the larger adults of the non-brooding *Crassostrea* genus (Strathmann & Strathmann, 1982). Non-brooding, oviparous species such as *C. gigas* have larvae with very high food requirements, that are dependent on plankton condition (i.e the availability of food) and suffer long-term exposure to predation (Thorson, 1950). In contrast brooded larvae are larger at release and feature lower food requirements resulting in a competitive advantage in conditions of low resources, and shorter exposure to predation (Thorson, 1950). Brooding will also reduce predation on eggs (Pechenik, 1999), however predation on adults subsequently has a high cost.

Brooding species such as *O. edulis* or *L. pedicellatus* are susceptible to low genetic diversity in local populations and are vulnerable to catastrophic local events (Buroker, 1985, Strathmann, 1985). Conversely brooding species will feature greater genetic diversity between distant populations than oviparous species. Work with lecithotrophic nudibranch larvae has shown that even local populations separated by as little as 100m can show significant heterogeneity in allele frequencies, suggesting these populations will receive many new larval

recruits from within that population (Lambert et al., 2003). This can be further complicated by introducing other factors such as species with very specific substratum requirements, whereby the rules, such as greater dispersal by species employing oviparous strategies, may not lead to greater genetic diversity (Buroker, 1985). Some brooders, such as the oyster *Tiostrea chilensis*, have modified the habit to enable brooding of larvae either to the point of settlement, or to release feeding planktotrophic larvae that can survive for a relatively long period in the plankton. This maintains gene flow between populations whilst enhancing dispersal (Cranfield & Michael, 1989, Kempf & Hadfield, 1985).

The spawning strategy shows variations of larval nutrition, larval dispersal potential and larval development site, that greatly influence the capabilities of the larvae produced, their relative mortality, and genetic diversity of adult populations through dispersal of larvae. The type of strategy varies according to species and varies across closely related genera. However, most bivalves do utilise a larval form. This larva will survive and disperse through the plankton and seek out a settlement site. The species of interest to this study were chosen as they show three contrasting examples of bivalve spawning strategies.

1.4 The bivalve veliger and the planktonic environment

The planktonic larva will disperse in the plankton prior to metamorphosis into the adult form, and thus this larva is adapted to fulfil two roles – dispersal via the plankton and survival within it. As Figure 1.1 shows, considerable larval growth occurs during the planktonic phase. Dispersal can be broadly divided into two aims - dispersal from the adult and dispersal from siblings (Strathmann, 1980). Understanding veliger anatomy and behaviour provides an understanding of how the veliger achieves this within the planktonic environment. In the plankton the larva must survive predation, overcome buoyancy issues, adapt to variations of temperature and light, currents, chemical cues and find food. All of these pressures influence the larval form. As a result there is a remarkable similarity in larval form between taxonomically diverse species with very different adult forms (Strathmann, 1993).

The planktonic larval form in the Bivalvia is the veliger (Figure 1.2). The veliger is typically associated with the Mollusca in general, but is only found in the gastropods and the bivalves (Nielsen & Nielsen, 1995). Within the Bivalvia rare specialised forms exist, such as the parasitic glochidium with its specialised hooks and hairs (Jupiter & Byrne, 1997), but the general veliger form is typical across most of the Bivalveia. The veliger is a shelled larva (Figure 1.2), formed after the trochophore developmental stage and characterised by the presence of the ciliated velum, a structure that fulfils both swimming and feeding roles for the larva within the water column.

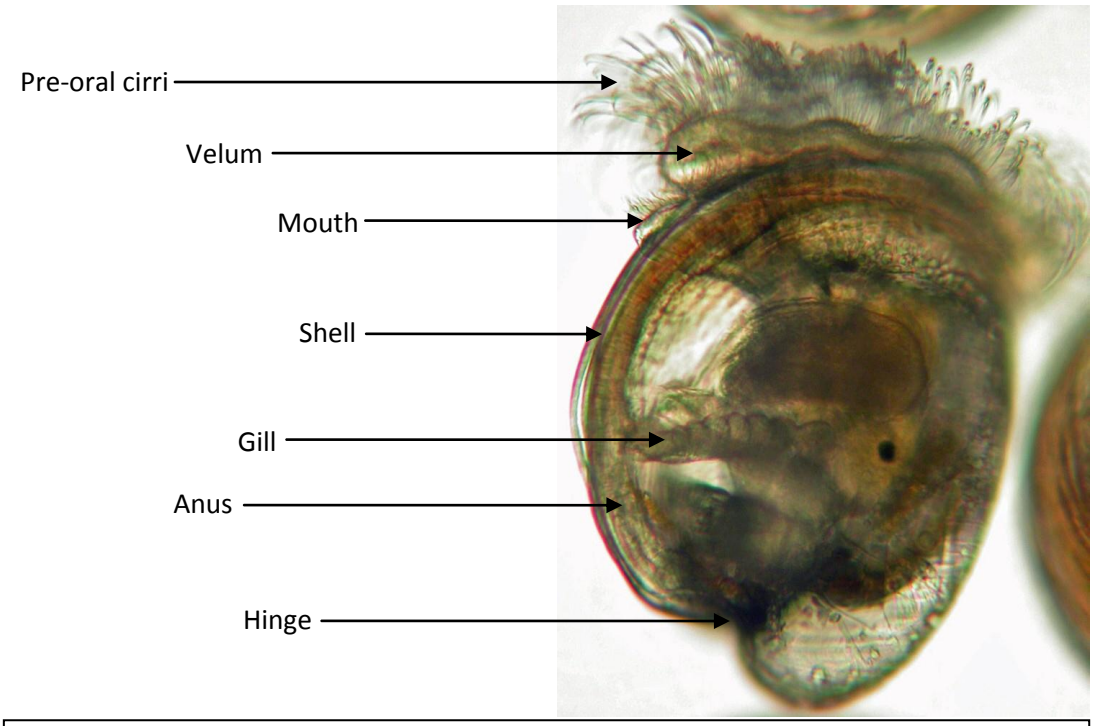

Figure 1.2 - *Crassostrea gigas* mid-stage veliger larva (Stanton, unpublished).

The large swimming/feeding organ, the velum, visible protruding from the shell valves, with the larval mouth just below. The digestive system is visible through the shell, as is the larval gill, in the posterior under the mouth and above the anus.

The velum stems from the prototroch, becoming flattened when viewed from the side and ovoid when viewed from above as the larva changes shape and the shell develops from secretions in the post-trochal region (Fioroni, 1982, Galtsoff, 1964). The ciliary arrangement around the velar rim generally comprises 4 rows of compound cilia (Waller, 1981). These rows provide the power stroke for larval swimming (Cragg & Gruffydd, 1975), and their beat achieves particle capture (Gallager, 1988). The latter is reflected in the rows being named according to their position relative to the larval mouth - the pre-oral, adoral and post-oral bands (Cragg, 1989,

Waller, 1981). The function of these rows for feeding follows the opposed band system of particle capture synonymous with protostomian downstream particle capture: a well documented feeding arrangement found in many planktonic invertebrate larvae (Riisgard & Larsen, 2001, Riisgard et al., 2000, Strathmann & Grunbaum, 2006), and one that is visible in the ciliary arrangement of the bivalve veliger velar edge (Ward et al., 1991). Bivalve veliger downstream particle capture has been filmed in the velar ciliation of *Mercenaria mercenaria* (Gallager, 1988, Ward et al., 1991), *Mya arenaria*, *Mytilus edulis* and *Placopecten magellanicus* (Ward et al., 1991). Having the velum for both swimming and feeding the veliger suffers from drag on the shell, hindrance from body weight, and the presence of oral ciliary bands beating in opposition to the swimming stroke - essentially by having good clearance rates for feeding, the veliger is a poorer swimmer (Strathmann & Grunbaum, 2006).

The ciliation of the velum does vary between species. It is generally accepted that the planktotrophic veliger with the opposed band ciliary layout is the primitive larval form (Cragg, 1996, Nielsen & Nielsen, 1995). Species with brooding habits often will show the loss of some velar ciliation, even between quite closely related species. For example *Ostrea chilensis* veligers can feed but have low clearance rates due to the loss of the post-oral band of cilia on the velum and are not released from the adult until ready to settle (Chaparro et al., 2006, Chaparro et al., 1999). In the gastropods, brooded versus encapsulated *Crepidula* larvae show inter-species velar ciliature modifications, again often involving the loss of the post-oral band or extension of the adoral band (Chaparro et al., 2002a, Chaparro et al., 2002b). This variation between species represents an area where anatomical information at the species level is still lacking, but also highlights the importance of collecting such information. Despite the general homology of the velum, species-specific variation is present. Knowledge of these species-specific variations and their links to reproductive strategies can feed into the debates surrounding the ancestry of the protostome larval form and the ancestry of the modification of the brooded velum, as well as expanding knowledge of the functional anatomy of the velar ciliation. The distribution of cilia on

the velum of *Crassostrea gigas, Ostrea edulis* and *Lyrodus pedicellatus* will be investigated in detail in **Chapter 3**.

On the velum, the central apical tuft probably fulfils a sensory function, as connections with the cerebral ganglion have been identified in the veliger larvae of the ostreids (Chaparro et al., 1999, Croll et al., 1997), pectinids (Croll et al., 1997) and Mytilidae (Flyachinskaya, 2000). Furthermore the apical tuft is found in other molluscan larvae such as gastropod veligers where it is also considered to have a sensory function (Croll, 2006, Hadfield et al., 2000, Hejnol et al., 2007, Kempf et al., 1992, Marois & Carew, 1997). The apical tuft is found across a diverse range of molluscan taxa (Page & Parries, 2000), but also across a wide range of invertebrate groups suggesting the tuft is probably ancestral (Young, 2002). The function of the apical tuft in the bivalve larva has not been fully determined experimentally (Cragg, 2006), but does bear structural comparison to chemosensory structures in other invertebrate larvae and experiments have suggested it becomes a receptor for settlement cues in the pediveliger (Hadfield et al., 2000).

In addition to the velar ciliature, the veliger larva has other attributes for survival within the plankton. The shell will act as an aid to orientation during swimming through the effects of gravity. This orientates the velum upwards, even before the larvae has developed the ability to detect gravity (Cragg, 1980). The larva has a well developed musculature for both retraction of the velum and the closing of the shell. The velum of *Pecten maximus* has 4 anterior retractor muscles and 3 posterior retractor muscles (Cragg, 1985), forming multiple branches where they contact the mantle lining the shell. This musculature enables the larva to not just retract the velum and close the shell, but to do so very rapidly causing the larva to sink. This reaction is one larval response to stimuli and others will be discussed in greater detail in **Chapter 4**.

Buoyancy is a problem the heavy, shelled veliger larva must overcome in order to favourably control its vertical position. Lecithotrophic larvae may utilise lipids for maintaining buoyancy, with the use and resulting loss of these lipids decreasing buoyancy by the late veliger stage (Levin & Bridges, 1995). However, in the case of those exclusively planktotrophic bivalve larvae, buoyancy probably is solely controlled by the physical retraction of the velum, and the

subsequent sinking through the weight of the shell, followed by active vertical swimming (Cragg & Gruffydd, 1975).

The veliger larva may have some chemosensory ability. This has been suggested by changes in swimming behaviour at differing concentrations of a chemical stimulant (Prael et al., 2001). However the chemosensory ability of veliger stage larvae still requires further research.

Predation is a significant problem for veligers in the plankton. The larvae of polynoid, spinoid and maldanid polychaetes are known to prey upon on *C. gigas* veligers (Johnson & Brink, 1998). In addition, the hydrodynamic disturbances caused by the beating of the cilia of the velum increase the chances of detection, with feeding larvae generating a larger field, making them more susceptible to predation by those planktonic organisms equipped with mechanoreceptors. Higher feeding rates will be attained when hovering, but the greater disturbance caused means hovering represents greater risk to the larvae from predators (Gallager, 1993, Pechenik, 1999).

The larval response both to the intensity and direction of light is an important factor for maintenance of the vertical position of the larva in the water column (Thorson, 1964). Most pelagic, veliger stage larvae are photopostive, tending to rise in the water in response to light, but showing a photonegative response to intense light and high temperature (Thorson, 1964) resulting in larvae often being limited to deeper waters during the day (Kaartvedt et al., 1987). However, larvae in a laboratory situation will maintain vertical swimming paths, regardless of the direction of illumination (Cragg & Gruffydd, 1975, Dekshenieks et al., 1996, Hoagland, 1986). Light also has been implicated in triggering the vertical migrations of larvae. Such migrations are probably due to more than just light stimuli, with tidal/diurnal cues, temperature, predator avoidance, food abundance and thermoclines all having an influence (Manuel & O'Dor, 1997, Manuel et al., 1997). In addition, veligers have also been shown to respond to changes in temperature and salinity, with extremes of high or low temperatures or salinities reducing the frequency of bouts of swimming (Galtsoff, 1928, Hidu & Haskin, 1978a). Larval detection and response to stimuli such as temperature and light, and the influence of this behaviour on larval population movements such as vertical migrations will be discussed further in **Chapter 4**.

1.5 The molluscan pediveliger and the benthic environment

The final larval stage before metamorphosis is the pediveliger (Figure 1.3). Whilst the veliger is adapted for the planktonic environment and its challenges, the pediveliger is adapted for the benthic environment. Anatomically the pediveliger is very similar to the veliger, still possessing a velum and the same organ systems. The pediveliger still feeds and swims in the water column (Hadfield & Koehl, 2004), but it will also crawl on the benthos using the larval foot to search out settlement sites (Cranfield, 1973b), a role vital to the long-term success of benthic populations.

The foot is the characteristic organ of the pediveliger. It exits between the shell valves dorsally from the mouth and above the anus, and has a profusely ciliated sole for propulsion (Cranfield, 1973a). The byssal duct opens on the heel of the foot (Figure 1.3) and the byssal groove runs along the sole towards the tip of the foot. This byssal region features various glands along its length capable of secreting mucus from the pedal glands on both the tip and anterior end of the foot (Cranfield, 1973c). These byssal regions are also the location for numerous neural pathways in pediveligers of both bivalves (Croll et al., 1997, Croll et al., 1995, Voronezhskaya et al., 2008) and gastropods (Dickinson & Croll, 2003, Hejnol et al., 2007, Kempf et al., 1992, Voronezhskaya et al., 1999). The surface texture of the benthos and the local hydrodynamics have an impact on pediveliger settlement in bivalves (Pearce et al., 2004) and gastropods (Fuchs et al., 2007, Koehl, 2007). Observations of *Ostrea edulis* pediveligers crawling show the larvae exhibit 6 phases of crawling when using the foot for searching out a settlement site - ciliary crawling, 4 phases of muscular crawling and cementing using byssal secretions (Cranfield, 1973a). Furthermore the larva will often swim with the foot extended and pointing towards the benthos (Cranfield, 1973c). These observations suggest the foot may have both chemosensory and mechanosensory capabilities allowing the larva to exert considerable control over its selection of a settlement site.

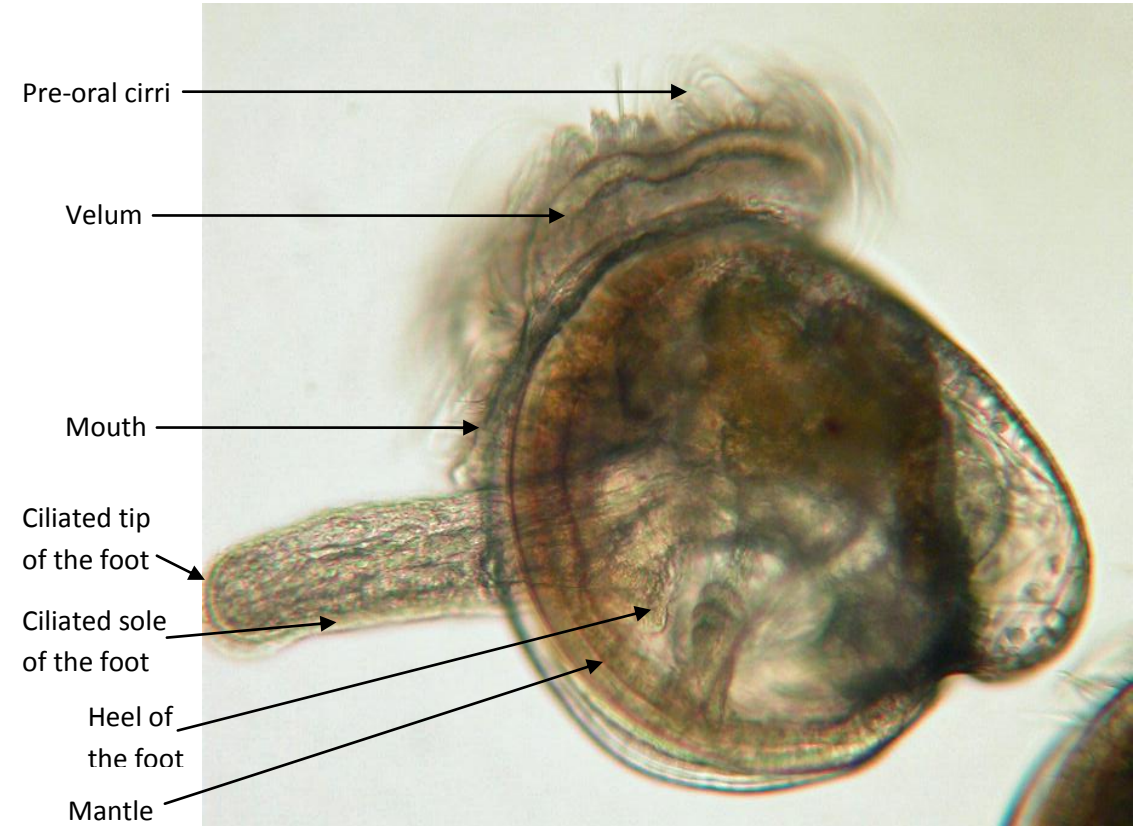

Figure 1.3 - *Crassostrea gigas* pediveliger (Stanton, unpublished).

The pediveliger foot can clearly be seen exiting the shell valves below the mouth, the velum and the pre-oral cirri (curved downwards showing the beat) are also visible. The heel of the foot and the tip of the foot have been labelled as these are the locations of pediveliger sensory cilia. The ciliated sole is labelled and this is the locomotory surface. The general appearance of the larva is similar to the veliger stage larva shown in Figure 1.2.

Figure 1.3 illustrates how close the mantle is to the surface of the benthos when the foot is extended and the larva is crawling on the ciliated sole. The pediveliger mantle probably has a role in attachment at settlement, just prior to metamorphosis, extending over the benthos and possibly being involved in attaching the larva to surfaces (Cranfield, 1974). However, whilst the presence of ciliation on the mantle of different bivalve pediveligers specifically on or near the mantle rim has been previously recorded (Bellolio et al., 1993, Cragg, 2006, Waller, 1981), there are few papers detailing this ciliation or speculating on its function. Any sensory ability afforded the larva from this mantle ciliation is currently unknown, although the close proximity of the mantle cilia to the benthos when a larva is crawling is suggestive.

To successfully find a settlement site, the pediveliger can detect water-borne cues specific for settlement. Larvae of *Crassostrea virginica* respond to such settlement cues in various hydrodynamic conditions by exhibiting downward swimming behaviour (Tamburri et al., 1996, Turner et al., 1994, Zimmer-Faust et al., 1997). Changes in swimming behaviour like this can prevent the pediveliger from being forced away from the site of the cue by changes in local hydrodynamic condition. This response can be rapid: nudibranch pediveliger larvae abruptly stop swimming and sink to the benthos when cues are detected (Hadfield & Koehl, 2004). Despite the sensory capability of the foot, ablating the apical organ of gastropod pediveligers inhibits the detection of settlement cues, indicating that the apical tuft has a role in detecting settlement cues (Hadfield et al., 2000).

As with the veliger, the pediveliger can detect salinity, temperature and light changes whilst either swimming or crawling, and the larval response to these stimuli often has an affect on pediveliger settlement potential by keeping the larva close to the benthos. Pediveligers have been recorded as being photonegative, showing the reverse of the veliger response to light (Thorson, 1964). Temperature and salinity have an affect on settlement potential: *Crassostrea iredelei* settlement was highest in optimum conditions of 20psu salinity and 30^{o}C (Devakie & Ali, 2000), while teredinid species such as *Teredo bartschi* and *Teredo navalis* have a wide tolerance for both temperature and salinity variations, but with poor settlement at the extremes of these variations (Hoagland, 1986). The pediveliger has some sensory capabilities specific to its benthic role. It can detect gravity through statocysts on the mantle (Cragg & Nott, 1977). These spherical sacks, containing sensory cilia and particles, are formed from an invagination of the epithelium of the foot, and are connected to the main mantle cavity via a ciliated canal (Cragg & Nott, 1977). The pediveliger larva probably use statocysts for orientation during crawling (Cragg & Nott, 1977).

1.6 The importance of cilia and the control of ciliary beat in the bivalve veliger

Cilia are important to many planktonic larvae, forming feeding, locomotory and sensory structures in a wide variety of invertebrate larvae (Young, 2002). Cilia in their various patterns

and different morphologies are of vital importance to the larval bivalve, lining the sole of the foot for motility when crawling, lining static ducts, covering the gill, lining the digestive tract and performing sensory and swimming roles for the organism (Cragg, 1989, Cragg, 2006, Cranfield, 1973b, Hadfield et al., 2000). Having considered the bivalve larva as an example of an invertebrate larva and examined the larva through veliger and pediveliger phases, this section will briefly consider the cilia themselves, and the methods of larval control of this ciliation. Cilia arise early on the evolutionary scale and are present in almost all animal groups, and in plants, formed of a bundle of protein tubules known as an axoneme (Leigh, 1962). The axoneme is comprised of 9 double tubules surrounding a central pair of single tubules - this makes up the characteristic 9+2 structure of cilia and flagellae (Haimo & Rosenbaum, 1981, Sleigh, 1962). The movement of cilia comprises an effective stroke (the power stroke) whereby the organelle moves rapidly to one side, followed by the recovery stroke where it moves back again along a similar/the same plane (Haimo & Rosenbaum, 1981, Satir, 1992, Sleigh, 1962) powered by the recovery of the sliding displacement of the microtubules within each axoneme (Haimo & Rosenbaum, 1981).

The characteristic organ of the bivalve veliger is the velum, using the opposing band system for swimming and feeding - it is the velum's use of ciliary effective and recovery strokes that make it so suited to its purpose. Ordered patterns of these effective and recovery strokes by the large pre-oral cilia of the velum rim provide the power stroke for larval swimming. Only small (less than 1mm) organisms can utilise cilia for locomotion owing to the low Reynolds numbers that operate at this scale. Bivalve larvae are also denser than seawater owing to the shell and as a result need to swim using the ciliary action of the velum to maintain their vertical position in the water column (Chia et al., 1984).

Ciliary feeding also utilises the power and recovery stroke of cilia in an ordered pattern on the velar rim. The pre-oral cilia will capture particles as they accelerate water during their power stroke (the effective stroke). As a result the particle is pushed out of the main water current and onto the adoral cilia at the end of the pre-oral cilia stroke. The opposing band of post-oral cilia prevent particle escape with their power stroke operating in the opposite plane to the pre-orals

and providing deflection onto the adoral tract of cilia. The adoral cilia beat around the velar rim towards the mouth - this opposed band system is found on almost all feeding bivalve veligers (Riisgard & Larsen, 2001, Strathmann et al., 1972).

Ciliary function within the gills of adult bivalves is known to be regulated by serotonin which raises cAMP levels in the gill (Stephens & Prior, 1992). There is neurally regulated catecholamine excitation of the swimming cilia in trochophore larvae (Marsden & Hassessian, 1986). These compounds have been identified in pediveliger stage larval bivalves, where they are known to act as morphogens influencing early development, and as triggers for settling and metamorphosis (Pires & Hadfield, 1991). Serotonin and catecholamines have been suggested as having roles in the control of larval ciliary activity (Beiras & Widdows, 1995) and both have been identified in the velum, mantle and foot of *Placopecten magellanicus* and *Mytilus edulis* pediveligers (Croll et al., 1997). In the velum of the gastropod *Ilyanassa obsoleta*, serotonin increases the beat frequency of pre-oral cirri whilst catecholamines decrease beat frequency and cause momentary arrests (Braubach et al., 2006). Velar activity in larval bivalves probably is regulated by both serotonin and catecholamines, and these compounds probably play a role in the behavioural regulation of ciliary beat, potentially illustrated by changes in larval swimming trajectories (Braubach et al., 2006, Croll et al., 1997).

This reliance on cilia for swimming and feeding extends beyond these two functions, with larvae having ciliated sensory organelles for settlement in the form of the apical organ of the gastropods (Hadfield et al., 2000), ciliated statocysts for gravity detection (Cragg & Nott, 1977), ciliated gills for respiratory demands (Beninger et al., 1994), and the little studied possibility of sensory ciliation on the mantle and mantle rim (Beninger & Veniot, 1999, Beninger et al., 1999, Cragg, 2006). Many of these structures have serotonin-containing or catecholamine-containing fibres or cells suggesting their ciliary beat is under nervous control (Braubach et al., 2006, Croll et al., 1997) but a connection between this anatomical and neural information has not yet been fully explored. Adult bivalves use specialised ciliary structures for sensory reception such as the abdominal sense organ in the scallops (Zhadan, 2005, Zhadan et al., 2004) or Stempell's organ in

Nucula (Haszprunar, 1985b, Haszprunar, 1987a). It is possible that some of the ciliary structures on the mantle of larval bivalves could be larval sense organs (Cragg, 2006, Cranfield, 1974, Haszprunar, 1985a) and that they are linked into larval behaviour.

It is important that inter-species variations in velar ciliary arrangements and the ciliation of the mantle be properly investigated in relation to their morphological variation and functional significance in order to fully understand the complex role of the external ciliation of the bivalve veliger larva.

1.7 The aims of this thesis

1.7.1 Context

During the course of this research the external ciliation found on brooded (*Lyrodus pedicellatus*), semi brooded (*Ostrea edulis*) and planktotrophic (*Crassostrea gigas*) bivalve larvae will be investigated in order to identify any differences or similarities that may be associated with the requirements placed upon the larvae by these specific reproductive strategies.

As has been discussed throughout this introduction, ciliation is of crucial importance to the bivalve larva. Comparisons of ciliary arrangements and forms can help elucidate the adaptations of larvae to the life histories and spawning strategies employed by specific marine bivalve species. Differences in the ciliation of the larval velum can reveal differences relating to larval feeding and swimming. These differences (if any are identified) may be related to the differing requirements of planktonic versus brooding stategies, or planktotrophic versus lecithotrophic forms of larval nutrition. Whilst the ciliary patterns of the velum have been documented for a few bivalve species (but not in detail for *C. gigas* or *L. pedicellatus*), another important ciliated larval organ, the mantle, has historically been overlooked. Ciliation of the bivalve larval mantle is poorly documented, despite evidence of several different groups on the mantle of larval Pectinids (Cragg, 2006). The larval mantle has mainly been considered for its role during settlement (Cranfield, 1974) and yet the ciliation it bears is exposed to the water column when the shell is open during veliger swimming and close to the benthos during pediveliger crawling. Therefore the presence of mantle ciliary groups may have a functional significance to

the larva, from the early swimming veliger stages through to settlement site searching pediveliger, which has previously been overlooked.

In addition to the functional significance of larval ciliation, anatomical studies also contribute evidence to evolutionary questions, such those surrounding the ancestry of planktotrophy/lecithotrophy within the Bilateria. The origin and final layout of ciliary bands contribute to these arguments, with the changes in the protoch and metatroch central to the question of the ancestral larval form. Furthermore, these discussions directly relate to the ancestry of feeding and development strategies, such as the ancestral nature of brooding, lecithotrophy and planktotrophy.

In all the above topics there is a lack of detailed anatomical information available on the larval stages of many bivalve species. These include species of considerable economic and ecosystem importance such as *Crassostrea gigas, Ostrea edulis* and *Lyrodus pedicellatus*. This research seeks to address some of these gaps in knowledge, specifically concerning larval ciliation, and provides a descriptive, comparative, functional and phylogenetic context for this additional information.

Anatomical studies of bivalve larvae often fail to incorporate this morphological knowledge within a behavioural context. The combination of larval behavioural knowledge with the information gathered by detailed anatomical studies of these larvae allows for a more detailed overview of the life histories and spawning strategies employed within the marine Bivalvia. For example, the ability of a larva to control ciliary beat may be a key factor influencing feeding, behavioural reactions and larval capability once released into the plankton. Behavioural studies of larval bivalves are rarely combined with detailed anatomical studies. This is probably due, at least in part, to the technical difficulty or expense of such studies. During this research an inexpensive method of filming larval behaviours was designed and used to collect information on larval swimming, in order to make this type of combined study more accessible.

1.7.2 Rationale

The morphology and pattern of the ciliation of the bivalve larval mantle and velum was investigated using a combination of light microscopy and scanning electron microscopy (SEM). This combination allowed for whole organism, sectional and confocal scanning laser microscopy techniques to be combined with the high resolution 3-dimensional imagery of SEM. Using SEM in this manner allowed for both contextual and high resolution imagery in order to investigate both the fine structure of the cilia themselves, and their location within the larva.

In addition a method of filming and analysing the swimming behaviour of the larvae using a video camera, standard macro lens and shareware software was developed and used to investigate any behavioural reactions of the larvae to changes in temperature. Temperature was chosen as an important stimulus encountered by the larvae when swimming: for example thermoclines have been identified as a factor affecting the vertical distribution of larval populations (Manuel et al., 2000). The larva has to be able to detect changes in temperature in order to affect a behavioural response. Temperature also is a variable whose effects on the properties of the water and the physiology of the cell will consequently affect the function of the ciliation examined elsewhere in the thesis. As a consequence some reaction to temperature could be reasonably expected, either behaviourally or physiologically. As such, temperature was determined an appropriate stimulus for the trial of a filming method designed to analyse for a change in ciliary swimming behaviours.

The brief listing below provides a summary of the central aims of this thesis, designed to inform the context described above in **1.7.1**.

1. Production of detailed descriptions of cilia morphology and distribution on the mantle of three species representing differing life history strategies - *Crassostrea gigas*, *Ostrea edulis* and *Lyrodus pedicellatus*. These descriptions will fill gaps in the current larval literature. This is examined in Chapter 2

2. Production of detailed descriptions of the ciliary arrangement and morphology on the velum of *Crassostrea gigas*, *Ostrea edulis* and *Lyrodus pedicellatus*. These descriptions will fill gaps in the literature. This is presented in Chapter 3.
3. Compare the information on mantle and velar ciliary arrangements of the larvae of these three species through development from early veliger to metamorphosis in consideration of the differing demands placed on the larvae by, for example, the length of planktonic or brooded periods. This is examined in Chapters 2 and 3.
4. Determine if there are any specialised sensory cilia on cilia mantle or velum of *Crassostrea gigas*, *Ostrea edulis* and *Lyrodus pedicellatus* larvae. This is examined in both Chapters 2 and 3.
5. Investigate the control of the beat of mantle and velar cilia by identifying the location of neurotransmitter compounds such as serotonin and catecholamines. This is examined in Chapters 2 and 3.
6. Investigate the ciliary swimming behaviour of a planktotrophic larva through the design of a simple and inexpensive method for the capture and analysis of film of larvae swimming in a controlled environment. This is explored during Chapter 4 through the following:
    i. Manipulation of water temperature to determine whether temperature has an effect on the swimming velocity of acclimated *Crassostrea gigas* larvae.
    ii. Expose swimming *Crassostrea gigas* larvae to rapid changes in temperature to investigate behavioural swimming response.

Chapter 2 - Ciliation of the bivalve larval mantle

2.1 Introduction

The mantle is an important organ in adult bivalves where it has a variety of significant roles, bearing sensory structures for detecting external stimuli, storing food reserves, secreting the shell and ejecting pseudofaeces from the body cavity (Beninger & Veniot, 1999). Despite this, the larval mantle has received relatively little attention. Studies of the larval mantle have been occasional over the last 40 years, with publications emerging as various tools useful for their study appeared: but the often predicted glut of information has not materialised. Papers tend to deal with the important role of the mantle in settlement prior to metamorphosis (Cranfield, 1973b, Cranfield, 1973c, Cranfield, 1974), shell secretion (Bubel, 1975, Cragg, 2006), or as the location for musculature attachments (Cragg, 1985). As a result, most papers giving mention to the larval anatomy of various bivalve species make only a passing reference to the cilia groupings of the mantle, despite the variations in the form and location of these groups, the changes they exhibit throughout the larva's development, and the potential for these cilia to be larval sense organs.

2.1.1 The larval mantle

The larval mantle encloses the body, containing the organs of the larva within the mantle cavity. It comprises a thin epithelium with its apical surface entirely covered by microvilli, lining the inner surface of each shell valve (Cragg, 2006), folding back on itself at the valve rim (shown in Figure 2.1). From here there are 2 folds just below the shell margin - the adult mantle has 3 folds. The outer of the two folds (i.e. the fold closest to the shell) is covered by a periostracum, which is known to be secreted by specialised cells at the base of the periostracal groove between the two mantle folds (Bellolio et al., 1993, Cranfield, 1974, Elston, 1980, Waller, 1981). Below these, the mantle epithelium merges with that of the velum and the foot, although it could be argued that both are formed via invaginations of the mantle. At the region closest to the hinge, the mantle forms a bridge between the two shell valves (Bellolio et al., 1993, Cragg, 2006).

2.1.2 Mantle ciliation in the literature

Several authors have noted the presence of cilia groups on the inner mantle fold of the bivalve veliger, however there are very few detailed descriptions of this ciliation. The cilia of these groups can occur either singularly or in compound form, and can be arranged in many different ways, from straight, beating tracts to round, stiff tufts. *Pecten maximus* larvae are noted as having five cilia groups visible on the inner mantle fold by the pediveliger stage (Figure 2.1), with these groups appearing from the veliger stage and diversifying through larval development (Cragg, 2006). Two cilia groups have been noted on the inner mantle fold of *Argopecten purpuratus*, occurring in an alternating pattern along the inner mantle fold rim (Bellolio et al., 1993). However Bellolio *et al.* (1993) attribute at least one of these groups to probably being developing adult structures as opposed to structures unique to the larval stage.

There is a little more literature available for the larval ostreid mantle ciliation. Only one detailed description of the mantle folds in *Ostrea edulis* notes the ciliation in the periostracal groove, sensory cilia on the apex of the inner fold and a band of cilia below the apex running around the mantle ((Cranfield, 1974) - Figure 2.1). However this information is based mainly on sectioning of the mantle, and reveals little about the morphology of the cilia themselves. Even quite comprehensive papers on the morphology and development of *Ostrea edulis* larva feature relatively little discussion of the mantle ciliation, describing the anal tuft in some detail and then referring only to scattered ciliation on the inner mantle fold margin relating to Cranfield's (1974) work on the mantle folds (Waller, 1981). *Crassostrea virginica* larvae have been described as having cilia at the gill bud/mantle join, an anal tuft and scattered cilia 'diffusely distributed on the epithelial surface of the mantle' (Elston, 1980), but the relevance of this ciliation to the larva is not discussed.

It is possible that the ciliation described on the mantle rim of *Ostrea edulis* is comparable to the type 2 and type 4 ciliation described for *Pecten maximus.* The *Pecten* cilia groups are on the inner mantle rim (Cragg, 2006), and cross sections of the mantle show ciliation in a very similar position to the mantle ciliation of *Ostrea*, as shown in Figure 2.1 and described by Waller

(1981). Furthermore the type 2 ciliation is arranged in discrete rows of cilia, and although this does not perfectly match the descriptions of *Ostrea edulis* mantle ciliation (Waller, 1981), it is comparable to that shown in Figure 2.1, if somewhat less profuse. The adult mantle of the two species is different, with the *Pecten maximus* mantle bearing specialised structures such as eyes (Brusca & Brusca, 1990), and the ostreid mantle being primarily concerned with particle selection and rejection (Beninger & Cannuel, 2006, Beninger & Veniot, 1999, Beninger et al., 1999). The potential for similarity in the ciliation of the larval mantle is interesting. Ciliation may be unique larval structures, or larval versions of these adult features. Currently there is insufficient information available on ostreid mantle ciliation to make an accurate comparison.

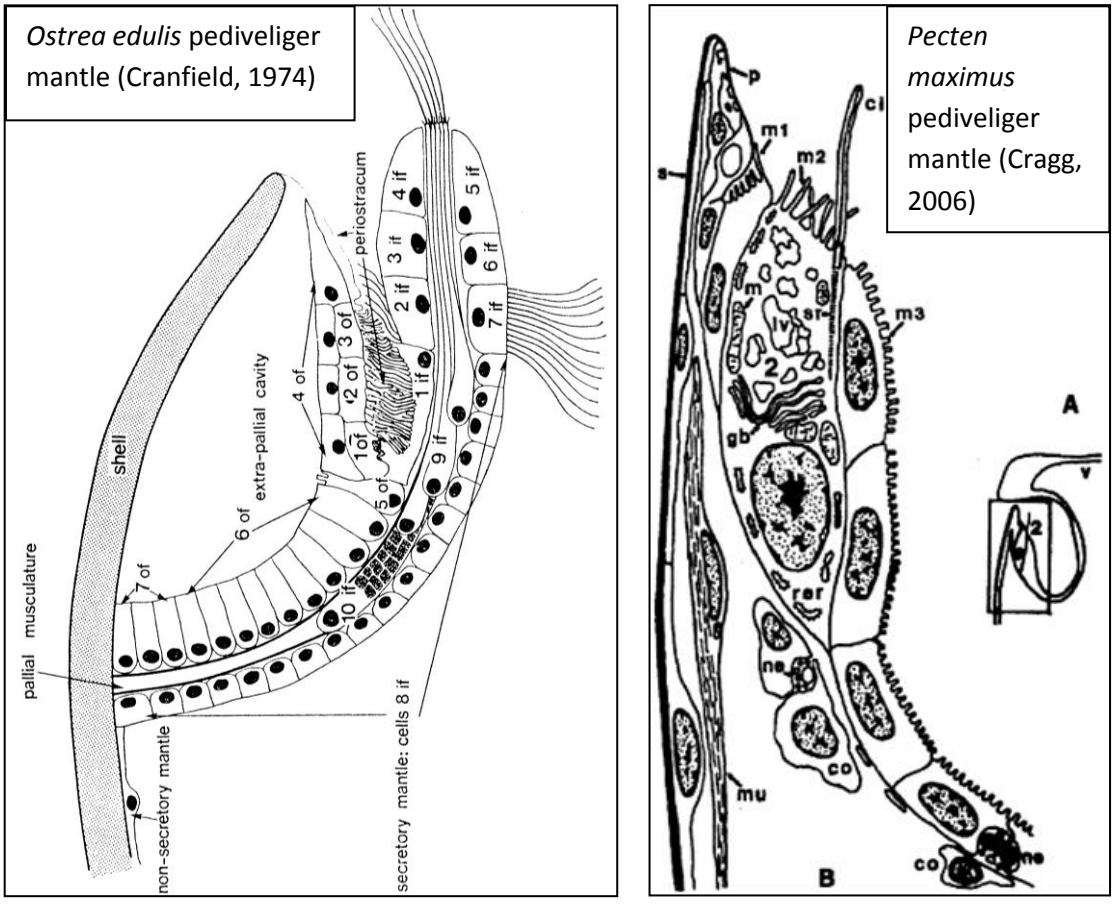

Figure 2.1 - Diagram of the mantle folds in *Ostrea edulis* (original image rotated for an easier comparison) and *Pecten maximus* pediveligers.

Ostrea edulis cilia occur in the periostracal groove on cell 2if (if=inner fold), on the apex between 4if and 5if and below the apex on cell 7if (Cranfield, 1974). *Pecten maximus* cilia occur in a similar location to the *Ostrea* cilia on cell 7if, but only one row is shown, with no cilia shown either on the apex or in the periostracal groove (Cragg, 2006).

The ciliation of the inner mantle fold of *Crassostrea gigas* has been highlighted for its potential to be a pseudofaeces rejection tract in the larva: a function of the adult mantle in many bivalve species (Beninger et al., 1994, Beninger & Veniot, 1999, Beninger et al., 1999). Beninger (2006) also points out the lack of study given to the ciliation of the larval mantle. Beninger describes a 'larval marginal ciliary tract' (Beninger & Cannuel, 2006): a pair of cilia tracts running along the ventral region which the author labels as rejection tracts, assumed to be larval versions of the adult structures, albeit potentially functional structures. During the present investigation of *Crassostrea gigas* larval mantle ciliation these tracts were found and fully described. Furthermore, this study examined the larval mantle of the closely related *Ostrea edulis* to see if these tracts are present, and attempted to show if these tracts act as rejection tracts for the larvae as opposed to simply being developing adult systems.

In the case of teredinid larvae there is very little information in the current literature regarding larval anatomy, and as a result no papers currently describing any ciliation of the mantle folds. Teredinids such as *Lyrodus pedicellatus* brood larvae until they are released as settlement-ready pediveligers and adult mantle ciliation is somewhat different from the ostreids or pectinids, with less profuse ciliation, although some species of *Teredo* do feature ciliated grooves (Nair, 1971). It may therefore be expected that the mantle ciliation of the larvae will be somewhat different from that of the ostreids or pectinids, partially due to the brooding habit, and partially (if larval ciliation is a larval version of adult forms) due to the difference in the adult mantle. However, currently there is no basis for comparison due to the lack of knowledge of the teredinid larval mantle.

In addition to the studies which are based on light and electron microscope observations, several papers have revealed neurons in the mantle, in those regions described by the previous authors as being locations of ciliary groupings. No information currently links the appearance of these neurons to the locations of ciliary groups, despite several neurological compounds being known for their roles in controlling ciliary beat.

Serotonin has been implicated in the control of ciliary activity in the veliger larvae of several members of the Mollusca, such as the bivalve *Mytilus edulis* (Beiras & Widdows, 1995), the gastropod *IIyanassa obsoleta* (Braubach et al., 2006, Braubach et al., 2005), molluscan embryos (Kuang & Goldberg, 2001) and in adult bivalve gills (Mackie, 1984). In these instances the increase in serotonin has been linked with an increase in ciliary activity (through an increase in beat frequency). Serotonin has been specifically located in the larval mantle of the mytilids and pectinids (Croll et al., 1997), but with direct reference to ciliation. In addition to serotonin, catecholamines have also been demonstrated as controlling ciliary activity in molluscs (Beiras & Widdows, 1995, Croll & Chiasson, 1990), specifically through the inhibition of ciliary beat. Catecholamines have been identified in the molluscan larval mantle in the ventral and brachial regions (Croll et al., 1997). Serotonin enhancement of ciliary beating in molluscs is likely mediated by an increase in intracellular calcium and activation of downstream messengers such as nitric oxide (Doran et al., 2004). The cellular actions of catecholamines are less well understood, however inhibition of serotonin pathways has been proposed (Cadet, 2004). In fact both serotonin and catecholamines may affect ciliary action through the changes in intracellular calcium (Beninger & Cannuel, 2006).

Whilst this is suggestive of both catecholamine and serotonin pathways having the potential to act as a method of control of ciliary beat, none of these papers link the presence of these neural compounds to the occurrence of ciliation on the mantle of larval bivalves, or offer any detailed exploration of any behavioural implications of the larvae having control over ciliary beat in these areas.

2.1.3 The objectives of this chapter

The mantle ciliation of *Crassostrea gigas* and *Ostrea edulis* larvae was examined from early veliger stage through to metamorphosis using scanning electron microscopy (SEM) to reveal the various ciliary groupings found throughout larval development. *Lyrodus pedicellatus* pediveligers were also examined.

These observations will provide evidence as to whether the ciliary groupings on the mantle are structures unique to the larvae, for example sensory structures, or larval versions of adult structures such as pseudofaeces rejection tracts. This will be the first detailed account of the cilia groups found on the mantle folds of these economically important species.

SEM was decided to be the most useful tool for the study of cilia as it enabled the examination of cilia groups in 3D at much higher resolution than with light microscopy, and allowed the appearance of the cilia to be examined. Whilst all the cilia using this method were fixed, their appearance can be very informative as it will show the cilia at a specific stage of their ciliary stroke (if one is present at all), providing both evidence of beat and a suggestion of direction. In turn, those cilia that appeared stiff and straight, or limp and without curvature when fixed were unlikely to have any beat at all. SEM will prove especially useful when these shelled larvae have been opened for examination of internal structures as it will allow the placement of groups of cilia in relation to each other and other organs within the mantle cavity.

Light microscopy has been used to take a series of images of the mantle rim cilia of *Crassostrea gigas* beating in water containing fluorescent beads. Video of the mantle ciliary beat will revealed the mantle cilia rejecting any beads that have become caught in the mantle cavity, visually supporting the ideas put forward by Beninger (2006) that mantle rim ciliation may serve as functioning larval versions of the adult rejection tracts.

The mantle of *Crassostrea gigas* was examined for catecholamines and serotonin using confocal microscope techniques. Glutaraldehye added to the fixative promoted the characteristic blue-green catecholamine fluorescence (Croll et al., 1997, Falck et al., 1982, Scholer & Armstrong, 1982), whereas serotonin was investigated using specific FITC-labelled goat anti-rabbit antibodies (Croll et al., 1997). This will provide the location of catecholamines and serotonin within the mantle which can be related to the areas where groups of mantle cilia were found with SEM, offering a suggestion as to the function and activity levels of the groups, and providing evidence that the larvae may be capable of a measure of control of the ciliary beat.

This information will expand on the electron microscope observations of the pectinid mantle (Cragg, 1985, Bellolio, 1993) by combining SEM information with that from fluorescence microscopy to provide evidence that these cilia groups have a sensory or functional significance. This is the first time electron microscopy, light microscopy and fluorescence methods will have been combined in one study to provide a detailed picture of the extent of the ciliation found on the larval mantle, the variation of this ciliation, how the ciliation changes with larval development from veliger stage to metamorphosis and combining this information to elucidate possible functions for these cilia groups.

2.2 Methods

2.2.1 Larval acclimation

Larvae of *Crassostrea gigas* and *Ostrea edulis* were obtained from the Kent-based firm SeaSalter Ltd. On arrival at our laboratory larvae were immediately placed in fine filtered 20^{o}C seawater (pH 7.99-8.02, salinity of 30.9-32.4$^{0}/_{00}$) from Langstone Harbour and very gently aerated through the use of a standard aquarium pump with a flow limiting crimp on the airline and a scrupulously clean glass Pasteur pipette over the outflow to introduce air to the bottom of the dish. Cultures were covered in foil to limit the chance of bacterial infection. Larvae were visually inspected for activity on arrival using a stereomicroscope to observe the general morphology and swimming or crawling patterns. This information was recorded for a basic comparison between batches. The culture was agitated prior to sampling to ensure specimens were taken from all regions of the culture (surface film, bottom, and water column). This enabled collection of a sample that was representative of all larval development stages that may be present in the culture - for example samples of late veligers would often show some pediveligers within the culture, and these may be crawling. The agitation of the culture prior to sampling ensured the collection of both swimming and crawling larvae.

Larvae sampled for electron microscopy, light microscopy and filming were transferred into shallow 2litre (190 mm x 90 mm) dishes containing 20^{o}C filtered Langstone Harbour seawater and left for another 1-2 hours before sampling to allow full velar extension.

2.2.2 Larval capture and culturing

Crassostrea gigas*: adult culture, early larvae collection and culture*

Adult *Crassostrea gigas* collected from groynes at Whitstable, Kent, were maintained in a 122cm (l) x 32cm (w) x 47cm (h) tank. Tank water was aerated, maintained at approximately 18^{o}C, and subject to a natural (ambient) photoperiod. Culture water was changed every 48 hours and replaced with fresh, unfiltered, seawater from Langstone Harbour. Water removed from the *C. gigas* tank was bleached prior to disposal. *C. gigas* adults were fed with 'Julian Sprungs' Marine

Snow (http://www.onlineaquariumstore.com/acatalog/Marine_Snow_250ml.html) every day. Spawning followed a period of warm weather. To collect the fertilised eggs and early larvae tank water was passed through a 50µm screen. A series of 30cm (l) x 15cm (w) x 20cm (h) tanks were set-up to grow early stage larvae and each tank was sampled every 24 hours using a 75µm screen. Collected samples were fixed in 4% glutaraldehye in 0.2M sodium cacodylate buffer (pH 7.8) for Scanning Electron Microscope (SEM) observation.

Crassostrea gigas *long term culture at SeaSalter Ltd*

Larvae at SeaSalter were cultured in a flow-through system that allows higher densities (and lower mortality rates) for commercial production. These flow-through cultures were fed directly from SeaSalter's own algal production facilities via a peristaltic pump, slowly introducing an algal mix into the larval tank. The larval flow-through is pictured below (Figure 2.2), the image reproduced from the FAO's (*Food and Agriculture Organization* of the United Nations) guide to the Hatchery Culture of Bivalves (Helm & Bourne, 2004). Larvae were cultured at 28°C.

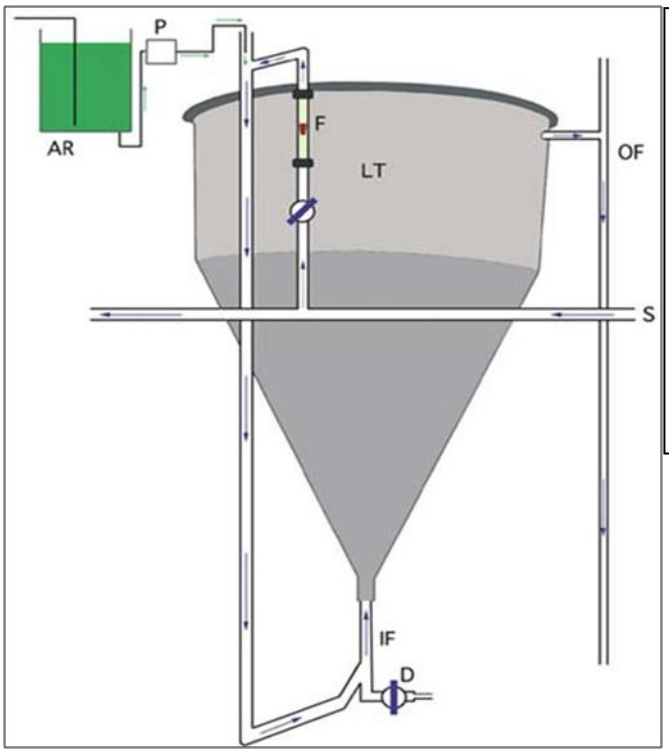

Figure 2.2 - Flow through culture set-up for *Crassostrea* larvae at SeaSalter.

AR is the algal tank, S the treated seawater, IF is the in-flow and OF the outflow, P the peristaltic pump and D the drain for draining of dead larvae and waste after a 'salt plug' of brine solution forces live larvae away from the drain (Helm & Bourne, 2004).

Crassostrea gigas short-term larval culture

Large batches of larvae that were kept for consecutive days of sampling were transferred to a 60cm X 30cm X 30cm tank containing freshly filtered seawater at 20°C (pH 7.99-8.02, salinity

of 30.9-32.4$^{0}/_{00}$). The culture was subjected to a 12 hour light and 12 hour dark photoperiod and maintained at an approximate density of 5 larvae per ml. The culture was aerated with an aquarium air-stone, with a flow limiting crimp on the airline to ensure gentle aeration. The tank was kept covered to limit the chance of bacterial infection. 50% water changes were conducted every day through the use of a siphon covered with 62µm plankton mesh to prevent loss of larvae. Larvae 'captured' during water changes were gently washed off the plankton mesh and back into the holding tank. The siphon was also used for sampling larvae from the tank for fixation prior to electron microscopy and light microscopy observations. Larvae were fed *Isochrysis* and *Tetraselmis* daily at concentration of approximately 50,000 algal cells per ml (Helm & Bourne, 2004). This is not the optimal diet for larvae of this size; however this larval culture was for short-term storage only, to enable the sampling of healthy as opposed to moribund larvae over a period of several days. This method was not intended to progress the larvae through to settlement, although some settlement on the tank glass was observed, demonstrating the health of the culture.

Lyrodus pedicellatus culturing and larval capture

Lyrodus pedicellatus adults were maintained in a seawater flow-through (approximately 25 litres per hour, seawater pH 7.99-8.02, salinity of 30.9-32.4$^{0}/_{00}$), and the tank was 'restocked' with fresh wood regularly to maintain a healthy population through the settlement of un-captured larvae. The tank was maintained at a constant temperature of 18^{o}C through the use of a 250W aquarium heater: set-up trials found this temperature to be the most productive for the collection of larvae (Stanton - unpublished observations). Spawning was stimulated via a full water change with fresh, unfiltered seawater at ambient temperature from Langstone Harbour. The resultant temperature drop down to around 12-15^{o} followed by a temperature rise stimulated the production of larvae. Larvae were captured using an aquarium box filter, modifying a technique used by (Eckelbarger, 1973) – bubbles of air were pushed into the filter box through a high, narrow tube and forced out through a second, lower and wider piece of tubing (uplift tube). This action generated a mild current of water being drawn into the filter box

through the slatted box lid, which was then pushed out with the air bubbles through the uplift tube. Larvae were drawn in with this gentle current of water, and pumped out with the water through the uplift tube (Figure 2.3). The end of the uplift tube was directed into a fixed piece of piping using some soft flexible tubing. One end of the larval collection piping was above the water line in the tank, whilst the other end was submerged, but screened with 63 micron plankton mesh. Larvae drawn by this gentle current passing through the system were trapped in this 'pool' in the collection pipe, and could be sampled at regular intervals. Gently lifting the piping from the water forced larvae onto the plankton mesh, the surface of which was washed into a shallow dish for extraction of larvae. Extraction of larvae from this shallow dish was complicated by the presence of suspended sediment from the collection pipe. As a result larvae had to be captured individually using a pipette.

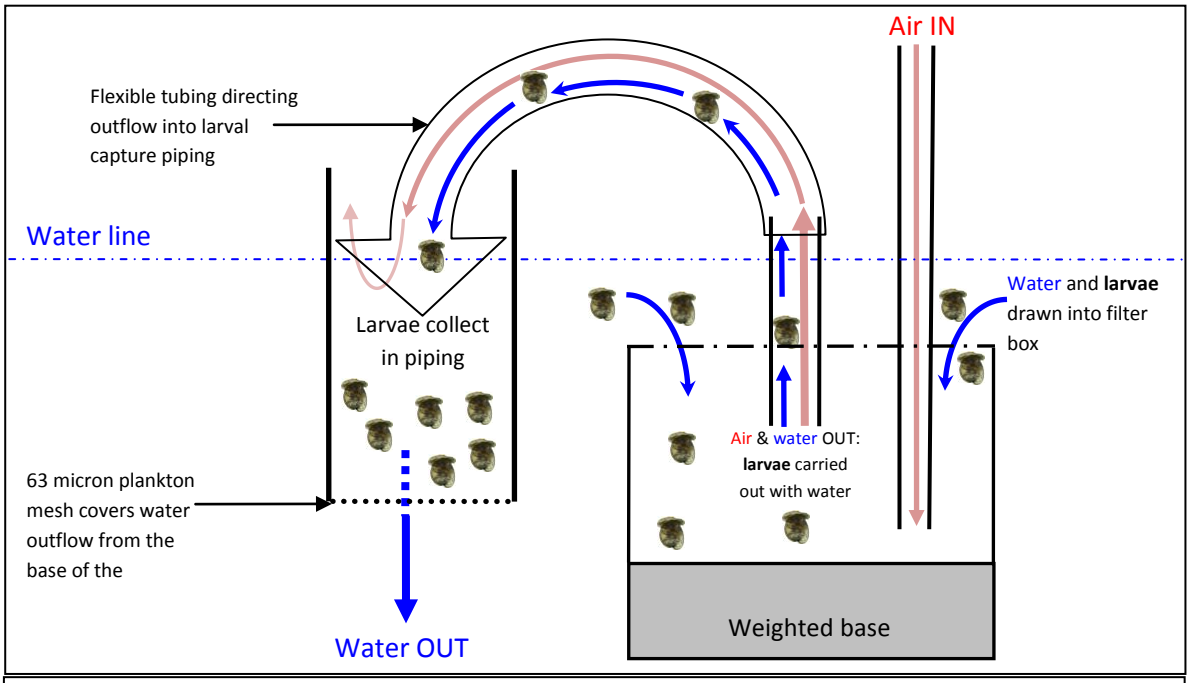

Figure 2.3 - *L.pedicellatus* larval capture

Larvae are drawn into the filter box through the grated top (dashed) via the action of air being pumped through the box. As the air exits the box through the short tube it carries a gentle water current with it. Larvae are drawn along by this current through a short piece of flexible hosing and into a short piece of piping. The piping has 63µm plankton mesh over the underwater exit (the other end being clear of the water), trapping larvae in the chamber until collected.

2.2.3 Narcotisation

Larvae sampled for electron microscopy (EM) were narcotised with 7.5% $MgCl_2$, to prevent the retraction of the velum on introduction of the primary fixative. Trials determined that a slow introduction of this solution via a strip of filter paper caused the least larval shell closing, and as a result gave a higher yield of larvae with extended velums. Narcotisation of larvae was confirmed after about 30 minutes under a low power microscope by disturbing the larvae with glass needles – if no retraction was observed larvae were adjudged narcotised. Once narcotised, larvae were transferred into glass vials for primary fixation.

2.2.4 General procedure for sample fixation for electron microscopy

Fixation for all EM preparations was accomplished by exposing larvae to 4% glutaraldehyde in a 0.2M cacodylate buffer for 1 hour. Fixation was confirmed under low power microscopy by observing the larvae to confirm that swimming, crawling and any ciliary beat had stopped. The fixed larvae were then rinsed in a 0.2M cacodylate buffer solution for two, 30 minute periods to ensure the complete removal of any remaining primary fixative. Secondary fixation was carried out for 30min – 1 hour using 1% osmium tetroxide in cacodylate buffer, in which the larvae were fully immersed. Larvae were given three further rinses in 0.2M cacodylate buffer following secondary fixation to remove any remaining osmium. For storage, samples were rinsed twice in 50% ethanol then moved into 70% ethanol and kept at 4^{o}C in the dark.

2.2.5 Scanning electron microscope (SEM) preparation

Following fixation, larvae were dehydrated in a graded ethanol series at room temperature. Excess buffer was pipetted out and larvae were immersed in 50% ethanol and rinsed twice more in 50% ethanol to ensure the removal of any excess cacodylate buffer solution. Larvae were then taken through a graded ethanol series – 50%, 70%, 80%, 90%, 100% – being immersed in each concentration in tightly covered vials for 30 minutes. The 90% and 100% ethanol stages were repeated twice. Following the 100% ethanol immersion, larvae were further dehydrated via either Hexamethyldisilazane (HMDS) as per (Bray et al., 1993), or Critical Point Drying (CPD) dehydration as per (Bellolio et al., 1993). These methods were used to provide a

comparison between the two in order to decide which method would be the most practical for standard use. Little difference was observed in the results. HMDS samples occasionally left a residue over fine structures but this was not common.

HMDS

Larvae were immersed in a 50:50 mix of 100% ethanol and 100% HMDS for half an hour, and then immersed in 100% HMDS for two 30 minute periods to remove any remaining ethanol. Larvae were kept tightly covered during all phases ensuring the specimens were kept wet at all times during these steps. Finally, larvae were immersed in 100% HMDS to a level just covering all the larvae and left uncovered to evaporate overnight in a fume hood at room temperature.

Critical point drying

Once in 100% alcohol, larvae were moved into 100% acetone via a 30 minute immersion in 50:50 ethanol and acetone solution. The 100% acetone was changed twice to completely remove any residual ethanol. Acetone was used as the intermediate fluid prior to the CO_2 transitional fluid for the critical point drying procedure. Larvae were dried in a CPD unit (Polaron Equipment Ltd E3000 Critical Point Dryer with E3500 Thermocirculator for temperature adjustment). Larvae were left for 45 minutes fully covered by liquid CO_2 to ensure full impregnation into the specimens. In order to contain the larvae during CPD dehydration they were placed into 80 micron plankton mesh within the CPD sample boat.

Specimen mounting

Dry larvae were transferred onto aluminium stubs. The brittle larvae were transferred to the surface of the stub using an artists brush with soft bristles. Care was taken to ensure a high proportion of larvae landed hinge down, making later processing easier. Larvae were affixed to the stub by use of sticky carbon tabs. Following attachment to the stub the larvae were cracked open using fine glass needles in a modification of the techniques first used by (Cragg, 1985) to reveal internal structure. Trials with cracking larval shells revealed that when a specific angle of

attack was used with the needle, greater exposure of relevant internal structures was achieved – simply cracking the larvae produced indifferent results. Gently tapping larvae on one of the shell valves in a direction away from the other shell valve would remove one side and expose the mantle rim of the opposing valve at a good angle for viewing with SEM. Larvae were coated with a gold/palladium mix for 2 ½ minutes in a sputter coating unit (Polaron Equipment Ltd, E5000). Larvae were then observed in an SEM (JEOL JSM-6060LV) at 15Kv.

Some larvae were immersed in liquid nitrogen for a few seconds, before being extracted and shattered - this procedure was used as an alternative to the glass needles. These shattered larvae were then mounted directly onto aluminium stubs using Araldite adhesive and sputter coated prior to being viewed in a Philips XL-30 Field Emission Scanning Electron Microscope.

2.2.6 Measurement in the scanning electron microscope

Measurements are provided for each style of cilia discussed in this chapter and Chapter 3. However, it should be noted that while these do provide a useful comparative tool, measurements are usually qualified as 'approximate'. This is due to the difficultly of obtaining accurate measurements for 3-dimensional structures within a scanning electron microscope, with the larvae not lying at known angles on the stubs, and thus not lending themselves to the carefully orientated pairs of images required for precise measurements (Minnich et al., 1999). However, the JEOL SEM 6060LV was calibrated prior to measurements being taken, in an effort to minimise the effect of the 3D environment, and to enable the most accurate comparisons between specimens.

2.2.7 Confocal laser scanning microscopy

Larvae intended for confocal laser scanning microscopy work were narcotised in shallow dishes with $MgCl_2$ prior to fixation, as with the EM sample description in **2.2.3**.

Aldehyde-induced catecholamine fluorescence

Narcotised larvae were moved into glass vials for fixation in 4% paraformaldehyde with 0.55% glutaraldehyde in 0.2M phosphate buffered saline solution (PBS) (Falck et al., 1982). Fixed

larvae were placed on glass slides and excess fluid was drawn off with strips of filter paper. Care was taken to draw fluid off evenly around the larvae, preventing them from clumping together on the slide. Slides were then desiccated in the dark, overnight, before the larvae were mounted in glycerol and observed on a confocal laser scanning microscope.

Serotonin staining

Narcotised larvae were fixed overnight in 4% paraformaldehyde in 0.2M PBS buffer. Larvae were rinsed in 0.2M PBS before being placed into 10% EDTA in 0.2M PBS for 20min. Following 2 washes in 0.2M PBS to remove residual EDTA, larvae were transferred to 4% Triton X-100 in 0.2M PBS overnight. Larvae were immersed in a 1:500 dilution of rabbit anti-serotonin (Invitrogen) in 0.2M PBS for 48 hours at 4^{o}C, before a 6 hour wash in 0.1M PBS, also at 4^{o}C. Finally larvae were incubated overnight at 4^{o}C in Fluorescein isothiocyanate (FITC) labelled goat anti-rabbit antibodies.

Both of the above methods are consistent with those used by Croll *et al*, 1997.

All of the larvae used in the methods above were examined on a Carl Zeiss LSM 510 confocal laser scanning microscope equipped with an AxioCam (HRc) camera.

Excitations and visualisation

Catecholamines: UV fluorescence, 488nm long pass filter and 355-425nm excitation.

Serotonin: argon laser, 488nm long pass filter, and emission visualised at 530nm.

2.2.9 Filming of larval particle selection and rejection

Following acclimation (as described in **2.2.3**), larvae were pipetted into a well-slide or small Petri dish and mounted onto a Leitz Dialux 22EB compound microscope fitted with a Nikon Coolpix 4500 camera, a transmitted halogen light source, and a mercury light source for

fluorescence imaging. Fluorescent beads or ink were added to the water, and the effect of the mantle and velum ciliary beat was filmed by capturing short MPEG files on the camera. Mantle cilia were filmed using larvae that were at least partially gaped and able to be viewed from an angle that allowed the movement of particles along the mantle rim cilia to be followed. Footage of velar beat was filmed by looking directly down onto the top of the larval velum, or from the side. To track the movements of the fluorescent beads (Duke Scientific, 10µm, green) more accurately the MPEG files were broken down into individual video frames and the passage of individual beads tracked through each video frame. Image collages were made from the video frames to illustrate the path taken by specific particles.

2.3 Results

The following descriptions are based on EM, LM and CLSM (Confocal Laser Scanning Microscopy) observations and are illustrated according to their anatomical positions in terms of the larval anterior-posterior and dorsal-ventral axis, these being fixed larval axes throughout the development stages considered here (see Figure 2.4 and Figure 2.5 for a diagrammatic representation of these axes - diagrams like these will provide orientation throughout the chapter). As each cilia group for each species is considered their consistency or variation of form and location throughout larval development will be illustrated and described. Larvae have been labelled according to their development stage. Age was not used as larvae were occasionally refrigerated by the hatchery, making 'days old' a less reliable gauge of larval development. Different cilia groups have been assigned numbers, for example the single tract of cilia in the antero-dorsal region of ostreid larvae is C1. Cilia unique to *Lyrodus* are designated with an L. *Please refer to Table 0.1, Table 0.2 and Table 0.4 in **Abbreviations** for a key to the labelling used in the images.*

Beat direction can be surmised from the SEM image. Cilia beat is an energetic process - fixation stops this process (Cragg, 1989), cilia fall to the end of their power stroke and are unable to perform the recovery stroke. Thus the angle and position of the cilia following fixation is assumed a useful gauge of the direction of the ciliary power stroke.

Summary of ostreid ciliation

Figure 2.4 and Figure 2.5 summarise the locations of the mantle cilia groups of the ostreid species throughout larval development, and are provided here as a reference for the descriptions and detailed images of each grouping presented in the following sections.

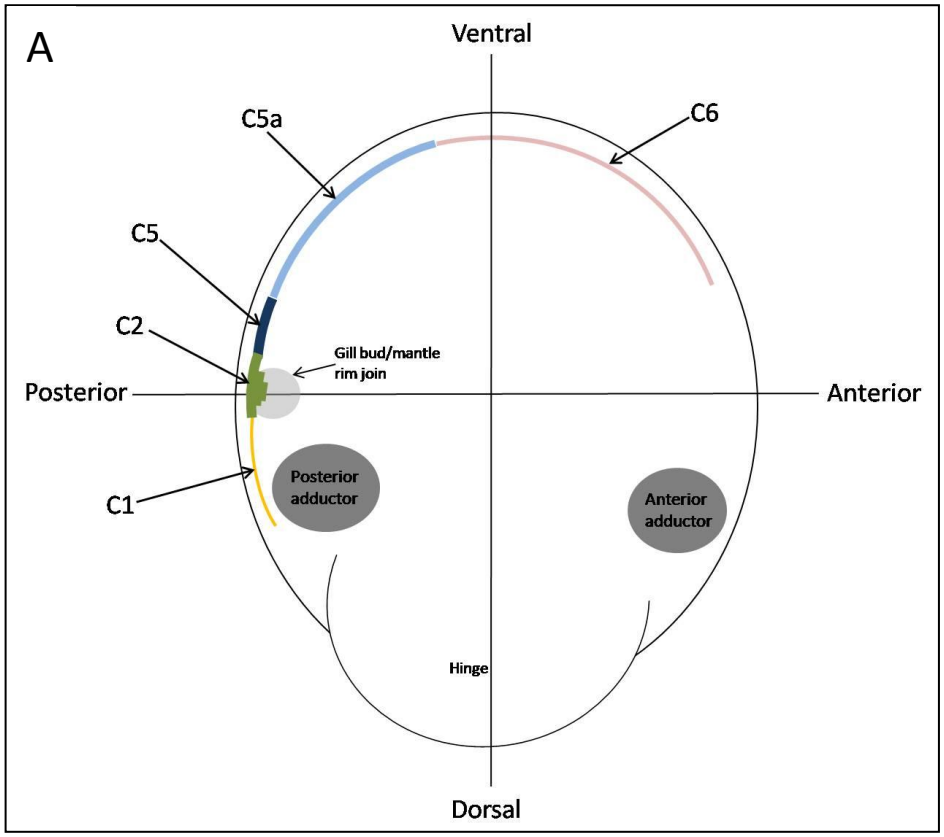

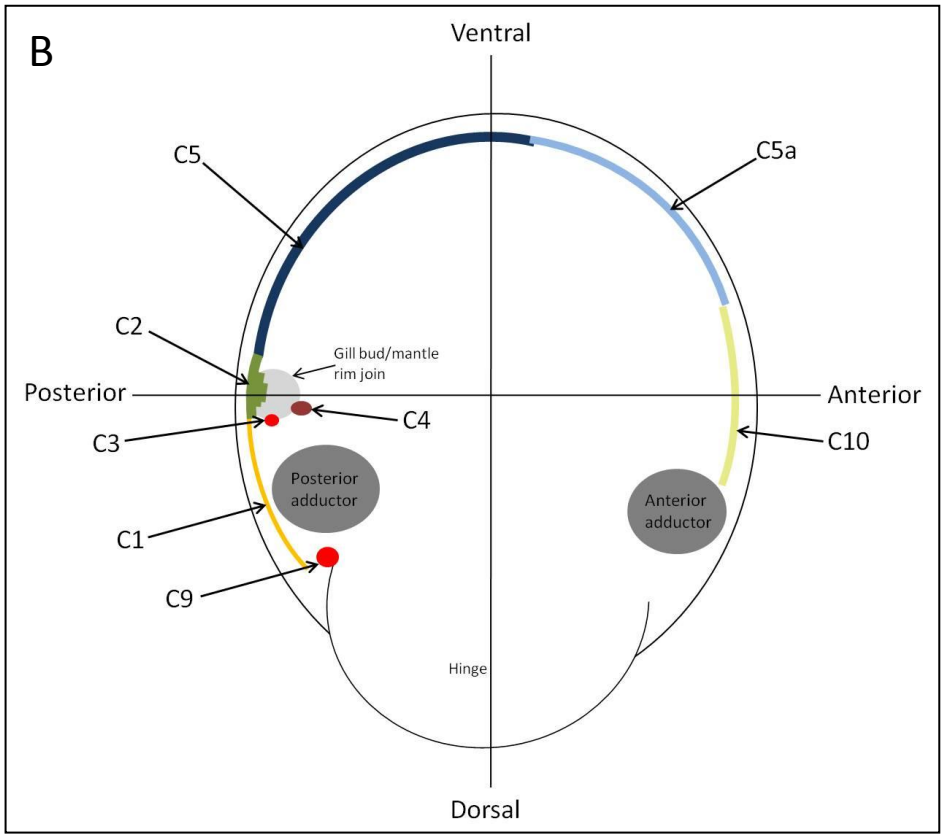

Figure 2.4 A & B - Diagram showing increase in ostreid mantle cilia complexity from early (A) to late (B) veliger.

The yellow colours are the C1 and C10 single cilia tracts, green the C2 ciliation, red the C3 and C9 cilia groups with rings of microvilli at the cilia bases, maroon the C4 group at the bottom of the gill bud, dark blue and blue the twin tracts C5 and C5a. This pair of diagrams should be viewed with the SEM images: Figure 2.6 and Figure 2.7.

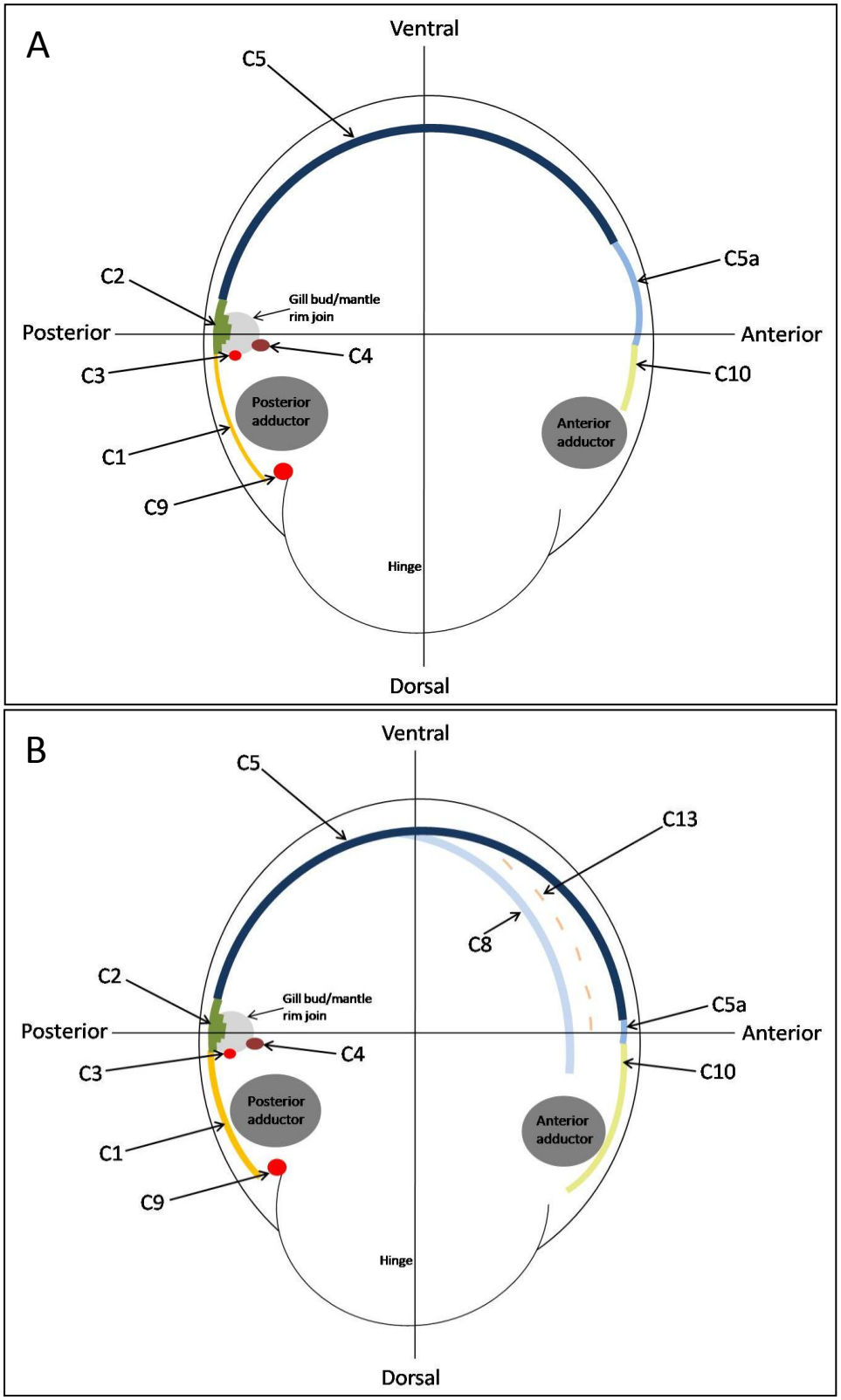

Figure 2.5 A & B - Diagram showing increase in ostreid mantle cilia complexity from early (A) to late (B) pediveliger.

The early pediveliger (A) shows the long C5 and short residual C5a region. The late pediveliger (B) shows the pre-metamorphosis complexity of mantle ciliation with the appearance of C8 and C13 cilia groups, finally resulting in 10 different cilia groups being present in set locations, and 3 more groups (C11, C12 and C7) spread around the rim. This pair of diagrams should be viewed with Figure 2.8.

A number of SEM stubs with larvae on were chosen to provide counts of mantle features, in order to estimate how common each feature was (as a percentage of larvae showing the group) across more than one broodstock. Three SEM stubs were chosen from each broodstock, divided into veliger or pediveliger stages of development. While counts were not made from every stub prepared, this method was considered suitable to provide an estimate of how common features were. Numbers of larvae on each stub ranged from ~133 to ~212 for ostreid larvae and ~20 to ~40 for *Lyrodus pedicellatus*. Orientation of specimens, sections of mantle, or the presence of damage was variable so counts were divided into positive and negative observations, shown in Table 2.1 to Table 2.5. The difficultly associated with finding specimens (or manipulating specimens) in the correct orientation is reflected in the lower n values, especially for some observations, such as the C3 cilia group, although it should be noted that these are representative counts and more larvae were examined during the course of the research.

Positive observations corresponded to those where the correct region of the larval mantle was visible along with the expected ciliary groupings (shown the summary diagrams Figure 2.4 and Figure 2.5). Negative observations were those where the appropriate region of the mantle was visible, but the expected ciliary groupings were not present. This was usually due to variations in development stage (which could be considerable within the same group of larvae) or potentially moribund larvae.

These counts allowed for an estimate of a percentage of larvae likely to display certain ciliary groups within these development stages. Larvae were sourced from fewer broodstocks for *O. edulis* due to poor commercial availability.

Mantle ciliary grouping	Number of broodstocks from which observations came	Number of Positive Observations (where region visible)	Number of Negative observations (where region visible)	Percentage of Individuals showing Ciliary grouping	Comments
1	3	33	10	76.7	
2	3	54	3	94.7	
3	3	7	0	100.0	Lower n values reflect difficulty of observing region
4	3	11	0	100.0	Lower n values reflect difficulty of observing region
5	3	93	3	96.9	
5a	3	47	10	82.5	
6	3	28	29	49.1	Low numbers due to the restriction of the group to early stage veligers
7	3	>93	0	100.0	
8	3	0	57	0.0	Not observed in any veliger stage larvae
9	3	29	0	100.0	Difficult region to collect images from
10	3	11	7	61.1	
11	3	18	1	94.7	Lower n values reflective of difficulty of observing region in veliger stage larvae
12	3	53	6	89.8	Less frequently obscured in veliger stage larvae
13	3	0	57	0.0	Not observed in any veliger stage larvae

Table 2.1- Number of observation of mantle features of *Crassostrea gigas* veliger stage larvae

Mantle ciliary grouping	Number of broodstocks from which observations came	Number of Positive Observations (where region visible)	Number of Negative observations (where region visible)	Percentage of Individuals showing Ciliary grouping	Comments
1	4	71	2	97.3	
2	4	38	1	97.4	
3	4	17	1	94.4	Lower n values reflect difficulty of observing region
4	4	17	1	94.4	Lower n values reflect difficulty of observing region
5	4	147	0	100.0	Length ranged from 180-250µm
5a	4	15	43	25.9	Less developed pediveligers show longer C5a. Length ranged from 10µm - 100µm
6	4	0	58	0.0	C5a occupy this place in pediveligers if C5 not present in anterio-ventral
7	4	>147	0	100.0	
8	4	24	4	85.7	Lower n values reflect difficulty of observing region
9	4	14	0	100.0	Lower n values reflect difficulty of observing region
10	4	44	4	91.7	
11	4	70	3	95.9	
12	4	15	0	100.0	Group is difficult to see when developed C5 are present
13	4	18	2	90.0	Only observed in one broodstock comprising pre-settlement pediveliger/early spat

Table 2.2 - Number of observation of mantle features of *Crassostrea gigas* pediveliger stage larvae

Mantle ciliary grouping	Number of broodstocks from which observations came	Number of Positive Observations (where region visible)	Number of Negative observations (where region visible)	Percentage of Individuals showing Ciliary grouping	Comments
1	2	16	0	100.0	
3	2	5	0	100.0	Lower n values reflect difficulty of observing region
4	2	5	0	100.0	Lower n values reflect difficulty of observing region
5	2	26	2	92.9	The 2 observations of no C5 and no C5a were recorded on the same individuals, possibly moribund larvae.
5a	2	22	2	91.7	
7	2	>20	0	100.0	
8	2	0	8	0.0	Group only occurs in pediveliger larvae
9	2	4	0	100.0	Lower n values reflect difficulty of observing the region
10	2	4	2	66.7	Area often obscured by the adductor muscle
11	2	16	1	94.1	
12	2	38	6	86.4	Area often difficult to resolve
13	2	0	25	0.0	Group only occurs in pediveliger larvae

Table 2.3 - Number of observation of mantle features of *Ostrea edulis* veliger stage larvae

Mantle ciliary grouping	Number of broodstocks from which observations came	Number of Positive Observations (where region visible)	Number of Negative observations (where region visible)	Percentage of Individuals showing Ciliary grouping	Comments
1	2	25	0	100.0	
3	2	2	0	100.0	Lower n values reflect difficulty of observing region
4	2	5	0	100.0	Lower n values reflect difficulty of observing region
5	2	42	1	97.7	
5a	2	9	18	33.3	Only less developed pediveligers show C5a.
7	2	>50	0	100.0	
8	2	5	0	100.0	Group only occurs in pediveliger larvae
9	2	5	0	100.0	Low n values reflect difficulty of observing the region.
10	2	12	1	92.3	Area often obscured by adductor muscle
11	2	22	0	100.0	
12	2	8	11	42.1	Group is difficult to see when developed C5 are present
13	2	5	18	21.7	Only observed in most developed individuals

Table 2.4- Number of observation of mantle features of *Ostrea edulis* pediveliger stage larvae

Mantle ciliary grouping	Number of broodstocks from which observations came	Number of Positive Observations (where region visible)	Number of Negative observations (where region visible)	Percentage of Individuals showing Ciliary grouping	Comments
L1	2	27	0	100.0	Lower n values reflective of difficult of observing region, and fewer numbers of larvae in comparison to commercially sourced larvae
L2	2	6	2	75.0	Lower n values reflective of difficult of observing region, and fewer numbers of larvae in comparison to commercially sourced larvae

Table 2.5 - Summary of *Lyrodus pedicellatus* mantle observations

2.3.1 Crassostrea gigas

Ciliation is mainly found on the rim of the inner fold of the mantle, although some ciliation is found on the mantle itself, especially in later stage larvae. Throughout larval development this ciliation increases in complexity until by the late pediveliger stage just prior to metamorphosis, larvae show 13 different ciliary groups separated either by form, location, or both. Observations of *Crassostrea gigas* larvae were made from early veliger larvae through to newly metamorphosed spat.

Figure 2.6, Figure 2.7, Figure 2.8 and Figure 2.9 illustrate the increase in complexity of the mantle ciliation on the inner mantle fold rim, providing an overview of the cilia groups present throughout larval ontogeny. The position of these groups is given relative to internal structures such as the gill bud or the adductors, and to each other. Full descriptions of each cilia group will be given later in this section.

In Figure 2.6 the early veliger has 5 cilia groupings, C1, C2, C5, C5a and C6. C1 cilia form a single tract of cilia on the inner mantle fold rim from the dorsal region to the gill bud/inner mantle fold rim junction. This join is covered with C2 cilia, covering both the mantle rim and the gill bud itself. C5 cilia form a very short twin tract moving ventrally from the bud, before decreasing in organization to become a long C5a tract through the ventral region. In the antero-ventral region the C5a ciliation gives way to a single tract of C6 cilia which spread from the end of the ventral region through the anterior towards the anterior adductor. The C6 tract is very variable in length between individuals, from very short 10µm tracts such as the one in Figure 2.6, to tracts that spread up to 30µm reaching the anterior adductor. This general pattern was observed in over 50 early veliger stage larvae, with the only variations being the length of the C5a tract and the length of the C6 tract.

In Figure 2.7 the late stage veliger larva has the same general pattern of ciliation on the inner mantle fold rim as the early veliger, beginning with the C1 cilia dorsal to the gill bud and C2 ciliation on the bud itself. However the cilia of the C5 region form a more densely ciliated tract than in the early veliger that reaches to the centre of the ventral region. The C5a ciliation spreads

from the centre of the ventral region through to the centre of the anterior region. As a result the single tract of cilia following the C5a ciliation is restricted entirely to the antero-dorsal region of the larva. This tract is much more densely packed with cilia than the C6 group found in the early veliger, which combined with the change of location, has resulted in this being classified as C10 ciliation which will persist in this form and approximate location until metamorphosis.

Figure 2.8 illustrates the ciliation of the mantle rim in a mid to late term pediveliger. C1 ciliation is present but somewhat denser, still spreading from the hinge, past the posterior adductor and terminating at the gill bud/mantle join. The C2 region is smaller and gives way to the very dense twin tract of C5 ciliation that runs all the way through the ventral region to the beginning of the anterior. The C5a region is typically shorter in the pediveliger, ≤~10µm long, and in was absent in 75% of the more developed pediveligers. Finally the C10 ciliation is denser and runs from the end of the anterior region to the dorsal mantle rim near the hinge.

In Figure 2.9 the C5 twin tracts are still visible on the mantle rim of the spat, and the C13 cilia are present on the mantle itself. The C1 and C8 cilia tracts are also retained post-metamorphosis, in the same locations on the mantle.

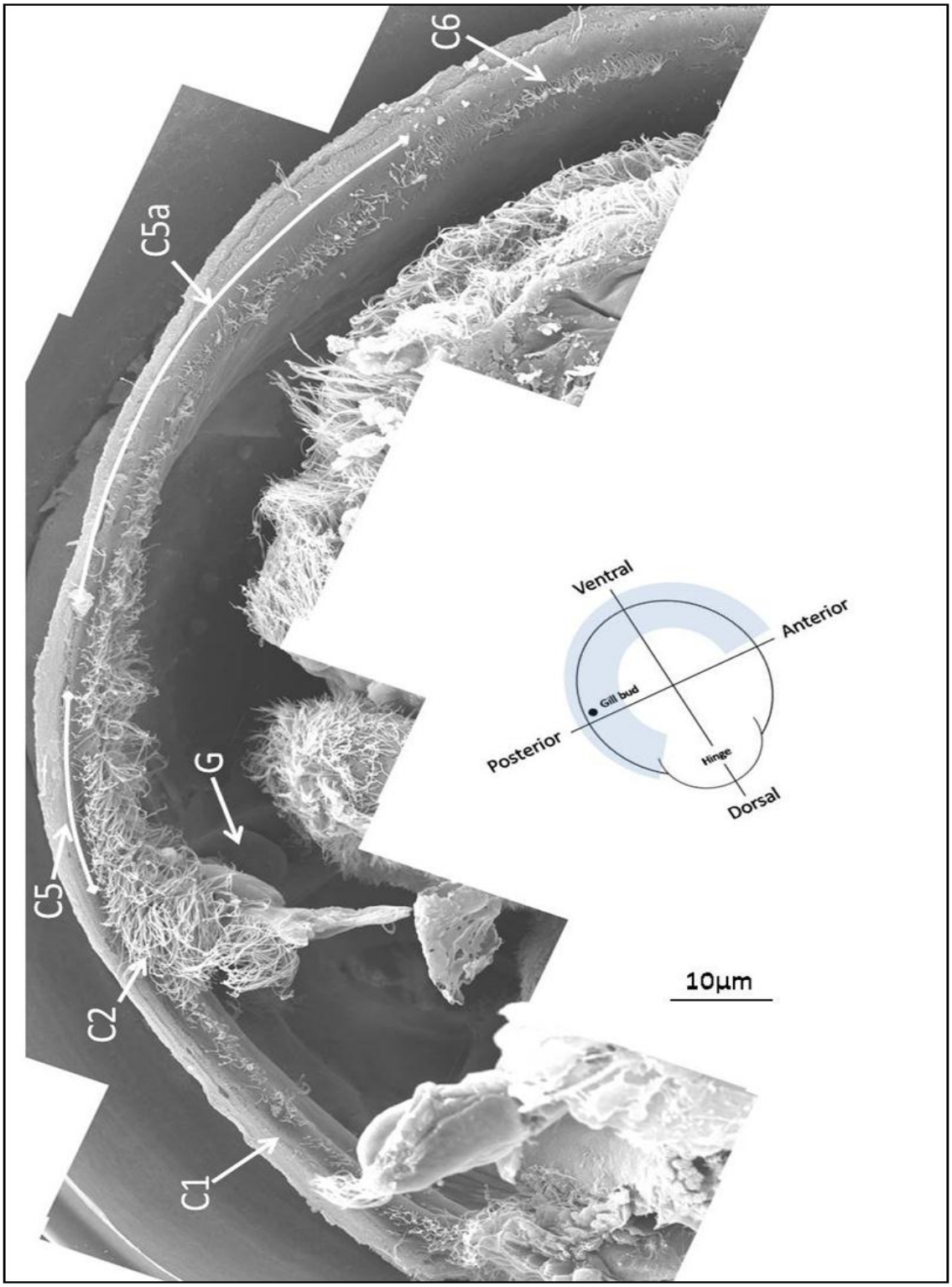

Figure 2.6 - Distribution of cilia around the inner mantle fold rim of early-stage *Crassostrea gigas* veliger.

Different cilia groups arise around the inner mantle fold rim in different locations; C1 cilia occupy the postero-dorsal region of the rim, C2 appear on the bud/mantle join, then C5 cilia and a large tract of C5a from the gill bud to the ventral, before ciliation becomes the sparser C6 group in the anterior mantle rim. This is an early veliger and it shows a very poorly developed C5 region, but a large area of C5a, representing a probable transition between the two. The larva has been dry fractured and imaged by SEM, the light blue shaded area of the inset diagram shows the area illustrated in the SEM pictures.

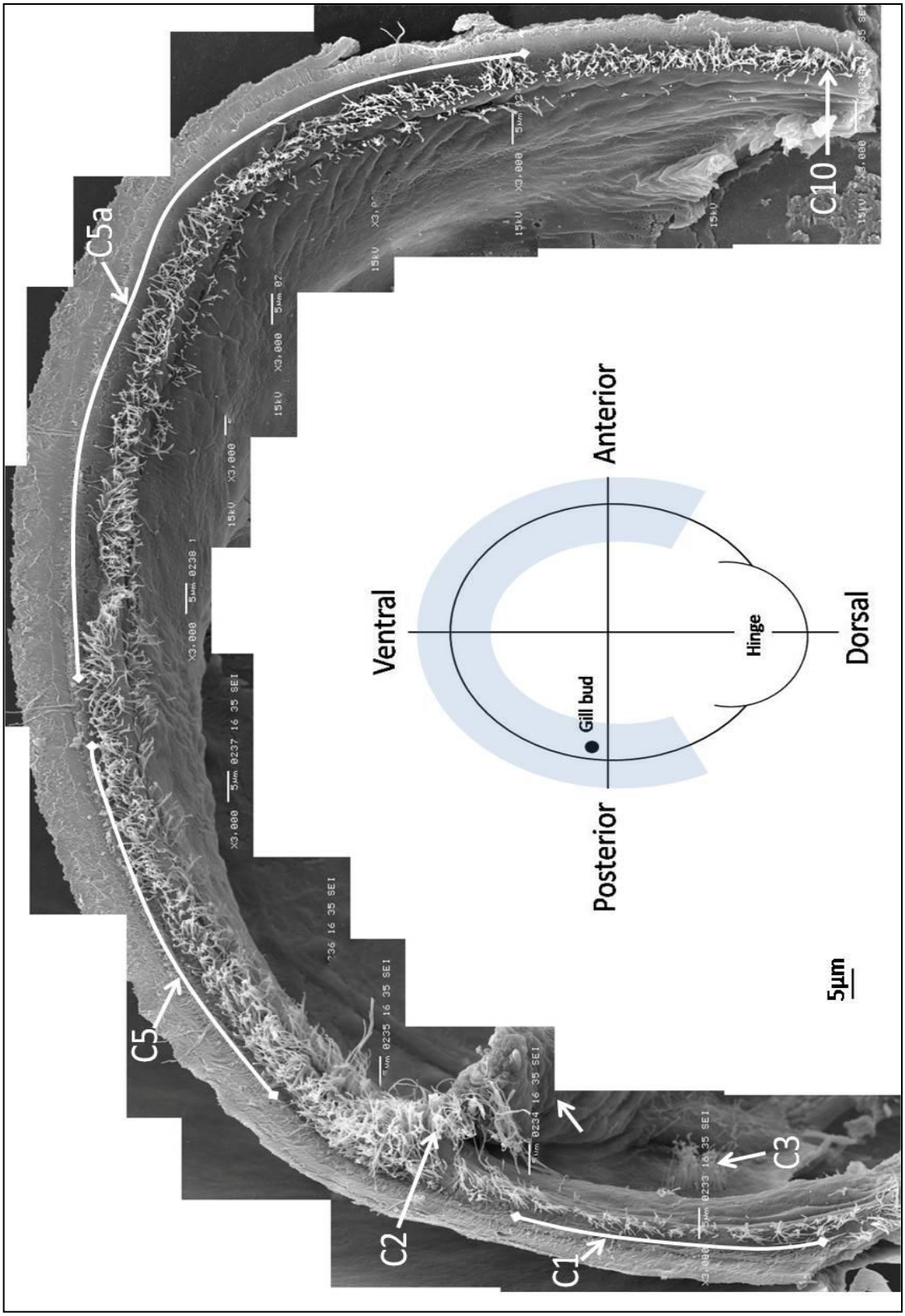

Figure 2.7 - Distribution of cilia around the inner mantle fold rim of a mid-stage *Crassostrea gigas* veliger.

The appearance of the cilia groups changes (starting from C1 cilia on the posterior-dorsal rim, to C2 on the bud/mantle join (arrowed), then C5 cilia and a tract of C5a, before the emergence of the C10 single tract cilia. This veliger shows a well developed, but short, C5 region and a long region of C5a. Note there are no C6 cilia, the C5a now leading straight into well developed C10 ciliation. The larva was dry fractured and imaged by SEM. The light blue shaded area of the inset diagram shows the area illustrated in the SEM pictures.

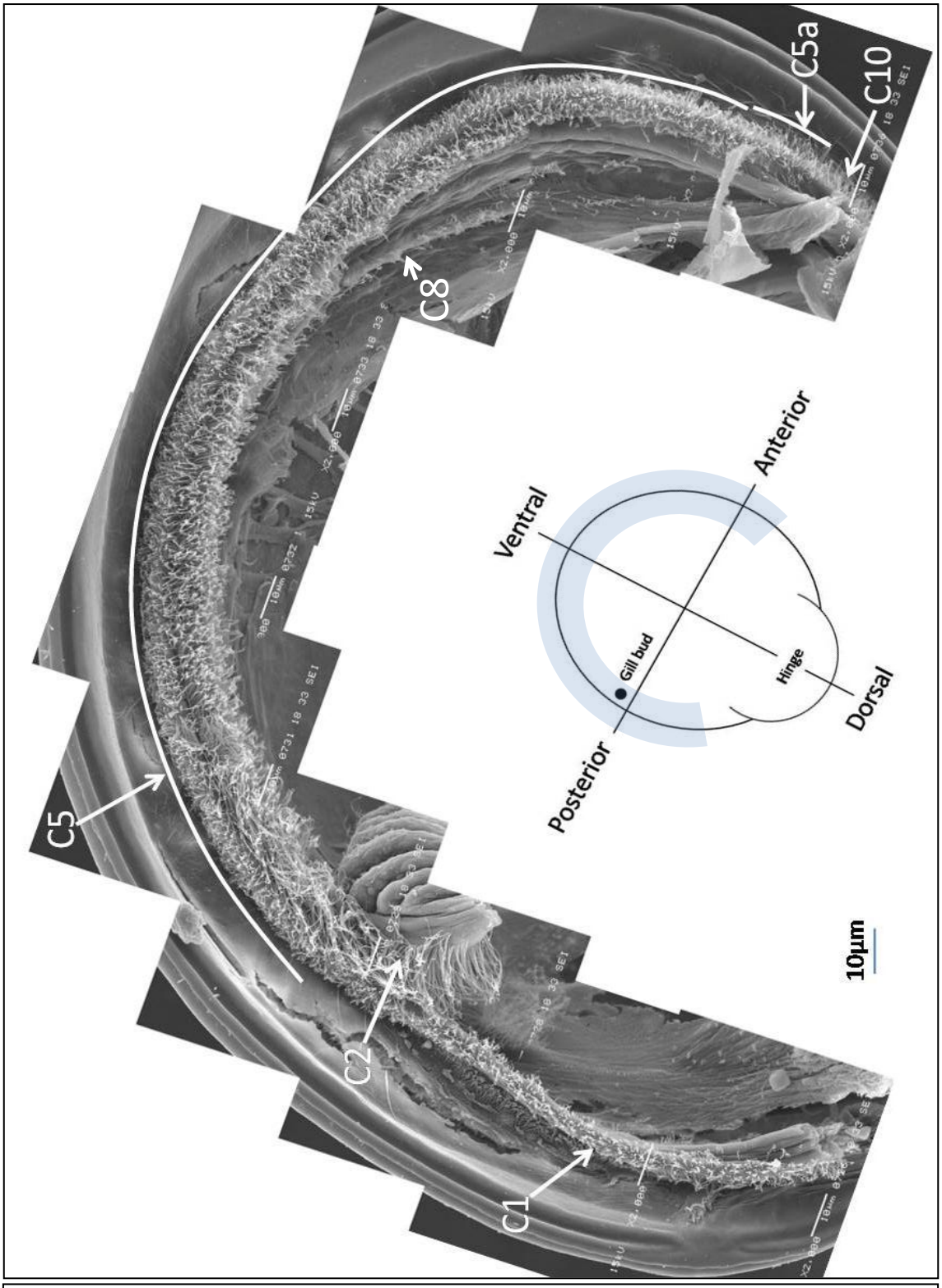

Figure 2.8 - Distribution of cilia around the inner mantle fold rim of a *Crassostrea gigas* pediveliger.

Going postero-dorsal to antero-dorsal, cilia groups change from C1 cilia on the postero-dorsal rim, to a brief region of C2 cilia on the bud/mantle join, then a large tract of C5 cilia, preceding a very short C5a cilia tract. Finally C10 ciliation is well developed, running right to the far dorsal edge of the mantle rim. This is a typical pediveliger and illustrates the length of the twin tract of C5 cilia found at this stage of development. The C5a cilia have almost disappeared, C5 cilia leading almost directly to C10 cilia. The C8 tract is visible on the mantle in the antero-ventral. The larva has been dry fractured and imaged by SEM, the light blue shaded area of the diagram shows the area illustrated by the SEM pictures.

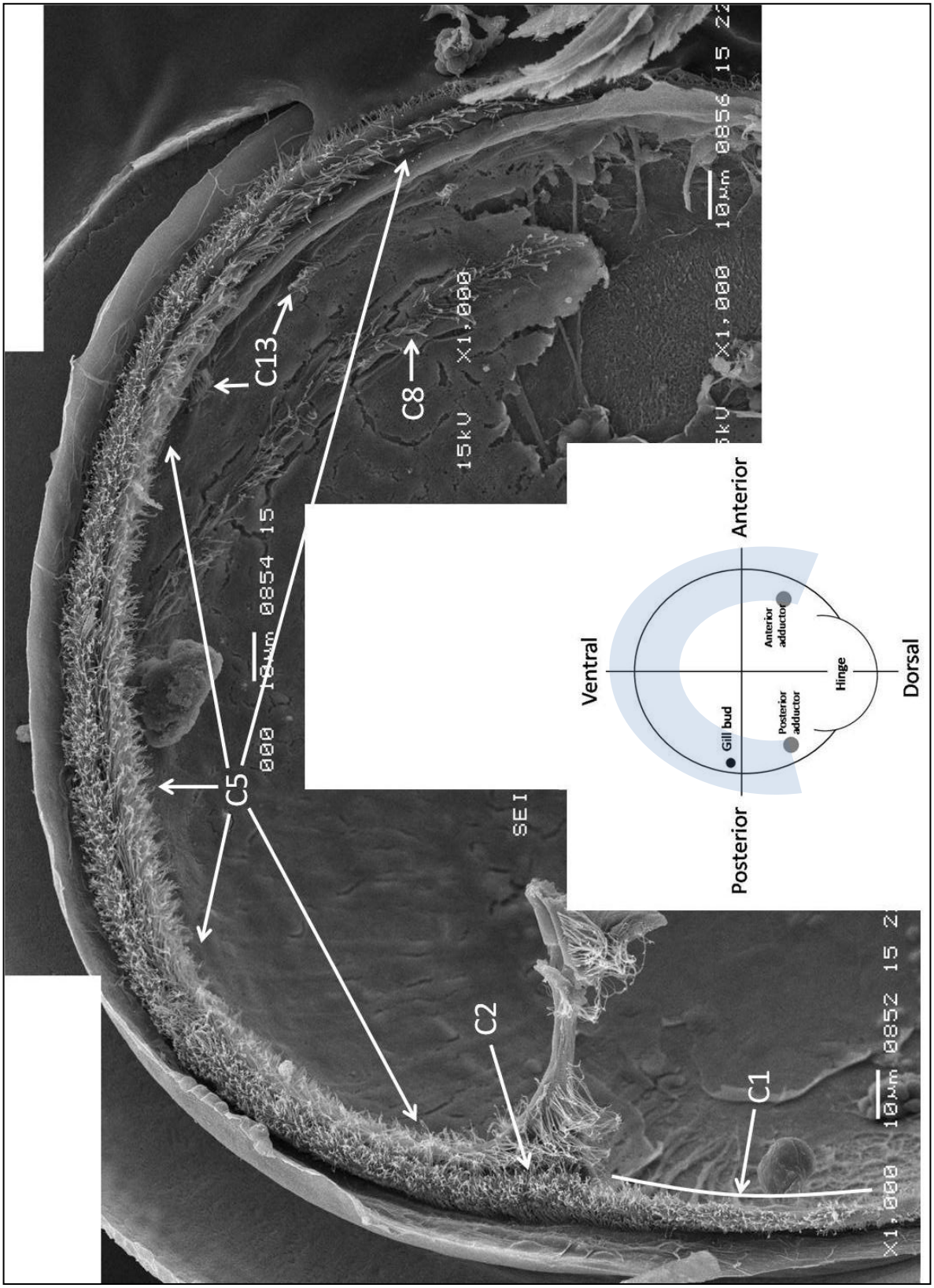

Figure 2.9 - Distribution of cilia on the mantle of an early *Crassostrea gigas* spat (1-3 hours post metamorphosis).

Moving from the postero-dorsal region there is a well developed C1 tract, a short area of C2 cilia and a long area C5 ciliation running around the rest of the mantle rim to the antero-dorsal region. Below the rim ciliation in the antero-ventral region there is a well developed tract of C8 cilia and several discrete sets of C13 cilia. This spat was dry fractured and imaged by SEM, the light blue shaded area of the diagram shows the area pictured.

Cilia of the postero-dorsal region

The mantle region from the hinge to the gill bud bears C1 ciliation on the inner mantle fold rim only, this being a single cilia tract running from the dorsal-most point of the rim to the gill bud/mantle rim junction. The C1 cilia tract is the only mantle rim ciliation present dorsal to the gill bud. The cilia vary from 2-5µm in length, emerging through the microvillous surface with no apparent organisation within the tract into clumps or lines in the veliger larvae, but organised as clumps in the pediveliger (Figure 2.11). The tract in the veliger (Figure 2.10) is sparse on the inner mantle fold rim, including many short cilia and showing a large variation in cilia length throughout the tract. By the pediveliger stage (Figure 2.11) the C1 tract is a dense line of ciliation covering the inner mantle fold rim. The C1 tract in the pediveliger shows less variation in cilia length with most of the tract made up of cilia around 5µm in length. The cilia do not appear stiff, but there is no uniform curvature to suggest any beat or beat direction. This group of cilia was observed in 77% of the veligers and 97% of the pediveligers used in this study where this region of the mantle rim was visible.

There is a group of cilia on an extrusion of mantle tissue next to the posterior adductor. This C9 grouping (Figure 2.12) is found dorsally from the anus, directly below the anal tuft on a protuberance of mantle tissue near to the hinge, forming a bridge between the right and left valves of the larval shell and directly below the posterodorsal notch in the shell as shown in Figure 2.12A. The posterodorsal notch is formed from a strong deflection of the shell edge of the left valve, resulting in a distinct notch in the shell. The right valve shows a slight deflection in some individuals. This notch results in a small gap in the shell when the valves are closed, this gap being located directly above the C9 cilia group, and varies (between individual larvae) in width form 1µm - 3µm. Despite the notch being close to the anus, it is not wide enough to serve as a method for faeces to exit when the valves are closed (or mostly closed): in fact some individuals were observed with faeces trapped in the notch. The C9 cilia grouping is comprised of between 20-30 cilia (Figure 2.12 A & B, specialised cilia are arrowed), separated from any other cilia groupings in the region by virtue of their position on the extrusion of mantle described earlier.

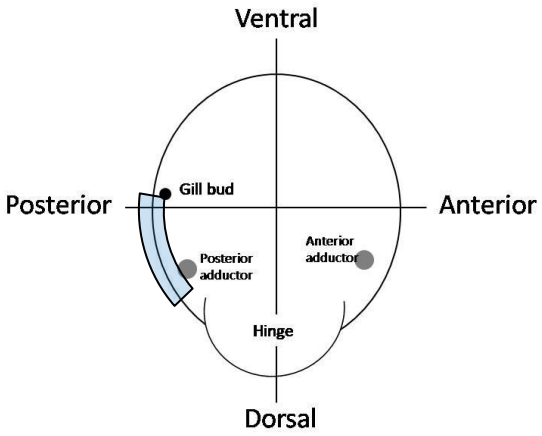

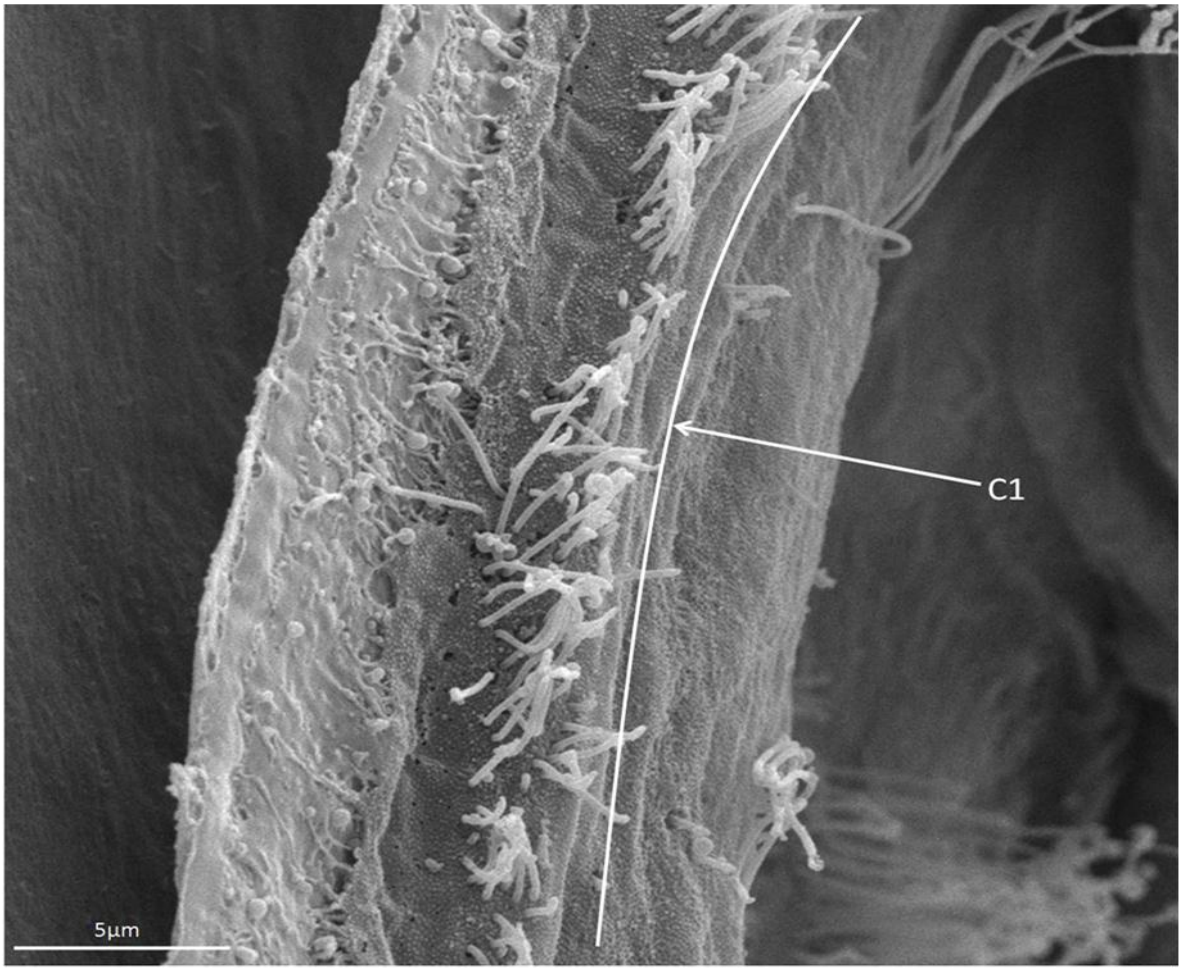

Figure 2.10 - C1 ciliation in the postero-dorsal region of the inner mantle fold rim of a mid-stage *Crassostrea gigas* veliger stage larva.

The image above is taken of a region of mantle rim located just dorsal of the gill bud (the diagram shows the location of the C1 group in the blue shaded area), the left side of the image is the shell and the dark area to the right is inside the larva, below the gill bud. C1 cilia emerge on the rim of the inner mantle fold below the gill bud/mantle join – the join is not visible in this image, but cilia arising on it can be seen at the top of the image. They form a loosely arranged single tract of cilia from the dorsal region of the mantle rim to the gill bud/mantle join (bottom → top of the image). Cilia range in length from approximately 2-5 µm and are directed straight out away from the rim showing no uniform curvature, but without appearing stiff. The larva has been dry fractured and imaged by SEM.

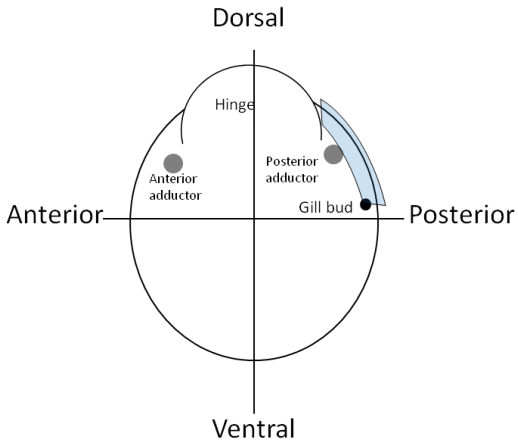

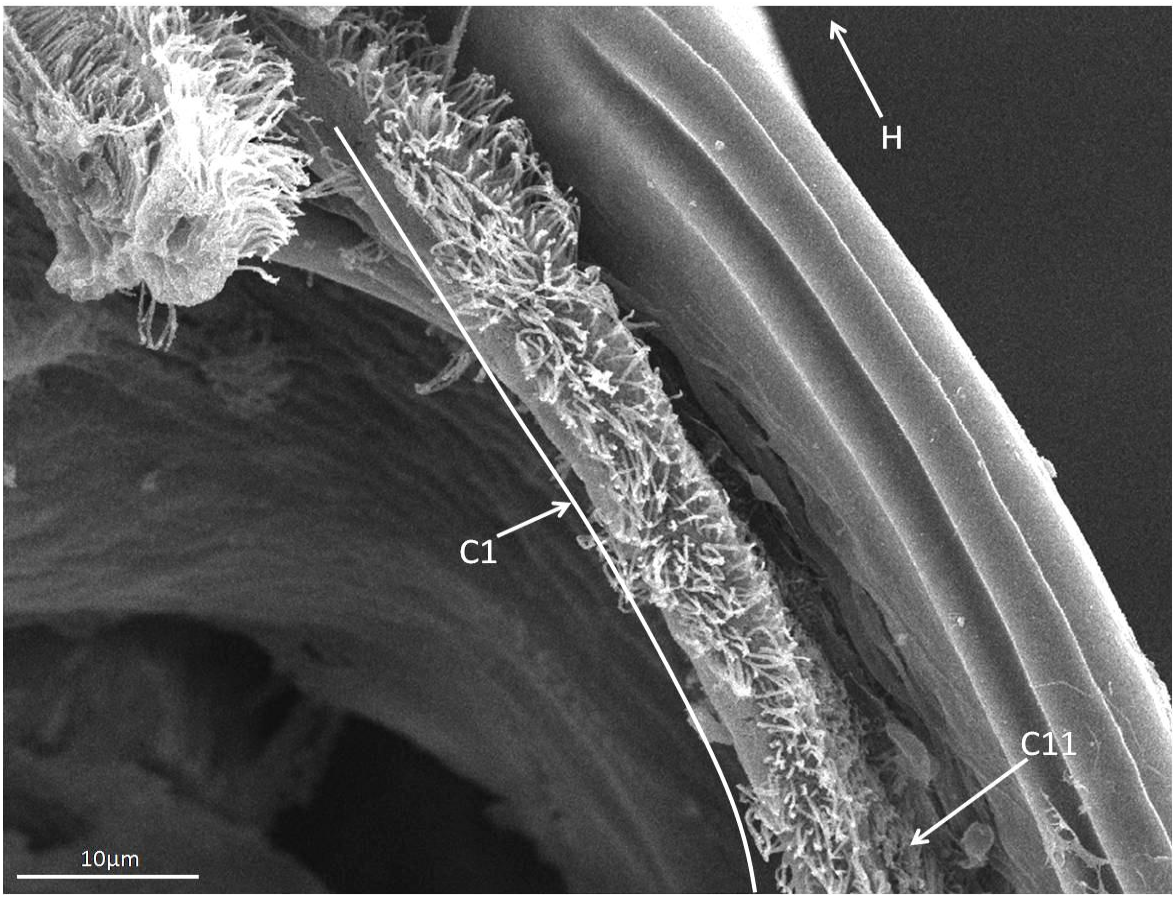

Figure 2.11 - Image of C1 ciliation on the inner mantle fold rim of a *Crassostrea gigas* pediveliger larva.

As shown previously on the veliger stage larva, C1 cilia arise on the inner mantle rim near the hinge (H).This ciliation spreads along the mantle rim until the junction between the rim and the gill bud (this description of ciliation corresponds to, bottom → top of the image). In comparison to Figure 2.10, the C1 ciliation is arranged more densely on the mantle rim of this pediveliger stage larva, but with cilia still arranged as a single tract. The larva has been dry fractured and imaged by SEM, and the area shown by the image is shaded blue in the diagram above.

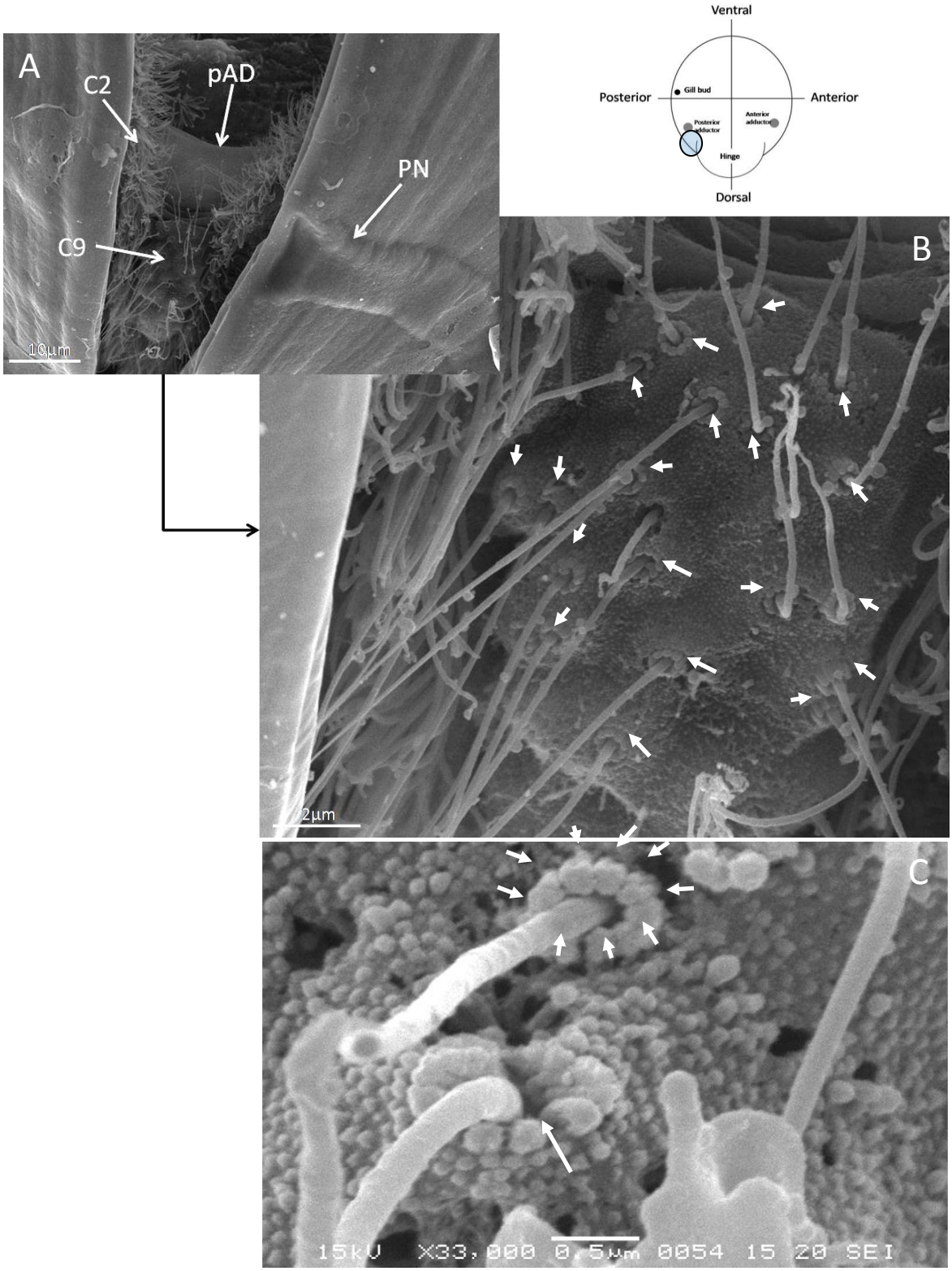

Figure 2.12 A, B & C - C9 cilia in the dorsal region of a *Crassostrea gigas* pediveliger larva.

The C9 cilia occur as a group of cilia on an extrusion of mantle tissue (shown in B) in the dorsal region of the larva just above the hinge and immediately adjacent to the posterior adductor muscle (pAD). This general location is shown in image A. The cilia of this group comprise a single long cilium of around 13µm, surrounded at the base by a ring of 9 microvilli (C shows two C9 cilia with microvilli at the base of the upper C9 cilium arrowed). C9 cilia are closely associated with the posterodorsal notch (PN) in the shell (seen in image A) and are just dorsal of the anal tuft. These cilia are long enough to protrude from the notch (which creates a slight gap in the shell directly above the group even when the valves are closed). This larva was imaged by SEM still intact, with the shell partially gaped - the blue shaded area on the inset diagram at the top gives the location the C9 cilia in the larva.

The long cilia of the C9 group show no curvature to suggest a beat direction and have a 0.7µm wide ring of microvilli at the base (Figure 2.12 C - arrowed). The ring is formed from 9 discrete microvilli: Figure 2.12C shows the individual microvilli (arrowed) have a triangular/heart shaped appearance when viewed from above, the indentation in the shape suggesting the microvilli may be composed of three individual units. The C9 cilia are noticeably longer than other groups found on the mantle rim at 13µm in length and are probably just able to extend out between the shell vales, through the postero-dorsal notch (Figure 2.12 A). C9 cilia were observed in individuals from different brood-stocks, in veliger through to late pediveliger stage larvae, and were present in 100% of individuals where the protrusion of mantle tissue was visible.

Details of the cilia groupings in the gill bud region

The gill bud region has 3 distinct cilia groups: C2 on the mantle rim where the gill bud fuses with the rim, C3 on the mantle below the rim at the base of the gill bud, between the bud and the posterior adductor and C4 on the mantle at the base of the gill bud itself (see Figure 2.12 for a view of the groups locations). In addition the gill bud is ciliated on the gill rudiments. The C5 grouping starts at the gill bud/mantle rim join at the appearance of the gill bud in the early veliger stage and spreads around the mantle rim during larval development. C2 cilia occur at the merging of the mantle rim to the gill bud and are grouped in short lines of 16-20 cilia scattered on the gill bud at its closest point to the mantle rim and also occur on the inner mantle fold rim (Figure 2.13 and Figure 2.14). The C2 cilia are limited to this area and extend no further along the mantle rim (Figure 2.14). C2 cilia are approximately 10µm in length, are not stiff and have no indication of a beat direction. This grouping was present in every specimen where the gill bud was observable.

Groups C3 and C4 are unusual in being well below the rim of the inner mantle fold - the rim being the location for much of the larval mantle ciliation. The C3 grouping (Figure 2.15) appears stiff, forming a round group of approximately 60 cilia projecting straight out from the mantle. The C3 grouping often features discocilia (possibly fixation artefacts). The cilia are approximately 10µm in length, although the presence of the discocilia makes length measurements difficult

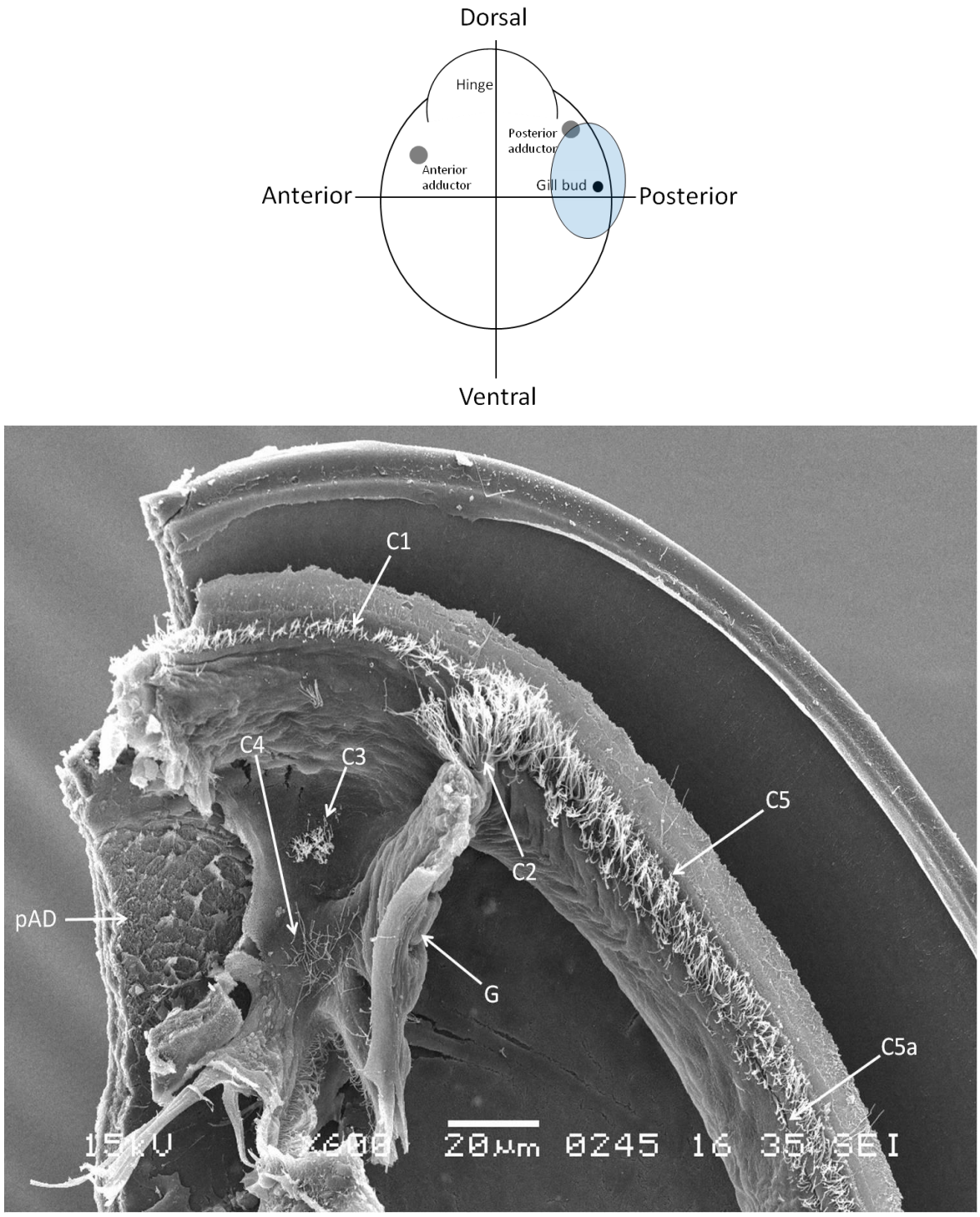

Figure 2.13 -SEM image summarising the ciliation found around the gill bud/mantle join in a *Crassostrea gigas* veliger stage larva.

The hinge, if visible, would be to the left of this image (see diagram at the top - the region shown by the SEM image is shaded light blue)., From the hinge, C1 ciliation spreads around the inner mantle fold rim until it reaches the gill bud/mantle join. This region is the location of several cilia groups, both on the mantle rim and on the mantle further into in the body cavity; C2 ciliation arises at the join, the C3 group is found below the gill bud (G) on the mantle itself and the C4 grouping is located at the base of the bud . From here the C5 ciliation can be seen extending along the mantle rim towards the ventral region. As this is a veliger stage larva, the C5 tract is short and fades into a C5a region quite close to the gill bud/mantle join. The C5a cilia are not obviously arranged into two discrete rows. This larva was dry fractured and imaged by SEM.

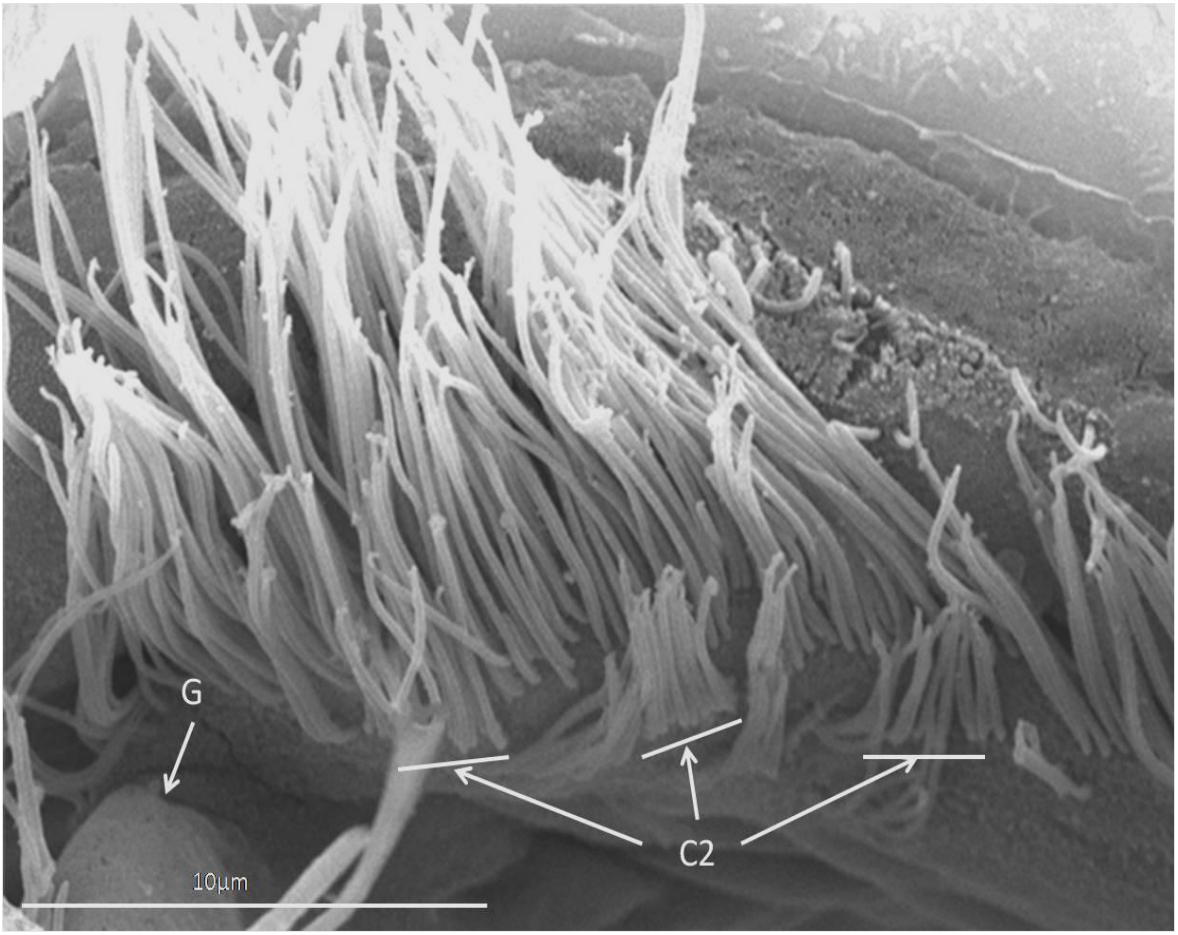

Figure 2.14 - C2 ciliation at the gill bud/inner mantle fold junction of an early *Crassostrea gigas* -stage veliger larva.

The C2 cilia are located where the gill bud (G) joins the inner mantle fold. They extend no further than the last group on the right of the image above and are found both on the gill bud and the inner mantle fold rim. The C2 cilia are arranged in discrete lines of roughly 16-20 cilia of up to approximately 10µm in length, which are scattered over the junction and not arranged into tracts or clumps. This larva has been dry fractured and imaged by SEM.

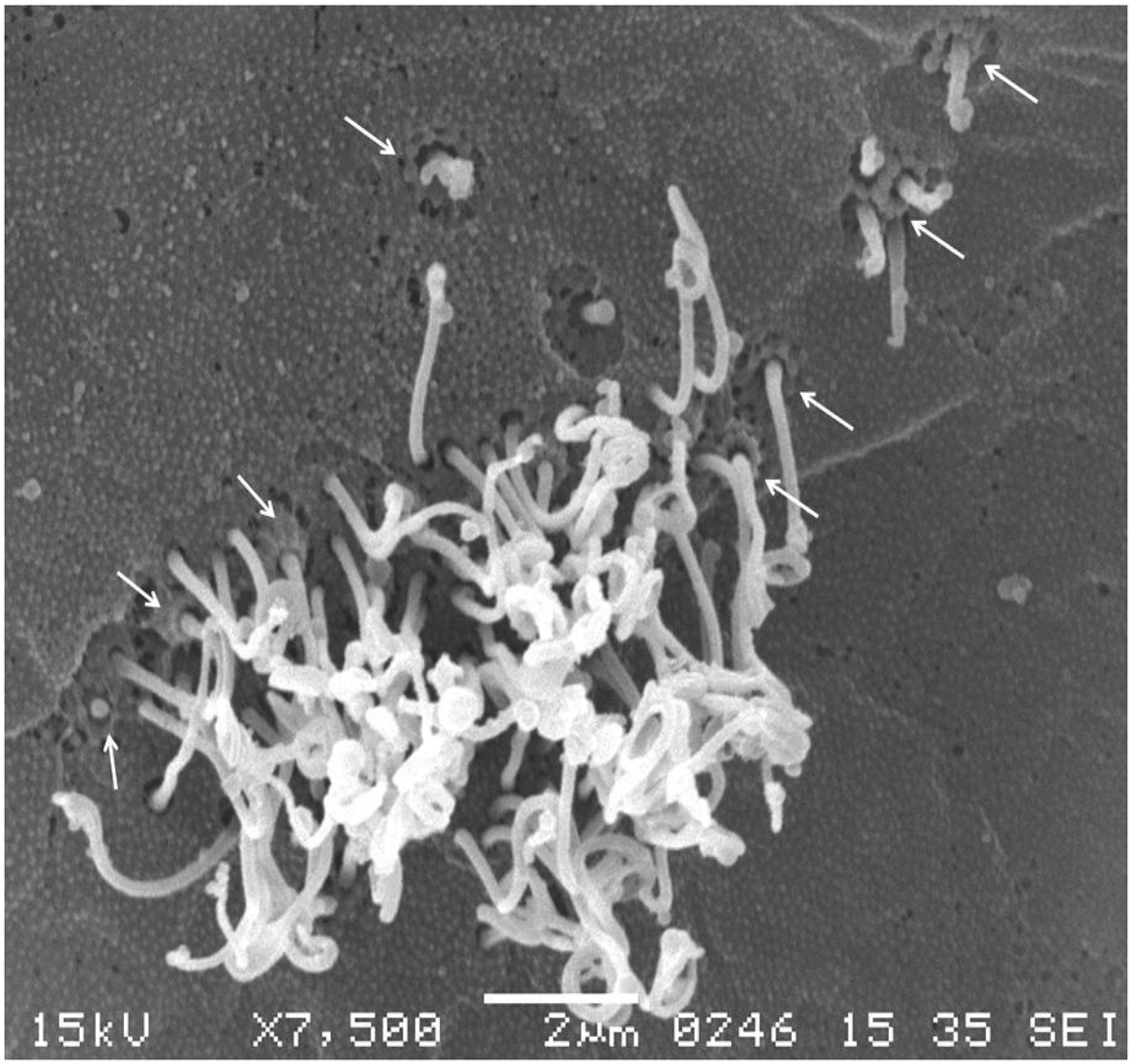

Figure 2.15 - C3 cilia group on the mantle of a *Crassostrea gigas* veliger stage larva.

The cilia of the C3 grouping typically have the stiff appearance after fixation shown in the image above. No beat direction is discernible from the appearance of the cilia. A number of cilia with a ring of 9 microvilli at the base (arrowed) appear around the edge of the group, with a few removed slightly from the main cilia cluster on the right of the image. The tips of the cilia in the main group show distinct discocilia, although these are most likely sample preparation artefacts (Short & Tamm, 1991). The grouping was revealed via dry fracturing the larva and then imaged by SEM.

The outer margin of the C3 grouping features numerous cilia bearing a ring of 9 microvilli at the base: these are arrowed in Figure 2.15. These cilia are similar to those of the C9 group but the cilium of C3 are shorter, those furthest away from the main group of cilia (and without discocilia) being less than 10µm in length.

The C4 cilium grouping occurs on the mantle where the gill bud fuses with the surface of the mantle (Figure 2.16). They form a loosely organised clump, not appearing stiff and tending to be laying flat on the surface of the mantle. Cilia vary in length from around 5µm to 10µm and lack any specialised bases or any indication of activity such as a beat direction. The grouping was present in 95% of pediveligers where this region of the mantle was visible and 100% of the veligers where the base of the gill bud could be observed.

Both C3 and C4 cilia groups have been observed in veliger and pediveliger stage larvae. Whilst their position often makes viewing difficult, both groups have been observed in numerous larvae from at least 3 different larval batches. The group does not change as the larva develops, being present over 95% of individuals (veliger or pediveliger) where this region of the mantle was visible.

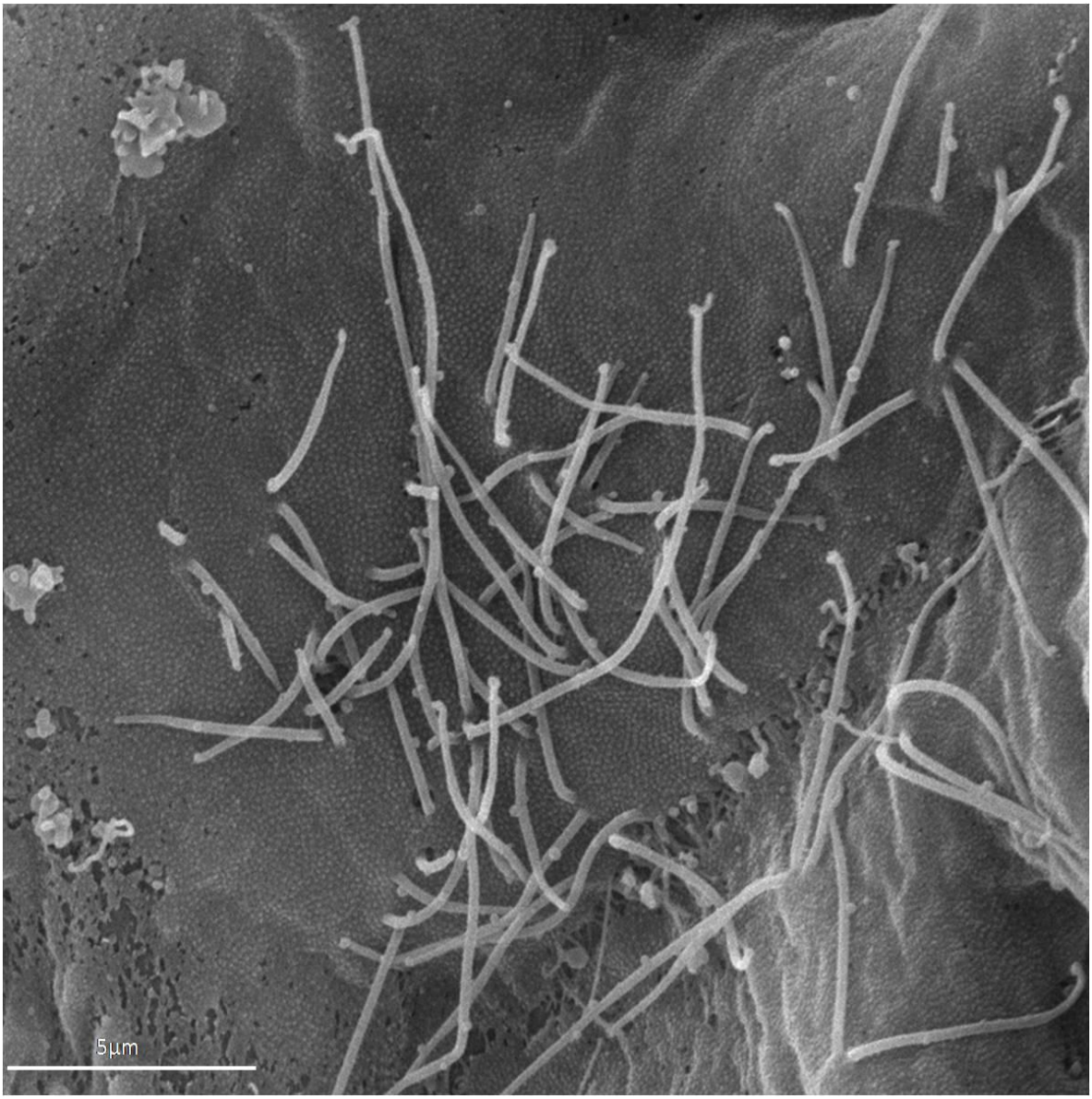

Figure 2.16 - C4 cilia at the base of the gill bud in a mid-stage *Crassostrea gigas* veliger.

The C4 grouping is located on the mantle at the base of the gill bud (gill bud is the raised area on the right of the image). As can be seen in the image above, the group is comprised of a number of cilia approximately 5-10µm long, loosely arranged and laying flat against the mantle surface when fixed. No specialised bases are visible. This larva was dry fractured and imaged by SEM.

Cilia groupings of the posterior to anterior axis (ventral region)

The ciliation of region is localised to the inner mantle fold rim - group C5 ciliation occurs as twin tracts of ciliation along the rim. These tracts develop significantly through larval development from veliger to late stage pediveliger and are dense enough to have been observed beating in live larvae using light microscopy (Figure 2.17, with the cilia tracts just visible on the mantle rim in the highlighted area).

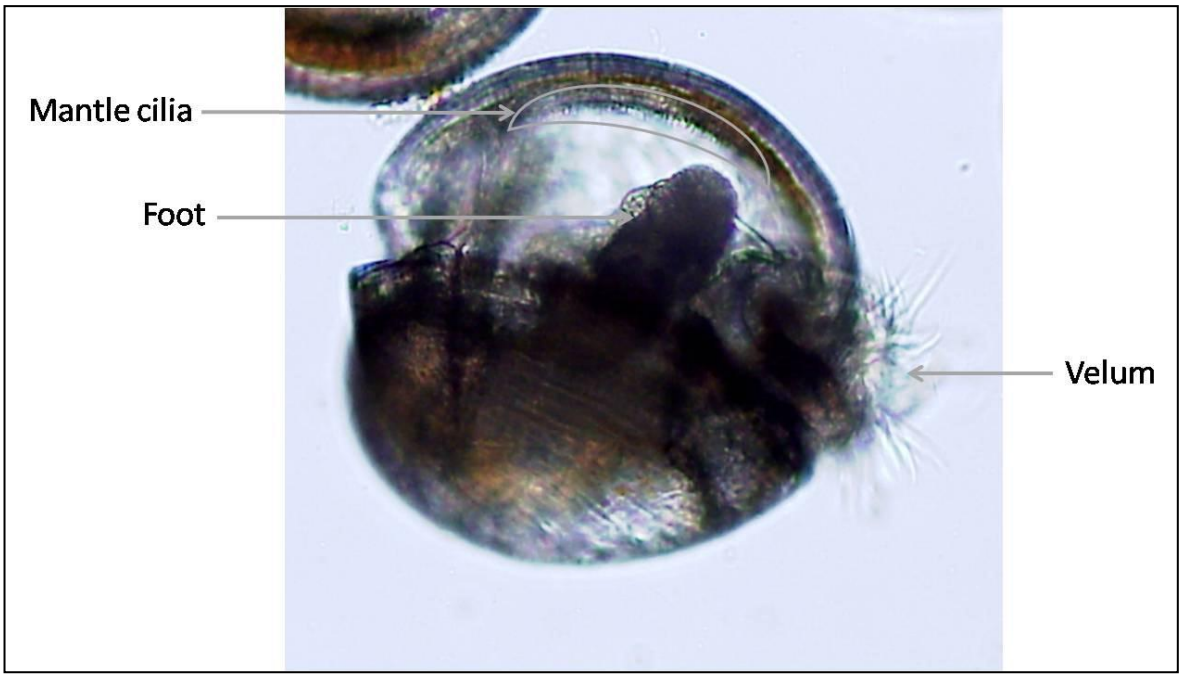

Figure 2.17 - *Crassostrea gigas* pediveliger, partially gaped with the foot partially extended.

This live larva was seen exhibiting both swimming and crawling behaviour, and when resting partially gaped, as in the image above, the mantle rim cilia could clearly be seen beating. The location of these eating mantle cilia suggests these are the C5 twin tract cilia. Note that these C5 cilia are in close proximity to the foot when it is extended or retracted.

C5 ciliation appears after the C2 cilia at the junction of the mantle rim and the gill bud. This cilia group is formed of two distinct tracts of cilia, one along the upper edge of the inner mantle fold rim, and a second tract just below (both tracts arrowed on Figure 2.18). There is a distinct gully about 5µm wide between the two cilia tracts. As can be seen in Figure 2.18, this gully often appears tightly folded in on itself when viewed in the SEM - this is probably an artefact of the specimen dehydration. The two tracts of the C5 group are formed of rows of cilia clumps - groups of 5-10 cilia form the clumps which are arranged closely together to form the tracts.

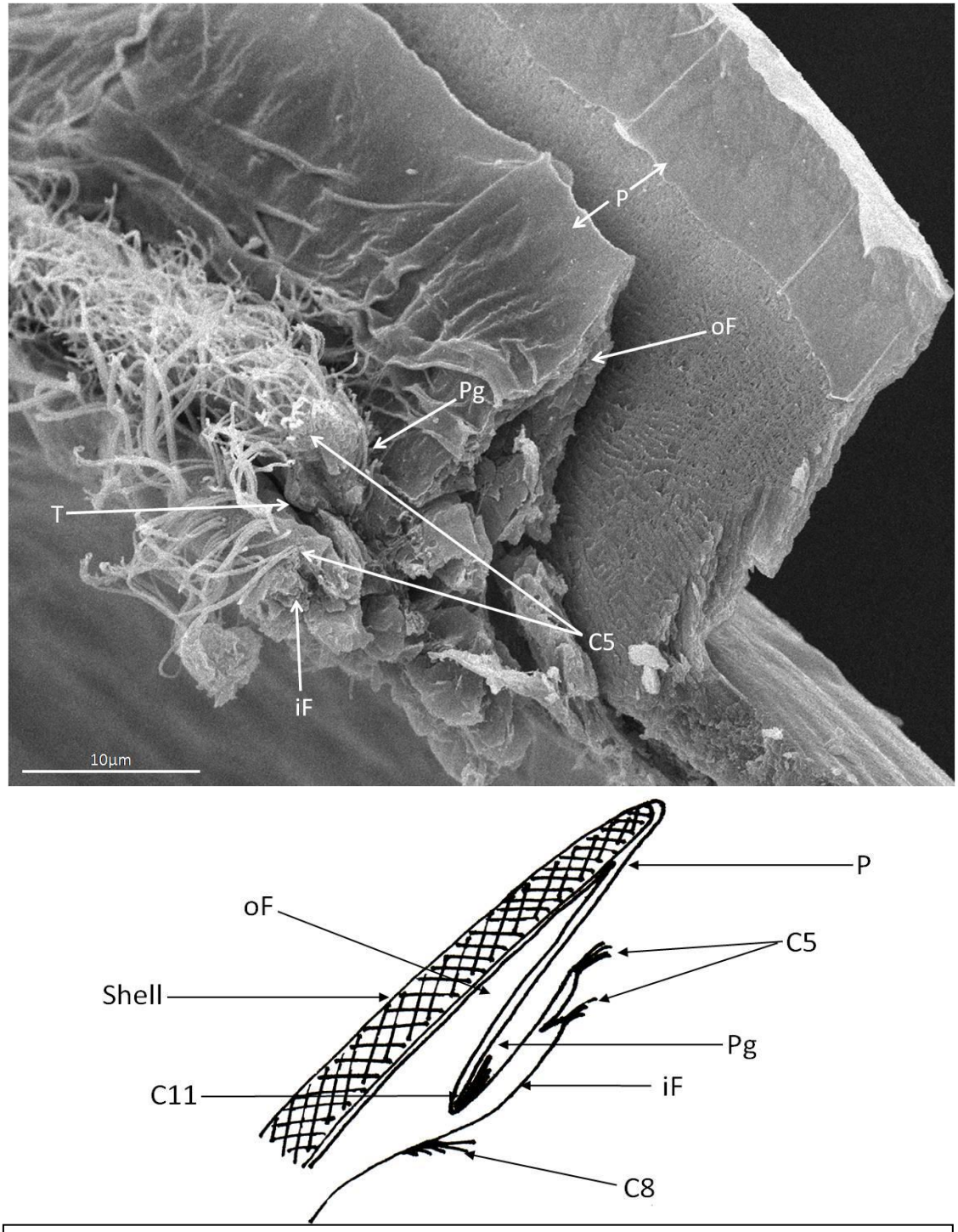

Figure 2.18 - Showing the mantle folds and their associated ciliation in the ventral region of a *Crassostrea gigas* pediveliger.

The C5 cilia form 2 tracts along the inner mantle fold (iF): one can be seen on the rim and the second below, with an un-ciliated tract in-between. The above image shows the space between the two cilia tracts as a deep fold (T), but this is likely accentuated by tissue shrinkage during dehydration. The periostracal groove (PG) between the inner and outer mantle folds is discernible, with the periostracum (P) emerging from here and covering the outer mantle fold (oF), which has torn away from the shell in the right side of the image above. This image provides a 3 dimensional view of the diagram by Cranfield (1974), reproduced in Figure 2.1. The diagram below the EM image illustrates the mantle folds as shown in the EM image above it, and using the information from LM sections and Cranfield's diagram. The larva was dry fractured and imaged with SEM.

Each cilium of the C5 tract forming clumps is around 8-10µm in length. When fixed the cilia of the tracts are often angled either posteriorly or anteriorly for most, or sections of their length, as is shown by the lower tract in Figure 2.19. This suggests the tracts have a directed beat - the tracts are large enough for this beat to have been observed in live larvae, especially in those larvae with the valves partially gaped and the velum either withdrawn or only semi-extruded. In experiments with introducing ink or fluorescent particles into the culture it was possible to see the dye/particles being pushed along the C5 tracts and extruded near the anus. The series of video frames and the explanatory diagram in Figure 2.20 illustrate this process. The C5 cilia tracts appear from the early veliger stage, being present in >95% of the individuals where their location was visible (although they may be absent from the earliest veligers but veliger still show >90% C5 presence), where they extend for a very short distance ventrally from the gill bud shown in Figure 2.6. By the late pediveliger stage these C5 tracts spread along the entire inner mantle fold from the gill bud to the anterior region of the larva, terminating next to the anterior adductor. This is shown in Figure 2.8. The C5 ciliation persists on the mantle rim in newly metamorphosed spat, as shown in Figure 2.9 and Figure 2.26.

In the ventral region of the veliger stage and in the antero-ventral region in the pediveliger stage, C5a ciliation occurs after the C5 twin tracts. The C5a is a transition region where the C5 tracts have not yet formed fully. As can be seen in Figure 2.21 the dividing gully between the tracts is barely visible (and never infolded) and the cilia are emerging individually through the microvilli, not in the form of clumps. The C5a cilia emerge on the inner mantle fold rim and on the inner mantle itself, as with the C5 cilia, but the ciliation on the rim is much denser than the lower ciliation on the mantle itself, suggesting the upper tract forms first. The cilia vary widely in length from less than 1µm to 8µm, with those cilia lower on the mantle tending to be shorter. 85% of veliger stage larvae observed showed a C5a region, although the length of this region varied between individuals from 20-120µm, and did not seem to be dependent on the size of the larva, only the development stage. This is compared to just 25% of pediveligers having a C5a group.

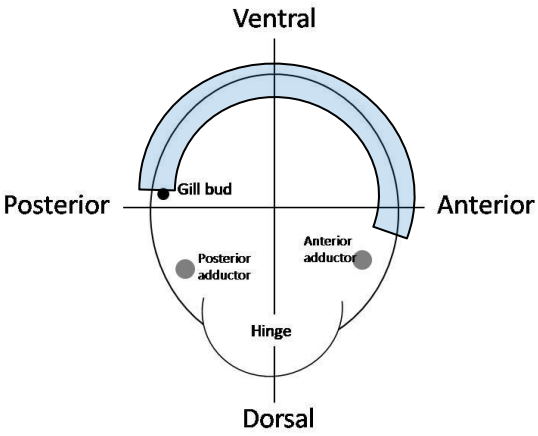

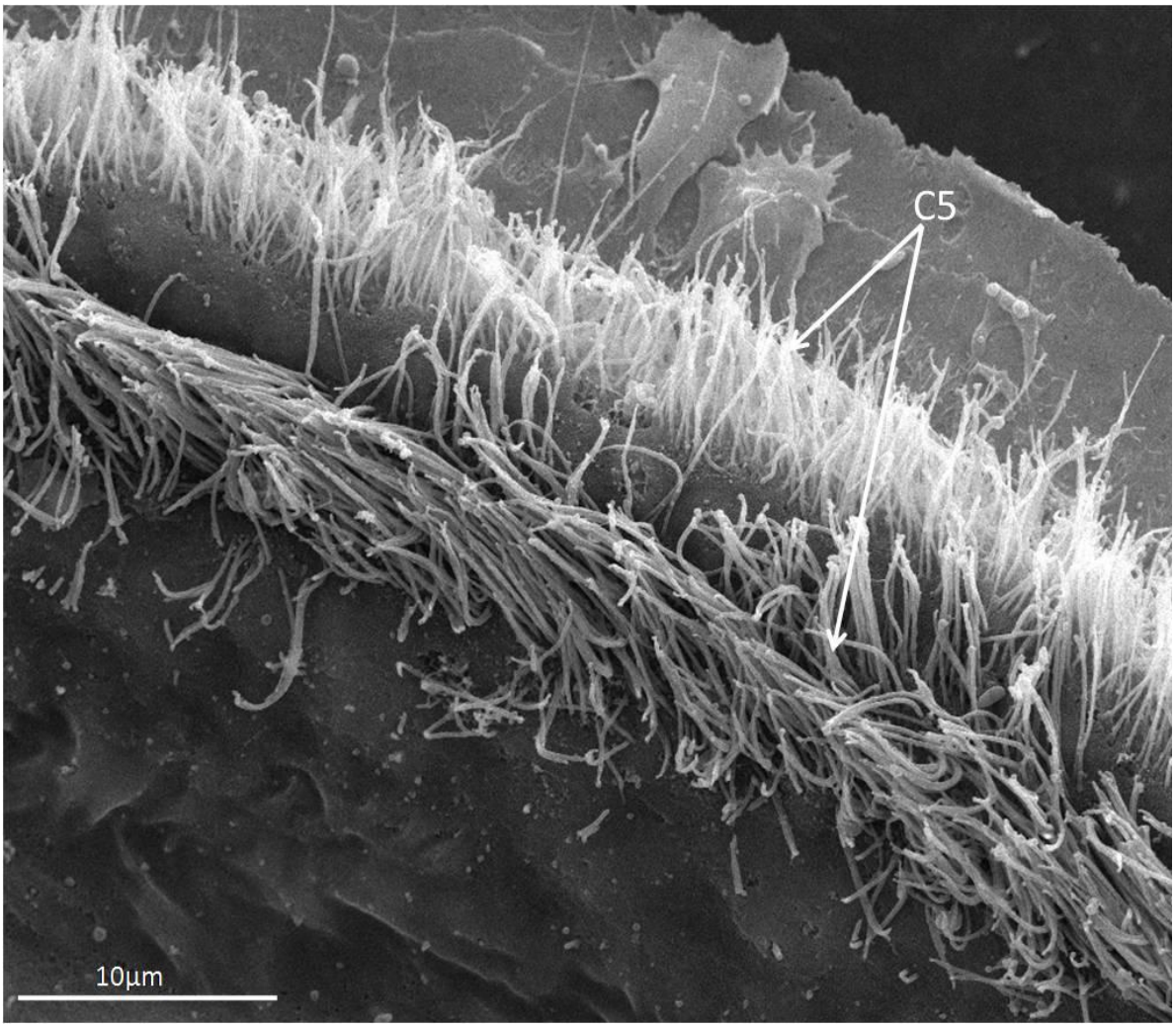

Figure 2.19 - C5 cilia on the inner mantle fold of a *Crassostrea gigas* pediveliger.

Two tracts of cilia run along the inner mantle fold, one on the edge of the rim and a second approximately 5µm below, labelled by two independent arrows. There is a distinct, microvilli covered tract between the two lines of cilia which indents where the lower tract of cilia emerges. The cilia of the tracts do not appear stiff when fixed and the consistent angle of the lower tract suggests the tract probably has a beat. The diagram above gives the location in blue shaded area of the pediveliger stage C5 ciliation shown in this SEM image. The larva was dry fractured and imaged by SEM.

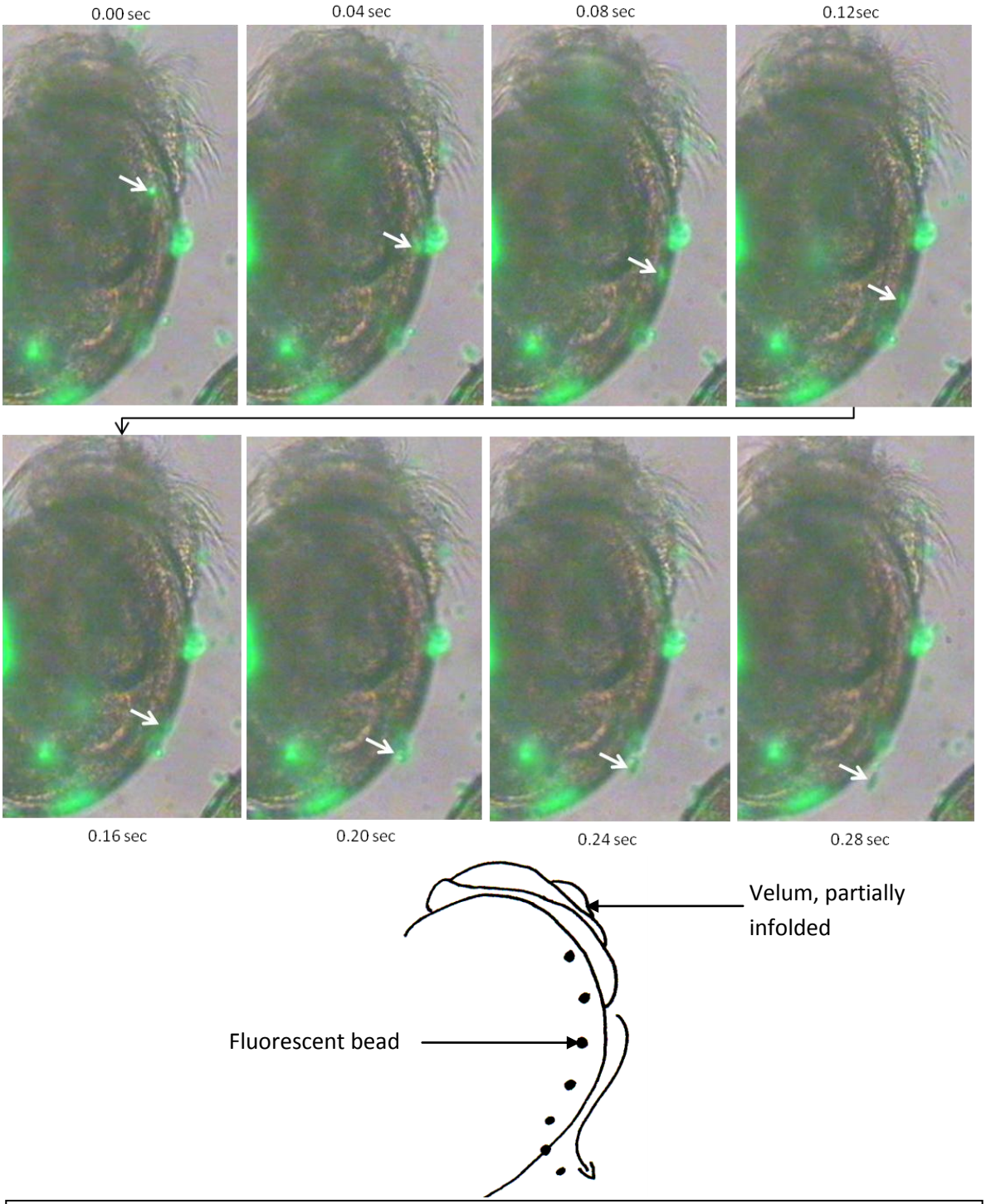

Figure 2.20 - Particle rejection by the C5 mantle cilia of a *Crassostrea gigas* pediveliger.

This sequence of video frames shows a fluorescent bead being rejected from the mantle cavity by the C5 cilia of the inner mantle fold rim. The bead is first visible in the mantle cavity just under the velum (0.00 sec), and is moved in a dorsal direction along the rim, before it exits the body cavity just above the hinge, where another bead (just out of focus) is trapped (possibly in debris accumulated around the posterodorsal notch). The bead continues to travel away from the larva after ejection, likely due to water movement generated by the pre-oral cirri on the velum. The diagram below the image series demonstrates the path (illustrated by the arrow) taken along the C5 cilia tracts by the fluorescent bead, before its ejection near the anus. This video was captured on a Nikon Coolpix 4500 attached to a compound microscope illuminated with a standard halogen transmitted light source and a mercury bulb to image the beads.

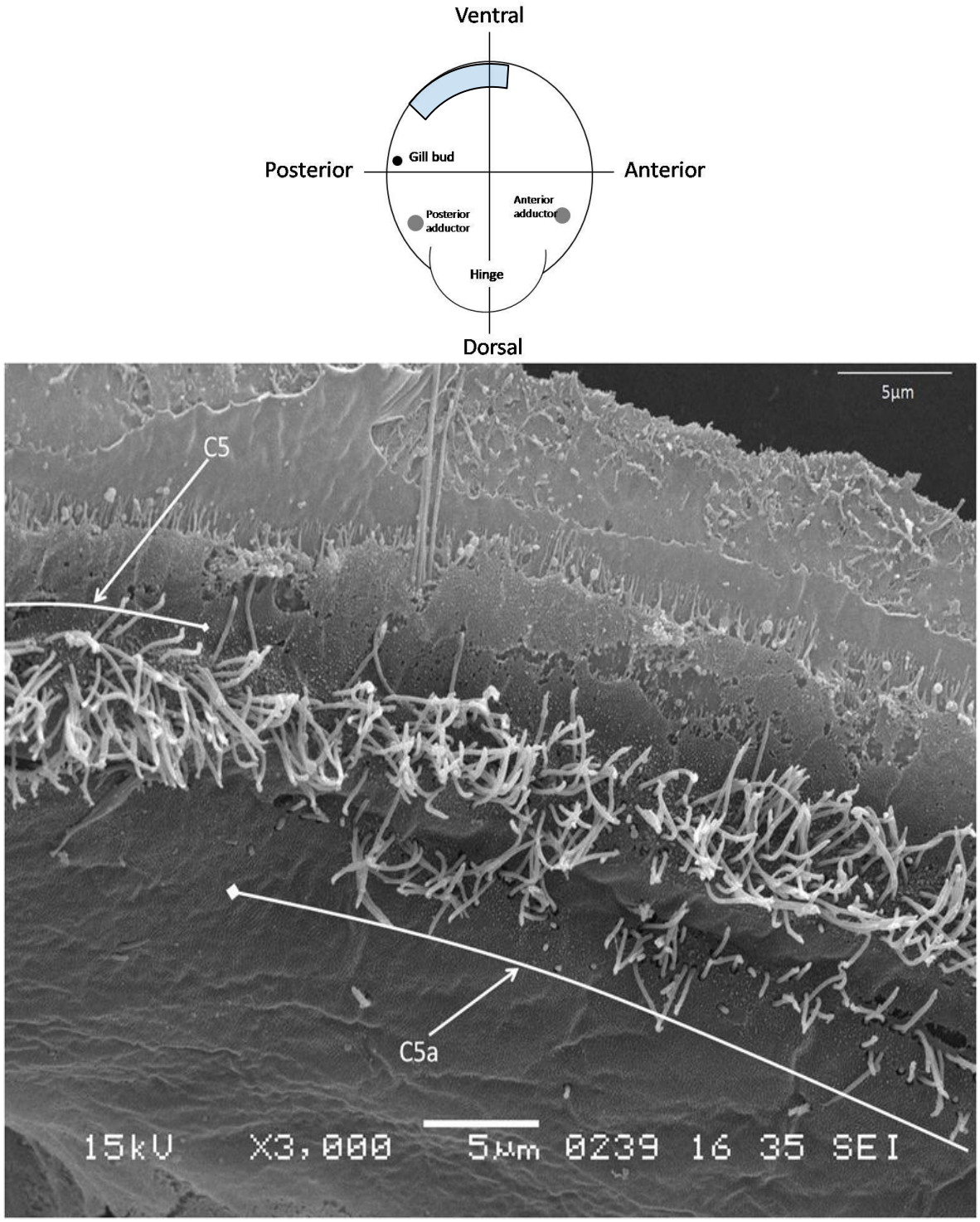

Figure 2.21 - C5a ciliation on the inner mantle fold of a mid-stage *Crassostrea gigas* veliger.

C5a ciliation is a transitional region were the distinct twin tract of C5 ciliation have not yet formed. The C5a cilia are in the ventral and anterior regions of the larva, depending on the level of larval development - see Figure 2.36 - in this case the ventral. The C5a cilia tract is less densely ciliated than the C5 tracts and the cilia vary considerably in length from 8µm down to less than 1µm. The ciliation on the rim is denser than that of the lower tract, but the dividing un-ciliated tract marking this as two rows of cilia is distinct. The diagram above shows the C5a group position in this larva in the blue shaded area. The larva was dry fractured and imaged by SEM.

In the late ventral/early anterior region of very early veliger stage larvae a single tract of cilia emerges after, or sometimes in place of, the C5a transition region. This short single tract of group C6 ciliation runs down towards the anterior region as far as the anterior adductor and is comprised of short, ungrouped cilia that vary widely in length from 1µm to 5µm (Figure 2.22). The tract of C6 cilia is often quite short: in some of the earliest veligers observed the tract was less than 15µm long. The C6 ciliation was observed only in those larvae that were early stage veligers, and disappeared quite quickly as soon as the C5a ciliation appeared more widely through the anterior and antero-ventral regions. No pediveligers had a C6 group and only 50% of veligers feature the group. The C6 cilia may be the early stage of the upper of the C5a tracts.

Short group C7 cilia are spread throughout the mantle rim from the posterior to anterior region (although they are most common in the ventral region). These cilia only just pierce the microvillous surface and are visible in Figure 2.22 and Figure 2.24, where they have been arrowed. The position of the C7 cilia in these figures illustrates that they are distinct from the other groups shown in these images. The C7 cilia are barely 0.5µm in length and appear to emerge through a distinct gap in the microvillous surface. C7 cilia occurred throughout all stages of larval development and were observed in 100% of the ostreid larva examined (>150 veliger and pediveligers from various broodstocks).

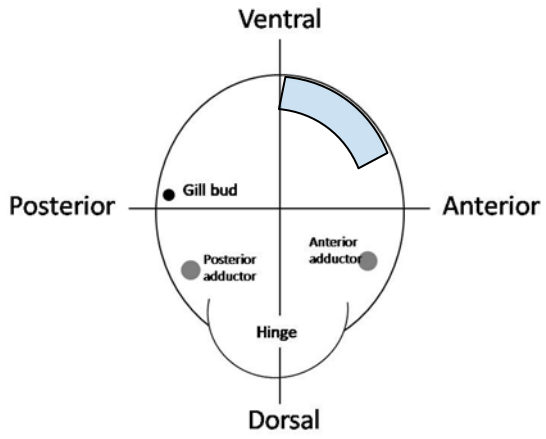

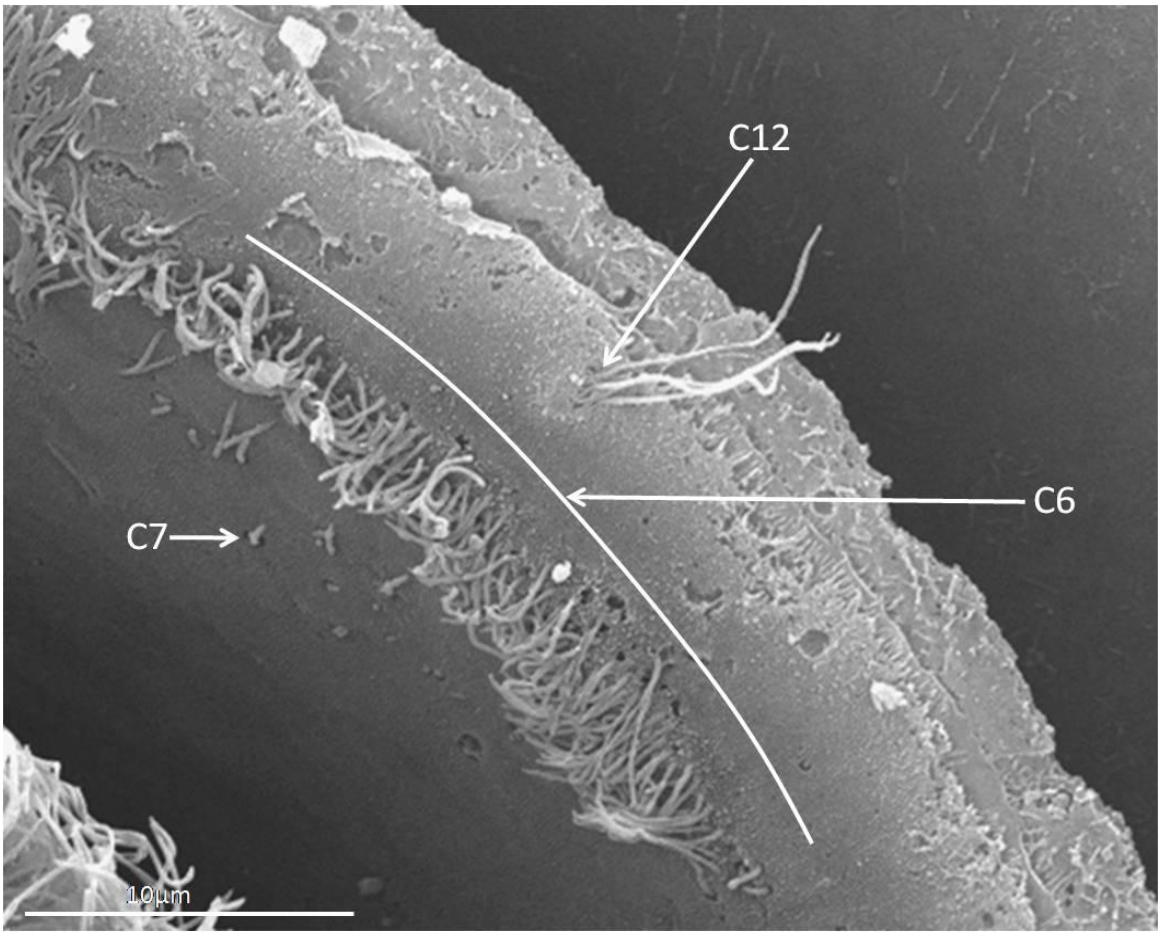

Figure 2.22 - C6, C7 and C12 ciliation on the inner mantle fold of an early stage *Crassostrea gigas* veliger.

C6 cilia form a short tract along the rim of the inner mantle fold in the antero-ventral region of early stage veliger larva only. The cilia comprising the tract are approximately 5µm in length and occur only in very early veligers. Note the presence of C7 cilia; short individual cilia appearing through the microvillous surface, below the main tract of cilia. C7 cilia also occur in late stage veligers and pediveligers, distributed widely over the inner mantle fold. C12 cilia are also labelled above, these being long cilia (around 12µm) arising from the outer fold of the mantle and extending out over the rim. The blue shaded area of the diagram above shows the region of the larva the SEM image is depicting. This larva was dry fractured and imaged by SEM.

Cilia groupings of the anterior-dorsal region

From the mid-veliger stage there is a single line of cilia on the inner mantle fold rim, beginning as C5a ciliation in the anterior region ends. This group C10 ciliation, shown in Figure 2.23, spreads down into the dorsal region, terminating at the end of the mantle rim near the hinge. The cilia of the C10 tract are approximately 5µm long, with relatively little variation in length. C10 cilia emerge through the epithelium individually, not as groups. These cilia are not stiff in appearance and are not consistently angled to suggest any beat direction. The C10 ciliation persists from the mid-veliger stage through until the late pediveliger, being present in ~60% of veligers but >90% of pediveligers. In the late pediveliger the C10 cilia tracts begin much further into the anterior of the larva, often not appearing until the area of the mantle rim adjacent to the anterior adductor, as in Figure 2.8. As a result the C10 tract is often very short (>10µm) in the late pediveliger, but is usually much more densely ciliated than at any other development stage.

Two more cilia groups arise on the mantle in the antero-dorsal region of the late pediveliger stage larva: C8 ciliation (Figure 2.24) runs from the ventral region to a location near the hinge, and is the only tract forming cilia group to be observed on the mantle itself and not on the inner fold rim. The C8 group forms a densely ciliated tract of cilia 8-10 µm in length, located 20-30µm below the lower row of the C5 group, stopping at the base of the anterior adductor - this endpoint is marked with an arrow in Figure 2.8. The C8 group was occasionally angled towards the ventral region, suggesting a beat in this direction in live larvae. C8 cilia were observed in 85%-100% of pediveliger larvae with this mantle region visible was, but 0% of veliger larvae, revealing this group to be unique to the pediveliger stages.

Group C13 cilia appear in the ventral to antero-dorsal region. The group is located between the C5 or C10 cilia groups on inner mantle fold rim and the C8 cilia tract on the mantle Figure 2.24. The group appears on the mantle at the location of the mantle/shell join - this often

appears to be the point where the mantle is peeling away from the shell in SEM images (probably a specimen dehydration artefact). Figure 2.25 shows the morphology of the C13 group in the pediveliger, formed of short lines of 15 to 30 cilia, 6µm in length, creating a grouping about 8µm wide laying flat against the mantle, directed towards the inner mantle fold rim. Figure 2.26 shows the C13 group comprised of over 30 cilia on the mantle of a newly metamorphosed spat (evidence of metamorphosis can be seen in the disappearance of the foot and the new shell growth extending past the mantle margin in Figure 2.26). As with the C8 grouping, C13 cilia appear in 0% of veligers but 90% of late stage pediveligers (figures from one broodstock where larvae sampled were just pre-metamorphosis), revealing this to be a group present only by the later pediveliger stage.

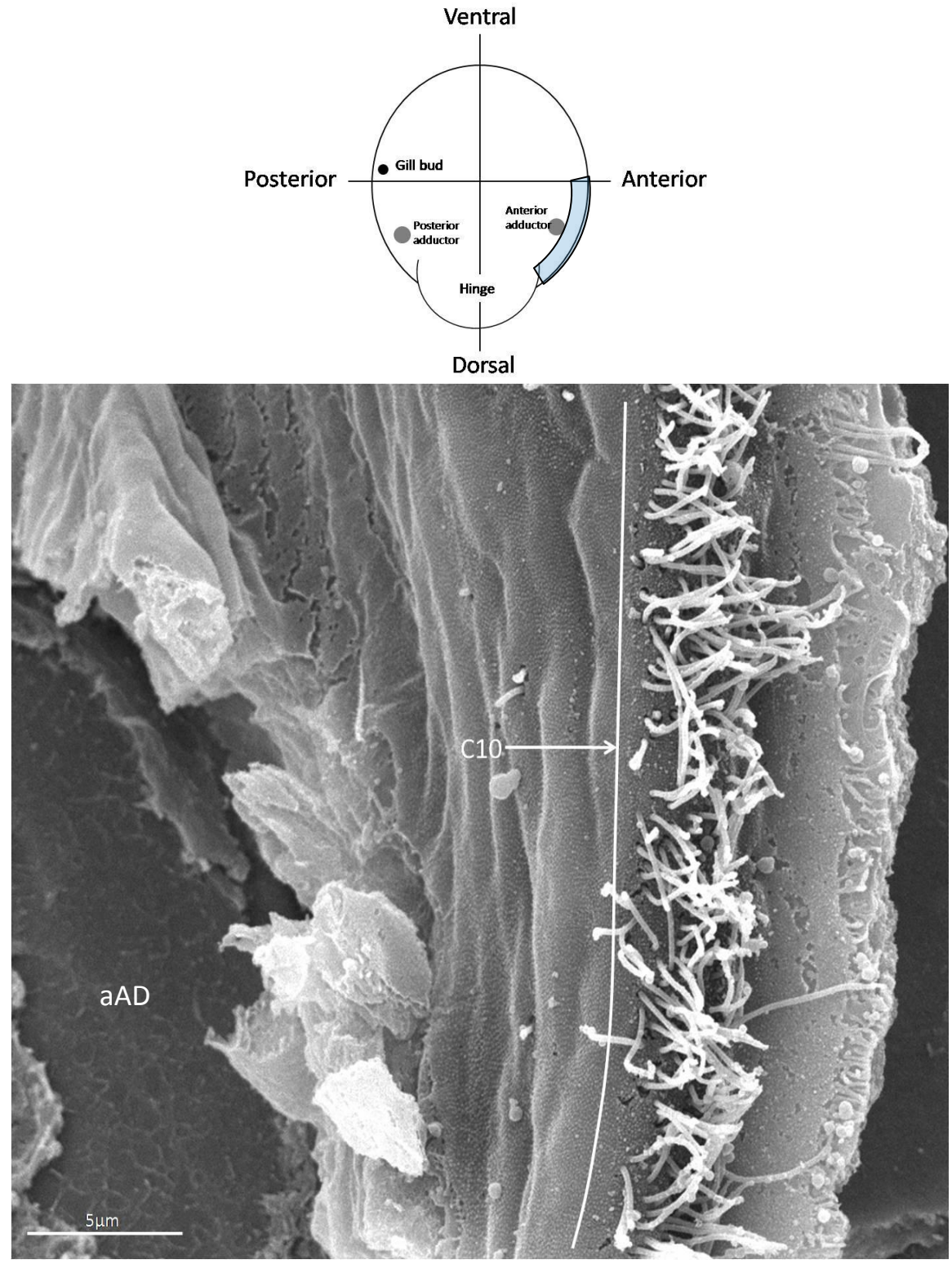

Figure 2.23 - C10 ciliation on the inner mantle fold of a late stage *Crassostrea gigas* veliger.

C10 cilia appear in the antero-dorsal region on the inner mantle fold rim . In the image above they form a single tract of cilia all approximately 5µm in length, and spreading past the anterior adductor (aAD marks the adductor scar). The inset diagram shows the group's location on the larva in the blue shaded area. The larva was dry fractured and imaged by SEM.

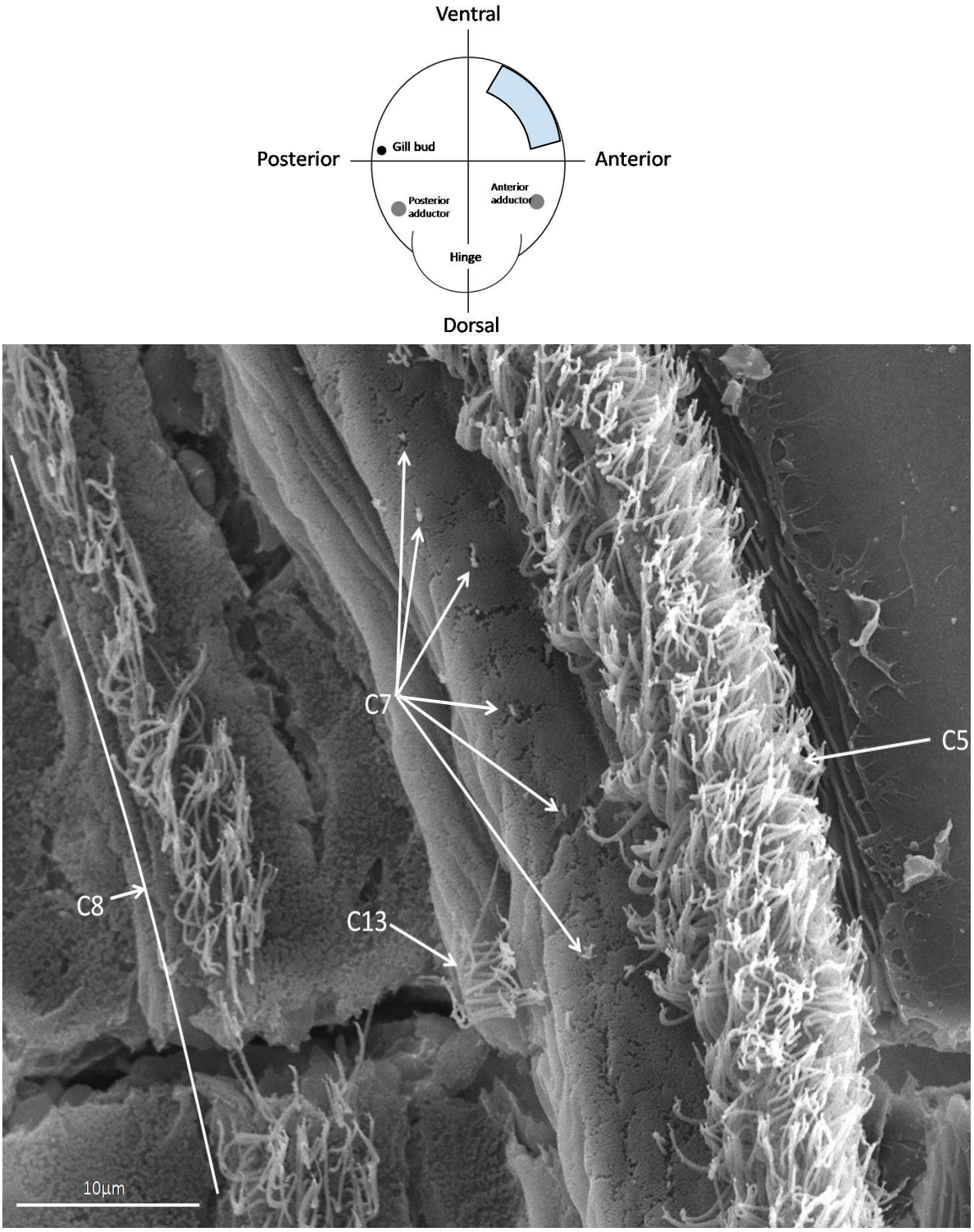

Figure 2.24 - C7 and C8 ciliation on the mantle of a late stage *Crassostrea gigas* pediveliger.

C7 cilia are approximately 0.5µm long, individually breaching the microvillus surface (never arranged as tracts) and scattered around the entire mantle rim, appearing in early veliger stage larvae (Figure 2.22) and persisting to metamorphosis. C8 ciliation can be seen on the above image on the mantle below the rim. They form a tract from the ventral region to the antero-dorsal region, almost to the hinge, in a single tract approximately 8 cilia wide. The blue shaded area on the diagram indicates the location of the SEM image. This image was obtained by dry fracturing the larva and imaged by SEM.

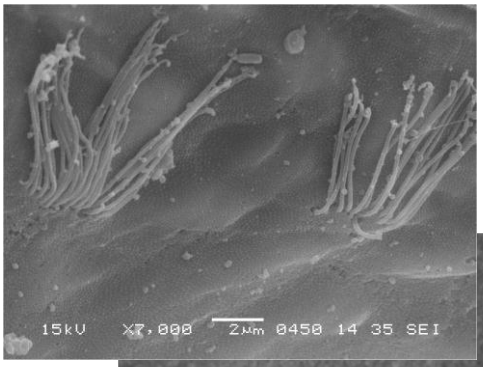

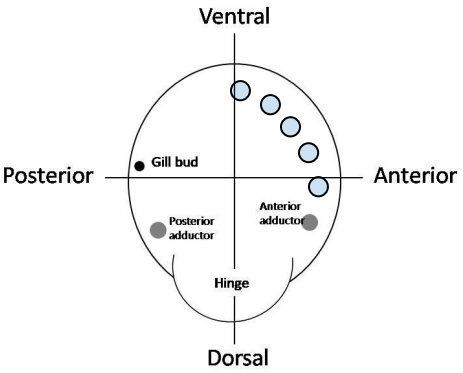

Figure 2.25 - C13 cilia group on the mantle of a late stage *Crassostrea gigas* pediveliger.

C13 ciliation is formed of short, straight lines of 15-30 cilia of approximately 6µm in length, located on the mantle below the C5 cilia tracts. Each 15-30 cilia group lays flat against the mantle surface when fixed, and are around 8µm apart (inset image). The C13 cilia occur from the ventral region, through the anterior (the focus of the above images) to the dorsal region - the inset diagram shows the position of the group with the shaded blue circles. This larva was dry fractured and imaged by SEM.

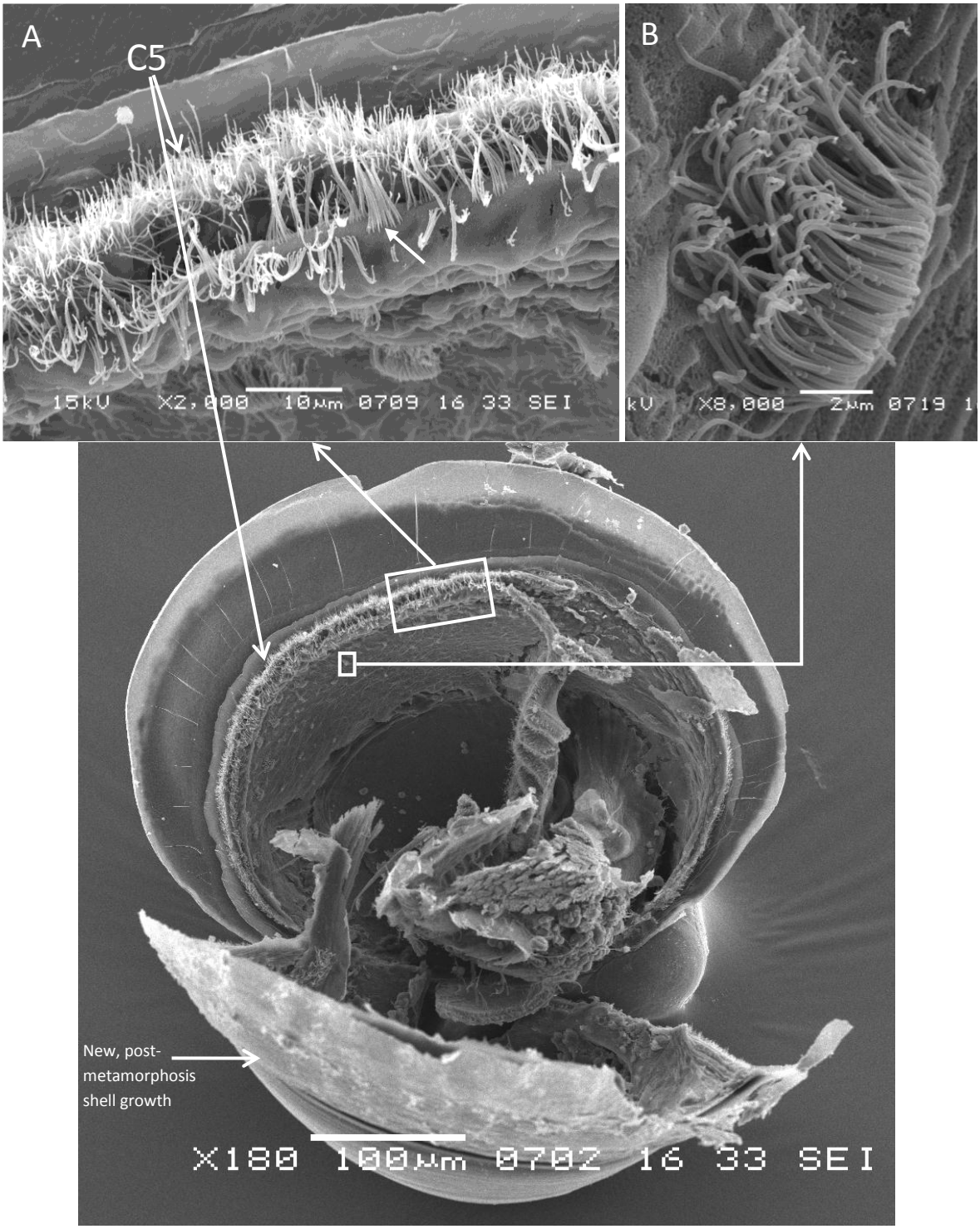

Figure 2.26 - *Crassostrea gigas* spat showing C5 and C13 mantle ciliation.

The spat has lost the larval foot and extensive new shell growth is visible above the mantle margin. The mantle rim is visible and still two tracts of C5 cilia in the ventral region (A). The lower tract is much less well developed than in the late pediveliger, with the cilia forming the row organised into discrete rows of approximately 30 cilia (arrowed in A). The C13 cilia are also present (B), but in higher numbers are composed of more cilia than the pediveliger C13 group. This spat was amongst pediveliger samples and was only a 1-3 hours post-metamorphosis, indicating that the mantle ciliation persists longer than true larval structures such as the velum or larval foot. This larva was imaged with SEM.

Additional cilia groupings of the mantle

Two further groupings of cilia have been identified on the mantle of *Crassostrea gigas* larvae. Figure 2.11 and Figure 2.27 show the group C11 ciliation in the periostracal groove between the inner and outer mantle folds. This ciliation does not become obvious until the late veliger stage larva, although it is present in 90% of veligers where the periostracal groove is visible (although the groove is often not visible in veliger larvae). The ciliation increases in density throughout larval development from veliger to late pediveliger, becoming more visible (95% of pediveliger feature the group, with higher n values - n=35 for veliger stage and n=95 for pediveliger). By the late pediveliger stage larva, group C11 is present throughout the entire periostracal groove from postero-dorsal to antero-dorsal. The cilia are formed into a tract comprised of cilia around 5µm in length that fill the entire width of the groove. The cilia do not appear stiff and are often angled, but not in a consistent direction. The angling of the C11 cilia varies in approximately 10-20µm sections alternating between those angled dorsally, and then the next 10-20µm length angled ventrally, indicating they may have a beat, but not a uniform one.

Group C12 cilia (Figure 2.22) were found on the outer mantle fold of veligers and early pediveligers (only very rarely in later stage larvae, although this was probably due to the more developed C5 cilia obscuring the group - Table 2.2). The group comprises of 2 or 4 cilia (more often 4, the 2 cilia groups were only observed in early veligers or rare individuals) on the outer fold of the mantle which come through the periostracum covering the fold, lay flat on the mantle, and extend over the edge of the outer fold. The cilia of the group are long, with a visible length of up to 15µm - these cilia were long enough to protrude from the shell valves when the larva was partially gaped, but they are likely much longer as the bases could not be seen by SEM due to their location within the periostracal groove.

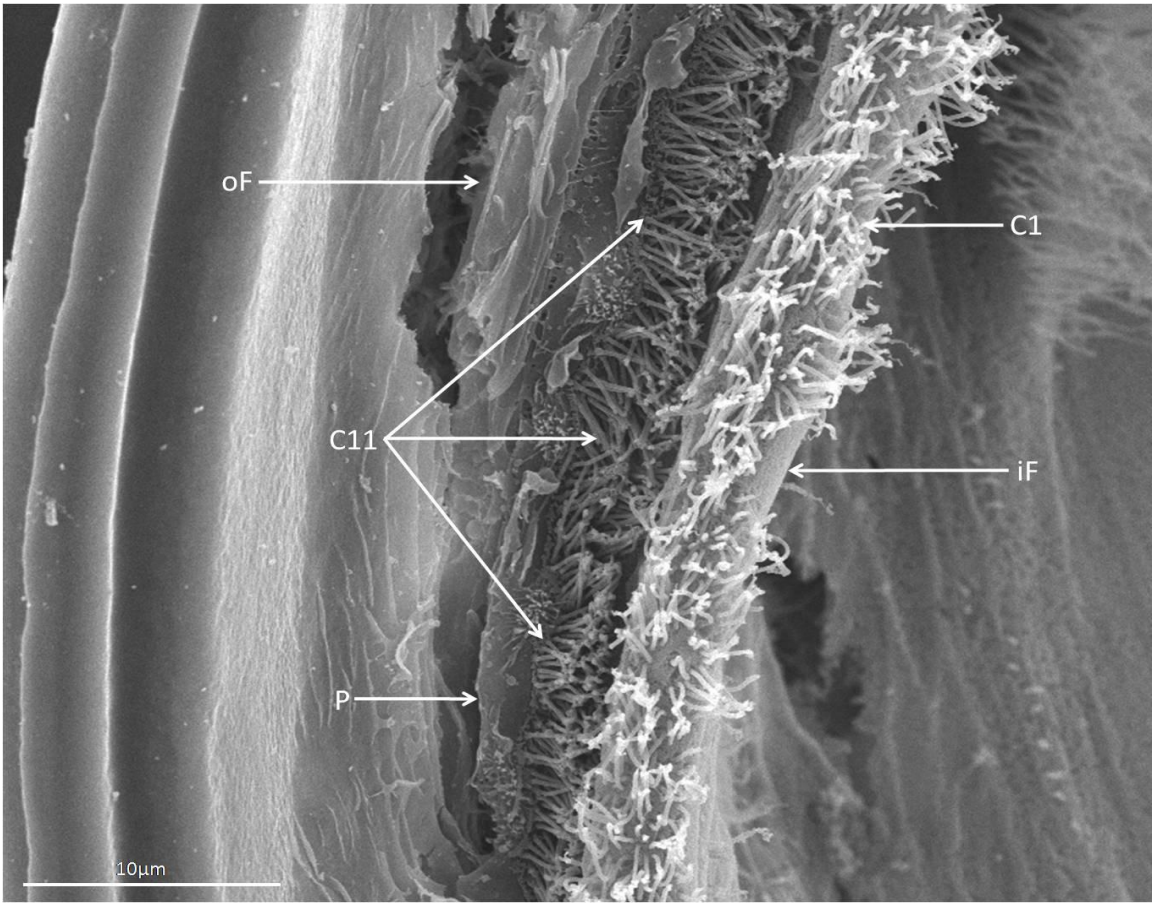

Figure 2.27 - C11 ciliation in the periostracal groove of a late stage *Crassostrea gigas* pediveliger.

C11 ciliation appears in the veliger stage and becomes quite profuse (as in the image above) by the late pediveliger stage. The C11 cilia arise in the periostracal groove between the inner (iF) and outer (oF) folds of the mantle and run from the postero-dorsal all the way around the mantle to the anterior region. These cilia appear to be approximately 5µm in length, comparable with most of the tract-forming cilia found on the larval mantle. In the above image the cilia are in the groove behind the C1 cilia of the posterior-dorsal inner mantle rim, and dorsal of the gill bud. The periostracum (P) can be seen running over the outer mantle fold and the shell on the left. A tear in the periostracum and the mantle allows the outer fold to be glimpsed under the periostracum. The larva has been dry fractured and imaged by SEM.

Fluorescence images of the mantle of Crassostrea gigas

Aldehyde-induced fluorescence of *Crassostrea gigas* larvae has revealed two specific areas of the blue-green fluorescence characteristic of catecholamines (Figure 2.28) in veligers and pediveligers. Dorsal to the larval gill bud and just above the hinge are 2-6 columnar shaped fluorescent cell bodies. The location of this signal can be compared to the locations of either the C1 or C10 groups of cilia, or the group C9 stereocilia (Figure 2.30).

There are also fluorescent columnar cell bodies in the ventral mantle. Up to 10 were observed in this location, localised to cells of the mantle rim (which is clearly discernible in the images shown in Figure 2.28 and in the location of the C5 cilia tracts described previously (Figure 2.30). Strong auto-fluorescence was also detected from the gut and intestine, likely from ingested algal cells. Negative controls fixed with 4% paraformaldehyde without glutaraldehye failed to exhibit any blue-green fluorescence under these conditions.

Serotonin labelling has revealed several fibres running in the mantle rim, or associated with mantle musculature locations in *Crassostrea gigas* pediveligers (Figure 2.29 and Figure 3.15). Figure 2.29 A&D show an immunoreactive fibre running from the area of the posterodorsal notch to the gill bud, and then branching into two directions. One branch travels down the gill bud itself whilst the other continues running along the mantle rim into the ventral region. The immunoreactive fibre is regularly interspersed with immunoreactive cell bodies. These bodies are especially evident as the fibre continues along the mantle ventral to the gill bud in Figure 2.29 B. The fibres run through the location of the C9, C1 and C5 ciliary groups described previously (Figure 2.30). The posterodorsal notch itself also emits a strong signal. The ventral region in Figure 2.29 A-D shows the presence of immunoreactive fibres both high on the mantle in the region of the mantle rim (the location of the C5 group tracts) and lower in the location of the mantle musculature attachments. These two fibres are linked several times by short, multi-branching immunoreactive fibres - Figure 2.29 C & D.

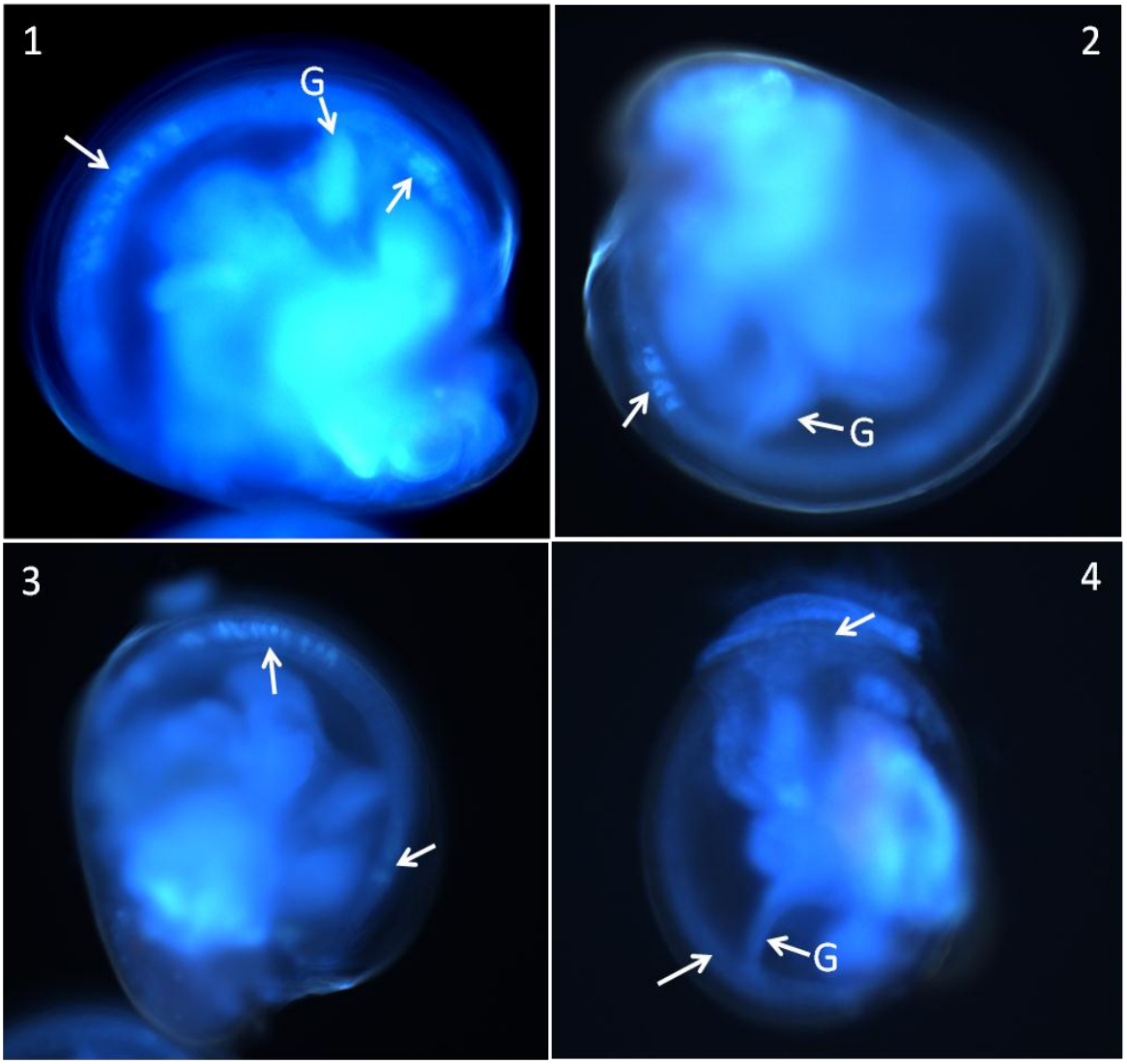

Figure 2.28 - Blue-green catecholamine fluorescence in *Crassostrea gigas* pediveliger larvae.

Areas of catecholamine fluorescence are arrowed, and the gill bud marked to provide some orientation. Columnar catecholamine containing cells appear in the mantle between the gill bud and the hinge. This is the probable location of the C9 cilia grouping identified by SEM. There is a second group of catecholamine containing cells located in the ventral mantle rim - these are all pediveliger stage larvae so this is the location of the C5 twin tract ciliation identified by SEM. Image 4 is a control prepared without glutaraldehyde, and the labelled areas show no cell specific fluorescence in the C9 or C5 locations. These images were captured on a Carl Zeiss LSM 510 confocal laser scanning microscope with AxioCam HRc camera using a 488nm long pass barrier and 355-425 nm excitation.

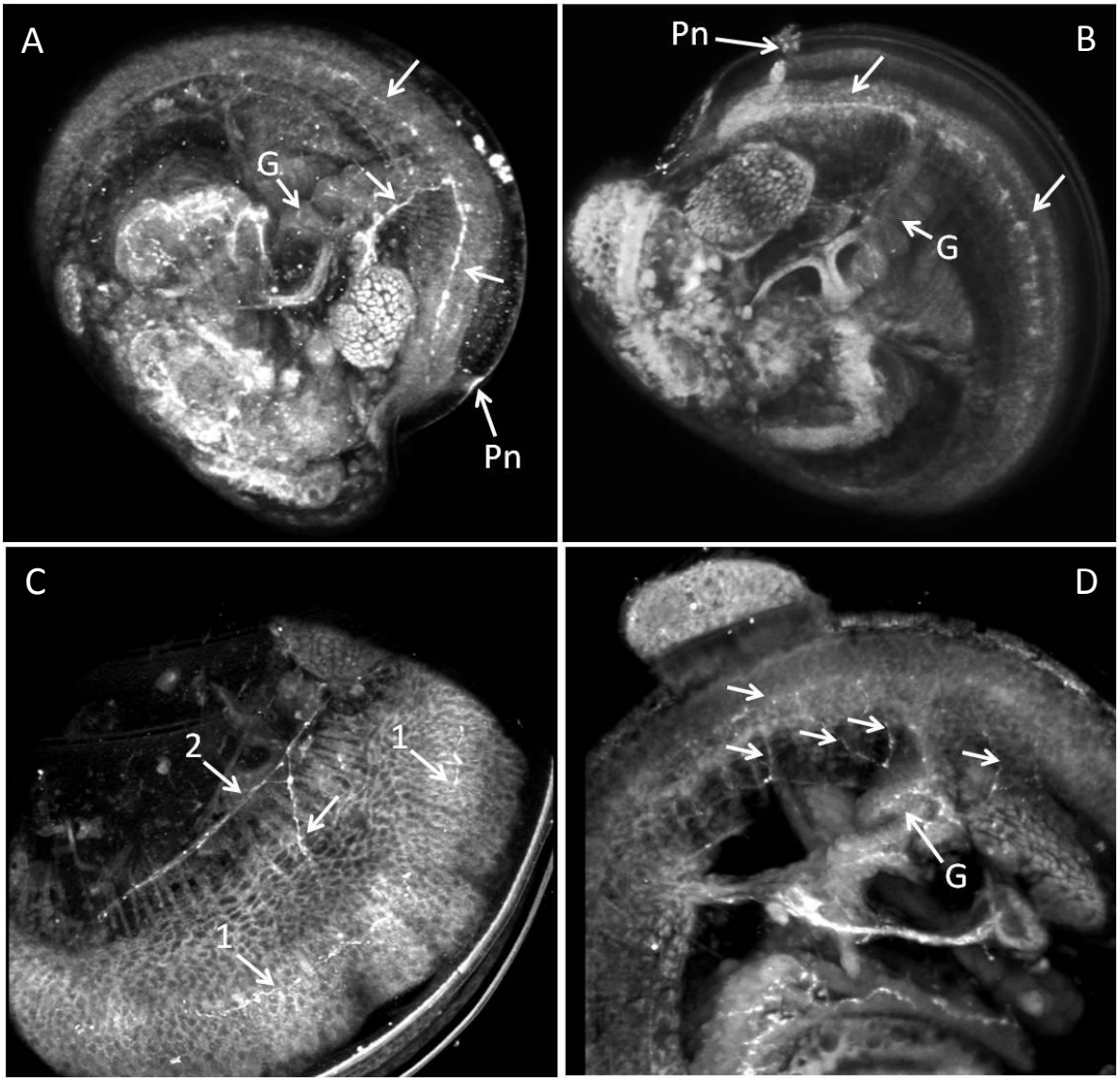

Figure 2.29 - Serotonin fluorescence in *Crassostrea gigas* veligers (A & B) and pediveligers (C & D).

Where visible the gill bud (G) has been marked to provide orientation. Images A and B show serotonin signal from the mantle rim region near the posterodorsal notch (Pn) running up to the gill bud. At the gill the serotonin fibre branches off down the gill bud and along the mantle rim into the ventral region (A & B). Images C and D show the route of the fibre branch that continues into the mantle in the ventral region of the larva. C shows the ventral region only, and signals can be seen near the mantle rim (1) and lower down where the mantle musculature attaches (2). Areas 1 and 2 are linked by another serotonin signal (arrowed). Image D shows a concentration of fibres around the gill bud, foot and adductor, and bears comparison to image C. Note all the fibres arrowed in D appear to link into the region around the gill bud. Specimens were observed in a Carl Zeiss LSM 510 confocal laser scanning microscope using a 488 nm argon laser, emission collected at 530 nm. The images above are comprised of a series of optical sections, projected as a 3 dimensional image using Zeiss LSM Image Browser.

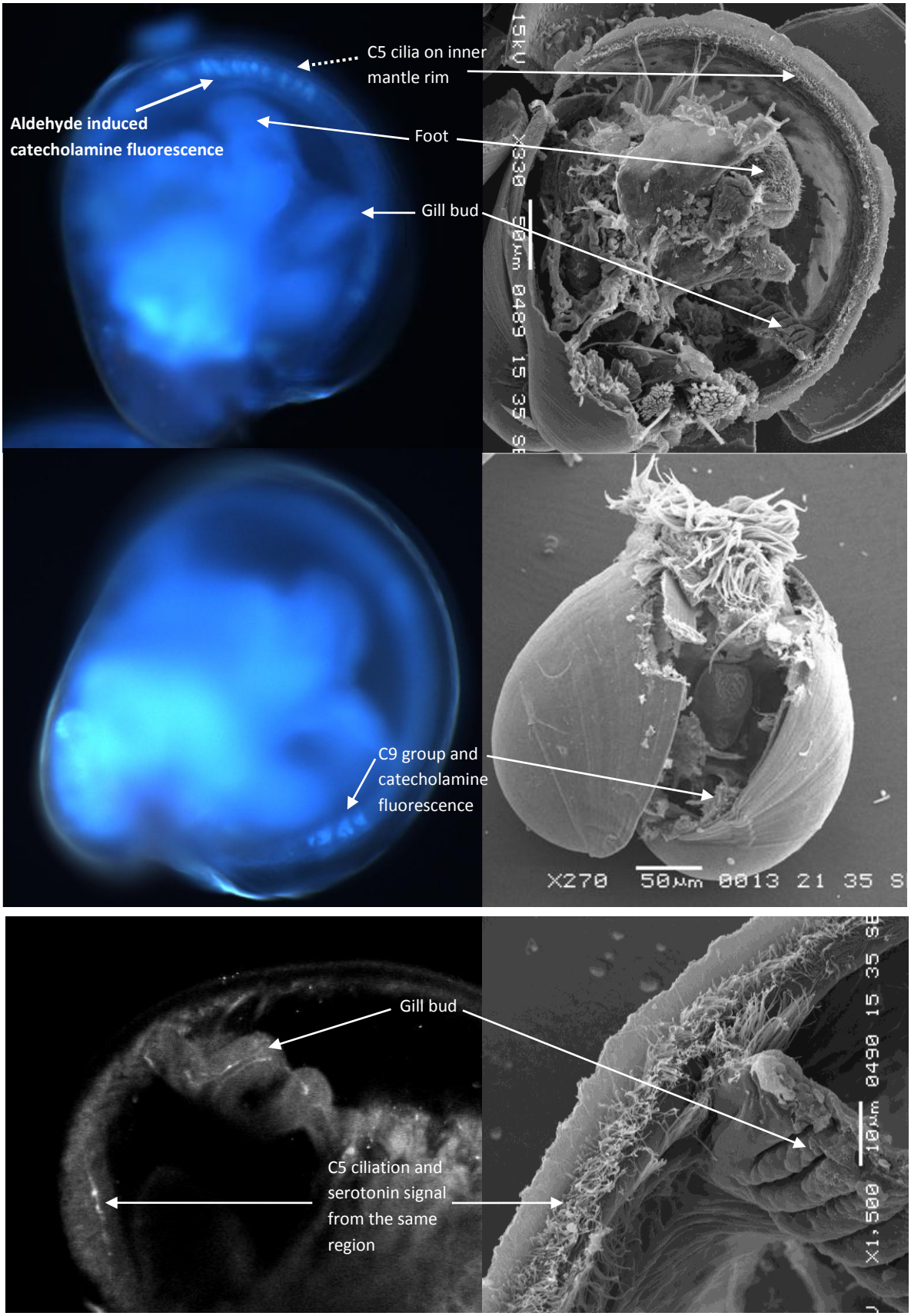

Figure 2.30 - Illustrating the locations of C5 and C9 cilia in comparison to catecholamine and serotonin signal. CLSM images are on the left and SEM images on the right.

The upper 4 images show the C5 and C9 cilia locations in the SEM images, both having catecholamine signal from their locations, although not for the entire length of the C5 tract. The lower image pair shows the serotonin signal from the gill bud and associated C5 cilia tract.

The extremely bright fluorescence from the gut and intestine of the larvae imaged in Figure 2.28 and Figure 2.30 is likely the auto-fluorescence of the algae in the gut: fluorescence from chlorophyll and its derivatives has been observed within the gut of *Crassostrea virginica* larvae (Babinchak & Ukeles, 1979), and illustrates that the larvae sampled from cultures were healthy, feeding larvae. Larvae could be starved prior to image collection, but this may lead to moribund larvae being imaged.

2.3.2 *Ostrea edulis*

The larvae of *Ostrea edulis* have most of the same mantle cilia groups as those of *Crassostrea gigas*, with cilia groups appearing at the veliger stage and becoming fully developed by the late pediveliger (Figure 2.31).

Figure 2.31 shows the dense ciliation present along the mantle rim of an *Ostrea edulis* pediveliger. Various cilia groups first appear in the early veliger around the larval gill bud, as shown in Figure 2.32 and Figure 2.33. Group C1 ciliation spreads from the dorsal region of the inner mantle fold rim by the hinge to the gill bud in the antero-dorsal. At the join of the gill bud to the inner mantle fold rim the C1 tract spreads around the mantle rim past the gill bud to become the top tract of the group C5 ciliation (Figure 2.32). Figure 2.33 shows group C3 and C4 cilia on the mantle at the base of the gill bud (C4) and on the mantle below the C1 tract and above the C4 group (C3).

Group C5 ciliation spreads ventrally along the inner mantle fold rim from its join with the gill bud, forming distinct twin tracts of cilia. In the veliger stage larvae this tract was followed by a section of group C5a ciliation in the ventral or anterior region, leading into the C6 or C10 ciliation. The pediveliger stage had no group C5a cilia. The C5 tracts are particularly dense in the pediveliger, running through the entire ventral region and terminating rather abruptly at the anterior adductor, as can be seen near the C10 label in Figure 2.31. From this point the single tract group C10 ciliation spreads dorsally down the remainder of the mantle rim to the hinge.

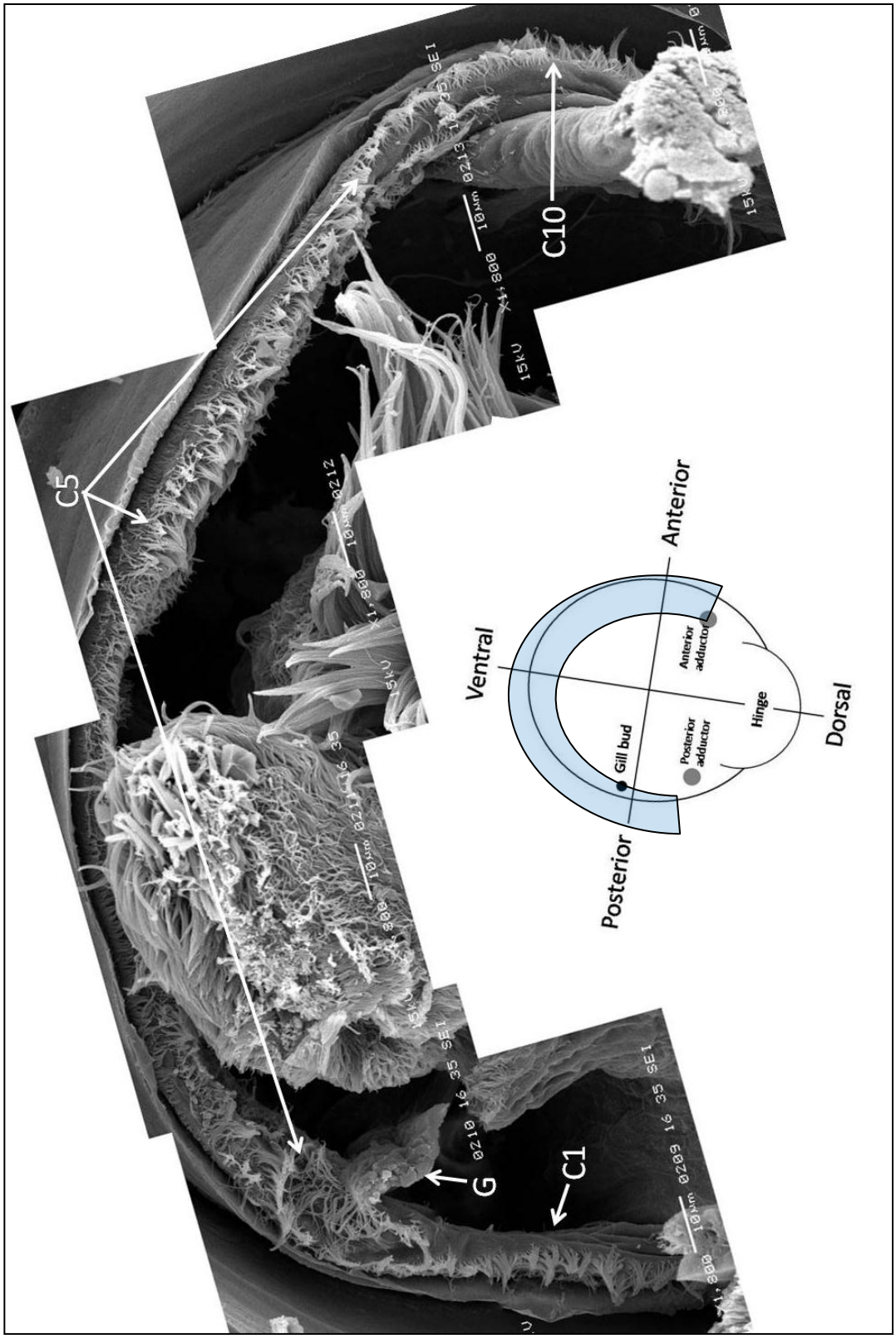

Figure 2.31 - Distribution of cilia on the mantle rim of an *Ostrea edulis* pediveliger.

This late-stage pediveliger shows profuse ciliation on the inner mantle fold rim, appearing to feature the same cilia groups as found in *C.gigas*. C1 cilia form a very dense single tract from the postero-dorsal region to the gill bud (G). Twin tract of C5 ciliation spread from the gill bud to the anterior adductor muscle. There is no C5a or C6 ciliation. A single tract of C10 ciliation occurs from the anterior adductor to the hinge region. The inset diagram shows the area of the larvae shown by the SEM images (shaded blue). This larva was dry fractured and imaged by SEM

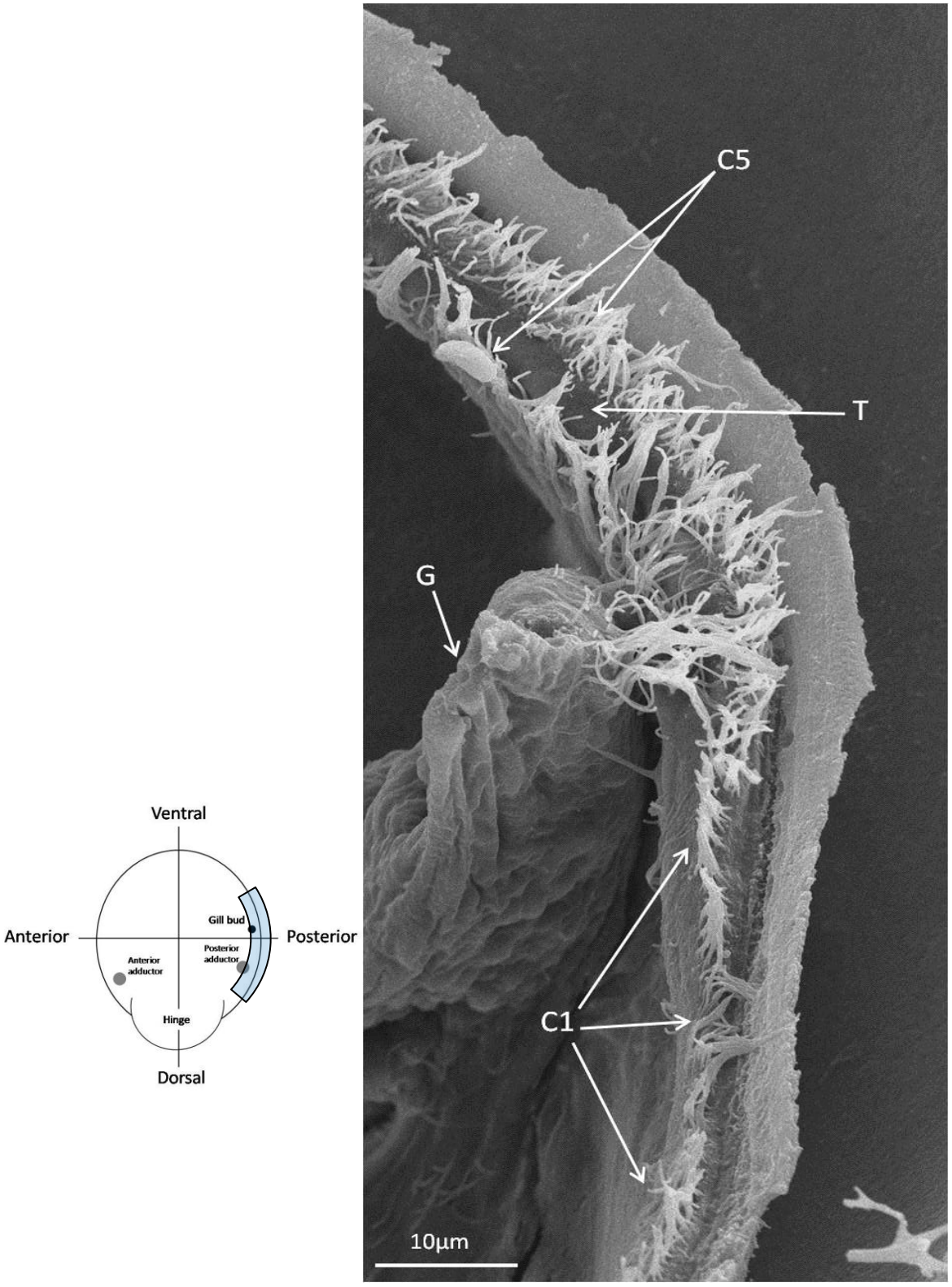

Figure 2.32 - C1 and C5 ciliation at the gill bud of an *Ostrea edulis* pediveliger larva.

The C1 cilia spread past the gill bud and eventually appear to form the upper tract of the C5 ciliation. As the cilia merge with the C5 tracts they increase in length and are arranged into the characteristic small clumps of 5-10 cilia that arrange to form the C5 tracts. The image above shows the change to twin tract is quite abrupt, occurring at the junction of the inner mantle fold rim and the gill bud (G). The diagram on the left provides orientation, the blue shaded region the area shown by the image. This larva was dry fractured and imaged by SEM.

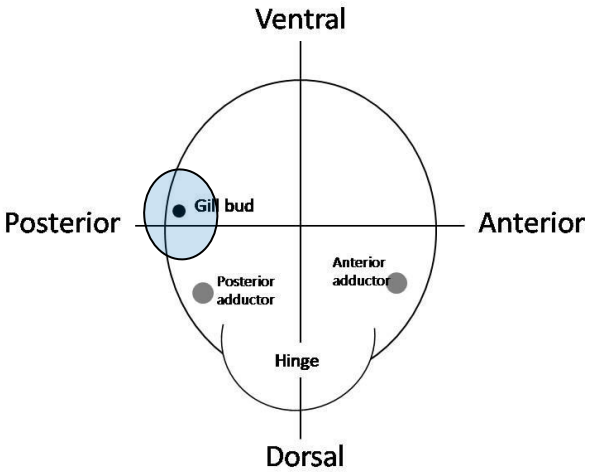

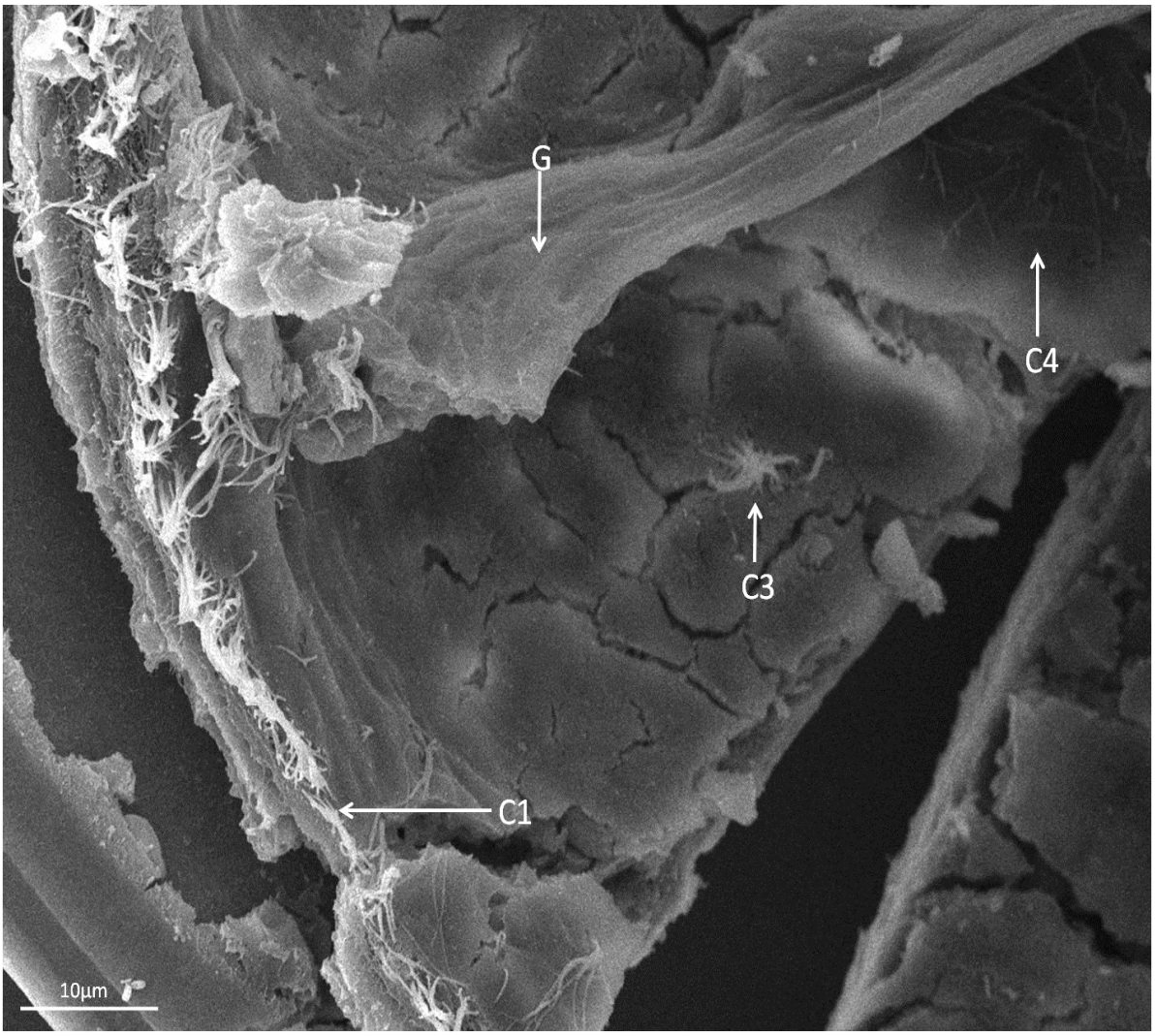

Figure 2.33 - The gill bud region of a mid-stage *Ostrea edulis* veliger.

The C3 cilia group and C4 cilia group can be seen below the gill bud (G) on the mantle in the same locations as these groups were found in *Crassostrea gigas*. The C3 group appears stiff after fixation and the C4 group is 'scattered' with no close clumping arrangement. In appearance both groups appear the same as those seen in *Crassostrea*. The location shown in this image is shaded blue in the diagram. The larva was dry fractured and imaged by SEM.

Cilia of the postero-dorsal region

The inner mantle fold rim in the postero-dorsal region, from the hinge to the gill bud, has 2 ciliary groups, C1 and C9 (in addition to the C3 and C4 groups on the mantle near the gill bud). Group C1 cilia, shown in Figure 2.33 in a veliger stage larvae and Figure 2.34 in a pediveliger stage larva, runs along the rim of the inner mantle fold, forming a single tract from the hinge to the gill bud. The tract is comprised of small, loosely arranged clumps of approximately 10 cilia, with the cilia varying from 5µm to 8µm in length. The cilia are not stiff in appearance and are not angled in any direction suggesting a beat direction. Over 90% of individuals observed had a C1 group.

The second group of cilia in this location is situated on a protuberance of mantle tissue next to the posterior adductor muscle. This piece of tissue forms a bridge between the left and right valves, shown in Figure 2.35, and bears a cluster of group C9 ciliation immediately dorsal of the anal tuft. These cilia have a ring of 9 microvilli at the base and are between 10-15µm in length. Figure 2.35B shows the group is located under the posterodorsal notch and that they are long enough to protrude from between the shell valves, through the notch, when the shell valves are closed (Figure 2.36). They show no curvature suggesting a beat direction, and are not stiff. 100% of individuals with this region observable had a C9 grouping.

Cilia groupings of the posterior to anterior axis (ventral region)

From the mid-late veliger stage through to late pediveliger this region is dominated by the twin tracts of group C5 cilia shown in Figure 2.37. One tract runs along the inner mantle fold rim, the second approximately 5µm below on the mantle, with a distinct (occasionally infolded) furrow between the two. The cilia of the tracts are similar in length, all being around 8-10µm long - those of the latest stage pediveliger are all at least 10µm long. The tracts are formed of small round clumps of approximately 10 cilia, emerging through the microvillous epithelium. From late veliger to the pre-metamorphosis pediveliger, C5 tracts were observed beating and especially in resting larvae with the valves partially gaped. Some individuals had particles in the tracts. By the pediveliger stage group C5 tracts run from the gill bud to the anterior adductor. The tracts of the late pediveliger were particularly densely ciliated. Veliger larvae had the group C5a ciliation seen in *Crassostrea gigas* larvae. 96.9% of veligers and 100% of pediveligers had a C5 tract.

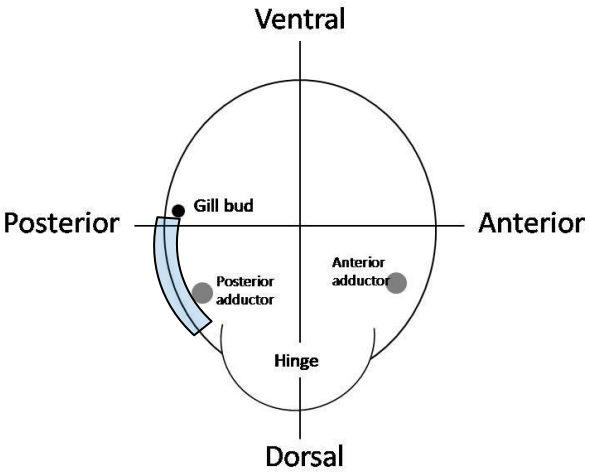

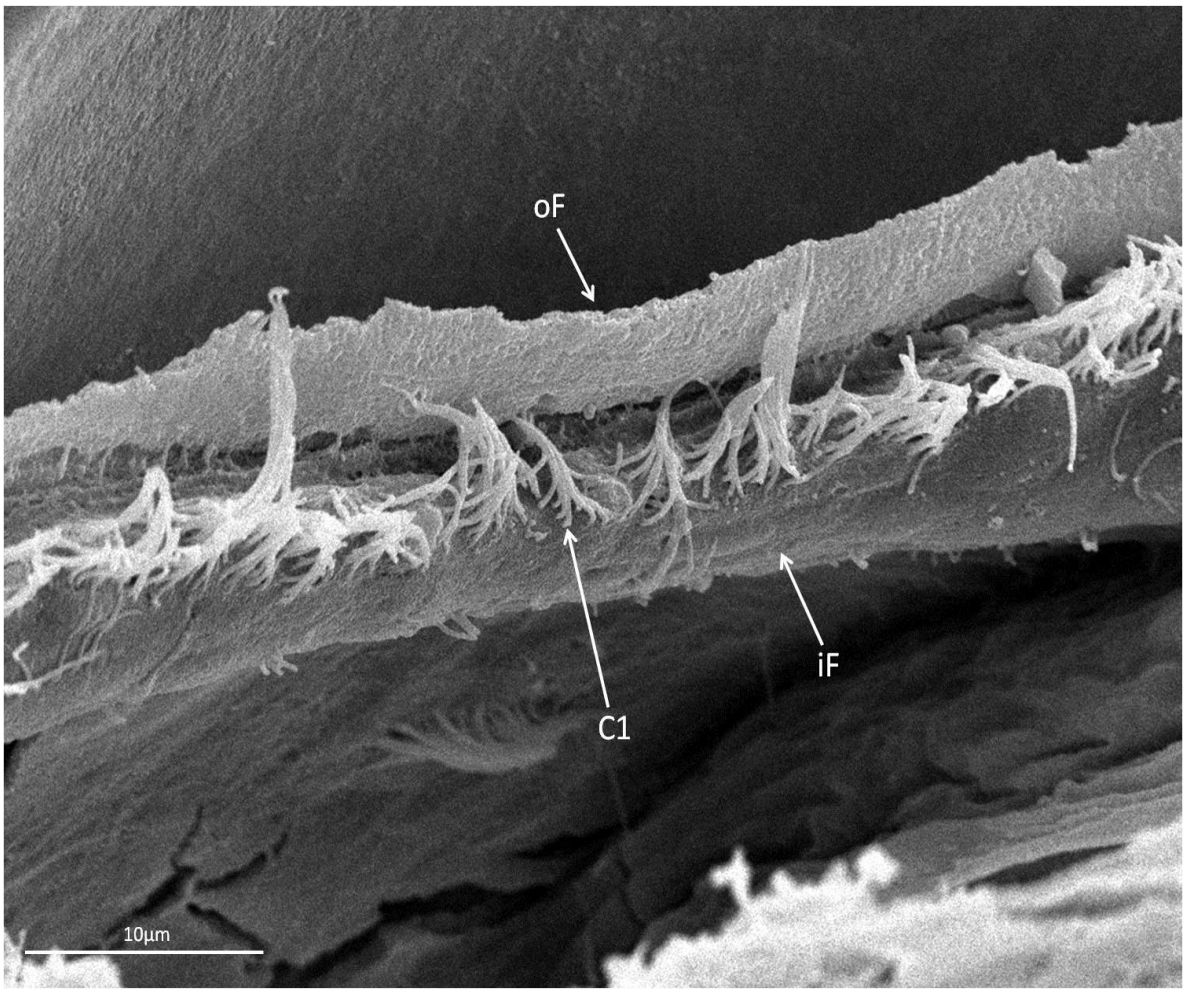

Figure 2.34 - C1 ciliation on the postero-dorsal inner mantle rim of a mid-stage *Ostrea edulis* pediveliger.

The C1 cilia can be seen forming a single tract of cilia on the rim of the inner mantle fold (iF). This tract occurs from the hinge to the gill bud - the location of this group in the larva is shaded blue in the diagram above. The C1 cilia are approximately 8µm in length and emerge through the microvillus epithelium as loose clumps. It is these clumps which can be seen forming the single tract on the inner mantle fold rim. This larva was dry fractured and imaged by SEM.

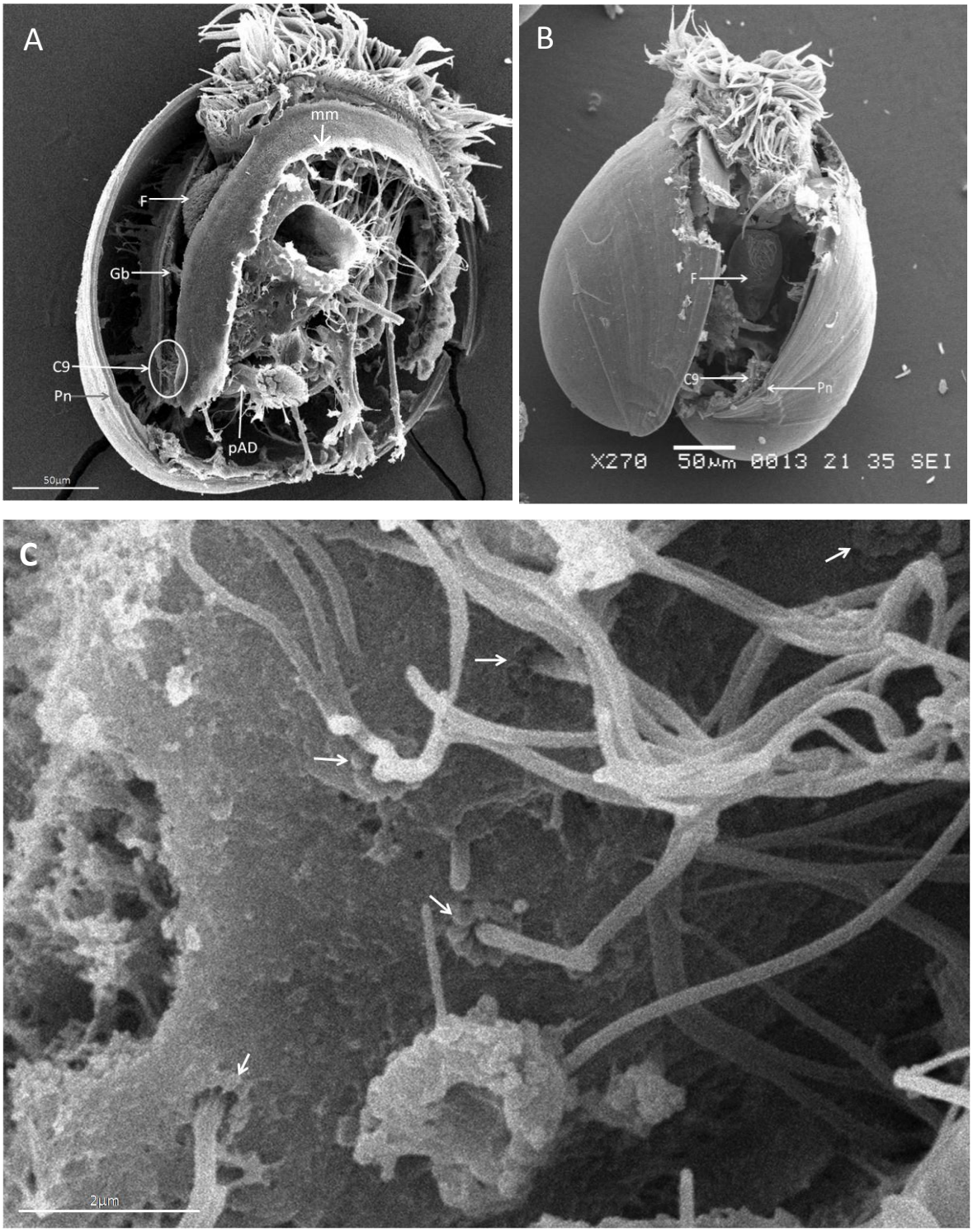

Figure 2.35 - The C9 cilia group on the mantle of an early stage *Ostrea edulis* pediveliger.

The C9 group is next to the posterior adductor (pAD in A) on an extrusion of mantle tissue below the anal tuft and in direct association with the posterodorsal notch in the shell, as shown in image B. Each unit of the group is comprised of one long cilium of around 10-15µm in length with a ring of 9 microvilli around the base (arrowed in C). These specialised cilia appear in no obvious pattern and all are located dorsally of the anal tuft, and directly under the posterodorsal notch (Pn). Note that the mantle musculature (mm) is visible, torn away from the shell in image A. The larva of image A was dry fractured, larva B was intact but with the shell partially gaped. Both were imaged by SEM.

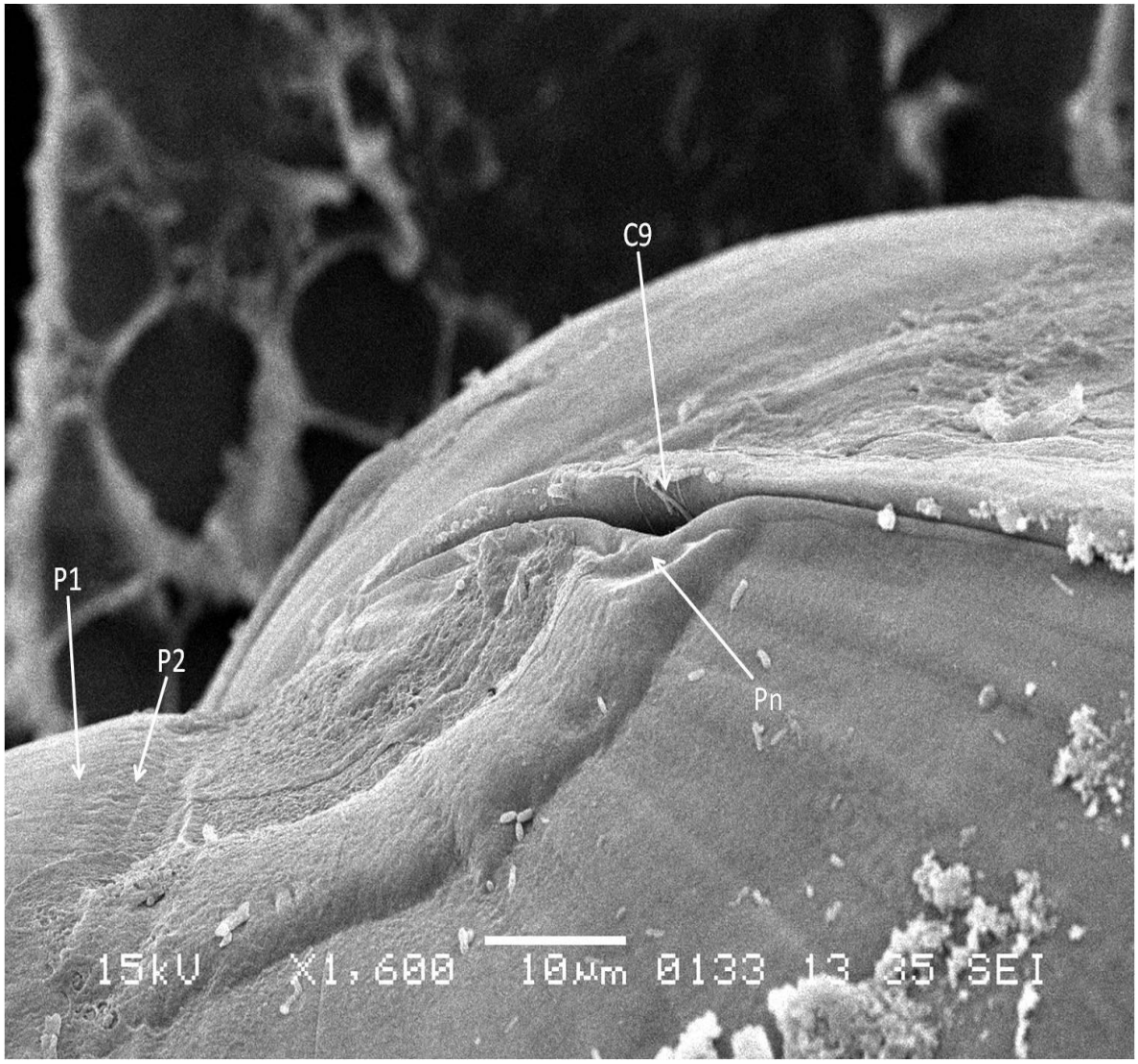

Figure 2.36 - Group C9 cilia and the posterodorsal notch on a mid-stage *Ostrea edulis* pediveliger.

The posterodorsal notch (Pn) of this *Ostrea edulis* pediveliger begins at the prodissoconch one and prodissoconch two boundaries (P1 and P2), creating a slight gap in the shell when it is closed. The size of this gap varied between individuals; this individual had a notch gap with shell closed of approximately 1µm but some individuals had gaps of up to 3µm. The top of the C9 cilia can just be seen protruding from the gap, stuck to the shell valve (probably as a result of sample preparation treatments). This intact larva was imaged using SEM.

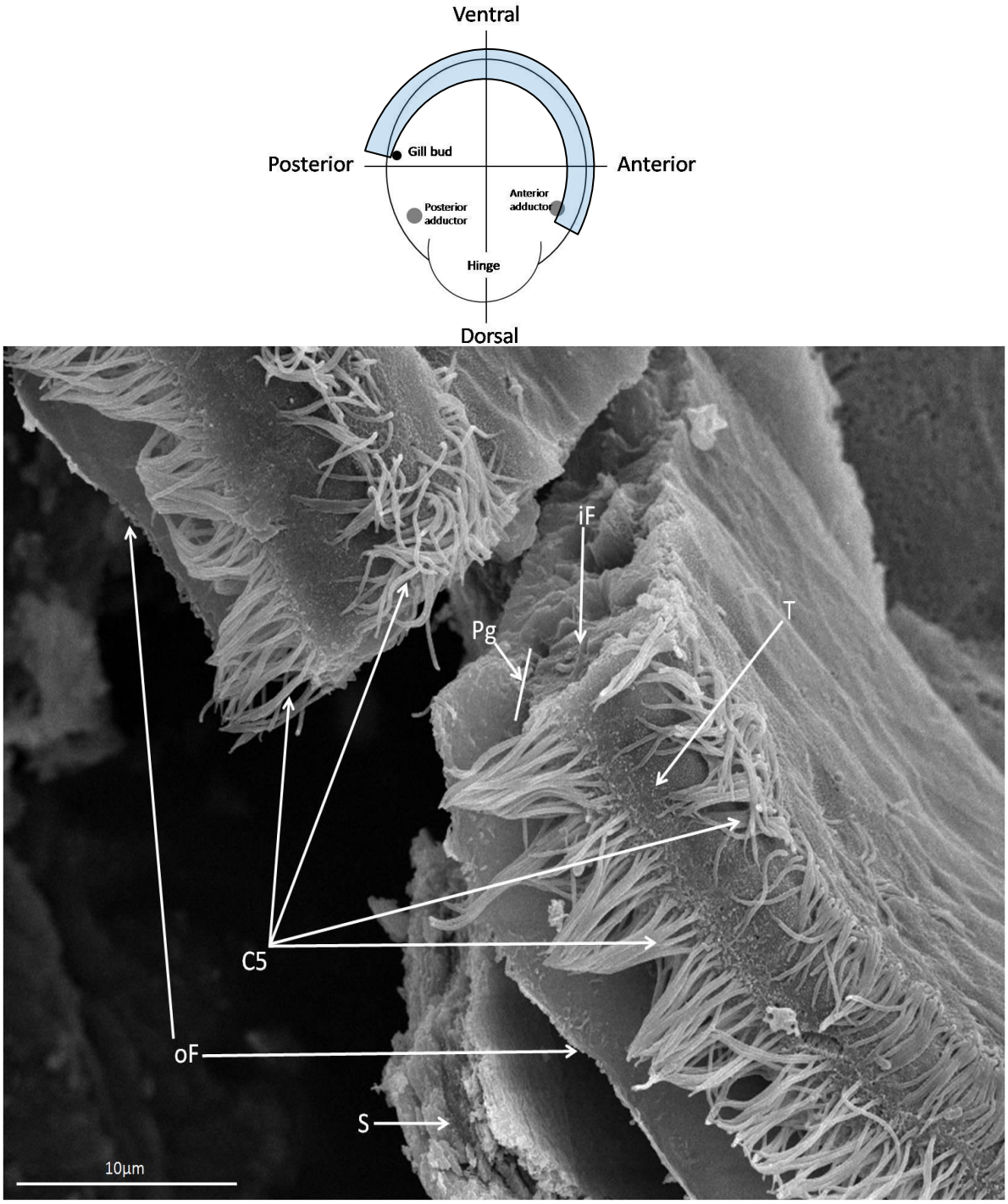

Figure 2.37 - C5 ciliation on an *Ostrea edulis* pediveliger.

The upper of the two C5 ciliation tracts can be seen running along the rim of the inner mantle fold. The second tract is also on the inner mantle fold about 5µm below the first, with a distinct tract (T) containing only microvilli running in-between. The arrangement of the cilia comprising the C5 tracts into small clumps is visible, showing the tracts to be made up of a series of small cilia units arranged closely together. Also visible are the mantle folds, with the outer fold of the mantle (oF) lying just apart from the shell (S) and the periostracal groove (Pg) visible between the inner and outer mantle folds. The region of the pediveliger stage larva featuring C5 cilia tracts is shaded blue on the diagram above. This larva was dry fractured and imaged by SEM.

The C5a ciliation shown in Figure 2.38 is an area in the ventral or antero-ventral and moves more antero-ventral as the larva develops from veliger to early pediveliger and the C5 tracts expand along the mantle rim. Group C5a ciliation has a tract on the inner mantle fold rim organised as described above for the C5 cilia group and a sparsely ciliated tract on the mantle below. The lower tract does not yet have cilia arranged in clumps, and the cilia comprising it vary widely in length from <1µm to 8µm. C5a ciliation was observed in on 33% of *Ostrea edulis* pediveligers, but was present in 92% of veligers.

Cilia groupings in the antero-dorsal region

The antero-dorsal region has a single line of cilia on the inner mantle fold rim. The group C5 cilia twin tracts of the pediveliger stop abruptly at the anterior adductor, as can be seen in Figure 2.31 and Figure 2.39, giving way to the single tract C10 ciliation that runs along the inner mantle fold rim dorsally to the hinge. In veliger larvae the group C10 cilia occur after the C5a cilia. The C10 group is similar to the C1 group, being a single tract of cilia comprised of small round cilia clumps of about 8µm in length arranged into a row. C10 cilia were observed in 66% of veliger stage larvae and 92% of pediveligers.

Additional cilia groupings from the mantle

There are two more cilia groups found on the larval mantle of *Ostrea edulis*. Group C11 ciliation (Figure 2.40) is found in the periostracal groove around the entire length of the mantle. By the late pediveliger, C11 cilia form a very densely ciliated tract within the periostracal groove.

C12 cilia (Figure 2.39) occur sporadically along the mantle, and appear less common as the larva develops, although this is probably due to the group C5 cilia obscuring the C12 cilia (Table 2.3 and Table 2.4). The C12 cilia are comprised of 1-4 long cilia arising from within the periostracal groove and extending over the edge of the outer mantle fold, as the single cilia is in Figure 2.39. The C12 cilia have a visible length of around 10µm, but are likely longer as the bases are somewhere within the periostracal groove and hidden by C11 ciliation or by the angle of the periostracal groove (Figure 2.39 is a good example of the difficulty of imaging an entire C12 group cilia).

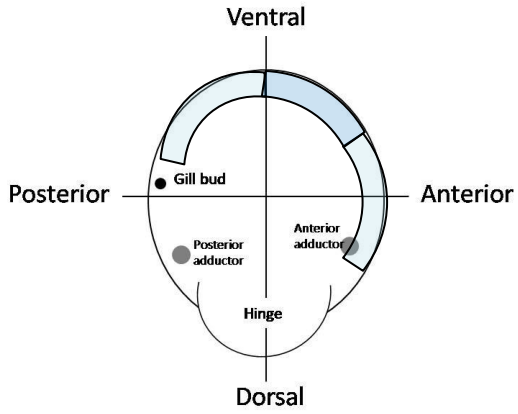

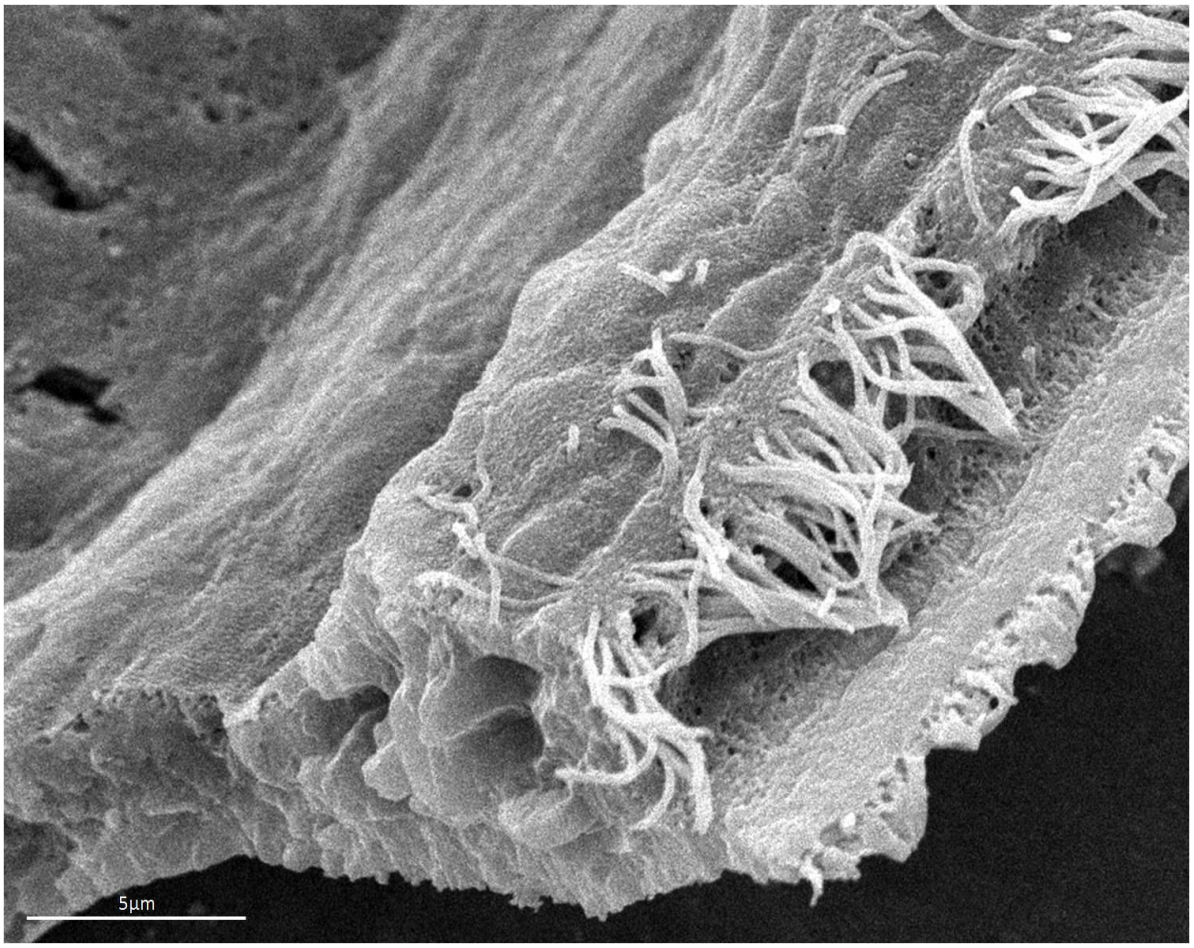

Figure 2.38 - C5a ciliation on the anterior mantle rim of a late stage *Ostrea edulis* veliger.

The tract of C5a ciliation shown above forms a transition region where the C5 twin tracts have not fully developed. The C5a comprise a fully formed single tract on the inner mantle fold rim and a scattered tract below it. The cilia of the lower tract show variation in length from less than 1µm to 8µm and are arranged less densely than those at the rim. The diagram at the top gives the location of this group in this particular *Ostrea edulis* veliger in the darker blue shading, and the lighter blue regions represent the potential locations for this group, depending on development stage. This larva was dry fractured and imaged by SEM.

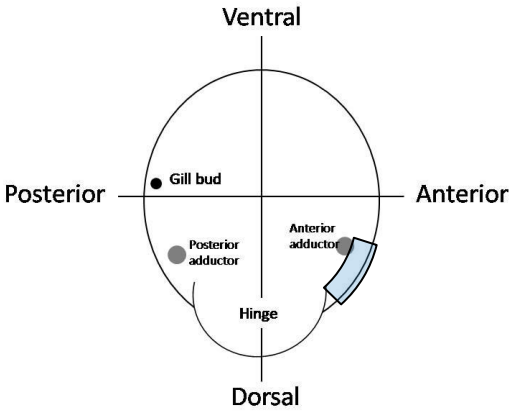

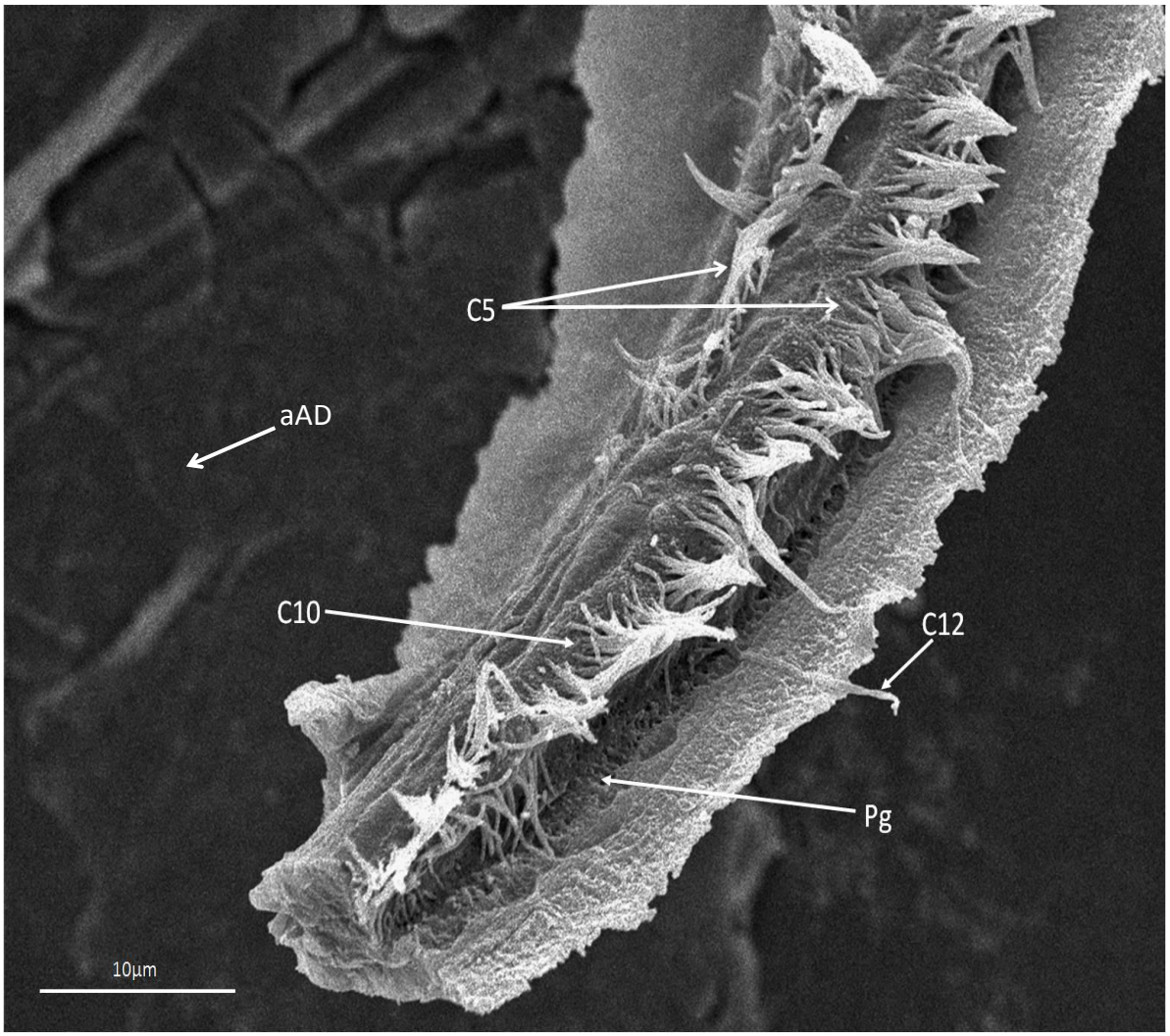

Figure 2.39 - C10 ciliation of an early stage *Ostrea edulis* pediveliger.

The twin tract arrangement of the C5 ciliation at the top of the image stops abruptly, with the upper tract becoming the single tract of group C10 ciliation that continues dorsally to the hinge. There is no region of C5a ciliation as found in earlier veliger stage larvae. Some pediveliger larvae did feature C5a ciliation (33%), but only in the earlier stages. The cilia form a single tract from a series of small round clumps of cilia arranged closely together along the rim of the inner fold of the mantle. The cilia of these clumps were all approximately 8µm in length. C10 ciliation arises next to the anterior adductor and stops at the end of the mantle near the hinge, shown by the blue shaded area of the diagram above. The scar of the anterior adductor is just visible in the image above, and has been labelled (aAD). The larva was dry fractured and imaged with SEM.

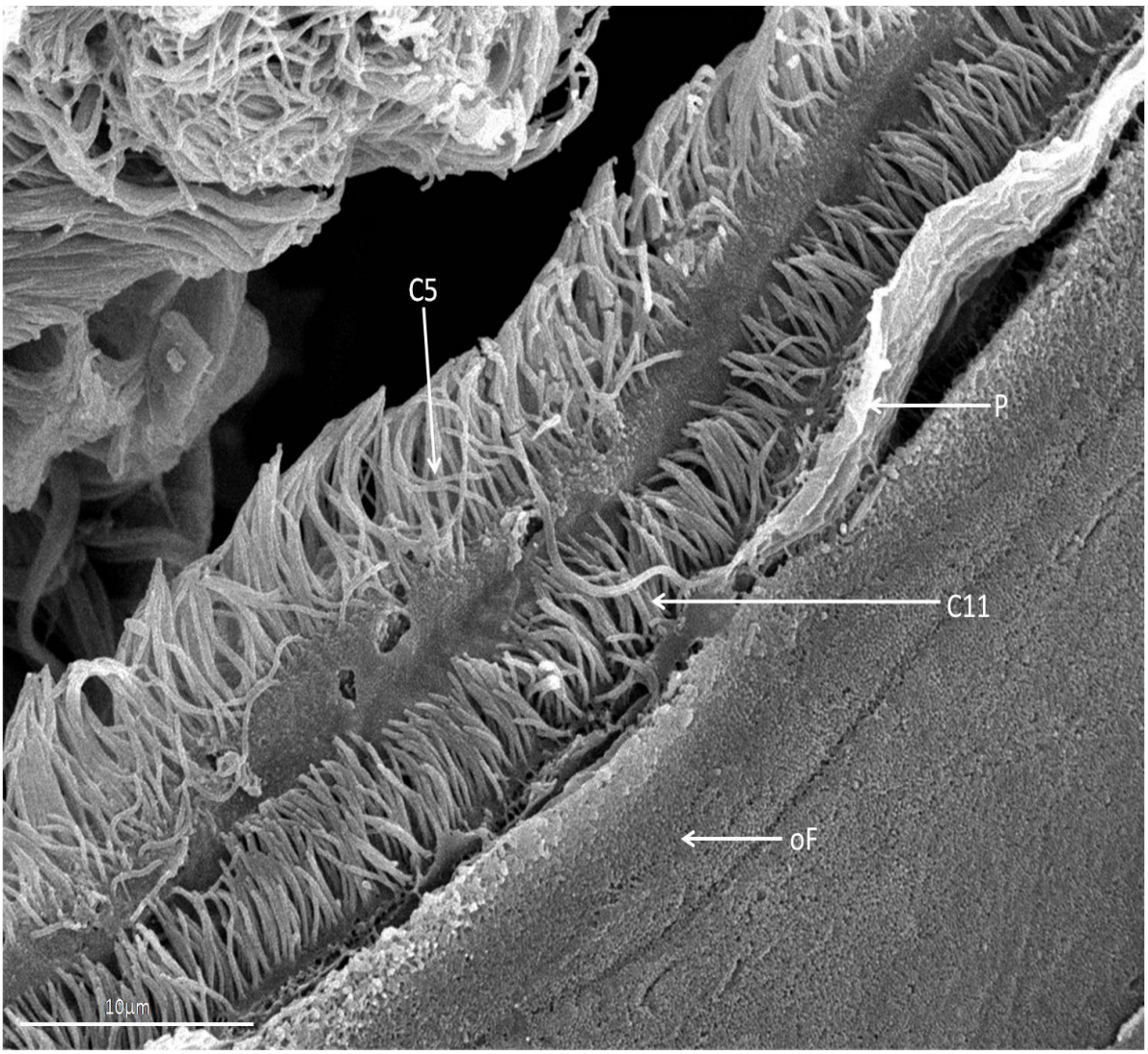

Figure 2.40 - group C11 cilia in the periostracal groove of a late stage *Ostrea edulis* pediveliger.

C11 cilia occur in the periostracal groove in all regions (postero-dorsal to antero-dorsal) of the pediveliger stage larva. In this late-stage pediveliger, C11 cilia are forming a dense tract of cilia between the inner and outer mantle folds in the periostracal groove. The periostracum (P) can be seen coming away slightly from the outer fold (oF) in the top right of the image, with the upper tract of C5 cilia visible on the inner fold rim. This larva was dry fractured and imaged by SEM.

2.3.3 Lyrodus pedicellatus

Lyrodus pedicellatus pediveligers were examined for mantle ciliation. Some pediveligers were extracted from brooding adults whilst pediveligers were captured after release from the adults. There was little/no difference in the size or development stage of these larvae.

SEM has revealed 2 cilia groupings on the mantle of *Lyrodus pedicellatus* pediveliger larvae. One group (L1) appears as discrete groups of cilia on the inner mantle fold rim (visible on 100% of larvae where this region of the mantle was visible), appearing near the hinge and occurring at intervals around the mantle rim towards the ventral region. Group L2 cilia appear on 75% of larvae, forming a line of cilia below the rim on the mantle emerging from a structure just ventral of the hinge and terminating in the antero-ventral region below the L1 cilia on the rim.

Group L1 cilia

The L1 cilia are found on the mantle rim from the dorsal region closest to the hinge where the mantle of the two valves fuses, as can be seen in Figure 2.42, to the ventral region, arising in small clumps from within hollows in the mantle epithelium. The clumps of L1 are more widely separated in the ventral regions. The clumps can comprise of up to 30 cilia, each group separated by around 10µm and comprised of cilia approximately 5µm in length. In the posterior and postero-dorsal region, especially near the anus, the L1 cilia are occasionally associated with a single cilium that has a ring of 9 microvilli at its base - see Figure 2.41 for detail. The L1 cilia in the ventral region are located slightly onto the back of the inner mantle fold rim, nearly into the periostracal groove as can be seen by their appearance in Figure 2.43. Consequently the ventral L1 groups are more on the shell-side of the inner mantle fold than the L1 groups found in more dorsal regions of the mantle. The L1 cilia are not stiff and are not regularly angled in one direction to suggest a beat.

Figure 2.41 - L1 cilia group on the dorsal mantle of a *Lyrodus pedicellatus* pediveliger.

The L1 group is a round group of approximately 30 cilia arising on the mantle rim. They do not appear stiff, or to have a consistent angle suggesting a beat. The group often features an associated cilium with a ring of 9 microvilli at the base, as arrowed in the image above. This is removed slightly from the main group of cilia. These cilia have only been observed in association with those L1 cilia found in the postero-dorsal to posterior regions of the mantle rim. The larva was imaged by FEG-SEM whilst partially gaped.

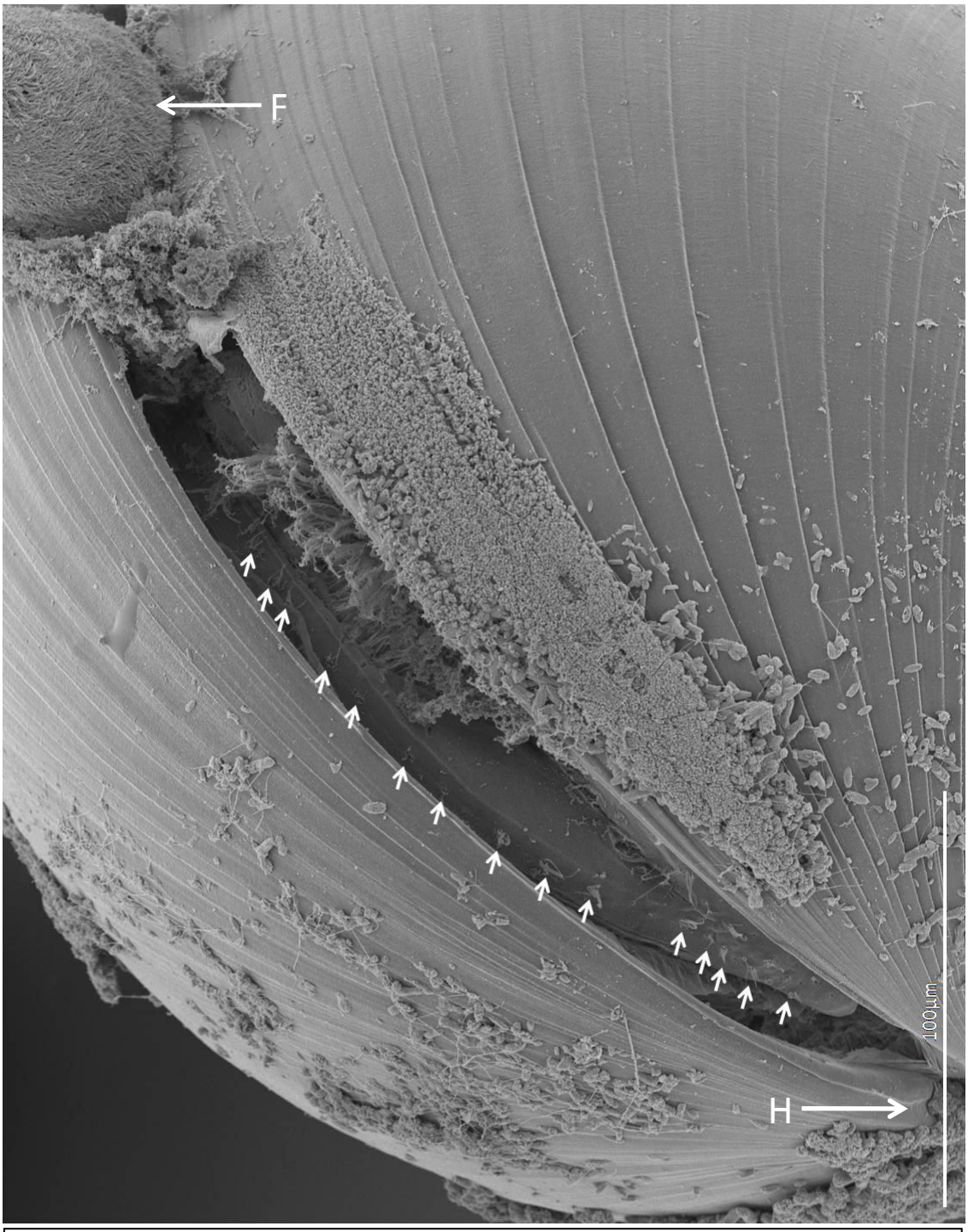

Figure 2.42 - Distribution of L1 cilia on the postero-dorsal and dorsal mantle rim.

Lyrodus pedicellatus pediveliger with L1 cilia groups occurring on the mantle of both valves from the hinge (H) region through to the posterior region where the foot (F) can be seen exiting the valves. This larva was imaged by FEG-SEM whilst intact and with the shell partially gaped open.

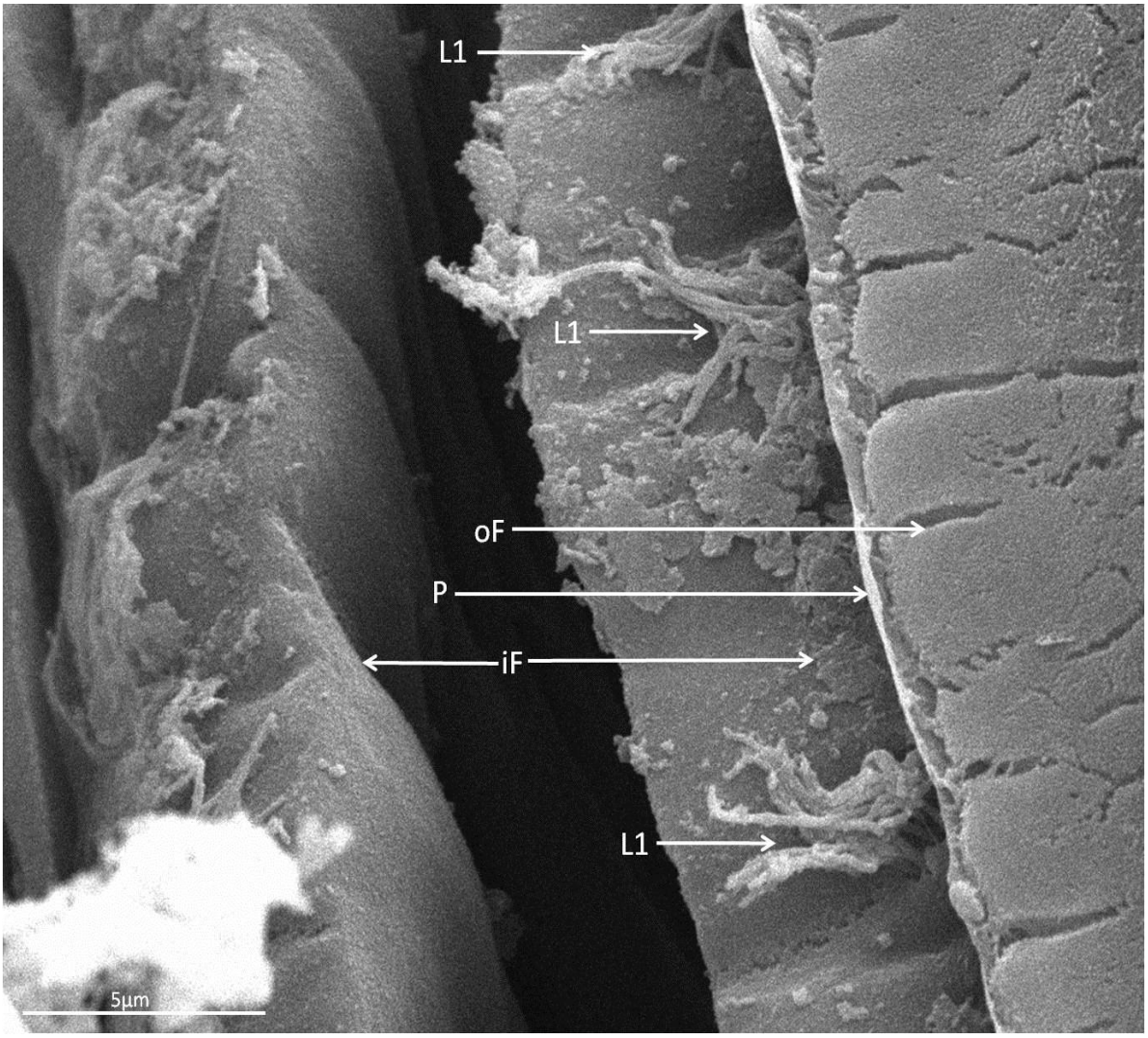

Figure 2.43 - L1 cilia in the ventral region of a *Lyrodus pedicellatus* pediveliger.

The L1 cilia can be seen arising on the rim of the inner mantle fold (iF), appearing as discrete groupings on the shell-side of the rim, just within the periostracal groove. The larva was imaged by FEG-SEM whilst partially gaped.

L2 ciliation

The single line of group L2 ciliation was found in all individuals where this region of the mantle was visible. The group L2 cilia form a single tract of cilia running from a ciliated structure near the base of the gill bud, possibly the opening of a static duct (marked with a '?' in Figure 2.44), along the mantle before curving up towards the mantle rim in the ventral region (Figure 2.44).

The cilia line stops below the mantle rim. The L2 cilia are long, approximately 15µm in length, and are not stiff in appearance. The tract itself varies between 70µm and 120µm in length, and was often seen laying almost flat on the surface, directed roughly towards the mantle fold rim, as in Figure 2.44.

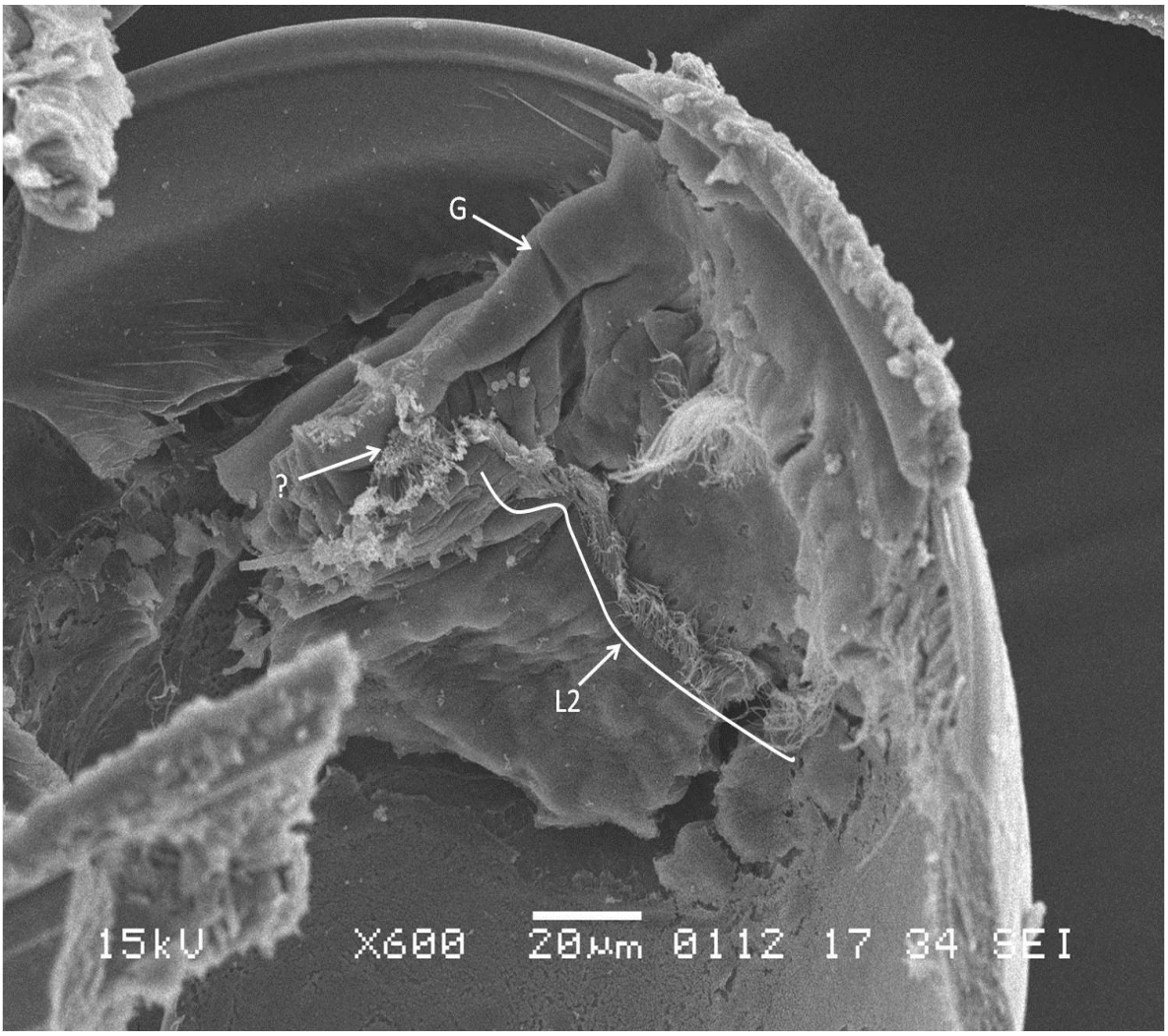

Figure 2.44 - L2 cilia group on the mantle of a *Lyrodus pedicellatus* pediveliger.

The tract of L2 cilia in the postero-ventral region runs from a ciliated structure (? on above image - possibly the opening to a static duct) at the base of the gill bud (G) ventrally along the mantle, before curving up towards the mantle rim. The tract does not appear to reach the mantle rim. The cilia are not stiff and are all angled towards the mantle rim, laying almost flat on the mantle surface, directed towards the mantle rim. This larva was dry fractured and imaged with SEM.

Summary of Lyrodus *mantle ciliation*

Figure 2.45 summarises the locations of the mantle cilia groups found on the mantle rim of *Lyrodus pedicellatus* in this study.

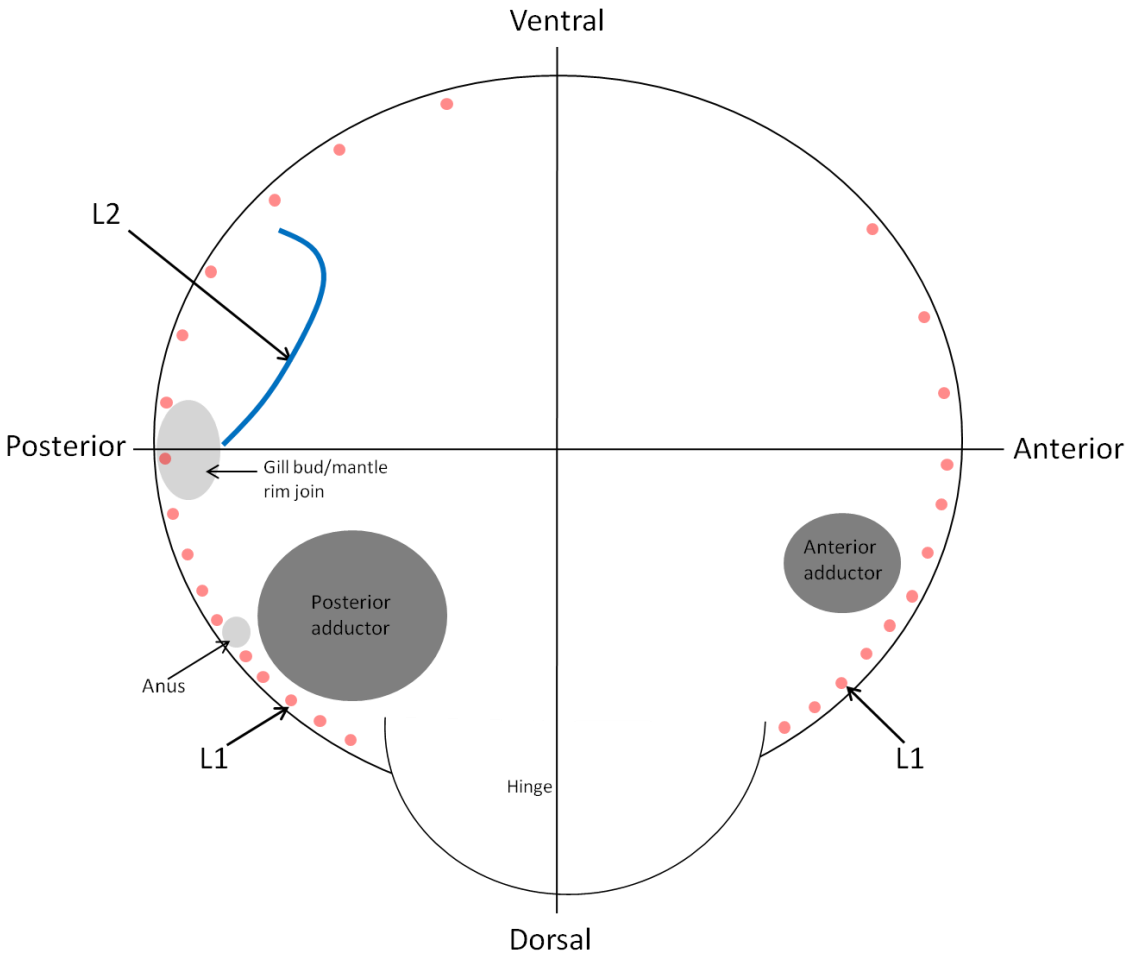

Figure 2.45 - Diagram showing the location of ciliary groups on the mantle of *Lyrodus pedicellatus* pediveliger larvae.

The L1 cilia group is present on the dorsal region of the mantle rim, being more frequent in this region and becoming more widely spaced as it occurs more ventrally. No L1 cilia were identified in the upper antero-ventral region. The group L1 ciliation often featured a single cilium slightly removed from the main group that had a ring of microvilli around its base. The L2 group is associated with the lower region of the gill bud, and continues a short distance ventrally along the mantle before curving up towards the rim.

2.4 Discussion

The ciliation of the mantle of both the ostreid species studied increased in complexity through larval development from veliger to late stage pediveliger, whilst the larval mantle of the *Lyrodus pedicellatus* pediveliger is comparatively sparsely ciliated. The location of some of the cilia groups (C5 and, possibly, C9) is closely linked to the location of catecholamines and serotonin containing cells in the mantle (Figure 2.30). The cilia observed here are comparable to similar structures observed by other authors in ostreid and pectinid larvae: however the extent, pattern and development of mantle ciliation in ostreids or teredinids has not previously been explored in the detail of this study. The cilia groupings observed through the larval development from early veliger to late pediveliger are summarised in Figure 2.4**,** Figure 2.5 and Figure 2.45, and tabulated in Table 2.7 and Table 2.6 (located after **2.4.1 Ontogeny**). The cilia groups found in *Crassostrea gigas* and *Ostrea edulis* are virtually identical, with the only exceptions being the C2, C6 and C8 cilia groups which were not identified in all the *O. edulis* specimens examined.

The larval mantle of the ostreid species investigated has a considerably greater range of cilia groups than previously reported. Cilia on the mantle edge have been recorded as diffuse tufts along the mantle edge (Elston, 1980), or localised tufts near the anus (Elston, 1980, Waller, 1981). Other cilia on the mantle have been observed as being in two tracts on the apex and just below this on the inner mantle rim fold (Beninger & Cannuel, 2006, Cranfield, 1974): Beninger's studies have shown the presence of the C5 cilia group further examined in this study. The appearance of cilia groups such as C3 and C4 around the gill bud has not been noted before, and there appears to be no account of the specialised C9 cilia group located under the posterodorsal notch, despite this shell feature having been indentified in SEM studies of oyster larvae before (Carriker, 1979, Waller, 1978, Waller, 1981).

2.4.1 Ontogeny of ostreid mantle ciliation from veliger to early spat

The ciliation on the mantle of ostreid larvae increases in abundance and complexity from early veliger to late pediveliger, with the pediveliger stage larva having densely ciliated groups such as the C5 tract, or groups that are unique to this larval stage, such as the C13 and C8 groups.

The C5 ciliary tracts in the earliest veliger stage larvae examined do not extend far from the gill bud. As such the early C5 tracts probably do not function as particle rejection tracts in the early veliger (see section **2.4.3**), although they may still beat, possibly simply preventing stagnation of water within the mantle cavity. As the larva develops from early veliger through to the pediveliger stage, the C5 tracts spread around the mantle rim from the gill bud towards the anterior adductor. The spread of these tracts is preceded in the early veliger by the C6 single tract in the antero-ventral, and later in development by the C5a tracts (Figure 2.4). The C5a tracts appear to be an early development stage of the C5 tracts, with the upper tract often being more developed than the lower one and the cilia of both upper and lower tracts varying in length. The C5a cilia are not organised into the regularly spaced clumps that form the main C5 tracts. Furthermore the tract between the upper and lower cilia rows is not very pronounced, suggesting that the C5/C5a tracts may develop as the two folds of the mantle itself continue to develop. By the mid-pediveliger stage there is a dense twin tract of cilia, formed of small clumps of cilia, running along the rim of the inner mantle fold from the gill bud to the anterior adductor. The tracts of the pediveliger were seen beating and rejecting particles from between the shell valves near the anus (Figure 2.20).

Shortly after metamorphosis, only the C5, C1, C2 and C8 tracts are still visible on the mantle rim (Figure 2.9). The C13 group appears on the mantle throughout the ventral region in higher numbers in the spat than it did in the pediveliger (Figure 2.26). The C5 tracts are probably a functional rejection tract in the larvae that is retained, at least for a short time, post-metamorphosis. It has been proposed these tracts undergo a reorganisation into the marginal rejection tracts of the adult mantle (Beninger & Cannuel, 2006), and this seems like a plausible explanation for the fate of this ciliation. The C1 and C10 single tracts are both present from the mid-veliger stage and both increase in density of ciliation during larval development. It is probable that these tracts, along with the C5 tracts, eventually form part of the adult marginal rejection tracts. The C8 cilia of the late pediveliger (Figure 2.24) are present after metamorphosis (Figure

2.9). The spat C8 tract is more densely ciliated than that of the pediveliger, suggesting this may develop to form the radial rejection tracts in the adult (Beninger & Cannuel, 2006).

Ciliary groups such as the C3 and C9 groups containing specialised cilia with rings of microvilli at the base are often difficult to image; further investigation is required to determine if these groups are truly unique to the larval form and are lost at metamorphosis. The C5 tracts undergo the most obvious change during larval ontogeny, becoming longer and more densely ciliated, although the length of the cilia forming the tracts does not appear to change. The C3 and C9 stereocilia appear identical in veliger larva to those groups in the late pediveliger larva: the ciliation is no denser and the group is no larger (Table 2.7 and Table 2.6). The lengths of the C9 cilia also appear comparable throughout all the stages of larval development investigated. This may suggest these groups are sensory cilia, likely mechanoreceptors (to be discussed shortly), unique to the larva, with the group probably being lost during metamorphosis.

Only the C6 (and in approximately 70% of individuals the C5a) ciliary group is lost during the development from veliger to pediveliger, with the general trend being for an increase in cilia complexity and diversity between these two development stages (Table 2.7 and Table 2.6). It is likely that the C6 cilia tract is an early development stage of what eventually becomes the C5 ciliation (via the C5a stage) as it occupies a location on the mantle rim that is, by the pediveliger stage, covered by the profuse twin tracts of the C5 cilia group.

Cilia Group	Location	Mantle fold	Mantle rim or mantle	Cilia length	Length variation	Cilia form	Cilia density (1-5)	Number of cilia	Directed beat	Stiff	Stereocilia	Discocilia
C1	Postero-dorsal	Inner	Rim	≈5µm	+	Single tract	3	n/a	-	-	-	-
C2	Gill bud/inner mantle fold junction	Inner	Rim	≈10µm	-	Short line	3	16-20	-	-	-	-
C3	Posterior	n/a	Mantle	≈10µm	-	Clump	n/a	≈60	-	+	+	+
C4	Posterior	n/a	Mantle	≈5-10µm	+	Loose clump	1	30-50	-	-	-	-
C5	Posterior	Inner	Rim	≈10µm	-	Twin tract	3	n/a	-	-	-	-
C5a	Ventral or antero-ventral	Inner	Rim	≈1-8µm	+	Twin tact (indistinct)	1	n/a	-	-	-	-
C6	Antero-ventral	Inner	Rim	≈1-5µm	+	Short line	n/a	n/a	-	-	-	-
C7	All	Inner	Rim and mantle	≈0.5µm	+	Single	n/a	n/a	n/a	-	-	-
C9	Postero-dorsal (under shell notch)	-	Neither - extrusion of mantle tissue	≈13µm	-	Clump	2	20-30	-	-	+	-
C10	Anterior	Inner	Rim	≈5µm	-	Single tract	3	n/a	-	-	-	-
C12	All	Outer	n/a	≈15µm	?	Clump	n/a	2-4	-	-	-	-

Table 2.6 - Summary of the cilia groups found on the mantle of the veliger stage ostreid larva. 'Cilia density' is an arbitrary scale with 1 being the least densely ciliated and 5 the most densely ciliated.

Cilia Group	Location	Mantle fold	Mantle rim or mantle	Cilia length	Length variation	Cilia form	Cilia density (1-5)	Number of cilia	Directed beat	Stiff	Stereocilia	Discocilia	Spat
C1	Postero-dorsal	Inner	Rim	≈5µm	+	Single tract	4	n/a	-	-	-	-	+
C2	Gill bud/inner mantle fold junction	Inner	Rim	≈10µm	-	Short line	3	16-20	-	-	-	-	-
C3	Posterior	-	Mantle	≈10µm	-	Clump	n/a	≈60	-	+	+	+	-
C4	Posterior	-	Mantle	≈5-10µm	+	Loose clump	1	30-50	-	-	-	-	-
C5	Posterior to anterior	Inner	Rim	≈10µm	-	Twin tract	5	n/a	+	-	-	-	+
C5a	Anterior	Inner	Rim	≈1-8µm	+	Twin tact (indistinct)	1	n/a	-	-	-	-	-
C7	All	Inner	Rim and mantle	≈0.5µm	+	Single	n/a	n/a	n/a	-	-	-	-
C8	Antero-ventral and anterior	-	Mantle	≈8-10µm	-	Single tract	3	n/a	+	-	-	-	+
C9	Postero-dorsal (under shell notch)	-	Neither - extrusion of mantle tissue	≈13µm	-	Clump	2	20-30	-	-	+	-	-
C10	Anterior	Inner	Rim	≈5µm	-	Single tract	4	n/a	-	-	-	-	+
C11	All	Periostrcal groove				Tract	5	n/a	+	-	-	-	-
C12	All	Outer	n/a	≈15µm	?	Clump	n/a	2-4	-	-	-	-	-
C13	Antero-ventral to antero-dorsal	-	Mantle	≈6µm	-	Short line	n/4	15-30	+	-	-	-	+

Table 2.7 - Summary of the cilia groups found on the mantle of the pediveliger stage ostreid larva. 'Cilia density' is an arbitrary scale with 1 being the least densely ciliated and 5 the most densely ciliated.

2.4.2 Comparative anatomy

The mantle ciliation of the bivalve larva has not been well documented. The ciliation of the ostreids can be compared to that recorded for the comparatively well studied and closely related pectinids, with 5 discrete groups of mantle cilia having been identified in *Pecten maximus* pediveligers (Cragg, 2006). Pectinids appear to not feature the long rejection tracts present in *Crassostrea gigas*. However, Cragg (2006) provides a layout map for pediveliger mantle ciliation which is similar to those in this study for the ostreids but less so to that of *Lyrodus pedicellatus,* as can be seen in Figure 2.46. The orientation of the larva is the same in each diagram in this figure.

Cilia tracts - the C5, C5a, C6, C1 and C10 groups

The C5 tracts are the largest and most striking cilia group observed on the inner mantle fold of the ostreid larvae in this study. The cilia making up the tracts for the C5 ciliation lack any specialised bases or structure suggesting that a sensory function is unlikely. Other authors have identified cilia in this location in ostreid larvae (Beninger & Cannuel, 2006, Cranfield, 1974, Waller, 1981), but only Beninger (2006) has identified the extent of ciliation seen in this study. The type 2 cilia of *Pecten maximus* pediveligers occupy the same location on the mantle rim (Figure 2.46) as the C5 twin tracts of the ostreid pediveligers (Cragg, 2006).

Descriptions of type 2 cilia in *Pecten maximus* depict the group as being arranged in discrete rows of up to 25 cilia, not in one long continuous row as is the case for all the tracts found in the ostreid larvae (C5, C5a, C1, C10 and C6), although the ostreid tracts are formed from close arrangements of small cilia clumps (Figure 2.37). The type 2 cilia lines of *P.maximus* do form an approximate tract that has been observed beating in live specimens, so can be considered broadly similar to the C5 tracts (Cragg, 2006). The type 2 ciliation also appears in the early *Pecten* veliger (Cragg, 2006), as was the case for C5 ciliation in *Crassostrea* and *Ostrea* larvae. Furthermore, identifying the same tracts in *Ostrea edulis,* but not in *Lyrodus pedicellatus* or in the literature for the more closely related pectinids, suggests that these tracts may be a 'phylogenetically new character in the Ostreidae' (Beninger & Cannuel, 2006).

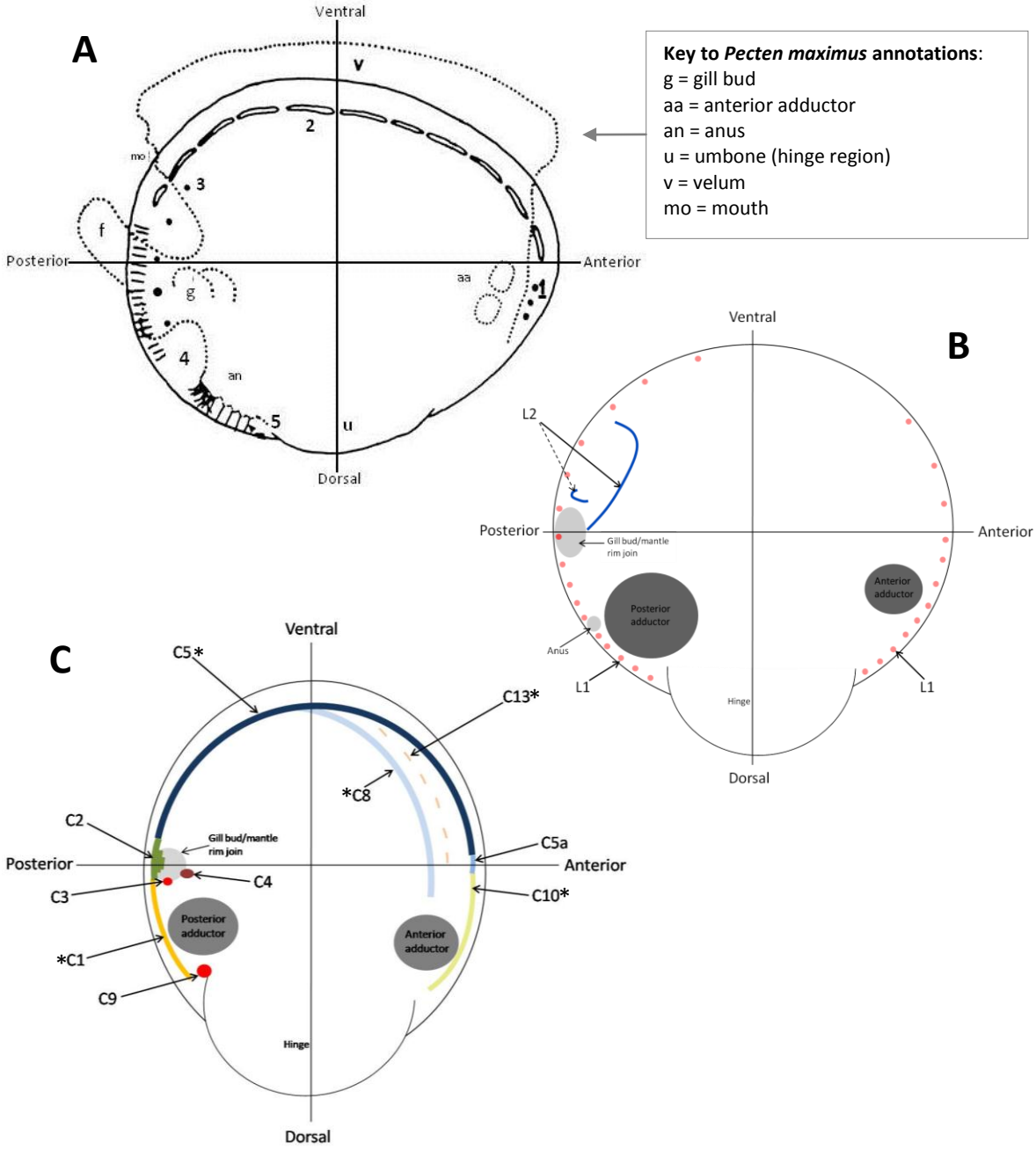

Figure 2.46 - Diagram comparing ciliation of the mantle of **A.** *Pecten maximus* pediveliger (Cragg, 2006), **B.** *Lyrodus pedicellatus* pediveliger and **C.** ostreid pediveliger larvae

The cilia are mostly located on the mantle rim for all species. *L. pedicellatus* has significantly less ciliation than the other two. The changes in the ciliation types on the mantle rim for of both *P.maximus* and *Crassostrea gigas* occur in almost exactly the same regions: *Pecten* type 2 = *Crassostrea* C5, *Pecten* type 4 = *Crassostrea* C1, *Pecten* type 5 = *Crassostrea* C9 and *Pecten* type 1 = *Crassostrea* C10. The descriptions of the cilia types do not match, suggesting they are differing arrangements of cilia, but in similar locations on the mantle rim. The C9 and type 5 ciliation may be an exception to this, appearing very similar whilst sharing a location. Those ciliary groups marked with an * in the ostreid diagram are the groups definitely retained 1-3 hours post-metamorphosis.

The type 1 cilia of the pectinids share a location with the C10 (or the C6 in the early *C. gigas* veliger) grouping in the antero-dorsal region of the mantle rim (Cragg, 2006). However the arrangement of the type 1 cilia group as short cilia in disparate groups (Cragg, 2006) is markedly different from the single tract found in this location in both *Crassostrea gigas* and *Ostrea edulis.*

The cilia groups bearing specialised cilia - C3, C9 and L1

The C3 grouping (Figure 2.15) has 3 distinct characteristics: the cilia with the ring of 9 microvilli at their base, the stiffness of the cilia and the presence of discocilia (Table 2.7 and Table 2.6). Discocilia have been seen in bivalve larvae before (Campos & Mann, 1974) but have been dismissed as artefacts produced from fixatives that are not correctly osmotically balanced (Short & Tamm, 1991). However, the C3 grouping was the only cilia group these discocilia were observed in, suggesting these cilia were more susceptible to the osmotic imbalance. The C3 grouping appears very similar to the type 3 ciliation of *Pecten maximus* pediveliger larvae (Bellolio et al., 1993, Cragg, 2006). The type 3 cilia are also stiff tufts, and are located in the posterior region (Figure 2.46) and most notably have specialised cilia with a ring of 9 microvilli at the base. As with the C3 group these cilia with microvilli at the base are slightly removed from the main grouping of cilia. The ostreids and the pectinids are closely related groups in the Pteriomorpha (Giribet & Wheeler, 2002). The shared location and similar appearance of a mantle ciliary group in two such relatively closely related species suggests this may be a homologous structure stemming from a shared ancestry.

The C9 cilia group also has cilia with a ring of microvilli at the base. Whilst the anal tuft in the general location of the C9 group is a well known ciliary feature both in ostreids (Elston, 1980, Waller, 1981) and pectinids (Bellolio et al., 1993, Cragg, 2006), there is no report of this group of cilia below the anal tuft and directly under the posterodorsal notch in ostreids. The site of the type 5 cilia on the bridge of mantle tissue between the shell valves of *P.maximus* pediveligers (Cragg, 2006), is exactly the same location as the C9 group observed in this study (Figure 2.46). The type 5 cilia of pectinids are not described as having any microvilli at the base, although the account does describe these cilia as arising from 'small hemispherical protuberances' (Cragg,

2006). From examination of the original SEM images of the type 5 cilia and, comparing these to the images of the C9 cilia, it is probable that these groups are very similar. The microvillous collar may not have been visible in the images of *Pecten maximus* type 5, either due to differences in equipment, preparation technique or the grouping simply not being viewed at an angle favourable to the imaging of the microvilli. Furthermore this location under the anus is comparable to that of the abdominal sense organ in the adults of both the ostreids and pectinids (Haszprunar, 1983). The development of this organ is homologous in the adults of the ostreids and pectinids (Haszprunar, 1983), raising the possibility that the C9 and type 5 ciliary grouping may be a larval form of this sense organ, or a developmental stage of the abdominal sense organ itself.

The pectinid type 1 cilia are formed of groups of up to ten cilia emerging from circular depressions, interspersed with a single cilium arising from circular depression. This group would appear to closely match, both in morphology and location, the L1 cilia of *Lyrodus pedicellatus* in Figure 2.41, Figure 2.42 and Figure 2.43. The life history strategies of the two species are different - *P.maximus* larvae are planktotrophic, featuring a long planktonic phase, whereas *L. pedicellatus* larvae are lecithotrophic, being brooded for some time and having a short planktonic phase (Pechenik et al., 1979). The disparity between these two bivalve genera, both in life history strategy and phylogeny, may suggest that while the ciliation is somewhat different in terms of the amount of cilia present on the mantle, the morphology of certain ciliary groupings is similar across taxonomically distant bivalve species. Mantle ciliation may be an ancestral trait that diversifies within the bivalve orders, and possibly within genera.

The cilia with a ring of microvilli at the base in the C3, C9 and L1 cilia groups are similar to those associated with the type 3 cilia in *P.maximus* (Cragg, 2006). These specialised cilia are referred to in the literature as collar cells (Crawford & Campbell, 1993) or stereocilia (Haszprunar, 1985a). For the purposes of this discussion these specialised cilia will be referred to as stereocilia, as their appearance is like the stereocilia in the Stempell's organ in adult *Nucula* bivalves (Haszprunar, 1985b). The term stereocilia should also be used with some caution, as it is used to

refer to very different structures within vertebrates and invertebrates that are not in the form of a cilium surrounded at the base by a ring of microvilli. There appears to be some confusion surrounding the use of the terms stereocilia, kinocilia or collar cell. When the term stereocilia is used in this study it describes a single cilium with a ring of 9 microvilli at the base.

The microvilli at the base of the stereocilia within Stempels organ are described as being triangular in cross section (Haszprunar, 1985b) - the appearance of the microvilli forming the collar in Figure 2.12 and Figure 2.35 are also triangular. Within the confines of this study, the appearance of stereocilia within similar ciliary groupings suggest this to be a feature that may be found throughout the larvae of the Bivalvia: *Lyrodus pedicellatus* is a member of the Order Myoidea (Giribet & Wheeler, 2002) and as such is phylogenetically distant from *Ostrea edulis* and *Crassostrea gigas*, with these species being found in the Ostreoida (Waller, 1981). These mantle stereocilia, in a similar ciliary grouping, also occur in *Pecten maximus* (Cragg, 2006), of the order Pectinoidea - this being a clade distinct from that including the Ostreidae (Giribet & Wheeler, 2002). These ciliary groupings with their associated stereocilia are therefore found in the veligers of the pteriomorph bivalves and veligers of the heterodont bivalves.

Furthermore the stereocilia are comparable to those occurring within the sensory structures of adult Pteriomorpha in specialised organs such as the abdominal sense organ or the mantle tentacles of adult scallops (Haszprunar, 1985a, Haszprunar, 1987a, Zhadan et al., 2004). The primitive bivalves also have stereocilia in the Stempels organ of adult *Nucula* (Haszprunar, 1985b).

Structures similar to those termed stereocilia in this study have been observed in the larvae of chitons (Haszprunar et al., 2002), nemerteans (Cantell et al., 1982), and asteroids (Crawford & Campbell, 1993), suggesting these stereocilia are found across a wide range of the Metazoa. The functional significance of larval stereocilia will be discussed in section **2.4.2,** and their phylogeny in **5.2.2**.

Summary of comparative anatomy

It is evident when comparing observations of the disposition of the cilia on the mantle of *Crassostrea gigas, Ostrea edulis* and *Lyrodus pedicellatus* (Figure 2.46) to published accounts of the pectinids (Bellolio et al., 1993, Cragg, 2006) that the location of the larval mantle ciliation of the ostreids and the pectinids is more comparable than to the larval mantle ciliation of the teredinids, reflecting the relatively close phylogenetic relationship of the former two families. However the fine structure of the cilia groups of both the ostreid species examined is different from that of the pectinids, and ciliation is considerably more profuse. The pectinids do not have the long twin tracts of cilia found in the ostreids and, where cilia rows are present, the cilia are not as densely packed: this may suggest a divergent evolution of the mantle ciliation between relatively closely related bivalve genera. Alternatively the adult mantle ciliation is somewhat different between the ostreids and the pectinids, if larval ciliation is not unique to the larval stage but a precursor to adult structures this may account for some of the variation seen.

Lyrodus pedicellatus is taxonomically distant from the other two species (Giribet & Wheeler, 2002), and yet while the extent and pattern of the ciliation is not comparable, the morphology of the cilia groups is. Whether the mantle ciliation of *L. pedicellatus* is comparable to other more closely related species is currently unknown, due to a lack of information concerning the mantle of larval teredinids. In all the species, the location for most of the cilia is the mantle rim.

Stereocilia are present on the mantle of all the species examined here and are generally similar in structure, consisting of a single long cilium with a ring of nine microvilli at the base, a structure that is characteristic of the stereocilia found in many invertebrate larval sensory structures (Cragg, 2006, Haszprunar et al., 2002). That the C3 group of cilia appears remarkably similar to the L1 of *L. pedicellatus* and the type 3 cilia recorded in the pectinids (Bellolio et al., 1993, Cragg, 2006) suggests this may be a ciliary arrangement found in the veligers of many phylogenetically distinct families of the Bivalvia, possibly indicating this group of mantle ciliation stems from an ancestral trait.

2.4.3 Functional anatomy

The C5, C5a, C1, C10 and C11 cilia tracts

The C5 ciliary tracts have recently been proposed to be pseudofaeces rejection tracts in the *Crassostrea gigas* pediveliger larva (Beninger & Cannuel, 2006). The tracts are very similar in appearance to the structures on the adult mantle with this function (Beninger & Veniot, 1999, Beninger et al., 1999).

Observations of live larvae in this study suggest this to be the probable function of the C5 tracts: video footage of larvae rejecting fluorescent particles from the mantle cavity suggests the C5 tracts are responsible for this particle movement (Figure 2.20). These particles are moved posteriorly along the mantle rim cilia tracts from within the mantle cavity under the velum, and expelled in the posterior near the anus, probably when they meet the anal tuft. Some larvae were fixed with particles still moving along the C5 tracts and an example of this has been provided here in Figure 2.47, in order to support the discussion of the functional anatomy of these cilia. The particles in Figure 2.47 are likely to be either algal strings or cyanobacteria. These particles are running along the twin tracts of cilia, between the upper and lowers lines of cilia indicating that they are being moved with the ciliary beat - there are 3 strings of particles visible in this image and none are laying across the C5 tracts, they are all roughly in line with the angle of the fixed cilia (indicating beat direction) and the path taken by the fluorescent bead in Figure 2.20. The C13 cilia seen below these C5 tracts may also aid particle rejection (Figure 2.25). The C13 cilia are always curved down onto the mantle, directed up towards the mantle rim (Figure 2.25), suggesting a beat in the direction of the C5 tracts, possibly to deflect any loose particles in the mantle cavity towards the C5 cilia. The C13 groups could be the beginnings of the complex radial rejection tracts found in adult *Crassostrea gigas* in addition to the marginal tracts (Beninger & Cannuel, 2006).

The C5 tracts could also serve to clean particles from the foot as it is retracted or extended between the shell valves - the close proximity of the most densely packed C5 tracts to the point of the foot entry and exit from the shell valves (Figure 2.17) lends some support to this

suggestion, although footage of live larvae was not conclusive for confirming this as a potential function. The C5 cilia tract may be a method to prevent water stagnation within the mantle cavity. This would be especially important when larvae are 'resting' with the velum partially retracted. This behaviour was common in larval cultures (Stanton - personal observations).

The C11 cilia group are found close to the C5 tracts, but their location within the periostracal groove, as seen in Figure 2.27, Figure 2.40 and Figure 2.47 is probably too sheltered for this group to be involved in pseudofaeces transport. It is only by the very late pediveliger stage that the tips of the C11 cilia exit the top of the groove as shown in Figure 2.47. The variation in the angling of the C11 cilia in the periostracal groove suggests that these cilia have a beat but that it is an irregular pattern, a side to side beat that is not regularly directed. It is possible the function of this grouping is simply to keep the periostracal groove clear of particles.

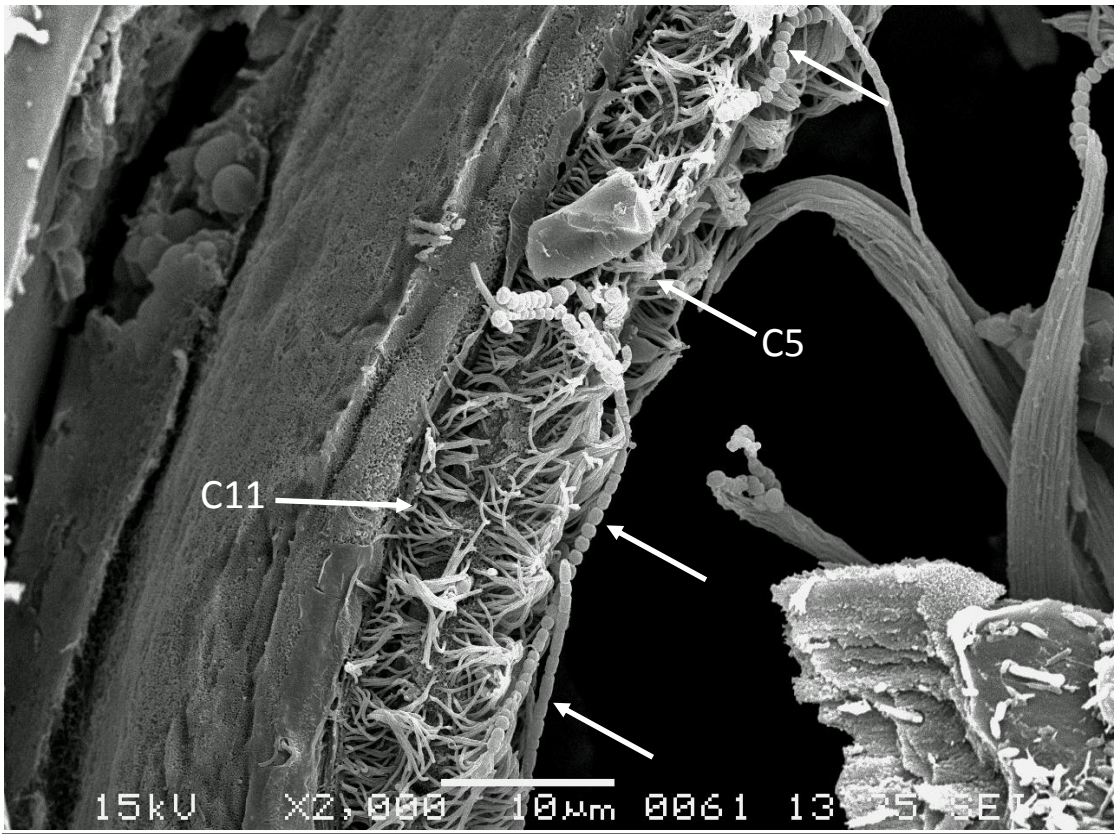

Figure 2.47 - C5 cilia tracts of an *Ostrea edulis* pediveliger larva.

The C5 tracts are clearly visible on the mantle rim (as are the C11 in the periostracal groove) with 3 string of algae or cyanobacteria (arrowed) caught between the upper and lower bands of the C5 tracts. The C5 cilia tracts have been postulated as being rejection tracts and this image, combined with live footage of particles travelling along these tracts, represents evidence for these tracts having a role in rejecting particles from the mantle cavity. This larva was dry fractured and imaged by SEM.

The C3, C9 and L1 stereocilia

Suggestions of function for the stereocilia primarily focus on these specialised cilia being invertebrate mechanoreceptors (Haszprunar, 1985a, Haszprunar, 1986, Haszprunar et al., 2002). Mechanoreceptive function of stereocilia is implicated by the central cilium moving against the microvilli at the base. This movement of the cilium probably generates a signal regarding the position of cilium, and thus enables the larvae to determine the position and direction of the cilium in relation to its stroke (Crawford & Campbell, 1993). The presence of neurotransmitter compounds such as serotonin and catecholamines may represent pathways by which the stereocilia sensory reception affects behavioural responses by the larva.

From the position of the C9 group in the ostreids examined here, a mechanoreceptory function would seem most likely, possibly to determine if excreted faeces are trapped in the posterodorsal notch, or to detect water-borne vibrations through the posterodorsal notch. The notch itself may serve as a method for water to escape the shell when it is rapidly closed, allowing pressures to equalise and facilitating rapid behavioural reactions such as the sinking response. The C9 mechanoreceptors may detect changes in water flow, for resulting from the notch being blocked or from successful shell closure, as has been suggested for other similar stereocilia in the Nuculidae (Haszprunar, 1983).

If the C9 group is involved with the C5 pseudofaeces rejection tracts then it may act as a mechanoreceptor that affects the beat of the C5 ciliary groups adjacent to it by detection of particles ejected from the tract, particles trapped in the notch above the C9 group or by sensing the strength of the water currents being generated. If this is the case then the group may also affect the rejection of faeces from the nearby anus and anal tuft (especially if particles have become lodged in the posterodorsal notch). However, the C9 cilia are not located directly adjacent to the C5 tracts, and may be too far from the anal tuft also to successfully fulfil this role.

A more probable role is as a mechanoreceptor for the detection of water-borne vibrations whilst swimming or crawling. The appearance of C9 cilia in early veligers suggests the group appears close to the formation of the posterodorsal notch in the shell, which itself appears at the

onset of Prodissoconch 2 and the truly planktonic phase. The C9 stereocilia may therefore be for the detection of water borne vibrations of importance to a planktonic organism, such as local hydrodynamic disturbances that would be caused by predators or other nearby larvae (Gallager, 1993). The presence of the larval fright reaction (rapid closing of the shell and sinking) when the nearby water is disturbed (Cragg, 1980) illustrates that larvae are capable of detecting such stimuli.

The position of the C3 group stereocilia within the mantle cavity and next to the gill bud could indicate they serve to detect stagnation of water in the mantle cavity. The location of this group is similar to that of the Stempels organ found in adult Nuclua (Haszprunar, 1985b). This organ acts as a mechanoreceptor, involved in the regulation of the water currents within the mantle cavity. It is very feasible that the C3 group could fulfil a similar function within larval bivalves, especially given the close proximity of this group, and the type 3 ciliation in pectinids, to the developing gill bud and the ciliation of the mantle rim (Cragg, 2006). The C3 ciliation could be a functional larval form of an adult organ such as Stempels organ (although Stempels organ is unique to the adult Nuculidae, which are taxonomically distant from either the ostreids or pectinids) or the abdominal sense organs found throughout the Pteriomorpha (Haszprunar, 1983). However, as discussed earlier, the location of the C9 ciliary group is a better fit with the ultimate location of the abdominal sense organ in the adult.

The stereocilia of the L1 cilia group in *Lyrodus pedicellatus* are exposed to the water column to a much greater degree than the C3 or C9 cilia groups. Their position below the region of the foot extension between the shell valves implies the most probable function of this group would be sensory reception when searching out a settlement site, either as mechanoreceptors for detecting surface topography or for a chemosensory role in site searching. Further investigation is required to positively determine the function of the C3, C9 and L1 cilia groups, especially when considering this similarity in their morphology, but disparity in their location.

2.4.4 The role of serotonin and catecholamines in the larval mantle

Serotonin-containing fibres can be seen running from the most dorsal point of the mantle through the mantle rim, past the gill bud and along the ventral mantle (Figure 2.29). The gill bud itself also shows a serotonin signal. *Mytilus edulis* and *Placopecten magellanicus* are bivalve species for which the presence of serotonin and catecholamines in the larval mantle has been investigated using confocal microscopy (Croll et al., 1997). Light and electron microscopy investigations have also revealed neurotransmitter-like vesicles in the ventral mantle rim of both *Pecten maximus* (Cragg, 2006) and *Placopecten magellanicus* (Croll et al., 1997). This region, the location of the C5 ciliary tracts, had both catecholamine fluorescent bodies and serotonin containing fibres in the pediveligers of *Crassostrea* gigas. However, Croll (1997) does not indicate the presence of aldehyde-induced fluorescence from the mantle of *M. edulis,* and *P.magellanicus* only has 3 catecholamine cells in the ventral mantle (although this is quite comparable to localised fluorescence found in *C. gigas* in this study) and none in the dorsal mantle (the region of the C9 grouping). Both *M. edulis* and *P.magellanicus* have serotonin signal running through the ventral mantle from the gill rudiment (Croll et al., 1995) as in *C. gigas* here. However there is little anatomical information relating to the ciliation of the larval mantle available in these species. As such it is not possible to know if the fluorescent cells correspond to mantle cilia locations, as can be shown for *Crassostrea gigas* in this study and using the anatomical information available for *Pecten maximus* pediveligers (Cragg, 2006).

Despite this lack of anatomical information, the presence of serotonin, and to an extent catecholamines, combined with the shared ancestry of *M. edulis* with the ostreids and pectinids within the Pteriomorpha (Giribet & Wheeler, 2002), indicate that it is probable that the mantle of the mytilids will have some ciliation. However the variation seen between the ostreid and pectinid mantle ciliary groups suggests the form of this ciliation may prove to be unique to the mytilids, and that the location of serotonin and catecholamines will reflect this.

Serotonin has been implicated in the control of ciliary activity in larvae of *Mytilus* (Beiras & Widdows, 1995), gastropod larvae (Mackie et al., 1976) and molluscan embryos (Kuang &

Goldberg, 2001), and is known to increase the beat frequency of velar ciliation (Braubach et al., 2006). Catecholamines have been implicated in the control of ciliary activity in molluscan larvae (Beiras & Widdows, 1995), probably through catecholamines reducing cilia beat frequency (Braubach *et al*., 2006). Brauchbach *et al* (2006) has shown that increased concentrations of serotonin lead to an increase in ciliary beating whilst catecholamines, in sufficient concentrations (~10^{-6}-10^{-9}mol l^{-1}), decreased the beat frequency of gastropod veliger ciliation. This was further examined on a whole organism view, with serotonin causing veligers to gather at the surface of the water column and catecholamines leading to a gather of veligers at the bottom of the water column. The authors further conclude that this is evidence of the potential for nervous control of behaviour in larvae, using serotonin and catecholamine pathways to control ciliary beat. As both compounds effect these changes by effecting intracellular calcium levels (Doran et al., 2004), it seems plausible that the compounds would work synergistically to change the beat frequencies of larval ciliation either on the velum or the mantle.

Catecholamines also have a major role in the induction and mediation of settlement and metamorphosis in the oyster *Crassostrea gigas* (Coon & Bonar, 1987), the scallop *Argopecten purpuratus* (Martinez et al., 1996), the gastropod *Phestilla sibogae* (Pires et al., 2000, Pires & Hadfield, 1991) and generally within the Mollusca (Croll & Dickinson, 2004). While the previous information indicates it is likely to find both of these compounds in a pre-settlement pediveliger stage larvae, the specific location of these near-mantle ciliation suggest they may have a role in regulating the beat of the ciliary tracts found in these locations (in addition to the mantle rim the gill bud itself is heavily ciliated).

The serotonin fibre imaged running below the mantle rim in Figure 2.29 is probably running along the point of mantle musculature-shell join. Possibly, serotonin is acting as a neurotransmitter for the contraction of the musculature here, allowing the outer fold of the mantle to move away from the shell slightly - the mantle was often pulled away from the inner shell surface in individuals observed with SEM, and while this is most likely an artefact of the specimen dehydration, it often reveals the mantle musculature and the mantle/shell join (Figure

2.35 - A). As well as its potential for influencing ciliary function (Beninger & Cannuel, 2006), serotonin has also been implicated in controlling the movement of muscular fibres in the velum of larval nudibranchs (Kempf et al., 1997), and nerve fibres have been imaged on the mantle near the velar retractors (Cragg, 1985), so the presence of fibres containing neurotransmitters on the mantle musculature of larval bivalves is not unexpected.

The SEM information collected in this study on the ciliary groups present on the mantle rim and the locations of the catecholamine-containing cells in the mantle is directly compared in Figure 2.30, and a correlation between the two seems probable. The catecholamine-containing cells of the ventral region (Figure 2.28) and the serotonin signal found in the ventral mantle rim could be attributed to control of the ciliary beat frequency of the C5 group. It has been suggested previously that cells showing catecholamine fluorescence from around the mouth of molluscan larva are controlling particle selection and rejection (Croll & Dickinson, 2004). This view would seem to support the theory that the C5 ciliary tracts are pseudofaeces rejection tracts, with the presence of both serotonin and catecholamine pathways potentially offering a method of control of ciliary beat (through increasing ciliary beat or reducing ciliary beat) such as that proposed for the control of velar ciliary beat in gastropod veligers (Braubach et al., 2006). Furthermore the presence of serotonin both in the mantle rim and in the location of the mantle musculature suggests these two could have a shared function. While the folding of the mantle away from the shell is assumed to be an artefact of SEM specimen preparation, being able to control the musculature of the mantle in relation to the beat of the C5 rejection tracts may be of benefit to the larva, helping to maintain particles within the rejection tracts, or collecting any stray particles from within the mantle cavity.

If the C9 stereocilia are mechanoreceptors for the detection of vibrations, such as local hydrodynamic disturbances that would be caused by predators or other nearby larvae (Gallager, 1993),the presence of serotonin fibres running from the location of the C9 group into the larva may imply a neural pathway to the musculature of the velum (Kempf et al., 1997). In this way the C9 group may act as a trigger for the larva to react to stimuli by the rapid retraction of the velum

and closing of the shell when a local hydrodynamic disturbance is detected. The C9 group could be a mechanism for predator detection in the veliger.

Alternatively the C9 group may act as a receptor for detecting surface topography or local hydrography in the pediveliger stage - gastropod pediveligers respond to cues by rapid retraction of the velum and sinking (Hadfield & Koehl, 2004), and the location of the C9 group is a feasible place for the detection of benthic stimuli when crawling or swimming near the benthos, despite the evidence that this role is primarily controlled by the apical organ (Hadfield et al., 2000).

2.5 Conclusions

The mantle ciliation pattern of the two species of ostreid larvae examined in this study are very similar, with 13 separate groupings having been identified on the mantle of *Crassostrea gigas* by the pediveliger stage, and most of the same groups being seen on the mantle of *Ostrea edulis*. The ciliation of the mantle increased both in its extent and its complexity as the larva develops from veliger to late pediveliger, but with only the cilia tracts on the mantle rim being retained in the post-metamorphosis spat. The mantle cilia groups bear comparison, both in morphology and location, to the larval mantle ciliation of the pectinids suggesting a shared ancestry for the mantle ciliation. However the mantle ciliation of the ostreids is greater than seen in the pectinids, suggesting some level of evolutionary divergence at the genera level.

The C5 cilia tracts run along the inner mantle rim as a twin tract that starts at the gill bud and spreads along the mantle rim towards the anterior adductor as the larva develops from veliger to metamorphosis. The C5 tracts have been imaged with particles in them and observed beating to eject fluorescent beads in live larvae, suggesting that they may function as a larval form of the adult pseudofaeces rejection tracts (Beninger & Cannuel, 2006, Beninger & Veniot, 1999). The C5 tracts are retained in the post-larva further suggesting the ontogeny of the pseudofaeces rejection tracts in ostreids as proposed by Beninger (2006). The location of the C5 mantle cilia tracts corresponds closely with the mantle locations of serotonin fibres and several

catecholamine-containing cells, suggesting that the larva may be able to control the frequency of the beat of the these cilia when ejecting particles.

The stereocilia of the C9 group have been identified in various sensory organs within the invertebrates as a mechanoreceptor. The location of this group in ostreids is the same as the type 5 cilia in pectinids. This location is the same as the abdominal sense organ in adult bivalves, but it is not yet known if this group is retained post-metamorphosis. The serotonin pathways and catecholamine containing cells in the location of this group of cilia also are linked to the pathways running into the mantle rim in the ventral region and further into the larva. This may suggest the C9 grouping is a sensory structure linked to either control of the ciliary beat of the C5 tracts or the larval sinking response (via musculature retraction of the velum) when water-borne vibrations are detected.

The mantle rim of *Lyrodus pedicellatus* is less profusely ciliated, but still has groups of cilia containing stereocilia that are similar in structure to those of the taxonomically distant ostreids and pectinids, albeit occupying a different location on the mantle rim to the C9 or C3 groups. The reduction in mantle ciliation may be an adaption to the brooded nature of *L. pedicellatus*, as similar modifications can often be found in the ciliation (usually the velar ciliation) of long-term brooded oysters (Chaparro et al., 1999). The similarity in the appearance of these cilia groups bearing stereocilia - the C3 cilia in ostreids, the type 3 in pectinids and L1 in Teredinidae - may indicate this mantle ciliary grouping is found throughout the veliger larvae of the Bivalvia.

Chapter 3 - Ciliation of the Bivalve Larval Velum

3.1 Introduction

Whilst the mantle and its associated ciliation may be the larval form of adult structures, the velum is the characteristic organ of the bivalve veliger, an anatomical adaptation that enables the larva to survive for a significant period of time in the planktonic environment. It is the most distinctive organ of the bivalve larva, developing from the D-larva stage and persisting until metamorphosis into the spat. The velum is lost during metamorphosis. During this time the velum is the organ used for swimming and feeding in the planktonic stages of the larvae, but it is still present in those larvae that are brooded for significant periods of time. Only the most extreme examples of the brooded condition, such as *Lasaea adansonii,* show a total loss of the velum (Altnoder & Haszprunar, 2008). As with the mantle described in the previous chapter, the velum has an array of ciliation equipping the larva for its planktonic existence.

3.1.1 The bivalve larval velum

The velum appears as a distinct organ during the larval development from trochophore to veliger, exiting the shell valves in the ventral to postero-ventral region opposite the hinge, as can be seen in Figure 1.2. It is formed as the pretrochal region becomes flattened, forming the top surface of the velum, and the prototroch dilates, forming the velar rim (Cragg, 2006). The velum may be formed of an infolding of the mantle itself (Cragg - unpublished). To begin with the velum is a relatively consolidated group of cells (Malakhov & Medvedeva, 1985). However the body cavity extends into the velum, and between D-larva and early veliger the larva becomes capable of rapidly withdrawing the velum into the shell through an ordered sequence of contractions by the velar retractor muscles (Cragg, 1985). The top surface of the velum and the epithelium that extends from the mantle is very thin, whilst the velar rim has a much thicker epithelium (Cragg, 1989).

The upper surface of the velum is relatively bare of cilia, with the exception of the apical tuft in the centre. The apical tuft of the apical organ is formed after the disappearance of the

apical flagellum and is composed of short cilia, not adhered together, and found within a shallow pit in the centre of the velum (Cragg, 2006, Hodgson & Burke, 1988). The apical organ itself is formed of a disk shaped region of thickened epithelium bearing short cilia and located directly overlaying a connective between two lobes of a cerebral ganglion (Cragg, 2006). The apical organ lies in a circular depression in the centre of the velum (Cragg, 2006) and probably is a sensory structure. The gastropod apical organ has been identified as a receptor for settlement cues, with ablation of the area preventing the metamorphic response to water-borne cues (Hadfield & Koehl, 2004, Hadfield et al., 2000). Nerve connections to the apical region have been preliminarily identified to the velar rim in *Placopecten* and *Mytilus* larvae (Croll et al., 1997, Raineri, 1995). These connections may suggest the apical region has a role in the regulation of ciliary beat. This brief overview is in no way sufficient to encompass the full breadth of information available for the apical organ; it is intended only to highlight the main features of this organ that may have relevance to the ciliary bands of the velum being investigated in this study.

The velar rim is profusely ciliated, and layout of these ciliary bands around the velar rim is well documented. The arrangement consists of four bands of cilia running around the circumference of the velum, named according to their position relative to the mouth as the larva swims (Cragg, 1989, Waller, 1978) - these bands are shown in Figure 3.1. From the upper velar surface down to the shell the four bands are:

1. The inner pre-oral band of cilia on the top surface of the velum just inside the top edge (a in Figure 3.1).
2. A band consisting of 2 rows of large pre-oral compound cilia (b1 and b2 in Figure 3.1), cirri, that beat downwards and are arranged out of register with each other (Cragg, 1989)
3. A wide tract of short, adoral cilia that beat towards the mouth (c in Figure 3.1)
4. On the lower edge of the velum a line of either compound cilia in ostreids (Waller, 1981) or single cilia in pectinids (Cragg, 1989) that beat up towards the adoral tract (d in Figure 3.1).

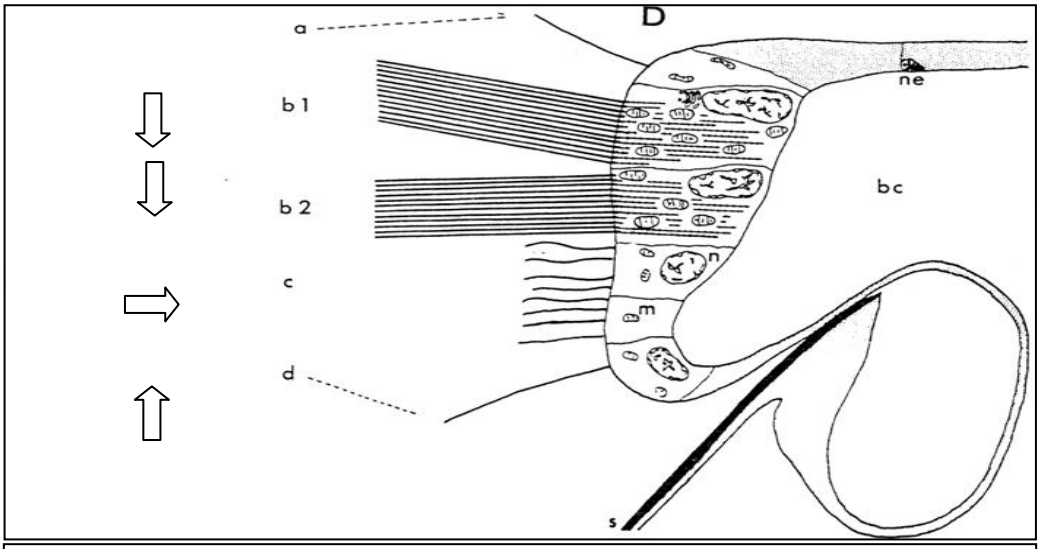

Figure 3.1 - The velar bands of a *Pecten maximus* pediveliger (Cragg, 1989)

The four bands of the velum are labelled above: a - the inner pre-oral band, b1&2 - the two pre-oral bands, c - the ad-oral band and d the post-oral band. The arrows to the left of the image show the direction of the ciliary beat, as used for particle capture in the opposed band method.

The larval mouth appears at the posterior end of the velum (visible in Figure 1.2 in section **1.3**), a ciliated opening in the adoral tract leading into the digestive tract (Bellolio et al., 1993). The mouth is sometimes accompanied by a tuft, such as in *Ostrea edulis* larvae (Waller, 1981) or compound cilia as in the case of *Pecten maximus* (Cragg, 2006) that have been suggested as having a particle selection or rejection function (Waller, 1981).

3.1.2 The velar function

The velum primarily fulfils two major functions of swimming and feeding, as well as serving as a surface area for gas exchange (Cragg, 2006), DOM uptake (Manahan, 1990), and a location for sensory structures such as the apical organ (Hadfield et al., 2000).

Swimming is fulfilled by the power stroke of the large pre-oral cirri running around the outer edge of the velum, which beat around the velar rim in a coordinated metachronal wave (Cragg, 1980, Knight-Jones, 1954), the recovery stroke being slightly oblique (Waller, 1981) and the out of register arrangement of the two rows of cirri serves to prevent interference between the two during recovery (Cragg, 1989). This is a vital function for those species, such as *Crassostrea gigas*, that have a long planktonic larval phase. The other cilia of the velum are, in

comparison to the pre-orals, too small and not numerous enough to be used for swimming; whilst sensory functions have been suggested (Waller, 1981), no evidence to support this has been found (Cragg, 1989). The larvae swim in an upwards helix with the velum on top but slightly inclined as a result of both the currents created by the adoral tract beating around the velum (Cragg, 1989), and the effect of gravity and drag on the shell (Cragg, 1980). Swimming maintains larval position within the water column, allowing behavioural responses to stimuli such as salinity changes, temperature and predator avoidance. Details of the behavioural swimming responses of the larvae when exposed to stimuli and the importance of these reactions to the planktonic larvae can be found in **Chapter 1** and **Chapter 4**.

The control of the beat of the pre-oral cirri for swimming is likely due to a mechanism comparable to that found in the gastropod veliger velum (Cragg, 2006). Cells bearing the pre-oral cirri are connected by gap junctions, and therefore are electrically coupled (Arkett et al., 1987). Arrests in ciliary beat are caused by Ca^{++}-dependent action potentials that probably are initiated from the cerebral ganglion (Arkett et al., 1987). Serotonin is known to affect changes in intracellular Ca, in turn affecting ciliary beating (Doran et al., 2004), making serotonin pathways likely candidates for velar ciliary control. Evidence of excitatory nervous control by serotoniergic cells has been obtained for molluscan embryos (Kuang & Goldberg, 2001), and dual serotoniergic excitation and dopaminergic inhibition has been found in the velum of *Mytilus edulis* (Beiras & Widdows, 1995) and prosobranch gastropods (Braubach et al., 2006).

Immunofluorescence reveals that the *M. edulis* velum contains cells on the velar edge containing catecholamines, but few pathways linking these to the ganglion at the apical organ have been located (Croll et al., 1997). Thus the abrupt cessations in ciliary beat that have been observed in swimming bivalve veligers (Cragg, 1989) probably are due to a system of nervous control based on serotoniergic and catecholamine pathways like those identified in *Mytilus edulis* larvae (Beiras & Widdows, 1995), and suspected in the gastropod *Ilyanassa obsoleta* (Braubach et al., 2006). Currently there is no information regarding the presence of either serotonin or

catecholamines in the velum of *Crassostrea gigas* larvae, and consequently knowledge of the nervous control of *Crassostrea* velar cilia beat is limited to assumptions based on other studies.

The cilia layout described earlier forms the basis for the 'opposed band' particle capture system (Strathmann et al., 1972). The downward beat of the pre-oral cirri accelerates passing particles by accelerating the water immediately around the cirri, concentrating particles in the faster moving water: these particles will then slow or, rarely, come to a halt with the water at the end of the cirri power stroke (Strathmann & Leise, 1979). The post-oral cirri beat in the opposing direction to the pre-oral cirri, beating upwards and preventing particle escape at the same time as deflecting the particles into the adoral tract (Strathmann & Leise, 1979). The adoral tract beats around the velum towards the mouth where particles are either selected or rejected. This sequence of ciliary beating on bivalve veliger velum conforms to the principle of 'ciliary downstream collection' (Riisgard et al., 2000). The principle of downstream collection transcends taxonomic boundaries, being found in many varied morphological forms across the taxonomic groups that use cilia for feeding (Riisgard & Larsen, 2001).

The downstream particle collection system is typical of protostome development and is an important factor in the phylogeny of the bivalve larvae, especially in relation to the debates surrounding the ancestry of the planktotrophic and lecithotrophic larva (Nielsen, 2004, Young, 2002). The complex arrangements of these ciliary bands into the downstream collection system have formed a crucial part of the argument for planktotrophy being the plesiomorphic condition, with many authors contending that the system is too complex to have evolved independently in so many disparate invertebrate groups (Haszprunar et al., 1995, Nielsen & Nielsen, 1995).

Detailed anatomical investigations into the velar bands of bivalve species showing different life history strategies can contribute important information to the debate over the ancestry of planktotrophic or lecithotrophic strategies, as well as expanding the knowledge of the functional anatomy of the ciliary bands.

3.1.3 The objectives of this chapter

The velar ciliation of *Crassostrea gigas, Ostrea edulis* and released (or near release) *Lyrodus pedicellatus* pediveliger larvae will be investigated using scanning electron microscopy (SEM) and light microscopy to examine the structure of the oral bands and the morphology of the cilia that comprise them. The species used in this study will provide a comparison between the velar ciliation of larvae representing three bivalve strategies: the planktotrophic larvae of *C. gigas,* the short-term brooded lecithotrophic larvae of *O. edulis* and the long term brooded larvae of *L. pedicellatus*. In addition to investigating adaptation of velar morphology, possibly due to spawning strategies, this chapter will also address the gaps in the knowledge of velar ciliation; while there is some literature describing the velar ciliation of *O. edulis* (Waller, 1981), there is very little concerning *C. gigas*, and even less detailing *L. pedicellatus* velar cilia.

The use of scanning electron microscopy allowed the morphology and appearance of the cilia when fixed to be examined showing the cilia at various stages during their power and recovery strokes, and enabling this information to be related to the velar function. Furthermore the use of SEM enabled accurate comparisons to be made with other SEM based reports of bivalve velar ciliation, such as those for the ostreids (Chaparro et al., 1999, Elston, 1980, Waller, 1981) or pectinids (Bellolio et al., 1993, Cragg, 1989, Hodgson & Burke, 1988). Cilia were removed from the velum of some specimens to reveal the cells bearing them, and the numbers of cilia comprising the compound cirri.

The presence of serotonin and catecholamines in the velum of fixed *Crassostrea gigas* larvae was investigated using confocal laser scanning microscopy. Information on the location of these compounds in relation to the oral bands may illustrate a potential mechanism of control of the velar ciliary beat. Glutaraldehye added to the fixative promoted blue-green catecholamine fluorescence (Croll et al., 1997, Falck et al., 1982, Scholer & Armstrong, 1982), and serotonin was investigated using specific FITC-labelled goat anti-rabbit antibodies (Croll et al., 1997). These methods are consistent with those used by Croll (1997) to enable accurate comparison to published findings of the presence of these compounds in the velum of other bivalve veligers.

The combination of immunofluorescence images with SEM images allowed for a consideration of the location of these compounds in relation to the ciliary bands of the velar rim. Studies have not previously combined these two techniques.

The velum was also examined using Topro-3 staining. Topro-3 is a cell nuclei stain and further revealed the arrangement of the cells bearing the ciliary bands of the velum.

Light microscope sections revealed the cells bearing the ciliary bands. Some dehydrated specimens were sectioned in wax for viewing in the SEM to further investigate the cells of the ciliary bands of the velar rim. SEM investigations of these larvae provided a 3-dimensional view of the structures revealed by light microscope sections and diagrams (such as Figure 3.1) given in the literature.

The velum was also filmed following the introduction of fluorescent beads into the water to view velar cilia capturing these particles. The movement of the beads around the velar rim is presented as a time series of video frames to visualise the beat of the velar ciliation.

3.2 Methods

All methods pertinent to this chapter are contained within **Chapter 2**, in **section 2.2 Methods.** Any additional methods used for the examination of the velum are described below.

3.2.1 Deciliation of the dehydrated velum

Those larvae with a well extended velum were treated with sticky tape to remove cilia. Tape (Sellotape) was carefully wrapped around the tip of a glass needle and gently rolled across the velar surface following critical point drying. The surface of the velum was then gently blown with air to remove any remaining debris. Alternatively, glass needles (made from heated Pasteur pipettes, stretched out to form fine glass points) were lightly scraped across the velar rim, and air lightly blown across afterwards to remove any obstructing debris.

3.2.2 Sectioning of larvae for SEM

As an alternative to cracking with glass needles some larvae were partially sectioned in wax prior to mounting. Larvae were dehydrated through an ethanol series to 100% ethanol, as described in **Chapter 2.2**. Larvae were immersed twice for 15 minutes in a 50:50 mix of 100% ethanol and Histoclear (non-toxic histological cleaning agent, Fisher Scientific) before being immersed into 100% Histoclear. The Histoclear was changed 3 times over a period of 2 ½ hours to remove any remaining ethanol residue before being placed into molten paraffin wax. Four further changes with molten wax removed any remaining Histoclear prior to the wax being poured off into moulds on a cold plate. Larvae sank close to the front of the wax block face before it cooled completely. This front portion of the block was then sectioned on a microtome until a large number of larvae were judged to be in the front face of the block – these were larvae that had been at least partially sectioned to varied thicknesses and at various angles, depending on the individual larva's fall through the wax. This front edge was trimmed off the block and the wax removed with xylene to leave the partially sectioned larvae free in solution. Xylene was changed for ethanol and samples were dehydrated from this stage through an ethanol series into HMDS as per **Chapter 2.2.5**, mounted on carbon tabs on aluminium stubs and viewed at 15KV in the SEM (JEOL JSM-6060LV).

3.2.3 Semi-thin sections of the velum for light microscopy

Larvae were decalcified in 5% ascorbic acid over an 8 hour period at room temperature. This was the most effective time-period and concentration to ensure complete removal of shell calcification. Decalcification was checked by cross-polar microscopy to determine success. Larvae were dehydrated in a graded ethanol series (50% - 100%) then embedded in either epoxy resin 812, or Agar low viscosity resin. The 812 resin was mixed hard or medium to account for the small size and relative toughness of samples (Bozzola & Russel, 1999), the Agar resin was used in a medium mixture as recommended by the manufacturer. The resin blocks were faced and shaped around individual larvae, with care being taken to ensure the specimen orientation was correct for sectioning.

Sections were cut semi-thin for light microscopy using a glass knife on a Reichert-Jung UltraCut-E Ultramicrotome, collected from the water boat behind the knife edge using a fine (000) paintbrush and dried onto a glass slide. Once firmly attached to the slide they were covered by a 1% Toluidine Blue on a hot plate for approximately 1 minute. Sections were viewed in a Leica DM LB2 light microscope, fitted with a JVC FY-F1030U digital camera.

3.2.4 Topro-3 staining

Narcotised larvae were moved into glass vials for fixation in 4% paraformaldehyde in 0.2M PBS buffer. Larvae were then given 3 rinses in 0.2M PBS to remove any remaining fixative. Post fixation larvae were incubated overnight in the dark at 4^{o}C in a solution of Topro-3 (Invitrogen), diluted 1:500 with 1% Triton X-100 (Fisher) in PBS. Specimens were very gently agitated throughout the overnight incubation on a specimen shaker. After incubation the larvae were given 5 washes, still in darkness, in 1% Triton X-100 in PBS for 10 minutes each wash. Larvae were then dehydrated through a graded methanol series and made transparent using Murray's Clear (a solution of 1 part benzyl alcohol to 2 benzyl benzoate (v/v) - referenced from (Dickie et al.)(2006), (product source: Sigma-Aldrich)). Finally larvae were mounted in Murray's Clear in a depression slide and viewed on the confocal laser scanning microscope using an argon laser for a 633nm excitation and emissions were visualised at 661nm.

3.3 Results

Observations were made of the velum of *Crassostrea gigas, Ostrea edulis* and *Lyrodus pedicellatus* larvae. The oral bands are described for each species investigated. These images should be viewed with the image keys provided in Table 0.3 and Table 0.4 in the **Abbreviations**. All descriptions of velar features are from observations of larvae from multiple broodstocks. All velar cilia described were present in all individuals, veliger and pediveliger, (across all broodstocks - corresponds to those listed in Table 2.1 - Table 2.5), provided the relevant region of the velum was observable.

3.3.1 *Crassostrea gigas*

The inner pre-oral band

The inner pre-oral band runs around the circumference of the velar surface, above the large pre-oral cirri and encircling the central apical tuft (Figure 3.2). The band is approximately 3-5 cilia wide at its densest points, forming a band usually less than 1µm wide. The cilia are between 10µm and 15µm in length, and do not appear stiff. In addition there is no indication of a beat direction, with the band lacking the metachronal wave seen in the pre-oral band, and no beat having been observed in live specimens. The transparent nature of the velum under the light microscope, combined with the beat of the pre-orals, made it difficult to resolve the inner pre-oral band in live animals.

The band of microvilli between the inner pre-oral cilia and the pre-oral cirri is composed of microvilli that are noticeably longer than those of the rest of the velar surface (Figure 3.3). This band of longer microvilli is approximately 5µm in width. There is a visible step in the microvillus epithelial surface directly above the pre-oral cirri (Labelled M2 on Figure 3.3) that signifies the beginning of the zone of longer microvilli.

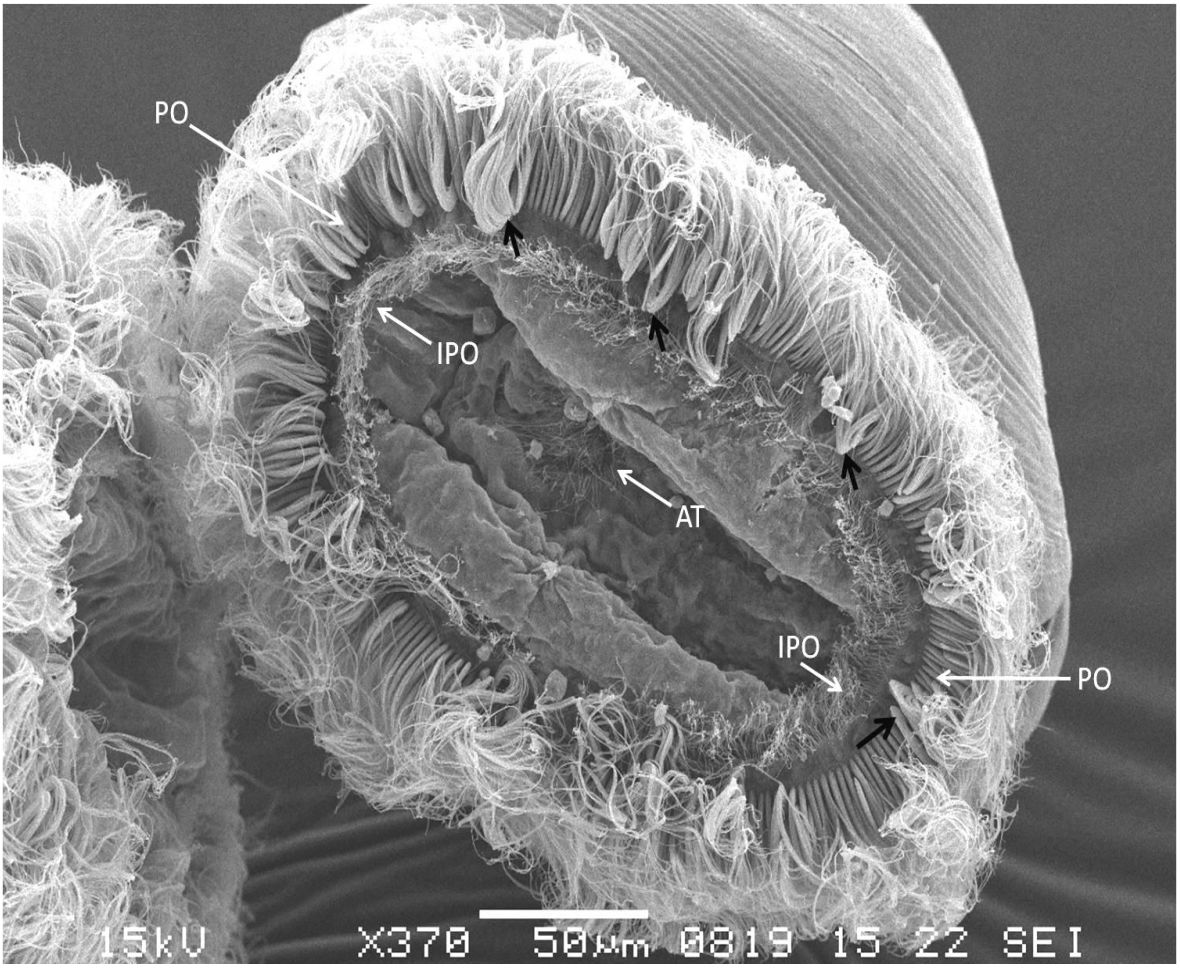

Figure 3.2 - *Crassostrea gigas* pediveliger stage larva with the velum extended.

This image is looking directly down onto the velum, showing the 3 types of cilia present on the upper region. The apical tuft (AT) is in the centre, the inner pre-oral row (IPO) runs around the edge of the upper surface and the large pre-oral row (PO) covers the top of the outer edge. Most of the pre-oral row is curved down over the ad-oral row. A few of the pre-oral cirri are bent back (black arrows) further than the cirri beside them, indicating these to be at a different stage of their beat, and possibly indicating the metachronal wave travelling around the velar edge. Note the inner pre-oral ring does not show any indication of beat, appearing limp or flat on the upper surface of the velum. This larva was imaged by SEM.

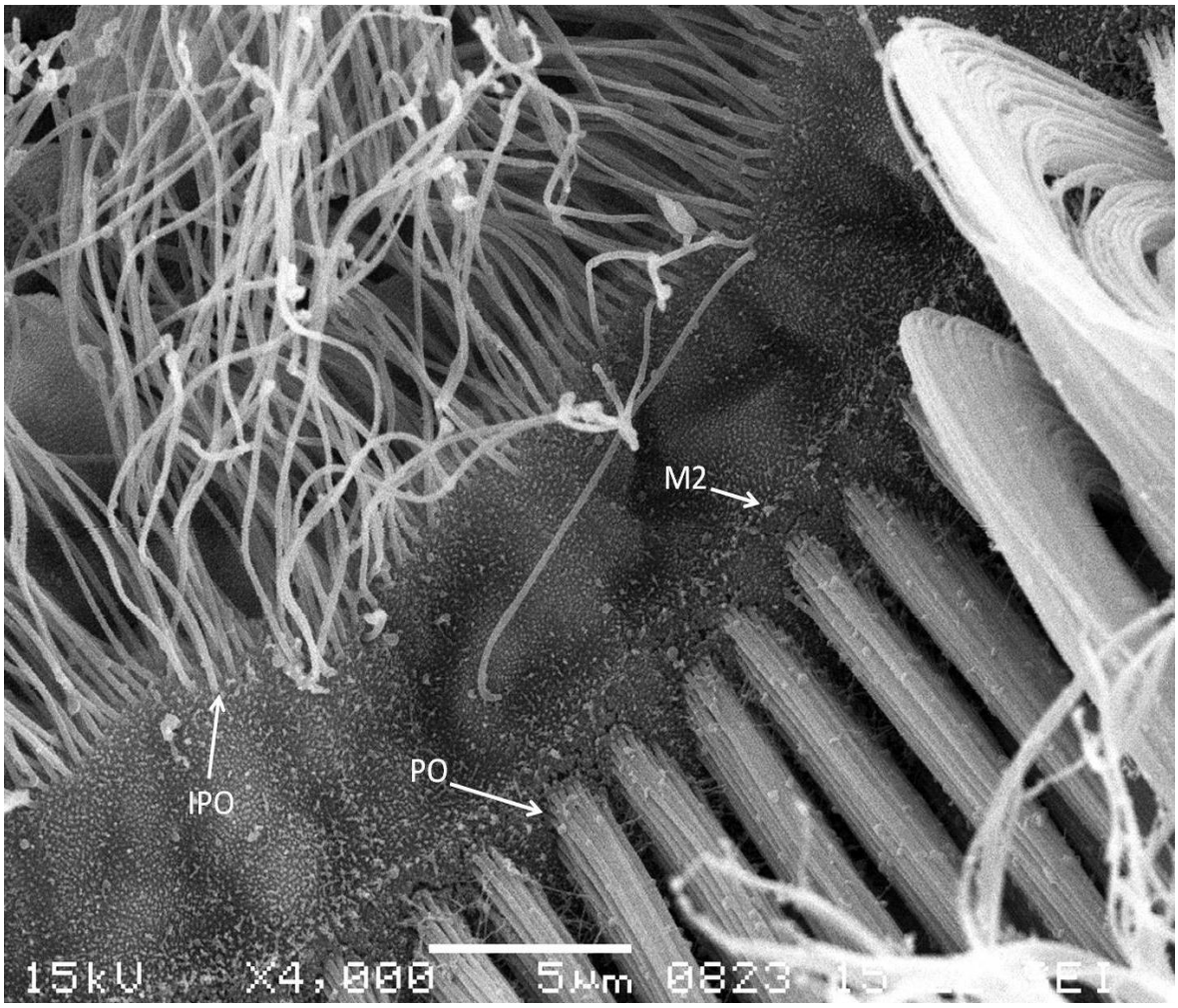

Figure 3.3 - detailed view of the inner pre-oral and pre-oral cilia bands of a *Crassostrea gigas* veliger.

The inner pre-oral band (IPO) is a row of simple cilia running around the top surface of the velum, about 5µm above the pre-oral band (PO). The microvilli between the two rows (M2) are longer than those on the rest of the velar surface, and there is a 'step' (marked by the M2 label) above the pre-oral cirri and before the inner pre-oral cilia. This boundary appears to mark the start of the zone of longer microvilli found in-between the IPO and PO rows. Note also the arched, beating, pre-oral cilia on the right of the image in comparison to the limp inner pre-oral row. This larva was imaged by SEM.

The pre-oral band

The pre-oral cirri dominate the velum, running around the top of the outer edge of the velum (Figure 3.2). The pre-oral band is composed of large compound cilia (cirri) made of multiple cilia (Figure 3.4) arising from two rows of cells, arranged in an alternating 'bricklaying' fashion along the velar edge (Figure 3.5). The total length of the cirri is approximately 50µm and 80µm. The veliger stage larvae examined generally had pre-oral cirri ranging from ~50µm to ~70µm, and pediveligers could range from ~60µm to ~80µm, although there was variation between individuals, reflected in the ranges given above, so it is difficult to quantify any increase in length within the ontogeny of the larval stages examined in this study. Furthermore it was difficult to accurately measure the pre-oral cilia, as it was rare to be able to see base to tip of any individual cirrus. The base each cirrus was 2-3 µm wide, equating to approximately 10 cilia.

The large cells from which the cilia arise are a diamond shape at the velar surface (Figure 3.5 and Figure 3.24), giving the cirri their blade-like appearance. Each cell giving rise to the cirri has between 110 and 140 cilia, the bases of which are visible in Figure 3.5, although each cirri splits giving the appearance of each pre-oral cirri blade being formed from only 20-30 cilia.

The splitting of the pre-oral cirri gives the cirri a 'ribbon-like' appearance towards the tips, such as those shown in Figure 3.4. This arises from the arrangement of the cilia forming each pre-oral cirrus, which split into more discrete units about a third of the way down the cirri length. These units take the form of thin lines, one cilia thick, but many wide, seen in Figure 3.4. These ribbons of cilia lay on top of each other to form the large pre-oral cirri that perform the power stroke. The cells bearing these cirri form a continuous line around the velar rim, broken only by the occasional microvilli arising between the cells bearing the pre-orals, as arrowed in Figure 3.5.

Staining with Topro-3 reveals the staggered arrangement of the cells bearing the pre-oral cirri seen in the SEM images. There are approximately 80 cells on the side of the velum imaged in Figure 3.6 (40 for each band).

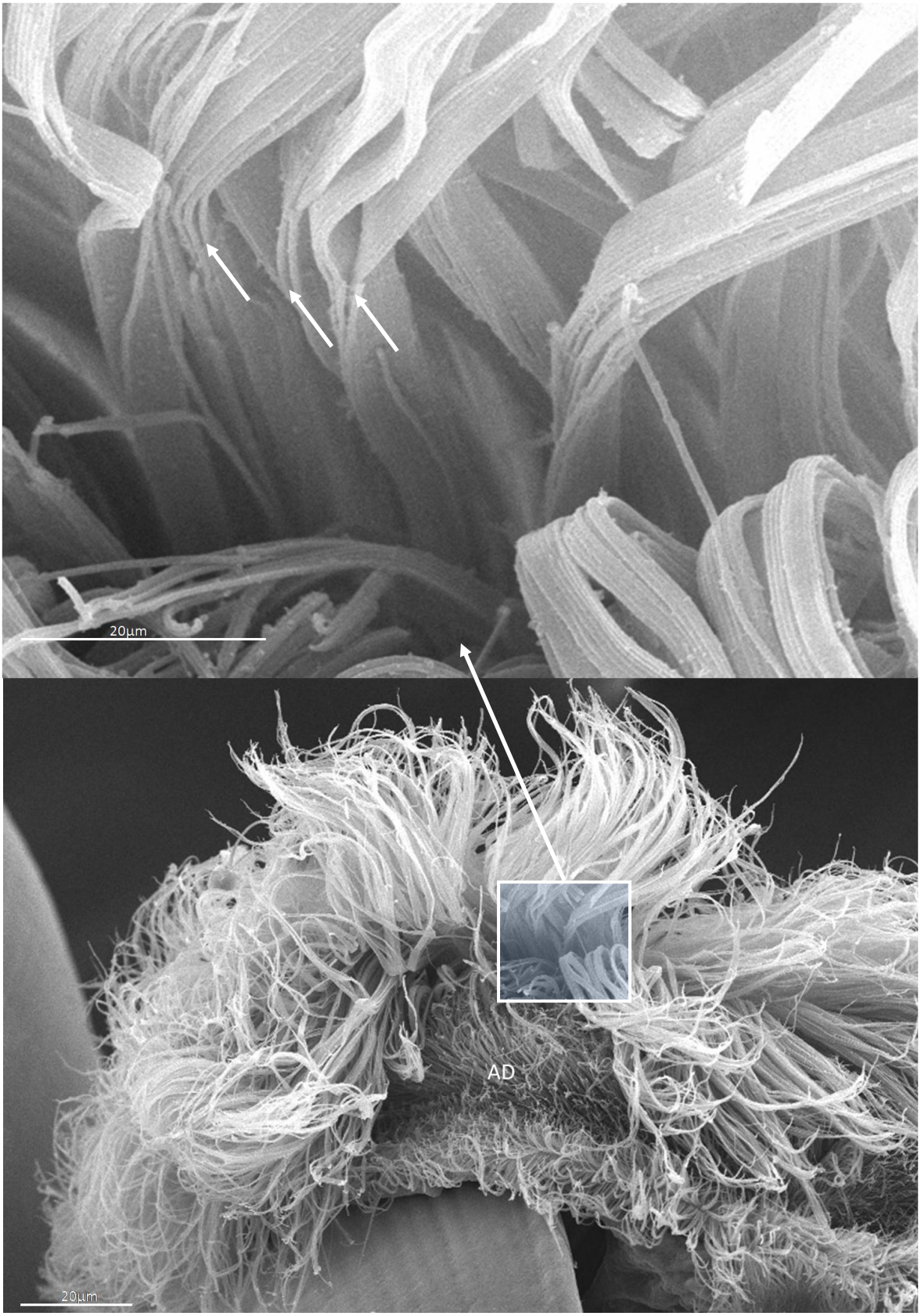

Figure 3.4 - Pre-oral cirri on the velar edge of a *Crassostrea gigas* veliger larva.

The upper image shows a detailed view of the pre-oral cirri splitting into thin, wide units of cilia to give their ribbon-like appearance at the tips. The cirri split about a 1/3 of the way along their length (the split is arrowed). The cirri are approximately 50-80 µm long. In the lower image the beat can be seen, the cirri in the centre having not quite completed the power stroke, exposing the ad-oral row (AD), whilst the pre-oral cirri to the left and the right are bent downwards at the bottom of their stroke. This larva was imaged by SEM.

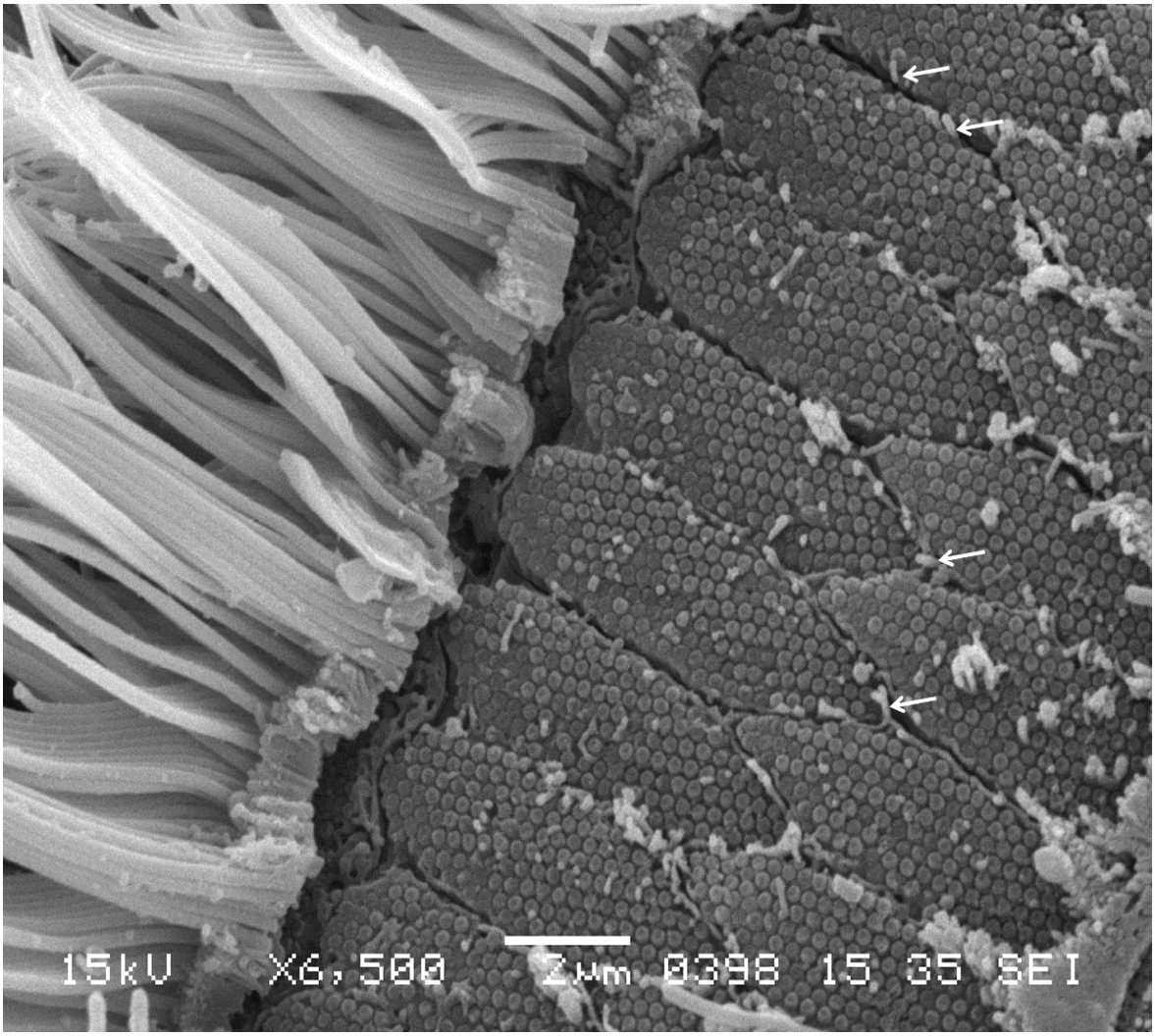

Figure 3.5 - The cells bearing the pre-oral cirri of a *Crassostrea gigas* larva.

The cells bearing the pre-oral cirri are visible after the removal of the cilia, exposing the basal bodies of the individual cilia emerging from the cells. The cells are arranged in two rows, arising in an alternating, 'bricklaying' pattern (see also diagram in Figure 3.24 for arrangement of cells bearing the ciliary bands). Counts of the cilia bases show each cell bears between 110 and 140 cilia making up the large cirri forming the pre-oral row. Microvilli occasionally appear between the pre-oral cells (arrowed). The pre-oral cilia were removed from a dehydrated larva using a glass needle and the velum then imaged by SEM.

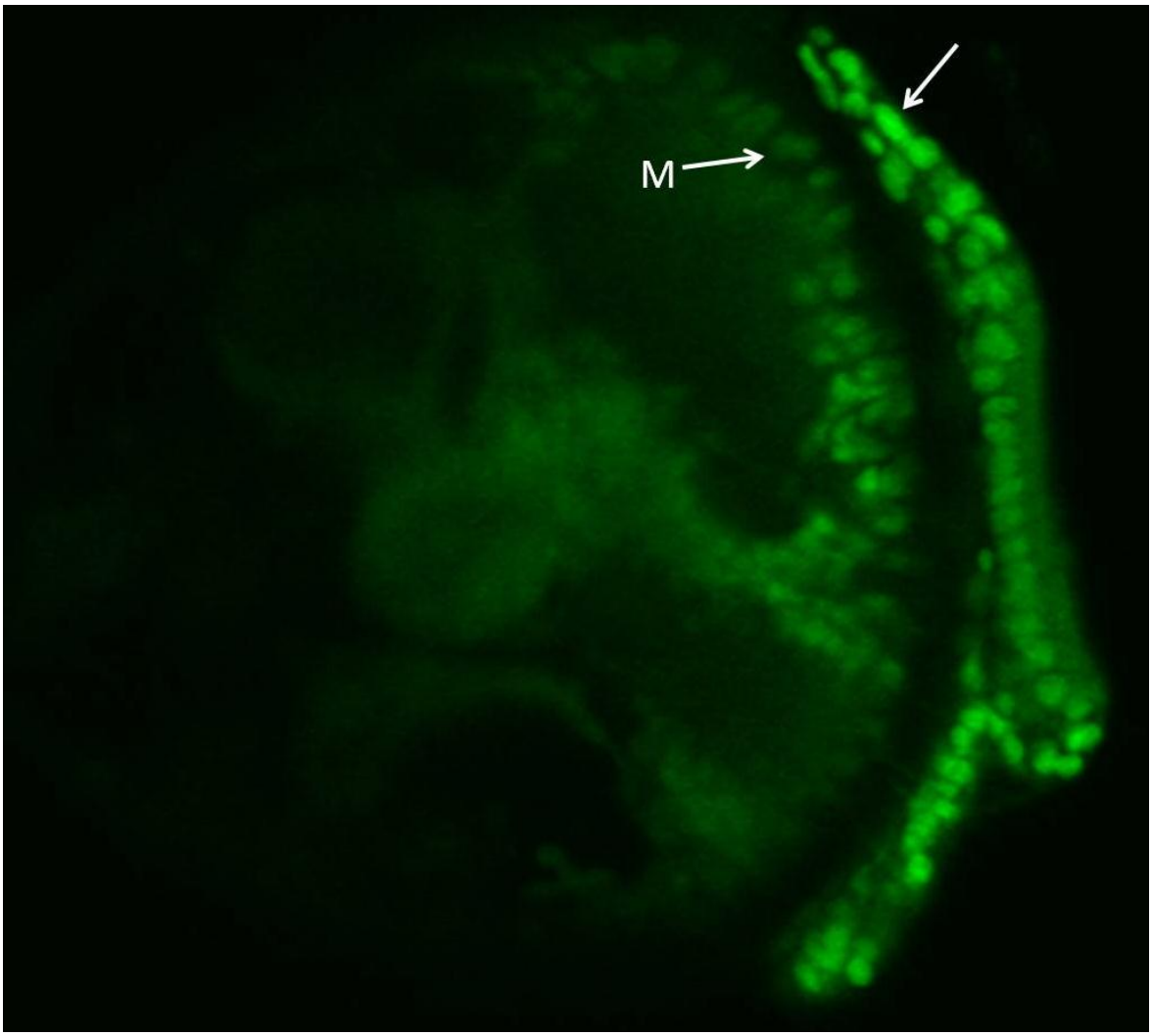

Figure 3.6- *Crassostrea gigas* larva with an extended velum stained with Topro-3.

Staining has revealed the nuclei of the large columnar cells bearing the pre-oral cirri on the velar edge (arrowed). The 2 rows of these cells, seen above in Figure 3.5, can be identified and approximately (precise counts are hampered by the folding of the velum) enumerated. Approximately 70 are visible on the edge imaged. Note also the cells bearing the C5 mantle ciliation (M). This larva was stained with Topro-3 and imaged on a Carl Zeiss LSM 510 confocal laser scanning microscope.

The minor pre-oral band

Located directly under the large pre-oral cirri is a single band of smaller cirri that comprise the minor pre-oral band. The band appears from early veliger and persists until metamorphosis. This band is located 1µm below the pre-oral band and 1µm above the adoral tract as shown in Figure 3.7 and is usually bent down over the top of the adoral tract, indicating this to be the probable direction of beat when live. The cirri of the minor pre-oral band are approximately 15µm-20µm in length and arise from a band of rectangular cells which are 4µm by 15µm, arranged lengthways along the rim (Figure 3.8). Figure 3.8 & Figure 3.9 show this band to be located between the diamond shaped cells of the pre-oral band and the less distinct cells of the adoral band. Each individual cell of the band gives rise to around 120 cilia: these then form the blades of the minor pre-oral cirri. Each of the cirri blades are comprised of around 20 cilia, resulting in around 6 minor pre-oral blades arising from each cell, shown in Figure 3.8.

The minor pre-oral cirri arise from columnar cells which, while smaller than those of the pre-oral band (Figure 3.7) are significantly larger than those of the adoral band. The cilia of the band arise through the microvillous surface of the velum - the microvilli are small branching structures which can be seen in Figure 3.10 covering the basal bodies at the base of the cilia, and have fine strings of mucus wrapped around the tips. Most of the branching microvilli occur between the oral bands of the velum, with individual un-branched microvilli such as those arrowed in Figure 3.5 arising around the bases of the cilia forming oral rows.

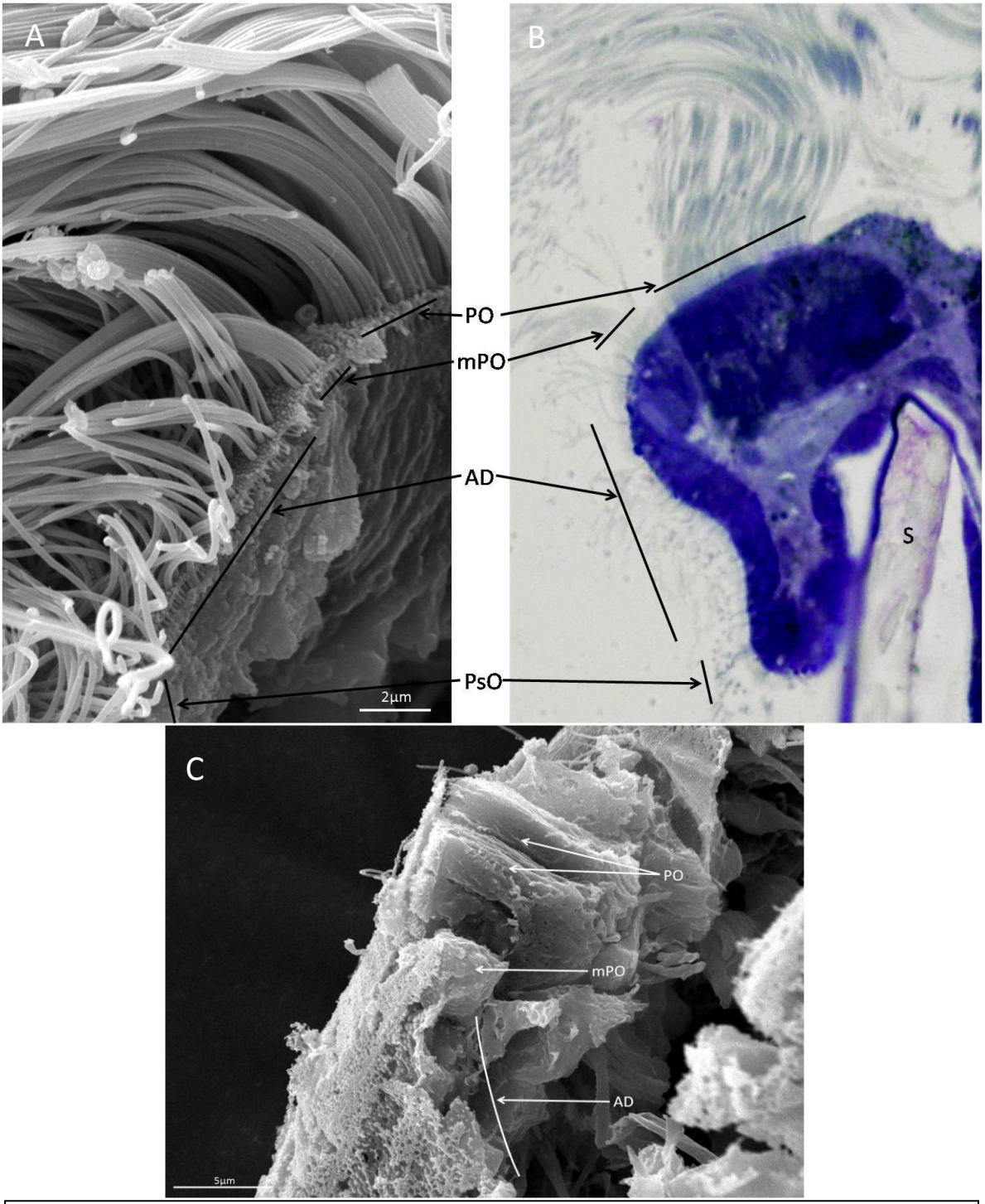

Figure 3.7 - Sections of *Crassostrea gigas* velum showing minor pre-oral and pre-oral bands.

A is an SEM image of a sectioned velum showing the presence of the minor pre-oral band (mPO) under the pre-oral band (PO) and above the adoral band (AD). The mPO is separated by ~1µm from both of the other oral rows. Image B is a light microscope section of the same area of the velar edge. The large columnar cells bearing the pre-oral cirri are obvious. The minor pre-oral cirri are carried by columnar cells which are slightly smaller than those of the pre-oral cirri but larger than those bearing the adoral cilia. The post-oral cirri (PsO) and their cells are just visible at the bottom curve of the velar edge, being of a similar size to those carrying the minor pre-oral cirri. The lower SEM image of a broken, deciliated velum shows the cells giving rise to the pre-oral and adoral bands seen in the sections above, these columnar cells being shorter than those of the pre-oral band but much bigger than those bearing the adorals.

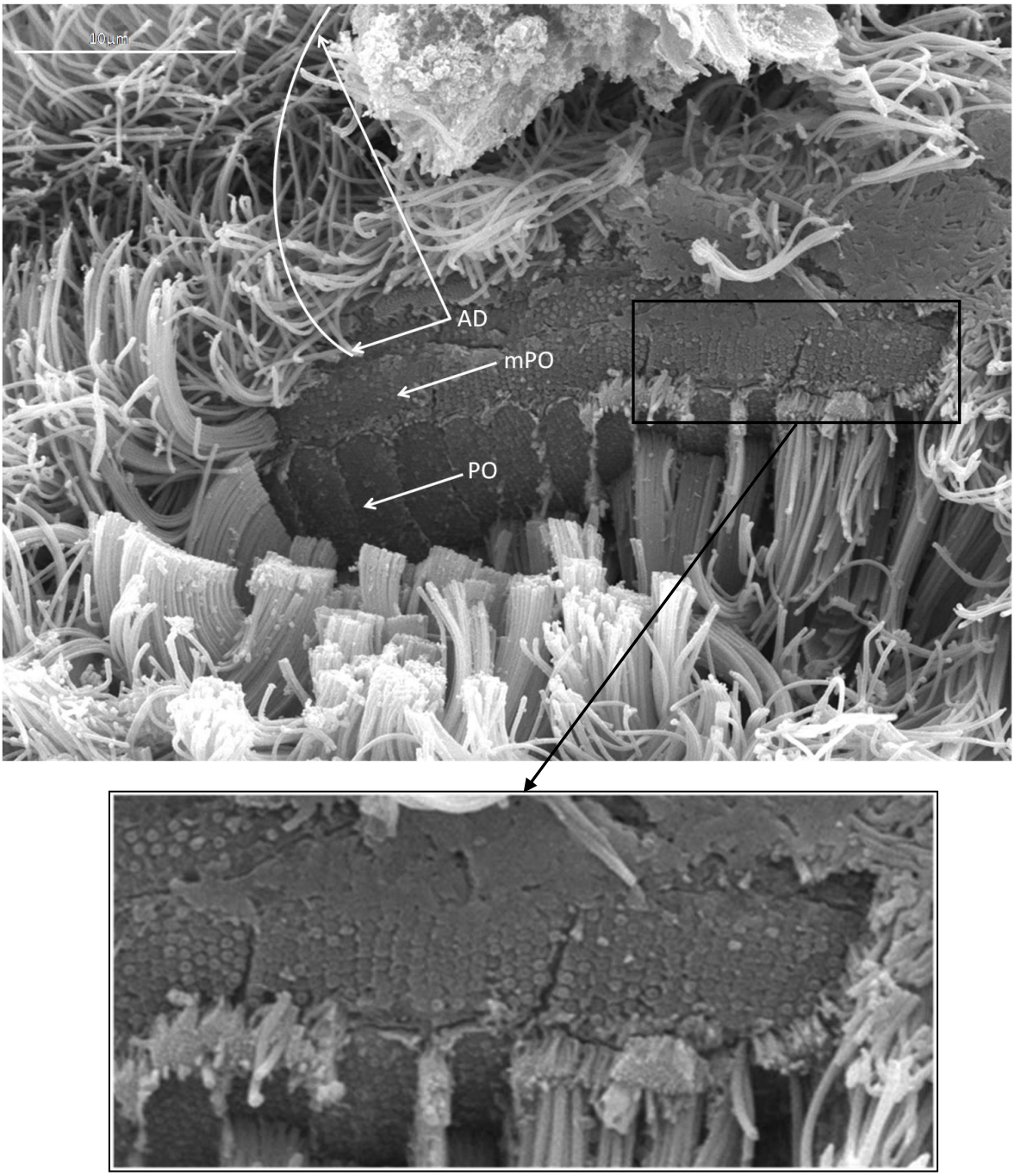

Figure 3.8 - *Crassostrea gigas* veliger velum showing pre-oral and minor pre-oral bands.

The arrangement of cells for the oral cilia bands can be seen above. The minor pre-oral band (mPO) is distinguishable from the cells bearing the cilia for the pre-oral cirri band (PO) and the individual adoral cilia (AD). The cells of the mPO band are approximately 4µm deep, as opposed to those of the pre-oral which are approximately 8µm. The minor pre-oral row cells are much wider than the cells of the pre-oral row (see inset) with one cell width being equal to up to ~3 pre-oral cells. This larval velum was scraped with a glass needle following dehydration then imaged by SEM.

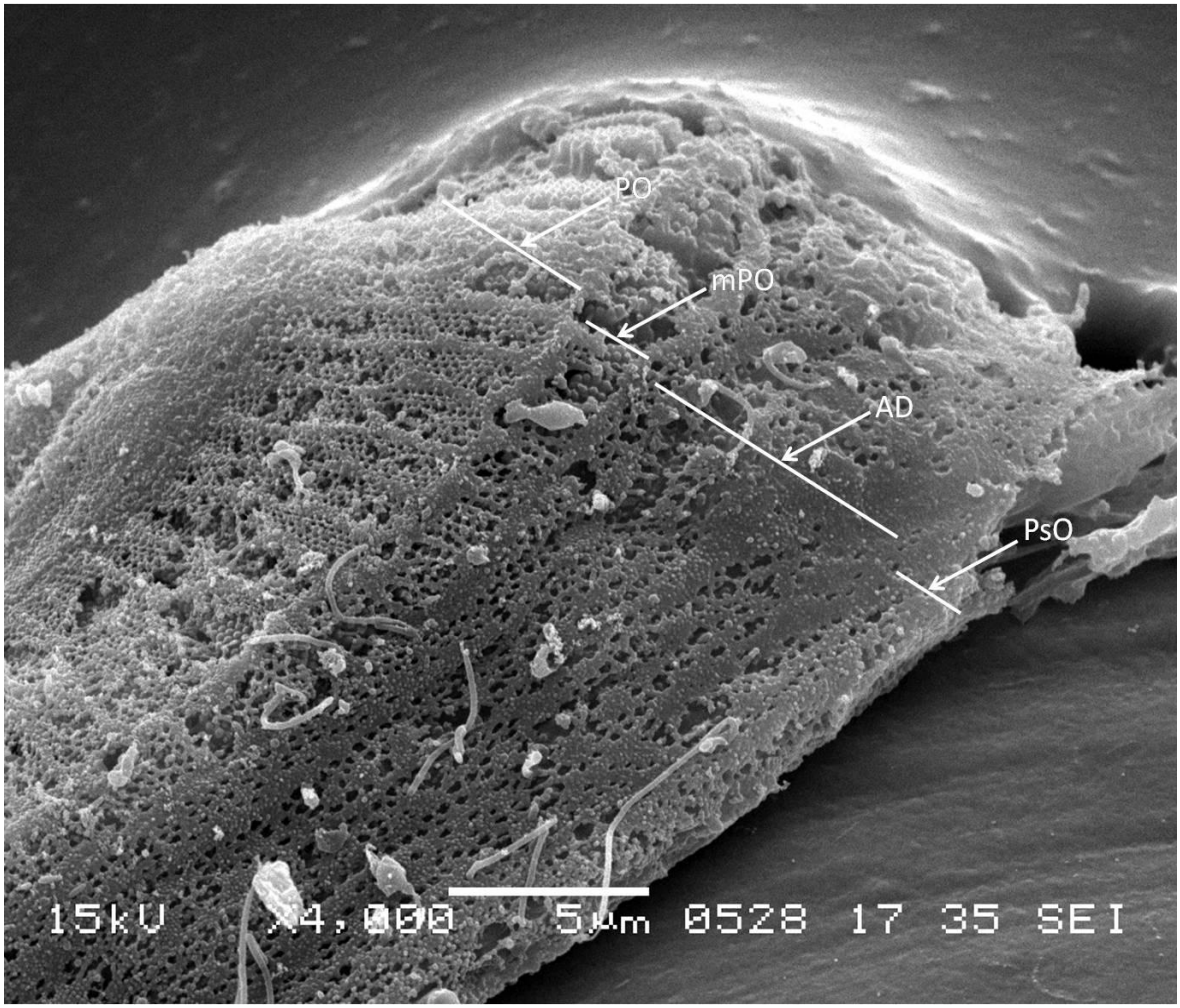

Figure 3.9 - Deciliated velum of a *Crassostrea gigas* veliger.

The holes indicate where the bases of the cilia comprising the oral bands emerge and reveal the arrangements of bands around the velar edge. 2 rows of pre-oral cells (PO) are followed by a narrow band of minor pre-oral cilia (mPO) bases, then the scattered cilia of the adoral band (AD), followed by the final post-oral band (PsO). This larva was deciliated with tape and imaged by SEM.

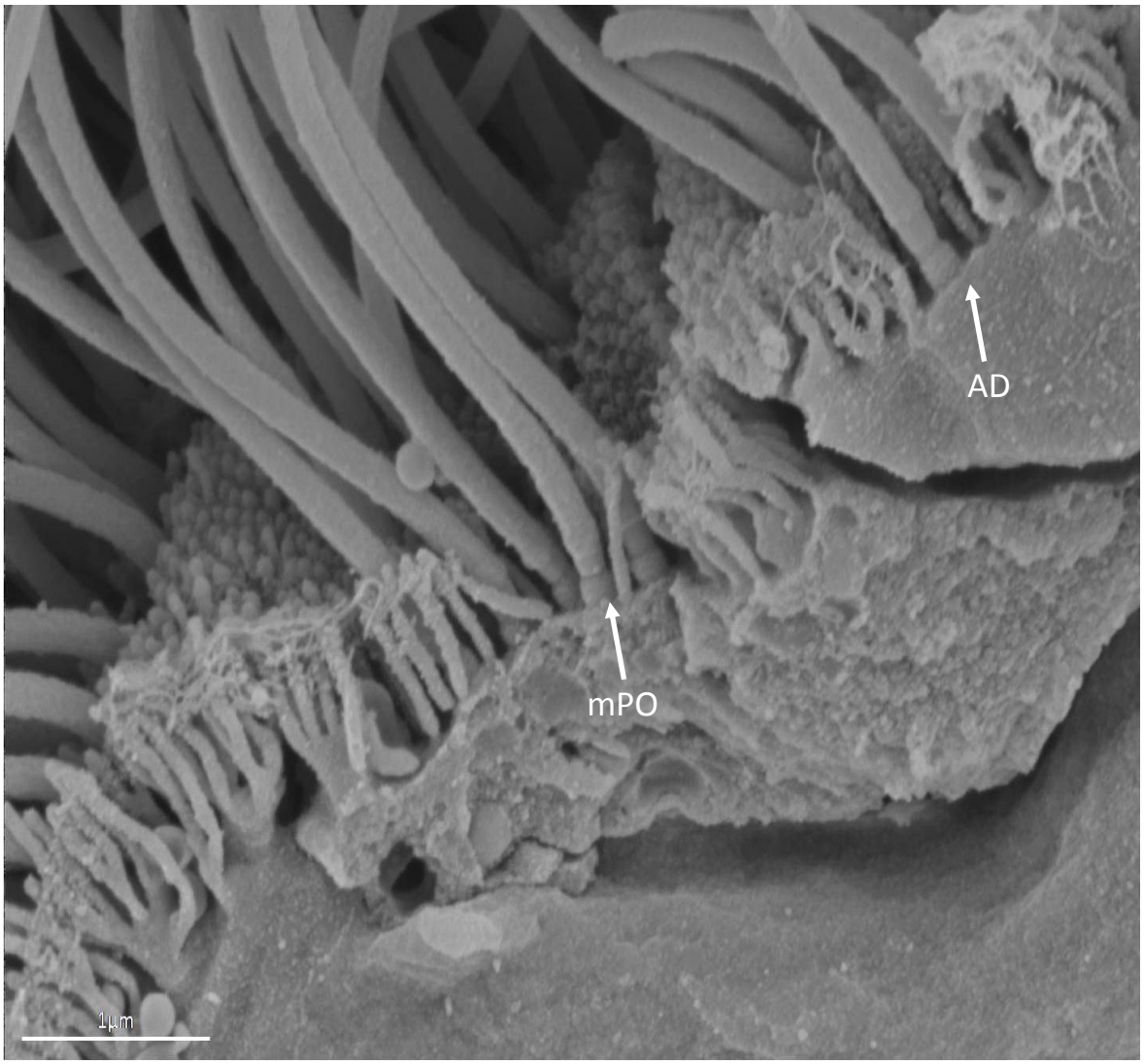

Figure 3.10 - Minor pre-oral cilia of a *Crassostrea gigas* veliger.

The joint of the cilia to the cell and the basal body at the surface of the cell can be seen. The microvilli covering the surface and emerging between the groups of cilia can be seen as branching structures, with fine strands of mucus running between the tips. This larva was dry fractured with liquid nitrogen and imaged by FESEM.

The adoral band

The adoral band runs around the edge of the velum (Figure 3.11) and is composed of scattered individual cilia, not the cirri blades of the previous two bands. The cilia are approximately 10µm in length and there is often a distinct tract in the centre of the group which is visible in Figure 3.11 and Figure 3.4, showing the direction of beat around the velum towards the mouth. The band of cilia is around 30-40µm wide by the late veliger stage larvae, although this varied between individuals. The band of the pediveliger was comparable in width.

Observations of fluorescent beads in the water around the pre-oral cirri revealed the acceleration of particles as they approach the velum and the beat of the adoral cirri towards the mouth as particles are deflected onto this row and then moved around the velar edge (Figure 3.12). In Figure 3.12 the captured bead can be seen to travel anteriorly along the tract towards the mouth. This particle was seen to be rejected once it arrived at the mouth, although the larval gut contained many beads that had been ingested. Note also in Figure 3.12 there are a few pre-oral cirri directly above the mouth that do not appear to beat during this sequence of video frames when pre-oral cirri next to them (to the right in these images) can clearly be seen beating throughout.

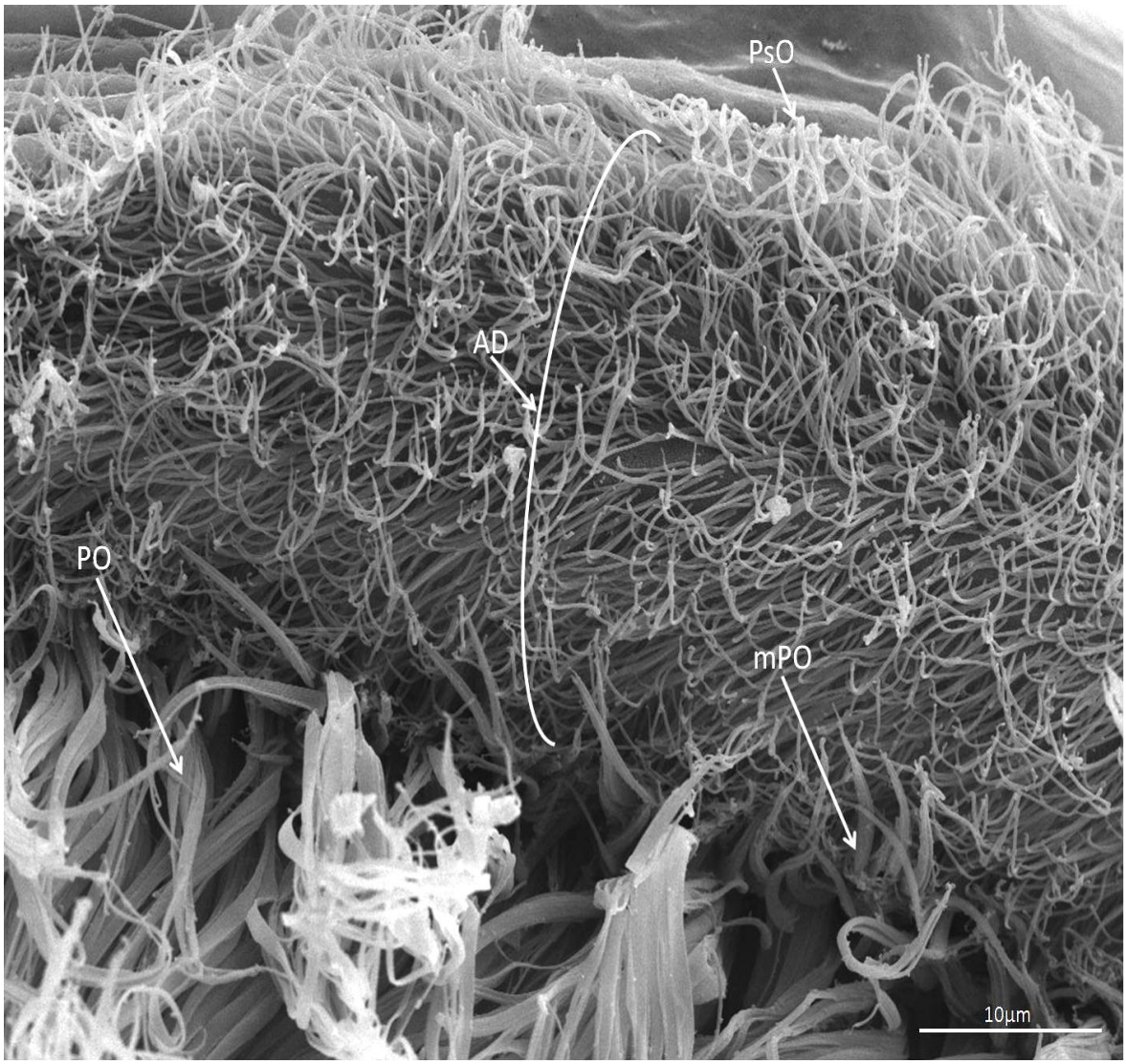

Figure 3.11 - The ad-oral band of a *Crassostrea gigas* veliger.

The ad-oral band (AD) forms a wide tract over the edge of the velum, composed of comparatively short 10µm cilia. The direction of the fixed cilia illustrates the beat, forming a line along the centre of the tract beating towards the mouth. The post-oral cirri (PsO) are also visible, bent over towards the adoral band indicating the beat direction. This larva was imaged by SEM

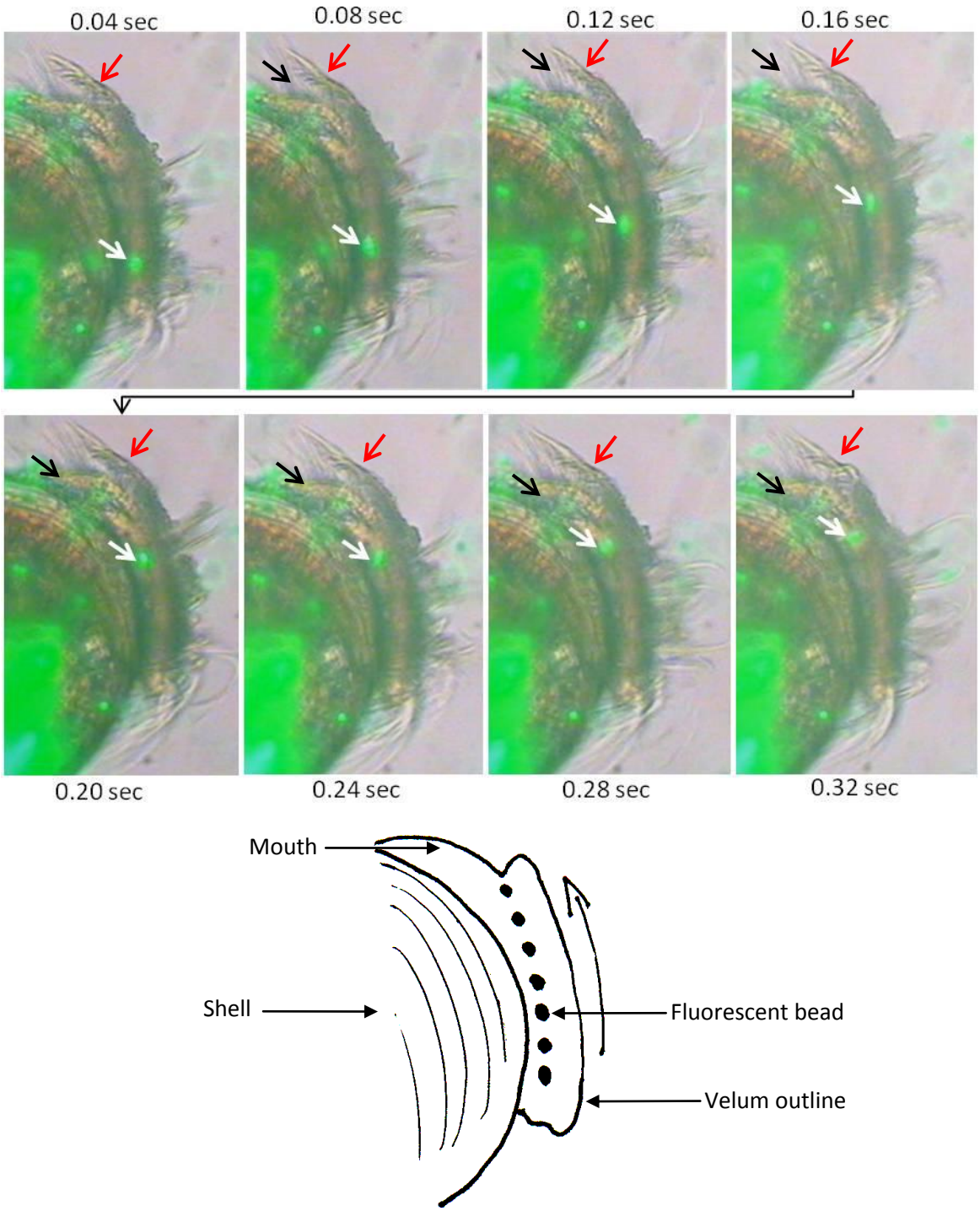

Figure 3.12 - Video frames showing particle capture and particle movement along the ad-oral band of a *Crassostrea gigas* veliger velum.

Sequence of images showing an amalgamation of 3 fluorescent beads after capture by the pre-oral cirri being moved along the adoral tract towards the mouth (black arrow). The large area of fluorescence at the bottom left of the image is beads which have been previously ingested by the larva, and are in the stomach or intestine. Note the pre-oral cirri above the mouth (red arrow) that do not beat during this sequence. The diagram below the time series is a copy of the larva in the images, the line of black dots and arrow above indicate the passage of the beads along the ad-oral tract towards the mouth. This image sequence is composed of individual video frames from an MPEG video captured on a Nikon Coolpix 4500, mounted on a compound microscope and illuminated with a mercury light.

The post-oral cirri band

The post-oral band is a single band of cirri, shown in Figure 3.13, directly below the adoral tract. Each cirrus is comprised of 5-30 cilia (this varied widely between individuals, and could only be estimated as the bases could not be counted as for the pre-oral and minor pre-oral bands), around 15µm-20µm in length and arising from a single band of cells on the lower edge of the velar rim. In most individuals these cirri were bent towards the adoral band, as in Figure 3.11, suggesting this as the direction of beat. In some specimens the band was laying back onto the surface of the shell.

Apical tuft cilia

The apical tuft was located in the centre of the velum on the upper surface (Figure 3.3 and Figure 3.14). It is formed of a dense group of cilia of approximately 20µm in length. Figure 3.14 shows that there appears to be a round, central group of cilia which may be slightly shorter, surrounded by an outer ring of cilia. No specialised bases were observed, although the top surface of the velum was often enfolded, making observations of the tuft, and especially the cilia bases, very difficult.

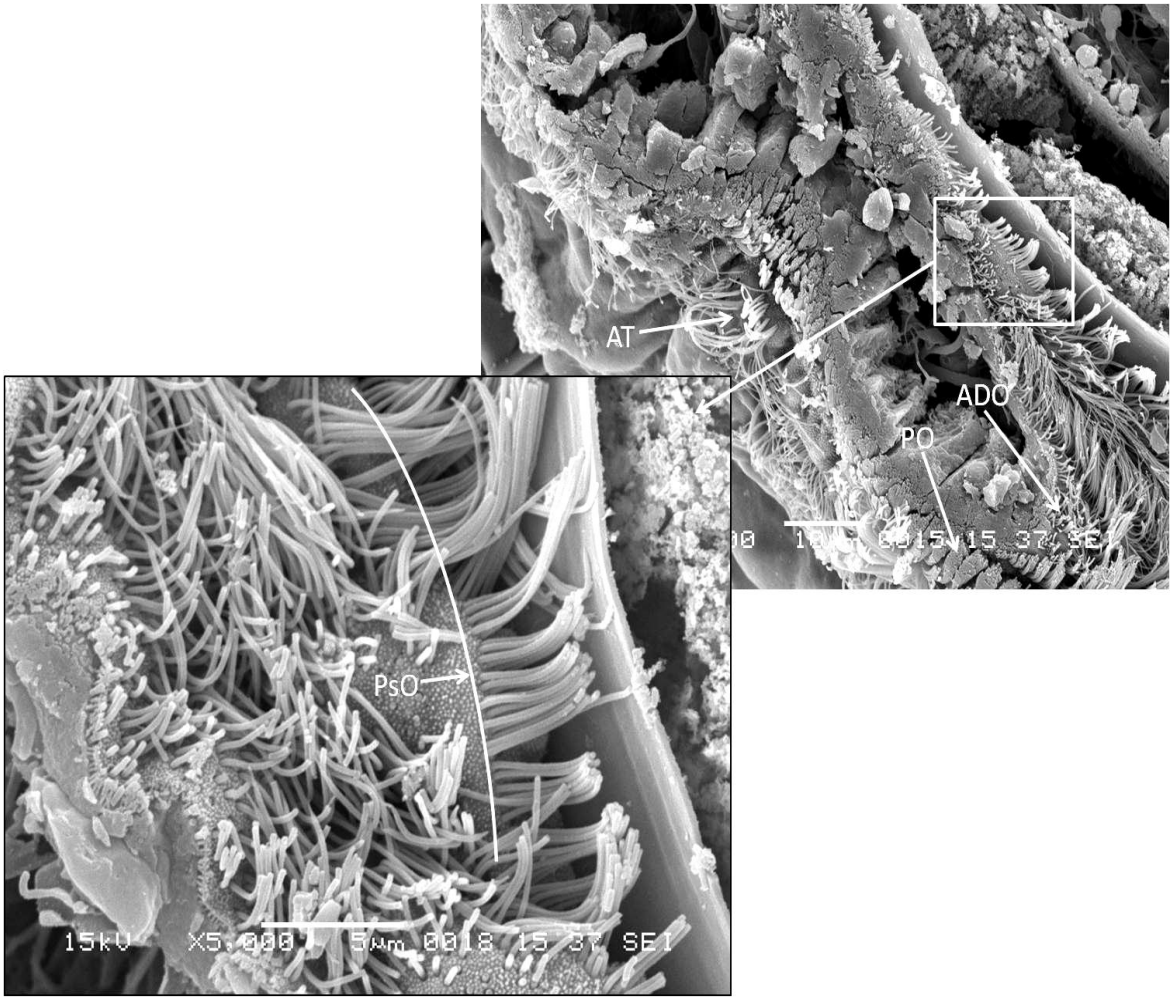

Figure 3.13 - Post-oral cilia band on a *Crassostrea gigas* velum.

This larva had been partially sectioned, obliquely cutting the velum to reveal the pre-oral, minor pre-oral, adoral and post-oral (PsO) bands visible in the lower magnification image at the top. The post-oral band can be seen beneath the ad-oral tract. The cilia are arranged in a similar manner to the minor pre-orals, with a single line of cells running along the lower edge of the velum, giving rise to the band of post-oral cirri. This larva was imaged by SEM.

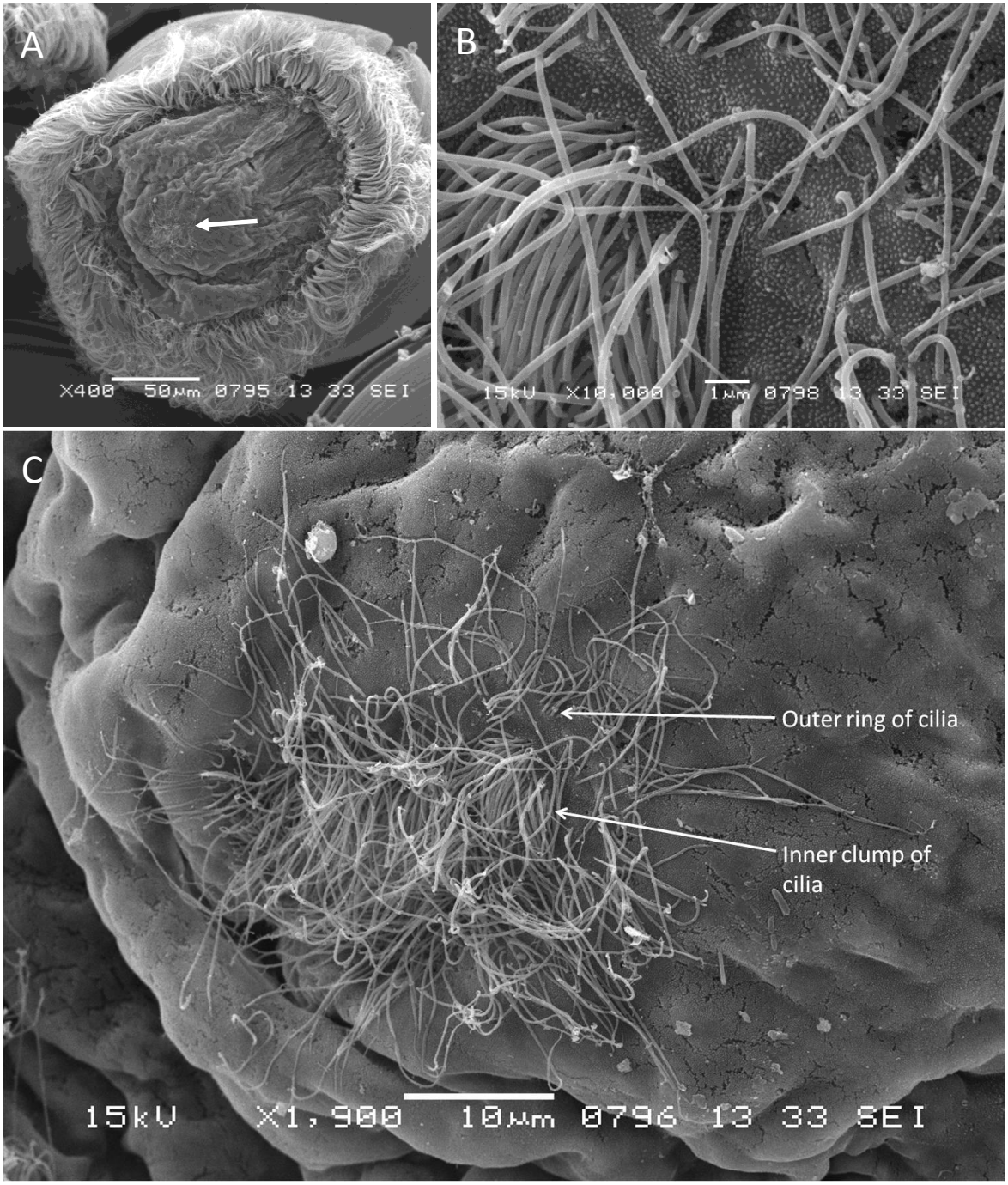

Figure 3.14 - Apical tuft on the velum of a *Crassostrea gigas* veliger larva.

The apical tuft is located in the centre of the velum (shown in image A), formed of a dense central clump of cilia and an outer ring (image C), but the cilia of the tuft appear to lack any specialised bases (images B and C). The cilia are approximately 20µm in length, do not appear stiff in appearance after fixation and occasionally feature discocilia artefacts. This larva was imaged by SEM.

Serotonin and catecholamines in the velum

The outer rim of the velum in Figure 3.15 and Figure 3.16 shows a strong serotonin signal after staining. There is a fibre running around the top outer edge where the pre-oral cilia were located. This fibre was interspersed at several points by spots of strong signal, seen in the image sequence in Figure 3.16, likely from specific cells along the top edge of the mantle rim.

There is another fibre running along the lower edge of the velum, arrowed in Figure 3.15, through the location of the post-oral cirri. Post-oral cells giving off strong localised signals were also observed in larvae with fully extended velums. These cells are also labelled in Figure 3.16, and are shown by those arrows with the solid heads.

Catecholamine fluorescence may be localised to a few cells of the velar rim. However, glutaraldehye induced methods generally produced a poor catecholamine signal in comparison to the results obtained for the mantle ciliation, and while images are suggestive of localised signal in the velar rim (Figure 3.17), further work will be required to verify these results.

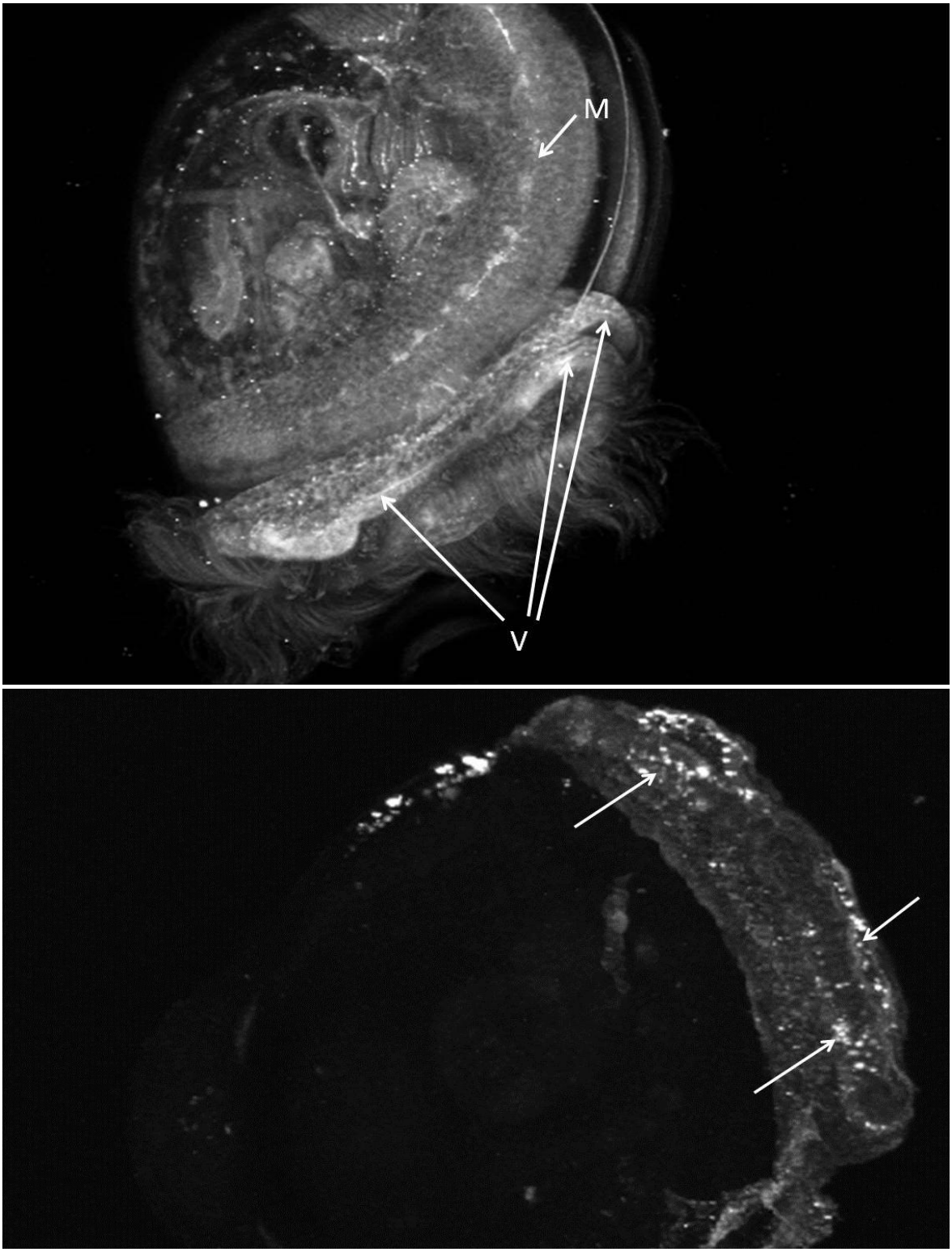

Figure 3.15 - Serotonin signal from the velar rim of two *Crassostrea gigas* larvae.

A single fibre runs around the top edge of the velum, interjected regularly by dense spots of signal, likely from specific cells. In the top image a fibre emitting a serotonin signal can also be seen running around the lower edge of the velum, through the location of the post-oral ciliary band. Specimens were observed in a Carl Zeiss LSM 510 confocal laser scanning microscope using a 488 nm argon laser, emission collected at 530 nm. The images above are comprised of a series of optical sections, projected as a 3 dimensional image using Zeiss LSM Image Browser, from which a 2D image is produced.

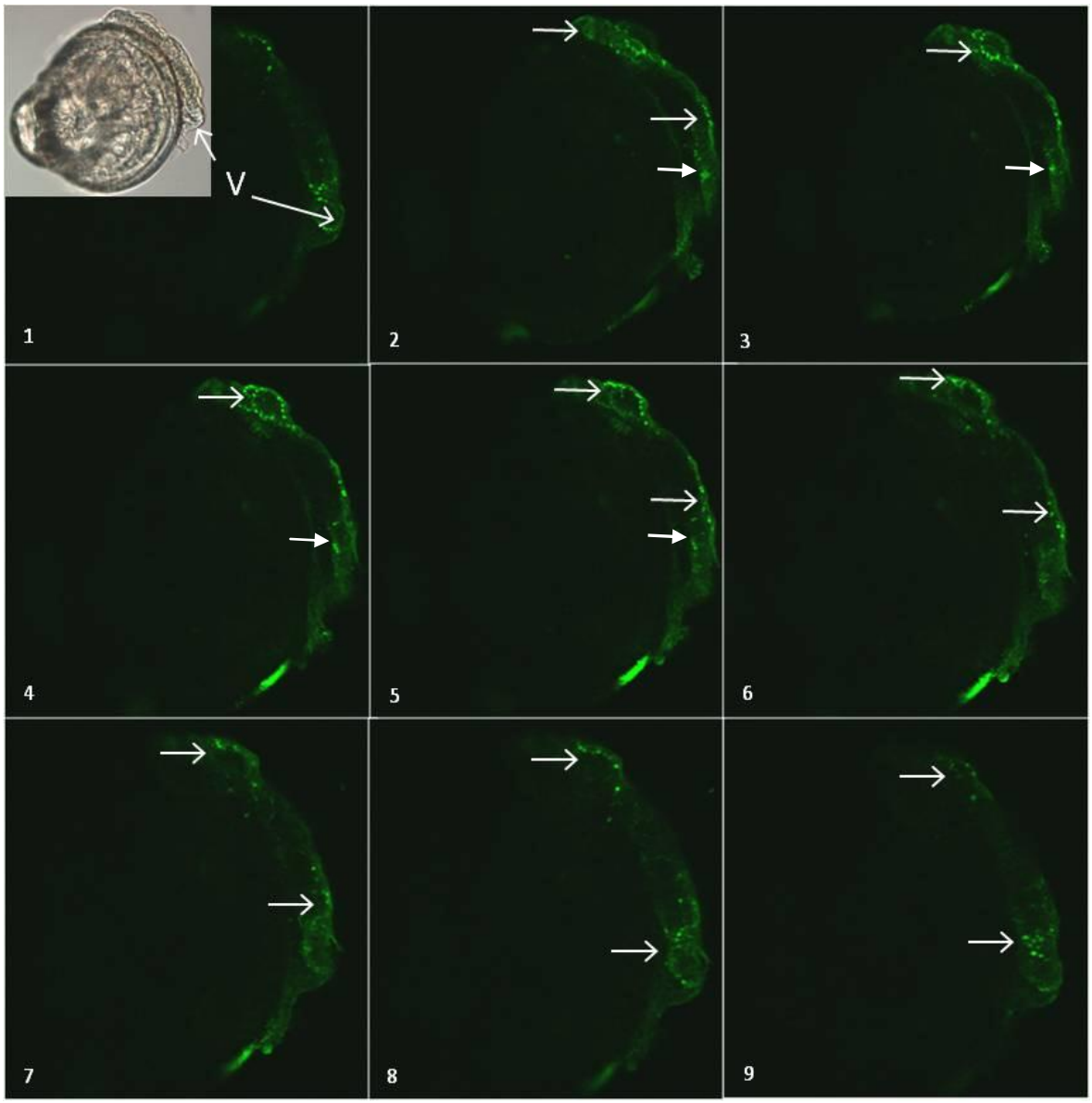

Figure 3.16 - Sequence of optical sections showing serotonin signal from the velar rim of *Crassostrea gigas* pediveliger

This image is a series of optical sections, numbered 1-9, stepping down through the larva revealing a ring of serotonin signal from the upper edge of the velum, in the locations of the pre-oral row (open headed arrows) and the post-oral row (solid headed arrows). Note the brightfield image of the same specimen prior to starting optical sectioning with the laser. This is provided for orientation, and reveals the larva to have its velum partially extended. The same area of the velum is labelled on the brightfield and laser image, again for orientation. Specimens were observed in a Carl Zeiss LSM 510 confocal laser scanning microscope using a 488 nm argon laser, emission collected at 530 nm.

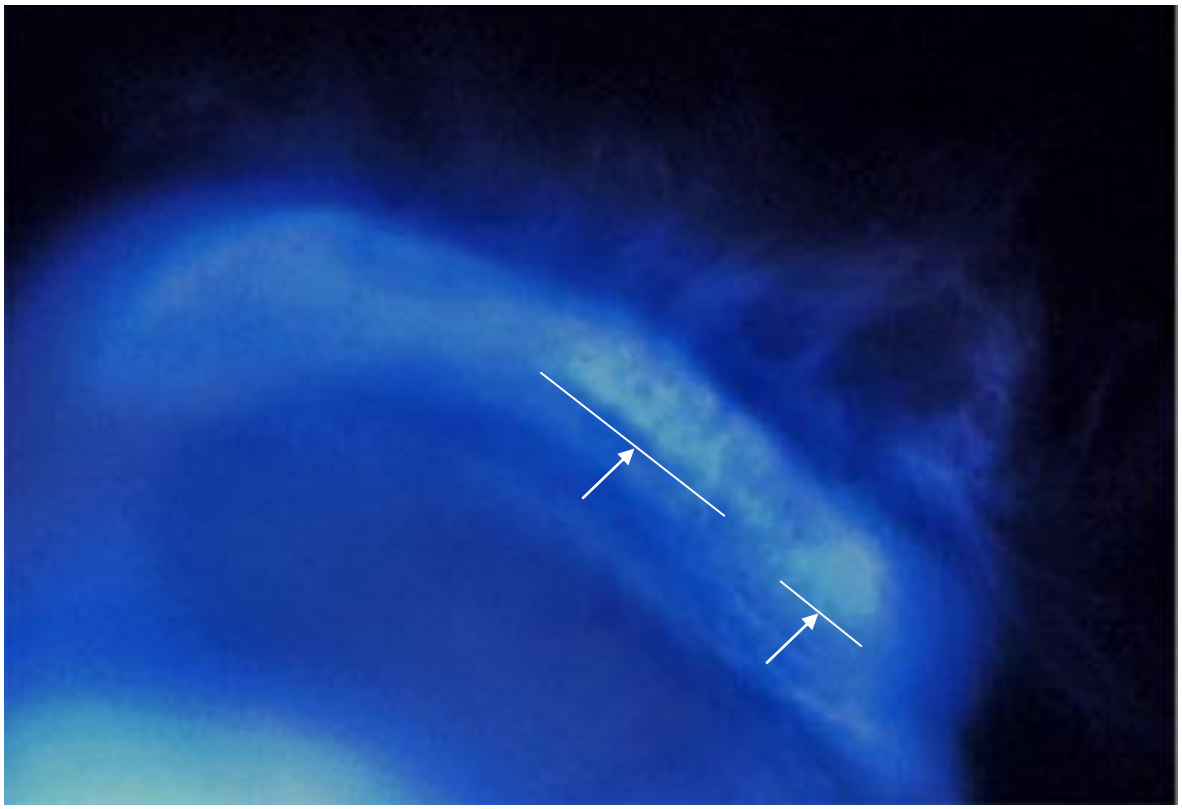

Figure 3.17 - weak catecholamine fluorescence in the velum of a *Crassostrea gigas* pediveliger.

The catecholamine fluorescence appears to be localised to cells in the region of the pre-oral cirri on the top edge of the velum, although signal from catecholamines was generally weak in comparison to the mantle cells. This image was captured on a Carl Zeiss LSM 510 confocal laser scanning microscope with AxioCam HRc camera using a 488nm long pass barrier and 355-425 nm excitation.

3.3.2 Ostrea edulis

The inner pre-oral band

The inner pre-oral band runs around the top of the velum, just above the velar rim and above the line of pre-oral cirri (Figure 3.18). The inner pre-oral band is composed of individual cilia arranged into a band that is never more than 4 cilia deep. The cilia are not stiff, and provide no indication as to a beat direction or coordinated metachronal movement. A discernible beat pattern was not observed in live larvae. The cilia of the band are approximately 10µm in length. The microvillus surface of the velum shows a marked change between the pre-oral cilia and inner pre-oral band with a distinct step (shown in Figure 3.18 and Figure 3.22) above the pre-oral band leading into a 5µm wide strip of longer microvilli running up to the inner pre-oral band.

The pre-oral cirri band

The pre-oral cirri run around the top outer edge of the velum (shown in Figure 3.19) and are broadly the same as the description already provided for *Crassostrea gigas*. These large cirri are composed of 110-140 cilia, with these cilia arising from cells on the top of the outer edge of the velum (Figure 3.20). Each cirrus is approximately 2-3µm (10 cilia) wide and ≈80µm in length, long enough to cover the adoral tract at the bottom of their down stroke (Figure 3.19). The cirri arise from 2 rows of cells arranged in the same alternating bricklaying pattern seen in *C. gigas*. The cells have a diamond shaped appearance at the surface of the velum, giving the pre-oral cirri a more hydrodynamic blade-like shape when all the cirri are gathered closely together. This is especially evident when the blade is bending on its down-stroke or return-stroke as seen in Figure 3.19. The cilia comprising each cirrus appear to 'stack' as the blade forms.

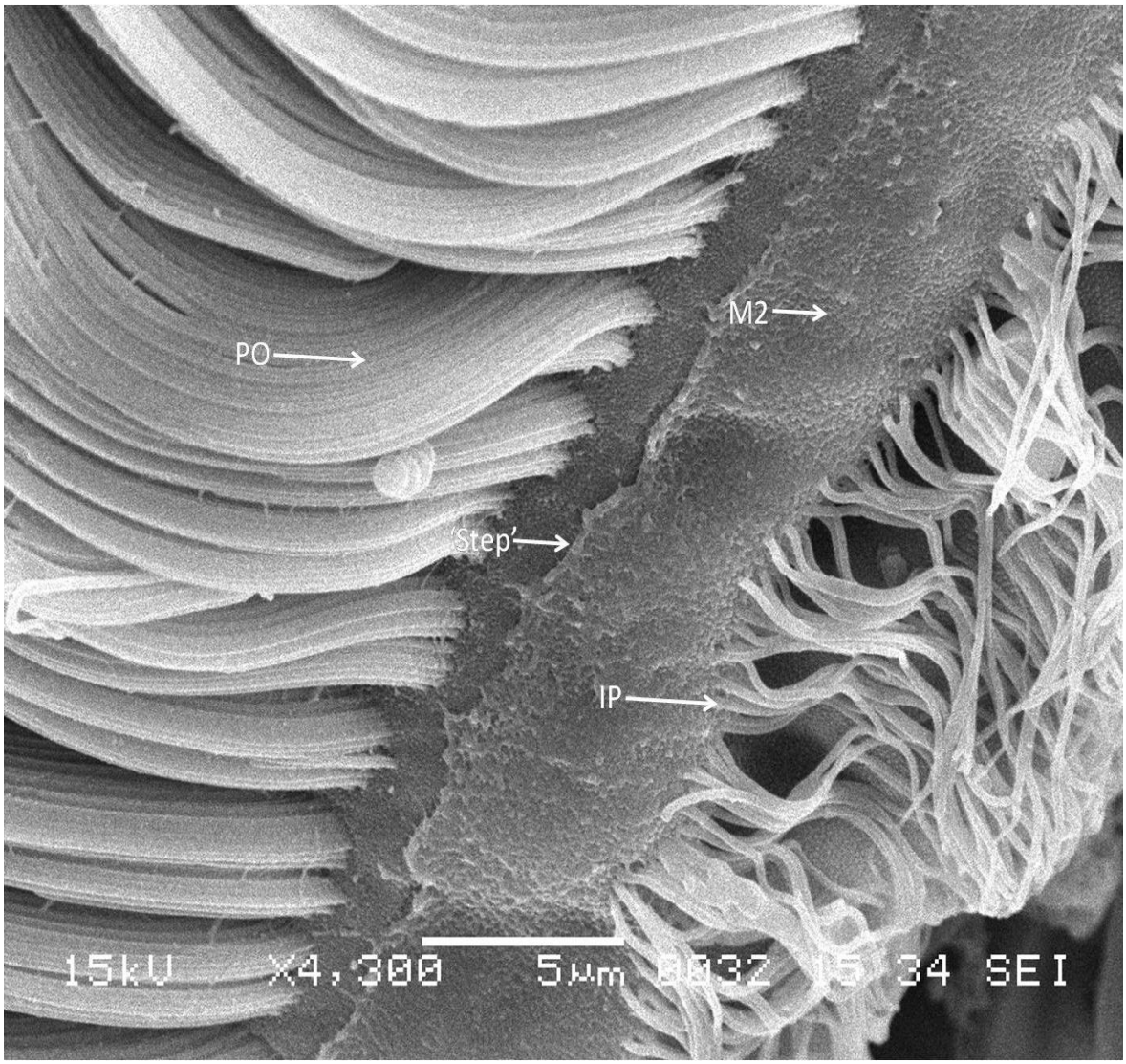

Figure 3.18 - high magnification image of the pre-oral and inner pre-oral ciliary bands on an *Ostrea edulis* pediveliger stage larval velum.

The inner pre-oral band of cilia (IP) occurs on the surface of the velum, above the pre-oral band (PO). This inner pre-oral band is formed of a single row of cilia, not collected together into cirri. These cilia appear limp following fixation, and lay back onto the surface of the velum, orientated away from the pre-oral cirri. Between the pre-oral and inner pre-oral band there is a 5µm wide region of microvilli which are longer (M2) than those found on the rest of the velar surface. There is a distinct step (labelled) marking the start of this region of longer microvilli. The longer microvilli stop at the inner pre-oral row. This larva was imaged by SEM.

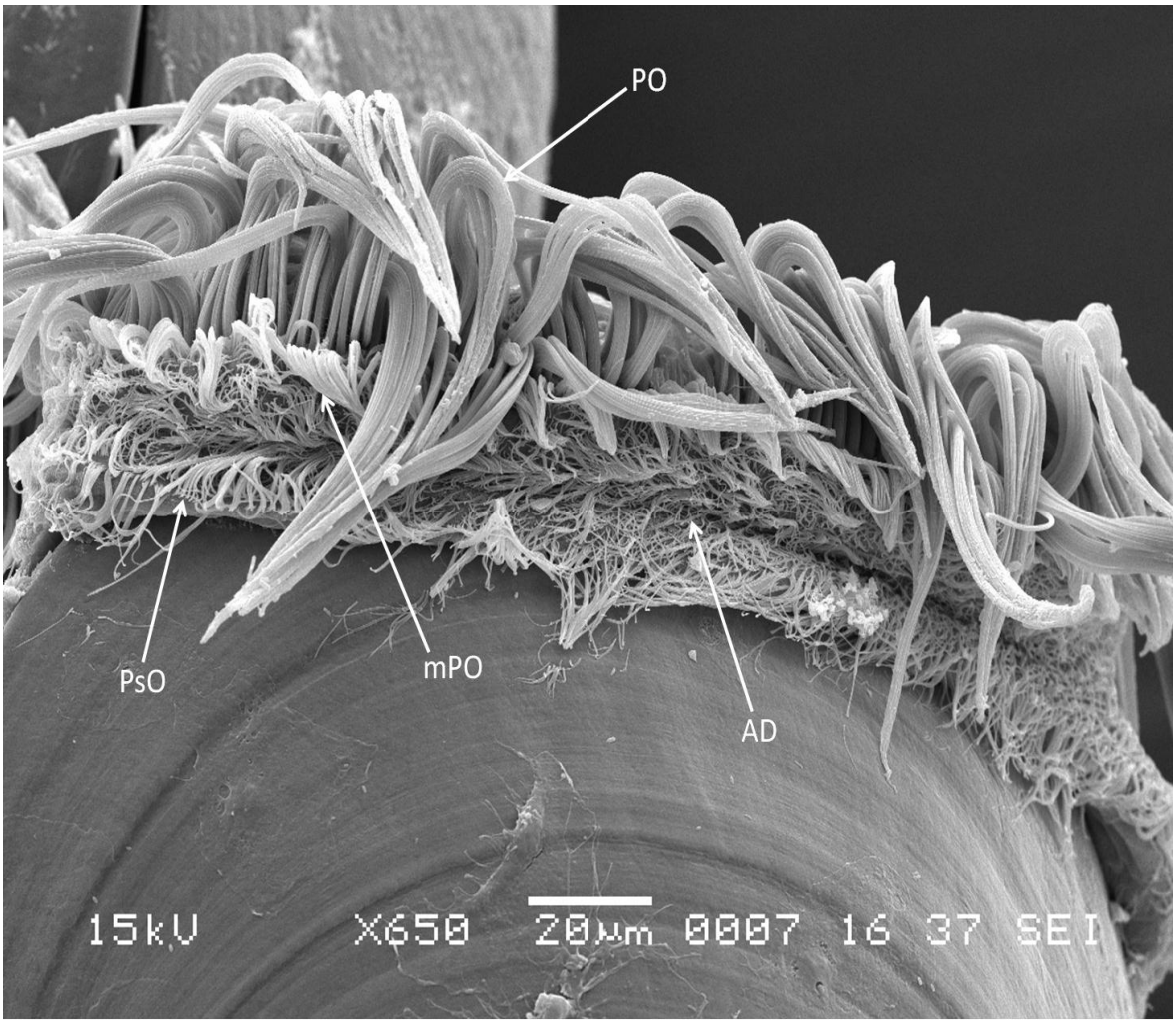

Figure 3.19 - The velar bands of an *Ostrea edulis* pediveliger.

The pre-oral cirri (PO) can be seen on the top edge of the velum. These are large cirri (approximately 60-80µm in length) comprised of multiple cilia, arising from two rows of cells running around the rim of the velum. Directly below the pre-oral cirri is the band of minor pre-oral cirri (mPO) above the adoral band (AD). The ad-oral band beats around the velar edge towards the mouth, the feeding groove this creates can be seen clearly in the image above. The post-oral cirri (PsO) are visible under the ad-oral tract, some angled upwards over the ad-oral tract (left edge on above image) and others lying on the shell (visible throughout). This larva was imaged with SEM.

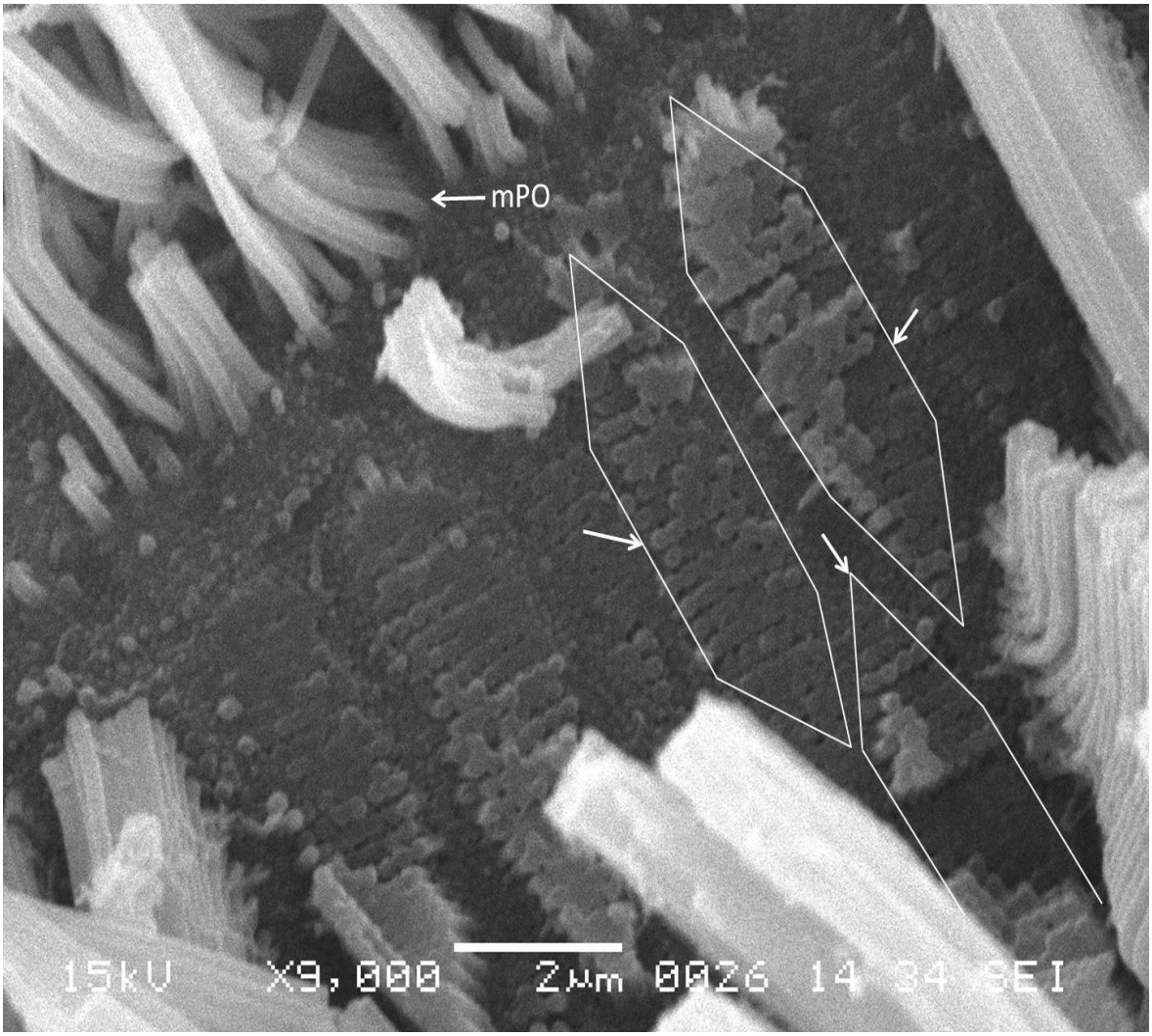

Figure 3.20 - Cells bearing the pre-oral cirri of an *Ostrea edulis* pediveliger.

The cirri of the pre-oral row can be seen to be composed of 110-140 cilia arising from cells that are diamond shaped at the velar surface, arranged in an alternating, 2 row pattern (marked, and slightly exaggerated to emphasise the shape in the image above). This cell shape is different to the shape of the cells bearing the minor pre-oral cirri (mPO), which can be seen to be more rectangular. This larva was dehydrated and the cells knocked away from the velar rim using glass needles before being imaged by SEM.

The minor pre-oral band

The minor pre-oral band is located directly under the pre-oral band and above the adoral tract (shown in Figure 3.20, Figure 3.21 and Figure 3.22) and is composed of cirri that are approximately 15µm in length, with each cirrus formed from around 20 cilia emerging through the microvillus velar epithelium. The minor pre-oral cirri form a band around the velar edge ~2.5µm in depth. Cirri arise from columnar cells smaller than those of the pre-oral cirri adjacent to them, but much larger and more distinct than the cells giving rise to the adoral tract, as can be seen in Figure 3.22. The minor pre-oral cirri are curved down towards the adoral band when fixed, indicating a probable direction of beat. When fully curved down the cirri reach the centre of the adoral band as in Figure 3.21.

The adoral band

The adoral band runs around the outer edge of the velum, being comprised of short cilia that beat around the velum towards the mouth, indicated by the angle of the cilia in tract that this beat direction forms in the centre of the velar edge in Figure 3.19 and Figure 3.21. The cilia are not arranged into cirri and show no other obvious form of organisation. The cilia of the adoral tract are approximately 5-10µm in length protruding through the microvillus surface of the velum (Figure 3.22). The entire tract varies in width between individuals, but is usually between 20µm to 30µm wide.

The post-oral cirri band

The post-oral band of cirri is located directly below the adoral band, separated by a narrow ~1µm gap covered with microvilli (Figure 3.21 and Figure 3.23). Each cirri of the post-oral band is composed of 3-4 cilia of approximately 10µm-15µm in length. These cilia are separate at the base but come together 1µm-2µm up their length to form the main cirrus. The cirri are not stiff in appearance and their positions when fixed show a beat direction towards the adoral band as seen in the left side of the velum in Figure 3.19 and in Figure 3.21. Some of the post-oral cirri were fixed lying on the shell apparently fixed when not beating (right side of Figure 3.19).

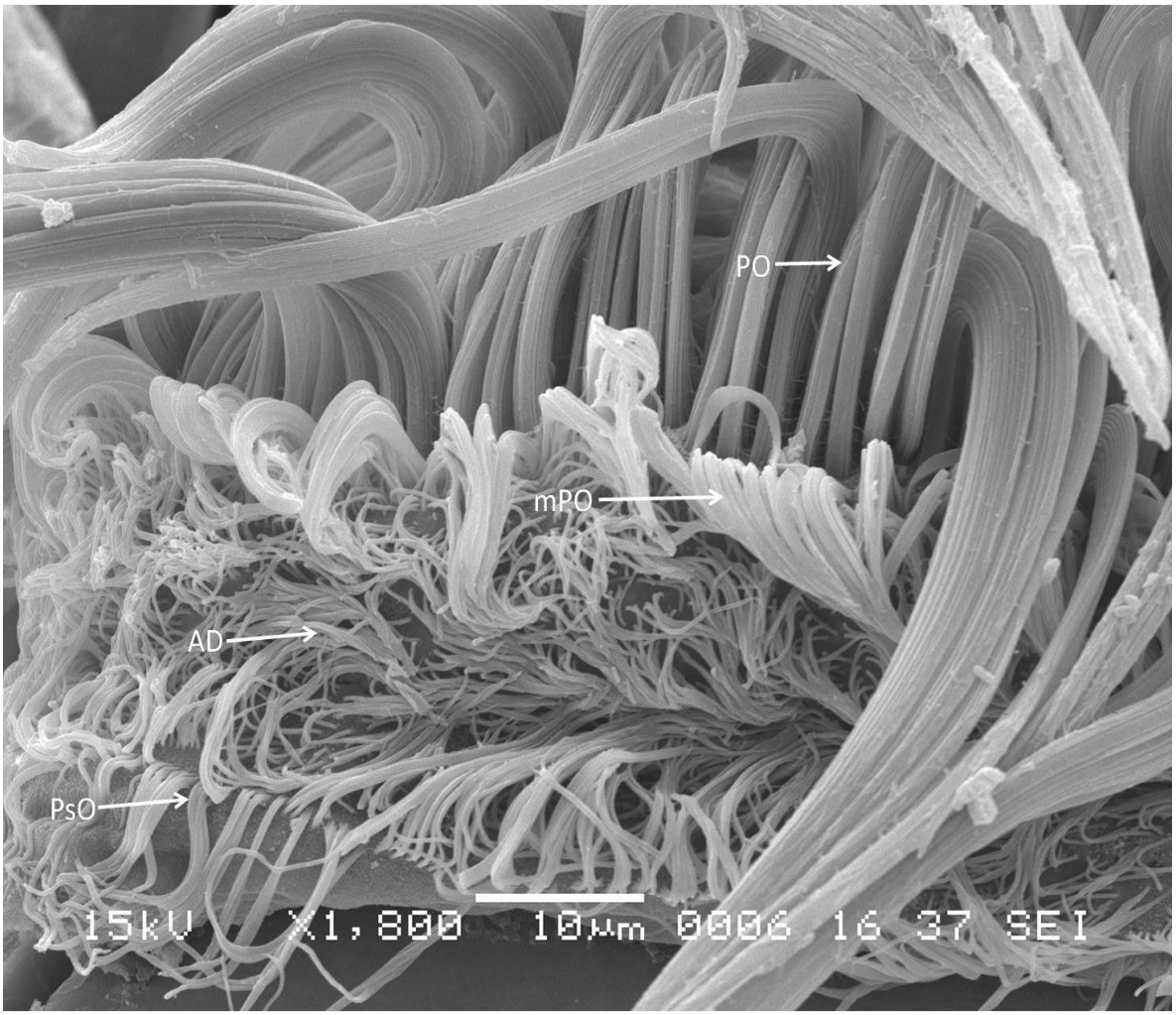

Figure 3.21 - The velar edge of an *Ostrea edulis* pediveliger showing the position of the minor pre-oral band in relation to the ad-oral and pre-oral bands.

The minor pre-oral band (mPO) is similar in appearance to the pre-oral band (PO) above it, and curled over the top of the adoral band (AD) indicating the downward beat. The minor pre-oral band is composed of cirri much wider and more substantial than those of the post-oral row (Pso), and appears to have a beat direction opposed to that of the post-oral band. This larva was imaged by SEM

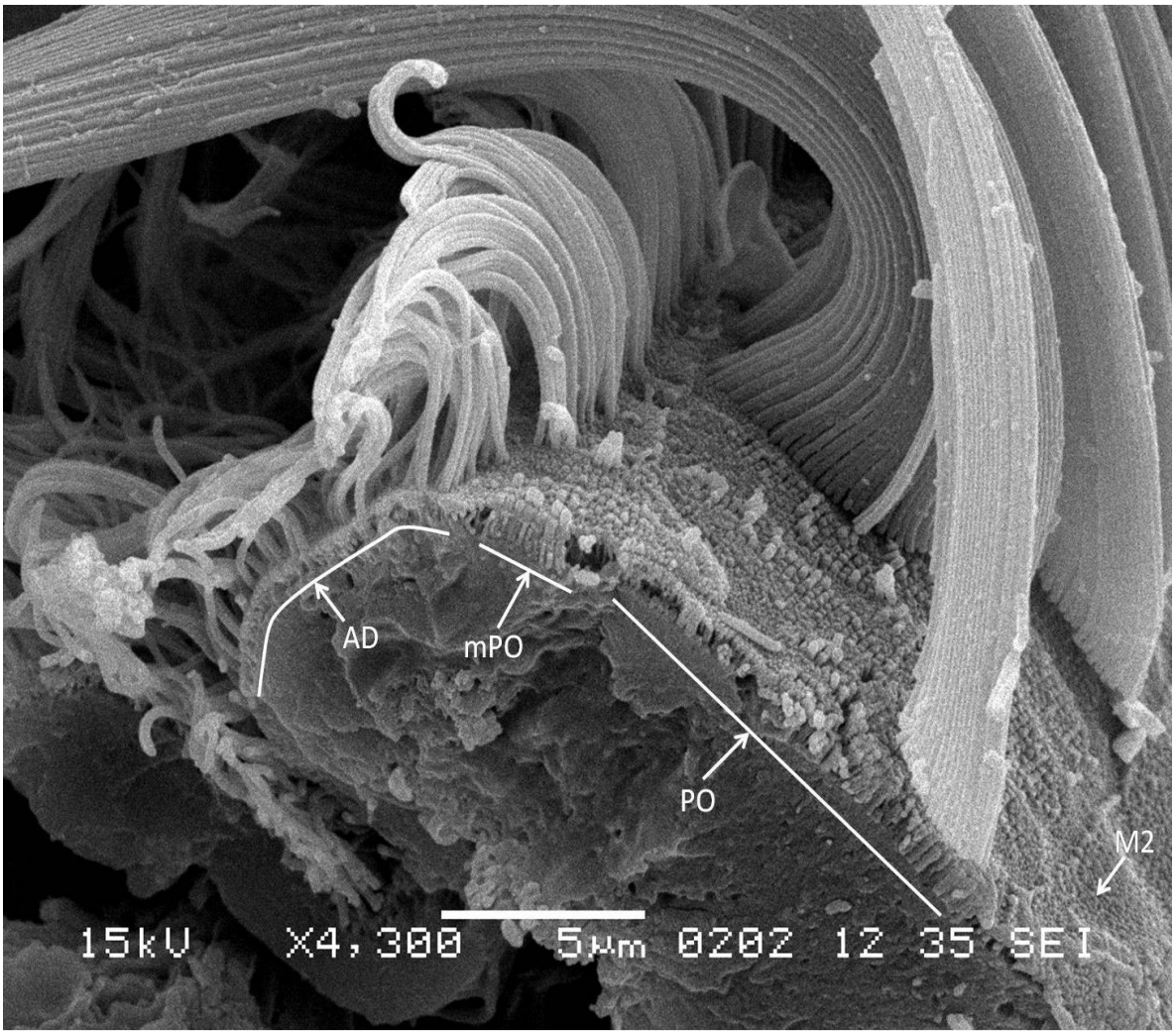

Figure 3.22 - Section of an *Ostrea edulis* pediveliger velum showing the oral bands.

Pre-oral cirri arise from 2 rows of cells (PO) bearing the cilia that comprise each cirrus. The minor pre-oral cirri (mPO) can be seen directly under the pre-oral row and before the ad-oral row (AD). The minor pre-oral cirri are curled down towards the ad-oral row after fixation, indicating this as the direction of their beat. Like the pre-oral cirri, the minor pre-oral cirri are composed of many cilia arising from cells arranged in a single row of ~2.5µm in width, running along the velar rim. Note also the step in the microvillous surface between the PO and the iPO is visible on this mantle section, to the right of the image. This larva was sectioned in wax and then imaged by SEM.

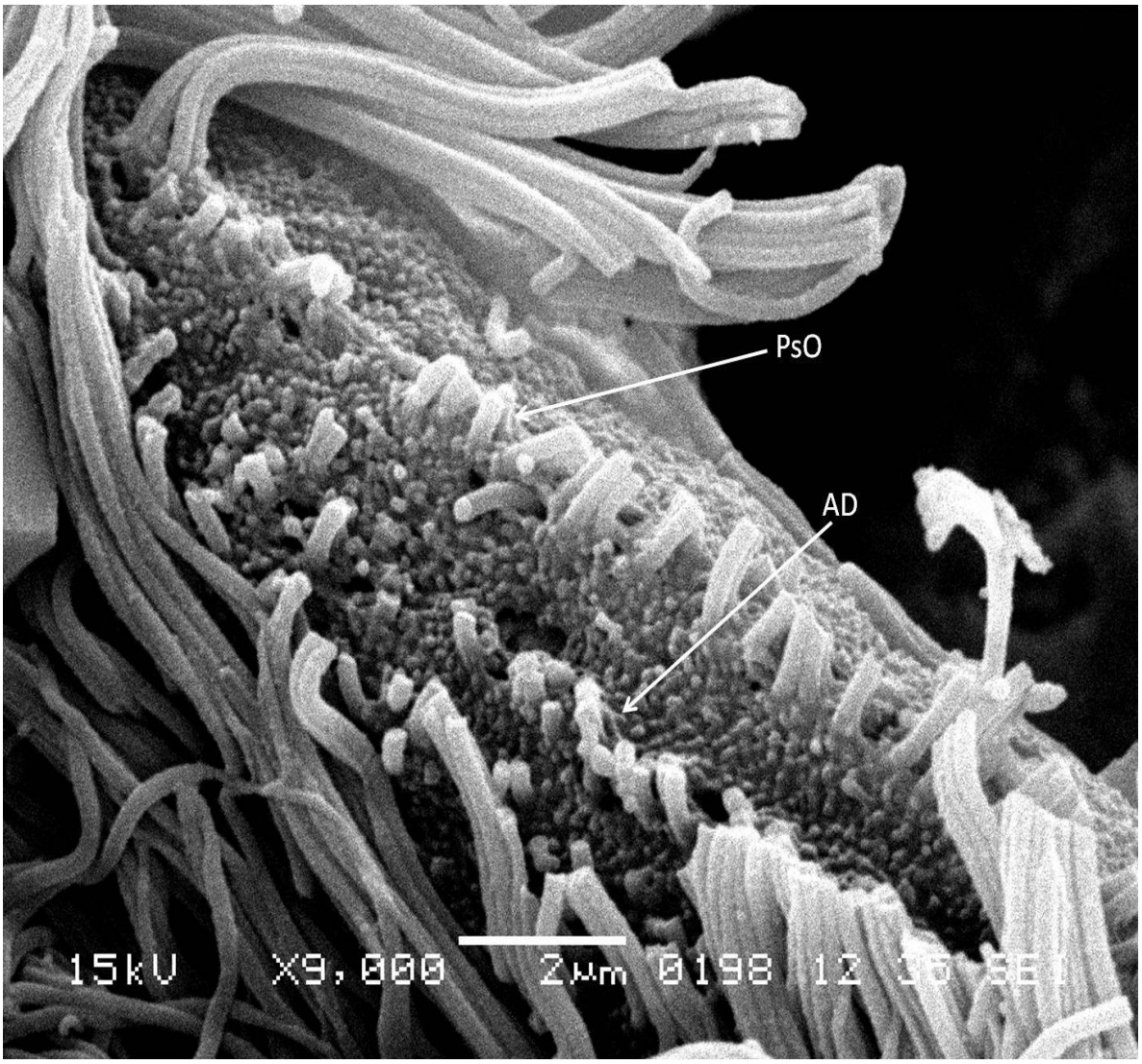

Figure 3.23 - The row of post-oral cilia on an *Ostrea edulis* pediveliger velum.

The post-oral row (PsO) can be seen below the ad-oral row on the bottom edge of the velar rim, forming a row distinctly separate from the less organised ad-oral (AD) ciliation above it. In this image the top of the cilia have been damaged during sample preparation, revealing the 3-4 cilia comprising each cirrus of the post-oral row. This larva was dry fractured and imaged by SEM.

Summary of ostreid velar ciliature

The diagram below (Figure 3.24) summarises the oral bands observed on the velar rim of ostreid larvae. There are 5 distinct bands, the inner pre-oral cilia, the pre-oral cirri, the minor pre-oral cirri, the adoral cilia and the post-oral cirri. Observations of live larvae and fixed specimens have indicated a probable downward beat of pre-orals and minor pre-orals cirri, the oral beat (around the velar rim) of the adoral tract and the occasional upstroke of the post-oral cirri.

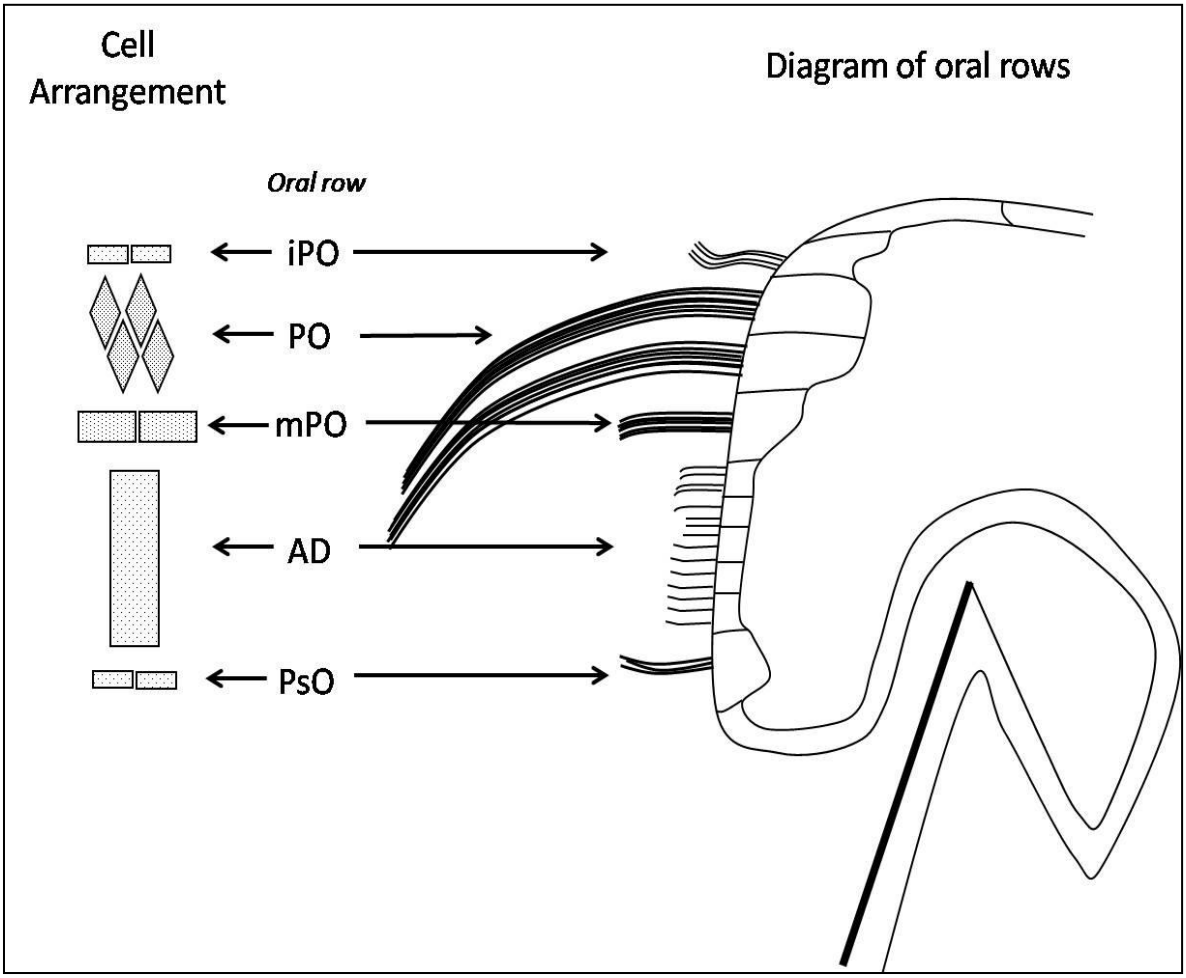

Figure 3.24 – Diagram illustrating the arrangement of the velar ciliature of ostreid larva.

The ostreid larval velum has 5 distinct bands of cilia: iPO – the inner pre-oral cilia, PO – the pre-oral cilia, mPO the minor pre-oral cirri, AD - the adoral row, and PsO - the post-oral row. The arrangement of the cells for each row is also provided in the key to the left. The arrangement of the PO cirri allows for the cirri to beat without obstructing its neighbour, facilitating an ordered rhythm of beating around the velar rim.

3.3.3 *Lyrodus pedicellatus*

The velum of *Lyrodus pedicellatus* has rarely been described in detail - the following description is based on SEM observations of pediveliger stage larvae collected from holding tanks at the University of Portsmouth.

The inner pre-oral band

The inner pre-oral band runs around the top outer edge of the velum, just above the large pre-oral cirri (Figure 3.26). The cilia of the band are ~8µm in length and arranged as a single line which can be up to 5 cilia deep. The inner pre-oral band occurs about 1µm above the large pre-oral band and was often seen angled onto the back of the pre-oral cirri so that the band is almost lying on the larger cirri. Just prior to the inner pre-oral band, above the pre-oral cirri, there is a distinct step in the velar surface, beyond it above the oral rows and covering the surface of the velum the microvilli are less distinct than the microvilli found at the bases of the oral rows (Figure 3.26 and Figure 3.27). The bases of the inner pre-oral cilia do not show any specialised structures, however the microvilli around the base of each cilium in Figure 3.10 appear to attach to the cilia shaft through slender fibres - these could be mucal threads, which have been seen running around the tips of the velar microvilli in *Crassostrea gigas* (Figure 3.10).

The pre-oral cirri band

The pre-oral band runs around the upper edge of the velum, formed of large cirri varying between ~50µm and ~80µm in length (Figure 3.25). These cirri are usually fixed at the bottom of their down-stroke and they almost totally cover the adoral cilia tract below them. The cirri appear to form two rows with the cirri of the upper band appearing shorter, although this is possibly due to the curvature of the cirri band extending over the lower band foreshortening the appearance of the upper cirri band on the 3-dimensional SEM image. The cirri of the pre-oral band are quite narrow, each being comprised of approximately 20 cilia, although the cilia bases are not visible to providing a more accurate count.

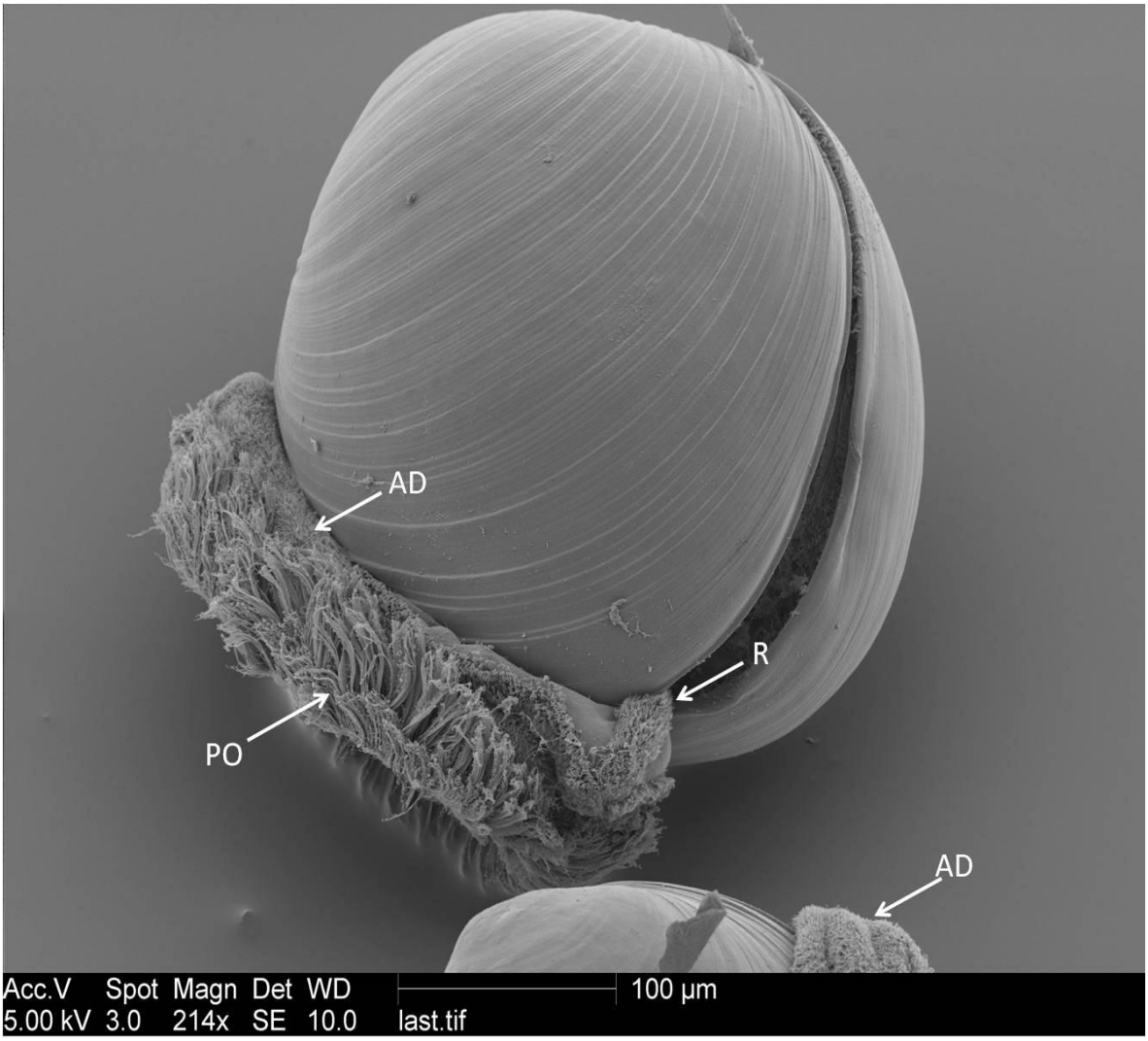

Figure 3.25 - *Lyrodus pedicellatus* pediveliger larva with extended velum.

The pre-oral cirri (PO) are over 50µm in length and almost entirely cover the ad-oral tract (AD) at the end of their down-stroke (where the cilia tend to have fallen post-fixation). The ad-oral tract is large, approximately 50µm-70µm in width. There is no obvious post-oral band in this image, and a rejection tract (R) is evident at the end of the velum. This larva was imaged by FESEM.

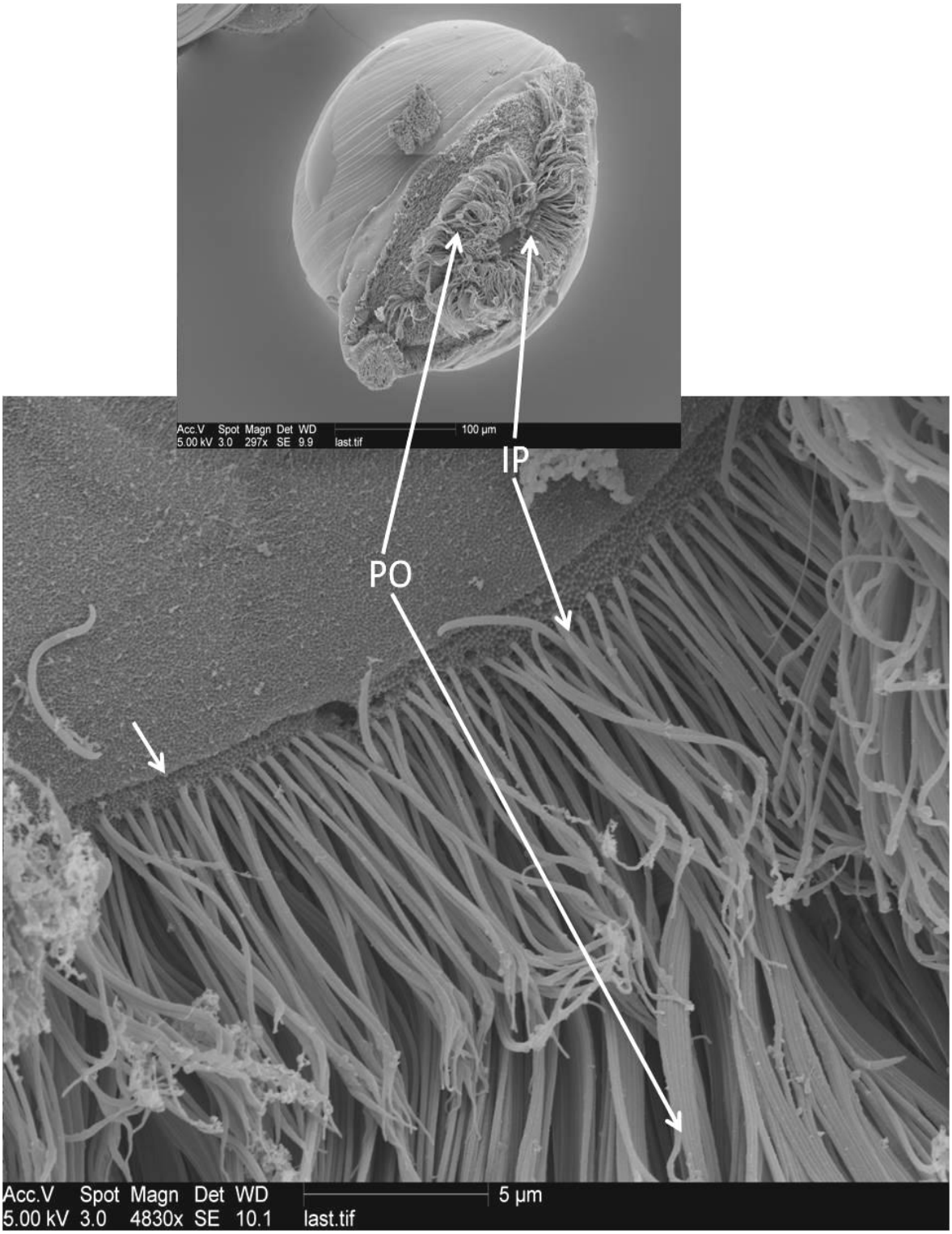

Figure 3.26 - The inner pre-oral band on the velum of a *Lyrodus pedicellatus* pediveliger.

The inner pre-oral band (iPO) is located on the velar surface above the pre-oral band (PO), formed of a row of cilia 5-6 deep, running around the entire circumference of the upper velar rim. The cilia comprising the row are ~8µm long and lay against the top of the pre-oral cirri. There is a distinct step in the surface of the velum (arrowed on the left) located just above the inner pre-oral row: the microvilli around the base of the oral rows below this step are more distinct than those on the top surface of the velum. This larva was imaged with FESEM.

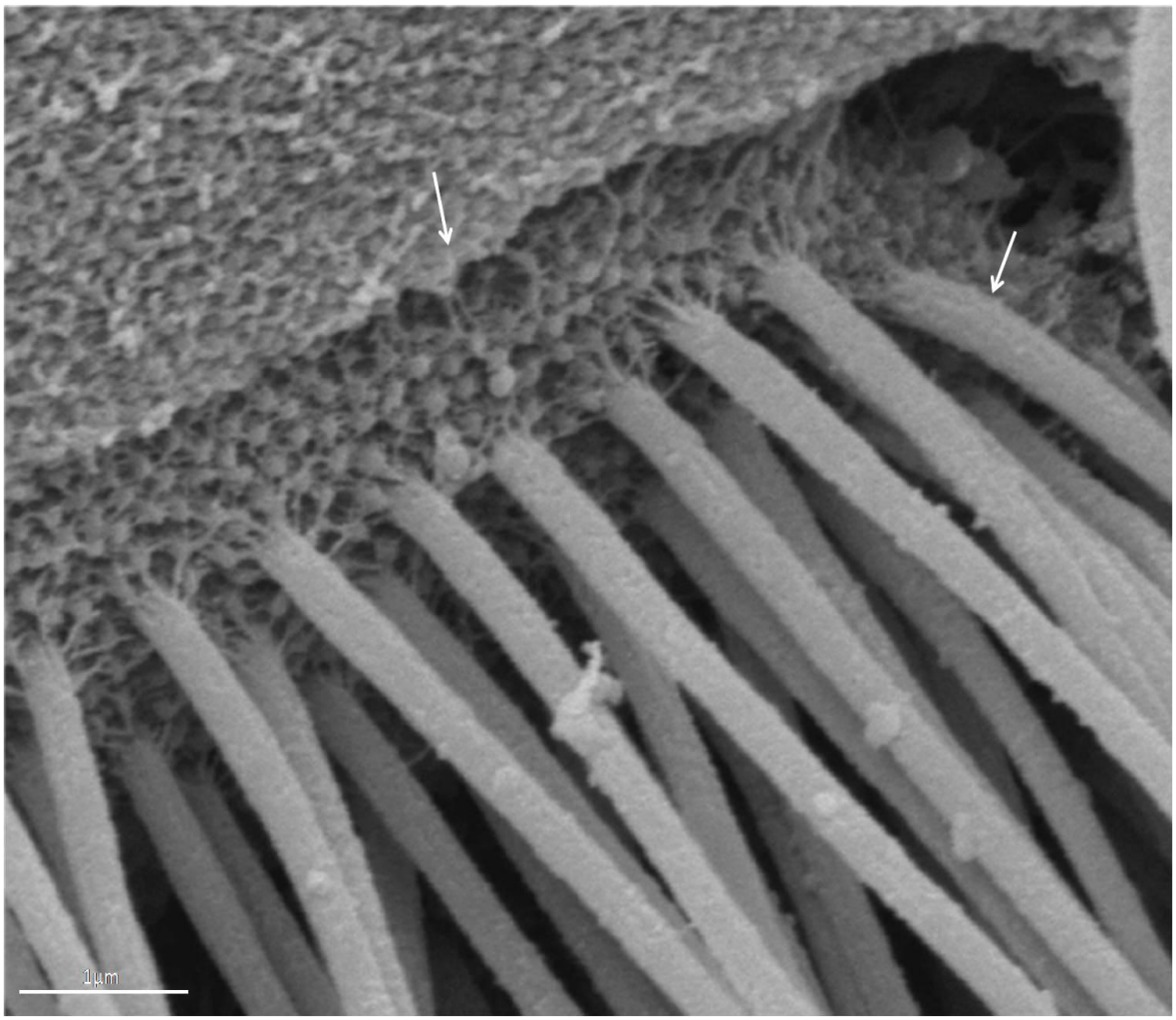

Figure 3.27 - The bases of the inner pre-oral cilia row.

The distinct step in the surface of the velum is clear - this occurs just above the inner pre-oral cilia. The microvilli on the inner pre-oral side of the step are more distinct than those of the velar surface above. The bases of the inner pre-oral cilia have fibres joining them from the surrounding microvilli; possibly these are the strands of mucus that run around the tops of the microvilli as seen in Figure 3.10. The appearance is not comparable to the sensory structures seen on the mantle in the previous chapter. This larva was imaged by FESEM.

The adoral band and rejection tract

The larvae of *Lyrodus pedicellatus* have a very wide adoral band without a post-oral band below it (Figure 3.28). The adoral band is directly below the pre-oral cirri and is comprised of individual cilia ~5µm in length, densely packed without any apparent organisation. The cilia are angled suggesting a beat direction towards the mouth - this is especially obvious in Figure 3.28 (lower image). The adoral tract extends across the entire velar edge of the larva and its size varied between individuals from ~50µm to ~100µm (this could be due to some variation in larval age when they are captured from holding tanks). The lower 10-20 cilia may be fixed curved upwards as in Figure 3.28, or angled towards the centre of the band. However there is no evidence to suggest this is a separate band. Approximately 0.5µm below the adoral tract there is another step in the surface of the velum similar to that found above the inner pre-oral band. There is no obvious difference in the microvilli surface either side of the step.

At the posterior end of the adoral tract there is a large rejection tract located directly below the mouth, shown in Figure 3.29. This tract is not connected to the adoral tract, as can be seen in Figure 3.28, but separated from it by a ~2.5µm tract of microvilli. This rejection tract has a wedge shaped top directly under the mouth, leading down into a straight tract ~20µm in width and ~30µm - 60µm in length (length may vary according to individuals, likely due to age, or simply due to difficulties and differences in viewing angles within the SEM). All the cilia throughout the length of the tract, when fixed, are directed down away from the mouth towards the shell. At the bottom of the tract the velum extrudes several strings of mucus (Figure 3.29) and finer mucal strands come off the tract itself onto the shell surface.

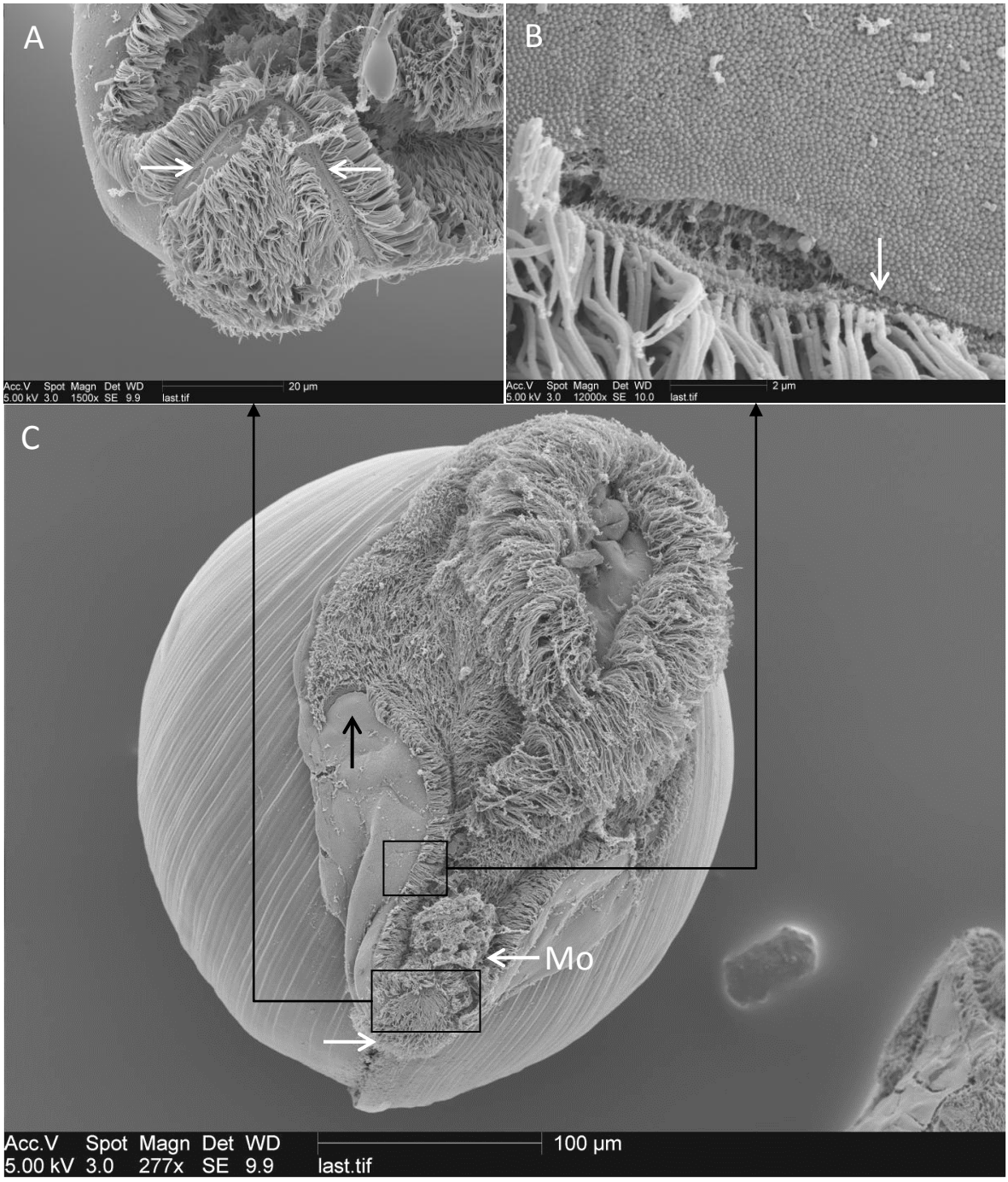

Figure 3.28 - *Lyrodus pedicellatus* pediveliger larva with rejection tract visible and illustrating the wide ad-oral tract.

In image C the rejection tract (white arrow) can be seen directly below the mouth (Mo). Note also the shape of the ad-oral band either side of the mouth and rejection tract, hooking round below the pre-oral band (black arrow). This may be an artefact of the velum not being fully extended - this shape is probably giving an indication of the distance that the rejection tract will extend down below the mouth and therefore the height of the velum when it is more fully extended. Image A has been provided to illustrate the separation of the rejection tract from the adjacent oral rows, with this gap arrowed for clarity. Image C highlights the step (arrowed) found in the velar microvilli between the bottom of the ad-oral band and the lower edge of the velum. In both image B and C there is no separate post-oral band, the ad-oral band extends to this step in the velar surface. This larva was imaged by FESEM.

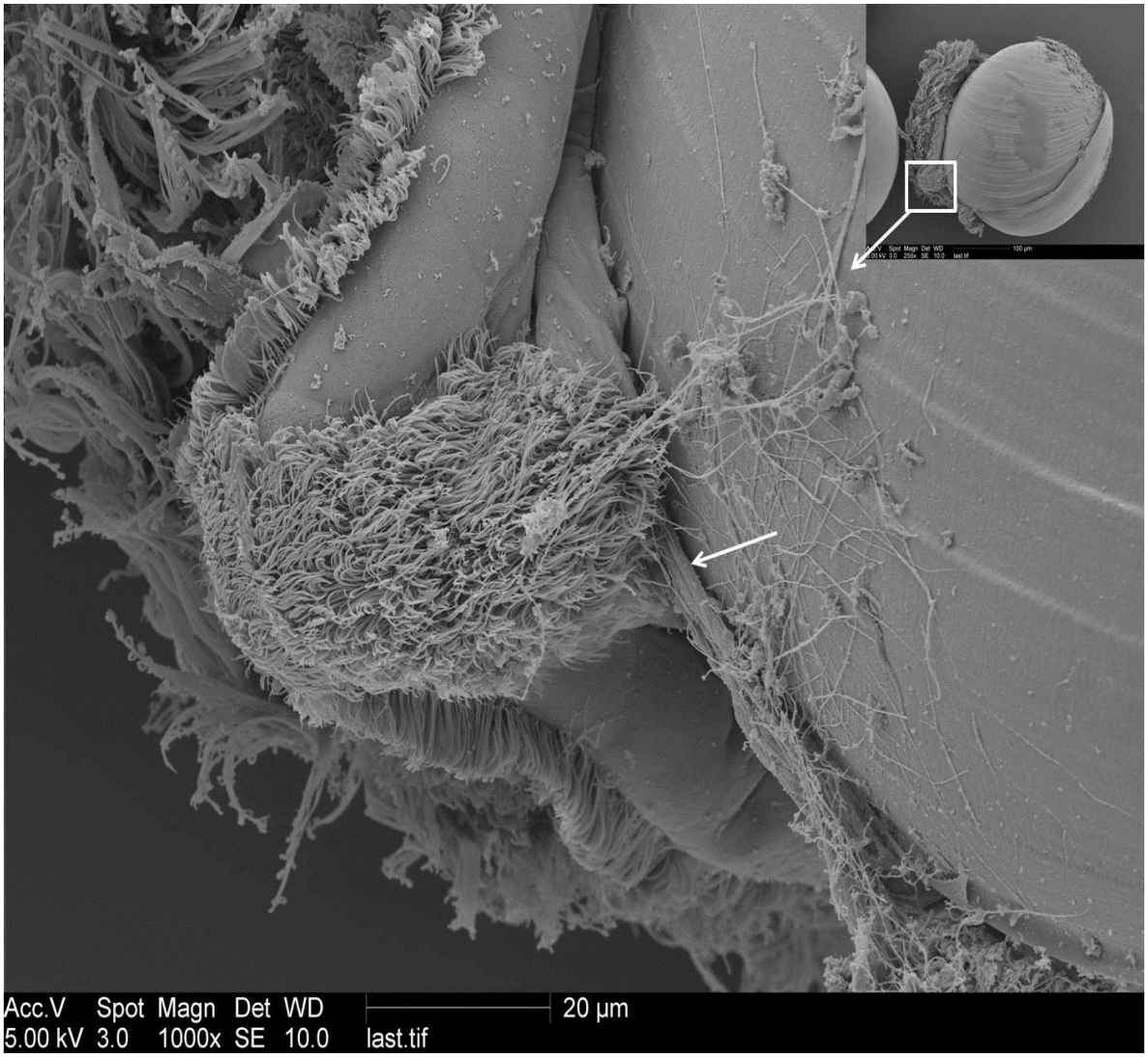

Figure 3.29 - The rejection tract on the velum of a *Lyrodus pedicellatus* pediveliger larva.

The cilia of the tract all are directed down, away from the velum, indicating the probable direction of beat. Note also the mucal threads being extruded from beneath the rejection tract (arrowed) and the strands of mucus on the shell and connected to the tract. These finer strands of mucus may have come from the cilia tract itself. This larva was imaged by FESEM.

Lyrodus pedicellatus *larval brood chambers*

The larvae of *Lyrodus pedicellatus* are held within the adult mantle cavity until their release as pediveliger stage larvae for settlement site searching. The larvae sit in pouches around the gills of the adult, the pouches appearing like sockets (Figure 3.30). Most of the larvae imaged were in pouches which cover approximately half of each individual larva. Some of the larvae were covered by a thin membrane around the entire larva, whilst still being held within the pouch (see the larva on the right of the image in Figure 3.30). In addition, three of the adults fixed, dissected and imaged had larvae that did not appear to be held at all, but were free in the mantle cavity. This could be as a result of the larvae being released through the sample preparation, moribund adults or that these larvae are not constrained to a pouch but free within the adult, possibly having been released. It is most likely all the larvae are fully encapsulated by this covering, but that the treatment for SEM has damaged the cover.

All the larvae imaged were ~300µm in diameter, being of pediveliger stage and therefore probably close to release. The larvae were often observed with their velums extended on specimens that would have been within the adult at the time of fixation - these individuals are arrowed in Figure 3.30.

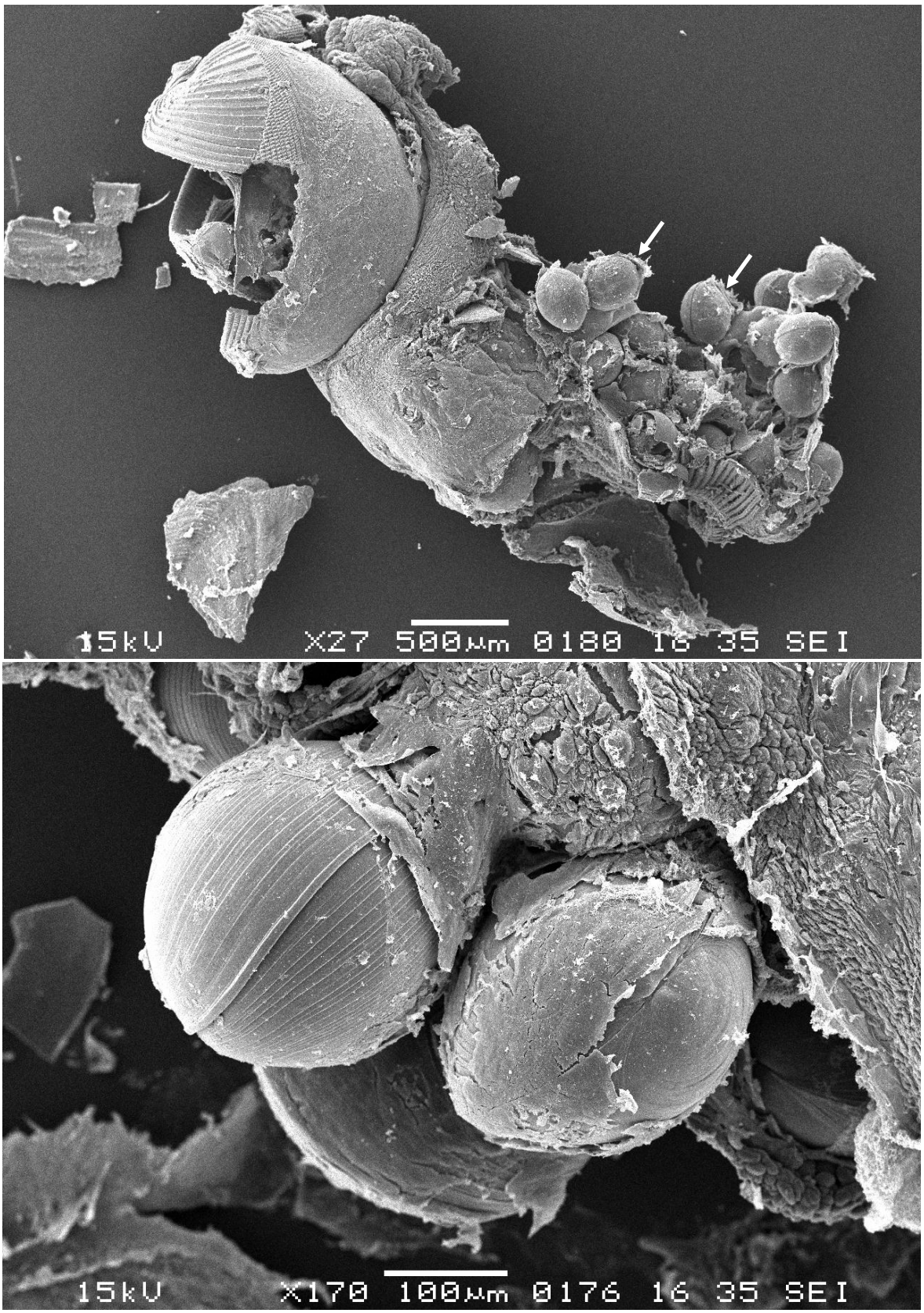

Figure 3.30 - *Lyrodus pedicellatus* larvae in adult brood pouches around the gill.

The brood pouches are located at the adult gill, shown in the upper image. The larvae feature a well developed velum (arrowed larvae in the top image had their velar extended at the time of fixation). These larvae are held within the adult body cavity and have not yet been released,. The adult was removed from a block of wood and fixed for electron microscopy, then cracked open after dehydration to reveal the larvae in the pouches seen above before being imaged with SEM. It is possible these were moribund adults unable to release the larvae.

3.4 Discussion

3.4.1 Comparative anatomy

This section will compare the observations of the ciliary bands of the velum of *Crassostrea gigas, Ostrea edulis* and *Lyrodus pedicellatus* described in this study with other records, looking in detail at each of the velar ciliary bands. A summary Figure 3.31 is provided at the end of **3.4.1**.

The inner pre-oral cilia

The inner pre-oral ring of ciliation differed only slightly between species, and appeared in all the veliger and pediveliger larvae investigated in this study. The inner pre-oral band in *Ostrea edulis* is recorded as being 8-10µm in width (Waller, 1981). Observations in this study found the band to only be 1-2 µm wide (equivalent to 4 cilia) at its deepest point and similar to the inner pre-oral band of *Crassostrea gigas*. The inner pre-oral band of *C. gigas* is no more than 1-2µm (4-5 cilia) wide, and comparable to that of *C.virginica* (Elston, 1980), *Ostrea chilensis* (Chaparro et al., 1999) and *Pecten maximus* (Cragg, 1989). The separation between the inner pre-oral and pre-oral band recorded in this study for both ostreid species is much larger (up to 10µm) than in any of the records for either ostreid or pectinid species, where in all cases the space is noted as being approximately 1µm-2µm.

The inner pre-oral band is not present in all bivalve larvae, with examples such as its absence in the larvae of the scallop *Chlamys hastata* (Hodgson & Burke, 1988), despite its presence in *Pecten maximus* (Cragg, 1989), suggesting that variation in the inner pre-oral can be found within families, at the species level. Furthermore both these species have planktotrophic larvae, indicating that the loss of this band may not be related to selection pressures from reproductive strategy. In this study the inner pre-oral band of *O. edulis* shows no significant difference to that of *C. gigas*, despite differences being recorded in the literature. This is suggestive that the variations reported in the literature could be a result of differences in equipment or sample preparation, and this should be noted when making such comparisons.

The inner pre-oral cilia of *Lyrodus pedicellatus* are orientated differently to the inner pre-oral cilia of the ostreid and pectinid larvae. Most SEM images show the ostreid inner pre-oral

band either directed away from the large pre-oral cirri with a distinct gap between the rows, or laying loosely on the velar surface (for example, Figure 3.2). In *L. pedicellatus* larvae the inner pre-oral band is located almost directly on top of the large pre-oral cilia (PO) and was always orientated down onto or along the pre-oral cirri themselves. This could suggest that in the case of *L. pedicellatus* the inner pre-oral cilia have an active beat, although as with all the bivalve larvae where the inner pre-oral band has been noted, the group was difficult to observe in live larvae (Cragg, 1989, Waller, 1981) so it was not possible to see any beat in live specimens. Furthermore, there were no observations of inner pre-oral cilia having any distinct curvature to suggest cilia fixed at the end of, or during a power stroke.

The change in microvilli between the inner pre-oral band and the pre-oral band, or the step in the velar surface between the two bands directly above the pre-oral band, has not been recorded on any bivalve larval velum before. Given that this feature was observed in both *Ostrea edulis* and *Crassostrea gigas*, and from different broodstocks, it is unlikely to be unique to the specimens used in this study. It is possible this is visible only because of improvements in image capture, or through differences in sample preparation. However this feature was visible in specimens prepared using either critical point drying or HMDS methods of sample dehydration. The JEOL JSM-6060LV used in this study was a new SEM, many of the previous studies incorporating images of velar ciliation were published during the early 1980's using scanning electron microscopes equipped with film cameras. The combination of new optics and higher resolution user interfaces has probably made the identification of this type of fine change in microvilli more readily identifiable. Whilst the film cameras on the older SEM's had excellent resolution the poor user interface screen may have led to a feature such as this change in microvilli being missed in previous investigations.

The pre-oral band

The pre-oral cirri of *C. gigas* and *O. edulis* show little variation; both have cirri composed of layers of cilia, are 2-3µm wide, approximately 10 cilia across and comparable in length. There appeared to be little difference in the band throughout larval ontogeny. The main difference in

the ostreid cirri was that those of *C. gigas* split approximately 1/3 of the way up the cirri length, giving them a thin, flattened, ribbon-like appearance when fixed (arrowed in Figure 3.4). The pre-oral blades of *O. edulis* do not split into ribbons but were fairly well consolidated for most of their length (Figure 3.4 and Figure 3.19). It is feasible this difference in appearance could be due to specimen preparation artefacts. However, this difference was seen throughout this study in larvae of different broodstocks and in larvae that were prepared for SEM using both critical point drying and HMDS methods of dehydration. This reduces the possibility of artefact being the cause, but it cannot be completely discounted.

The ribbon-like appearance of *C. gigas* pre-oral cirri closely matches the appearance of the pre-oral band in *Crassostrea virginica* (Elston, 1980). However it should be noted that the pre-oral cilia of *O. edulis* have been recorded as splitting apart towards the tips of the cirri (Waller, 1981). However when examining the published photographs the pre-oral cirri are still different in appearance to those of *C. gigas* in this study, or those of *C. virginica* (Elston, 1980), with the pre-oral cirri not having the fine appearance of the *Crassostrea* species. It is possible that the lack of splitting down the length of the pre-oral cirri is caused by the presence of a greater amount of mucus on the velum of *O. edulis*. Mucus often performs a cleaning function, and whilst such a role cannot be discounted here, it is extremely expensive metabolically (Cannuel & Beninger, 2007). It has been suggested that brooded larvae may use mucus on the velum to enhance the capture of food from the adult (Chaparro et al., 1993, Hodgson & Burke, 1988). It is possible that the splitting of the pre-oral cirri in non-brooded, planktotrophic species such as *C. gigas* may afford benefits to swimming efficiency, or that the more splayed tips may improve particle collection. However mucus does not greatly aid particle capture at the low Reynolds numbers found in ciliary systems (Hodgson & Burke, 1988), possibly making preparation artefact a more plausible explanation for this difference in the appearance of the pre-oral cirri of *O. edulis* and *C. gigas*, despite the consistency of the observation.

Whilst the pre-oral band shows a stability of form across species (and consequently across various breeding strategies e.g. brooded versus non-brooded), with most authors recording

similar cirrus lengths (80µm by the pediveliger stage) and widths (approximately 3µm), there is some variation in the numbers of cilia comprising each pre-oral cirri. The composition of *Pecten* pre-oral cirri is 15-20 cilia (Cragg, 1989), 20-80 cilia per each cirri in *O. edulis* (Waller, 1981), 50-100 cilia compose the pre-oral cirri of *Ostrea chilensis* (Chaparro et al., 1999), *Tivela mactroides* pre-oral cirri are composed of just 4-5 cilia (Silberfeld & Gros, 2006), and approximately 10 cilia per cirrus in *Mercenaria mercenaria* (Gallager, 1988). *Argopecten purpuratus* is listed as having only 12 cilia per cirri, but in this case the author attributed 5-6 cirri to each cell - these cirri may also be splitting like those of *C. gigas* in this study, giving the impression they are formed of smaller units (Bellolio et al., 1993). The variation in these numbers may be due, at least in part, to differences in technique and equipment enabling more (or less) accurate counts of cilia to be made. Few studies have exposed the cells bearing the pre-oral cirri in the manner of this study to enable more accurate counts of cilia bases to be made.

Irrespective of the variation in cilia per cirrus, there is consistency in the form of the pre-oral cirri between bivalve species and families. This consistency could be expected when considering the function of the pre-oral cirri is broadly the same across species, fulfilling both swimming and feeding roles (although some lecithotrophic larvae may only use this ciliation for swimming). However, that this form is still the same even when there is little evidence of planktonic feeding, such as in the case of *L. pedicellatus* (Pechenik et al., 1979), may further indicate a shared ancestry for the pre-oral band throughout the Bivalvia. The pre-oral band stems from the prototroch and probably represents the plesiomorphic condition (Nielsen, 2004).

The consistent selection pressures of the planktonic environment have not resulted in a modification of the pre-oral cilia in those species with a free-swimming planktonic larval stage: in the majority of these species the pre-oral cirri are used for both the swimming power stroke and the opposed band method of particle capture. Having a dual role forces a design that is a balance between the two functions; longer cirri provide higher flow rates but are less efficient at capturing particles (Strathmann & Leise, 1979). Furthermore cilia lose the power of the flex in their effective stroke if the length exceeds 150µm, resulting in a loss of swimming efficiency (Chia

et al., 1984). It is probable that the combination of feeding and swimming pressures have forced this optimisation in cirri form to be reflected across all the bivalve species with a feeding planktonic veliger. That this is probably the plesiomorphic condition also seems likely when considering that most modifications of this band involve the loss of structures for brooding (Nielsen, 2004). Examples such as the loss of the velum in *Lasaea adansonii* (Altnoder & Haszprunar, 2008) or very late development of ciliation in *Ostrea chilensis* (Chaparro et al., 1999), are usually found in species that have specialised in the brooding strategy, holding larvae within the body cavity for most of their development and having a very short larval planktonic phase.

The minor pre-oral band

The minor pre-oral cirri arise under the pre-oral cirri (Figure 3.31), and have been imaged on the velum of ostreid larvae for the first time in this study. The band was seen on larvae from several different broodstocks (and present in all individuals where this region of the velum was visible) making it unlikely to be a mutation unique to the larvae of one broodstock. Some studies identify a ciliated gap of 4µm -10µm between the pre-oral and the adoral rows on ostreid larvae (Chaparro et al., 1999, Waller, 1981), but do not note the minor pre-oral row. However there do appear to be images in the literature that show the minor pre-oral band on bivalve veliger velum. Most authors have attributed these to pre-oral cirri fixed towards the end of their recovery stroke, with only the tips showing through the rest of the pre-oral band (Gallager, 1988). The large pre-oral cirri often protrude through the rest of the row at the back of their recovery stroke (Figure 3.32) but, as in Figure 3.21, these cirri are distinct from those of the minor pre-oral band. Close examination of the images presented of the *Mercenaria mercenaria* velum (Gallager, 1988) reveals the bases of the minor pre-oral cirri appear to be visible. This identifies the band as separate from the pre-oral cirri above, comparable to the arrangement presented in Figure 3.21 and proposed in Figure 3.31. Minor pre-oral cirri also appear to be visible on SEM micrographs of the velum of *Spisula solidissima* (Campos & Mann, 1988). This suggests that the minor pre-oral band may not be limited to ostreids, but found in other members of the Bivalvia. Examination of the ciliary bands of other Protostome larvae such as polychaete larvae has not yet revealed the

presence of this band (Nielsen, 2004, Nielsen & Nielsen, 1995, Young, 2002), although the possibility cannot be discounted. The minor pre-oral band has a power stroke, as do the pre-oral and post-oral bands, and may suggest a particle capture system more complex than the original Strathmann (1972) model (discussed in 3.4.2 Functional anatomy).

The adoral band

The form of the adoral band appears consistent across the veliger larvae of the Bivalvia. The earliest observations of a current directing particles to the mouth identify the adoral row this function (Yonge, 1926). The adoral band appears almost identical in all the bivalve larvae for which there are detailed accounts of the group, with the main inter-species difference being the overall width of the band itself. The adoral bands of *C. gigas* and *O. edulis* adhere to this trend, both being composed of scattered cilia 5µm -10µm in length and having a band ~20µm-40µm wide. For both species the curvature of the fixed cilia indicate the beat of the AD is towards the mouth (Figure 3.11, Figure 3.19 and Figure 3.21). The appearance of the cilia comprising the adoral band of *L. pedicellatus* pediveliger was the same as the ostreid species, both in beat direction (shown via the angle of the fixed cilia) and cilia size. However the band tended to be wider than in the ostreid species, being between 50µm and 100µm.

The post-oral band

As seen in the other oral bands, the post-oral band is very similar in *Crassostrea gigas* and *Ostrea edulis*; however the post-oral cirri of *C. gigas* had more cilia per cirrus than those of *O. edulis*. These observations broadly agree with records of the ostreid post-oral cirri: the post-oral band of *Ostrea chilensis* (Chaparro et al., 1999) and *Ostrea edulis* (Waller, 1981) vary from those of *Crassostrea virginica* (Elston, 1980, Galtsoff, 1964), whose post-oral band is almost identical to that of *C. gigas* reported here. The post-oral band of *Pecten* larvae is comprised of simple cilia (Cragg, 1989). Simple post-oral cirri have also been seen in other scallops (Hodgson & Burke, 1988) and possibly represent an ancestral post-oral band, with the post-oral band of the ostreids being a modification of the original form (Cragg, 1989). The *L. pedicellatus* pediveliger did not have a post-oral band, with a velum very similar in appearance to that of the long term brooded

oyster *Ostrea chilensis* pediveliger (Chaparro et al., 1999): this will be further discussed in **3.4.2** when considering the function of the post-oral band.

Summary of comparative anatomy

The appearance of the oral rows of the species with a planktonic phase (such as *C. gigas* and *O. edulis*) appears quite consistent, both between species and when compared with reports of the velar bands of other species with a similar planktonic phase. Modification of these bands is mainly found in lecithotrophic larvae or those species that utilise a longer brooded phase, and commonly involves the loss of some rows. This may support the view that the bands forming the downstream collection method are representative of the ancestral trait, and that the modification of the velum, such as the loss of the post-oral band, is an adaptation of the ancestral condition, as has been argued by Nielsen (2004).

The minor pre-oral band may be a modification of the opposed band system of planktotrophic larvae. The addition of a row, in this instance the mPO band, appears to shed doubt on the downstream collection ciliary arrangement being the plesiomorphic condition. However this may not be the gain of a row, but a band that has simply been lost in other planktotrophic larvae, or not previously been noted; the apparent confusion around the appearance of this row on other larvae (where it appears to have been imaged but not recorded by other authors), makes it difficult to draw conclusions on the ancestry of the minor pre-oral band.

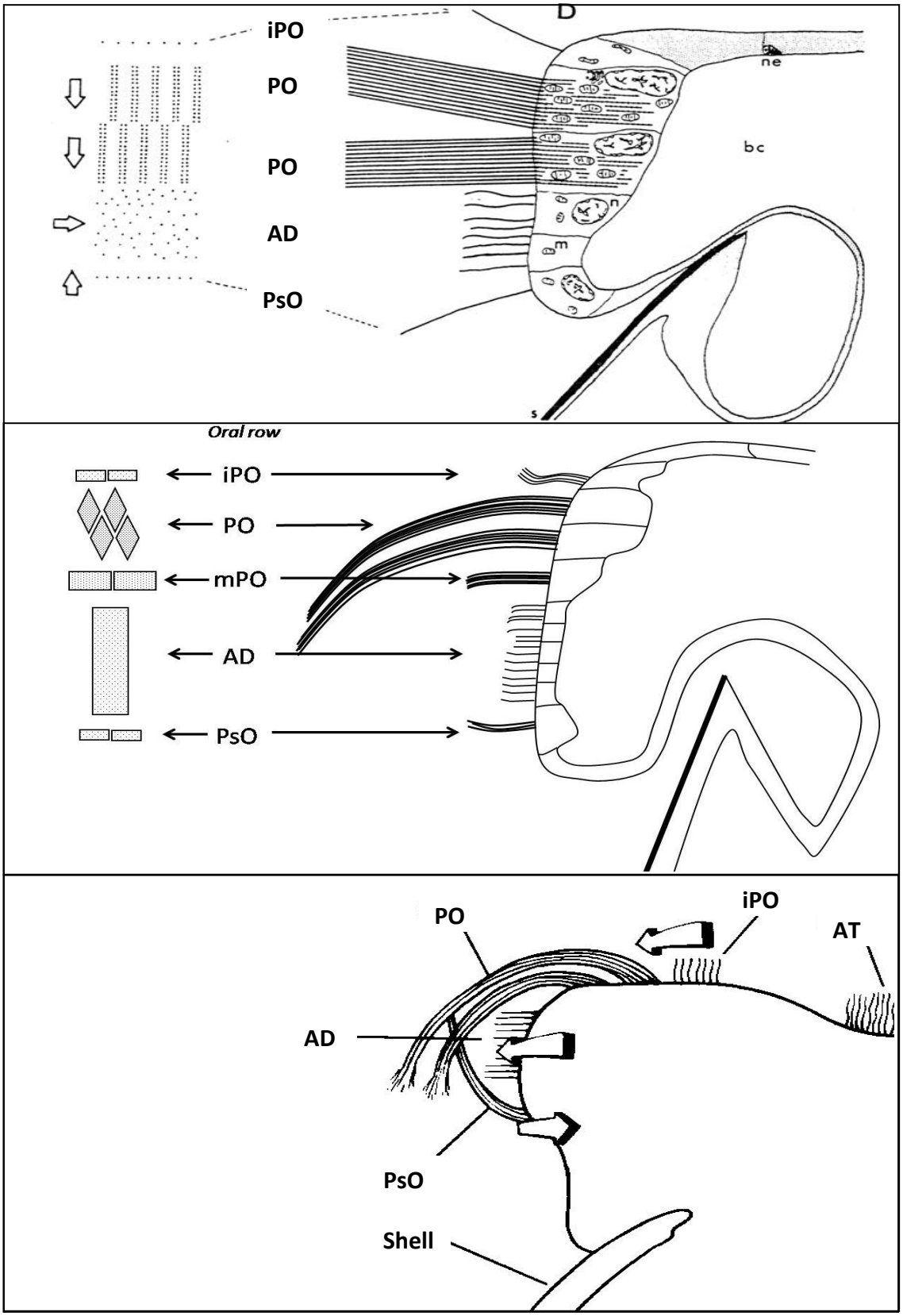

Figure 3.31 – Inter-species comparison of velar cilia layout.

Figures, from top to bottom, of *Pecten* (Cragg, 1989), the new ostreid layout identified in this study and *Ostrea edulis* (Waller, 1981). Labelling has been changed from the author's originals to suit the definitions used in this study. The cell arrangement of *Pecten* and *Ostrea* appears broadly the same, with *Ostrea* featuring diamond shaped cells at the velar surface, giving rise to the pre-oral cirri blade shape. The minor pre-oral cirri identified during this investigation does not appear on the diagrams provided by the other authors. Waller (1981) suggests a wider inner pre-oral row in *O.edulis* than was seen in this study.

3.4.2 Functional anatomy

Functional anatomy will be considered with regard to each of the ciliary bands identified on the velar rim, considering both feeding and swimming roles.

The inner pre-oral cilia

A definite function for the inner pre-oral ring has not yet been determined. The inner pre-oral ring occurs across varied life history strategies - all three species in this study show the inner pre-oral band, *Crassostrea gigas* being planktotrophic, *Ostrea edulis* is lecithotrophic/brooded for at least half its larval development (Waller, 1981) and *Lyrodus pedicellatus* is a long term brooder releasing pediveligers competent to settle (Isham & Tierney, 1953). In addition, observations of the velum of a long-term brooded ostreid larva, *Ostrea chilensis*, also reveal the presence of an inner pre-oral band (Chaparro et al., 1999). This may suggest the inner pre-oral band is either not related to feeding - brooded larvae often do not need the more complex patterns of ciliary bands required for extended periods feeding in the plankton (Chaparro et al., 1999). In addition the appearance of the fixed cilia in the SEM images does not show any consistent angle to suggest a beat direction. Examining the inner pre-oral cilia in Figure 3.2 and Figure 3.3 illustrates the somewhat limp appearance of the cilia, and contrasts against the curvature of the pre-oral cilia in the same images.

Suggestions of a mechanoreceptive function (Waller, 1981) are more plausible than the inner pre-oral ring forming a part of the feeding or swimming structure, but this proposition is not yet proven. The lack of any specialised structures at the base of the cilia, or any difference in the morphology of the cilia themselves, sheds doubt on the band having a sensory function. Alternatively the inner pre-oral band may simply be an ancestral carry-over; one that has not been lost in the manner the post-oral row is in some long-term brooders (Chaparro et al., 1999, Nielsen, 2004).

The inner pre-oral band of *Lyrodus pedicellatus* appears different to that of the ostreids, with SEM images consistently showing the cilia laying flat against the top of the large pre-oral cirri. Whilst this may suggest the inner pre-oral cilia have a beat orientated towards the pre-oral

cirri, there is still no curvature evident in the cilia, it is perhaps more likely they are simply closer to the pre-oral band than is seen in ostreids. It is possible these cilia have a cleaning function in *Lyrodus pedicellatus* - the inner pre-oral cirri will be in close contact with the pre-oral cirri at the end of the recovery stroke (Figure 3.32), being forced in-between the larger pre-oral cirri. This would strip any remaining small particles from the pre-oral cirri and onto the inner pre-oral band. The inner pre-oral cilia in Figure 3.26 have several small particles attached to them. However it is difficult to confirm this cleaning function without further work.

This work should include both the observation of live larvae (although the transparent nature of the velum makes this difficult) and further examinations of the velum using SEM after the larvae have been swimming in water that is known to contain some very small particulate matter (i.e. lightly filtered seawater). Care would have to be taken to ensure these particles were identifiable, for example the use of small silica beads (ThermoScientific, USA). The regular shape of these beads would ensure they were identifiable in the SEM; however the 10µm beads used for particle capture experiment would be too large. Beads of ~0.49 µm would probably provide a good starting point for such an investigation.

The pre-oral band

The layering of cilia in each pre-oral cirrus gives the cirri a greater rigidity (Cragg, 1989) and thus enables a shelled larva to be heavier (Cragg, 1980), but probably also provides this more solid structure with a greater degree of flexible power. When the cirri are at their most curved at the start of the recovery stroke, the layers of cilia can be clearly seen, such as the pre-oral cirrus at the top right of Figure 3.3 or the pre-oral cirri in Figure 3.22. The appearance of the layering when the cirri are curved suggests the layers of cilia must slide against each other in order to maintain contact, and thus the cirrus shape, whilst the cirri beat. This system would seem to mirror the system of movement inside the cilia as the sliding displacement of the microtubules within the axoneme powers the beat of the cilia themselves (Haimo & Rosenbaum, 1981, Satir, 1992). This system would allow the rigid structure of the cirri to remain flexible, whilst increasing the power of each cirrus stroke.

The cells of the pre-oral band show the staggered arrangement seen in veligers of *Pecten* (Cragg, 1989) and *Mercenaria* (Gallager, 1988) and the angle of the fixed pre-oral cirri shows the plane of beat of the cirri to be slightly oblique to the line of the velar edge, as shown for *Pecten maximus* (Cragg, 1989), *Crassostrea virginica* (Elston, 1980), *Mercenaria mercenaria* (Gallager, 1988) and *Ostrea edulis* (Waller, 1981). The alternate arrangement of the cells of the pre-oral row prevents the cirri from interfering with each other during their beat pattern (Figure 3.31). This alternating arrangement can be seen clearly in Figure 3.5 and Figure 3.6 for *C. gigas* and Figure 3.20 for *O. edulis*. As a result of this arrangement, when one cirrus is at the bottom of its power stroke it is not impeded by either of the neighbouring cirri - Figure 3.21 shows a pre-oral cirrus at the bottom of its power stroke (to the right of the image) clearly passing through the neighbouring cirri without being restricted.

The angle and arrangement of the pre-oral cirri observed in all the species in this study show evidence of the metachronal waves passing around the rim of the velum at a right angle to the plane of beat of each cirrus. This organised velar ciliary beat is known as diaplectic metachrony (Gallager, 1988, Knight-Jones, 1954); the cells bearing the pre-oral cirri form a single 'orthoplectic' band parallel to the fluid movement generated by the cirri beat (fluid is accelerated downward with the beat of the cirri). The pre-oral cirri within the orthoplectic band are arranged as two 'diaplectic' rows, perpendicular to the fluid flow generated by the pre-oral cirri beating. It is the bricklaying pattern of organisation of the cells of the two diaplectic rows, as shown in a diagram in Figure 3.24, and in the SEM image in Figure 3.9, that allows the cirri of these rows to beat without interfering with their neighbours. The organised beat of these diaplectic rows within the orthoplectic band is termed diaplectic metachrony. The cirri beat in an organised sequence of alternation of the two diaplectic rows around the velum, making the ciliary beat appear to move like a wave around the velar rim. This metachronal beat propels the veliger upwards, but with a slight spin generated by the diaplectic arrangement of the cells and the beating of the adoral band (Cragg, 1980, Cragg, 1989).

This beat pattern is visible in Figure 3.2 and Figure 3.21 with some pre-oral cilia at the end of their recovery stroke and others at the end of the power stroke (pre-oral cilia were only imaged fixed at the end of the power or recovery strokes, at the end of energetic processes), illustrating the 'wave' of pre-oral ciliary beat spreading around the velum. This organisation of beat progressed clockwise around the velum. Figure 3.19 also shows neighbouring pre-oral cirri at different stages of their stroke, but not interfering with each other. This movement of the metachronal waves is common where diaplectic metachronism occurs, for example in polychaete trochophore, gastropod veligers, phoronis larvae, or other bivalve larvae (Knight-Jones, 1954).

The pre-oral cirri have, in most cases, been fixed either at the end of the power stroke or at the beginning of the recovery stroke. No SEM images were captured of the cirri fully extended. This suggests the mechanism of ciliary beat stopped at the bottom of the power stroke following fixation. This is possibly due to the energetic requirements of withdrawing the cilia. TEM investigations of the cells bearing the pre-oral cilia indicate high numbers of mitochondria (Cragg, 1989, Elston, 1980): if fixation has stopped the energetic processes in the cell, then the cilia may have simply continued to fall to the end of their stroke, being unable to complete the energetic processes of the recovery stroke.

The minor pre-oral band

The opposed band system of particle capture often has been described in the larvae of many different bivalve families with reports of its use within larvae of the venerids (Altnoder & Haszprunar, 2008, Kang et al., 2004, Moueza et al., 1999), mytilids (Bayne, 1976), pectinids (Bellolio et al., 1993, Cragg, 1989), ostreids (Chaparro et al., 1999, Waller, 1981) and teredinids (Culliney, 1975). It is the standard model of downstream particle capture utilised by the molluscan veliger (Nielsen & Nielsen, 1995, Strathmann et al., 1972, Strathmann & Leise, 1979, Young, 2002).

Figure 3.31 illustrates the position of the minor pre-oral cirri in relation to the known layout of the bivalve velum, and compared against the diagrams provided by Cragg (1989) of *Pecten maximus* and Waller (1981) for *Ostrea edulis* - all the larvae are active feeders within the

plankton. Given the consistent downward curvature of the fixed minor pre-oral cirri over the adoral tract, this is the most likely direction of beat for this band of cirri.

This band may have a dual role. First, it will provide a refinement to the opposed band particle capture method (see **3.1**, for a description), serving as a final deflection onto the adoral tract after the deflection from the post-oral band. Second, the minor pre-oral band may also serve to prevent particles becoming lost or trapped in the pre-oral cirri during their recovery stroke, effectively keeping the tips of the pre-oral cirri clean for a more effective power stroke - these functions are illustrated in Figure 3.32, showing how the pre-oral cirri have to pass either through or across the minor pre-oral cirri during the recovery stroke. This will concentrate particles below the minor pre-oral cirri (illustrated by the black dots) whose downward beat will deflect the particles onto the adoral band below. As such it could be argued that these functions are two aspects of increasing efficiency of particle capture, and that the cleaning of the pre-oral cirri is an added benefit. The interaction of the minor pre-oral cirri with the adoral band is clearly shown in the upper left image of Figure 3.7, and the close proximity of the pre-oral cirri to the minor pre-oral cirri during their recovery stroke can be seen in Figure 3.22. That this band is found on the velum of the ostreid species with a feeding planktonic stage may suggest, if the band increases particle capture efficiency, the appearance of the band stems from the selection pressures in the plankton.

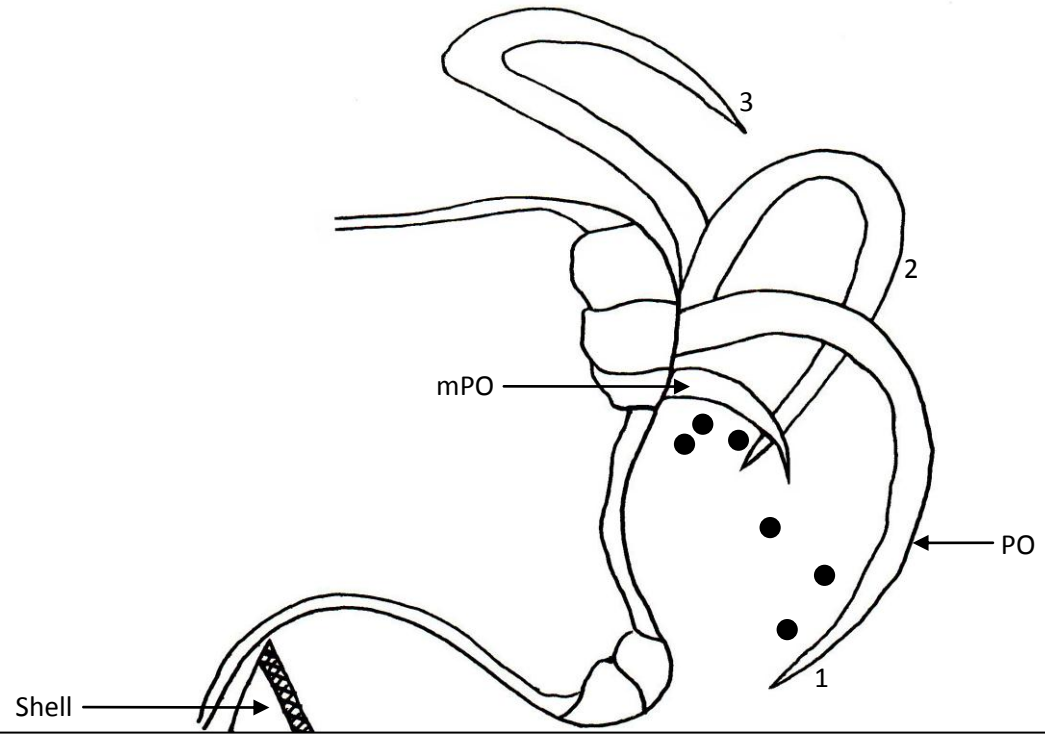

Figure 3.32 - Diagram showing possible function of the minor pre-oral cirri.

As the pre-oral cirri (PO) go through the recovery stroke, whose path is marked by the numbered pre-oral cirri, 1 → 2 → 3 (the final position of the recovery stroke), the tips will pass though the minor pre-oral band (mPO) in position 2. Particles will concentrate below the minor pre-oral band (back dots) and be deflected onto the ad-oral band as minor pre-oral cirri beat downwards. The minor pre-oral band will also concentrate particles through their own beat, as a refinement of the opposed band capture system.

The adoral band

For all the species examined in this study the position of the fixed cilia clearly indicate the beat of the adoral cilia towards the mouth, and a groove is prominent in the centre of the adoral band, shown clearly in Figure 3.4, Figure 3.19 and Figure 3.21. Particles were observed moving around the velum in this groove (Figure 3.12**)**. There was nothing remarkable about the adoral tract in either of the ostreid larvae examined; the function of this tract in passing particles around to the mouth is the final phase of the opposed band method of particle capture (Riisgard et al., 2000, Strathmann et al., 1972).

The presence of a large adoral tract in the *Lyrodus pedicellatus* pediveliger may be unexpected when considering evidence presented that the larvae of *L. pedicellatus* do not actively feed on phytoplankton (Pechenik et al., 1979) and thus would not require such a large adoral tract during their short planktonic phase. However, the presence of a large prodissoconch II (Young,

2002) would seem to suggest the larva does feed at some stage. A large prodissoconch I typically is associated with lecithotrophic development, deriving nutrition from yolk, whilst a large prodissoconch II usually signifies a planktotrophic development mode (Cragg, 2006, Young, 2002). That the larvae of *L. pedicellatus* have such a large prodissoconch II despite being a long-term brooded larva suggests there may be significant growth outside of the adult brood chamber after the lecithotrophic phase, possibly indicating a change in feeding to a planktotrophic phase (although it is not possible to discount yolk still being used, especially in light of the evidence presented by Pechenik *et al*, 1979).

The angle of the adoral cilia on the fixed velum of *Lyrodus pedicellatus* indicates a beat around the velum towards the mouth, implying the tract fulfils the same function as the Crassostrea *gigas* adoral tract in Figure 3.12. In addition the velum has a distinct tract of cilia under the mouth. All the cilia of this tract are fixed, in all specimens examined, curved away from the mouth (Figure 3.29). If, as with the pre-oral cilia, these cilia have been fixed at the end of their power stroke this may indicate this as the direction of beat, and suggest this is a rejection tract. In addition there are thick mucal strands extruded from under this rejection tract and fine mucal strands running through the cilia of the rejection tract and the adoral tract (Figure 3.29). While mucus on the velum has been suggested as a means of ensuring adhesion of particles to cilia during capture, at the low Reynolds numbers obtained during ciliary movements for particle capture, mucus is probably not needed for aiding particle adhesion to cilia (Hodgson & Burke, 1988). It is possible the mucus is there to bind particles being rejected under the mouth, or an artefact of a system for collecting cells released by the adult when the larva is being brooded. Mucus may also be fulfilling a cleaning function, keeping the cilia of the velar rim free of nuisance particles, and increasing swimming efficiency. However, as previously discussed in section 3.4.1, mucus is extremely expensive metabolically (Cannuel & Beninger, 2007) and therefore unlikely to be used by a developing larva.

The veliger larvae of some bivalves do actively feed by capturing particles whilst being brooded within the mantle cavity (although solely lecithotrophic larvae will have no need to feed).

Even extreme (long term) brooders such as *Ostrea chilensis* (Chaparro et al., 1993) and *Ostrea circumpicta* (Kang et al., 2004) can retain particles, capturing particles concentrated around the gills by the parent. Both *Ostrea chilensis* and *Ostrea circumpicta* lack any specialised structures for holding larvae whilst brooding. It is possible that *L. pedicellatus* is further adapted to the brooding habit, as is suggested by the pouches the larvae are held in (Figure 3.30) which are very similar to the brood pouches seen in *Teredo* sp. (Morse & Zardus, 1997). The *L. pedicellatus* larvae may therefore derive its nutrition from the parent using the modified velar structure (Turner & Boyle, 1974). The brooded larva may also be capable of the uptake of dissolved organic matter (DOM) whilst encapsulated within the brood pouches, in a manner comparable to that seen in encapsulated gastropod larvae (Martinez et al., 2008).

The appearance of the adoral tract and the rejection tract with its distinct curve (Figure 3.28) in the *Lyrodus pedicellatus* pediveliger suggests this may be an artefact of the extended velar structure seen in the brooded veliger stage larva (Turner & Boyle, 1974) that is retained in the non-feeding, released pediveliger larva. The velar structure of the released pediveliger is probably a reduced form of the modified veliger velum that is more suited to swimming and that therefore echoes the ancestral ciliary layout (Nielsen & Nielsen, 1995).

The post-oral band

The cilia of the post-oral band were fixed in two positions, predominantly curled up towards the adoral tract and frequently angled down over the shell, as has been reported for *Pecten* larvae (Cragg, 1989). There was no evidence of the metachronal beat pattern like that seen in the pre-oral cirri. As the opposed band system used to capture particles in the velum is well documented, it can be assumed that those cirri not beating towards the adoral tract at the time they were fixed were either not beating, or fixed at a point in their beat where the cirri fell back down over the shell (Cragg, 1989). In contrast to the influence of fixation on the pre-oral cirri, where their position is likely a result of fixation stopping the energetic process of ciliary beat, those cirri laying on the shell were probably not beating when fixed - veliger larva are known to stop the beat of the post-oral tract when swimming without feeding (Strathmann et al., 1972).

The lack of any post-oral band of cilia in *Lyrodus pedicellatus* appears to be a common adaptation of brooded larvae. The velum of the released pediveliger larvae of *L. pedicellatus* is comparable to the pediveliger velum of the brooded *Ostrea chilensis* (Chaparro et al., 1999). The veliger stage velum of these two brooded larvae is very different (although both are highly modified), with ciliation appearing very late on the velum of *O. chilensis* while the *L. pedicellatus* veliger has a large, ciliated, modified velum (Chaparro et al., 1999, Turner & Boyle, 1974). The lack of a post-oral band may benefit a long-term brooded larva. It does not require the band for feeding and losing the band may increase swimming efficiency. That both pediveliger stages resemble the appearance of the planktotrophic opposed band despite earlier modification for brooding in the veliger suggests the opposed band system is an ancestral trait that has been modified for brooding (Nielsen & Nielsen, 1995).

3.4.3 Neural control of the velum

Crassostrea gigas had serotonin fibres and cells in the velar rim. Results for catecholamine compounds were less distinct, and although suggestive, will need further experimental work to verify, probably by using specific stains like those used for serotonin (for example dopamine has previously been linked with ciliary control by Beiras & Widdows, 1995). The locations of these nerve systems have mostly been attributed to the large cells bearing the pre-oral ring, but the boundary between the inner pre-oral and pre-oral is so slight that some of these fibres could be associated with the inner pre-oral band not the pre-oral band. This localised distribution of serotonin and catecholamine containing fibres and cells in the velar rim is consistent with published accounts from across the phylum Mollusca, with serotonin and/or catecholamines having been found in the velar rim of the bivalves *Mytilus edulis* (Beiras & Widdows, 1995, Croll et al., 1997, Croll et al., 1995), *Mytilus trossulus* (Voronezhskaya et al., 2008), *Placopecten magellanicus* (Croll et al., 1997, Croll et al., 1995, Smith et al., 1998), as well as being recorded in opisthobranch larvae (Croll, 2006, Kempf et al., 1992, Kempf & Page, 2005, Kempf et al., 1997, Pires et al., 1997), prosobranch gastropod veligers (Dickinson & Croll, 2003) and heterobranch gastropod embryos (Voronezhskaya et al., 1999).

Serotonin is known to have a role in the control of ciliary activity in molluscan veligers through affecting changes (usually increases) in ciliary beat frequencies (Beiras & Widdows, 1995, Croll & Dickinson, 2004, Mackie et al., 1976). Catecholamines have also been implicated in the control of velar cilia activity in mollusc larvae (Croll & Dickinson, 2004, Croll et al., 1997), and are known to inhibit ciliary beat in concentration of ~10^{-6}-10^{-9}mol l^{-1} (Braubach et al., 2006). Both of these compounds effect the Ca levels in the intracellular spaces (Doran et al., 2004), therefore the presence of both serotonin and catecholamine compounds could be implicated for localised ciliary control through stimulating or inhibiting ciliary beat (Beiras & Widdows, 1995). While this has not been demonstrated experimentally for ostreid larvae, the combination of serotonin excitation and dopaminergic inhibition has been implicated in controlling the frequency of velar ciliary beat in *Mytilus edulis* (Beiras & Widdows, 1995) and the gastropod veliger *Ilyanassa obsoleta* (Braubach et al., 2006). *I.obsoleta* larvae vertical distributions were altered by differing concentrations of these compounds, probably through changes in velar cilia beat frequencies (Braubach et al., 2006).

The presence of serotonin and catecholamines in the location of the pre-oral and post-oral cirri of *Crassostrea gigas* (Figure 3.15 and Figure 3.17), suggests that the larva may have a measure of control over the beat of these cirri. Controlling pre-oral ciliary beat frequency would allow the larva to effect various swimming trajectories through increasing or reducing beat frequency to control a fall through the water or simply beating more rapidly to negate the helical pattern usually observed (Cragg, 1980).

In the series of video frames in Figure 3.12 there is a group of pre-oral cirri whose beat is inhibited throughout the course of the video. The location of the serotonin, and possibly catecholamines at the velar edge, combined with this video footage showing inhibited pre-oral beat in this region, may provide preliminary evidence for inhibition of the pre-oral band in *Crassostrea gigas* veligers, similarly to that of *I.obsoleta* veligers (Braubach et al., 2006). The pre-oral cirri either side of the stationary cirri beat throughout the video, only those cirri directly above the mouth are inhibited. The larva was seen to reject the particles moving along the adoral

tract in the video, suggesting the cessation of the pre-oral beat may be linked to particle selection and rejection at the mouth (Croll & Dickinson, 2004), possibly preventing the beating of the pre-oral cirri from blocking the escape trajectory of rejected particles. Furthermore, the larva has strong fluorescence from beads in the stomach and intestinal tract, indicating this was not a moribund larva, but one that had previously selected beads.

Catecholamine inhibition of the post-oral band (or the lack of serotonin stimulus) may indicate the method by which this band can be stopped when the larva is swimming and not feeding, although no video footage was captured of non-beating post-oral cirri. However it has been suggested that bivalve veligers can stop the beat of the post-oral band to increase the efficiency of swimming with the pre-oral cirri by removing the beat of the opposing post-oral band (Strathmann et al., 1972). Some of the SEM images in this study show post-oral cilia fixed beating towards the adoral band (Figure 3.4, Figure 3.13 and Figure 3.19), and some of which show the band laying back on the shell (Figure 3.13 and some of the post-oral cilia in Figure 3.19). The presence of both serotonin and catecholamines in the velar rim of many molluscan larvae may suggest that control of the ciliary beat of the oral bands is a trait that is found across the veliger larvae of the Mollusca, although nervous connection between the velar rim and apical region has been suggested in some studies (Beiras & Widdows, 1995, Croll & Dickinson, 2004, Croll et al., 1997), this still cannot be confirmed in *Crassostrea gigas* veligers.

3.5 Conclusions

There is a striking consistency in the arrangements of the cilia around the velar rim of the planktotrophic bivalve veliger. The velar ciliation has to fulfil both feeding and swimming roles and the evolution towards an effective compromise between these roles has given rise to a structure in planktotrophic larva that has seen few modifications. This consistency is found across families, and may suggest the opposed band system is ancestral. However there are still gaps in the knowledge of the velum at the species level; for example this study has revealed the velum of both *Crassostrea gigas* and *Ostrea edulis* have an additional band of oral cilia. This band of minor

pre-oral cirri probably increases the efficiency of particle capture, although further investigation is required to confirm this. In addition the minor pre-oral cirri may also clean the pre-oral cirri tips during their recovery stroke, maintaining maximum swimming efficiency. It is difficult to draw conclusions as to the ancestry of this band (and whether this band has been gained by ostreids, or lost by other larvae) until more information is available regarding its presence of absence in other larvae.

The velum of *Lyrodus pedicellatus* reflects the brooding habit having lost the post-oral band and having a large adoral band with a rejection tract. The velum of the released pediveliger is very similar to that of pediveliger larvae of *Ostrea chilensis* despite differences in the veliger stage. This suggests a shared ancestral form that has been modified for brooding. *L. pedicellatus* larvae have a wider adoral band than the ostreid larvae, with this adoral band and rejection tract probably being an artefact of the modified velum of the brooded veliger stage.

The presence of compounds known to change the frequency of ciliary beat in larval molluscs - serotonin and catecholamines - is comparable to the location of the ciliary bands seen in the SEM images. It is possible that the larva can control the frequency of the beat of the pre-oral cirri and the post-oral band. Observations of different swimming trajectories reflect fluctuations in the frequency of the beat of pre-oral cirri and images of irregular ciliary beat were recorded from the velar rim of a feeding larva. SEM images of post-oral cilia lying flat on the shell surface may indicate that ciliary beat was being inhibited when the larva was fixed.

Chapter 4 - Investigation of ciliary swimming through the development of a filming technique

4.1 Introduction

Applying the knowledge gained from anatomical studies of minute organisms, such as that presented in the preceding chapters, within a behavioural context presents significant methodological challenges. Investigations of bivalve larval swimming behaviours, effected through changes in the beat of the velar cilia, provide a suitable subject for the development of an inexpensive methodology for the capture and analysis of digital film of larval swimming.

An individual larva can control its vertical position within the water column, and will respond to external stimulus. Observations of larval population movements in mesocosms following exposure to stimuli such as light, salinity, pressure or temperature have revealed probable behavioural reactions to such stimuli (Mann et al., 1991, Mann & Wolf, 1983, Manuel & O'Dor, 1997, Manuel et al., 2000). Careful observations of larval swimming patterns in well slides or larger containers have documented general swimming paths and fright responses (Cragg, 1980).

Developing a method of filming these swimming behaviours in both controlled and altered environments will enable both a visualisation and analysis of these reactions. The collection of such data, combined with careful observations of swimming larvae, will to add to knowledge of larval competence in the plankton, relate to control of velar ciliation for swimming, and potentially contribute to models of larval dispersal and recruitment (Fuchs et al., 2010).

4.1.1 Current approaches to filming planktonic organisms

Techniques for collecting specific data on the behavioural swimming of planktonic animals such as bivalve larvae are often reliant on specialised microscope cameras tied to expensive software packages. However these products are often subject to lengthy development periods, and consequently require researchers to purchase expensive licences. Free software options

usually feature less usable interfaces, or require specialist knowledge from the user. As a result studies utilising such analysis software are often not economically or academically viable for many researchers. There are several software solutions that have been used for interpreting video of the swimming behaviour of marine invertebrate larvae.

The Ethovision® (Noldus, USA) software is a widely used commercial solution by larval researchers and has been used to analyse the reaction of cyprid larvae to various antifouling products (Aldred et al., 2010, Aldred et al., 2008, Marechal et al., 2004), as well as the behavioural reactions of terrestrial insect larvae (Porcel et al., 2011) and adult Zebrafish (Wong et al., 2010). The developer of this software has further extended this solution to incorporate the EthoVision software within a bespoke filming and animal tracking chamber (DanioVision). While effective, easy to use (the system automates many processes) and known to have produced peer-reviewed data for behavioural analysis of planktonic organisms, the licence cost for usage of such software is usually high.

Two other commercial alternatives are ActualAnalytics® (iBehave group, University of Edinburgh) and Able Particle Tracker (Mu Labs, Slovenia). The ActualAnalytics software is still under development and unlike Ethovision neither has been used to produce peer-reviewed data relating to larval behaviours. Furthermore, whilst both are less expensive options, both still requires licence fees. While potentially applicable to smaller members of the plankton, current versions of the software are primarily concerned with tracking larger organisms (Zebrafish larvae), using multi-point tracking (for example with adult Zebrafish; head, centre of mass and tail).

More complex, less user friendly commercial solutions involve the use of programming environments such as Matlab (MathWorks, Massachusetts, USA), IDL (Exelis Visual Information Solutions Inc, Colorado, USA) or LabVIEW (Texas, USA) for the creation of the user's own algorithms for tracking the subject, or in which to run published algorithms (such as Crocker & Grier, 1996) in software programmed by the user. These programming environments have been used to create algorithms that have produced tracking data for fluorescent particles, barnacle cyprids and gastropod larvae (Crocker & Grier, 1996, Fuchs et al., 2004, Pradhan et al., 2011,

Valentine et al., 2001). The user is required to be familiar with the design of complex mathematical models (Fuchs et al., 2004) or computer programming (Crocker & Grier, 1996, Pradhan et al., 2011, Valentine et al., 2001). Pradhan *et al* (2011) focus specifically on the design of an automated, real-time tracking algorithm for analysing cyprid settlement behaviours.

The approach taken during this chapter focuses on a more accessible solution whereby video data collected using less specialised laboratory equipment can subsequently be interrogated to produce robust data describing larval swimming behaviours. The shareware software ImageJ 1.42q (ImageJ is a public domain, Java-based image processing program developed at the National Institute of Health that provides extensibility via Java plug-ins and recordable macros - http://rsbweb.nih.gov/ij/) is an excellent tool for image analysis with users able to upload macros suitable for specific image analysis tasks. No specialised mathematical or programming knowledge is required. The ImageJ plug-in ParticleTracker (developed by MOSAIC group, Zurich) is designed to track particle trajectories through image sequences using a feature point and tracking algorithm (Sbalzarini & Koumoutsakos, 2005). The software has no specialised computing requirements and can analyse standard image formats (such as JPEG) generated from general photographic equipment. Although designed for cell biology, the adjustments available in the program for detecting low-intensity fluorescence in cell biology (i.e. the ability to select and analyse specific particles) may suit the requirements of analysing the swimming velocities and behaviours of bivalve larvae.

4.1.2 The importance of behavioural swimming responses

Understanding how an individual larva will respond to specific stimuli is important for understanding larval competence in the plankton and for predicting the movements of larval populations and their dispersal from natal populations. The bivalve larva fulfils two roles during its development:

1. The veliger stage larva must be able to swim, feed (if planktotrophic) and avoid predators within the plankton.
2. The pediveliger larva must find a suitable site for metamorphosis into the adult form.

During both veliger and pediveliger larval development stages the larva will swim actively in the plankton, although pediveliger larvae will alternate between swimming in the water column and crawling on the benthos (Cragg, 2006). When either swimming or crawling the larva has the ability to both sense stimuli within its environment and, if necessary, effect a behavioural response to the stimulus (Hadfield & Koehl, 2004). These reactions will ultimately lead to the success or failure of the larvae to find a site to settle and metamorphose, and directly influence larval dispersal (Fuchs et al., 2010).

4.1.3 The responses of the swimming veliger larva to environmental stimuli

The veliger larva is subjected to various environmental stimuli throughout both its planktonic and settlement site searching phases. These stimuli will evoke either a directional taxis or general kinesis response from the veliger. It is still unclear how much the individual larval response to stimuli can influence the position of larval populations in the water column, largely due to a lack of species-specific data concerning these reactions (Baker, 2003, Fuchs et al., 2010). However, information from *Placopecten* veligers indicates these responses contribute to the ability of individual larvae to control their position within water column for avoidance of predators, unfavourable stimuli and maintaining position in feeding zones (Manuel et al., 1996, Manuel et al., 2000, Manuel et al., 1997). Larvae are subject to both vector and scalar stimuli.

Vector stimuli

Vector stimuli such as light or gravity can be vital for the veliger larva to maintain its vertical position within the water, or conversely for the pediveliger to maintain contact with the benthos. Veligers have a phototaxic response to light. *Pecten maximus* and *Placopecten magellanicus* veliger stage larvae move away from strong sources of irradiation, resulting in larvae tending to be closer to the surface in darkness and vertical distributions being highly dependent on prevailing light levels (Kaartvedt et al., 1987, Manuel et al., 1996). Environmental vector stimuli are also important for the pediveliger stage larva. Pediveligers of *Crassostrea virginica* will respond to chemical settlement cues with either downward swimming or rapid sinking (Tamburri et al., 1996, Turner et al., 1994). Such rapid responses to settlement cues are not limited to the

bivalve veliger: the pediveliger larvae of the nudibranch *Phestilla sibogae* respond within seconds to the presence of settlement cues, ceasing swimming and dropping, even in turbulent flows (Hadfield & Koehl, 2004, Pawlik, 1992). Pediveliger larvae of *Pecten maximus* use statocysts to detect gravity for orientation of the larva whilst crawling because the effect of gravity on the shell is no longer consistent when crawling instead of swimming (Cragg & Nott, 1977). Both veliger and pediveliger *Crassostrea virginica* larvae will respond to adverse chemical cues, closing the shell and sinking when exposed to traces of formalin (Hidu & Haskin, 1978a), although this may not be a directed chemotactic response but a chemokinesis.

Scalar stimuli

Larvae also encounter less directed scalar cues such as temperature gradients, pressure, salinity changes, currents and tidal or diurnal cues. Larvae of *Crassostrea virginica* are capable of responding to changes in salinity, increasing swimming in higher salinities (Hidu & Haskin, 1978b). This response contributes to the maintenance of larval populations within areas such as bays and estuaries by, to a limited extent, counteracting the influence of tides and currents by controlling larval vertical position in the water column (Wood & Hargis, 1971). Much research has centred on the movement of estuarine larval populations due to the coastal nature of economically important molluscan species such as *Crassostrea virginica* or *Crassostrea gigas*, and the relative ease of successfully collecting larvae from these restricted field sample sites. However, there is still transport of larvae out of estuaries, because while veligers are capable of responding to salinity through changes in swimming velocity (Hidu & Haskin, 1978b) or vertical position (Wood & Hargis, 1971), larvae still are subject to passive transport via the patterns of local currents (Verwey, 1966). The issue of larval behaviour affecting larval retention in estuarine situations is still somewhat contentious, with arguments against behaviour having a significant effect stating that swimming capabilities will only influence retention in estuaries if the flow is below 0.15m s^{-1} (Roegner, 2000).

Coastal upwelling and downwellings have also been implicated in larval distribution, with larval behaviour greatly influencing the extent to which these hydrodynamic factors affect, or do

not affect, the larval distribution (Shanks & Brink, 2005). Upwellings or downwellings may overwhelm the behavioural reactions of smaller larvae (Dekshenieks et al., 1996), as has also been suggested for estuarine water movements (Roegner, 2000). Furthermore several authors have suggested that the effect of behaviour will likely vary significantly between species, as the intensity and type of reaction varies between species (Ma et al., 2006, North et al., 2008, Shanks & Brink, 2005).

Pressure is an important stimulus for its relation to depth. Veliger larvae of *Arctica islandica* will respond to increases in pressure by increasing the diameter of the swimming helix, and as a result tend to show an increase in upward movement (Mann & Wolf, 1983). This response plays a key role in determining the depth of the veliger population, as does the larva's reaction to local thermoclines.

Temperature variability will typically be encountered by the larvae when swimming brings them into contact with thermoclines. In the coastal areas where many large bivalve populations are located, these thermoclines can be as much as 5.5^{o}C within a 10m depth, although there will probably be associated salinity changes as well (Tremblay et al., 1994). *Placopecten* veligers are capable of detecting relatively sharp 1.5 degree thermoclines (Manuel et al., 2000), and have been shown to not cross thermoclines of more than 5^{o}C (Gallager et al., 1996) and to swim vertically in response to colder waters (Manuel et al., 2000). *Placopecten* pediveligers can detect similar gradients, with larvae responding by showing a preference for favourable temperature regimes for settlement (Pearce et al., 2004). It is not known if bivalve larvae are capable of rapid responses when detecting unfavourable temperature stimuli. The mechanism of detection of thermal cues is also unknown (Manuel et al., 2000).

The reaction to thermoclines is especially important as veliger larvae are known to undertake significant vertical migrations as a behavioural reaction to scalar stimuli such as diurnal cycles or currents (Manuel & O'Dor, 1997, Manuel et al., 1997). Veligers of the scallop *Placopecten magellanicus* respond both to diurnal and tidal cues by rising or falling in the water, to keep a population within a favourable area whilst having the additional advantage to the larva

of avoiding predators and finding food (Manuel & O'Dor, 1997, Manuel et al., 1997). During these migrations larvae will encounter and probably cross thermoclines. Indeed this means the thermocline is not a physical barrier to the migrations, and could even be an additional trigger for them (Manuel et al., 2000).

4.1.4 The importance of collecting laboratory data on molluscan larval behaviour; modelling dispersal

Larval responses to stimuli have to be considered when creating complex simulations of bivalve larval distribution or dispersal within hydrodynamic models. Modelling often relies on laboratory data of larval behaviour, or data from field sampling, and subsequently incorporating this into known tidal movements or simulated conditions (Fuchs et al., 2010), Dekshenieks et al., 1996). For example, laboratory studies of the reactions of gastropod larvae to turbulence reveal species-specific reactions to these conditions (Fuchs et al., 2010). Inclusion of these data into local hydrographic models reveals these reactions contribute to suitable site selection for each species (Fuchs et al., 2007, Fuchs et al., 2010). Such informative, species-specific data is not currently available for many bivalve larvae (or indeed many molluscan larvae).

Often it is too complex to incorporate every aspect of larval behaviour so specific responses appropriate for the models are used: for example pediveliger responses to light have been incorporated into models of larval settlement in turbulent/turbid water (Eckman et al., 1994), or reactions of gastropod larvae to turbulence incorporated into site selection models in estuaries (Fuchs et al., 2010). Attempts have been made to model larval dispersal within an estuarine environment incorporating multiple behavioural assumptions from laboratory observations and literature sources (North et al., 2008). The authors note that behaviour has a significant effect, and that this will vary between species. Consequently this is problematic if species specific data are not available.

Swimming velocities are a good example of such a gap in knowledge of a larval behaviour that will exert considerable influence on larval distributions. Whilst there are published data on species specific swimming velocities (Chia et al., 1984, Mileikovsky, 1973), this does not cover

many species likely to be the object of models, i.e. those economically important species. For example there is little information in the literature on the swimming velocities of *Crassostrea gigas* larvae. As a result any subsequent effect on these velocities from larval responses to environmental stimuli are also unknown and will hamper the effectiveness of these distribution models (Baker, 2003, North et al., 2008). Consequently there is a requirement for the design of effective methods of collecting species-specific larval swimming data following exposure to stimulus likely to be encountered in the environmental, such as temperature.

4.1.5 The use of temperature to investigate behavioural responses in the laboratory

Temperature is a tractable stimulus for investigating the effectiveness of a method for analysing a behavioural or physiological reaction in bivalve larval swimming, as at least a physiological response could be expected (Rico-Villa et al., 2009). Furthermore results for *Crassostrea virginica* larval swimming in differing temperature regimes indicate that a swimming velocity and behavioural response in *C. gigas* larvae is probable (Hidu & Haskin, 1978a). It is also a variable that is fairly simple to control within a laboratory, and will therefore suit a method development.

Salinity and temperature are two key environmental stimuli and are usually present in the hydrographical aspects of larval distribution models. As a result species behavioural reactions to these stimuli, if available, should also be included. Information is available on the effect of both temperature and salinity on the successful hatchery production of larvae (His et al., 1989, Robert et al., 1988), or the changes in development pattern as a result of suboptimal salinity and temperature conditions (Dekshenieks et al., 1996, Dove & O'Connor, 2007, Drent, 2002, Gruffydd, 1976, His et al., 1989, His & Seaman, 1992, Hoagland, 1986, Pechenik, 1999). Information is also available for salinity and temperature effects on the settlement rate of bivalve larvae in commercial culture (Devakie & Ali, 2000, Rico-Villa et al., 2009).

Knowledge of species specific behavioural reactions to either temperature or salinity for the incorporation into models is currently limited, mainly to *Crassostrea virginica* (Baker, 1997, Baker, 2003, Hidu & Haskin, 1978a, Turner et al., 1994, Wood & Hargis, 1971) and *Placopecten*

magellanicus (Gallager et al., 1996, Manuel et al., 2000, Tremblay et al., 1994). The importance of this information for distribution modelling is evident when considering that veligers of *Crassostrea virginica* are known to be tolerant of a wide thermal range (Hidu et al., 1973), and to swim more quickly at higher temperatures (Finelli & Wethey, 2003, Gallager, 1993, Hadfield & Koehl, 2004, Hidu & Haskin, 1978a, Tamburri et al., 1996, Turner et al., 1994). These data for *C.virginica* swimming in differing thermal condition will also provide a comparative tool for the data to be collected using the filming design and ImageJ image processing proposed.

4.1.6 The effect of temperature on cilia

There is considerable information on the increase in the filtration rate of ciliary suspension feeding in bivalves with increasing temperature (Galtsoff, 1928, Haure et al., 1998, Jørgensen, 1966, Leigh, 1962, Sylvester et al., 2005), although incorrect methods or differing experimental conditions have led to some inconsistent results (Riisgard, 2001). Furthermore the metabolic effects on the poikilothermic bivalve larva when water temperature increases should result in an increase in ciliary beat (Riisgard, 2001) until the optimum for bivalve ciliary beat, ~30^{o}C, is reached (Galtsoff, 1928, Haure et al., 1998). Thus a higher swimming velocity is expected as the water temperature increases, as a result of an increase in the frequency of the metachronal beat of the pre-oral cirri on the velar rim.

Also to be considered are the changes in the physical properties of the seawater during this temperature change, with viscosity falling as temperature rises (Podolsky & Emlet, 1993). This fall in viscosity has been shown to affect bio-mechanical activity, as a ciliary beat increases at higher temperatures and cilia have to work less in the lower viscosity (Larsen & Riisgård, 2009). In fact decreased seawater viscosity is likely to be a more important factor on the increase of ciliary beat in higher temperatures than the physiological effects of the higher temperature (Larsen & Riisgård, 2009, Riisgard & Larsen, 2009). It is difficult to positively distinguish between the direct physiological effect of temperature and the effect of viscosity on cilia as temperature induced viscosity changes do not always show exactly the same results as temperature controlled viscosity experiments (Larsen & Riisgård, 2009). However, viscosity has been shown to have a

major influence on the swimming velocity of a wide range of small planktonic organisms such as: fish larvae (Podolsky & Emlet, 1993, von Herbing & Keating, 2003), polychaete larvae (Bolton & Havenhand, 1997), copepods (Larsen et al., 2008) and ciliates (Riisgard & Larsen, 2009). Although viscosity effects have not yet been verified for molluscan larvae it seems likely that viscosity changes associated with changing water temperatures would probably affect swimming velocity through the physical effects on the action of the pre-oral cirri of the velum. However this lack of literature does not preclude a behavioural response to the detection of either viscosity or temperature change.

4.1.7 The objectives of this chapter

Field experiments with the behaviour of bivalve larvae present considerable practical difficulties, especially when investigating specific variables such as velocity that will be affected by environmental conditions. Laboratory models offer a controlled environment in which to manipulate the environmental variables of interest allowing analysis of behavioural change. However the design and interpretation of associated experiments have considerable practical and financial difficulties to overcome. To test the effectiveness of an inexpensive and relatively straightforward method of investigating larval behaviour, digital film was collected of larvae swimming in constant and manipulated water temperatures. Experiments were conducted in a purpose-built temperature-controlled water bath that allowed control of the water temperature the larvae were exposed to. Individual larval swimming paths and velocities were extracted from film using ImageJ.

Temperature is a key variable in the larval environment (Drent, 2002, Hoagland, 1986, Larsen et al., 2008, Mann & Wolf, 1983, Tremblay & Sinclair, 1992, von Herbing & Keating, 2003). Swimming velocity change is a measurable and an expected outcome of temperature change (Hidu & Haskin, 1978a), either through a behavioural response, physiological change within the larva (Rico-Villa et al., 2009) or physical changes in water viscosity (Riisgard & Larsen, 2009). As such temperature is considered a suitable variable through which the effectiveness of this method of data collection can be investigated.

There are no published data on the swimming velocity of *Crassostrea gigas* larvae, or details of any behavioural responses to the detection of sudden temperature changes. However, there are swimming velocity data for other closely related oyster species such as *Crassostrea virginica* (Hidu & Haskin, 1978a). Such data can be used for comparative purposes, both to validate the method and provide some application for the results obtained in this chapter.

Developing effective methods of generating data on larval behaviours is vital to enable incorporation of swimming velocity or behavioural data as variables in mathematical models of larval population distribution and dispersal. Such data may both increase knowledge of the larval capability within the planktonic environment, and improve the accuracy of such models (Fuchs et al., 2010). Furthermore the effects of temperature have a direct bearing on the function of the velar ciliation described in the previous chapter. The use of computer analysis of swimming velocity in water held at culture temperature has the potential to be used as a behavioural assay for gauging larval fitness within a hatchery situation. A series of questions have been considered to guide the trial of the method devised:

What is the swimming velocity of temperature acclimated* Crassostrea gigas *larvae?

The veliger and pediveliger larvae of *Crassostrea gigas* were filmed throughout a controlled temperature range, by filming the larvae swimming after a period of acclimation to a series of water temperatures. Temperature control will be achieved through the design of a flow-through water bath. This was capable of both effecting changes to the larval environment, and of holding a steady temperature. Video footage was analysed using ImageJ software to select those larval trajectories composed of only vertical swimming - upward swimming is a behavioural action with speed and direction being controlled by the individual larva, thus the ability to select for these data is appropriate. Falling is often achieved by larvae simply closing the shell, or by using the velum to intermittently control the larva's descent (Cragg, 1980). Furthermore, free-falling will be affected by physical factors such as variation in size of individuals: thus velocity measurements from falling larvae are considered a less useful measure of behavioural velocities, i.e. those swimming velocities controlled by the larva.

What is the thermal tolerance of temperature acclimated larvae?

It is postulated that the swimming of larvae that have been acclimated to a temperature will show the thermal tolerance of the larvae. Velocities of acclimated larvae were collected at a variety of steady temperatures. These have enabled the reactions of the larvae in behavioural experiments to be considered against the physiological capability of the larva to swim at a certain temperature.

Can the methodology reveal behavioural reactions to temperatures changes?

Larvae were also exposed to rapid changes of temperature to see if there is a behavioural response to the detection of the exaggerated temperature change. Two types of data were collected and investigated - vertical swimming velocity change and changes in swimming pattern. These responses were examined by filming larval swimming patterns following the exposure to rapid temperature change for comparisons to constant temperature controls. Vertical swimming velocities were recorded following the rapid temperature change.

Veliger and pediveliger stage larvae were used in experiments. It is proposed that there may be variation between planktonic veliger stage larvae and the more benthic pediveliger larvae, potentially adding a further layer of complexity to the interpretation of behavioural responses. Furthermore there is a notable difference in the sizes of the two development stages. This a relevant consideration if this filming technique is to be applicable to a range of planktonic studies and as thus a range of planktonic sizes classes, not limited to only bivalve larvae.

4.2 Materials and Methods

Overview of filming design

Larvae were filmed in 4ml spectrophotometer cuvettes, held in a bespoke temperature controlled water bath, for either 2 or 5 minute time periods to measure swimming velocities of individual larvae, and to observe individual larval swimming behaviours. These observations were divided into three categories:

1. Swimming velocities of acclimated larvae. Two minute films recorded for measurement of larval vertical swimming velocities at a series of stable temperatures, following a period of time where the larvae acclimated to the water temperature.
2. Swimming velocities following rapid temperature change. Five minute films of larval vertical swimming velocity changes following the detection of a rapid alteration in water temperature.
3. Larval behavioural responses. 5 minute films of larval swimming where behaviour types were recorded following exposure to rapid changes in temperature.

4.2.1 Larval sampling

Larvae of *Crassostrea gigas* were sampled directly from the culture bins within SeaSalter Shellfish's hatchery facility. Sampling at the hatchery was conducted on several different occasions resulting in sampling from several different broodstocks. Larvae had been reared at 26-28^{o}C in the aerated flow-through system described in Chapter 2, section **2.2**. Larvae were collected from the culture bins before each session of filming and maintained in glass beakers at 26^{o}C until required for filming work. Beakers were covered and left in clean environments in order to exclude, as far as was practicable, dust particles that would interfere with the tracking software when video footage was analysed. Larvae in the beakers were regularly checked using a dissecting microscope to ensure swimming was being maintained. Prior to each filming run, beakers were agitated to ensure even sampling of larvae and approximately 4ml of seawater containing larvae placed into 4ml polystyrene spectrophotometer cuvettes (internal dimensions -

height 42mm, width 10mm, depth 10mm) within a temperature controlled filming chamber. These were left for 20 minutes to allow the larvae to acclimatise to the cuvette environment. The cuvettes were even sided, not tapering, and had two clear sides for filming.

4.2.2 Filming chamber and filming equipment

A bespoke filming chamber was constructed for video capture. This comprised a Perspex® water bath containing 5 plastic spectrophotometer cuvettes of the dimensions provided above. Water was fed into the bath through a perforated tube behind the cuvettes ensuring water was delivered evenly throughout the chamber, avoiding hot or cold spots near the cuvettes. A diagram of this chamber is provided overleaf in Figure 4.1.

A heater-chiller unit with a temperature control unit (Model G heater/chiller with model D1 controller, Haake Ltd, Denmark) was used to pump water through the filming chamber, controlling the temperature in the chamber to within ±1^{o}C (determined though constant temperature trials of 5 minutes to 4 hours). A flow-limiting crimp on the inflow maintained a gentle flow-through. The chamber temperature was held at 28^{o}C when larvae were inserted into the cuvettes and the chamber temperature subsequently raised or lowered to the level required for filming. Larval acclimation began once the water in the cuvettes in the filming chamber had reached the filming temperature set by the heater-chiller unit. Larvae were acclimatised to the cuvette and chamber for 20 minutes. Filming was conducted at 2^{o}C intervals from 10^{o}C to 38^{o}C.

For rapid temperature change experiments the heater-chiller was used to warm or chill the water in the filming chamber whilst larvae were held in cuvettes in the laboratory, outside of the chamber, in hatchery seawater for a 20 minute, 26^{o}C acclimation period. Following acclimation the cuvettes containing larvae were placed into the filming chamber. For temperature reduction experiments the water in the chamber was maintained at 10^{o}C, for temperature increase experiments the filming chamber was stable at 40^{o}C. Filming began immediately the cuvettes were placed into the filming chamber. This method was used in preference to altering temperature whilst the cuvettes were in place as the heater-chiller unit did not heat or cool quickly enough. Figure 4.2 summarises the sequence of events for video capture.

Filming chamber viewed from above

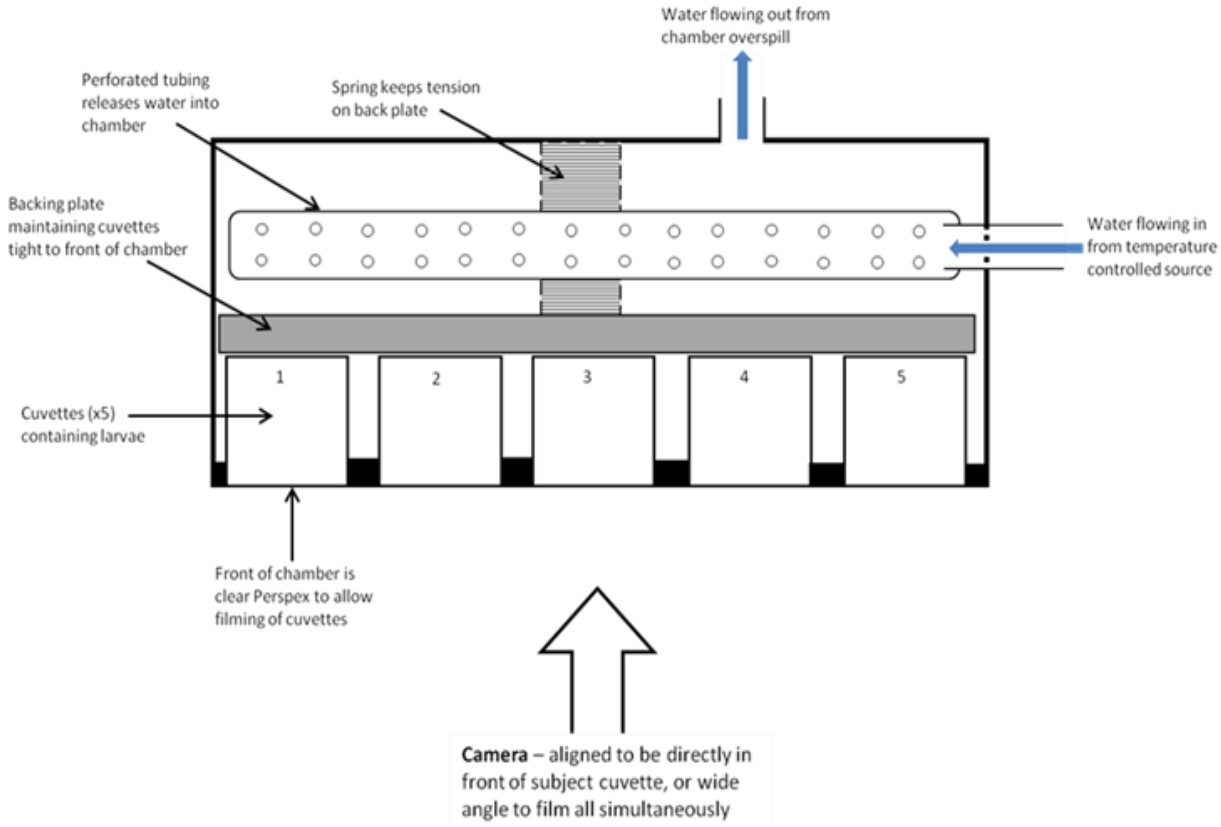

Filming chamber viewed from front (the filming face)

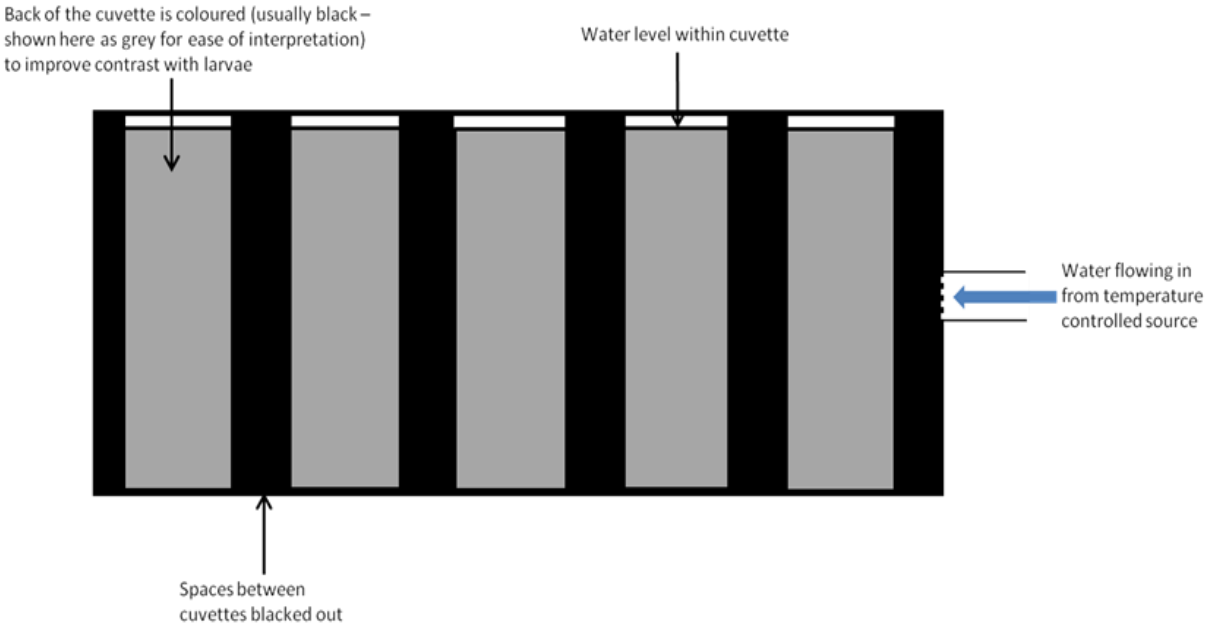

Figure 4.1 - Diagram of the larval filming chamber

The chamber was constructed from Perspex® sheets and designed to give an even distribution of heat to all 5 cuvettes. The top diagram shows the layout of the cuvettes within the chamber, and the arrangement of the cuvettes flush to the face of the chamber. This was designed to minimise any distortion of the image captured. When the camera was aligned in front of the filming chamber (giving the view shown in the bottom diagram) cuvettes could be filmed in high magnification singly, or the three central cuvette filmed.

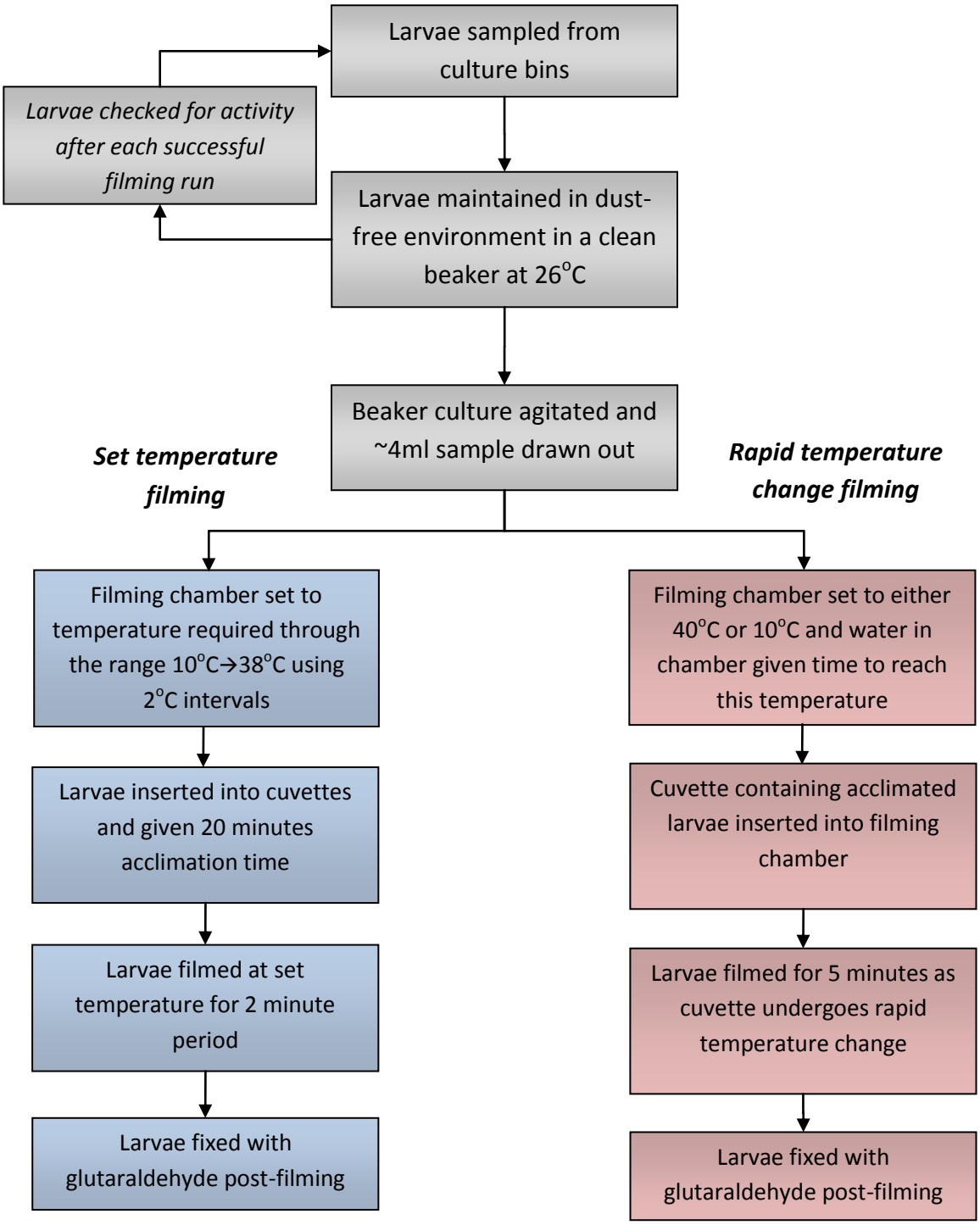

Figure 4.2 - Work-flow for filming larval swimming behaviours and velocities in respect to water temperature.

This work-flow summarises the approaches taken to collect; film of acclimated larvae for information on swimming velocities at set temperatures, film for any velocity response of larvae during rapid temperature change and film of behavioural reactions during rapid changes in water temperature.

The filming chamber was illuminated using a cold light source (so as to minimise heat being introduced from light sources) with flexible fibre optic arms to evenly direct the light into the chamber. Filters were placed over the ends of the optic arms to evenly distribute the light from these point-light sources. Care was taken to ensure the lighting did not come from either one of the sides or from above or below to prevent larval phototaxis.

The back of each cuvette was painted matt black to provide better contrast with the larvae, which appeared as bright white specks on the video when the chamber was lit. Trials were conducted with background colour; white provided good contrast, larvae appearing black, however even matt whites produced some glare on the image. The ImageJ analysis software was more successful identifying larvae against a black background. Greyscales were not suitable with larvae being difficult to identify on the video.

All of the 5 cuvettes contained larvae in seawater and all were filmed. The three central cuvettes were used as replicates for velocity or behavioural experiments. The outer two cuvettes were used to monitor water temperatures (using a K-type probe) within the cuvettes during filming. The water temperature within the filming chamber was also monitored.

4.2.3 Video capture of larvae swimming in cuvettes

Larval swimming within the cuvettes was filmed using a digital camera (JVC TK-C1381, 470,000 pixels) with an SLR macro-lens (focal length 100mm) attached by a C mount converter, with the whole assembly mounted on a tripod facing the filming chamber. The adjustable tripod allowed the lenses to be set perfectly horizontal. The video output was captured onto a computer using a USB video creator (Dazzle USB, Pinnacle, USA). All of these pieces of video capture equipment are suitable for general use photography. They are available to most researchers for a relatively low cost in comparison to more specialised microscopy cameras. Constraints of the equipment resulted in it being more practical for filming to begin at the colder temperatures, as chilling water took significantly longer than heating.

For acclimated larvae in steady temperature regimes, filming started at the lowest filming temperature, and the temperature was raised by 2 degrees for each filming interval. Each filming

interval was 2 minutes of video capture of larval swimming in the cuvettes, at the temperature controlled by the water bath. Fresh larvae, from the same original culture, were used for each filming interval. This length of film was a suitable compromise between adequate records of larval swimming for velocity measurements, combined with a manageable file size (2 minutes of video generated ~3000 frames of video for later processing).

Rapid temperature change experiments were filmed for 5 minutes in order to observe larval behavioural responses and provide reactions over a significant period of temperature change. To provide an example of normal larval swimming behaviours, 5 minutes of film was captured for each of the cuvettes at 26-28^{o}C, these temperatures corresponding to those used within the hatchery cultures. This film was used as a control for larval behavioural and velocity measurements. At the end of each filming run the larvae from each cuvette were fixed with 4% glutaraldehyde in a 0.2M cacodylate buffer to allow the number present in each cuvette to be counted for calculating the percentage of the population actively swimming during filming.

4.2.4 Raw processing of video files

Following capture of video, the files required some treatment before larval trajectories could be extracted. The video creator captured un-finalised video files which were converted into MPEG-2 files using the Dazzle software. In final filming trips these videos showed all cuvettes (earlier trials successfully captured higher magnification videos of single cuvettes, but there was no difference in the subsequent processing due to the limits of the digital resolution of the camera - capturing all three cuvettes simultaneously subsequently streamlined film collection work and allowed for more data to be collected). These files were cropped into separate files, one for each individual replicate (cuvette) and exported as image sequences using the freeware programme VirtualDub64 1.8.8 (http://www.virtualdub.org/). The image sequence saved comprised the individual frames of the video captured - 3000 JPEG files per 2 minutes of footage, per replicate (video capture frame rate 25fps), or 7500 JPEG files for the 5 minutes of rapid temperature change footage.

These image sequences were imported into ImageJ 1.42q (64 bit version - ImageJ is a public domain, Java-based image processing program developed at the National Institute of Health that provides extensibility via Java plug-ins and recordable macros - http://rsbweb.nih.gov/ij/) and converted to greyscale to reduce file size for ease of processing. In the case of the 5 minute videos, the image sequences were imported as 750 frame (30 second) sections - the full 7500 image sequence was too demanding on computer memory (>8 gigabytes was required) to be processed as one entire sequence.

Brightness, contrast and noise adjustments were made to ensure the larvae stood out as clearly as possible from the background, and the image was enlarged to make the larvae easier to pick out. Once enlarged, a line of known length was drawn across the image and used to calibrate a scale. This scale was calculated for each set of films from each visit to the hatchery to take into account any slight differences in the set-up of the filming equipment (for example, distance of the camera from the filming chamber).

4.2.5 Image analysis

Extracting velocity data

The ImageJ plug-in ParticleTracker (http://rsbweb.nih.gov/ij/plugins/index.html) was used to analyse the larval swimming image sequences created by VirtualDub. These sequences were imported into ImageJ and ParticleTracker identified swimming larvae by means of user-defined pixel size and light intensity. Individual larvae were then tracked through an image sequence (i.e. through a filming interval) using a feature point detection and tracking algorithm (Sbalzarini & Koumoutsakos, 2005). The number of pixels of movement of a particle (larva) between frames and the number of frames used to track a particle could be user-defined to increase the accuracy of larval tracking. Once all images in a sequence were analysed, ParticleTracker generated an *All Trajectories* visualisation showing all the individual larval paths in a replicate over either the 2 minutes of filming (Figure 4.3), or the 30 second (750 frames) clips used for the 5 minute video analysis. The tracking of larvae through a sequence and consequent generation of the *All Trajectories Visual* was fairly computationally demanding requiring, ideally, a quad core processor

(Intel® Q9550 or similar specification) and a minimum of 2-4 gigabytes of memory (4-6 gigabytes if some memory is reserved for the graphics card). Processing was possible on a lower specification computer, but was significantly slower (often ≥1hour per sequence).

Figure 4.3 - An *All Trajectories Visual* screenshot

This screenshot shows all the tracked particles (larvae and any dust contamination) in a single cuvette at 18°C. This image has had a filter applied to it to remove any trajectories less than 75 frames (3 seconds) in length. The multi-coloured lines are the paths taken by individual larvae within the 2 minute filming period. Without the filter it is impossible to discern these individual trajectories.

A filter was applied to the All Trajectories image cutting out image sequences shorter than 75 frames to eliminate short tracks that included those made by dust particles. Without this filter every speck on the screen was tracked, even if it occurred for just 2 frames (or 0.08 seconds). A sequence of 75 frames (3 seconds) provided an acceptable balance between a manageable number of trajectories and the collection of larval velocities. For the 30 second sequences from the longer video sequences a 50 frame filter was applied. All the upward swimming individual larval trajectories were selected from the 'All Trajectories Visual' screen (aided by playing the

sequence), shown in Figure 4.3. The image sequence of each selected trajectory was manually played as a video to check that it tracked only one larva. In addition the user could ensure the trajectory was that of a larva that maintained upward swimming. When the trajectories were viewed in this manner ParticleTracker overlaid a line indicating the object being tracked and its path (Figure 4.4). This was particularly informative for investigating larval swimming patterns, and for validating trajectories to be used for analysis.

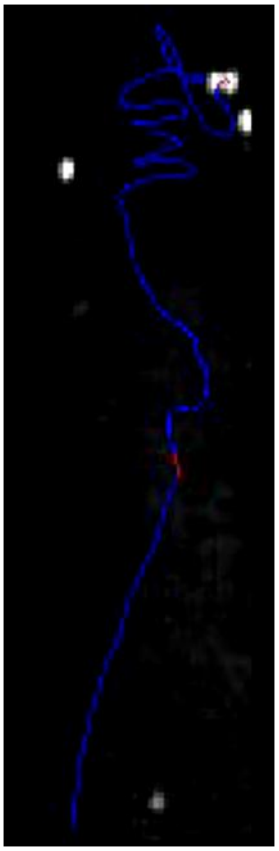

Figure 4.4 - ImageJ screen-grab of a single trajectory.

This trajectory is selected from a visualisation such as the one in Figure 4.3. The white spots are the larvae and the blue line indicates the individual path of the tracked larva. In this instance the larva has begun at the bottom of the image and swum upward with little deviation before swimming in a helical pattern at the top of the image.

Once trajectories had been validated, X and Y coordinates for the larva were generated from each image in the sequence and these were outputted into a Notepad document. Any discrepancies in the dataset (such as a larva falling at the beginning or end of the track) were cut out at this point. This procedure was then repeated for every trajectory shown in the visualisation (Figure 4.3) until a set of frame-by-frame coordinates was obtained for each upward swimming larva in each cuvette. Data were imported from Notepad into an Excel spreadsheet (post Excel 2007 it was possible to output straight from ImageJ to Excel) as comma delimited data

and the displacement (in pixels) between particle coordinates in consecutive frames (images) was calculated using a simple Pythagoras equation. The pixel displacement between the two images gave a distance, which was converted from pixels to mm using the scale calculated earlier. Video sequences were recorded at 25fps, giving 0.04 seconds between successive images. The displacement between 2 images therefore gave the distance moved in 0.04 seconds. Total time for each larval trajectory was calculated by multiplying total number of images by 0.04. Total distance moved by the larva was calculated by summing the displacement values for each video frame. Velocity of each trajectory was calculated in mm s^{-1}. Each larval trajectory was recorded in this manner giving a comprehensive velocity record for every upward swimming larva in every cuvette at every temperature.

4.2.6 Behavioural measurements - counts of rising, descending and falling larvae

Counts were made of the number of larvae swimming past a mid-line that was drawn across the video at the precise half-depth of each cuvette, and the video played - larvae that crossed this line were counted. Counts were separated into 10 second segments of the 5 minute video sequence. Three specific types of larval movement were counted to assess larval behaviour as well as activity:

1. *Rising* - larvae actively swimming upwards.
2. *Descending* - larvae controlling a fall through the water column using the velum.
3. *Falling* - larvae with closed shells falling rapidly and uncontrolled.

4.2.7 Counting of larvae from filming cuvettes

A procedure for automating counting large numbers of larvae was also developed. Fixed larvae were washed from the cuvettes into separate chambers in a well-tray and gently shaken to prevent clumps of larvae. These circular wells were drained of excessive fluid to reduce image distortion and photographed from precisely above the well. This image was then imported into ImageJ. The circular well was cut out from the image, converted to an 8-bit image and thresholding applied to the image so that larvae appeared as black dots on a white background.

In areas where thresholding led to small groups of larvae being regarded as a large gathering of pixels, the image was adjusted to resolve each larva. ImageJ produced a count of the number of larvae. To ensure accuracy, several manual counts were also conducted for comparison to Image J results. This process is summarised below in Figure 4.5.

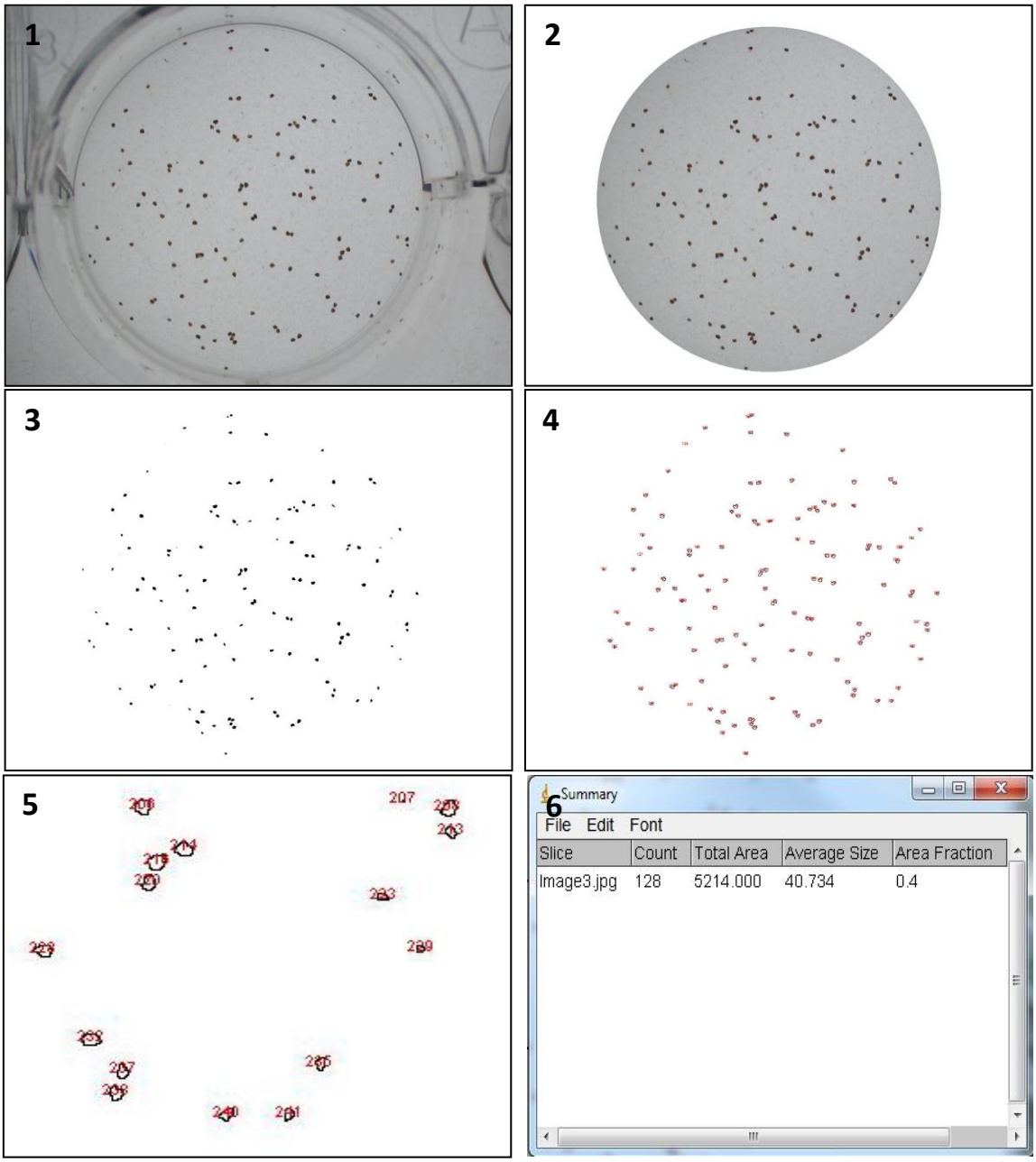

Figure 4.5 - ImageJ screen grabs showing the digital counting of larvae.

1) The original image of the well containing larvae from a cuvette. **2**) The cut-out image of the inside of the well. **3)** The cut-out image after thresholding. **4)** Visualisation of ImageJ count. **5)** An enlargement of **4** showing the larvae being picked out and counted. **6)** The final summary given after the count analysis.

4.3 Results

4.3.1 Observations of Larval swimming patterns

Larvae swam in three distinct patterns: upwards swimming in a helix pattern, descending using the beat of the pre-oral cirri to control falling and horizontal swimming across the cuvette. Some larvae also swam upwards without deviation or fell rapidly by retracting the velum and falling freely. These patterns are illustrated in Figure 4.6**,** a series of screenshots from the ImageJ software. The software was able to successfully track and illustrate the swimming path of multiple individuals within the same cuvette.

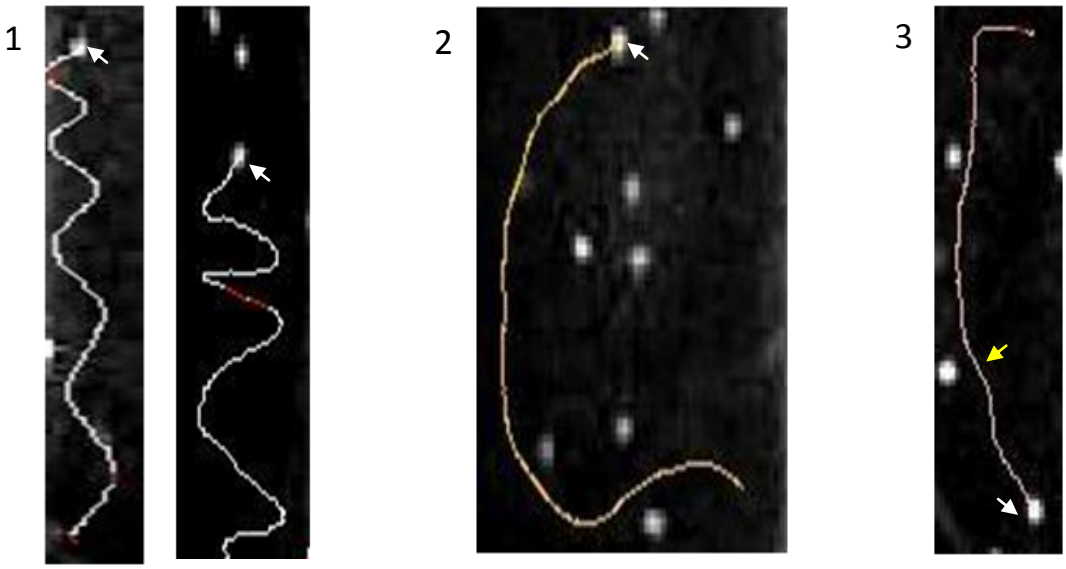

Figure 4.6 - Series of ImageJ screenshots showing larval swimming patterns

Each image illustrates the end of a filming video: the computer has overlaid a line as it has tracked the larva through its swimming path. Larvae are arrowed in each image, with the arrow representing the larva's final position at the end of the swimming video.

1. Larvae swimming upwards in a helical pattern.

2. Larva swam along a horizontal path from right to left, swimming upwards along a curved, not helical, path for the remainder of the video.

3. This larva swam briefly horizontally from right to left before descending using the velum. The curve of the fall, punctuated by occasional slight changes in the swimming path (yellow arrow), indicates the larva using the velum to control its descent as opposed to falling simply through retracting the velum and closing the shell. It is possible these changes reflect the detection of the neighbouring larvae, with the descending larva detecting the vibration of the ciliary beat of these larvae and effecting a change in the path of descent to avoid them.

4.3.2 Swimming velocities of temperature acclimated larvae

During the development of this filming methodology, some data have been generated on the swimming velocities of *Crassostrea gigas* larvae. The investigation of these data is valuable for assessing the usefulness of the filming and data extraction techniques, and for guiding the future development of this method. Two statistical packages have been used for this analysis, Minitab® 14 Statistical Software (Minitab Inc, UK) and GenStat® 13 (VSN International Ltd, UK - some notes on the regression analysis used by this package are provided on p238).

The larvae were acclimated to stable temperatures (10°C-38°C) and filmed swimming. Four different batches of larvae were filmed for the collection of vertical swimming velocities with mean batch sizes of: 250µm (batch 1), 213µm (batch 2), 257µm (batch 3), and 180µm (batch 4). Batch 1 was filmed in a range from 16-30°C, batch 2 in 20°C to 38°C, batch 3 in 24°C to 38°C and batch 4 in 10°C to 38°C. The difference in the temperature ranges was a result of the method development - rapidly cooling water was found to be more difficult than warming water (batch 4 being the final data collection trial, with the largest temperature range).

Overall 1139 individual larval swimming velocities were recorded, with an overall trend for an increase in swimming velocity through the ascending temperature regime from 12°C to 22°C (below the culture temperature, no larvae were observed swimming in <10°C), with no obvious trend in the 24°C-38°C range. Figure 4.7 presents velocity data that has been transformed to $\log_e$ to ensure the data was normally distributed. Seawater viscosity change with temperature has also been presented on a second axis for context.

These data are not appropriate to be modelled in terms of larval dispersal. Swimming velocity datum of this type, generated using this method, are most suitable for incorporation as a factor in such mathematical models. It provides larval movement potential in specific water temperature ranges; however, it does not provide (as yet) sufficient data to be modelled in independently. This will be considered more in the discussion.

Following examination of the data presented in Figure 4.7, the analysis of set-temperature swimming velocities has been split into two areas for investigation. This interim analysis is the most appropriate at this stage of method development, indentifying general patterns or flaws within these data to guide further enhancements of the data collection methodology. The two areas investigated are:

- Analysis of the apparently linear trend for velocity increase with increasing temperature in lower temperature range (Figure 4.7). The maximum temperature range included in this analysis was determined through a series of regression analyses (examining R^2_{adj} and standard error values - Table 4.1)
- Analysis of the upper temperature range. This analysis takes two forms:
    - Regression analysis of velocity versus temperature
    - ANOVA between larval batches

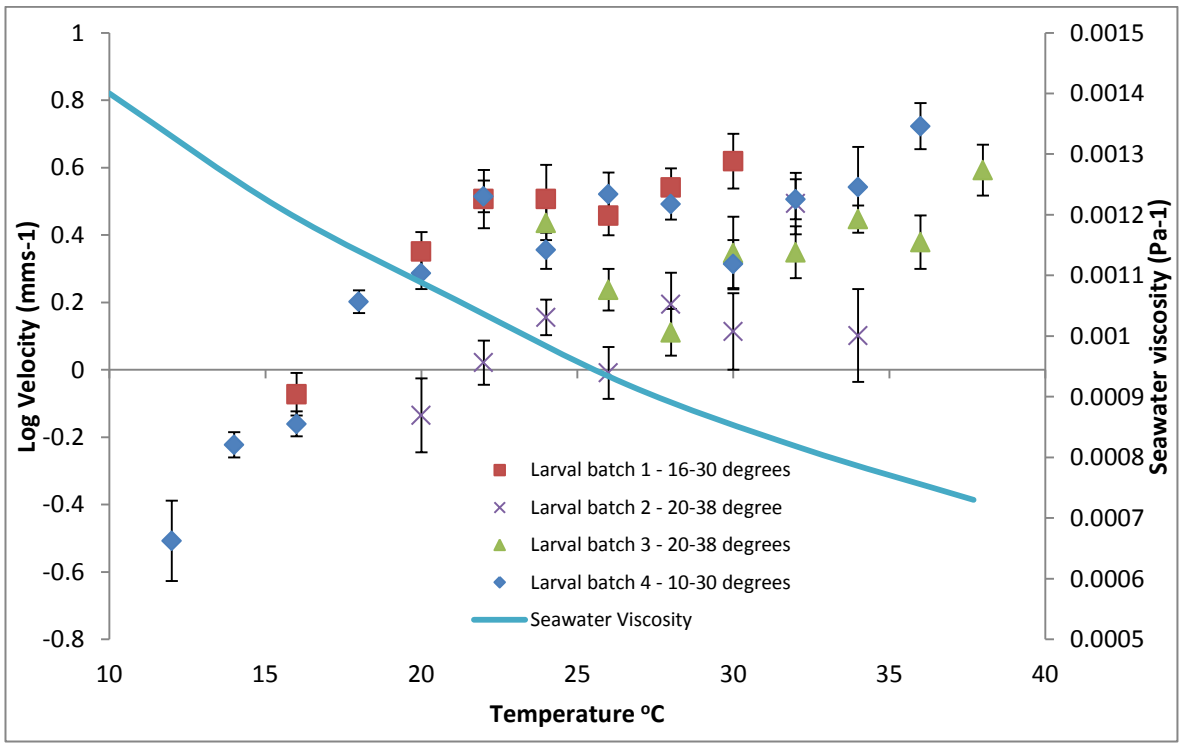

Figure 4.7- Mean $\log_e$ larval batch velocity versus temperature for the range 12°C-38°C, +/- 1 SE

Larval velocity increases from 12°C to 22°C from approximately 0.5mms^{-1} to approximately 1.8mms^{-1}. From 22°C there is no obvious trend for increase in velocity versus temperature for any larval batch (10°C-38°C, total n = 1139, n batch 1 = 132, n batch 2 = 169, n batch 3 = 324, n batch 4 = 514).

Examining the 12°C to 22°C temperature range - larvae of batches 1 and 4

All velocity data was transformed to $\log_e$. Raw data was not normally distributed - normal probability plots indicated a positive skew, and a Box-Cox analysis (Minitab 14) indicated that $\log_e$ was the most appropriate transformation to stabilise the variance. An analysis of variance (ANOVA) test was performed to determine if there was a significant difference between the datasets from larval batches 1 and 4, these being the only datasets with velocity data below 20°C. The ANOVA indicated that there was no significant difference ($F_{1, 329}$=3.98, p>0.05) in the velocities of batches 1 and 4 through the temperature range 12°C-22°C (Figure 4.8).

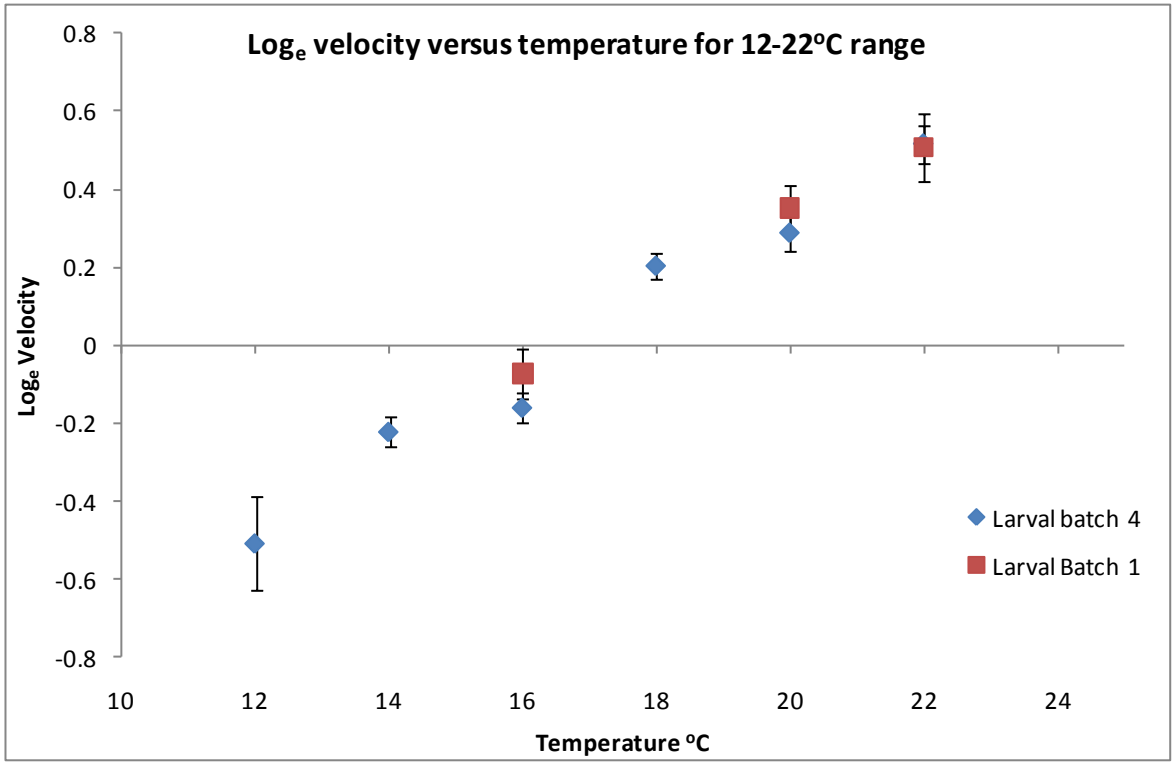

Figure 4.8 - Mean increase in swimming velocities from 12°C to 22°C, +/- 1 SE

Larval velocity increased in this pattern in the 12°C to 22°C range for larvae of batch 1 and 4 (n=338). An ANOVA indicated that there was no statistically significant difference ($F_{1, 329}$=3.98, p=0.182) between the larval batches 1 & 4 in the temperature range 12-24°C.

These datasets were combined for a regression analysis of velocity versus temperature in order to determine the T_D value for these data. It is proposed a T_D value would correspond with the temperature increase required to double the swimming velocity during this period. This variable could be used to summarise the effect of temperature on larval *C. gigas* swimming

velocity, allowing comparison with future experiments that include this temperature range (as part of the continued development), or for comparisons between species (using this methodology).

In order to determine the most suitable temperature range for this analysis, a series of regressions analyses were performed to determine the best fit to the lower temperature range. Table 4.1 presents the results of this analysis. The temperature range 12°C-22°C appeared most suitable for a regression analysis of these combined datasets, with a lower error than encountered when incorporating the data from higher temperatures. Error increased and the R^2_{adj} reduced sharply when incorporating temperatures above 24°C.

Temperature range (°C)	Standard error of the estimate	R^2_{adj}	T_D (°C)
12 to 20	0.28	38%	6
12 to 22	0.29	48%	7
12 to 24	0.32	40%	9

Table 4.1 - Analysis of temperature ranges to determine the best fit for determination of T_D

Regression analysis of 12-22°C temperature range versus swimming velocity:

This regression used the natural log of 338 individual larval velocities from the 12°C-22°C range.

- There was a significant ($F_{1\text{-}329}$ = 304, p< 0.001) linear regression of natural log of velocity against temperature (°C) (Equation 1)
- *In(Velocity) = - 1.65 + 0.0985 Temperature coefficient* (Equation 2 - the regression equation)
- Forty eight percent of the variation in Log_e(velocity) was accounted for by variation in temperature (R^2_{adj} = 48%). The remaining variation is assumed to be variation between individuals.

There is scatter about the linear regression line, evident in Figure 4.9, and this is probably due to the variation between individuals discussed above.

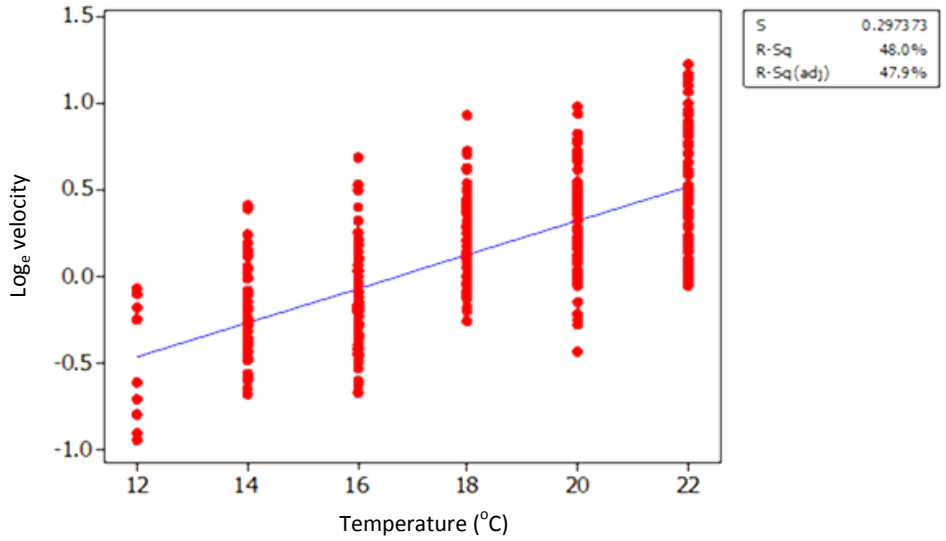

Figure 4.9 – Regression (Minitab 14) of swimming velocity in the 12°C to 22°C temperature range

There is a linear trend for increase in swimming velocity with increase in temperature. The R^2_{adj} of 47.9% indicates forty eight percent of the variation is due to temperature; however there is still considerable scatter due to variation between individuals.

Calculation of T_D for 12°C-22°C velocity/temperature increase

The equation for the velocity temperature increase curve:

$V = Ae^{(kT)}$

Where *V* is the swimming velocity, *T* is the temperature, *A* is the swimming velocity at 0°C, and *k* is the fractional temperature coefficient *In(Velocity) = - 1.65 + 0.0985 Temperature coefficient* (Equation 2).

Therefore for natural log data:

$Log_e(V) = Log_e(A) + KT$

The doubling temperature (T_D) is calculated by solving these equations to

$$\frac{Log_e 2}{k} = T_D \ (C^o)$$

The T_D value for the increase in larval swimming velocity in the 12°-22°C range is 7, i.e. 7°C temperature increase doubles the larval swimming velocity in the range from 12°C-22°C. While this temperature range is below the culture temperature being employed at SeaSalter, it is a

relevant value to calculate here; the figure provides a 'benchmark' against which future refinements of the method could be assessed.

Analysis of the 24°C-38°C temperature range velocity data

Regression analysis versus velocity

An increase in swimming velocity with increasing temperature was not observed in the 24°C to 38°C range (Figure 4.7). In 3 larval batches a regression analysis of $\log_e$ velocity (mms^{-1}), transformed to normalise the variance, against temperature (C^o) was not significant at the 5% level; Batch 1 $F_{1, 69}$=1.42, p=0.237; Batch 2 $F_{1, 105}$=1.53, p=0.219; Batch 3 $F_{1, 322}$=2.25, p=0.134;

Batch 4 indicated a possible significant relationship at the 0.5% level between temperature and velocity ($F_{1, 238}$=8.21, p=0.005). A straight line regression analysis indicated that the relationship was poorly defined. The relationship between temperature and velocity accounted for <3% of the variation (R^2_{adj} 2.9).

For all larval batches a p value of >0.001 indicated no significant relationship at the 0.1% level between temperature and velocity above 24°C, and an R^2_{adj} less than 3 was observed, for all batches, indicating a maximum of 3% of the variation in Log_e (velocity) was accounted for by temperature. In batches 1, 2 and 3 R^2_{adj} was less than 1%.

Across the 24°-38°C temperature range average velocities varied from 1.1mm s^{-1} ± 0.2 for batch 2 to 1.7mm s^{-1} ± 0.6 in batches 1 and 4. Batch 3 had an average in between this range of 1.55mms^{-1} ± 0.13. Higher temperatures saw several individual larvae achieve velocities of around 4mm s^{-1}, with some individuals achieving velocities in excess of 5mm s^{-1}, leading to increased variation and bias in these ranges.

Analysis of variance between larval batches in the 24°C-38°C range

Each larval batch corresponds to a different larval broodstock. An ANOVA test was used to determine if there was significant variation between the velocities of these different larval batches, within the temperature range where the previous analysis had shown no relationship

between velocity and temperature. This temperature range had the most data available for this analysis, with all 4 batches having a number of velocity records. In total 742 individual larval velocities were analysed across the 4 separate larval batches:

Normal probability plots of the residuals in an ANOVA of the raw velocities indicated that the velocities were not normally distributed, and a plot of the residuals versus fitted values indicated that the variance was not homogeneous.

The equivalent plots for $\log_e$ of the velocities indicated that the transformation had stabilised the variance, and that the $\log_e$ values were approximately normally distributed. The ANOVA was therefore undertaken using the transformed velocities. There was a significant ($F_{3, 738} = 20.89$, $p<0.001$) difference between at least two of the $\log_e$ mean maximum velocities in the four batches -batch 1 = 0.52, batch 2 = 0.15, batch 3 = 0.35, and batch 4 = 0.48. A conservative *post hoc* test (Tukey-Kramer) indicated that batches 2 and 3 were significantly different from all the other batches, and then from one another at the 5% level (Minitab output);

```
Batch    N    Mean   StDev  -----+---------+---------+---------+----
1       71  0.5280  0.3056                          (-----*-----)
2      107  0.1459  0.3825  (----*----)
3      324  0.3506  0.4438                (--*--)
4      240  0.4818  0.3787                          (--*---)
                            -----+---------+---------+---------+----
                               0.15      0.30      0.45      0.60
```

The Log_e mean maximum velocity of batch 2 was the lowest of the 4 batches. There was no correlation between size and Log_e mean maximum velocity - batch 2 were not the smallest or largest larvae, but were significantly slower than all the other batches.

4.3.3 Larval swimming velocities when exposed to rapid temperature change

Pediveliger larvae and veliger larvae show different reactions in their velocities following exposure to rapid changes of temperature (Figure 4.11-Figure 4.10). Both development stages show a reaction to rapid temperature change, but the veliger stage larvae continued to swim more consistently. Velocity means are presented with ± standard error of the mean.

Swimming velocity in controls cuvettes

Pediveliger larvae swam actively in the cuvette throughout the 5 minutes (10, 30 second intervals) of filming of larvae under a constant temperature regime (Figure 4.10). Velocity ranged from a few very slow individuals moving at 0.6mm s^{-1} to a few very fast individuals moving at between 4.5mm s^{-1} to 5.5mm s^{-1} (one individual recorded a velocity of 7.04mm s^{-1}). In most individuals velocity was maintained at approximately 1.7-2.3mm s^{-1}, with an actual average across the time period of 2.6mm s^{-1} ±0.4. These infrequent, very fast swimming individual larvae were observed in in all the experiments conducted in the cuvettes, and was also observed in the beaker cultures being sampled for filming. The appearance of fast individuals showed no trend linked with time or temperature.

Veliger stage larvae swam actively in all areas of the cuvette throughout the 5 minutes of constant temperature filming (Figure 4.10). Velocities ranged from 0.95 mm s^{-1} to 4.3 mm s^{-1}, with an average velocity across the 5 minutes of film of 1.79 mm s^{-1} ±0.2. There are peaks in velocity in the 60-90 seconds and 150-80 seconds brackets.

Regression analysis of velocity controls

Pediveliger - A straight line regression of $\log_{10}$ velocity (mms^{-1}), transformed to normalise the variance, against time (seconds) was not significant at the 5% level ($F_{1, 158}$ = 0.03, p=0.860), indicating that no systematic linear trend was present in the data.

Veliger - A similar analysis of $\log_{10}$ velocity (mms^{-1}), transformed to normalise the variance, showed no significant ($F_{1, 94}$ = 0.02, p=0.900) trend in the veliger swimming velocities with elapsed time in the experiment.

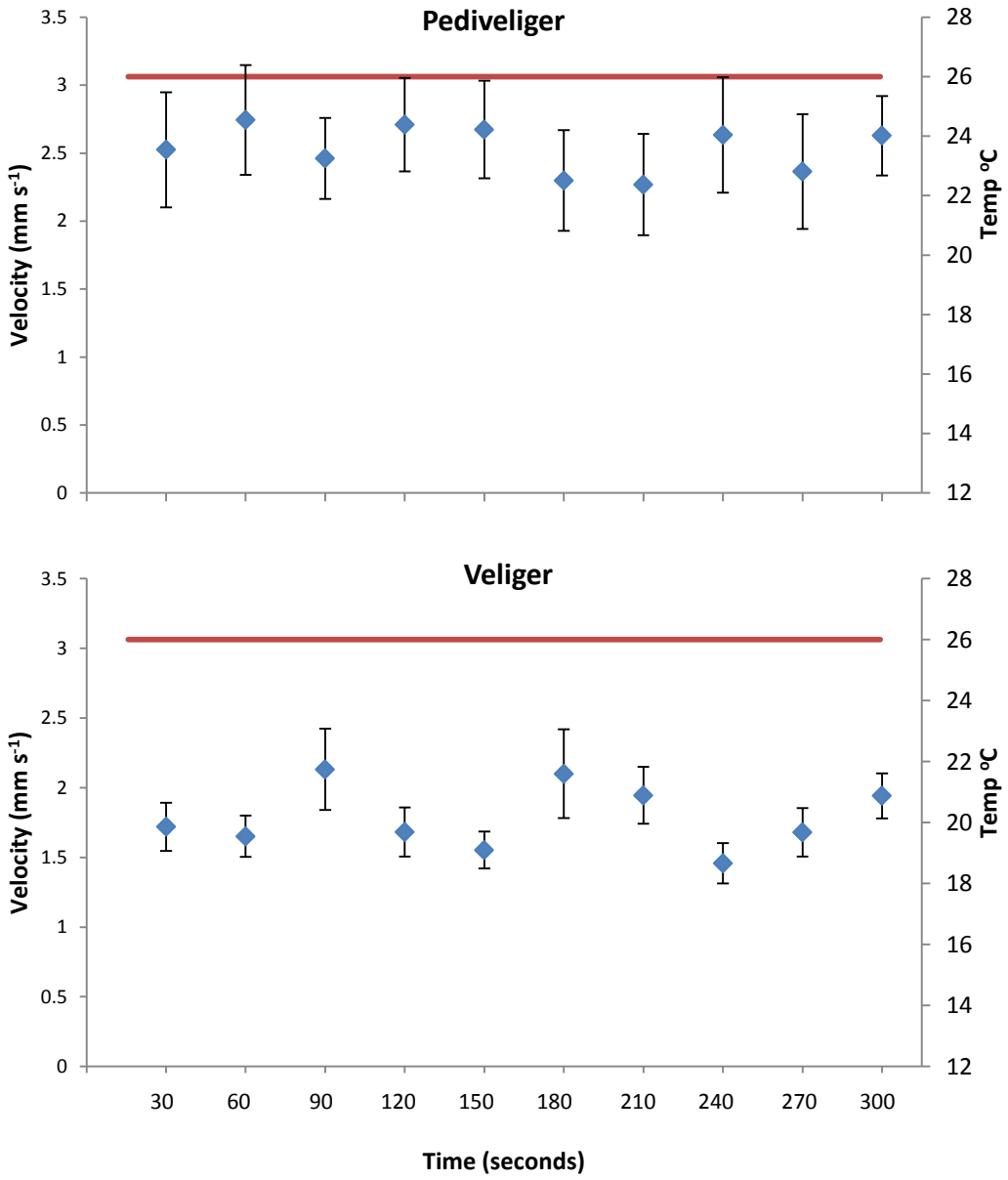

Figure 4.10- Mean larval velocities within control cuvettes, +/- 1 SE.

Swimming velocities of pediveliger and veliger larvae (mean ±SE, left axis) during stable temperature (red line, right axis) regime. Pediveliger velocity (n=160) remains fairly constant throughout the filming period at an average of 2.6 mm s^{-1}±0.4. Veliger velocity (n=138) remains fairly constant throughout the filming period, showing some peaks and troughs, but with no overall trend. Average velocity for the veliger stage larvae was 1.79 mm s^{-1}±0.2.

Larval swimming velocity responses to rapid temperature rise

Pediveliger larvae

Figure 4.11 shows pediveliger larvae exposed to a rapid rising of temperature from 26°C to 37.5°C featured no change in swimming velocity with mean velocities only varying from 2.43mm s^{-1} to 2.19mm s^{-1} during the initial 10°C temperature rise (the first 120 seconds of exposure). Following this velocity fell to 1.67 mm s^{-1} ±0.90 during the next 2°C rise (120-50 seconds) before falling to 0.25 mm s^{-1} ±0.25 mm s^{-1} when the temperature reaches 36.5°C. No change in swimming pattern was observed, with straight line swimming, helical swimming and falling were all observed throughout the filming period. Larval activity observed in the cuvette fell during the filming period (this trend is investigated in section 4.3.3). When 36°C is reached (after 180 seconds), larvae swimming upwards in the cuvette were rare with only one slowly swimming individual moving at 0.48 mm s^{-1} being recorded in the 210-240 seconds time interval at 36.9°C. There was no further activity in the cuvettes once the temperature went over 37°C (240 seconds after the start of filming).

Veliger larvae

Veliger stage larvae swam throughout the 11.5 degree temperature rise (300 seconds filming period) with swimming velocity increasing slightly by the end of the experiment (Figure 4.11). Mean velocity during the initial 3.3°C temperature rise (the first 30 seconds) remained close to that seen in the controls (Figure 4.10) at 1.97 mm s^{-1} ±0.18, dropping slightly in the next 2.5°C rise (30-60 seconds) to 1.86 mm s^{-1} ±0.19. Velocity rose steadily over the next 5°C of temperature rise reaching a mean velocity of 2.58 mm s^{-1} ±0.59 after 150 seconds when the temperature reached 36.6°C. Velocity drops slightly during the next 0.2°C rise before reaching a high for the experimental period of 3.16 mm s^{-1} ±0.36 at 36.8°C during the 180-210 seconds period. Both this temperature and the following temperature of 37.1°C had individuals reaching 5.7 and 5.9 mm s^{-1}. Larval velocity at the conclusion of the filming period at a final temperature of 37.5°C was a mean of 2.44 mm s^{-1} ±0.22, higher than the 26°C velocity of veligers in the controls in Figure 4.10 and at the start of the graph in Figure 4.11.

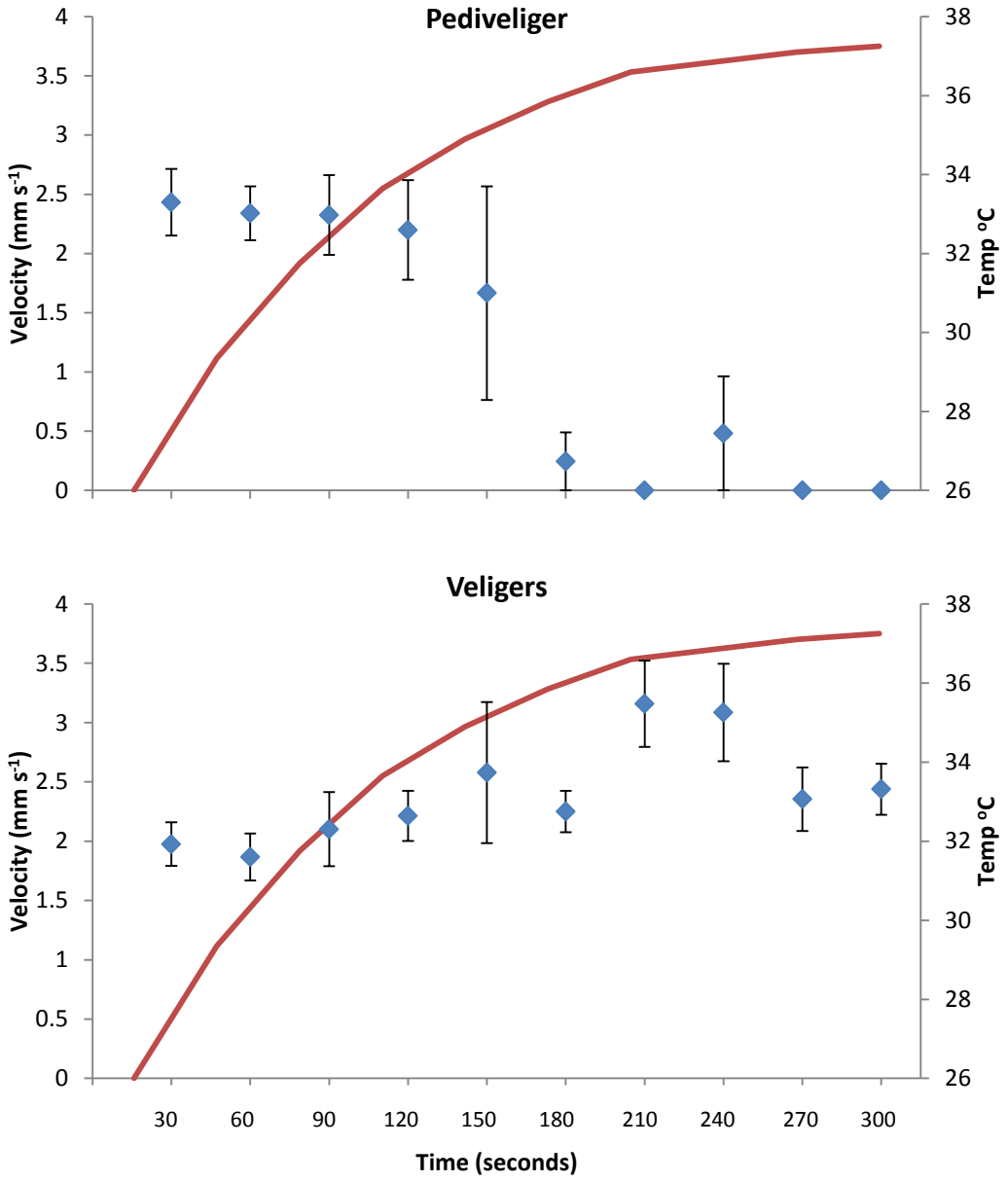

Figure 4.11 - Mean larval velocities during rapid temperature rise, +/- 1 SE.

Change in swimming velocity of pediveliger and veliger larvae (mean ±SE, left axis) with increase in temperature (red line, right axis). Pediveliger velocities (n=84) drop sharply as swimming activity falls. Veliger swimming velocity (n=127) gradually rises throughout the 11°C temperature rise, reaching 2.44 mm s^{-1}±0.22 at the end of filming.

Regression analysis of larval swimming velocities following rapid temperature rise

Pediveliger larvae

Investigation of pediveliger larval swimming reveals velocities to be consistent until approximately 120 seconds into the exposure (~35°C) when swimming stopped (Figure 4.11). A regression analysis (performed on $\log_{10}$ transformed velocities to normalise the variance) revealed no significant ($F_{2, 108}$ = 1.31, p = 0.275) relationship between velocity and increasing temperature across the whole 5 minutes of exposure. In order to ensure no bias was introduced by the few slow swimming velocity records found above 36°C, the regression was also performed only on the first 5 time periods. This analysis still illustrated no significant ($F_{1, 108}$= 2.25, p = 0.136) relationship at the 5% level between exposure time (and thus increasing temperature) with velocity.

Veliger larvae

Initial investigations of veliger swimming velocities suggested a rise in velocity with temperature increase (Figure 4.11). A regression analysis of $\log_{10}$ velocity (mms^{-1}), transformed to normalise the variance, against time (corresponding to temperature rise) was significant at the 1% level ($F_{2, 123}$ = 5.18, p=0.007). Whilst this p value is low the analysis indicated that only 6.3% of the variation was explained by this relationship. The remaining 93.7% was probably due to variation between individuals - there is a large scatter about the fitted line plot (Figure 4.12) and the trend is poorly defined.

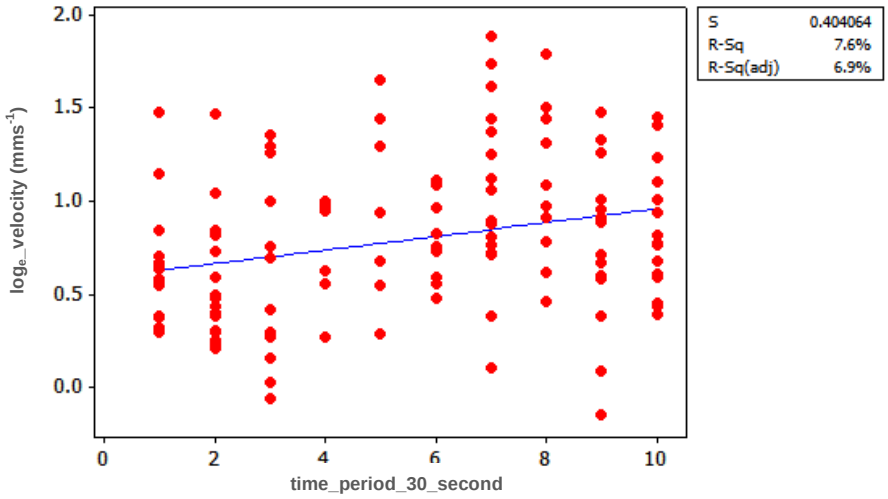

Figure 4.12 – Regression (Minitab 14) of $\log_e$ veliger swimming velocity when exposed to an increase in temperature

Larval swimming velocity responses to rapid temperature drop

Pediveliger larvae

Figure 4.13 illustrates pediveliger larvae exposed to a rapid decrease in temperature showed a drop in velocity during the first 11°C drop in temperature (the first 150 seconds of exposure). The initial 4°C drop (during the first 30 seconds of exposure) had a mean swimming velocity of 2.38 mm s^{-1} ±0.70, decreasing to 1.68 mm s^{-1} ±0.16 in the next 3°C drop (30-60 seconds). During the following 3.5°C fall no further significant decrease was noted with a mean velocity of 1.20 mm s^{-1} ±013 for 60-90 seconds and 1.16 mm s^{-1} ±0.16 for 90-120 seconds. From 14.8°C to 12°C there was little difference in those filming time intervals that record larval velocities and no velocity greater than 0.42 mm s^{-1} recorded. Larval activity was noticeably reduced in the final stages of filming with two time intervals, 180-210 seconds (13.35°C - 12.5°C) and 270-300 seconds (12.25°C-12°C) featuring no upward swimming velocities. Those larvae that were swimming in the water column moved at a velocity that was visibly slower than the larvae observed at the beginning of the filming period. Large numbers of apparently active larvae were observed on the base of the cuvette.

Veliger larvae

Figure 4.13 shows a gradual fall in veliger swimming velocity during the first 10°C drop in temperature (the first 120 seconds of the filming period). Velocity in the initial 4°C drop (0-30 seconds) was a mean of 2.02mm s^{-1} ±0.17, slightly above the control, dropping to 1.42 mm s^{-1} ±0.10 during the next 3°C fall, 1.14 mm s^{-1} ±0.06 during the fall from 18°C-16°C and 1.06 mm s^{-1} ±0.08 during 16°C-14.8°C. From 14°C to the end of the filming period at 12°C the larval velocity remained between 0.82 mm s^{-1} and 0.66 mm s^{-1}. Larval activity was reduced in the cuvettes during the last 180 seconds (14.8°C-12°C), but larvae still maintained upward swimming.

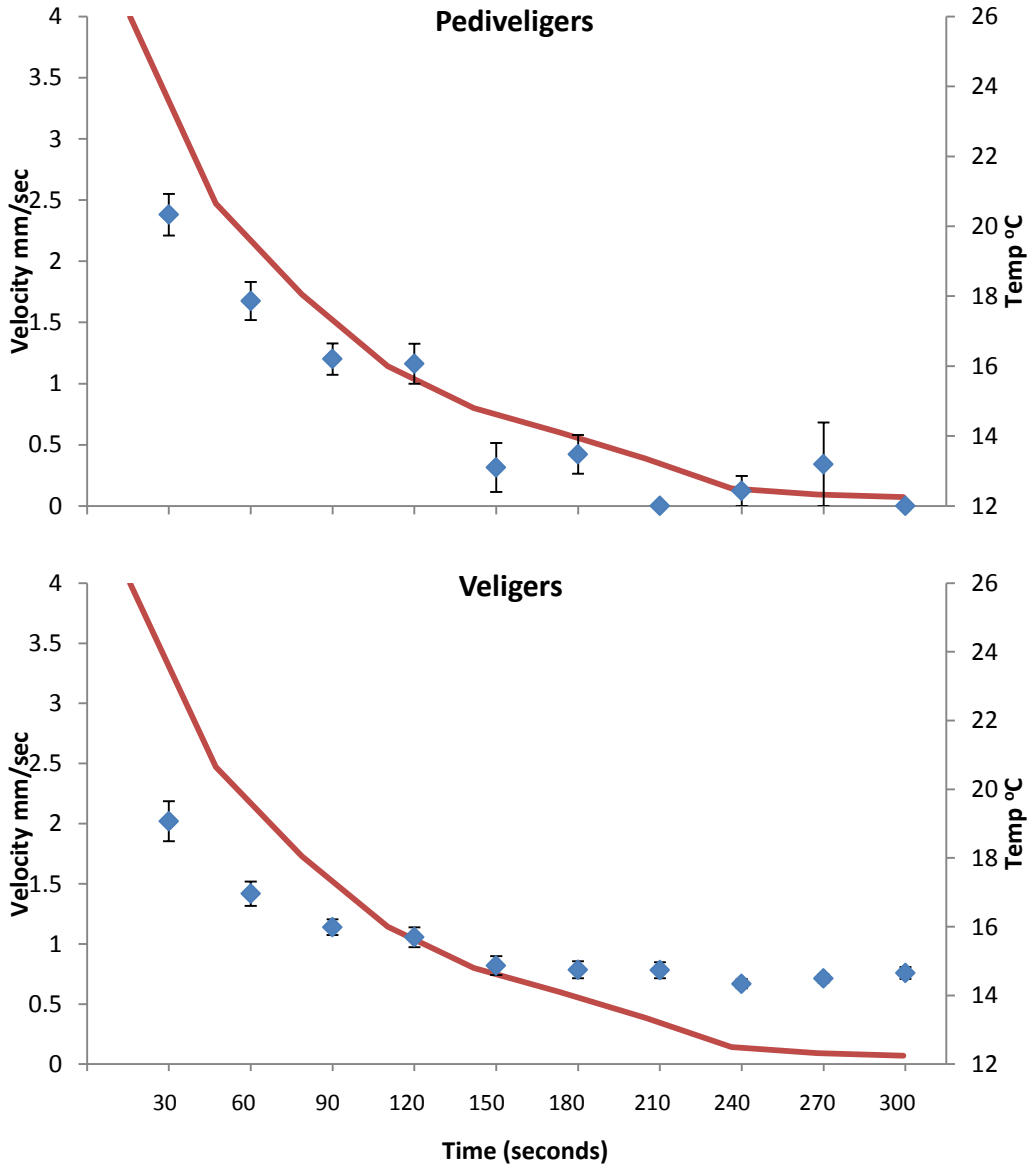

Figure 4.13 - Larval velocities during rapid temperature drop, +/- 1 SE.

Change in swimming velocity of pediveliger and veliger larvae (mean ±SE, left axis) with decrease in temperature (red line, right axis). Pediveliger velocities (n=55) fell sharply, dropping to a minimum of 0.122 mm s^{-1}±0.12, with 2 time intervals having no upwards swimming larvae present to collect velocity data from. Veliger velocity (n=95) falls for the first 10°C drop, then remained steady at an average of 0.75 mm s^{-1} ±0.05 for the final 4°C drop.

Regression analysis of larval swimming velocities following rapid temperature drop

Pediveliger

An analysis of $\log_{10}$ velocity (mms^{-1}), transformed to normalise the variance, against time (seconds) indicated the decrease in swimming velocity with decreasing temperature observed in Figure 4.13 is significant at the 0.1% level ($F_{2, 92} = 31.08$, $p<0.001$). This analysis accounted for 39.5% of the variation. In order to investigate if there was a behavioural 'lag phase', exponential and logistic functions were fitted, but there was little difference between the two approaches - a comparison is presented below. Analysis of the curves (Figures 4.13 and 4.14) reveals considerable scatter (less than 40% of the variation was accounted for by the regression, and the remaining 60% is probably due to variation between individuals), and few records in the later time (lower temperatures) range, making the fit relatively poorly defined.

	Exponential Function			Logistic Function		
	D.f	**F**	**p**	**D.f**	**F**	**p**
Regression	2	31.08	<.001	3	20.75	<.001
Residual	90			89		
Total	92			92		
% Variance	39.5			39.2		
S.e. of the estimate	0.203			0.203		
	Estimates of parameters:					
	Estimate		**s.e.**	**Estimate**		**s.e.**
	R	0.803	0.119	B	-0.589	0.629
	B	0.932	0.273	M	2.28	2.43
	A	-0.419	0.328	C	0.888	0.839
				A	-0.281	0.196

Table 4.2 - Summary of exponential and logistic regressions for pediveliger rising behaviour following rapid temperature drop.

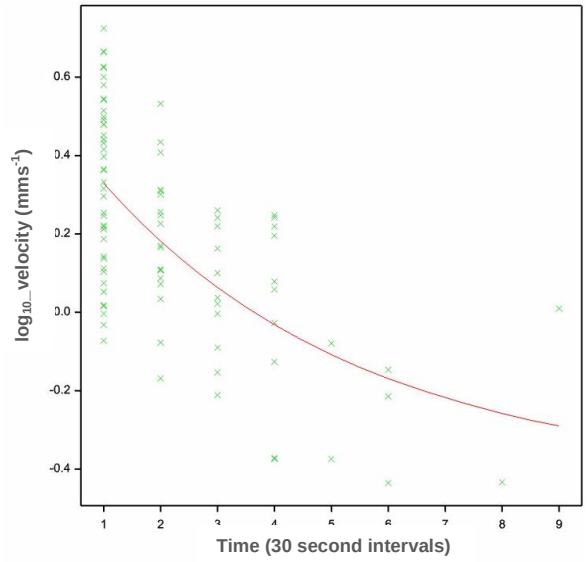

Figure 4.14 - Exponential regression of pediveliger swimming velocity following exposure to a sudden fall in temperature.

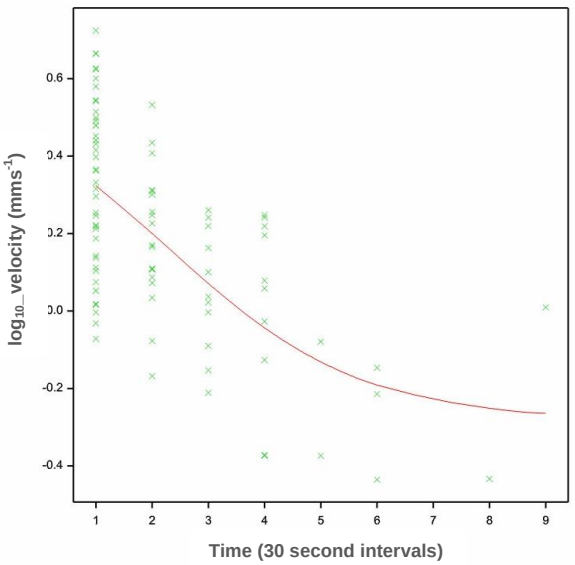

Figure 4.15 - Logistic regression of pediveliger swimming velocity following exposure to a sudden temperature drop.

Veliger

Analysis of $\log_{10}$ velocity (mms^{-1}), transformed to normalise the variance, against time (seconds) indicated a significant (at the 0.1% level-Table 4.3) decrease in swimming velocity with decreasing temperature. As for the pediveliger data, both exponential and logistic functions were fitted, with little difference between the two approaches - a comparison is presented below. The analysis explains <50% of the variation, despite there being more data in the lower temperature range. Investigating the curves (Figure 4.16 and Figure 4.17) reveals considerable scatter, with variation between individuals probably explaining the remaining 50% of variation.

	Exponential Function			Logistic Function		
	D.f	F	p	D.f	F	p
Regression	2	84.49	<.001	3	56.29	<.001
Residual	166			165		
Total	168			168		
% Variance	49.8			49.7		
S.e. of the estimate	0.141			0.141		
	Estimates of parameters:					
	Estimate		s.e.	Estimate		s.e.
	R	0.687	0.0565	B	-0.572	0.334
	B	0.668	0.0606	M	0.82	3.61
	A	-0.183	0.0351	C	0.91	1.04
				A	-0.1649	0.036

Table 4.3 - Summary of exponential and logistic regressions for veliger velocities following rapid temperature drop

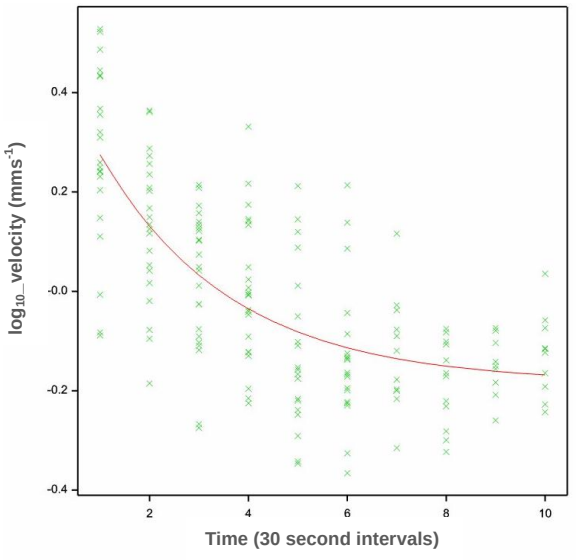

Figure 4.16 - Exponential regression of veliger swimming velocity following exposure to a sudden decrease in temperature.

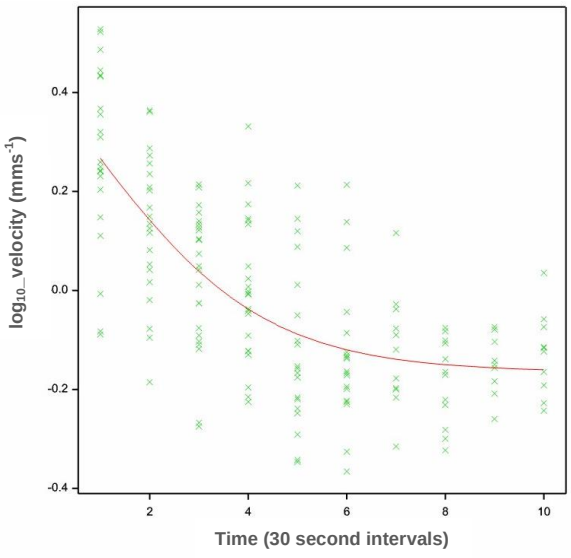

Figure 4.17 - Logistic regression of veliger swimming velocity following exposure to a sudden decrease in temperature.

4.3.4 Investigating larval behavioural responses to rapid temperature change

The behaviours investigated here comprise of 3 types of larval swimming: larvae swimming upwards (rising), descending (larvae controlling their fall through the water column using the velum) and falling (simple closed shell falling through the water column). Two batches of larvae were studied to enable a comparison between pediveliger (a mean larval size of 257µm) and veliger (a mean larval size of 180µm) larvae. Results are presented with ±standard error of the mean.

The preliminary results from this filming technique are presented here in two forms:

- First the raw counts of larval activity are presented in terms of the percentage of the larval populations of the cuvettes demonstrating one of the three types of behaviour (rising, descending and falling).
- Secondly a regression analysis has been performed to investigate any relationship between the temperature change over the filming period and the change in these larval activities. This analysis was considered more appropriate for identifying trends in these data than, for example, a repeated measures ANOVA. All data have been Log_{10} transformed in order to achieve a normal distribution. Two forms of regression curve have been fitted to each dataset using the statistics package GenStat® - exponential and logistic. While there are other analyses that may be considered appropriate for such a dataset, the combination of these two interpretations may provide evidence of a behavioural reaction within the current data. If a logistic curve provides the best fit to the data, this may suggest a 'lag phase' at the beginning of the reaction (the reaction being a reduction in any of the activities). If an exponential curve provides a better fits for these data, the response may be assumed more likely a physiological reaction, or one that is the result of the viscosity changes in the water.

Notes on the GenStat® package and the regression equations

The asymptotic decline model and the ordinary logistic function were fitted to the data using the maximum likelihood general non-linear regression routine available in Genstat 13.

The asymptotic model ($y= a + be^{-kx} + \varepsilon$) is fitted using the form ($y= a + br^{x} + \varepsilon$), where $r=e^{(-k)}$. This device is used in Genstat to avoid problems with large values of k (the first order rate constant), and k is calculated as $\log_e r$.

The ordinary logistic function $y=a+c/[1+e^{-b(x-m)}]$) where a is the lower asymptote, (a+c) is the upper asymptote, m is the value of x when y = a + c/2 (i.e., the midpoint), and b is a rate constant.

The routine provides estimates of the parameters with standard errors, and calculates r^2 as the regression sum of squares divided by the total sum of squares. The latter provides a measure of the proportion of the total variation accounted for by the fitted function.

Observations of larval behaviour in steady temperature control filming

Controls were larvae filmed within the cuvette maintained at the culture temperature and not subjected to any rapid temperature changes. The controls show slight reductions in activity during the 300 seconds filming period with no pronounced decreases or increases in any specific behaviour (Figure 4.18 and Figure 4.19). Due to the constant temperature regime in the controls results in this section are described in time intervals not temperature change.

Rising behaviour in steady temperature control cuvettes

There was gradual loss of rising behaviour in the pediveliger larvae during the course of filming, and generally less activity from the overall pediveliger cuvette population during the first 30 seconds of filming (Figure 4.18). Overall rising activity was 10.4%±0.8 in the first 30 seconds of filming, and gradually fell to 5.7%±0.2 at the end of the 300 second filming period, with no obvious peaks or troughs throughout the filming period.

Veliger stage larvae cuvette had some variation between time intervals, but with an overall slight decline in rising behaviour (Figure 4.19) by the end of filming. In the initial 30 seconds of filming 7.9%±1.3 of the larvae were rising, but this proportion fell to 5.2%±0.9 by the end of the 300 seconds filming period. Rising activity during the filming period reached a high of 8.8%±0.8 of the larvae rising during the 30-60 seconds interval and a low of 4.0%±1.6 rising during the 210-240 seconds interval.

Descending behaviour in steady temperature control cuvettes

Control cuvettes for the percentage for the pediveliger larvae descending in steady temperatures had a less regular trend, but with a lower percentage of the larvae descending by the end of the 300 seconds of filming (Figure 4.18). 16.0%±0.8 of the pediveliger larvae were descending in the first 30 seconds, reducing to 5.7%±0.2 by the end of filming. The numbers descending fell from 16.7%±0.8 in the first 30 seconds to 8.5%±0.2 in the 30-60 seconds phase, before rising again in the 60-90 seconds period to 14.6%±0.2 of the larvae. After this rise the percentage descending fell again to 10.0%±0.2 in the 90-120 seconds time frame, and stayed between 6.9%±0.2 and 7.5%±1.1 for the 120-210 seconds filming period. There was a sharp drop in numbers descending in the 210-240 period with a fall to 2.5%±1.3, followed by another sharp rise to 7.5%±1.1 before reaching 5.6%±0.2 of the larvae descending at the end of filming. Visual observations of the larval descending in the controls noted that the larvae often descended in large groups, at any time throughout the 300 second period. This was not observed in any of the rapid temperature change experiments.

Veliger larvae showing descending behaviour during steady temperature filming show little difference from the initial 30 seconds of filming (6.4%±1.2 of veligers) to the final 270-300 seconds bracket of filming (6.3%±0.9 of veligers). There was one large drop in descending behaviour noted at 240-270 seconds where the percentage of the veligers descending fell to 1.9%±1.3, before rising up again for the final filming interval (Figure 4.19).

Closed shell falling in steady temperature control cuvettes

The percentage of pediveliger larvae falling remained below 0.4% throughout the filming period (Figure 4.18), with falling being limited to occasional individuals.

The percentage of veliger larvae falling varied between 0% and 1.1% throughout the filming period, with falling limited to infrequent individuals or pairs of larvae (Figure 4.19).

Total activity of larvae in steady temperature control cuvettes

The total percentage of the pediveliger larvae within control cuvettes showing any activity fell from 27.2%±2.2 in the first 30 seconds to 11.7%±1.7 at the end of the 5 minute filming period (Figure 4.18). The decrease in activity was steady, with one exceptional drop in activity to 6.3%±2.7 during the 210-240 seconds filming period that was followed by a sharp rise back to an activity of 12.5%±1.6.

Overall activity of veliger larvae remained constant with only slight drops during the course of the 300 seconds of filming (Figure 4.19). 15.4%2.7 of veligers were active during the first 30 seconds and activity fell to 12.5%±0.6 at the end of the 300 seconds of filming. Throughout the filming period, larval activity varied from a peak of 17.3%±2.9 active during 60-90 seconds to a low of 8.8%±2.3 in the 240-270 second period.

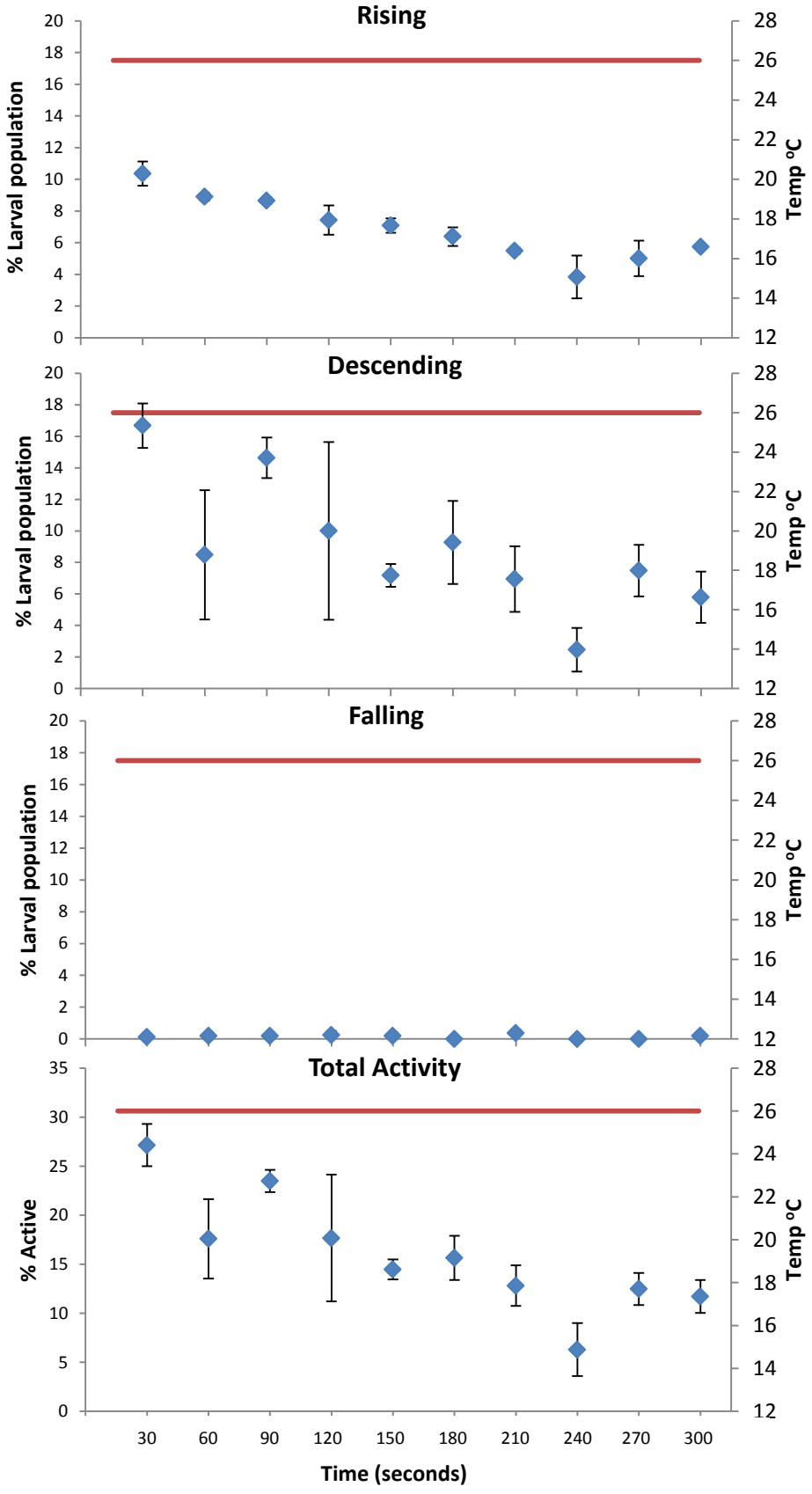

Figure 4.18 - Mean of cuvette population swimming behaviour of pediveliger larvae in steady temperature controls, +/- 1 SE.

The percentage of the larval population (left axis) either rising, descending or falling (shell closed) is displayed against time with steady temperature (right axis, red line) during the 5 minute filming period. The lower graph shows the total level of larval activity (left axis) during the filming period.

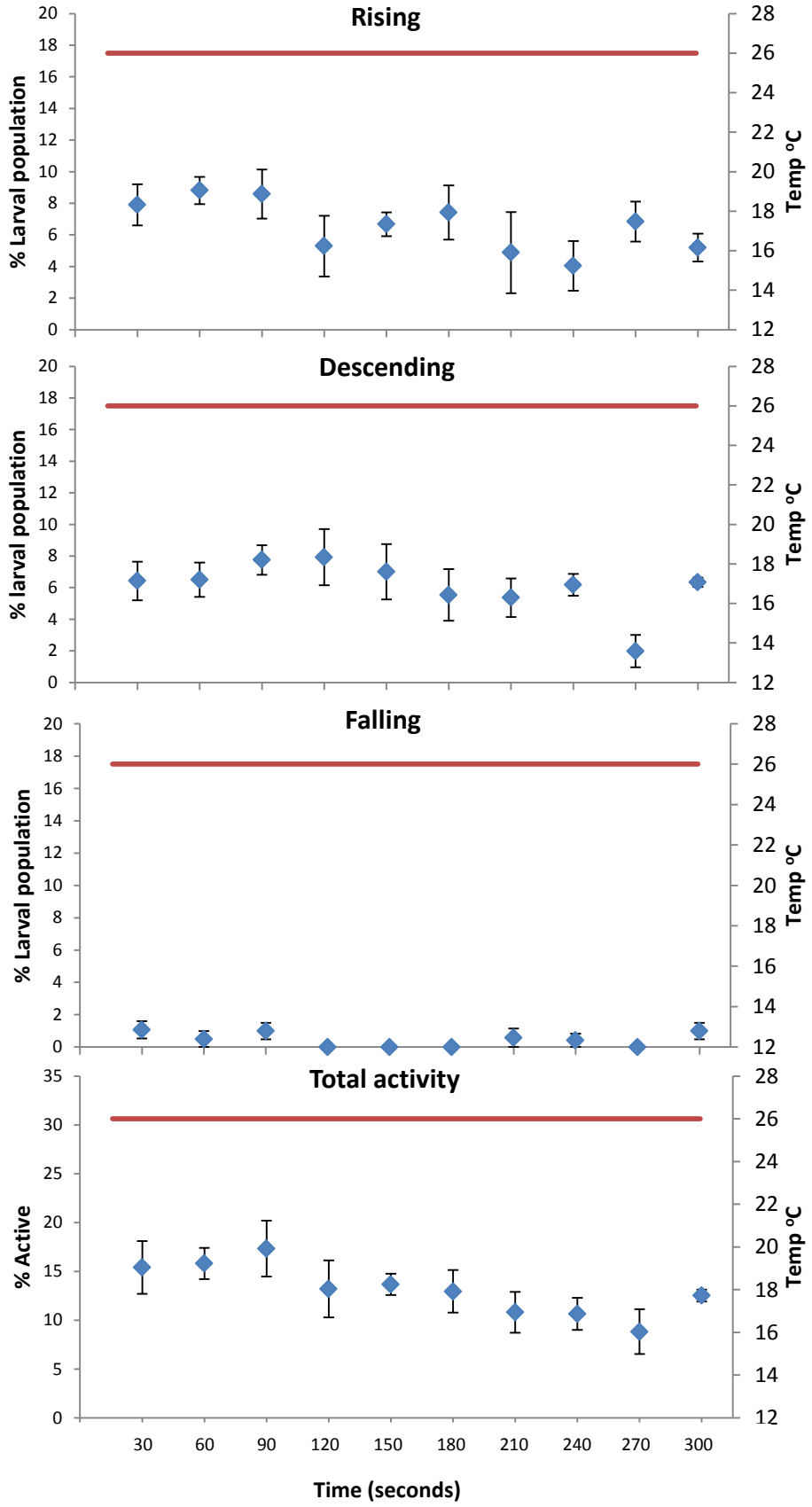

Figure 4.19 - Mean percentage swimming behaviour of veliger larvae population in steady temperature controls, +/- 1 SE.

The percentage of the larval population (left axis) either rising, descending or falling (shell closed) is displayed against time with steady temperature (right axis, red line) during the 5 minute filming period. The lower graph shows the total level of larval activity (left axis) during the filming period.

Regression analysis of behavioural controls

RISING BEHAVIOUR

Pediveliger larvae

Investigation of the percentage population data presented previously suggests the pediveliger larvae may show a decline in rising activity in the controls during the filming period. Exponential and logistic regressions have been employed to test the significance of this relationship. GenStat outputs are provided and briefly interpreted below:

	Exponential Function, A+ B*(R**X)			Logistic Function, A + C/(1 + EXP(-B*(X - M)))		
	D.f	**F**	**p**	**D.f**	**F**	**p**
Regression	2	43.33	<.001	3	30.02	<.001
Residual	53			52		
Total	55			55		
% Variance	60.6			61.3		
S.e. of the estimate	0.272			0.270		
	Estimates of parameters:					
	Estimate		**s.e.**	**Estimate**		**s.e.**
	R	0.8182	0.0763	B	-1.180	0.558
	B	1.566	0.205	M	4.289	0.440
	A	-0.146	0.284	C	0.877	0.153
				A	0.1296	0.0715

Table 4.4 - Summary of exponential and logistic regressions for pediveliger rising behaviour in steady temperature controls

The exponential function may fit the data reasonably well (60.6% variation accounted for), with the $p<0.001$ indicating significant relationship between a reduction in rising activity versus time in a shallow curve throughout the 5 minute filming period (Figure 4.20). However, there is considerable scatter in the data (39.4% of the variation is not accounted for; probably reflecting large variation between individuals).

The logistic function fits the data slightly better than the exponential approach (61.3% variation accounted for), again showing significant (at the 0.1% level) reduction in rising activity throughout the 5 minute filming period, as indicated by $p<0.001$. The logistic curve also suffers from high scatter, especially in the later time periods (Figure 4.21).

Regression curves for both approaches are provided overleaf:

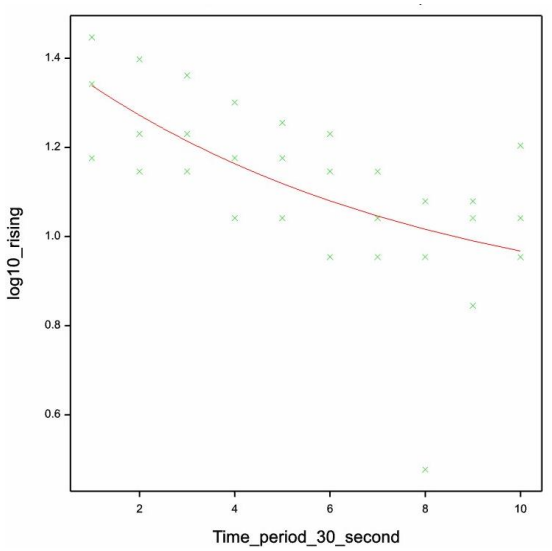

Figure 4.20 - Exponential regression of rising pediveliger larvae in steady temperature controls.

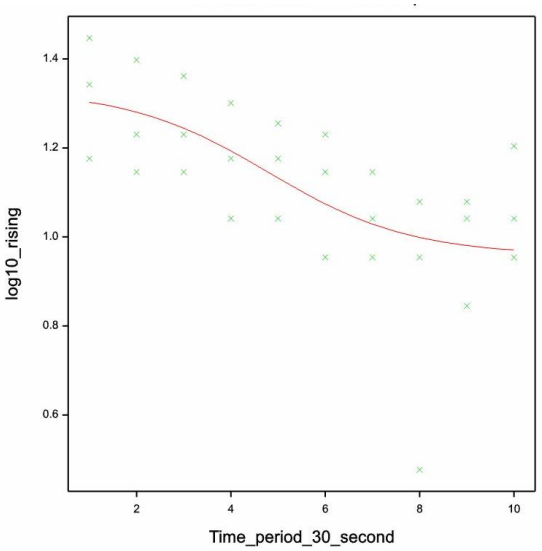

Figure 4.21 - Logistic regression of rising pediveliger larvae in steady temperature controls.

There is no obvious lag phase indicated in the logistic curve above, and the fit is poor.

Veliger larvae

No trend is visible in the percentage population data for the veliger larvae. Exponential and logistic regressions have been employed to test for any significant trend in larval rising behaviour during the control filming period.

	Exponential Function, A+ B*(RX)**			**Logistic Function, A + C/(1 + EXP(-B*(X - M)))**		
	D.f	**F**	**p**	**D.f**	**F**	**p**
Regression	2	9.22	<.001	3	6.44	0.002
Residual	27			26		
Total	29			29		
% Variance	36.2			36.0		
S.e. of the estimate	0.151			0.151		
	Estimates of parameters:					
	Estimate		**s.e.**	**Estimate**		**s.e.**
	R	0.875	0.168	B	-0.6712	Unable to calculate
	B	0.606	0.358	M	4.803	
	A	0.808	0.442	C	0.3691	
				A	0.9600	

Table 4.5 - Summary of exponential and logistic regressions of veliger rising behaviour in steady temperature controls

The exponential function fits poorly; indicating only 36% of the variation is explained by time. Although $p<0.001$ suggests a significant regression, the fit is generally poor with variation between individuals producing scatter about the curve (Figure 4.22).

Although the regression was significant at the 0.2% level, the fit of the logistic model was ill conditioned for this data set, and GenStat was unable to calculate standard errors. Examining the curve reveals no lag phase and considerable scatter (Figure 4.23).

Regression curves for both approaches are provided below:

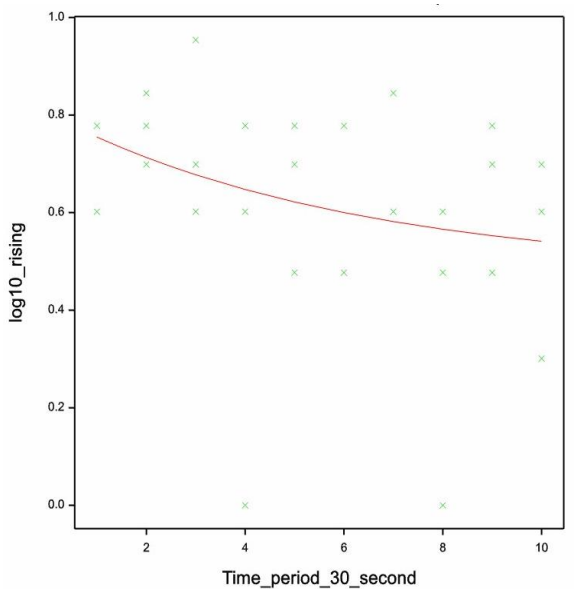

Figure 4.22 - Exponential regression of rising veliger larvae in steady temperature controls.

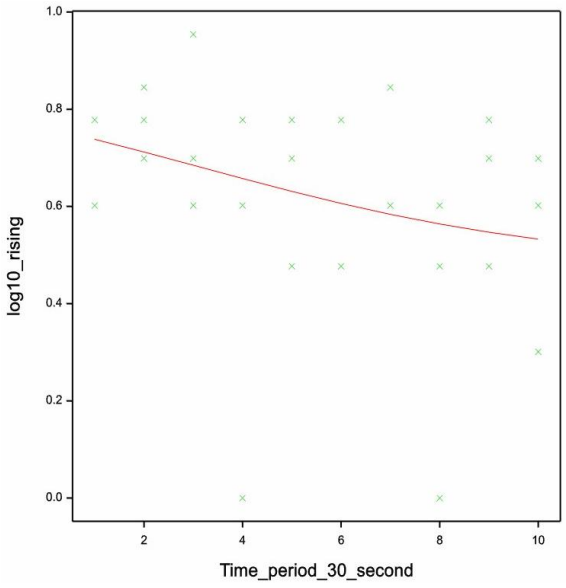

Figure 4.23 - Logistic regression of rising veliger larvae in steady temperature controls.

DESCENDING BEHAVIOUR

Pediveliger larvae

Examination of the percentage population data reveals pediveliger larvae descending activity declines in the controls during the filming period. Exponential and logistic regressions have been employed to test the significance of this relationship. GenStat® outputs are provided and briefly interpreted overleaf.

	Exponential Function, A+ B*(R**X)			Logistic Function, A + C/(1 + EXP(-B*(X - M)))		
	D.f	F	p	D.f	F	p
Regression	2	58.19	<.001	3	29.20	<.001
Residual	48			47		
Total	50			50		
% Variance	69.6			62.8		
S.e. of the estimate	0.257			0.284		
	Estimates of parameters:					
	Estimate		**s.e.**	**Estimate**		**s.e.**
	R	0.4708	0.0809	B	-0.3600	Unable to calculate
	B	2.563	0.509	M	-8.864	
	A	0.3026	0.0561	C	42.78	
				A	0.1379	

Table 4.6 - Summary of exponential and logistic regressions for pediveliger descending behaviour in steady temperature controls

The exponential function explains 69.6% of the variation and a p value of <0.001 indicates a significant regression at the 0.1% level between the number of larvae exhibiting descending behaviour and time. Examining the regression curve (Figure 4.24) shows there is considerable scatter around the curve, likely due to the groups of individuals seen falling in the control experiments, described earlier.

Again, despite the significant regression, the logistic model was ill conditioned for this data set, and GenStat® was unable to calculate standard errors (Table 4.6). Exponential and logistic curves are provided below:

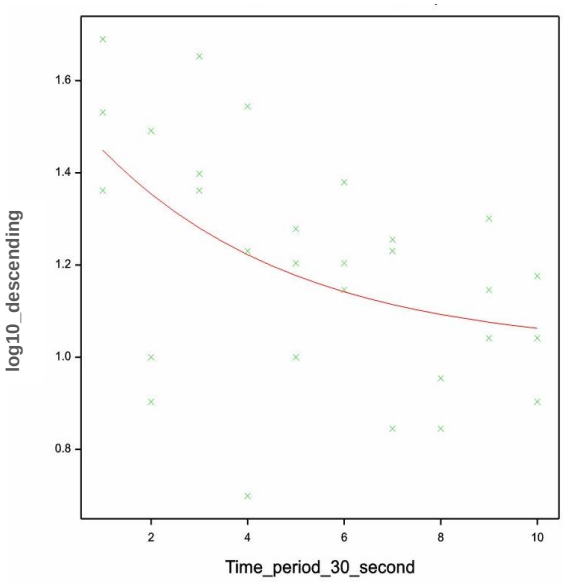

Figure 4.24 - Exponential regression of descending pediveliger larvae in steady temperature controls.

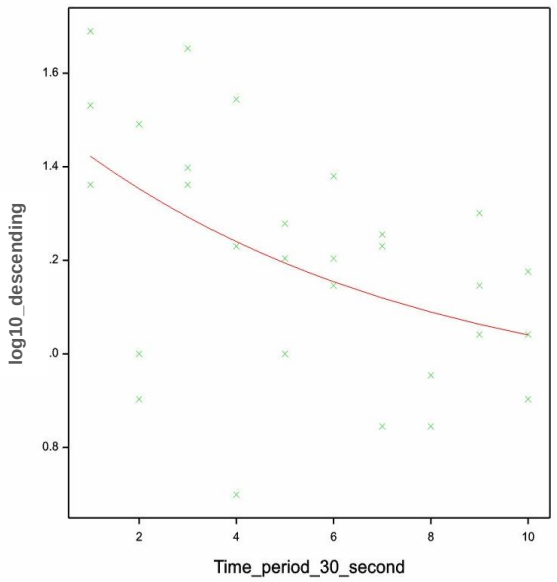

Figure 4.25 - Logistic regression of descending pediveliger larvae in steady temperature controls.

Veliger larvae

Initial examination of the percentage population data (Figure 4.19) does not indicate any decline or increase in descending behaviour in the film of the control cuvettes. Exponential and logistic regression analyses have been conducted to examine these data for any trends in descending behaviour during the control filming.

	Exponential Function, A+ B*(R**X)			Logistic Function, A + C/(1 + EXP(-B*(X - M)))		
	D.f	**F**	**p**	**D.f**	**F**	**p**
Regression	2	4.24	0.025	3	2.67	0.069
Residual	26			25		
Total	28			28		
% Variance	18.8			15.2		
S.e. of the estimate	0.227			0.232		

Estimates of parameters:					
Estimate		**s.e.**	**Estimate**		**s.e.**
R	0.781	0.241	B	-0.1447	Unable to calculate
B	0.555	0.191	M	-22.16	
A	1.016	0.221	C	15.65	
			A	0.8928	

Table 4.7 - Summary of exponential and logistic regressions for descending veliger larvae in steady temperature controls

Neither the exponential nor the logistic regressions indicate any relationship between number of larvae descending and time for veliger larvae in the steady temperature control filming experiments. The percentage of the variation explained by this relationship is poor in both cases (18.8% and 15.2% respectively), and the p value of >0.025 indicates a significant exponential relationship at the 5% level between time and descending larvae. However, for the logistic function there was no significant (at the 5% level) relationship. Examination of both curves (provided overleaf) reveals this poor fit to these data.

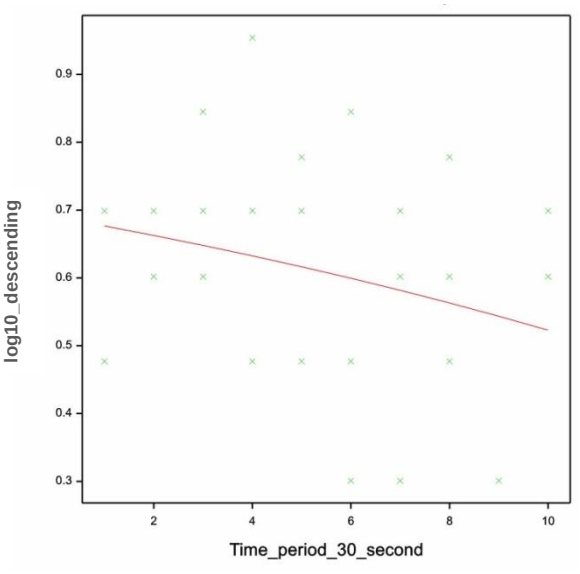

Figure 4.26 - Exponential regression of descending veliger larvae in steady temperature controls.

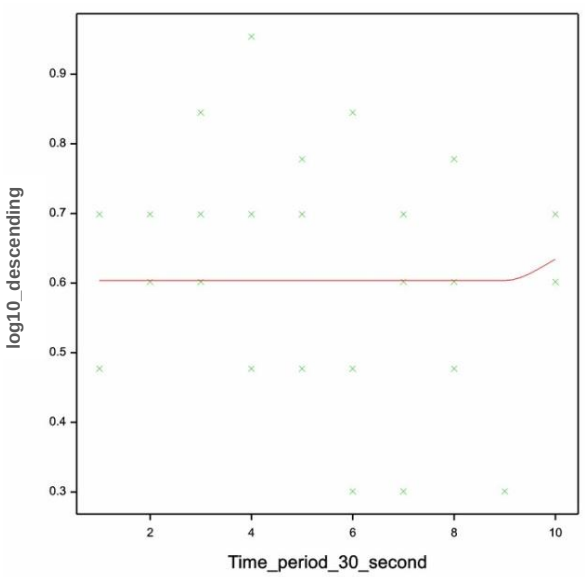

Figure 4.27 - Logistic regression of descending veliger larvae in steady temperature controls.

Neither pediveliger nor veliger control data had sufficient instances of falling larvae for a regression analysis.

Observations of larval behaviour following rapid temperature rise

Larvae of all development stages show a response during the first 10°C-13°C rise in temperature (the first 90 seconds). Both the number of larvae rising and the numbers descending alter during the larva's exposure to the rapid temperature increase (Figure 4.28 and Figure 4.29).

Rising Behaviour

The number of pediveliger larvae rising reduced sharply from 10.0%±1.0 of the cuvette population during the initial 4°C temperature increase (the first 30 seconds of exposure) to 6.8%±1.5 by 31.75°C (Figure 4.28). This trend continued to fall to 3.4%±0.6 rising by 34.5°C and just 1.6%±0.5 rising when 35°C was reached. Beyond 35°C less than 1% of the larvae were rising, with the percentage rising varying between 0.08% and 0.4%. Observations during filming show these percentages came from occasional individuals spread across the replicates, giving rise to high variance at these temperatures.

There was a sharp drop in veliger rising behaviour, reducing from 7.5%±1.7 during the initial 4°C rise, to 3.7%±1.4 in the next 3°C rise and 1.8%±0.6 in the next 2°C increase to 33.6°C (Figure 4.29). From 33.6°C to the end of filming at 37.5°C there was no little difference in the percentage of veligers showing rising behaviour with figures ranging between 1.0%±0.4 and 1.3%±0.4 in the remaining time intervals. This was more than double that shown by the pediveligers in the same time period.

Descending Behaviour

Figure 4.28 shows 15.4%±1.7 of the pediveligers descending during the first 4°C rise in temperature, falling to just 9.7%±0.8 by 32°C (at the end of the first 60 seconds). The 32°C-33.6°C rise (~90 seconds into filming) saw only a minor fall to 7.9%±0.9 of the pediveligers descending, before another large fall to 4.06%±0.69 descending during the 33.6°C-35°C temperature rise (~120 seconds into filming). This was followed by another fall as only 1.7%±0.4 of the larvae descended as the temperature rose to 35.8°C. The final 1.7°C rise saw all results being below

0.5% of larvae descending past the midline. Observations during filming show this number to come from occasional individuals descending from the surface, spread across all the replicates.

There was a gradual reduction in the numbers of veliger larvae descending (Figure 4.29) during the 11°C (300 second) temperature rise. During the initial 4°C rise (30 second), 9.5%±2.0 of the larvae were descending, decreasing to 7.2%±2.4 in the next 3°C rise to 33°C, 5.2%±1.9 by the time 33.8°C is reached and falling further to 2.9%±1.1 descending by 34.9°C (120 seconds into exposure). From 34.9°C to the end of the 300 second filming period at 37.5°C there was little variation in the percentage of larvae descending with numbers varying between 1.4%±0.6 and 0.8%±0.4. As with the rising veliger larvae data, the low percentages are generated from infrequent individuals descending during the final phase of the filming.

Falling larvae

The percentage of pediveligers falling shows a slight decline from 2.7%±0.6 during the first 4°C rise to 1.1%±0.3 after a 9.5°C rise. Post 35°C the percentage of pediveligers falling is below 0.5% and limited to infrequent individuals (Figure 4.28).

In veliger larvae the first 4°C rise had 2.7%±0.8 of the larvae showing falling. This dropped sharply to 0.2%±0.1 of veligers for the next 3°C increase, and remained below 0.5% of larvae falling during the rest of the filming period (Figure 4.29).

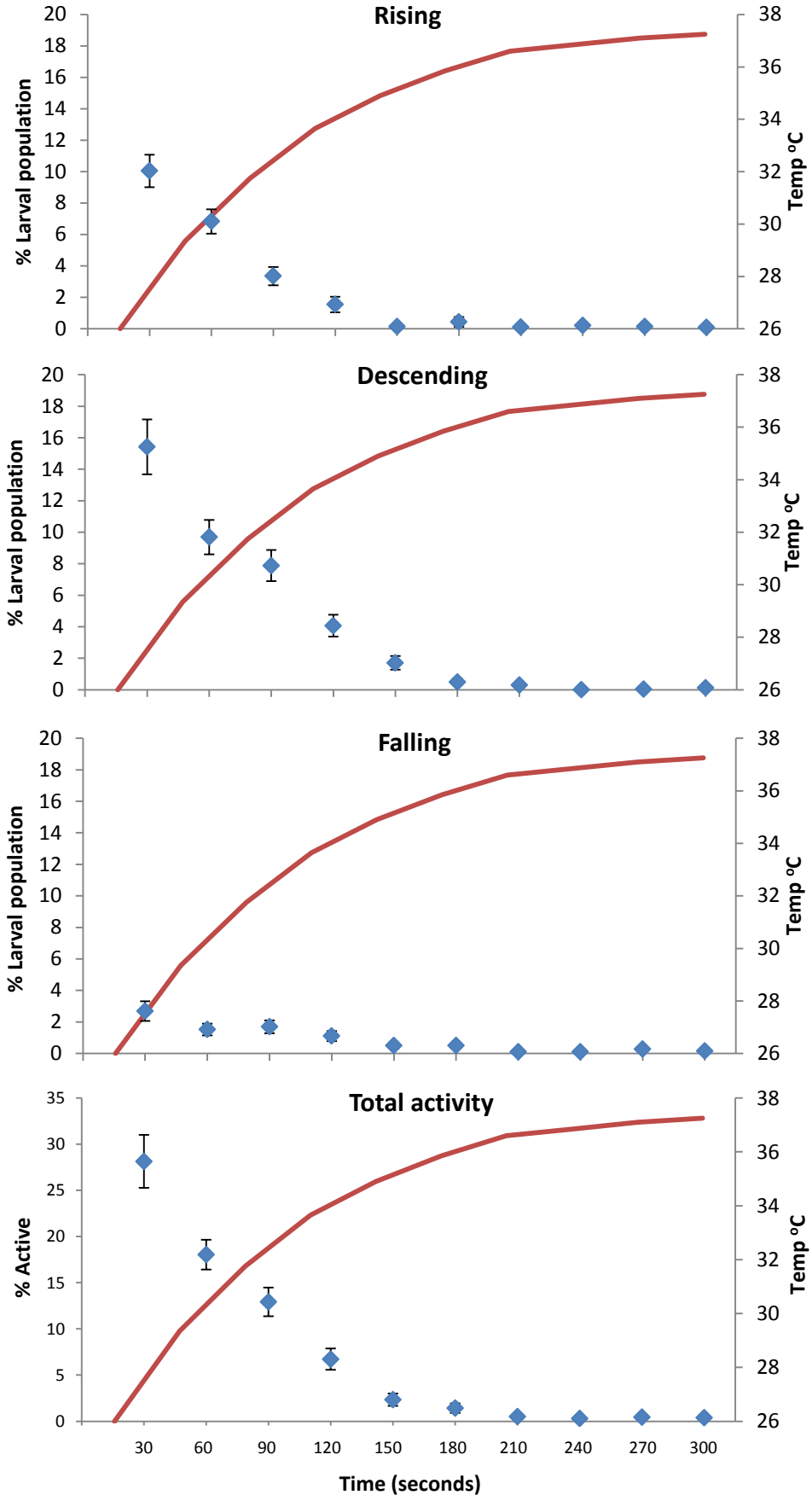

Figure 4.28 - Mean pediveliger larvae behaviours during rapid temperature rise, +/- 1 SE.

The percentage of the larval population (left axis) either rising, descending or falling (shell closed) is displayed against time and increasing temperature (right axis, red line) during the 11°C temperature change. The lower graph shows the total percentage of larval activity (left axis) during the temperature increase.

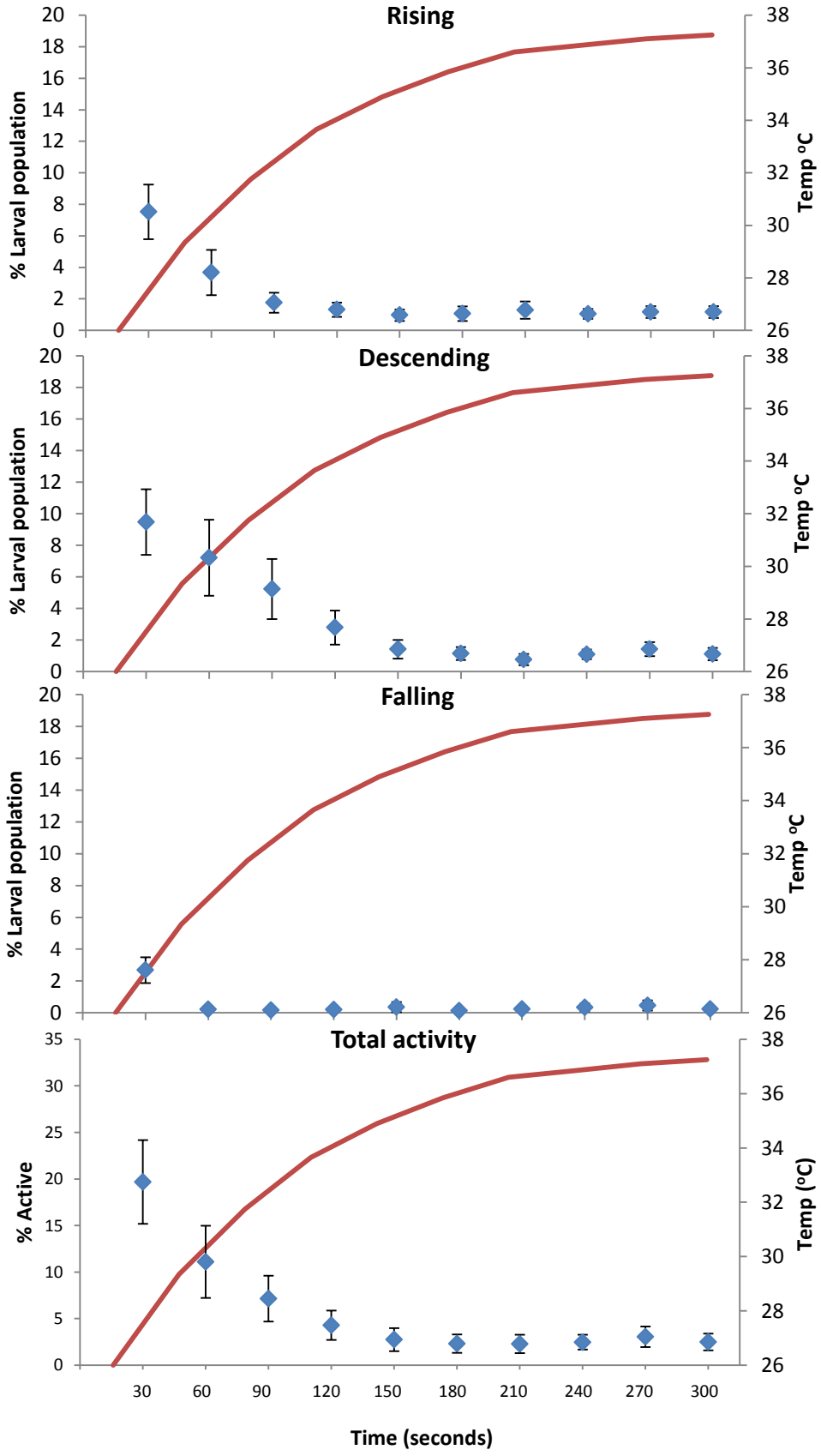

Figure 4.29 - Mean veliger larvae behaviours during rapid temperature rise, +/- 1 SE.

The percentage of the larval population (left axis) either rising, descending or falling (shell closed) is displayed against time and increasing temperature (right axis, red line) during the 11°C temperature change. The lower graph shows the total percentage of larval activity (left axis) during the temperature increase.

Regression analysis of larval behaviours following rapid temperature increase

RISING BEHAVIOUR

Pediveliger larvae

Initial examination of the percentage population data indicates a sharp decline in rising behaviour by pediveliger larvae following a rapid temperature increase.

	Exponential Function, A+ B*(R**X)			Logistic Function, A + C/(1 + EXP(-B*(X - M)))		
	D.f	F	p	D.f	F	p
Regression	2	55.45	<.001	3	41.46	<.001
Residual	63			62		
Total	65			65		
% Variance	62.6			65.1		
S.e. of the estimate	0.255			0.247		
	Estimates of parameters:					
	Estimate		**s.e.**	**Estimate**		**s.e.**
	R	0.7525	0.0699	B	-1.404	0.530
	B	1.545	0.153	M	3.043	0.284
	A	-0.060	0.187	C	0.956	0.155
				A	0.1388	0.0776

Table 4.8 - Summary of exponential and logistic regressions for pediveliger larvae rising behaviour versus time (and corresponding temperature elevation).

The exponential function indicates a significant relationship at the 0.1% level between number of larvae rising and time (during which temperature rises). Investigation of the exponential curve shows scatter giving a poor fit to these data in the later time periods (Figure 4.30). The occasional individuals rising described in the description of the observations probably cause this variance.

The logistic function indicates a similar pattern to the exponential, accounting for marginally better percentage of the variation, though is not an important increase give that the logistic function contains one extra parameter. The $p<0.001$ indicates a significant relationship between number of larvae rising and time (i.e temperature increase) at the 0.1% level. Examination of the logistic curve (Figure 4.31) reveals scatter in the later time (higher temperature) ranges due to the low numbers of swimming larvae. The logistic curve straightens

above 34°C (time period 4), probably due to these occasional swimming individuals spread across the replicates giving high variability at the high temperatures.

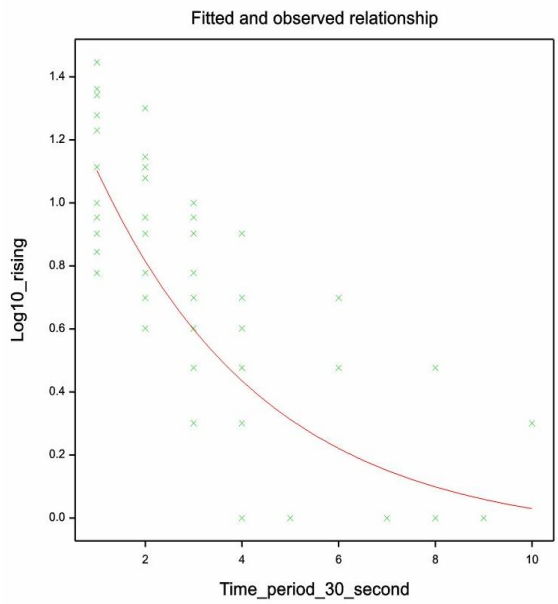

Figure 4.30 - Exponential regression of rising pediveliger larvae against time when exposed to rapid rise in temperature

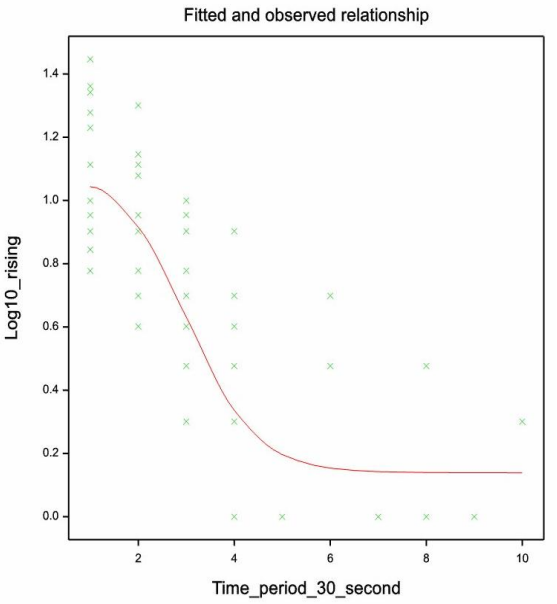

Figure 4.31 - Logistic regression of rising pediveliger larvae against time when exposed to rapid rise in temperature.

The apparently stability during the later time periods (higher temperatures) is probably due to having so few records of swimming at the end of the experiment.

Veliger larvae

Percentage cuvette population data (Figure 4.29) indicates veliger rising behaviour reduces following exposure to rapid temperature increase. A small percentage of veliger larvae maintained rising behaviour throughout the filming period.

	Exponential Function, A+ B*(R**X)			Logistic Function, A + C/(1 + EXP(-B*(X - M)))		
	D.f	**F**	**p**	**D.f**	**F**	**p**
Regression	2	40.81	<.001	3	23.07	<.001
Residual	80			79		
Total	82			82		
% Variance	49.3			44.7		
S.e. of the estimate	0.283			0.296		
	Estimates of parameters:					

Estimate		s.e.	Estimate		s.e.
R	0.4293	0.0960	B	-0.4752	
B	2.099	0.540	M	-8.328	
A	0.4101	0.0450	C	73.35	
			A	0.3392	

Table 4.9 - Summary of exponential and logistic regressions for veliger larvae rising behaviour versus time (and corresponding temperature elevation).

Both exponential and logistic functions indicate a significant relationship between reduction in number of larvae rising and increase in time of exposure at the 0.1% level with a p value of <0.001. However, in both instances the regression accounts for <50% of the variation. . Examining Figure 4.32 and Figure 4.33 reveals considerable scatter around both the exponential and logistic curves, but with a similar curve shown by both. The fit to the logistic function was ill conditioned, and GenStat was unable to calculate standard errors of the estimate for the logistic function indicating that this is an inappropriate model for these data. In both examples the curve begins to straighten at ~time period 4, or ~34^{o}C, probably due to the small number of larvae that maintained rising behaviour.

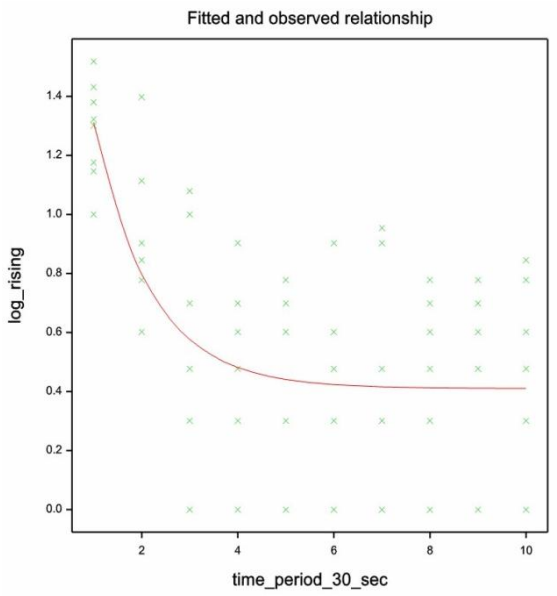

Figure 4.32 - Exponential regression of rising veliger larvae against time when exposed to rapid rise in temperature.

There are more records of swimming larvae in the later time period (higher temperatures) seen in the pediveliger larvae.

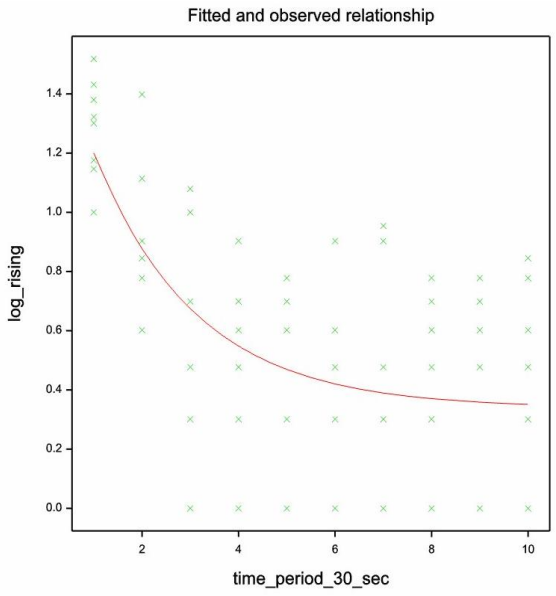

Figure 4.33 - Logistic regression curve of rising veliger larvae against time when exposed to rapid rise in temperature

DESCENDING BEHAVIOUR

Pediveliger larvae

The percentage population data shows a decline in descending behaviour as the temperature increases with exposure time (Figure 4.29).

	Exponential Function, A+ B*(R**X)			Logistic Function, A + C/(1 + EXP(-B*(X - M)))		
	D.f	**F**	**p**	**D.f**	**F**	**p**
Regression	2	80.77	<.001	3	57.87	<.001
Residual	77			76		
Total	79			79		
% Variance	66.9			68.4		
S.e. of the estimate	0.255			0.250		

Estimates of parameters:					
Estimate		**s.e.**	**Estimate**		**s.e.**
R	2.00	2.45	B	0.750	0.276
B	3.51	2.38	M	4.125	0.422
A	0.9330	0.0595	C	0.046	0.177
			A	1.379	0.304

Table 4.10 - Summary of exponential and logistic regressions for pediveliger larvae descending behaviour versus time (and corresponding temperature elevation).

Both approaches indicate a significant relationship between number of larvae descending and increasing time (=increasing temperature) at the 0.1% level with p values of <0.001.

The logistic function is a slightly better fit to the data, accounting for a higher percentage of variation. Both functions have considerable variance at the later time periods (higher temperatures), again probably due to the infrequent number of individuals recorded in the observations, and causing the scatter in the later time periods in Figure 4.34 and Figure 4.35.

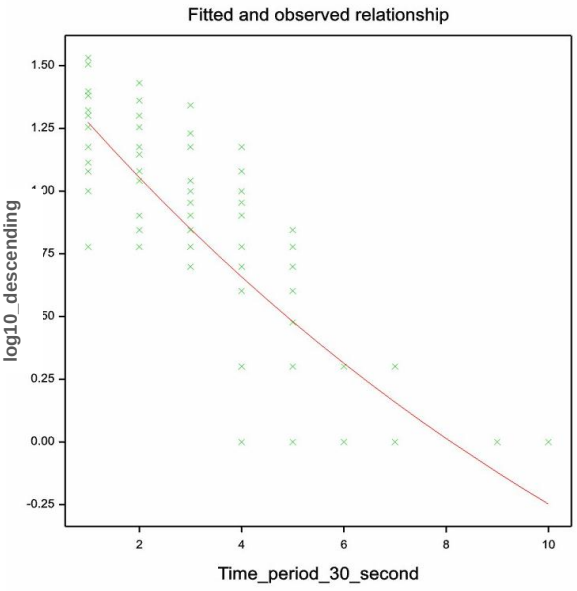

Figure 4.34 - Exponential regression curve of descending pediveliger larvae against time when exposed to rapid rise in temperature

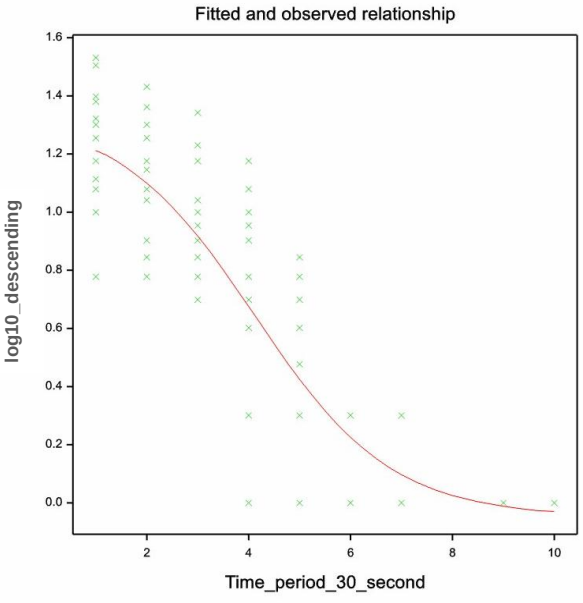

Figure 4.35 - Logistic regression curve of descending pediveliger larvae against time when exposed to rapid rise in temperature

Veliger larvae

Figure 4.29 shows the percentage of veliger larvae exhibiting descending behaviour decreases throughout the filming period/temperature increase.

	Exponential Function, A+ B*(R**X)			Logistic Function, A + C/(1 + EXP(-B*(X - M)))		
	D.f	**F**	**p**	**D.f**	**F**	**p**
Regression	2	51.45	<.001	3	42.21	<.001
Residual	80			79		
Total	82			82		
% Variance	55.2			60.1		
S.e. of the estimate	0.311			0.294		

Estimates of parameters:					
Estimate		**s.e.**	**Estimate**		**s.e.**
R	0.3688	0.0896	B	1.701	0.696
B	1.694	0.224	M	3.347	0.284
A	0.6623	0.0737	C	0.936	0.126
			A	0.4296	0.0483

Table 4.11 - Summary of exponential and logistic regressions for veliger larvae descending behaviour versus time (and corresponding temperature elevation).

The logistic approach appears to provide a better fit to the data, accounting for a greater proportion of the variation, though the increase is small considering that the logistic function contains one extra parameter. Both approaches indicate a significant (at the 0.1% level) relationship between time (=temperature rise) and a reduction in rising behaviour. Examining the logistic curve shows high scatter around the later time period, but a possible lag phase during the initial 5^{O}C temperature rise (30-60 seconds).

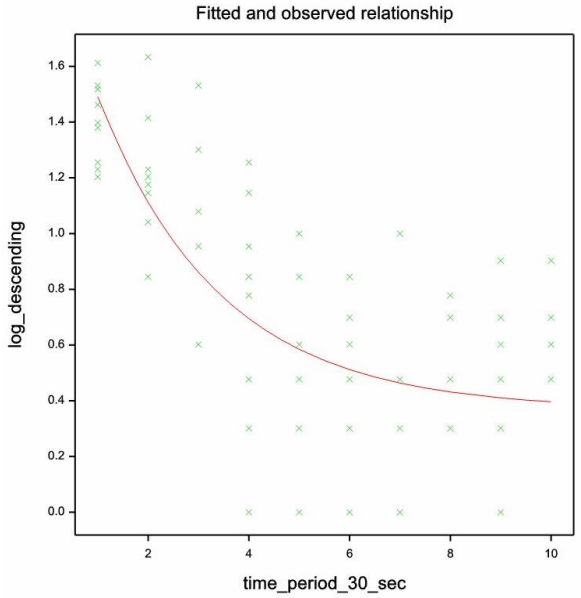

Figure 4.36 - Exponential regression curve of descending veliger larvae against time when exposed to rapid rise in temperature

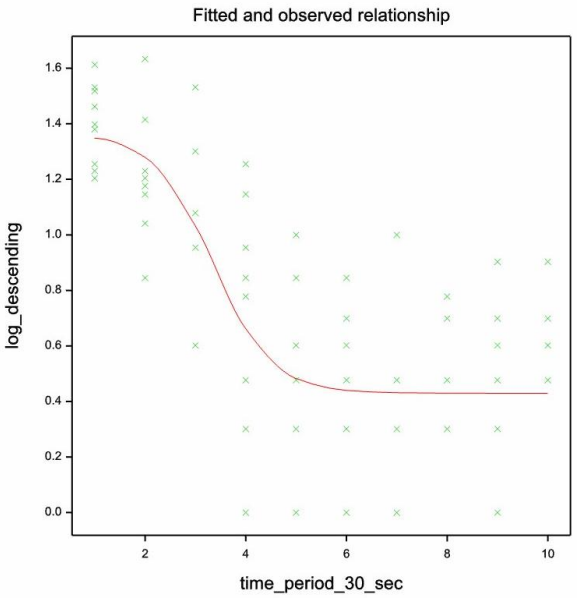

Figure 4.37 - Logistic regression curve of descending veliger larvae against time when exposed to rapid rise in temperature

Neither pediveliger nor veliger rapid temperature rise experiments had sufficient instances of falling larvae to allow a regression analysis.

Observations of larval behaviours following rapid temperature reduction

Larvae subjected to a rapid drop in temperature showed a decline in the numbers of individuals rising, descending and falling within the first 13°C (180 seconds) temperature reduction (Figure 4.38 and Figure 4.39), with this trend being especially pronounced in veliger stage larvae.

Rising Behaviour

The number of pediveliger larvae rising fell from 11.3%±3.0 during the first 4°C drop to 3.8%±1.2 in the following 3°C fall, and fell again to 1.7%±0.8 after the next 2°C fall to 17°C (Figure 4.38). From 16°C, rising activity falls to 0.6%±0.4 and for the next 180 seconds of filming as the temperature fell to a low of 12°C, the percentage of pediveligers rising did not get higher than 0.4%±0.4. As with previous experiments, the low percentages for the final 180 seconds of filming can be attributed to occasional individuals.

The percentage of veliger larvae rising fell steadily throughout the 11°C temperature drop (Figure 4.39). 5.0%±1.3 of veligers were rising during first 4°C drop (0-30 seconds of filming), falling to 1.8%±0.6 by 18°C, and rising again to 3.2%±0.9 when 16°C is reached (90 seconds after exposure). From 16°C, 1.61%±030 of veliger larvae were rising, falling to 0.89%±0.25 during the fall from 14.8°-14°C, 0.58%±0.19 from 14°C-13.3°C and 0.5%±0.1 in 13.3°C-12.5°C. The remaining 0.5°C temperature drop (final 90 seconds of filming) has less than 0.5% of veliger larvae rising.

Descending Behaviour

The number of pediveliger larvae descending fell steadily throughout the 11°C temperature drop (Figure 4.38). The first 4°C drop in temperature saw 9.7%±3.4 of pediveligers descending, followed by a sharp drop to 4.7%±1.2 during the following 3°C drop. In the next 2°C fall to 17°C (60-90 seconds phase) the number of pediveliger larvae descending rose slightly to 7.3%±2.8. From 16°C the percentage larvae descending fell steadily from 7.3% to a final percentage of 1.3%±0.4 at 12°C. There was little difference in the percentage of pediveligers descending during the final 0.5°C of temperature decrease, with numbers staying below 1.0%.

Numbers of descending veliger larvae underwent a very sharp decline after the first 4°C drop in temperature, during the first 30 seconds of exposure, with 10.2%±2.0 of veligers descending, dropping to 3.3%±1.0 after the next 3°C fall to 19°C (Figure 4.39). From 18°C to the end of the filming period another sharp drop occurred with less than 1.0% of the larval population descending, and this low percentage continued for the remainder of the temperature drop to 12°C.

Falling larvae

Numbers of pediveliger larvae falling dropped from 1.8%±0.9 of the larvae in the first 4°C fall, to 0.2%±0.1 during the next 3°C temperature drop. Numbers of falling larvae stayed under 0.5% for the rest of the temperature change (Figure 4.38).

Numbers of falling veligers decreased sharply after the first 4°C drop (in the first 30 seconds), during which 10.9%±1.8 of the larvae fell with closed shells (Figure 4.39). In the following 3°C decrease 0.6%±0.4 of the larvae were falling. The percentage population of veligers falling did not exceed 0.3%±0.1 for the remainder of the filming period as the temperature fell by another 7°C to 12°C.

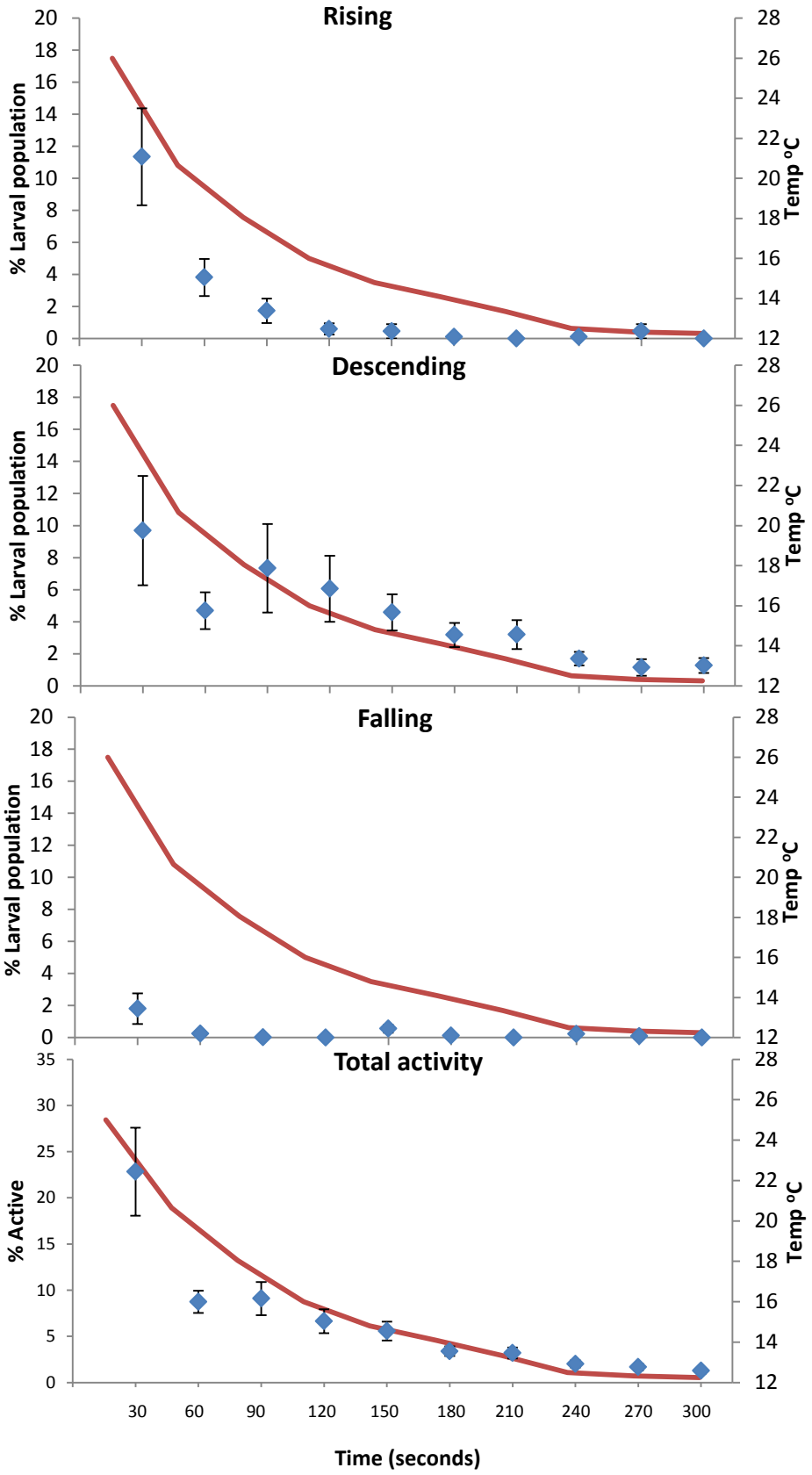

Figure 4.38 - Mean of pediveliger larvae behaviours during rapid temperature drop, +/- 1 SE.

The percentage of the larval population (left axis) either rising, descending or falling (shell closed) is displayed against time and decreasing temperature (right axis, red line) during the 11°C temperature change. The lower graph shows the total percentage of larval activity (left axis) during the temperature fall.

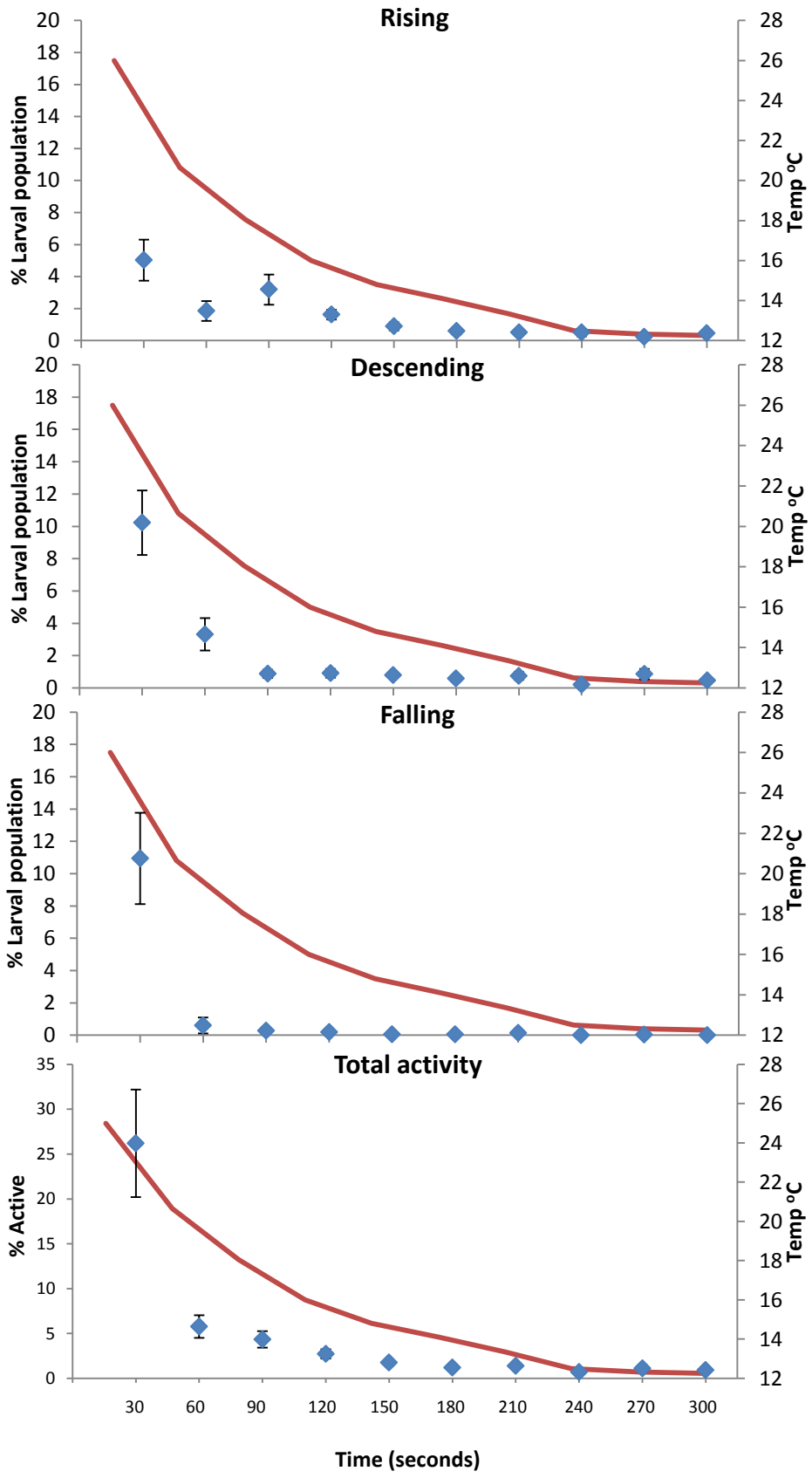

Figure 4.39 - Mean veliger larvae behaviours during rapid temperature drop, +/- 1 SE.

The percentage of the larval population (left axis) either rising, descending or falling (shell closed) is displayed against time and decreasing temperature (right axis, red line) during the 11°C temperature change. The lower graph shows the total percentage of larval activity (left axis) during the temperature fall.

Regression analysis of larval behaviours following rapid temperature decrease

RISING BEHAVIOUR

Pediveliger larvae

Figure 4.38 indicates the number of pediveliger larvae exhibiting rising behaviour fell sharply during the first 5^{o}C temperature decrease (30 seconds), and continued to fall throughout the temperature decrease.

	Exponential Function, A+ B*(R**X)			Logistic Function, A + C/(1 + EXP(-B*(X - M)))		
	D.f	**F**	**p**	**D.f**	**F**	**P**
Regression	2	36.20	<.001	3	23.40	<.001
Residual	30			29		
Total	32			32		
% Variance	68.8			67.7		
S.e. of the estimate	0.260			0.264		

Estimates of parameters:					
Estimate		**s.e.**	**Estimate**		**s.e.**
R	0.618	0.104	B	-0.624	0.708
B	1.929	0.254	M	3.9	14.3
A	-0.094	0.187	C	-0.36	9.66
			A	-0.064	0.221

Table 4.12 - Summary of exponential and logistic regressions for pediveliger larvae rising behaviour versus time (and corresponding temperature reduction).

The fits to both models indicate the relationship between changing temperature (time) and the reduction in rising behaviour shown in Figure 4.44 is significant at the 0.1% level. This relationship explains ~69% of the variance (a comparable value to the pediveliger reaction to temperature rise), with the remaining 31% probably due to variation between individuals. There is considerable scatter about the line, as seen previously this is most obvious during the latter time periods (lower temperature ranges) where fewer larvae are recorded swimming, contributing to high variance in these ranges.

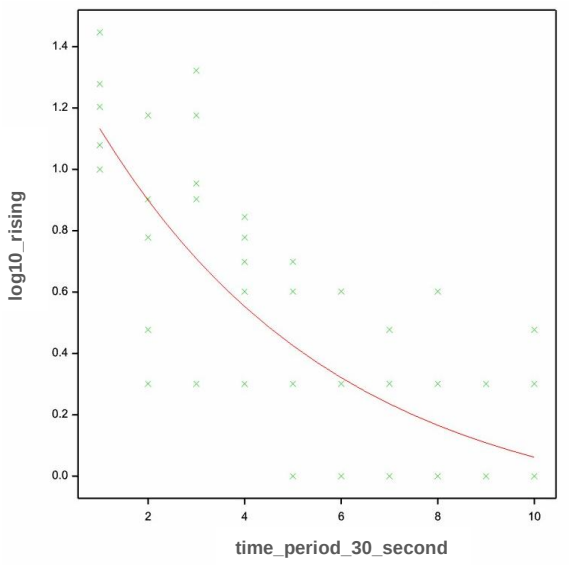

Figure 4.40 - Exponential regression curve of rising pediveliger larvae against time when exposed to rapid decrease in temperature

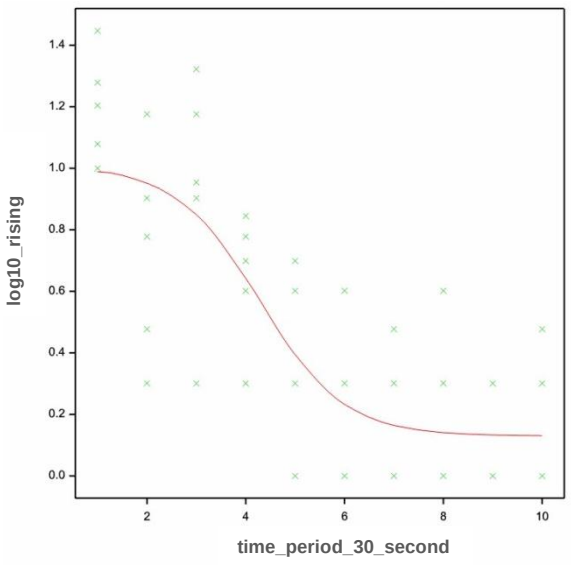

Figure 4.41 - Logistic regression curve of rising pediveliger larvae against time when exposed to rapid decrease in temperature

Veliger larvae

The number of rising veliger stage larvae displays a gradual decrease during the rapid reduction in temperature (Figure 4.44).

	Exponential Function, A+ B*(R**X)			Logistic Function, A + C/(1 + EXP(-B*(X - M)))		
	D.f	F	p	D.f	F	p
Regression	2	52.08	<.001	3	34.65	<.001
Residual	57			56		
Total	59			59		
% Variance	63.4			63.1		
S.e. of the estimate	0.218			0.219		
	Estimates of parameters:					
	Estimate		**s.e.**	**Estimate**		**s.e.**
	R	0.8407	0.070	B	-0.551	0.350
	B	1.359	0.202	M	3.57	1.50
	A	0.012	0.277	C	1.067	0.515
				A	0.246	0.177

Table 4.13 - Summary of exponential and logistic regressions for veliger larvae rising behaviour versus time (and corresponding temperature reduction) following temperature reduction.

The fits to both models show a relationship, significant at the 0.1% level, between reduced rising behaviour and reduction in temperature during the 5 minute filming period. This

relationship explains 63% of the variance, with some scatter about the fit (due to variation between individuals) evident in Figure 4.42 and Figure 4.43.

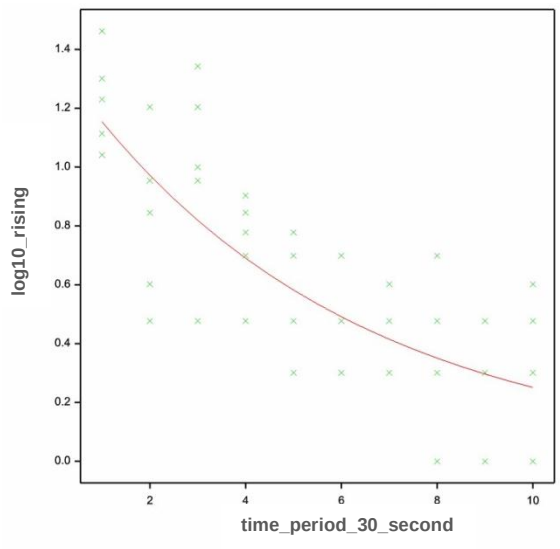

Figure 4.42 - Exponential regression curve of rising veliger larvae against time when exposed to rapid decrease in temperature

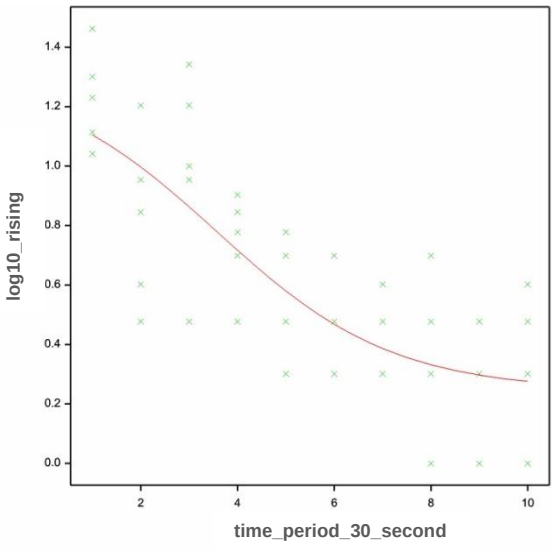

Figure 4.43 - Logistic regression curve of rising veliger larvae against time when exposed to rapid decrease in temperature

DESCENDING BEHAVIOUR

Pediveliger larvae

Figure 4.38 indicates a more gradual reduction in the numbers of pediveliger larvae descending when compared to previous treatments.

	Exponential Function, A+ B*(R**X)			Logistic Function, A + C/(1 + EXP(-B*(X - M)))		
	D.f	F	p	D.f	F	P
Regression	2	15.07	<.001	3	10.32	<.001
Residual	81			80		
Total	83			83		
% Variance	25.3			25.2		
S.e. of the estimate	0.411			0.411		
	Estimates of parameters:					
	Estimate		**s.e.**	**Estimate**		**s.e.**
	R	1.093	0.158	B	-0.909	0.748
	B	-0.59	1.49	M	6.519	0.984
	A	1.59	1.60	C	0.700	0.259
				A	0.173	0.202

Table 4.14 - Summary of exponential and logistic regressions for pediveliger larvae descending behaviour versus time (and corresponding temperature elevation).

Both approaches show a significant (at 0.1% level) relationship between reducing descending behaviour and time/temperature drop. However both exponential and logistic functions account for just 25% of the variation, and examination of the curves presented in Figure 4.44 and Figure 4.45 reveal a large amount of scatter. These fits are poorly defined.

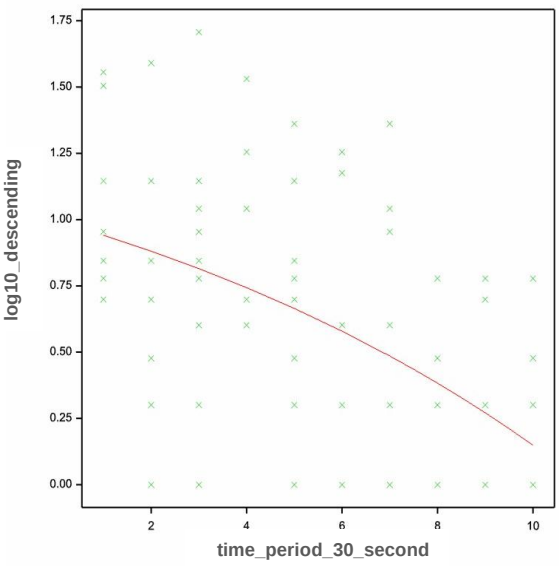

Figure 4.44 - Exponential regression curve of descending pediveliger larvae against time when exposed to rapid decrease in

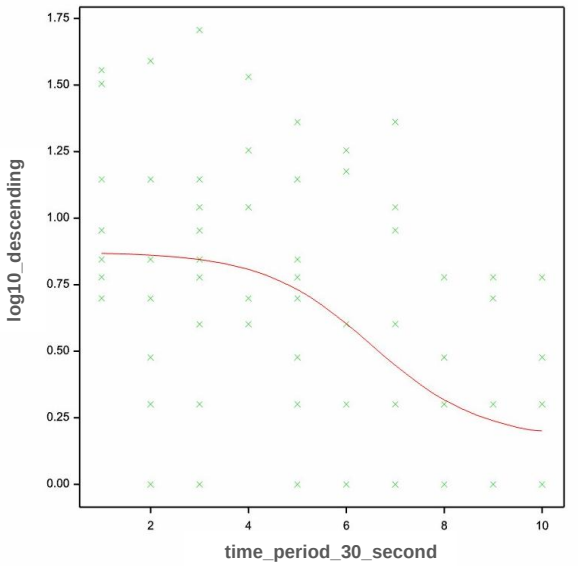

Figure 4.45 - Logistic regression curve of descending pediveliger larvae against time when exposed to rapid decrease in temperature

Veliger larvae

Figure 4.39 indicates that the descending behaviour of veliger larvae reducing sharply following exposure to a sudden reduction in temperature.

	Exponential Function, A+ B*(R**X)			Logistic Function, A + C/(1 + EXP(-B*(X - M)))		
	D.f	**F**	**p**	**D.f**	**F**	**p**
Regression	2	54.61	<.001	3	35.28	<.001
Residual	57			56		
Total	59			59		
% Variance	64.5			63.5		
S.e. of the estimate	0.258			0.261		
	Estimates of parameters:					
	Estimate		**s.e.**	**Estimate**		**s.e.**
	R	0.4723	0.0802	B	-0.6359	Unable to calculate
	B	2.416	0.490	M	-6.653	
	A	0.3814	0.0497	C	148.0	
				A	0.3570	

Table 4.15 - Summary of exponential and logistic regressions for veliger larvae descending behaviour versus time (and corresponding temperature reduction).

Both models show a significant (at the 0.1% level) relationship between the reduction in descending behaviour and time/reducing temperature. The analysis accounted for 64% of the variation, the remaining 34% being variation between individuals. However, the fit of the logistic function was ill conditioned, and GenStat® was unable to calculate standard error of the estimates for the logistic function.

As with previous analyses, there is significant scatter in the later time periods/lowest temperatures (Figure 4.46 and Figure 4.47) contributing to this variation. A second analysis, removing the results past time period 4 (~15°C), also indicated a significant regression ($F_{1, 22}$ = 39.7, p<0.001), and only accounted for 64.5% of the variation. There was still significant variation between individuals during the initial 10°C drop in temperature.

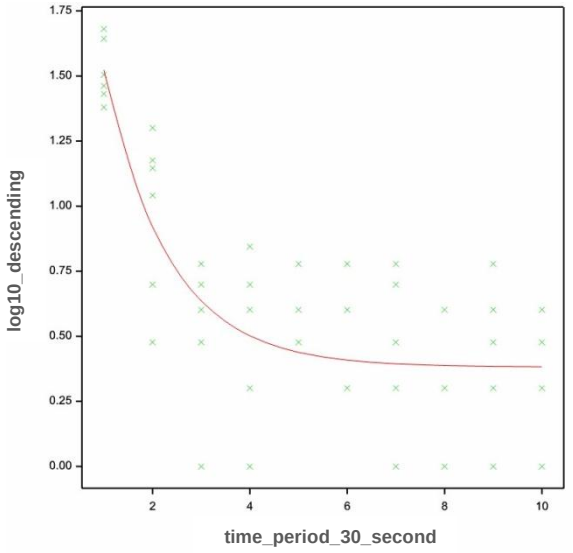

Figure 4.46 - Exponential regression curve of descending veliger larvae against time when exposed to rapid decrease in temperature

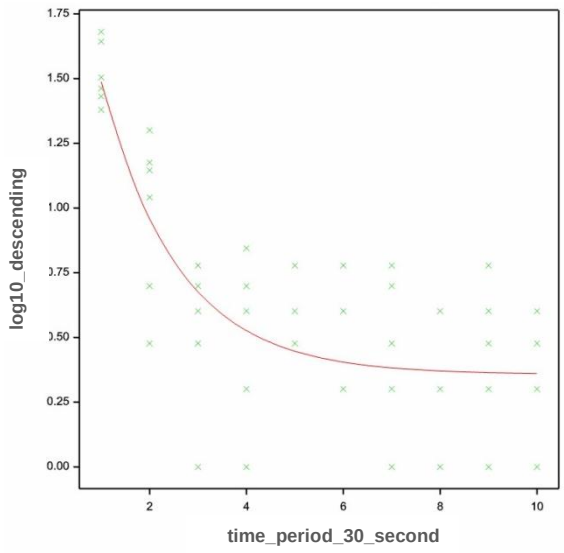

Figure 4.47 - Logistic regression curve of descending veliger larvae against time when exposed to rapid decrease in temperature

Neither pediveliger nor veliger rapid temperature rise experiments had sufficient instances of falling larvae to allow a regression analysis.

General summary of observations of larval activity following rapid temperature change; a description of the overall trends

There was a sharp decline in the total activity of the larval populations of the cuvettes (based on the three observed behaviours) following exposure to either rapidly rising or decreasing water temperatures (Figure 4.28 - Figure 4.39).

Rapid temperature increase

The percentage of active larvae in the cuvettes in the heat shock experiments fell from 28.1%±2.9 active in the first 4^{o}C rise to 18.0%±1.6 during the next 3^{o}C rise (30-60 seconds time interval, Figure 4.28). Activity continued to reduce, dropping to 12.9%±1.6 by 33.6^{o}C, 6.7%±1.2 by 35^{o}C, 2.3%±0.7 by 36^{o}C and just 1.4%±0.5 of the cuvette population by 36.6^{o}C. From 36.6^{o}C onwards (180 second after into exposure) the percentage population active was consistently less than 0.5%.

During filming of the first 4^{o}C rise, 19.7%±4.5 of the veligers were active, falling to 11.1%±3.8 in the next 3^{o}C rise during the 30-60 seconds time-frame (Figure 4.29). Total activity continued to fall, dropping from 7.1%±2.4 in the rise from 32^{o}C-33.6^{o}C to 4.3%±1.5 when 35^{o}C was reached. The remaining 2.5^{o}C increase saw an average of 2.6%±0.9 of the larvae active until the end of filming, higher than in the pediveliger experiments.

Rapid temperature reduction

The percentage of pediveligers active in the temperature reduction experiments fell from 22.8%±7.1 during the first 4^{o}C drop to 8.7%±1.8 during the next 3^{o}C (Figure 4.38). This sharp decline was typically followed by a more gradual decline in activity from 9.0%±2.8 of larvae in to 1.1%±0.4 by the end of the 5 minute filming period /~12^{o}C temperature reduction.

The veliger stage larvae dropped from 26.29%±5.9 active in the 0-30 seconds time period to 5.8%±1.3 after 60 seconds (8^{o}C, Figure 4.39). The remainder of the filming period saw a more gradual decline in overall activity, falling from 4.3%±0.9 at 16^{o}C, to 1.2%±0.3 when 13.3^{o}C is reached. The remaining 0.5^{o}C fall in temperature of saw 1.0%±0.3 of the cuvette population remaining active.

	Rapid Temperature Rise			Rapid Temperature Drop			
Larvae	**Velocity**	**Behaviour**	**Population characteristics**	**Velocity**	**Behaviour**	**Population characteristics**	**Controls**
Pediveliger	No significant rise in velocity during first 10°C rise ($F_{1, 108}$ = 2.25, p = 0.136). Swimming stops after a 10°C rise in temperature. (Figure 4.11)	Steep falls in both rising and descending behaviour (Figure 4.28). Both are significant at 0.1% level (Table 4.8 and Table 4.10) with the regression explaining 60-70% of the variation.	Population activity falls from an initial 28% to less than 0.5%. (Figure 4.28)	Sharp reduction in swimming velocity. Falls below 0.4mms^{-1} by the end of filming with few individuals swimming. (Figure 4.13) Significant ($F_{2, 92}$ = 31.08, p<0.001) relationship between velocity and time (temperature change), but only explains ~40% of variance. Fit is poor due to lack of swimming in lower temperatures	Sharp decline in rising larvae during initial 10°C temperature reduction (Figure 4.38). Significant at 0.1% level with ~69% variation explained. Descending behaviour shows a steady decline (Figure 4.38). Significant at 0.1% level, but with only 25% variation explained. Poor fit to the data. A lot of variation between individuals	Population activity falls from 23% active to 1%. The largest fall is during the initial 4oC drop. (Figure 4.38)	No significant change in velocity over filming period ($F_{1, 94}$ = 0.02, p=0.900) Significant reduction in rising behaviour (Table 4.4). ~60% variation accounted for by regression against filming time. Significant reduction in rising behaviour (Table 4.6). ~70% variation accounted for by exponential regression.
Veliger	Slight increase in velocity during the 5 minute filming period (Figure 4.11), significant at the 1% level. 93.7% of variance probably due to variation between individuals	Shallower decline in rising and descending behaviours (Figure 4.29). Both significant at the 0.1% (Table 4.9 and Table 4.11) level. Relationship between reduction in behaviours and time (temperature change) explains ~49% of variation in rising experiments, and 55% in descending.	Population activity falls from 20% to 2.5% (Figure 4.29)	Gradual reduction in swimming velocity to 0.8mms^{-1} (Figure 4.13). Significant fall (Table 4.3) with ~50% of variation accounted for.	Gradual reduction in rising throughout the temperature fall (Figure 4.39). Significant at the 0.1% level with this relationship explaining ~63% of the variation. Sharp fall in descending behaviour (Figure 4.39). Significant at the 0.1% level with this relationship explaining ~64% of the variation.	Population activity falls from 26% active to 1% active during the final stages of the temperature fall (Figure 4.39).	No significant change in velocity over filming period ($F_{1, 158}$ = 0.03, p=0.860) Possible significant changes in behaviour (Table 4.7and Table 4.9) but with very poor fit to data and high variation between individuals (Figure 4.22 and Figure 4.26)

Table 4.16 - Summary of the reactions recorded in the veliger and pediveliger larvae exposed to rapid temperature changes

4.4 Discussion

Larval dispersal is affected by both hydrodynamic transport and larval behaviours, however little is known about how behaviours may affect dispersal and recruitment patterns (Fuchs et al., 2010). Data on behavioural reactions can be difficult to collect, but the method developed here potentially provides an accessible way of collecting information on larval reactions to specific variables, such as temperature, that can be incorporated into dispersal models.

4.4.1 A consideration of the method

Prior to discussion of the results generated, it is important to evaluate the filming technique; the results should be considered as part of this method development process. Suggestions for future applications for the method have been provided in section **4.4.9** and further comment on the method is provided during the discussion of the results.

The use of cuvettes

Spectrophotometer cuvettes were chosen to contain the larvae for filming as these allowed a high magnification view of swimming whilst offering a controlled environment where temperature could be altered rapidly. Furthermore the clear face of the spectrophotometer cuvettes did not distort the image whilst filming with a macro lens. Other filming techniques have used small (5ml) wells (Fuchs et al., 2010, Hidu & Haskin, 1978a), but these have curved sides which are difficult to film other than from above, thus not allowing collection of film of vertical movements. Another alternative was to tether larvae (Gallager, 1993, Hadfield & Koehl, 2004), but this was too restrictive on larval movement and methodologically challenging - an important aspect of the design was ease of replication.

The flat front face of the cuvette did not distort the image, and the volume allowed for a good range of larval movements to be captured (Figure 4.6). The cuvette was ideal for filming singly, or for filming several replicates together. However the cuvette, while allowing collection of fairly long larval trajectories, was still a fairly restricted environment. Larger (up to 9m)

mesocosms have been used for investigating larval reactions to thermoclines (Manuel et al., 1996, Manuel et al., 2000, Pearce et al., 2004), but while less restrictive these large chambers would be extremely difficult to track individual larvae in. However the restricted cuvette environment did limit possible distance of travel, and resulted in occasional collisions between larvae. These collisions have been noted as problematic in other larval studies were small (5ml) wells have been used for filming (Hidu & Haskin, 1978a). However it should also be noted that the trajectories visualised by ImageJ do provide a method of viewing these reactions by individual larvae (Figure 4.6). The cuvette was a compromise between obtaining detailed information on larval swimming trajectories and sufficient volume to allow relatively uninhibited swimming, and in this regard was fairly successful. Some larvae may have been caught in the surface tension either at the water surface, or potentially in the cuvette corners resulting in some very fast moving individuals. This was also noted by Hidu (1978) when using wells for filming.

The cuvette environment was easy to consistently alter for, in this case, temperature. While the cuvette did have a slight insulation effect (it was always 1-2^{o}C cooler/hotter than the water bath) this was constant and easily monitored. There was no evidence of thermoclines in the cuvettes in the final design. Early filming efforts had a thermal effect that was visible when filming, but redesigning the filming chamber to ensure even introduction of the heating/cooling water removed this effect. The possibility of the larvae showing a response to the cuvette environment when held at steady temperatures, possibly seen in Figure 4.18 to Figure 4.27, is considered in section **4.4.7**.

Underestimating the helix?

Filming from only the front face of the cuvette was most practical, but could result in an underestimation of the helical movement of the larvae (Cragg, 1980). By calculating the distance moved in pixels between video frames this gave a two dimensional movement, not incorporating the helical swimming path (if the larva had swum in this manner - Figure 4.6). It is not possible to discount this effect at this stage of development; changes in the size of the helix may still have an

influence on the swimming velocities recorded. Future iterations of the method would require filming from above in order to entirely discount or incorporate the influence of the helix.

Software

The combination of the VirtualDub and ImageJ shareware software packages was extremely effective, if rather computationally demanding, for extracting velocity and trajectory information. The selection of individual larval paths in ImageJ was a particularly powerful tool. However the method, in current form, is somewhat dependent on user input. As a consequence processing a large number of trajectories is extremely time-consuming. Incorporation of a number of short macros designed to extract only those coordinates from ImageJ spread sheets that represented vertical swimming would allow some degree of automation, bringing the method closer to some of the commercial software solutions such as Ethovision® and ActualAnalytics®. However, in comparison to the licence costs of such software, this use of ImageJ and ParticleTracker provided a viable alternative.

4.4.2 Swimming velocity of temperature acclimated *Crassostrea gigas* larvae

The filming method has provided specific information on the larval swimming velocities of *C. gigas* through a temperature range that includes the species optimum spawning temperature range. Although 23^{o}C is considered the optimum environmental temperature for *C. gigas* larval growth (Kobayashi et al., 1997, Quayle, 1988), many hatcheries employ higher temperatures for rapid growth to settlement (Rico-Villa et al., 2009). Average velocities through the 20-38^{o}C temperature range varied from 1.1mms^{-1} to 1.7mms^{-1} depending on the larval batch (Figure 4.7). There are no previous velocity records available for *C. gigas* larvae through the temperature range investigated in this study. These results provide an insight into larval swimming competence through a wide range of temperature regimes.

The change in the swimming velocity of acclimated veligers as temperature increases can clearly be divided into two relationships - an exponential response in the 12^{o}C-22^{o}C range and a period of relatively stable velocity during the 24^{o}C-38^{o}C range. It should be noted here that while the regression indicated a relationship between increasing temperature and increasing velocity in

the 12°C-22°C range (R^2_{adj} value of 48%, F_{1-329} = 304 and $p < 0.001$), the considerable remaining variation, 52%, can probably be assigned to differences between individual larvae. This variation was a theme of all the results collected, and has been noted in previous studies of larval swimming (Hidu & Haskin, 1978). Above 22°C there was no significant trend for an increase in velocity with temperature, and data start to deviate from the exponential relationship observed over the lower temperature range (with a high variation between individuals). This may indicate that the animals are moving into a zone where normal functioning is disrupted. This could be due to processes such as damage to temperature sensitive proteins, and changes in membrane fluidity. However, this is probably not the case as the 26-28°C range for the culturing of *C. gigas* ensures maximum larval growth (Helm & Bourne, 2004, Helm & Millican, 1977), and optimum settlement (Ben Kheder et al., 2010). Furthermore, larvae are still competent to settle in high numbers at 32°C, metabolising even moderate lipid reserves for settlement and metamorphosis (Ben Kheder et al., 2010).

The lack of a significant relationship between velocity and temperature increase post 22°C probably suggests the larvae enter a period of tolerance to temperature - a range where they reach their metabolic limit (prior to this becoming lethal) for the speed capable of being achieved by the larva through ciliary swimming (Hidu et al., 1973). Although temperatures within the 24-38°C range have previously been indicated as optimal for *C. gigas* larval development, there is variance in the specific temperatures reported from 23°C (Quayle, 1988) to 27°C (Ben Kheder et al., 2010, Rico-Villa et al., 2009) and 28°C (Helm & Bourne, 2004). This disparity may be a result of variation between individuals (and probably broodstocks), evidenced throughout the results presented in this chapter. Large variation between individuals has been noted before in larval studies (Hidu & Haskin 1978a, Cragg, 1980).

4.4.3 The physiological effect of temperature on the larvae - thermal tolerance within the cuvette environment

The metabolic rate of the larvae will increase with the rise in water temperature (Beiras et al., 1995, Rico-Villa et al., 2009). This physiological effect would have probably been more

pronounced on the temperature acclimated larvae than those used in the behavioural work as they were exposed to the changes in temperature for a longer period of time, in order to allow larvae to acclimate to these temperatures within the cuvette. The increase in growth rates, settlement rates and, in this study, velocity with rising temperature may therefore be a simple stimulation of the larval metabolism (Rico-Villa et al., 2009).

Increase in temperature will see an increase in swimming velocity through the physiological effect of temperature on the ciliated cells of the velum (increase in metabolic rate resulting in increase in cilia beat frequency) that is probably most obvious in the linear increase in velocity from 12-22^{o}C (Beiras et al., 1995, Hidu & Haskin, 1978a). A rise in temperature to 32^{o}C will stimulate the bivalve larval metabolism without causing significant mortality (Ben Kheder et al., 2010).

The point at which temperature becomes inhibitory to *C. gigas* larval swimming (for larvae that have been afforded time to acclimatise) is not reached during the current study. Given that the filming period was 2 minutes, plus the acclimation time of 20 minutes, the results indicate *C. gigas* larvae can tolerate, albeit with reduced swimming activity, temperatures of up to 38^{o}C for at least 22 minutes. While there was reduced swimming in the water column of the cuvette, it was noted that larvae were still active on the base of the cuvette. Given that some individuals were still active in the water column at the end of filming, and the remainder appeared active on the base, it is probable that *C. gigas* larvae are tolerant of ≥38^{o}C for a period of time in excess of 22 minutes.

C. gigas larval thermal tolerances (usually measured though mortality or settlement investigations) have previously been reported at a low of 15^{o}C (Diederich et al., 2005) and a high of 35^{o}C (Rico-Villa et al., 2009). Lower temperature ranges (<22^{o}C) delay settlement and metamorphosis (Ben Kheder et al., 2010). Growth is reduced at these lower temperatures, and mortality increases sharply above 35^{o}C (Rico-Villa et al., 2009). However, defined upper and lower thermal limits for *C. gigas* larvae have not yet been fully established. Results from this study may suggest that this tolerance will be correlated with time of the exposure period.

Longer filming periods will be required in order to use this method to assess thermal tolerance (although this will generate problems of file size for processing). Whilst these data do indicate *C. gigas* larvae are tolerant of ≥38°C for ≥22minutes, significant mortality in veligers of *Crassostrea virginica* when exposed to temperatures of >30°C does not occur until exposure periods of 2 hours are reached (Hidu et al., 1973). Conversely significant mortality in *C.virginica* does occurs in 10 seconds in water temperatures of >40°C (Hidu et al., 1973). However, other studies have suggested that low mortality may be maintained in *Crassostrea virginica* for as long as 2 hours in 40°C-41°C water (Wright et al., 1983). As with the variations in temperature optimum records, this may be explained through variation between individuals or variation between larval batches/broodstocks.

Larvae of some other temperate/warm temperate bivalve species also show considerable tolerance to higher temperatures, although this is again linked to the exposure period. Veligers of *Mercenaria mercenaria* and *Mulinia lateralis* withstand temperatures up to 41°C for a over an hour (Wright et al., 1983). This is not true of all temperate bivalve species, *Sipisula solidissima* veligers are less tolerant, surviving in these extremes for approximately 10 minutes (Wright et al., 1983). This temperature tolerance is probably linked to the natural ranges of the species (Wright et al., 1983), but with some variation between species and broodstocks (potentially even within broodstocks).

This method of filming could be simply modified to further investigate this thermal limit. Exposure periods can be increased and swimming competence investigated through a longer filming period, recording any changes in velocity or behaviours during this time. Settlement (and related behaviours) could be recorded within the filming chamber (a cuvette or similar, possibly larger vessel) throughout a wide range of temperatures. This would enable a comparison between those temperatures at which larvae were capable of swimming, but not competent to settle. The collection of such information would be important for consideration of the spread of species outside of their existing ranges, such as the spread of *C. gigas* into UK waters - this is considered further in **4.4.8**.

However, when considering the effects of temperature the physiological changes within the larvae must be considered against the physical changes in the water in the cuvette. Changes in water viscosity with temperature have consequences for ciliary swimming.

4.4.4 Ciliary action is affected by changes in water temperature and viscosity

Sharp rises in temperature will increase the rate of ciliary beat (Haure et al., 1998, Jørgensen, 1966, Sylvester et al., 2005). There is a rise in the beat frequency of oyster ciliation with increasing water temperature - the ciliary activity in bivalve gills peaks at around 30^{o}C for both *Crassostrea virginica* (Galtsoff, 1928) and *Ostrea edulis* (Haure et al., 1998). In planktonic organisms the rate of water movement can be used as a guide of food collection capacity in ciliary feeding mechanisms through the use of clearance rates: this information shows that over increasing temperatures clearance rates increase (Riisgard & Larsen, 2001, Strathmann et al., 1972). In bivalve larvae, as pre-oral ciliary beat increases, so does the clearance of water, and as a result the collection rate of food will be higher in warmer waters (Rico-Villa et al., 2009). Bivalve larvae use the pre-oral cirri for swimming as well as feeding so an increase in temperature will result in swimming velocity increasing due to an increase in the beat of the pre-oral cilia.

In colder temperatures cilia effectiveness is reduced markedly when the temperature drops below 15^{o}C (Leigh, 1962). This suggests the sharp drop-off in larval swimming velocity shown in Figure 4.13 to Figure 4.17 when temperatures drop from 26^{o}C to 10^{o}C could be due, at least in part, to the low temperatures affecting the beat of the pre-oral cilia. As discussed in **Chapter 3** the length of the pre-oral cilia is a compromise between what is suitable for swimming and what is suitable for feeding (Strathmann & Grunbaum, 2006), but the compound nature of the pre-oral cilia allows the shelled bivalve larvae to be heavier (Cragg, 1989). If the colder temperatures are reducing the efficiency of the large pre-oral cirri then the shelled larvae will be slowed dramatically as the weight and drag from the shell becomes more pronounced in the higher viscosities present at lower water temperatures (Cragg, 1989, Podolsky & Emlet, 1993). Furthermore swimming would become more metabolically demanding in these lower temperatures (Rico-Villa et al., 2009). The colder temperature range of this study may therefore

have a more pronounced effect on ciliary swimming than the higher range. Analysis indicated a significant reduction in velocity with temperature in both veliger and pediveligers (Figure 4.14 to Figure 4.17). The presence of a rise or fall in velocity with temperature could therefore be expected through the physical effects of temperature on the metabolism of the larva (Rico-Villa et al., 2009) and thus the beat frequency of the pre-oral cilia of the larval velum. However this is probably in combination with viscosity effects causing increased drag in colder water (further work should investigate this trend in coldwater bivalve species to see if the effect of temperature reduction is as pronounced as in *C. gigas*).

The viscosity of seawater reduces as temperature increases, and increases as temperature falls (Podolsky & Emlet, 1993). In Figure 4.7 the trend of larval swimming is shown with the trend of reducing viscosity - viscosity was not measured directly during these experiments (although will need to be investigated during future developments of the method), but has been provided for context. An initial investigation of this graph indicates that velocity increase mirrors the viscosity decrease. Viscosity has a major influence on the swimming velocity of planktonic fish larvae, often accounting for as much as 40-50% of the change in swimming velocity over a 10^{o}C temperature drop (Podolsky & Emlet, 1993, von Herbing & Keating, 2003). Viscosity may be the major factor in the effect of temperature on ciliary swimming in planktonic organisms (Riisgard & Larsen, 2009), although the authors also highlight the difficulty of separating viscosity effects from temperature, and the inconsistency of results from differing species (highlighted by the authors using ciliates). As such it is impossible to consider the larval reaction to temperature without also considering seawater viscosity changes. The difficulties of separating the effect of viscosity from temperature mean that, for example, larger larvae may stop swimming as a result of both the effectiveness of the pre-oral cirri being reduced by lower temperatures and by viscosity having a greater drag effect than on the smaller larvae (Strathmann & Grunbaum, 2006).

The methodology used in this chapter collected swimming data in normal seawater. The discrete, temperature controlled cuvettes may offer a convenient way of investigating ciliary

swimming in altered viscosities. Riisgard (2009) offers an approach for creating solutions with artificially adjusted viscosities, in order to separate viscosity effects from those of temperature. The methodology developed here would allow filming of larvae within these solutions within the current filming chamber. Using the same environment would allow a comparison to other results from the same chamber generated from temperature adjusted seawater. Trials with solutions could also take place in these chambers, and larval behaviours and velocities compared to seawater controls - it would be possible to film cuvettes side-by-side for simultaneous comparison. Part of the development of this filming technique, if used for further temperature investigations, should incorporate trials with viscosity adjusted solutions.

4.4.5 Comparisons with records of swimming velocities of other bivalve larvae

There is a limited amount of data available for swimming velocities of related oyster larvae that occupy similar temperature ranges to *C. gigas*. Those swimming velocities that are available closely match those recorded in this study. In the 20°C-28°C temperature range *Crassostrea virginica* veligers swam in a velocity range of between 0.83mm s^{-1} and 2.3 mm s^{-1} (Finelli & Wethey, 2003, Hidu & Haskin, 1978a, Turner et al., 1994, Wood & Hargis, 1971) and *Ostrea edulis* larvae (although generally found in slightly cooler, ~15°C waters) swam at a mean of 1.23mm s^{-1} (Cragg & Gruffydd, 1975). Both occur within the velocity ranges recorded in this study at comparable temperatures (Figure 4.7). Furthermore, that the velocity records gathered here do not show a large disparity to published records for related warm temperate species such as *C.virginica*, gives some confidence to the information produced from this filming methodology.

Hidu (1978) also provides evidence that *C.virginica* larvae swim faster when acclimated to higher temperatures, in a pattern that echoes the significant rise shown in Figure 4.7 and Figure 4.8. Between 15°C and 25°C *C.virginica* veligers increased swimming velocity by 1.5mms^{-1} from 0.83mm s^{-1} to 2.3mms^{-1} (Hidu & Haskin, 1978a). This is comparable to the 1.2mms^{-1} rise in velocity during the 12-22°C temperature increase shown by *C. gigas* larvae in Figure 4.8.

Records of bivalve veliger swimming speeds belonging to other temperate species, and recorded at ~20-24°C, fall within a similar range: *Pecten maximus* larvae have a velocity of

approximately 1.4mm s^{-1} (Cragg, 1980), *Placopecten magellanicus* larvae have a mean velocity of 1.5mm s^{-1} (Manuel et al., 2000) and *Mercenaria mercenaria* a larval velocity of 1.3mm s^{-1} (Chia et al., 1984). There are notable exceptions to this such as the slow 0.28mm s^{-1} speeds found in veligers of the cold water species *Arctica islandica* (Mann & Wolf, 1983) and the rapid 7.7mm s^{-1} shown by veligers of the tropical species *Teredo bartschi* (Isham & Tierney, 1953). However**,** **v**ariation according to natural temperature ranges is probably to be expected (Wright et al., 1983).

The larval velocity records from oyster species that live in similar water temperatures, such as the records available for *C.virginica* (Hidu & Haskin, 1978a, Hidu et al., 1973), provide a suitable comparison with the swimming velocities of *C. gigas* larvae recorded here. This filming method could be used to gather more complete datasets on species occupying similar or neighbouring temperature zones. Comparison of the temperature response curves such those presented in Figure **4**.**7**, and throughout section **4.3.4**, would provide valuable information on the swimming competence of these larvae. Such information would, for example, be invaluable for estimating the potential for the spread of non-native species as local sea temperatures change, especially when combined with the settlement studies suggested previously. Furthermore if other species show an exponential relationship between velocity and temperature in the lower temperature ranges, then it may be possible to use the calculation of T_D values as a comparative tool (of both species responses and for method development).

4.4.6 Variation in larval batches

It could be expected the larger larvae would swim faster than the smaller, as is the case for *Crassostrea virginica* larvae (Hidu & Haskin, 1978a), *Arctica islandica* (Mann & Wolf, 1983) and *Pecten maximus* (Cragg, 1980). While batches 1, 3 and 4 show some (not significant) variation from each other, batch 2 larvae were significantly (at the 0.1% level) slower than all the other batches. Batch 2 larvae were not the smallest larvae. There was no evidence from the acclimated larvae swimming velocities to suggest the smallest larvae (batch 4 - 180µm) swam more slowly than the largest (batch 1 - 250µm) with an ANOVA showing no significant difference between

these two batches ($F_{1, 329}$=3.98, p>0.05). The size difference in this study is not as large as in those where a size difference versus swimming speed has been recorded; 75µm *Crassostrea virginica* larvae swim slower than 300µm larvae (Hidu & Haskin, 1978a). This author does note that 'there was a plateau of swimming speeds reached with the intermediate sized (100µm and 250µm) larvae' (Hidu & Haskin, 1978a). As such the variation between batches may infer a variation in fitness between larval batches as opposed to variation caused by size. Future filming designs should incorporate larger differences in larval size for a further analysis of this variable.

In contrast to the acclimated larvae results the velocity of the pediveligers in the velocity control cuvettes (Figure 4.10) are higher than that of the veliger larvae, and higher than for the same larvae, from the same batch, in the temperature acclimated experiments, albeit by only 0.6mm s^{-1}. Figure 4.10 shows there is a slight difference in the velocities of the larger pediveliger stage (batch 1) larvae to that of the smaller veliger stage (batch 4) larvae, despite there being no difference between these batches when allowed 20 minutes acclimation time. As part of the experimental design these larvae had less time in the cuvette prior to filming (approx 10/15minutes), as being filmed at their cultured temperature, they needed no time to acclimate to temperature only to cuvette conditions. This may suggest that there is a variation in swimming velocities between these batches/larval sizes when given less time to acclimate to the cuvette, and that in future designs a longer cuvette acclimation is required.

Commercially produced larval batches, such as those sampled in this study, frequently suffer high levels of variation in larval fitness. High mortality and inconsistencies between batches are a frequent problem in the hatchery production of bivalve larvae (Robert & Gerard, 1999, Utting & Millican, 1997, Utting & Spencer, 1991) and are especially common in the production of *Crassostrea* gigas larvae (Helm & Bourne, 2004, Robert & Gerard, 1999). This variation would seem a plausible explanation for variation between batches where there is significant difference between the swimming speeds of similarly sized batches. Furthermore all of the results throughout this chapter show high levels of variation, probably as a result of variation between individuals.

These results raise the possibility that a future direction for this method of video analysis could be as a relatively quick assay for determining the fitness or health of larval batches within hatcheries, based on swimming velocities. Velocities for healthy larvae of some commonly cultured species such as *Crassostrea virginica* (Hidu & Haskin, 1978a), or *Pecten maximus* (Cragg, 1980) have been documented and, as has been discussed here, are quite comparable Furthermore hatcheries could build their own datasets on swimming velocities. If larval batches were found to be significantly slower than reported or historic figures despite favourable conditions, such as is the case for the larvae of batch 2 in this study, this may suggest an unhealthy batch, either unable to rapidly acclimate to the cuvette or simply swimming at speeds slower than expected.

4.4.7 Consideration of the results of *Crassostrea gigas* larval swimming behaviour investigations

Larval behaviours in steady temperature controls

Examining the larval activity in the steady temperature control cuvettes reveals that veliger and pediveliger larvae swim constantly throughout with more larvae swimming in the later time periods than when larvae were exposed to temperature change (Figure 4.18 and Figure 4.19). However the activity of the pediveliger larvae fell significantly during the filming period (Figure 4.20, Figure 4.21, Figure 4.24 and Figure 4.25). This fall in pediveliger larval activity, while significant (at the 0.1% level), was less pronounced than in the temperature change experiments - for example comparing Figure 4.20 with either Figure 4.30 or Figure 4.40 reveals a much shallower curve, with more data in the later time periods. Analysis of veliger larvae controls also indicated a significant ($F_{2, 27}$ = 9.2 p=<0.001) reduction in rising behaviour (but not descending) in the controls, but this analysis explained only 36% of the variation, with a very shallow, poorly fitted curve. The large amount of scatter about the line indicated a large amount of variation between individuals.

However, these results do indicate that there may be some effect on the larvae from the cuvette environment. Although having ~20% of the population actively swimming is consistent

with other such laboratory trials with gastropod larave (Fuchs et al., 2010) further investigation into the severity of the effect will be required (longer filming periods may reveal if this was a short-term effect). However the data from the controls are still markedly different from that of the rapid temperature change experiments.

Swimming velocity was consistent in both sets of steady temperature experiments (Figure 4.10), with no systematic trends in the data. The less pronounced declines in larval activity, combined with the consistent velocities, suggest the sudden responses of the larvae in the rapid temperature change experiments (Figure 4.28 to Figure 4.47) to be as a result of the larva's detection of the temperature change within the cuvette. The response is probably the individual larva's behavioural or physiological response to this change. Furthermore the results from the temperature acclimated larvae (Figure 4.7) show the larvae to be capable of swimming in temperatures as low as 12^{o}C and as high as 38^{o}C, within the same cuvette environment, suggesting these responses are possibly behavioural. A summary of the larval responses to temperature is provided in Table 4.16 at the end of the results section.

Falling in all experiments, excluding the veliger's initial reaction to cold, was very rare. When it did occur it was usually the result of larval collisions (Figure 4.6) or when no contact was obvious, was possibly a result of the detection of the hydrodynamic disturbances of a swimming larva (Gallager, 1993) nearby in the cuvette.

The decline in both rising and descending activity from pediveligers within the steady temperature experiments (Figure 4.20, Figure 4.21, Figure 4.24 and Figure 4.25) probably indicate that *C. gigas* pediveliger larvae tended to gather on the base of the cuvette. This tendency for downward shift in pediveliger larvae in laboratory experiments has also been noted for the pediveligers, but not the veligers, of *Crassostrea virginica* (Finelli & Wethey, 2003). The downward shift by pediveligers when not exposed to rapid temperature change suggests that this behaviour is perhaps exaggerated by the rapid temperature change, as opposed to induced by it. It is contrasted by the veliger larvae being more consistently active, with a shallower decline in activity.

This difference in larval behaviour between veliger and pediveliger larvae in the constant temperature situations may not be unexpected when considering the function of these two larval stages. The settlement site searching pediveliger, whilst intermittently active within the plankton, is less likely to be active in the water column and will tend to gather close to the benthos. Models of larval distribution suggest this change in vertical distribution serves to increase the rate of contact with the benthos for the pediveliger, increasing the likelihood of detection of settlement stimuli by the larva, consequently increasing rates and/or success of larval settlement (Eckman et al., 1994, Gross et al., 1992). The veliger is the planktonic form of the larva, living entirely in the water column (Finelli & Wethey, 2003, Strathmann, 1980). Furthermore several authors hypothesise the descending of pediveliger larvae seen in the constant temperature cuvettes is at least partly due to the increased influence of specific gravity on the largest larvae, and that this aids settlement and settlement timing, especially amongst larvae of a similar size (Chia et al., 1984, Finelli & Wethey, 2003, Hidu & Haskin, 1978a). The results from the control cuvettes may be an expression of these differences between the veliger and pediveliger stages.

Also worthy of note is the occasional presence of very fast moving individuals, usually swimming upwards, noted in both the controls and the beakers containing larvae to be sampled. This larval behaviour was also noted by Hidu (1978) in *C.virginica* larvae in both the author's cultures and experimental chambers. These larvae recorded velocities of over 7.5mm s^{-1}, more than double the velocities recorded in the steady temperature controls, and making them occasional outliers from the normal distribution of the larval velocities. These records are also significantly above (more than double) the velocities reported for bivalve larvae from other studies of warm temperate species and listed earlier in this discussion. These larvae did not occur regularly with a maximum of 3 in any one experiment, and some moved at a velocity too great to be calculated with the other larval velocities. As with the fast moving *Crassostrea virginica* veligers observed by His (1978) these larvae were often near to the edge of the glass or surface of the water, so swimming speed is likely to have been increased through a surface tension effect.

Larval behaviours following temperature change

Filming revealed pediveliger and veliger larvae had different velocity responses to rapid changes of water temperature. In both rising and falling temperatures, pediveliger larvae stopped almost all upward swimming in the cuvette two minutes into the temperature change (Figure 4.11 and Figure 4.13). The pediveliger larvae had a significant drop in velocity during the temperature decrease prior to the cessation of swimming (Table 4.2, Figure 4.14 and Figure 4.15). Veliger larvae swimming velocity significantly ($F_{2, 123} = 5.18$, $p = <0.001$) increased during temperature rise and significantly ($F_{2, 166} = 84.49$, $p = <0.001$) decreased during temperature reduction. The results of the behavioural observations reveal a similar pattern to that seen in the velocity experiments, with the first 8°C-10°C (~120 second) of rapid temperature change appearing to have the most marked response from both pediveligers and veligers (Figure 4.28 - Figure 4.39).

In none of the behavioural experiments (or controls) was the logistic function a markedly better fit to the data than the exponential function. This indicated a (potentially behavioural) lag phase was not present at the start of the response to the temperature change. This does not discount a behavioural reaction, but may make a physiological/physical one more probable.

Behaviours following temperature rise

The temperature rise experiments saw both rising and descending behaviour reducing significantly in both pediveligers and veligers by the end of the first 10°C of temperature increase (Table 4.8 - Table 4.11 and Figure 4.28 - Figure 4.37), with slightly more veligers maintaining swimming in the higher temperatures.

The velocity response of veliger larvae to the increase in temperature was a slight increase in velocity over the 10°C rise (Figure 4.11). While the increase in swimming velocity with increasing temperature was significant at the 0.1% level, there was large scatter (Figure 4.12); analysis indicated only 6.3% of the variation was explained by the relationship to temperature. Whilst this relationship was not well defined, it may be either a short-term effect on the physiology of the ciliated cells of the velum causing increased beat frequencies (Galtsoff, 1928, Hidu & Haskin, 1978a), physiological stress on the whole larva (Beiras, 1995), a behavioural

response, or a results of reduced viscosity in the cuvette (Riisgard & Larsen, 2009). Pediveligers did not show the same response, swimming simply stopped after a 10°C rise, with no increase in velocity preceding this.

Behaviours following temperature reduction

Temperature reduction saw a similar trend in rising behaviour to that seen in the temperature increase experiments with the end of the initial 8°C-10°C temperature fall signifying a marked reduction in rising behaviour from both pediveliger and veliger larvae. This was significant at the 0.1% level, with a high percentage of the variation explained by this relationship.

Pediveliger larvae reduced vertical swimming 10°C into the temperature reduction and thus recorded few swimming velocities at the colder temperatures. There was a significant ($F_{2, 92}$ = 31.08, $p<0.001$) reduction in swimming velocity with temperature prior to the cessation in swimming. As with all the results of the behavioural experiments there was a large amount of variation unaccounted for by this analysis, probably variation between individuals.

The number of veliger larvae swimming reduced but those individuals that maintained swimming saw a significant (Table 4.3) drop in velocity, particularly marked during the first 10°C of temperature reduction (Figure 4.16 and Figure 4.17). Swimming velocity was stable after the initial 10°C fall at ~0.7mm s^{-1} for the remainder of the experiment. This velocity is half the rate recorded for the veliger larvae in the stable temperature controls, but is comparable to the velocity seen at 12°C-14°C in the acclimated larvae from the same batch 4 veligers (Figure 4.7). Both this and the velocity results from the temperature rise may suggest that some veligers were capable of acclimating more rapidly to temperature change than the pediveligers.

The veliger descending behavioural (Figure 4.46) response to the fall in temperature was particularly striking when compared to either the rising behaviour (Figure 4.42) or descending following temperature rise (Figure 4.36). A large number of veligers descend during the first 4°C fall producing a steep initial decline in descending behaviour. This is a much more marked reaction than the shallow decline shown by the pediveliger larvae, as can be seen when comparing Figure 4.44 with Figure 4.46. Few veligers descended at all after the initial 7°C of

temperature change (60 seconds exposure), with few rising throughout, suggesting the veligers rapidly gathered on the bottom of the cuvette. Temperature drop was also the only experiment where a large percentage of veligers fell with closed shells during the first 4^{o}C of change (Figure 4.39). This response may be a reaction to the sudden change in viscosity, or a sudden physiological response to drop in temperature.

The gradual decline in pediveligers descending suggested a steadier movement of the pediveligers to the base of the cuvette throughout the temperature drop, as opposed to a sudden cessation the sudden fall to the base suggested by the veliger results. This is probably a slight exaggeration of the pediveligers tendency for downward shift shown in the control cuvettes (Figure 4.24). It is possible the larger pediveliger may be better able to respond to the higher energetic demand of swimming in lower temperature (high energetic demand)/higher viscosity (increased drag) water (Riisgard & Larsen, 2009). It is noteworthy that temperature drop was the only condition where pediveligers did not show a sharp decline in descending - perhaps the energetic demand for rising was too great, but pediveligers were still able to perform a controlled descent.

Veligers may suffer a more significant physiological effect than the larger pediveliger, as suggested by Figure 4.11 and Figure 4.13 where veliger velocity is altered by temperature change, but stable after 10^{o}C. Investigation of the regression curves in Figure 4.16 and Figure 4.17 shows the curve flattening towards the end of filming, still with a large scatter. If the physiological effect of rapid temperature drop is more significant for the veliger larvae than the physical effects of the viscosity change this may explain the sudden drop in activity shown by the veligers at the beginning of the sudden temperature decrease experiments. The logistic function (which would show a lag phase) is not a better fit to the data than the exponential, possibly suggesting a physiological reaction may be more probable than a behavioural one. However, the data presented in Figure 4.7, 4.13, 4.16 and 4.17 indicated the veliger larvae were still capable of swimming in these temperatures once acclimated. It is not possible to discount that such a rapid response may be a behavioural one.

Summary of behavioural observations

This combination of filming technique and ImageJ video analysis is not yet able to discern if larval responses to sudden changes in temperature are behavioural or due to factors such as physiology and viscosity (for example, exponential and logistic functions fit similarly). However, analysis of the video data has indicated a clear, rapid and significant larval reaction when exposed to sudden temperature change which contrasted with the behaviours and velocities recorded in the steady temperature control cuvettes.

4.4.8 The importance of laboratory studies in understanding larval reactions to stimuli

Temperature was chosen as a suitable variable for testing a method for filming larval swimming in the laboratory because a reaction could be expected (through simple metabolic effects, Rico-Villa et al, 2009), and because it is a stimulus likely to by encountered by a swimming larva. The reaction to temperature stimulus shown by both veliger and pediveliger stage larvae has implications for the distribution of larval populations within the water column. These reactions may be explained by a combination of physical and physiological effects, or these sudden alterations in swimming paths and velocities may be a behavioural response; this filming technique is currently unable to discriminate between these factors. In either case, the vertical distribution of larvae in the plankton is likely to change in reaction to detection of a stimulus such as temperature. Information gathered from laboratory investigations can inform these responses.

Crassostrea virginica pediveligers are known to respond rapidly when detecting vector stimuli such as chemical cues within a water flow, either by stopping swimming and falling, or rapidly increasing vertical swimming within small (5ml) wells (Turner et al., 1994). However, thermal stimuli are scalar and will be encountered by the larvae in the form of both permanent and seasonal thermoclines and sharp, localised regions of unnatural temperature variation in areas influenced by man such as power station outfalls (Hidu et al., 1973, Wright et al., 1983). Natural thermoclines can be distinct with changes of up to 5.5^{o}C over 10-20m having been reported in areas of interest to studies of bivalve veligers, such as Georges Bank (Tremblay et al., 1994), and temperatures to 40^{o}C near power stations or in power station cooling ducts (Hidu et

al., 1973). Larvae will most likely encounter natural thermoclines whilst undergoing vertical migrations (Manuel & O'Dor, 1997, Manuel et al., 2000, Manuel et al., 1997), but the ability to respond to these changes in temperature affects the larva's vertical position, and subsequently its capability to either remain in the surface waters and feed, or sink to find a suitable settlement spot.

Laboratory studies have produced varied results regarding bivalve larval reaction to temperature, with some indicating temperature detection is only present in mid-pelagic (veliger) stage bivalve larvae (Kingsford et al., 2002), capable of responding to thermoclines as low as 1^{o}C (Manuel et al., 2000). More severe 11^{o}C gradients in larger 9m mesocosms have found that the veligers of *Placopecten magellanicus* did not penetrate a thermocline from 5^{o}C-16^{o}C, staying in the warmer layer above the thermocline and causing the authors to suggest the viscosity change prohibited larvae from crossing the thermocline (Gallager et al., 1996). By combining experiments with acclimated larvae and temperature shocked larvae (as has been done in this study), reactions can be gauged against temperatures in which larvae are known to still be competent to swim. There was no vertical swimming in both veligers and pediveligers of *C. gigas* when acclimated to temperatures below 12^{o}C (Figure 4.7), suggesting there is a physical point at which *C. gigas* larval swimming is not possible, probably due to viscosity and physiological effects. However, the reaction of the larvae when exposed to a sharp drop or increase in temperature illustrates the larva will respond, either behaviourally, physiologically or physically to a non-directed (i.e. not a depth associated) temperature change within the first 4^{o}C, even if they are still capable of swimming in these conditions once acclimated.

Other laboratory studies of the bivalve larval response to thermal stimuli have shown responses to >1^{o}C thermoclines from *Placopecten magellanicus* veligers (Gallager et al., 1996, Manuel et al., 2000, Pearce et al., 2004). Field studies indicate that veligers make vertical migrations at times when light cannot be the main cue (Manuel & O'Dor, 1997, Manuel et al., 1997). When taken in conjunction with the results presented the current study, and other laboratory work (Manuel et al., 2000), these findings may indicate a thermal response in bivalve

veligers. Such a response would indicate that larvae will regulate their vertical position within the water to some degree in response to thermal cues, and independent of the physical or physiological effects of less severe temperature changes. Velocity increases at higher water temperatures may have the effect of assisting veliger larvae to stay in the (generally) warmer, more productive surface waters when a thermocline is detected. It is surprising that the veliger reaction to the temperature drop was to descend (Figure 4.39). Other laboratory studies have shown that on the detection of colder waters *Placopecten* veligers rise to maintain their position for feeding in the surface layers (Manuel et al., 2000). It is possible that the rapid temperature change used in this experiment reveals only a thermokinetic 'fright' response and not a directional thermotactic response. Further method development using differing rates of temperature change may elucidate any directional element of the response, in conjunction with attempts to isolate any effect from viscosity changes. The method of perception of thermal gradients has not yet been discovered (Manuel et al., 2000), but it is possible that the detection is one of viscosity and not temperature itself, with mechanoreceptive stereocilia such as those on the mantle rim of all the larval species examined in **Chapter 2** (Figure 2.12) potentially fulfilling this role.

Such behavioural responses will affect the distribution of larval populations and should be considered when attempting to model the distributions and movements of larval populations (Fuchs et al., 2010). Previously, salinity has been considered a more important influence in larval vertical stratification within the water column than temperature (Dekshenieks et al., 1996). As a result of this, larval reaction to salinity during tidal cycles has been assumed to prove the greatest influence on larval distribution (Wood & Hargis, 1971), combined with the sinking of larger larvae nearing settlement (Dekshenieks et al., 1996, Hidu & Haskin, 1978a). Temperature has often been considered more for larval survival when rearing within a hatchery or laboratory scenario (Beiras et al., 1995, His & Seaman, 1992, Rico-Villa et al., 2009, Robert et al., 1988), than for specific behavioural response of larvae to temperature. The current level of understanding of the thermal response of larval bivalves is not sufficient for incorporating into modelling of the distribution of larval bivalve populations. Species specific studies into the behavioural reactions

to all variables such as temperature are required (Baker, 2003, Finelli & Wethey, 2003, Ma et al., 2006). Evidence of a thermokinetic response in larval bivalves could have significant implications for these models. If veliger larvae are responding to thermal cues to stay in the surface waters for feeding they will be more susceptible to wind influenced movements or local surface currents such as freshwater run-offs. Greater knowledge of this thermokinetic response at the species level is required before reliable models of larval distributions can be produced. The methods used in this study, with some refinement, represent an inexpensive laboratory technique for investigating thermal responses, and potentially other environmental stimuli. More information must be collected on the reactions of larvae to specific environmental variables in order to accurately model dispersal and recruitment (Fuchs et al., 2010), and the development of effective and accessible methods, such as this one, will facilitate the collection of such data. The swimming velocity and behavioural information collected here is not suitable to be modelled independently. However it does provide detailed information on factors such as velocities and potential (thermal) reactions that can be incorporated into models built on known environmental and hydrographical factors from the regions where such distribution models are to be applied.

Information gathered from filming and analysing larval swimming is not limited to dispersal modelling applications, but can also inform, in this example, larval thermal tolerances. Data such as these presented in Figure 4.7 add to the knowledge of larval swimming competence within a thermal range. This is especially relevant in the case of *C. gigas* - this is a non-native UK species, whose spread is linked to the water temperatures required for spawning and settlement (Spencer et al., 1994). Native populations are establishing in areas where water temperature were believed the limiting factor for larval dispersal and settlement, with warm summers usually implicated in the sporadic spatfalls (Diederich et al., 2005, Spencer et al., 1994). Settlement in laboratory scenarios tends to reduce at temperatures of ≤17^{o}C (Rico-Villa et al., 2009). While the information on swimming velocities collected using this filming methodology does not indicate whether larvae would be competent to settle, they do provide information on swimming competence and, potentially, mortality. This filming method could be applied to capture footage

of larval settlement in varying environmental conditions, informing the spread of non-native species where the effects of environmental variables on the larvae are limiting factors.

4.4.9 Future application for this filming technique

While the results collected during the development of this filming technique are informative themselves, they also reveal the method is probably suitable for producing useful and replicable data on larval behaviours in various scenarios. Some future directions and applications for this combination of filming hardware and ImageJ analysis are considered below.

In order to investigate the effect (if any) of helical larval swimming on the results, a second camera could be mounted above the cuvette in order to utilise the three-dimensional particle tracking plug-in for ImageJ. This uses the same algorithm as the 2 dimensional version (Sbalzarini & Koumoutsakos, 2005), but allows for incorporation of a z axis. However, isolating the same individual larva on both cameras is potentially challenging and care would have to be taken to ensure cuvettes were not over-crowded with larvae; ParticleTracker may struggle to identify the same larva on both images. Such a method may be more suited to filming individual larvae in wells (Hidu & Haskin, 1978a) or single, shallower (for depth of focus problems) cuvettes.

For development of the filming method, reactions to a sudden change in temperature were used. The method of filming using cuvettes contained within the manipulable environment of the filming chamber would be equally suitable for investigating slower or directed temperature changes. This method could be combined with altered light regimes to replicate diurnal conditions and thermoclines, potentially simulating vertical migrations or phototaxis behaviours.

Filming and enumeration of settlement of within cuvettes through various differing temperatures may provide information on the potential spread of species outside of their natural ranges as local water temperatures change; for example comparing swimming competence with settlement competence of *C. gigas* larvae. While other methods (such as monitoring settlement in temperature controlled rooms/tanks) offer alternatives, the use of the cuvettes, filming chamber and ImageJ analysis offers a convenient method of gathering information on individual larval swimming paths and settlement behaviours within a controllable environment.

Such investigations need not be limited to temperature investigations. Cuvettes of varying salinity would provide data both on swimming competence, behaviours and velocity. Larval reactions to neurotransmitter compounds such serotonin and catecholamines could be recorded in a manner similar to investigations of gastropod larval movements following exposure (Braubach et al., 2006). However, in addition to the information presented by Braubach (2006), this filming method would allow a more detailed investigation of changes in swimming behaviour or velocity. Such information could be related to changes in pre-oral ciliary beat frequencies (Braubach et al., 2006). Varying electromagnetic fields (EMF) fields could be introduced into the chamber and velocities, behaviours and settlement monitored; this is especially relevant given the upsurge in coastal wind farm construction, and lack of data of EMF effects on shellfish spatfall.

Adaptation of the cuvettes would allow flow-through experiments. Replacing the sides with a rigid mesh would allow investigation of reactions in flow through scenarios; for example recording individual larval trajectories following the introduction of settlement stimulus (Finelli & Wethey, 2003) or differences in trajectories between species when exposed to differing turbulent flows (Fuchs et al., 2004, Fuchs et al., 2007, Fuchs et al., 2010).

Although further investigation into the slight decline in behaviours noted in the control cuvettes is still necessary, the combination of a controlled environment and VirtualDub/ImageJ software analysis offers an accessible way of generating data on bivalve larval behaviours.

4.5 Conclusions

The filming methodology developed is capable of collecting a large amount of information relating to larval swimming velocities, swimming patterns, environmental tolerances and reactions to environmental variables such as temperature. This novel method of combining non-specialised photographic equipment with shareware software packages has the potential to make the collection of data on planktonic organisms more accessible to the research community. The data obtained is comparable to that gathered from other laboratory studies (Hidu & Haskin, 1978a). The methodology still requires some refinement, notably in consideration of any affect on larvae from being in the cuvettes and into the potential for automation of image processing.

Crassostrea gigas larvae were tolerant of a temperature range of 12-38^{o}C, and swimming velocities saw a sharp increase from 12^{o}C to 22^{o}C. From 24^{o}C to 38^{o}C larval swimming velocities were not linked to increasing temperature and saw wide variation between individuals. This information can inform larval thermal tolerances. *C. gigas* swimming velocities appear similar to records from species occupying similar thermal ranges, but it is difficult to separate the effects of viscosity from physiology when considering the effects of temperature on larval swimming.

Velocities collected in this manner could reveal difference s in the swimming velocities of larvae from different broodstocks. One batch of larvae had significantly slower swimming speeds than the other 4, and this was not linked to larval size suggesting the filming technique used in this study could be used as a rapid, routine assay for the assessment of the fitness of larval batches within a hatchery.

Veliger and pediveliger larvae have a thermokinetic response to the detection of changes in temperature, and this may aid the larva in favourably regulating its vertical position. This reaction is likely to be different in different larval stages; pediveligers stopped swimming and gathered in the base of the cuvette, veligers usually maintained some swimming but had a more marked reaction to decreases than increases in temperature. All results saw a large scatter probably accounted for by variation between individuals and not the time in cuvette or temperature relationships. Further work is required to isolate the effect of viscosity and to determine if there is a difference in its effect on veliger or pediveliger stage larvae.

Thermokinetic responses in the environment may help to maintain veliger larvae amongst regions of high chlorophyll productivity for feeding, and increase the chances of successful settlement for pediveliger larvae. The method by which larvae detect thermal cues is unknown, but further investigation into the stereocilia on the mantle of bivalve larvae is merited, as is further investigation of the inner pre-oral band of cilia on the velum, to determine if these are mechanoreceptors sensitive to viscosity changes. The development of laboratory methods such as this one that can reveal larval reactions following the detection of environmental variables is an important step in providing data for models of larval dispersal and recruitment.

Chapter 5 - General Discussion

5.1 Larval ciliature

Cilia are of vital importance to veliger larvae. On the velum, ciliary action is used for both locomotion and feeding. The general pattern of the velar ciliary bands is quite consistent across the Bivalvia. However this study has revealed that the velum of the ostreids has a band not previously recorded, and has shown the ciliation of the velum of *Lyrodus pedicellatus* to be modified, probably as a result of the brooding habit. Furthermore, observations of the swimming patterns and behavioural responses of *Crassostrea gigas* larvae (Figure 4.6) indicate that there larvae probably have some control of the frequency of the beat of velar ciliation, possibly through the use of the serotonin pathways and catecholamine containing cells that have been located in the velar rim. This still requires further investigation.

The bivalve larval mantle, especially the rim of the inner mantle fold, is profusely ciliated, with this ciliation increasing in density and complexity in the ostreids as the larva develops. These ciliary arrangements are much more complex than has been previously recorded. No study has described the extent of ciliation found on the rim of *Crassostrea gigas* and *Ostrea edulis* in this investigation, and few studies speculate on a function for this ciliation. The cilia groups found on the mantle of *Lyrodus pedicellatus* are described here for the first time, being less extensive than those of the ostreid species, but still mainly located on the mantle rim and containing sensory stereocilia. The development of a method of Investigating larval swimming and behavioural responses has revealed that the *Crassostrea gigas* larva responds to thermal stimuli, and that such investigations are possible using fairly simple software and hardware solutions.

5.1.1 Functional significance of larval stereocilia

The appearance of some of the cilia groups identified on the mantle with collars of microvilli at their base has been identified before in invertebrate larvae and have been termed as either collar cilia (Crawford & Campbell, 1993) or stereocilia (Haszprunar, 1985a). These specialised cilia structures are usually associated with invertebrate sensory organs, such as those

found in the Stempell's organ of adult *Nucula* (Haszprunar, 1985b). The stereocilia recorded in **Chapter 2** are similar to those seen in the group 3 cilia of *Pecten maximus* veligers (Cragg, 2006), chiton larvae (Haszprunar et al., 2002), asteroid larvae (Crawford & Campbell, 1993) and in adult bivalves (Haszprunar, 1985a, Haszprunar, 1986, Haszprunar, 1987b). The potential phylogenetic significance of these stereocilia will be considered in **5.2**.

All of the stereocilia found in the larvae investigated in this study (the C3, C9 and L1 groups) bear structural comparison to those in the abdominal sense organs (ASO) found across the Bivalvia, and are known to be used for detecting water borne vibrations (Zhadan, 2005). The location of the C9 stereocilia is comparable to the location of the ASO in adult ostreids and pectinids (Haszprunar, 1983). It is possible that these are larval forms of this type of sensory system, either detecting water movements externally, within the mantle cavity or associated with the movement of particles along the C5 pseudofaeces rejection tracts.

Those stereocilia with a location more exposed to the water column, the L1 and C9 groups, may have a mechanoreceptive function related to external water-borne vibration. As such, these groups would detect changes in water currents that relate to the presence of predators or other larvae - larvae are known to have a 'fright reaction' to such cues whereby they will rapidly retract the velum and close the shell (Cragg, 1980). This reaction was observed in larvae that were close to each other in the filming cuvettes used in **Chapter 4** (Figure 4.6**)**, but did not always appear to be triggered by physical contact. This may indicate the detection of the water-borne vibrations emitted by the swimming larvae (Gallager, 1993). The presence of serotonin fibres running from stereocilia locations along the mantle, branching off into the mantle musculature and further into the larva itself, reveals that the larval nervous system is connected to the locations of the stereocilia, and may reveal the mechanism by which this larval fright reaction is triggered, although no connections to larval ganglion have yet been observed.

Alternatively the stereocilia could detect currents or water movement changes brought on by temperature altering the water viscosity. Mechanoreceptors are a plausible receptor for such cues and stereocilia with a structure comparable to those identified in this study have been

implicated in detecting water movements in adult *Nucula* (Haszprunar, 1985b). These stereocilia could therefore be implicated in detecting the temperature stimuli and affecting the thermokinetic response reported in **Chapter 4**. The larval behavioural reaction to sharp changes in temperature involve changes in swimming trajectory and velocity, both of which imply a change in ciliary beat, or falling through musculature velar retraction. If stereocilia are responsible for the detection of such stimuli, then the serotonin pathways may affect the response and may be one of the mechanisms by which the larva responds to thermal cues. Further investigations into the potential for connections from both the *C. gigas* larval mantle and velum to the larval ganglion (especially in the apical region) are warranted.

The L1 stereocilia of *Lyrodus* may have a role in settlement site selection (possibly in addition to the above). They are located on the mantle rim, in the region where the foot is extended and retracted through the shell valves. As a result when larvae are crawling using the foot these stereocilia will be in close proximity to the benthos. If the group come into contact either with the benthos itself, or the layer of water just above it, they may provide some sensory function to augment the sensory suite found on the larval foot (Cranfield, 1973a). As these are stereocilia this is probably through mechanoreception (Haszprunar, 1985b) of surface topography or although reception of chemical cues in the water cannot be discounted. Fluorescence investigations into connections to the pedal ganglion from the location of the L1 would be valid.

The C3 cilia group is located on the mantle itself and is stiffer in appearance than the stereocilia groups. This location is very suggestive of the C3 group having a mechanoreceptive role relating to the movement of water within the mantle cavity, possibly preventing stagnation, similar to the Stempels organ found in adult *Nucula* (Haszprunar, 1985b).

5.1.2 Pseudofaeces rejection in ostreid larvae

The extensive C5 twin tracts of cilia running along the rim of the mantle from the gill bud to the anterior adductor are known to be present in *Crassostrea gigas* (Beninger & Cannuel, 2006) but had not previously been identified in *Ostrea edulis* larvae. The presence of particles in these tracts when fixed (Figure 2.42), combined with the observations of particles moving down beating

C5 tracts in live larvae (Figure 2.16) suggest these tracts function as larval precursors to the adult pseudofaeces rejection tracts that are then retained post metamorphosis. The presence of identical tracts on the mantle rim of both *Ostrea edulis* and *Crassostrea gigas*, but not on the mantle of the pectinids or teredinids, seems to agree with Beninger's (2006) proposal that these are a 'phylogenetically new characteristic of the Ostreidae'. The phylogenetic implications of similarities and differences in mantle ciliation are considered in **5.2**.

This extensive and varied ciliation of the mantle suggests the role of the mantle changes throughout larval development. Where it is initially concerned with the secretion of prodissoconch II (Waller, 1981), by the veliger stage the presence of these disparate groups of cilia suggests the mantle role has changed. It now bears sensory structures that are likely unique to the larval stage as discussed above, and ciliated tracts for evacuating pseudofaeces and preventing stagnation of the mantle cavity (Beninger & Cannuel, 2006). The ciliation of the mantle during the planktonic stage of development can therefore be considered as important as that of the velum, and while the velum is lost in metamorphosis, the mantle persists though to the adult where some of this ciliation is retained and develops further to suit the requirements of the sessile adult form.

5.1.3 Modification of the velar ciliature

Species-specific differences in the cilia patterns of the velum were also observed. The additional band of compound cilia on the ostreid velum (the minor pre-oral cilia) has not been previously recorded. This band is located under the pre-oral cirri and probably beats down onto the adoral tract increasing the efficiency of the opposed band system of particle capture, serving as a final deflection onto the adoral band, or a means of keeping particles within the adoral band (Figure 3.32). In addition, the recovery stroke of the large pre-oral cirri above will bring the cirri tips through the minor pre-oral band, dislodging any particles that may have become attached to the cirri during their beat. If the larva has stopped the beat of the post-oral band and is swimming but not actively feeding (Strathmann & Grunbaum, 2006) this band may perform a cleaning function, maintaining the efficiency of the beat of the pre-oral band.

The velum of the long-term brooded larvae of *Lyrodus pedicellatus* does not have a post-oral band, suggesting that this band is not necessary for a larva that does not feed in the plankton. Such modification of the pediveliger velum is also seen in the brooded larvae of *Ostrea chilensis* (Chaparro et al., 2006), and it is likely that this is a modification brought about by the differing selection pressures of the brooding strategy. The post-oral band probably reduces the efficiency of the swimming stroke as it beats against that of the pre-oral band (Cragg, 1989), so the loss of this band in larva that has to swim but not feed in the plankton may afford an advantage when settlement site searching through an increase in swimming efficiency. This increase in swimming efficiency is especially important when considering that brooded larvae will probably not disperse as far as larvae that develop entirely in the plankton (Strathmann & Grunbaum, 2006). This raises the possibility that the loss of the post-oral band is not a change in the velar ciliature to suit the larva whilst it is being brooded, but may be to increase the dispersal potential of brooded larvae through increased swimming efficiency when they are released.

5.1.4 Larval control of ciliary beat

The ability of the larva to control the frequency of the beat of velar and mantle cilia is suggested by the presence of the ciliary control compounds serotonin and catecholamines (Croll & Dickinson, 2004) in the velar rim and the mantle. Whilst the larva may control the beat of the C5 tracts (Figure 2.20) through the presence of these compounds, ciliary control was much more evident in the velum. Observations of larval swimming saw larvae fall through the water column both following retraction of the velum (Cragg, 1980) and with a controlled fall slowed by velar cilia beat. Through filming individual larvae it was possible to observe larvae swimming not just in the reported helical pattern (Cragg, 1980), but along horizontal and vertical trajectories without helical deviations (Figure 4.6). Whilst none of these swimming trajectories were maintained for extended periods of time (although was probably limited by the size of the cuvette in the observations recorded in **Chapter 4**) they suggest that control of the velar ciliary beat may give the veliger considerable control over its swimming trajectory. Such control may enable a larva to stay within feeding zones and respond to stimuli in more ways than a simple vertical helical

swimming path punctuated by closing of the shell and falling. Gastropod veligers are known to use serotonin to increase the frequency of ciliary beat and catecholamines will reduce the frequency of ciliary beat, consequently changing the vertical distribution of larvae in containers in the laboratory (Braubach et al., 2006).

The presence of both compounds in the velum of *Crassostrea gigas* larvae (although results for catecholamines in the velum were much less conclusive than for those of the mantle) suggests a similar method of ciliary control. Many of the swimming patterns observed would require this type of ciliary control. Furthermore the presence of both compounds in the velum (and mantle) of many bivalve veligers (Beiras & Widdows, 1995, Croll et al., 1995, Voronezhskaya et al., 2008) and gastropod veligers (Croll, 2001, Croll, 2006, Croll et al., 1997, Page & Parries, 2000, Voronezhskaya et al., 1999), and in ciliated molluscan embryos (Kuang & Goldberg, 2001), suggests this may be a method of ciliary control common throughout the larvae of the Mollusca.

The inner pre-oral ciliation was not observed to beat either in live larvae (although examination of this group is extremely difficult in live larvae due to the transparent nature of the velum), or through examining the curvature of the fixed cilia in the SEM images. The lack of any microvillous ring around the ciliary bases such as seen around the stereocilia on the mantle sheds doubt on the notation of the inner pre-oral cilia having a sensory function (Waller, 1981). However the group appears from the early veliger stage in all the species where this stage was examined suggesting either the band must have a function that is still has to be discovered, or it is an ancestral feature.

5.2 A consideration of phylogeny

5.2.1 Patterns of mantle ciliation within the Bivalvia

The mantle and the velar ciliation show variations between diverse taxonomic groups, however there are some shared characteristics that appear to cross relatively large divides (Figure 5.1 - this diagram has been chosen as the relationships are based on a combination of morphology and genetic techniques). The ciliation of the mantle is very rarely mentioned in studies concerning the phylogeny of the Bivalvia, within even very comprehensive studies

focusing only on the development of the mantle itself, or the development of the shell gland (Nielsen, 2004). This is somewhat surprising given the potential for some variation between species, as has been discussed in this thesis, and the relative importance given to the potential homologous ancestry of other ciliary arrangements such as the prototroch and metatroch (Henry et al., 2007, Nielsen, 2004). It may be that mantle ciliation has simply been overlooked, or that there is not currently enough anatomical information available for authors to begin forming opinions on its potential importance (or lack thereof) in phylogeny.

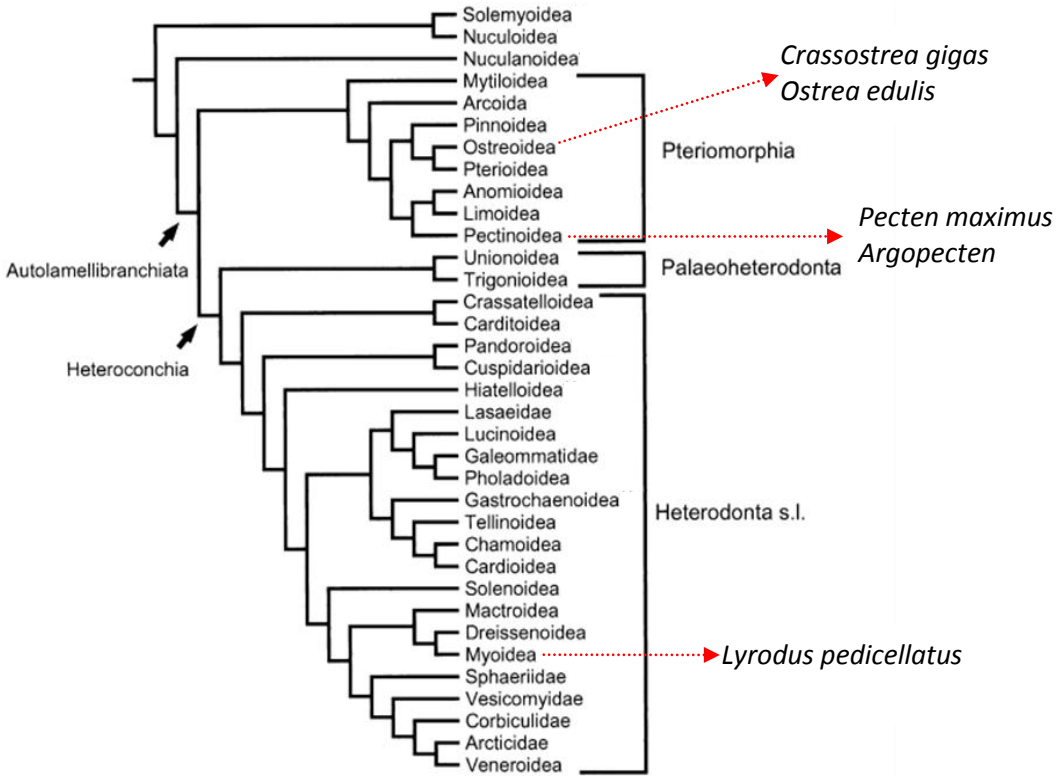

Figure 5.1 - Cladistic diagram of the Bivalvia - modified from (Giribet & Wheeler, 2002).

The species used in this study are labelled to illustrate how close or distant their clades are.

The heterodont Myoidea (including *Lyrodus pedicellatus*) have very different mantle ciliation to the pteriomorphan Ostreoidea (*Crassostrea gigas* and *Ostrea edulis*) and Pectinoidea (*Pecten maximus* - Cragg, 2006 and *Placopecten* - Bellolio, 1993). However the mantle ciliature of the Ostreoidea is similar to that of the Pectinoidea. The groups of cilia occur in almost identical positions around the mantle rim, although there is variation in the morphology of these groups - cilia lengths appear similar but the cilia patterns and arrangements are different. This suggests that while the origins of the mantle ciliation may be shared within the Pteriomorpha, there is

probably divergent evolution of this ciliation between the clades, possibly due to the selection pressures related to breeding strategy, or the variations in the ciliation found on the adult mantle.

Further work is required to determine the extent of the similarities between the clades of the Pteriomorpha, and to determine if differences are as a result of these mantle cilia developing into different adult organs in the different families (such as the rejection tracts in *Crassostrea*), or if selection pressures stemming from breeding strategy are responsible. Investigating the mantle ciliation of some longer-term brooded ostreids such as *Ostrea chilensis* and contrasting this with planktotrophic species such as *Crassostrea gigas*, might reveal variation between fairly closely related species brought about by selection pressures acting on the larva as a result of breeding strategy. There is evidence suggesting such variation can travel down to a species level in the differing reports of mantle ciliation in *Pecten maximus* (Cragg, 2006) and *Argopecten* (Bellolio et al., 1993).

5.2.2 Stereocilia

Crassostrea gigas, Ostrea edulis, Lyrodus pedicellatus and *Pecten maximus* all have groups of stereocilia within similar cilia groups, despite the general difference in the patterns of mantle ciliation between the Pteriomorpha and the Heterodonta. This cilia arrangement is identified as type 3 in pectinids (Cragg, 2006), C3 and C9 in ostreids (this study) and L1 in the teredinids (this study). This suggests the stereocilia group in the Bivalvia either originates from a common ancestor or is the product of convergent evolution brought about by the selection pressures of the plankton. It is however, difficult to draw firm conclusions from the mantle ciliation in the teredinids without more knowledge of the mantle ciliation of more heterodont bivalves.

The term stereocilia, as stated in **Chapter 2**, should be treated with some caution due to its inconsistent use between authors. When the term stereocilia is used in this study it is referring to a single cilium with a ring of 9 microvilli at the base. These stereocilia are found in both the ostreids and teredinids in this study and occur widely across the Mollusca within the Docoglossa (subpallial stripe), Vetigastropoda (epipodial sense organs), the Pteriomorpha (abdominal sense organs), and Stempell's organ in the *Nucula* (Cragg, 1996, Haszprunar, 1985a, Haszprunar, 1986,

Haszprunar, 1987a, Haszprunar, 1987b). Stereocilia do not just occur within the Mollusca, but in several other major phyla: tubellarians (Sopott-Ehlers, 1984), gastrotichs (Teuchert, 1976), cnidaria (Golz & Thurm, 1993, Westfall et al., 1998), echinodermata (Crawford & Campbell, 1993), nemertea (Cantell et al., 1982), hemichordata (Dilly, 1972). This indicates that the stereocilia are found across a wide range of taxa as illustrated in Figure 5.2 (Dunn et al., 2008).

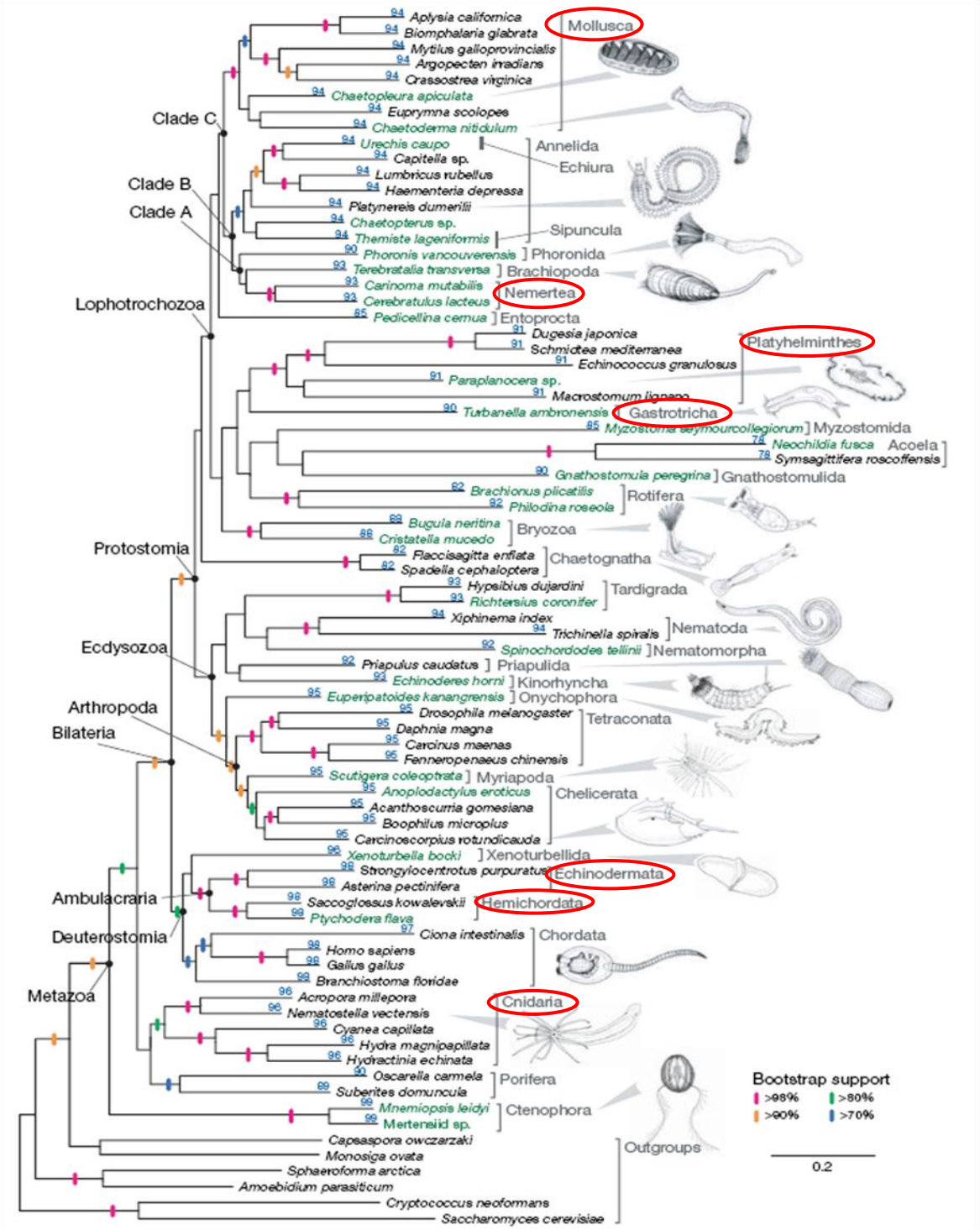

Figure 5.2 - Tree illustrating those taxa (ringed) with stereocilia of the same appearance as those identified in this study (Dunn et al., 2008).

These stereocilia are not limited to large protostome groups such as the lophotrochozoa, with examples in the Echinodermata and Hemichordata. Stereocilia appear to not be limited to the Bilateria, owing to their appearance in the Cnidaria. It has been proposed that similarities in the structures bearing stereocilia have arisen from either convergence or a shared genetic linage for the structures expressed under specific evolutionary pressures (Haszprunar, 1985a, Haszprunar, 1985b). However this suggestion does not discount the possibility of the stereocilia themselves being ancestral, as indicated by their presence throughout the metazoa.

5.2.3 Velar ciliation

The ciliary bands of larval molluscs have been afforded a limited importance in the phylogeny of the Mollusca, with the arrangement of a downstream ciliary collection system consisting of prototroch (pre-oral band), adoral band and metatroch (post-oral band) being found in the gastropods and bivalves (Nielsen, 2004). However the cell linage leading to the formation of the protoch is still not confirmed (Nielsen, 2004). The appearance of these three rows is consistent throughout the planktonic veligers of the Bivalvia, with this layout probably the ancestral one (Nielsen, 2004). However it has been argued that the prevalence of lecithotrophy and brooding within the Mollusca suggests that lecithotrophy is the plesiomorphic condition, and that the downstream collection system is the product of parallel evolution in the bivalves and the gastropods (Haszprunar et al., 1995). This would suggest the selection pressures of the planktonic environment have given rise to the downstream collection system. The apparent lack of a mPO band in other groups that are generally consider homologous (e.g. polychaeta) may further support Haszprunar's (1995) suggestion of parallel evolution. The disparity of mPO observations, even with the Bivalvia, currently makes such comparisons problematic.

The ostreid and pectinid velar cilia layout is very similar, and shows no significant variation from other members of the Pteriomorphia such as the Mytiloidea *Mytilus edulis* (Bayne, 1976), generally following the accepted ciliary layout of planktotrophic larval velar ciliary bands. However, there are examples within the ostreids of altered ciliary arrangements on the velum in species such as *Ostrea chilensis* that show the brooding trait (Chaparro et al., 1999). These

changes are very similar to those of the taxonomically distant *Lyrodus pedicellatus*, with the loss of the post-oral band and wide adoral tract. It is difficult to suggest loss of the post-oral band is an ancestral trait related to brooding, it is generally accepted that the planktotrophic condition is the ancestral trait and that brooding is a newer strategy (Nielsen, 2004). However if the theory of lecithotrophy being ancestral is accepted then the similarity between these two brooded vela takes on more importance, and may provide further evidence towards this being the ancestral trait (Haszprunar et al., 1995). It is perhaps more probable that these shared modifications of the velar ciliation are the result of convergent evolution stemming from the selection pressures unique to the brooding strategy - the conjecture that lecithotrophy is the ancestral trait is largely based on an assumption that downstream feeding is just as easy to evolve as to lose, but closer analysis of some gastropod clades has shown non-planktotrophy has evolved repeatedly from a planktotrophic ancestor (Nielsen, 2004, Strathmann, 1978). Furthermore the appearance of the velum in the earlier stages of the development of *Lyrodus pedicellatus* and *Ostrea chilensis* is very different, suggesting their similarity in appearance by the pediveliger stage may be an expression of the ancestral trait (Chaparro et al., 1999, Turner & Boyle, 1974). As such the loss of the post-oral band in *Lyrodus pedicellatus* is probably a modification of the ancestral trait of planktotrophy, brought about by the evolution to a brooding, lecithotrophic, strategy, and leading to the loss of the metatroch.

Few conclusions can be drawn about the ancestry of the minor pre-oral band on the velum of the ostreid larvae as although the feature has not been recorded on the velum of other bivalve larvae it is probable that it has been overlooked in other studies. The band can be seen in images of the *Mercenaria mercenaria* velum (Gallager, 1988), and *Spisula solidissima* (Campos & Mann, 1988) although it was not noted by either author. *Mercenaria* is of the Order Veneroidea and *Spisula* of the Order Mactroidea, and as such both are quite distant from the Ostreidae (Giribet & Wheeler, 2002). As this is the only evidence currently available for the presence of the minor pre-oral band, it is not yet possible to isolate the trait solely to either planktotrophic members of the Ostreidae or to planktotrophic bivalve larvae in general. Thus it is not yet

possible to draw conclusions regarding the possibility of this bands appearance being linked to selection pressures relating to breeding strategy modifying the ancestral trait.

5.3 Laboratory studies of larval swimming; the importance of collecting data on larval responses to environmental stimuli

Knowledge of the swimming velocity of the larvae of species of economic or environmental importance, combined with knowledge of individual larval reactions to stimuli in the plankton, have important implications for the modelling of movements of populations; these responses probably vary at a species level, increasing the error in generalised larval distribution models (Baker, 2003, Stobutzki, 2001). Laboratory studies provide a convenient way of studying these reactions, offering a controlled environment in which reactions to specific stimulus can be investigated. Identifying the mechanism by which larvae regulate their vertical position in order to avoid hydrographical features, predators, or simply to remain in feeding zones is a recurring theme in modelling studies (Stobutzki, 2001). Species-specific larval vertical distributions are consistently implicated in the regulation position, but a lack of data means authors are often unable to identify the mechanism larvae are using to effect these responses (Baker, 2003, Yoshinaga et al., 2010).

Through the design of a filming methodology, this study has provided evidence that one method by which bivalve larvae will regulate their vertical position is through the use of thermal cues, as has also been reported in laboratory studies on the veligers of *Placopecten magellanicus* (Manuel et al., 2000, Pearce et al., 2004). To date the details of thermal sensitivity have only been reported for a few species. However the information available from these studies, and this study, does suggest that larvae, when held within a controlled environment, will display a reaction a thermal stimulus, and that this reaction is probably different depending on the development stage of the larva or the species.

It is still to be experimentally determined if these reactions are specific to species, or if different life history stages will show different thermal preferences across species. Some of the lack of information regarding these reactions is probably due to the difficulties of collecting data

on larval reactions to stimuli; commercial solutions for studying the behaviour of planktonic organisms in the laboratory are often expensive or computationally complex (Pradhan et al., 2011). The combination of photography equipment, controlled environment (the filming chamber and cuvettes) and ImageJ data extraction detailed in **Chapter 4** provides a simple way of collecting data on and visualising larval reactions. This laboratory techniques, or similar techniques, are easily replicable enabling more data to be generated on species-specific reactions to typical environmental stimulus such as temperature, salinity or turbulence. It is difficult to collect such detailed information regarding larval swimming in the field, however laboratory methods are known to offer a convenient way of comparing reactions observed in the laboratory with the distribution of larvae sampled in the field (Fuchs et al., 2010).

Collecting data in the laboratory, whilst more practical than field experiments, must overcome some further challenges. For example, in the development of the method described in **Chapter 4** it was identified that the effect of temperature has more variables than just a potential larval behavioural response. Viscosity changes at higher and lower temperatures will affect the functioning of the pre-oral cirri of the velum. It is likely that the larger pediveliger, with its slightly larger velum and more developed organ systems producing more energy for the larva, would be able to offset the higher physiological energy demand in the higher viscosities found at lower temperatures. Temperature will also exert a physiological affect on the cells bearing these cirri, either increasing or decreasing their capability. This would be further influenced by the fitness of the larvae (which is known to vary between larval batches, Helm & Bourne, 2004), and the larval development stage. Further investigation is required to isolate the effects of temperature from viscosity on larvae swimming, and to determine if these factors are affected by the contained environments (such as a cuvettes) used for filming. It is also plausible that it is viscosity change that is detected by larval mechanoreceptors, and not temperature itself, and that it is this which triggers a behavioural response - studies isolating viscosity and filming reactions would also clarify this. It should also be considered that viscosity will vary with temperature in the environment also, but the influence of the enclosed confines of laboratories studies must be investigated

before swimming information can be compared across different species and reliably related to environmental scenarios.

Crassostrea gigas displays a planktonic larva, with a planktotrophic strategy. That both this larva and the larva of another planktonic member of the Pteriomorpha, *Placopecten magellanicus*, demonstrate a distinct behavioural reaction to temperature change (Manuel et al., 2000) may suggest this to be a common response amongst planktotrophic bivalve veligers. This warrants further investigation in the laboratory in order to produce data that can be incorporated into modelling of larval distributions - this is especially relevant for those species with purely planktotrophic strategies whose larvae may be subject to greater dispersal (Levin, 2006).

Such investigations need to cover a wider range of bivalve orders to determine if this is a trait unique to the larvae of the Pteriomorpha, or if the trait is found throughout the Bivalvia. This work will also need to focus within orders and families to investigate if larvae that are brooded still have similar responses to such stimuli when swimming outside of the mantle cavity. This knowledge is important for various applications. Such data will lead to more accurate dispersal models that can incorporate known larval responses and swimming velocities for the exact species of interest, something currently only possible for a few species. The successful reintroduction of species where local populations have been reduced will be considerably improved through knowledge of larval responses (Leverone et al., 2010). Accurately forecasting larval reactions to known hydrographic conditions within the local area being targeted for re-introduction will greatly increase recruitment. Alternatively such models can provide information on the spread of non-native species (Diederich et al., 2005). Currently available data on larval reactions is limited but the design practical methods of generating these data in the laboratory can facilitate a rapid expansion of the information available.

5.4 Future work

5.4.1 Further investigations into larval ciliature

Further anatomical investigations into ciliation of the larval mantle should include investigations into the fate of the groupings to determine if these are purely larval structures that

at lost at metamorphosis or larval versions of adult organs (retained ciliation is marked in Figure 2.46). The C5 and C8 tracts are still present in the 3 hours post-settlement, as are the C13 groups (although these are not yet showing any indication of being organised into tracts) and probably become the adult radial rejection tracts (Beninger & Cannuel, 2006). However these results suggest that these structures undergo considerable change following metamorphosis, so while the C5 tracts do probably become the adult marginal tract (Beninger & Cannuel, 2006), they are sufficiently altered in the larval form to be considered functional larval pseudofaeces rejection tracts in their own right.

Sampling of spat at short intervals for several days after metamorphosis would allow for examination of the ciliary tracts as they change in the juvenile bivalves. Furthermore, the fate of specialised C3 and C9 groups in the spat should be investigated in the same manner to discover if these are larval sense organs lost after metamorphosis, or early manifestations of adult sensory structures, such as abdominal sense organs.

Both the investigations of the velar ciliation and the mantle ciliation would benefit from the use of transmission electron microscopy (TEM), because TEM will reveal the cellular contents of the cells bearing the cilia. TEM would enable the roots of the cilia to be investigated (Cranfield, 1974) to see if any row has deeper roots. The mitochondrial content of the cell will indicate the energetic demands placed on the cell (Cragg, 2006): more mitochondria suggest a higher metabolic demand is placed on the cell. It would be interesting to compare the mitochondrial content of the cells bearing the minor pre-oral band with that of the pre-oral and post-oral bands. This would enable a comparison of energy demand placed on the cells of the minor pre-oral band with those bearing the large, highly active pre-oral cilia.

TEM of the C5 mantle cilia tracts would provide similar information, as well as allowing for an examination of the mantle folds in cross section in order to confirm the positions of the ciliary rows suggested in Figure 2.18. TEM investigations may determine the 9+2 structure of the C3 and C9 stereocilia, as well as permitting investigation of the nervous connections from which the catecholamine and serotonin fluorescence arises. Precise sectioning of the locations of the C3

and C9 groupings will be extremely difficult due to the problem of orientating the larvae with the hinge towards the face of the resin blocks when embedding. In the case of the C9 group, it may be possible to use the weight of the shell as a means of orientation in the resin by allowing larvae to fall through an unset resin before hardening, in a manner similar to the one employed in **Chapter 3** when sectioning larvae in wax. This would ensure the hinge would be at the face of the block and less sectioning would be required to reach the C9 group. Decalcification would also be extremely important as the mantle ciliation is always near the shell, and any remaining calcification would spoil the mantle sections.

The possible appearance of the C9 group at the start of prodissoconch II stage when the posterodorsal notch is first formed is curious, with the group having been seen in early veliger larvae. The potential mechanoreceptive function of this group could be investigated using tethered larvae - a method which has been successfully employed with *Mercenaria mercenaria* and *Phestilla sibogae* (Gallager, 1993, Hadfield & Koehl, 2004) - by attempting to instigate the fright response. It may be that the appearance of this group marks the point at which the larva is capable of rapidly retracting the velum. A method of ablating the C9 cilia group, similar to the bleaching used on *Phestilla sibogae* (Hadfield et al., 2000), used in conjunction with tethered larvae and a vibration stimulus would test the C9 role as a mechanoreceptor. However ablating the C9 group would present significantly more technical challenges than ablating the apical sense organ on the centre of the large velum of *Phestilla sibogae* due to the small size of the area.

Finally, more filming work with fluorescent beads may, at higher magnifications than those available to this study, provide clues as to whether the C9 group has a role in the rejection of pseudofaeces - for example determining whether expulsion is triggered when particles reach the C9 group, or whether the shell opens if particles become trapped in the posterodorsal notch.

The use of fluorescent beads may also prove useful for the further investigation of the minor pre-oral band if used in conjunction with the high speed video microscopy techniques used in the study of *Mercenaria mercenaria* feeding (Gallager, 1988) and zooplankton swimming (Gallager, 1993). This would enable the deflection of particles to be followed, and allow for the

comparison of particle paths in species with and without the minor pre-oral band. Furthermore, the particle tracking software used in **Chapter 4** may be able to track the trajectories of particles captured or deflected by tethered larvae and provide a visualisation and a measurement of the particle paths in a similar manner to the projections of swimming paths in Figure 4.6.

The function of live filming of *Lyrodus pedicellatus* larvae would give a valuable insight into the function of the L1 stereocilia. The location of these cilia near the region of the foot exit suggests they would be held very close to the substrate when the larva is crawling. Filming crawling behaviour on different surfaces, with either varied topography or chemical covering, will show if these surface elicit a behavioural response from either surface type. However it will be difficult to positively identify this as being due to the mantle cilia and not the sensory reception of the foot. It may be possible to ablate the sensory cilia of the foot to isolate the reception capabilities of the mantle ciliation.

5.4.2 The expansion of this filming design for further investigations into thermokinesis

While temperate provided a suitable variable for testing the development of a filming method, future development can also be addressed through further investigation into questions raised by the results. The design used in **Chapter 4** investigated reaction to thermal stimuli through a rapid temperature change. The purpose of a rapidly changing temperature regime versus a stable temperature regime was to illicit a behavioural response; to compare swimming once acclimated to a stable temperature in the cuvette with swimming of larvae exposed to a sudden change in temperature. This revealed a probable thermokinetic response in the larvae, and provided data on swimming velocities through a thermal range. However in order to positively link this response with the thermal stratification of larval populations discussed elsewhere the method requires further development to investigate variables not included in the previous design:

1. Slower temperature change, possibly from a specific direction (although this may generate hot-spots in the cuvette) to see if larvae show a thermotactic response

through either a change in swimming velocity or a behavioural change in swimming trajectory.

2. The use of a thermocline within a mesocosm to see if the reactions of *Crassostrea gigas* are similar to those published for *Placopecten magellanicus* (Manuel et al., 2000, Pearce & Bourget, 1996, Pearce et al., 2004). This would involve using the same photographic equipment and software, but requires a larger environment. As such this would also test the adaptability of the technique to see if the ParticleTracker plug-in will still identify individual swimming paths at a lower magnification.
3. Separation of temperature-controlled viscosity effects by using steady water temperatures but artificial viscosity adjustments as suggest by Riisgard (2009).
4. Use a wider range of larval development stages to investigate if reactions to thermal cues change.

These investigations should include several different larval batches, if hatchery-produced larvae are used, in order to attempt to gauge the effect of variations of larval fitness between batches.

Furthermore investigations should also include an investigation of the responses of larvae with differing strategies; for example do planktotrophic larvae respond differently to long-term brooded larvae? While the species in this study (and those investigated in larval literature) are predominately planktotrophic bivalve species there is evidence to suggest the behavioural responses of pelagic lecithotrophic mollusc veligers may be different from planktotrophic veligers.

The planktonic stage of the lecithotrophic, intertidal, nudibranch *Adalaria proxima* is behaviourally adapted to avoid dispersal in the water column, being capable of crawling or swimming on release, with these behaviours promoting local recruitment and thus suggesting its planktonic phase may not be purely for dispersal (Todd et al., 1998). This is contrasted with another intertidal, but planktotrophic, nudibranch, *Goniodoris nodosa,* whose longer planktonic stage conforms to the expectations of high larval dispersal (Todd et al., 1998). However there is also significant variation between siblings of *A. proxima* ensuring there is some dispersal from natal sites (Lambert et al., 2003). Larval of gastropod species that occupy different coastal

habitats and that represent different larval strategies have different swimming responses to the detection of turbulence (Fuchs et al., 2004, Fuchs et al., 2007, Fuchs et al., 2010). This filming technique could capture larval swimming trajectories in differing turbulent flows. The larvae of bivalve species that show different strategies within similar local areas (for example *Crassostrea gigas* and *Ostrea edulis*) should be investigated to reveal if there are similar variations in larval behavioural responses that may be related to strategy.

Experiments of differing species swimming velocities in conditions where viscosity is altered under a constant temperature should be compared with anatomical investigations of the pre-oral cirri of the velum - for example does the brooded velum of species such as *Lyrodus* suffer any more or less effect from viscosity following the loss of the post-oral band or by having a large adoral band? Variations in pre-oral cirri morphology between species could be a hugely relevant factor in the effect of viscosity. If the velar ciliature of *Crassostrea gigas* is indeed finer than that of *Ostrea edulis*, as indicated in **Chapter 3**, does this affect their swimming capability? The investigation of the velar ciliature of different species in relation to swimming should be further extended to consider the effect of ontogeny. This investigation should include consideration of a connection between development stage and larval response, such as the reaction to cold water shown by veliger stage larvae in this study.

5.6 Larval swimming velocities as a routine larval assay?

The method of analysing digital video using the ImageJ software provided swimming velocity figures that were comparable to values published in the literature, suggesting the method is successful at generating robust velocity data. However if it is to be used as an assay for assessing the health of larval batches, as suggested in **Chapter 4**, it requires some refinement. As the method has been developed currently, the system of tracking particles through a large number of video frames is demanding on computer memory, often requiring in excess of 6 gigabytes of physical RAM, and is heavily reliant on data inputs from the user. The 1139 larval trajectories used to gather the velocity data presented in **4.2** represent some 1500 hours of video processing (discounting the design of the physical filming apparatus), and this would not be cost

effective as an assay of batch vigour. However having refined this experimental approach throughout the course of this thesis the processing time has been greatly reduced, although further refinements considered below will reduce processing time even more significantly.

The user is required to select larval swimming paths of interest before velocities can be obtained, as well as setting parameters for tracking. The system of reducing video footage down to its constituent frames is done rapidly through the use of software such as VirtualDub. Given that the ParticleTracker plug-in for ImageJ is a macro-based software based on a published feature point detection and tracking algorithm (Sbalzarini & Koumoutsakos, 2005), it should be possible to refine the system through the construction of macros to select only vertical trajectories after particle tracking was completed. This, combined with a set of standard settings for both video camera set-up and ParticleTracker, could automate a large amount of the tracking work (also making the software package more comparable to those such as Ethovision®). The use of a permanent static station where a camera is set-up on a fixed stand in front of a cuvette, and samples simply pipetted in as they are required to be checked - the water bath set-up used in **Chapter 4** would not be required for such short video capture - would make the experiment easier to execute, and therefore more useful to hatcheries. Excel has the capability to automatically calculate displacements and provide velocities, again through the use of macros.

The ImageJ plug-in ParticleTracker proved any easy interface to use, without requiring a licence to run programming environments such as MatLab or IDL. This ease of use was considered extremely important for development of an assay for commercial hatcheries.

This method has the potential to be used as an easy, and free, method of gauging larval fitness through the refinement of the software routine for collecting larval velocities. Ultimately the system should simply involve a small sample of larvae being filmed for 1 or 2 minutes, and this video then being analysed for swimming velocity extraction. Published velocities like those discussed in **4.4.5** can be used for checking data from broodstocks against (until a hatchery has collected enough velocity data to enable comparison within its own datasets), potentially allowing the quick identification of possible unhealthy batches of larvae.

5.7 Main conclusions

The mantle of the bivalve larvae has been shown to be profusely ciliated in the larvae of the ostreids, with ciliation increasing in density as the larva develops from early veliger to metamorphosis. Larvae of *Crassostrea gigas* and *Ostrea edulis* have larval pseudofaeces rejection tracts running along the mantle rim from the gill bud, the cilia of the tracts eventually reaching the anterior adductor by the late pediveliger stage. These are probably functional larval structures that are then retained and modified in the adult. Furthermore the mantle is a site for ciliated sensory structures in the bivalve larva, with 2 distinct stereocilia groups being identified on the mantle and mantle rim. These are most likely mechanoreceptors.

The mantle of the brooded larva of *Lyrodus pedicellatus*, was less profusely ciliated but still with discrete groups of cilia on the mantle rim. These groups also have sensory stereocilia, similar in appearance to those seen in *Pecten maximus*.

The larval mantle also has serotonin and catecholamine containing fibres in the rim and dorsal regions. The locations of these compounds can be closely matched to the locations of the C5 and C9 ciliary groups. Both compounds affect ciliary beat so their presence in ciliated regions may suggest the larva has a measure of control over the frequency of beat of these ciliary groups, or receives some sensory input from them. The locations of the mantle ciliary groups are comparable between some species, and may have some implications for bivalve phylogeny.

The velar ciliation of *Crassostrea gigas* and *Ostrea edulis* is similar to that found in most descriptions of the bivalve velum with the exception of both of those species having a previously unrecorded band of compound cilia under the main pre-oral band. This band is most likely to be a modification of the opposed band method of particle capture, serving as a final deflection onto the adoral tract, as indicated by the curvature of the minor pre-oral cilia over the adoral tract. Further work is required to elucidate the potential phylogenetic importance of the minor pre-oral band.

The velum of *Crassostrea gigas* was shown to contain serotonin and possibly catecholamines in the rim, in the region of the pre-oral cirri and the post-oral cirri. This may

represent a mechanism for the control the of velar ciliary beat frequency as these neurotransmitter compounds have been shown to either stimulate or inhibit the velar ciliary beat of larval bivalves (Beiras & Widdows, 1995, Croll et al., 1997, Raineri, 1995, Voronezhskaya et al., 2008) and gastropods (Braubach et al., 2006, Kempf et al., 1997). This is further evidenced by SEM images of the post-oral band appearing to have not been beating at fixation, and observations of variations in swimming patterns in live larvae. Connections from the velar rim to the apical ganglion in *C. gigas* have not yet been found.

The velum of the brooded larvae of *Lyrodus pedicellatus* does not have a post-oral band by the pediveliger stage, but does feature a large adoral band and a well developed rejection tract under the mouth. This indicates the pediveliger larva to have a velum modified for brooding, as seen in species such as *Ostrea chilensis*. The presence of enclosed brood pouches suggests the larva may ingest cells released from the parent whilst brooded, and thus not feed on phytoplankton once released into the plankton (Pechenik et al., 1979), and that the appearance of the pediveliger velum is a result of the reduced veliger velum. These velar characteristics should be considered for their phylogenetic implications, the loss of the post-oral band suggesting a modification of the ancestral trait, as suggested by Nielsen (2004).

The velum in all the species examined had the large pre-oral swimming cilia typical of the ancestral planktonic veliger larval form, and observations of live larvae swimming saw individual larva effect several distinct swimming trajectories, often with very abrupt changes in direction indicating the larvae were responding to some external stimulus.

The development of a method of capture and analysis of digital film of larval swimming revealed the planktonic larvae of *Crassostrea gigas* have a distinct reaction to temperature stimulus, and provided data on larval swimming velocity and competence through a steady temperature range. Acclimated *Crassostrea gigas* larvae tolerated a temperature range of 12-38^{o}C, but swimming velocities varied throughout this range, probably due to a combination of physiological effects on the cells of the velum and viscosity affecting the pre-oral cirri. The general trend was for an increase in swimming velocity with increasing temperature during the

rise from 12°C to 22°C, with no significant increase in velocity with increasing temperature after this point. As in other studies investigating bivalve larval swimming, there was large variation between individuals (Cragg, 1980, Hidu & Haskin, 1978a).

The method used for capturing larval swimming velocities also has the potential to be used as a quick assay to gauge the fitness of larval batches within a hatchery, through collection of swimming velocities.

The filming technique allowed for capture and analysis of digital film of larval swimming behaviours. This analysis of larval swimming velocities and trajectories revealed a rapid response to sudden changes in temperature, with this response varying slightly depending on the larval development stage. This indicated the larvae probably possess a thermokinetic response. Further method development using temperature as a variable and ImageJ to extract larval swimming data, combined with modification to the filming chamber, has the potential to reveal if there is a directional component to this thermal response. These developments may elucidate the potential for this reaction, and reactions other environmental stimuli, to affect the vertical distribution of larval populations in the water column.

The design of accessible laboratory methods such as that presented in **Chapter 4** have an important role in increasing the available information on larval swimming behaviours in response specific environmental stimulus. Such methods have the potential to provide robust data for incorporation into models of larval distribution.

References

Acarli, S. & Lok, A., 2009. Larvae development stages of the European flat oyster (*Ostrea edulis*). *Israeli Journal of Aquaculture*, **61**(2), 114-120.

Aldred, N., Li, G.Z., Gao, Y., Clare, A.S. & Jiang, S.Y., 2010. Modulation of barnacle (Balanus amphitrite Darwin) cyprid settlement behavior by sulfobetaine and carboxybetaine methacrylate polymer coatings. *Biofouling*, **26**(6), 673-683.

Aldred, N., Phang, I.Y., Conlan, S.L., Clare, A.S. & Vancso, G.J., 2008. The effects of a serine protease, Alcalase (R), on the adhesives of barnacle cyprids (Balanus amphitrite). *Biofouling*, **24**(2), 97-107.

Altnoder, A. & Haszprunar, G., 2008. Larval morphology of the brooding clam Lasaea adansonii (Gmelin, 1791) (Bivalvia, Heterodonta, Galeommatoidea). *Journal of Morphology*, **269**(6), 762-774.

Arkett, S.A., Mackie, G.O. & Singla, C.L., 1987. Neuronal control of ciliary locomotion in a gastropod veliger (Calliostoma). *Biological Bulletin*, **173**(3), 513-526.

Babinchak, J. & Ukeles, R., 1979. Epifluorescence microscopy, a technique for the study of feeding in *Crassostrea virginica* veliger larvae. *Marine Biology*, **51**(1), 69-76.

Baker, P., 1997. Settlement site selection by oyster larvae, *Crassostrea virginica*: Evidence for geotaxis. *Journal of Shellfish Research*, **16**(1), 125-128.

Baker, P., 2003. Two species of oyster larvae show different depth distributions in a shallow, well-mixed estuary. *Journal of Shellfish Research*, **22**(3), 733-736.

Bayne, B.L., 1976. The biology of mussel larvae. In *Marine mussels, their ecology and physiology*, (ed. B.L. Bayne), pp. 81-120. Cambridge University Press.

Beiras, R., Camacho, A.P. & Albentosa, M., 1995. Short-term and long-term alterations in the energy budget of young oyster *Ostrea edulis* in response to temperature change. *Journal of Experimental Marine Biology and Ecology*, **186**(2), 221-236.

Beiras, R. & Widdows, J., 1995. Effect of the neurotransmitters dopamine, serotonin and norepinephrine on the ciliary activity of mussel (*Mytilus edulis*) larvae. *Marine Biology*, **122**(4), 597-603.

Bellolio, G., Lohrmann, K. & Dupre, E., 1993. Larval morphology of the scallop *Argopecten purpuratus* as revealed by scanning electron microscopy. *Veliger*, **36**(4), 332-342.

Ben Kheder, R., Moal, J. & Robert, R., 2010. Impact of temperature on larval development and evolution of physiological indices in Crassostrea gigas. *Aquaculture*, **309**(1-4), 286-289.

Beninger, P.G. & Cannuel, R., 2006. Acquisition of particle processing capability in the oyster *Crassostrea gigas*: ontogeny of the mantle pseudofeces rejection tracts. *Marine Ecology Progress Series*, **325**, 153-163.

Beninger, P.G., Dwiono, S.A.P. & Le Pennec, M., 1994. Early development of the gill and implications for feeding in *Pecten maximus* (Bivalvia, Pectinidae). *Marine Biology*, **119**(3), 405-412.

Beninger, P.G. & Veniot, A., 1999. The oyster proves the rule: mechanisms of pseudofeces transport and rejection on the mantle of *Crassostrea virginica* and *Crassostrea gigas*. *Marine Ecology-Progress Series*, **190**, 179-188.

Beninger, P.G., Veniot, A. & Poussart, Y., 1999. Principles of pseudofeces rejection on the bivalve mantle: integration in particle processing. *Marine Ecology Progress Series*, **178**, 259-269.

Bolton, T.F. & Havenhand, J.N., 1997. Physiological versus viscosity induced effects of water temperature on the swimming and sinking velocity of larvae of the serpulid polychaete *Galeolaria caespitosa*. *Marine Ecology-Progress Series*, **159**, 209-218.

Bozzola, J.J. & Russel, L.D., 1999. *Electron Microscopy - Principles and Techniques for Biologists*. Jones and Bartlett.

Braubach, O.R., Dickinson, A.J.G., Evans, C.C.E. & Croll, R.P., 2006. Neural control of the velum in larvae of the gastropod, *Ilyanassa obsoleta*. *Journal of Experimental Biology*, **209**(23), 4676-4689.

Braubach, O.R., Dickinson, A.J.G., Evans, C.E. & Croll, R.P., 2005. Neural control of the velum in larvae of the gastropod, *Ilyanassa obsoleta*. *Integrative and Comparative Biology*, **45**(6), 1113-1113.

Bray, D.F., Bagu, J. & Koegler, P., 1993. Comparison of hexamethyldisilazane (HMDS), Peldri-Ii, and critical point drying methods for scanning electron microscopy of biological specimens. *Microscopy Research and Technique*, **26**(6), 489-495.

Brusca, R.C. & Brusca, G.J., 1990. Invertebrates. In *Brusca, R. C. and G. J. Brusca. Invertebrates. Xix+922p. Sinauer Associates, Inc.: Sunderland, Massachusetts, USA. Illus*, pp. XIX+922P.

Bubel, A., 1975. An ultrastructural study of the mantle of the barnacle, *Elminius modestus* (Darwin) in relation to shell formation. *Journal of Experimental Marine Biology and Ecology*, **20**(3), 287-324.

Buroker, N.E., 1985. Evolutionary patterns in the family Ostreidae - larviparity vs oviparity. *Journal of Experimental Marine Biology and Ecology*, **90**(3), 233-247.

Cadet, P., 2004. Nitric oxide modulates the physiological control of ciliary activity in the marine mussel Mytilus edulis via morphine: Novel mu opiate receptor splice variants. *Neuroendocrinology Letters*, **25**(3), 184-190.

Campos, B. & Mann, R., 1974. Discocilia and paddle cilia in the larvae of *Mulinia lateralis* and *Spisula solidissima* (Mollusca: Bivalvia). *Biological Bulletin*, **175**(3), 343-348.

Campos, B. & Mann, R., 1988. Discocilia and paddle cilia in the larvae of *Mulinia lateralis* and *Spisula solidissima* (Mollusca, Bivalvia). *Biological Bulletin*, **175**(3), 343-348.

Cannuel, R. & Beninger, P.G., 2007. Acquisition of particle processing capability in juvenile oyster *Crassostrea gigas*: ontogeny of gill mucocytes. *Marine Biology*, **151**(3), 897-905.

Cantell, C.E., Franzen, A. & Sensenbaugh, T., 1982. Ultrastructure of multi ciliated collar cells in the pilidium larva of *Lineus bilineatus* (Nemertini). *Zoomorphology*, **101**(1), 1-15.

Carriker, M.R., 1979. Ultrastructural morphogenesis of prodissoconch and early dissoconch valves of the oyster *Crassostrea virginica*. *Proceedings National Shellfisheries Association*, **69**, 103-128.

Chaparro, O.R., Charpentier, J.L. & Collin, R., 2002a. Embryonic velar structure and function of two sibling species of *Crepidula* with different modes of development *Biol. Bull.*, **203**(1), 80-86.

Chaparro, O.R., Navarrete, L.R. & Thompson, R.J., 2006. The physiology of the larva of the Chilean oyster *Ostrea chilensis* and the utilisation of biochemical energy reserves during development: An extreme case of the brooding habit. *Journal of Sea Research*, **55**(4), 292-300.

Chaparro, O.R., Soto, A.E. & Bertran, C.E., 2002b. Velar characteristics and feeding capacity of encapsulated and pelagic larvae of *Crepidula fecunda* Gallardo, 1979 (Gastropoda, Calyptraeidae). *Journal of Shellfish Research*, **21**(1), 233-237.

Chaparro, O.R., Thompson, R.J. & Emerson, C.J., 1999. The velar ciliature in the brooded larva of the Chilean oyster *Ostrea chilensis* (Philippi, 1845). *Biological Bulletin*, **197**(1), 104-111.

Chaparro, O.R., Thompson, R.J. & Ward, J.E., 1993. In vivo observations of larval brooding in the Chilean oyster, *Ostrea chilensis* Philippi, 1845. *Biological Bulletin*, **185**(3), 365-372.

Chia, F.S., Buckland-Nicks, J. & Young, C.M., 1984. Locomotion of marine invertebrate larvae - a review. *Canadian Journal of Zoology*, **62**(7), 1205-1222.

Child, A.R., Papageorgiou, P. & Beaumont, A.R., 1995. Pacific Oysters Crassostrea-Gigas (Thunberg) of Possible French Origin in Natural Spat in the British-Isles. *Aquatic Conservation-Marine and Freshwater Ecosystems*, **5**(3), 173-177.

Coon, S.L. & Bonar, D.B., 1987. The role of dopa and dopamine in oyster settlement behavior. *American Zoologist*, **27**(4), A128-A128.

Cragg, S.M., 1980. Swimming behaviour of the larvae of *Pecten maximus* (L.) (Bivalvia). *Journal of the Marine Biological Association of the United Kingdom*, **60**, 551-564.

Cragg, S.M., 1985. The adductor and retractor muscles of the veliger of *Pecten maximus* (L) (Bivalvia). *Journal of Molluscan Studies*, **51**, 276-283.

Cragg, S.M., 1989. The ciliated rim of the velum of larvae of *Pecten maximus* (Bivalvia, Pectinidae). *Journal of Molluscan Studies*, **55**, 497-508.

Cragg, S.M., 1996. The phylogenetic significance of some anatomical features of Bivalve veliger larvae. *Origin and evolutionary radiation of the Mollusca*, 371-380.

Cragg, S.M., 2006. Chapter 2 Development, physiology, behaviour and ecology of scallop larvae. In *Developments in Aquaculture and Fisheries Science*, vol. Volume 35 (eds. E.S. Sandra and G.J. Parsons), pp. 45-122. Elsevier.

Cragg, S.M. & Gruffydd, L.D., 1975. The swimming behaviour and the pressure responses of the veliconchia larvae of *Ostrea edulis* L. *Proceedings of the 9th European Marine Biological Symposium*, 43-57.

Cragg, S.M. & Nott, J.A., 1977. The ultrastructure of the statocysts in the pediveliger larvae of *Pecten maximus* (L.) (Bivalvia). *Journal of Experimental Marine Biology and Ecology*, **27**(1), 23-36.

Cranfield, H.J., 1973a. Observations on function of glands of foot of pediveliger of *Ostrea edulis* during settlement. *Marine Biology*, **22**(3), 211-223.

Cranfield, H.J., 1973b. Observations on the behaviour of the pediveliger of *Ostrea edulis* during attachment and cementing. *Marine Biology*, **22**, 203-209.

Cranfield, H.J., 1973c. Observations on the function glands of the foot of the pediveliger of *Ostrea edulis* during settlement. *Marine Biology*, **22**, 211-223.

Cranfield, H.J., 1974. Observations on the morphology of the mantle folds of the pediveliger of *Ostrea edulis* L. and their function during settlement. *Journal of the Marine Biological Association of the United Kingdom*, **54**, 1-12.

Cranfield, H.J. & Michael, K.P., 1989. Larvae of the incubatory oyster *Tiostrea chilensis* (Bivalvia, Ostreidae) in the plankton of central and southern New Zealand. *New Zealand Journal of Marine and Freshwater Research*, **23**(1), 51-60.

Crawford, B.J. & Campbell, S.S., 1993. The microvilli and hyaline layer of embryonic asteroid epithelial collar cells - a sensory structure to determine the position of locomotory cilia. *Anatomical Record*, **236**(4), 697-709.

Crocker, J.C. & Grier, D.G., 1996. Methods of Digital Video Microscopy for Colloidal Studies. *Journal of Colloid and Interface Science*, **179**(1), 298-310.

Croll, R.P., 2001. Catecholamine containing cells in the central nervous system and periphery of *Aplysia californica*. *Journal of Comparative Neurology*, **441**(2), 91-105.

Croll, R.P., 2006. Development of embryonic and larval cells containing serotonin, catecholamines, and FMRFamide related peptides in the gastropod mollusc *Phestilla sibogae*. *Biol Bull*, **211**(3), 232-247.

Croll, R.P. & Chiasson, B.J., 1990. Distribution of catecholamines and of immunoreactivity to substances like vertebrate enzymes for the synthesis of catecholamines within the central nervous system of the snail, *Lymnaea stagnalis*. *Brain Research*, **525**(1), 101-114.

Croll, R.P. & Dickinson, A.J.G., 2004. Form and function of the larval nervous system in molluscs. *Invertebrate Reproduction & Development*, **46**(2-3), 173-187.

Croll, R.P., Jackson, D.L. & Voronezhskaya, E.E., 1997. Catecholamine containing cells in larval and postlarval bivalve molluscs. *Biological Bulletin*, **193**(2), 116-124.

Croll, R.P., Too, C.K.L., Pani, A.K. & Nason, J., 1995. Distribution of serotonin in the sea scallop *Placopecten magellanicus*. *Invertebrate Reproduction & Development*, **28**(2), 125-135.

Culliney, J.L., 1975. Comparative larval development of shipworms *Bankia gouldi* and *Teredo navalis*. *Marine Biology*, **29**(3), 245-251.

Dekshenieks, M.M., Hofmann, E.E., Klinck, J.M. & Powell, E.N., 1996. Modeling the vertical distribution of oyster larvae in response to environmental conditions. *Marine Ecology-Progress Series*, **136**(1-3), 97-110.

Devakie, M.N. & Ali, A.B., 2000. Salinity, temperature and nutritional effects on the setting rate of larvae of the tropical oyster, *Crassostrea iredalei* (Faustino). *Aquaculture*, **184**(1-2), 105-114.

Dickie, R., Bachoo, R.M., Rupnick, M.A., Dallabrida, S.M., DeLoid, G.M., Lai, J., DePinho, R.A. & Rogers, R.A., 2006. Three-dimensional visualization of microvessel architecture of whole-mount tissue by confocal microscopy. *Microvascular Research*, **72**(1-2), 20-26.

Dickinson, A.J.G. & Croll, R.P., 2003. Development of the larval nervous system of the gastropod *Ilyanassa obsoleta*. *Journal of Comparative Neurology*, **466**(2), 197-218.

Diederich, S., Nehls, G., van Beusekom, J.E.E. & Reise, K., 2005. Introduced Pacific oysters (Crassostrea gigas) in the northern Wadden Sea: invasion accelerated by warm summers? *Helgoland Marine Research*, **59**(2), 97-106.

Dilly, P.N., 1972. Structures of tentacles of *Rhabdopleura compacta* (Hemichordata) with special reference to neurociliary control. *Zeitschrift Fur Zellforschung Und Mikroskopische Anatomie*, **129**(1), 20-&.

Doran, S.A., Koss, R., Tran, C.H., Christopher, K.J., Gallin, W.J. & Goldberg, J.I., 2004. Effect of serotonin on ciliary beating and intracellular calcium concentration in identified populations of embryonic ciliary cells. *Journal of Experimental Biology*, **207**(8), 1415-1429.

Dove, M.C. & O'Connor, W.A., 2007. Salinity and temperature tolerance of Sydney rock oysters *Saccostrea glomerata* during early ontogeny. *Journal of Shellfish Research*, **26**(4), 939-947.

Drent, J., 2002. Temperature responses in larvae of *Macoma balthica* from a northerly and southerly population of the European distribution range. *Journal of Experimental Marine Biology and Ecology*, **275**(2), 117-129.

Dunn, C.W., Hejnol, A., Matus, D.Q., Pang, K., Browne, W.E., Smith, S.A., Seaver, E., Rouse, G.W., Obst, M., Edgecombe, G.D., Sorensen, M.V., Haddock, S.H.D., Schmidt-Rhaesa, A., Okusu, A., Kristensen, R.M., Wheeler, W.C., Martindale, M.Q. & Giribet, G., 2008. Broad phylogenomic sampling improves resolution of the animal tree of life. *Nature*, **452**(7188), 745-U745.

Eckelbarger, K.J., 1973. A device for collecting free swimming bivalve larvae from laboratory aquaria. *Veliger*, **15**(3), 256-257.

Eckman, J.E., Werner, F.E. & Gross, T.F., 1994. Modelling some effects of behaviour on larval settlement in a turbulent boundary layer. *Deep Sea Research Part II: Topical Studies in Oceanography*, **41**(1), 185-208.

Elston, R., 1980. Functional anatomy, histology and ultrastructure of the soft tissues of the larval American oyster, *Crassostrea virginica*. *Proceedings of the National Shellfisheries Association*, **70**, 65-93.

Falck, B., Hillarp, N.A., Thieme, G. & Torp, A., 1982. Fluorescence of catecholamines and related compounds condensed with formaldehyde. *Brain Research Bulletin*, **9**(1-6), R11-R15.

Finelli, C.M. & Wethey, D.S., 2003. Behaviour of oyster (*Crassostrea virginica*) larvae in flume boundary layer flows. *Marine Biology*, **143**(4), 703-711.

Fioroni, P., 1982. Larval organs, larvae, metamorphosis and types of development of mollusca - a comprehensive review. *Zool. Jb. Anat.*, **108**, 375-420.

Flyachinskaya, L.P., 2000. Localization of serotonin and FMRFamide in the bivalve mollusc *Mytilis edulis* at early stages of its development. *Journal of Evolutionary Biochemistry and Physiology*, **36**(1), 66-70.

Foighil, D.O. & Taylor, D.J., 2000. Evolution of parental care and ovulation behavior in oysters. *Molecular Phylogenetics and Evolution*, **15**(2), 301-313.

Fuchs, H.L., Mullineaux, L.S. & Solow, A.R., 2004. Sinking behavior of gastropod larvae (Ilyanassa obsoleta) in turbulence. *Limnology and Oceanography*, **49**(6), 1937-1948.

Fuchs, H.L., Neubert, M.G. & Mullineaux, L.S., 2007. Effects of turbulence mediated larval behavior on larval supply and settlement in tidal currents. *Limnology and Oceanography*, **52**(3), 1156-1165.

Fuchs, H.L., Solow, A.R. & Mullineaux, L.S., 2010. Larval responses to turbulence and temperature in a tidal inlet: Habitat selection by dispersing gastropods? *Journal of Marine Research*, **68**(1), 153-188.

Gabbot, 1973. Growth and metabolism of *Ostrea edulis* larvae. *Nature*, **241**(5390), 475-476.

Gallager, S.M., 1988. Visual observations of particle manipulation during feeding in larvae of a bivalve mollusc. *Bulletin of Marine Science*, **43**(3), 344-365.

Gallager, S.M., 1993. Hydrodynamic disturbances produced by small zooplankton - case study for the veliger larva of a bivalve mollusk. *Journal of Plankton Research*, **15**(11), 1277-1296.

Gallager, S.M., Manuel, J.L., Manning, D.A. & Odor, R., 1996. Ontogenetic changes in the vertical distribution of giant scallop larvae, *Placopecten magellanicus*, in 9-m deep mesocosms as a function of light, food, and temperature stratification. *Marine Biology*, **124**(4), 679-692.

Galtsoff, P.S., 1928. The effect of temperature on the mechanical activity of the gills of the oyster (*Ostrea virginica* Gm). *The Journal of General Physiology*, **11**(4), 415-431.

Galtsoff, P.S., 1964. The American Oyster *Crassostrea virginica* Gmelin. *Fishery Bulletin of the Fish and Wildlife Service*, **64**, 1-487.

Giribet, G. & Wheeler, W., 2002. On bivalve phylogeny: a high-level analysis of the Bivalvia (Mollusca) based on combined morphology and DNA sequence data. *Invertebrate Biology*, **121**(4), 271-324.

Golz, R. & Thurm, U., 1993. Ultrastructural evidence for the occurrence of 3 types of mechanosensitive cells in the tentacles of the cubozoan polyp *Carybdea marsupialis*. *Protoplasma*, **173**(1-2), 13-22.

Gross, T.F., Werner, F.E. & Eckman, J.E., 1992. Numerical modeling of larval settlement in turbulent bottom boundary layers. *Journal of Marine Research*, **50**, 611-642.

Gruffydd, L.D., 1976. The development of the larva of *Chlamys islandica* in the plankton and its salinity tolerance in the laboratory (Lamellibranchia, Pectinidae). *Astarte*, **8**, 61-67.

Hadfield, M.G. & Koehl, M.A.R., 2004. Rapid behavioural responses of an invertebrate larva to dissolved settlement cue. *Biological Bulletin*, **207**(1), 28-43.

Hadfield, M.G., Meleshkevitch, E.A. & Boudko, D.Y., 2000. The apical sensory organ of a gastropod veliger is a receptor for settlement cues. *Biological Bulletin*, **198**(1), 67-76.

Haimo, L.T. & Rosenbaum, J.L., 1981. Cilia, flagella, and microtubules. *Journal of Cell Biology*, **91**(3), S125-S130.

Haszprunar, G., 1983. Comparative analysis of the abdominal sense organs of Pteriomorpha (Bivalvia). *Journal of Molluscan Studies*, (12A), 47-50.

Haszprunar, G., 1985a. The fine structure of the abdominal sense organs of Pteriomorpha (Mollusca, Bivalvia). *Journal of Molluscan Studies*, **51**, 315-319.

Haszprunar, G., 1985b. On the anatomy and fine structure of a peculiar sense organ in *Nucula* (Bivalvia, Protobranchia). *Veliger*, **28**(1), 52-62.

Haszprunar, G., 1986. Fine morphological investigations on sensory structures of primitive solenogastres (Mollusca). *Zoologischer Anzeiger*, **217**(5-6), 345-362.

Haszprunar, G., 1987a. The fine morphology of the osphradial sense organs of the Mollusca .3. Placophora and Bivalvia. *Philosophical Transactions of the Royal Society of London Series B-Biological Sciences*, **315**(1169), 37-&.

Haszprunar, G., 1987b. The fine structure of the ctenidial sense organs (bursicles) of Vetigastropoda (Zeugobranchia, Trochoidea) and their functional and phylogenetic significance. *Journal of Molluscan Studies*, **53**, 46-51.

Haszprunar, G., Friedrich, S., Wanninger, A. & Ruthensteiner, B., 2002. Fine structure and immunocytochemistry of a new chemosensory system in the chiton larva (Mollusca : Polyplacophora). *Journal of Morphology*, **251**(2), 210-218.

Haszprunar, G., Vonsalviniplawen, L. & Rieger, R.M., 1995. Larval planktotrophy - a primitive Trait in the Bilateria. *Acta Zoologica*, **76**(2), 141-154.

Haure, J., Penisson, C., Bougrier, S. & Baud, J.P., 1998. Influence of temperature on clearance and oxygen consumption rates of the flat oyster *Ostrea edulis*: determination of allometric coefficients. *Aquaculture*, **169**(3-4), 211-224.

Hejnol, A., Martindale, M.Q. & Henry, J.Q., 2007. High-resolution fate map of the snail *Crepidula fornicata*: The origins of ciliary bands, nervous system, and muscular elements. *Developmental Biology*, **305**(1), 63-76.

Helm, M.M. & Bourne, N., 2004. Hatchery culture of bivalves. A practical manual. *FAO Fisheries Technical Paper*, **471**, 177pp.

Helm, M.M. & Millican, P.F., 1977. Experiments in the hatchery rearing of Pacific oyster larvae (*Crassostrea gigas,* Thunberg). *Aquaculture*, **11**(1), 1-12.

Henry, J.Q., Hejnol, A., Perry, K.J. & Martindale, M.Q., 2007. Homology of ciliary bands in spiralian trochophores. *Integrative and Comparative Biology*, **47**(6), 865-871.

Hidu, H. & Haskin, H., 1978a. Swimming speeds of oyster larvae *Crassostrea virginica* in different salinities and temperatures. *Estuaries and Coasts*, **1**(4), 252-255.

Hidu, H. & Haskin, H.H., 1978b. Swimming Speeds of Oyster Larvae Crassostrea-Virginica in Different Salinities and Temperatures. *Estuaries*, **1**(4), 252-255.

Hidu, H., Roosenburg, W.H., Drobeck, K.G., McErlean, A.J. & Mihursky, J.A., 1973. Thermal tolerance of oyster larvae *Crassostrea virginica* as related to power plant operation. *Proceedings National Shellfisheries Association*, **64**, 102-110.

His, E., Robert, R. & Dinet, A., 1989. Combined effects of temperature and salinity on fed and starved larvae of the Mediterranean mussel *Mytilus galloprovincialis* and the Japanese oyster *Crassostrea gigas*. *Marine Biology*, **100**(4), 455-463.

His, E. & Seaman, M.N.L., 1992. Effects of temporary starvation on the survival, and on subsequent feeding and growth, of oyster (*Crassostrea gigas*) Larvae. *Marine Biology*, **114**(2), 277-279.

Hoagland, K.E., 1986. Effects of temperature, salinity and substratum on larvae of the shipworms *Teredo bartschi*, Clapp and *Teredo navalis,* Linnaeus (Bivalvia, Teredinidae). *American Malacological Bulletin*, **4**(1), 89-99.

Hodgson, C.A. & Burke, R.D., 1988. Development and larval morphology of the spiny scallop, *Chlamys hastata*. *Biological Bulletin*, **174**(3), 303-318.

Isham, L.B. & Tierney, J.Q., 1953. Some aspects of the larval development and metamorphosis of *Teredo* (*Lyrodus*) *pedicellata* de Quatrefages. *Bulletin of Marine*

Science of the Gulf and Caribbean, **2**(4), 574-589.

Jaeckle, W.B. & Manahan, D.T., 1989. Growth and energy imbalance during the development of a lecithotrophic molluscan larva (*Haliotis rufescens*). *Biological Bulletin*, **177**(2), 237-246.

Johnson, K.B. & Brink, L.A., 1998. Predation on bivalve veligers by polychaete larvae. *Biological Bulletin*, **194**(3), 297-303.

Jørgensen, C.B., 1966. Biology of suspension feeding. vol. 46 pp. 762-762. Pergamon Press, Oxford.

Jupiter, S.D. & Byrne, M., 1997. Light and scanning electron microscopy of the embryos and glochidia larvae of the Australian freshwater bivalve *Hyridella depressa* (Hyriidae). *Invertebrate Reproduction & Development*, **32**(2), 177-186.

Kaartvedt, S., Aksnes, D.L. & Egge, J.K., 1987. Effect of light on the vertical distribution of *Pecten maximus* larvae. *Marine Ecology Progress Series*, **40**(1-2), 195-197.

Kang, D.H., Kim, S.J. & Choi, K.S., 2004. Microscopic observations of larval *Ostrea circumpicta* (Bivalve:Ostreidae) in brood chambers. *Journal of Shellfish Research*, **23**(2), 411-415.

Kempf, S.C., Chun, G.V. & Hadfield, M.G., 1992. An immunocytochemical search for potential neurotransmitters in larvae of *Phestilla sibogae* (Gastropoda, Opisthobranchia). *Comparative Biochemistry and Physiology Pharmacology Toxicology & Endocrinology*, **101**(2), 299-305.

Kempf, S.C. & Hadfield, M.G., 1985. Planktotrophy by the lecithotrophic larvae of a Nudibranch, *Phestilla sibogae* (Gastropoda). *Biological Bulletin*, **169**(1), 119-130.

Kempf, S.C. & Page, L.R., 2005. Anti-tubulin labelling reveals ampullary neuron ciliary bundles in opisthobranch larvae and a new putative neural structure associated with the apical ganglion. *Biological Bulletin*, **208**(3), 169-182.

Kempf, S.C., Page, L.R. & Pires, A., 1997. Development of serotonin like immunoreactivity in the embryos and larvae of nudibranch mollusks with emphasis on the structure and possible function of the apical sensory organ. *Journal of Comparative Neurology*, **386**(3), 507-528.

Kingsford, M.J., Leis, J.M., Shanks, A., C, L.K., M, M.S. & Pineda, J., 2002. Sensory environments, larval abilities and local self-recruitment. *Bulletin of Marine Science*, **70**(1), 309-340.

Knight-Jones, E.W., 1954. Relations between metachronism and the direction of ciliary beat in Metazoa. *Quarterly Journal of Microscopical Science*, **s3-95**(32), 503-521.

Kobayashi, M., Hofmann, E.E., Powell, E.N., Klinck, J.M. & Kusaka, K., 1997. A population dynamics model for the Japanese oyster, Crassostrea gigas. *Aquaculture*, **149**(3-4), 285-321.

Koehl, M.A.R., 2007. Mini review: hydrodynamics of larval settlement into fouling communities. *Biofouling*, **23**(5), 357-368.

Kuang, S.H. & Goldberg, J.I., 2001. Laser ablation reveals regulation of ciliary activity by serotonergic neurons in molluscan embryos. *Journal of Neurobiology*, **47**(1), 1-15.

Laing, I., Walker, P. & Areal, F., 2006. Return of the native. Is European oyster (Ostrea edulis) stock restoration in the UK feasible? vol. 19 pp. 283-287. Cambridge Journals Online.

Lambert, W.J., Todd, C.D. & Thorpe, J.P., 2003. Genetic population structure of two intertidal nudibranch molluscs with contrasting larval types: temporal variation and transplant experiments. *Marine Biology*, **142**(3), 461-471.

Larsen, P.S., Madsen, C.V. & Riisgård, H.U., 2008. Effect of temperature and viscosity on swimming velocity of the copepod *Acartia tonsa*, brine shrimp *Artemia salina* and rotifer *Brachionus plicatilis*. *Aquatic Biology*, **4**(1), 47-54.

Larsen, P.S. & Riisgård, H.U., 2009. Viscosity and not biological mechanisms often controls the effects of temperature on ciliary activity and swimming velocity of small aquatic organisms. *Journal of Experimental Marine Biology and Ecology*, **381**(2), 67-73.

Le Pennec, M., Paugam, A. & Le Pennec, G., 2003. The pelagic life of the pectinid *Pecten maximus* - a review. vol. 60 pp. 211-233.

Leigh, M.D., 1962. Cilia, ciliated epithelium and ciliary activity. . vol. 15 pp. 885.

Leverone, J.R., Geiger, S.P., Stephenson, S.P. & Arnold, W.S., 2010. Increase in bay scallop (*Argopecten Irradians*) populations following releases of competent larvae in two west florida estuaries. *Journal of Shellfish Research*, **29**(2), 395-406.

Levin, L.A., 2006. Recent progress in understanding larval dispersal: new directions and digressions. vol. 46 pp. 282-297.

Levin, L.A. & Bridges, T.S., 1995. Pattern and diversity in reproduction and development. In *Ecology of Marine Invertebrate Larvae*, (ed. L.R. McEdward), pp. 1-49.

Ma, H.G., Grassle, J.P. & Chant, R.J., 2006. Vertical distribution of bivalve larvae along a cross-shelf transect during summer upwelling and downwelling. *Marine Biology*, **149**(5), 1123-1138.

Mackie, G.L., 1984. Bivalves. In *Mollusca*, vol. 7. Reproduction (ed. M.V.D. Biggelaar), pp. 351-418. Academic Press.

Mackie, G.O., Singla, C.L. & Thiriot-Quievreux, C., 1976. Nervous control of ciliary activity in gastropod larvae. *Biological Bulletin*, **151**(1), 182-199.

Malakhov, A.A. & Medvedeva, L.A., 1985. Embryonic development of giant oysters. *The Soviet Journal of Marine Biology*, **11**, 39-45.

Manahan, D.T., 1983. The uptake and metabolism of dissolved amino acids by bivalve larvae. *Biological Bulletin*, **164**(2), 236-250.

Manahan, D.T., 1990. Adaptations by invertebrate larvae for nutrient acquisition from seawater. *American Zoologist*, **30**(1), 147-160.

Manahan, D.T. & Crisp, D.J., 1983. Autoradiographic studies on the uptake of dissolved amino acids from seawater by bivalve larvae. *Journal of the Marine Biological Association of the United Kingdom*, **63**(3), 673-682.

Mann, R. & Wolf, C.C., 1983. Swimming behaviour of larvae of the ocean quahog *Arctica islandica* in response to pressure and temperature. *Marine Ecology Progress Series*, **13**(2-3), 211-218.

Manuel, J.L., Gallager, S.M., Pearce, C.M., Manning, D.A. & Odor, R.K., 1996. Veligers from different populations of sea scallop *Placopecten magellanicus* have different vertical migration patterns. *Marine Ecology Progress Series*, **142**(1-3), 147-163.

Manuel, J.L. & O'Dor, R.K., 1997. Vertical migration for horizontal transport while avoiding predators: A tidal/diel model. *Journal of Plankton Research*, **19**(12), 1929-1947.

Manuel, J.L., Pearce, C.M., Manning, D.A. & O'Dor, R.K., 2000. The response of sea scallop (*Placopecten magellanicus*) veligers to a weak thermocline in 9-m deep mesocosms. *Marine Biology*, **137**(1), 169-175.

Manuel, J.L., Pearce, C.M. & O'Dor, R.K., 1997. Vertical migration for horizontal transport while avoiding predators: II. Evidence for the tidal/diel model from two populations of scallop (*Placopecten magellanicus*) veligers. *Journal of Plankton Research*, **19**(12), 1949-1973.

Marechal, J.P., Hellio, C., Sebire, M. & Clare, A.S., 2004. Settlement behaviour of marine invertebrate larvae measured by EthoVision 3.0. *Biofouling*, **20**(4-5), 211-217.

Marois, R. & Carew, T.J., 1997. Fine structure of the apical ganglion and its serotonergic cells in the larva of *Aplysia californica*. *Biological Bulletin*, **192**(3), 388-398.

Marsden, J.R. & Hassessian, H., 1986. Effects of Ca2+ and catecholamines on swimming cilia of the trochophore larva of the polychaete Spirobranchus giganteus (Pallas). *Journal of Experimental Marine Biology and Ecology*, **95**(3), 245-255.

Martinez, G., Garrote, C., Mettifogo, L., Perez, H. & Uribe, E., 1996. Monoamines and prostaglandin E(2) as inducers of the spawning of the scallop, *Argopecten purpuratus* Lamarck. *Journal of Shellfish Research*, **15**(2), 245-249.

Martinez, G., Lopez, V., Mettifogo, L. & Cancino, J.M., 2008. Energy source utilization by embryos and larvae of the muricid snail *Chorus giganteus* (Lesson, 1829). *Journal of Experimental Marine Biology and Ecology*, **354**(1), 65-80.

McEdward, L.R. & Chia, F.-S., 1991. Size and energy content of eggs from echinoderms with pelagic lecithotrophic development. *Journal of Experimental Marine Biology and Ecology*, **147**(1), 95-102.

Mileikovsky, S.A., 1973. Speed of active movement of pelagic larvae of marine bottom invertebrates and their ability to regulate their vertical position. *Marine Biology*, **23**(1), 11-17.

Minnich, Leeb, Bernroider & Lametschwandtner, 1999. Three-dimensional morphometry in scanning electron microscopy: a technique for accurate dimensional and angular measurements of microstructures using stereopaired digitized images and digital image analysis. *J Microsc*, **195**(1), 23-33.

Morse, M.P. & Zardus, J.D., 1997. Bivalvia. In *Microscopic Anatomy of Invertebrates*, vol. 6A pp. 7-118. Wiley-Liss, Inc.

Moueza, M., Gros, O. & Frenkiel, L., 1999. Embryonic, larval and postlarval development of the tropical clam, *Anomalocardia brasiliana* (Bivalvia, Veneridae). *Journal of Molluscan Studies*, **65**, 73-88.

Nair, N.B., 1971. Biology of wood boring teredinid molluscs. *Advances in Marine Biology*, **9**, 335-&.

Nielsen, C., 2004. Trochophora larvae: cell-lineages, ciliary bands, and body regions. 1. Annelida and Mollusca. *Journal of Experimental Zoology Part B: Molecular and Developmental Evolution*, **302B**(1), 35-68.

Nielsen, C. & Nielsen, C., 1995. Animal evolution: Interrelationships of the living phyla. In *Animal evolution: Interrelationships of the living phyla*, pp. ix+467p. Oxford University Press; Oxford University Press, Inc.

North, E.W., Schlag, Z., Hood, R.R., Li, M., Zhong, L., Gross, T. & Kennedy, V.S., 2008. Vertical swimming behaviour influences the dispersal of simulated oyster larvae in a coupled particle-tracking and hydrodynamic model of Chesapeake Bay. *Marine Ecology Progress Series*, **359**, 99-115.

Page, L.R. & Parries, S.C., 2000. Comparative study of the apical ganglion in planktotrophic caenogastropod larvae: ultrastructure and immunoreactivity to serotonin. *Journal of Comparative Neurology*, **418**(4), 383-401.

Pawlik, J.R., 1992. Chemical ecology of the settlement of benthic marine invertebrates. *Oceanography and Marine Biology*, **30**, 273-335.

Pearce, C.M. & Bourget, E., 1996. Settlement of larvae of the giant scallop, *Placopecten magellanicus* (Gmelin), on various artificial and natural substrata under hatchery-type conditions. *Aquaculture*, **141**(3-4), 201-221.

Pearce, C.M., Manuel, J.L., Gallager, S.M., Manning, D.A., O'Dor, R.K. & Bourget, E., 2004. Depth and timing of settlement of veligers from different populations of giant scallop, *Placopecten magellanicus* (Gmelin), in thermally stratified mesocosms. *Journal of Experimental Marine Biology and Ecology*, **312**(1), 187-214.

Pechenik, J.A., 1999. On the advantages and disadvantages of larval stages in benthic marine invertebrate life cycles. *Marine Ecology-Progress Series*, **177**, 269-297.

Pechenik, J.A., Perron, F.E. & Turner, R.D., 1979. The role of phytoplankton in the diets of adult and larval shipworms, *Lyrodus pedicellatus* (Bivalvia: Teredinidae). *Estuaries*, **2**(1), 58-60.

Pires, A., Coon, S.L. & Hadfield, M.G., 1997. Catecholamines and dihydroxyphenylalanine in metamorphosing larvae of the nudibranch *Phestilla sibogae* Bergh (Gastropoda: Opisthobranchia). *Journal of Comparative Physiology*, **181**(3), 187-194.

Pires, A., Croll, R.P. & Hadfield, M.G., 2000. Catecholamines modulate metamorphosis in the opisthobranch gastropod *Phestilla sibogae*. *Biological Bulletin*, **198**(3), 319-331.

Pires, A. & Hadfield, M.G., 1991. Oxidative breakdown products of catecholamines and hydrogen peroxide induce partial metamorphosis in the Nudibranch *Phestilla sibogae* Bergh (Gastropoda, Opisthobranchia). *Biological Bulletin*, **180**(2), 310-317.

Podolsky, R.D. & Emlet, R.B., 1993. Separating the effects of temperature and viscosity on swimming and water movement by sand dollar larvae (*Dendraster excentricus*). *Journal of Experimental Biology*, **176**, 207-221.

Porcel, M., Cotes, B. & Campos, M., 2011. Biological and behavioral effects of kaolin particle film on larvae and adults of Chrysoperla carnea (Neuroptera: Chrysopidae). *Biological Control*, **59**(2), 98-105.

Pradhan, N.N., Gohad, N.V., Orihuela, B., Burg, T.C., Birchfield, S.T., Rittschof, D. & Mount, A.S., 2011. Development of an automated algorithm for tracking and quantifying Barnacle cyprid settlement behavior. *Journal of Experimental Marine Biology and Ecology*, **410**, 21-28.

Prael, A., Cragg, S.M. & Henderson, S.M., 2001. Behavioural responses of veliger larvae of *Crassostrea gigas* to leachate from wood treated with copper-chrome-arsenic (CCA): A potential bioassay of sublethal environmental effects of contaminants. *Journal of Shellfish Research*, **20**(1), 267-273.

Quayle, D.B., 1988. Pacific Oyster Culture in British Columbia Canada. *Canadian Bulletin of Fisheries and Aquatic Sciences*, (218), I.

Raineri, M., 1995. Is a mollusk an evolved bent metatrochophore - a histochemical investigation of neurogenesis in *Mytilus* (Mollusca, Bivalvia). *Journal of the Marine Biological Association of the United Kingdom*, **75**(3), 571-592.

Rico-Villa, B., Pouvreau, S. & Robert, R., 2009. Influence of food density and temperature on ingestion, growth and settlement of Pacific oyster larvae, *Crassostrea gigas*. *Aquaculture*, **287**(3-4), 395-401.

Riisgard, H.U., 2001. On measurement of filtration rates in bivalves - the stony road to reliable data: review and interpretation. *Marine Ecology-Progress Series*, **211**, 275-291.

Riisgard, H.U. & Larsen, P.S., 2001. Minireview: ciliary filter feeding and bio-fluid mechanics - present understanding and unsolved problems. *Limnology and Oceanography*, **46**(4), 882-891.

Riisgard, H.U. & Larsen, P.S., 2009. Ciliary-propelling mechanism, effect of temperature and viscosity on swimming speed, and adaptive significance of 'jumping' in the ciliate *Mesodinium rubrum*. *Marine Biology Research*, **5**(6), 585-595.

Riisgard, H.U., Nielsen, C. & Larsen, P.S., 2000. Downstream collecting in ciliary suspension feeders: the catch- up principle. *Marine Ecology-Progress Series*, **207**, 33-51.

Robert, R. & Gerard, A., 1999. Bivalve hatchery technology: the current situation for the Pacific oyster *Crassostrea gigas* and the scallop *Pecten maximus* in France. *Aquatic Living Resources*, **12**(2), 121-130.

Robert, R., His, E. & Dinet, A., 1988. Combined effects of temperature and salinity on fed and starved larvae of the european flat oyster *Ostrea edulis*. *Marine Biology*, **97**(1), 95-100.

Roegner, G.C., 2000. Transport of molluscan larvae through a shallow estuary. vol. 22 pp. 1779-1800.

Satir, P., 1992. Mechanisms of ciliary movement - contributions from electron microscopy. *Scanning Microscopy*, **6**(2), 573-579.

Sbalzarini, I.F. & Koumoutsakos, P., 2005. Feature point tracking and trajectory analysis for video imaging in cell biology. *Journal of Structural Biology*, **151**(2), 182-195.

Scheltema, R.S., 1995. The Relevance of Passive Dispersal for the Biogeography of Caribbean Mollusks. *American Malacological Bulletin*, **11**(2), 99-115.

Scholer, J. & Armstrong, W.E., 1982. Aqueous aldehyde (Faglu) histofluorescence for catecholamines in 2 Mu-M sections using polyethylene glycol embedding. *Brain Research Bulletin*, **9**(1-6), 27-31.

Shanks, A.L. & Brink, L., 2005. Upwelling, downwelling, and cross-shelf transport of bivalve larvae: test of a hypothesis. *Marine Ecology-Progress Series*, **302**, 1-12.

Short, G. & Tamm, S.L., 1991. On the nature of paddle cilia and discocilia. *Biological Bulletin*, **180**(3), 466-474.

Silberfeld, T. & Gros, O., 2006. Embryonic development of the tropical bivalve *Tivela mactroides* (Born, 1778) (Veneridae : subfamily Meretricinae): a SEM study. *Cahiers De Biologie Marine*, **47**(3), 243-251.

Sleigh, M.A., 1962. *The biology of cilia and flagella*. Oxford: New York, Paris : Pergamon press.

Smith, S.A., Nason, J. & Croll, R.P., 1998. Distribution of catecholamines in the sea scallop, *Placopecten magellanicus*. *Canadian Journal of Zoology*, **76**(7), 1254-1262.

Sopott-Ehlers, B., 1984. Epidermal collar receptors of the Nematoplanidae and the Polystyliphoridae (Plathelminthes, Unguiphora). *Zoomorphology*, **104**(4), 226-230.

Spencer, B.E., Edwards, D.B., Kaiser, M.J. & Richardson, C.A., 1994. Spatfalls of the non-native Pacific oyster, Crassostrea gigas, in British waters. *Aquatic Conservation: Marine and Freshwater Ecosystems*, **4**(3), 203-217.

Stephens, R.E. & Prior, G., 1992. Dynein from serotonin-activated cilia and flagella: extraction characteristics and distinct sites for cAMP-dependent protein phosphorylation. vol. 103 pp. 999-1012.

Stobutzki, I.C., 2001. Marine reserves and the complexity of larval dispersal. *Reviews in Fish Biology and Fisheries*, **10**(4), 515-518.

Strathmann, R.R., 1978. The evolution and loss of feeding larval stages of marine invertebrates. *Evolution*, **32**(4), 894-906.

Strathmann, R.R., 1980. Why does a larva swim so long. *Paleobiology*, **6**(4), 373-376.

Strathmann, R.R., 1985. Feeding and non-feeding larval development and life history evolution in marine invertebrates. *Annual Review of Ecology and Systematics*, **16**, 339-361.

Strathmann, R.R., 1993. Hypotheses on the origins of marine larvae. *Annual Review of Ecology and Systematics*, **24**, 89-117.

Strathmann, R.R., Fonseca, J.R.C. & Jahn, T.L., 1972. Suspension feeding by marine invertebrate larvae - clearance of particles by ciliated bands of a rotifer, pluteus, and trochophore. *Biological Bulletin*, **142**(3), 505-&.

Strathmann, R.R. & Grunbaum, D., 2006. Good eaters, poor swimmers: compromises in larval form. *Integrative and Comparative Biology*, **46**(3), 312-322.

Strathmann, R.R. & Leise, E., 1979. Feeding mechanisms and clearance rates of molluscan veligers. *Biological Bulletin*, **157**(3), 524-535.

Strathmann, R.R. & Strathmann, M.F., 1982. The relationship between adult size and brooding in marine invertebrates. *American Naturalist*, **119**(1), 91-101.

Sylvester, F., Dorado, J., Boltovskoy, D., Juarez, A. & Cataldo, D., 2005. Filtration rates of the invasive pest bivalve *Limnoperna fortunei* as a function of size and temperature. *Hydrobiologia*, **534**(1-3), 71-80.

Tamburri, M.N., Finelli, C.M., Wethey, D.S. & ZimmerFaust, R.K., 1996. Chemical induction of larval settlement behaviour in flow. *Biological Bulletin*, **191**(3), 367-373.

Teuchert, G., 1976. Sensory devices in *Turbanella cornuta* Remane (Gastrotricha). *Zoomorphologie*, **83**(2), 193-207.

Thorson, G., 1950. Reproductive and larval ecology of marine bottom invertebrates. *Biol. Rev*, **25**, 1-45.

Thorson, G., 1964. Light as an ecological factor in the dispersal and settlement of larvae of marine bottom invertebrates. *Ophelia*, **1**, 167-208.

Todd, C.D., J. Lambert, W. & Thorpe, J.P., 1998. The genetic structure of intertidal populations of two species of nudibranch molluscs with planktotrophic and pelagic lecithotrophic larval stages: are pelagic larvae "for" dispersal? *Journal of Experimental Marine Biology and Ecology*, **228**(1), 1-28.

Tremblay, M.J., Loder, J.W., Werner, F.E., Naimie, C.E., Page, F.H. & Sinclair, M.M., 1994. Drift of sea scallop larvae *Placopecten magellanicus* on Georges Bank - a model study of the roles of mean advection, larval behaviour and larval origin. *Deep Sea Research Part ii - Topical Studies in Oceanography*, **41**(1), 7-49.

Tremblay, M.J. & Sinclair, M., 1992. Planktonic sea scallop larvae (*Placopecten magellanicus*) in the Georges Bank region - broadscale distribution in relation to physical oceanography. *Canadian Journal of Fisheries and Aquatic Sciences*, **49**(8), 1597-1615.

Turner, E.J., Zimmer-Faust, R.K., Palmer, M.A., Luckenbach, M. & Pentcheff, N.D., 1994. Settlement of oyster (*Crassostrea virginica*) larvae: effects of water flow and a water soluble chemical cue. *Limnology and Oceanography*, **39**(7), 1579-1593.

Turner, R.D. & Boyle, P.J., 1974. Studies of bivalve larvae using the scanning electron microscope and critical point drying. *Bulletin of the American Malacological Union*, **40**, 59-65.

Turner, R.D. & Johnson, A.C., 1971. Biology of marine wood boring molluscs. In *Marine borers, fungi and fouling organisms of wood*, (eds. E.B.G. Jones and S.K. Eltringham), pp. 259-301.

Utting, S.D. & Millican, P.F., 1997. Techniques for the hatchery conditioning of bivalve broodstocks and the subsequent effect on egg quality and larval viability. *Aquaculture*, **155**(1-4), 45-54.

Utting, S.D. & Spencer, B.E., 1991. The hatchery culture of bivalve mollusc larvae and juveniles. *Laboratory leaflet, MAFF fisheries research*, **68**, 1-31.

Valentine, M.T., Kaplan, P.D., Thota, D., Crocker, J.C., Gisler, T., Prud'homme, R.K., Beck, M. & Weitz, D.A., 2001. Investigating the microenvironments of inhomogeneous soft materials with multiple particle tracking. *Physical Review E*, **64**(6), 9.

Verwey, J., 1966. The role of some external factors in the vertical migration of marine animals. *Netherlands Journal of Sea Research*, **3**(2), 245-266, IN241-IN244.

von Herbing, I.H. & Keating, K., 2003. Temperature induced changes in viscosity and its effects on swimming speed in larval haddock. In *The big fish bang: Proceedings of the 26th Annual Larval Fish Conference*, pp. 23-34. Institute of Marine Research (Norway).

Voronezhskaya, E.E., Hiripi, L., Elekes, K. & Croll, R.P., 1999. Development of catecholaminergic neurons in the pond snail, *Lymnaea stagnalis*: I. Embryonic development of dopamine containing neurons and dopamine dependent behaviours. *Journal of Comparative Neurology*, **404**(3), 285-296.

Voronezhskaya, E.E., Nezlin, L.P., Odintsova, N.A., Plummer, J.T. & Croll, R.P., 2008. Neuronal development in larval mussel *Mytilus trossulus* (Mollusca : Bivalvia). *Zoomorphology*, **127**(2), 97-110.

Waller, T.R., 1978. Formation of a posterodorsal notch in larval oyster shells and the prodissoconch I/II boundary in the Bivalvia. *The Bulletin of the American Malacological Society*, 55-56.

Waller, T.R., 1981. Functional morphology and development of veliger larvae of the European oyster, *Ostrea edulis* Linne. *Smithsonian Contibutions to Zoology*, (328), 1-70.

Ward, J.E., Beninger, P.G., Macdonald, B.A. & Thompson, R.J., 1991. Direct observations of feeding structures and mechanisms in bivalve mollusks using endoscopic examination and video image analysis. *Marine Biology*, **111**(2), 287-291.

Westfall, J.A., Sayyar, K.L. & Elliott, C.F., 1998. Cellular origins of kinocilia, stereocilia, and microvilli on tentacles of sea anemones of the genus Calliactis (Cnidaria: Anthozoa). *Invertebrate Biology*, **117**(3), 186-193.

Wong, K., Stewart, A., Gilder, T., Wu, N., Frank, K., Gaikwad, S., Suciu, C., Dileo, J., Utterback, E., Chang, K., Grossman, L., Cachat, J. & Kalueff, A.V., 2010. Modeling seizure-related behavioral and endocrine phenotypes in adult zebrafish. *Brain Research*, **1348**, 209-215.

Wood, L. & Hargis, W.J.J., 1971. Transport of bivalve larvae in a tidal estuary. In *4th European Marine Biology Symposium*, (ed. D.J. Crisp), pp. 29-44.

Wright, D.A., Kennedy, V.S., Roosenburg, W.H., Castagna, M. & Mihursky, J.A., 1983. Temperature tolerance of embryos and larvae of five bivalve species under simulated power plant entrainment conditions: a synthesis. *Marine Biology*, **77**(3), 271-278.

Yonge, C.M., 1926. Structure and physiology of the organs of feeding and digestion in *Ostrea edulis*. vol. 14 pp. 295-386. Cambridge Journals Online.

Yoshinaga, M.Y., Sumida, P.Y.G., Silveira, I.C.A., Ciotti, A.M., Gaeta, S.A., Pacheco, L. & Koettker, A.G., 2010. Vertical distribution of benthic invertebrate larvae during an upwelling event along a transect off the tropical Brazilian continental margin. *Journal of Marine Systems*, **79**(1-2), 124-133.

Young, C.M. (ed.), 2002. *Atlas of Marine Invertebrate Larvae*. Academic Press.

Zhadan, P.M., 2005. Directional sensitivity of the Japanese scallop *Mizuhopecten yessoensis* and Swift scallop *Chlamys swifti* to water-borne vibrations. *Russian Journal of Marine Biology*, **31**(1), 28-35.

Zhadan, P.M., Sizov, A.V. & Dautov, S.S., 2004. Ultrastructure of the abdominal sense organ of the scallop *Mizuchopecten yessoensis* (Jay). *Cell and Tissue Research*, **318**(3), 617-629.

Zimmer-Faust, R.K., Tamburri, M.N. & Decho, A.W., 1997. Chemosensory ecology of oyster larvae: benthic-pelagic coupling. In *Sensory Ecology and Physiology of Zooplankton*, (eds. D.L. Hartline, P. Lenz and J.E. Purcell), pp. 37–50. Toronto: Gordon and Breach.